

Topics in Organometallic Chemistry 48

Christian Bruneau
Pierre H. Dixneuf *Editors*

Ruthenium in Catalysis

 Springer

Topics in Organometallic Chemistry

Series Editors

Frank Glorius, Münster, Germany

Jun Okuda, Aachen, Germany

Editorial Board

M. Beller, Rostock, Germany

J.M. Brown, Oxford, United Kingdom

P.H. Dixneuf, Rennes, France

J. Dupont, Porto Alegre, Brazil

A. Fürstner, Mülheim, Germany

L.J. Gooßen, Kaiserslautern, Germany

T. Ikariya, Tokyo, Japan

S. Nolan, St Andrews, United Kingdom

L.A. Oro, Zaragoza, Spain

Q.-L. Zhou, Tianjin, China

Aims and Scope

The series *Topics in Organometallic Chemistry* presents critical overviews of research results in organometallic chemistry. As our understanding of organometallic structure, properties and mechanisms increases, new ways are opened for the design of organometallic compounds and reactions tailored to the needs of such diverse areas as organic synthesis, medical research, biology and materials science. Thus the scope of coverage includes a broad range of topics of pure and applied organometallic chemistry, where new breakthroughs are being achieved that are of significance to a larger scientific audience.

The individual volumes of *Topics in Organometallic Chemistry* are thematic. Review articles are generally invited by the volume editors. All chapters from *Topics in Organometallic Chemistry* are published OnlineFirst with an individual DOI. In references, *Topics in Organometallic Chemistry* is abbreviated as Top Organomet Chem and cited as a journal.

More information about this series at
<http://www.springer.com/series/3418>

Christian Bruneau · Pierre H. Dixneuf
Editors

Ruthenium in Catalysis

With contributions by

M. Akita · P.G. Alsabeh · E. Balaraman · M. Beller ·
C. Bruneau · V. Cadierno · B. Chaudret · P. Crochet ·
S. Dérien · P.H. Dixneuf · C. González-Rodríguez ·
R.H. Grubbs · M.B. Herbert · H. Junge · T. Koike ·
B. Li · P. Lignier · V.M. Marx · D. Mellmann · D. Milstein ·
K. Philippot · L.E. Rosebrugh · C. Saá · J.A. Varela

 Springer

Editors

Christian Bruneau
Pierre H. Dixneuf
Inst. des Sciences Chimiques de Rennes
UMR 6226 CNRS-Université Rennes1
Rennes
France

ISSN 1436-6002 ISSN 1616-8534 (electronic)
ISBN 978-3-319-08481-7 ISBN 978-3-319-08482-4 (eBook)
DOI 10.1007/978-3-319-08482-4
Springer Cham Heidelberg New York Dordrecht London

Library of Congress Control Number: 2014951202

© Springer International Publishing Switzerland 2014

This work is subject to copyright. All rights are reserved by the Publisher, whether the whole or part of the material is concerned, specifically the rights of translation, reprinting, reuse of illustrations, recitation, broadcasting, reproduction on microfilms or in any other physical way, and transmission or information storage and retrieval, electronic adaptation, computer software, or by similar or dissimilar methodology now known or hereafter developed. Exempted from this legal reservation are brief excerpts in connection with reviews or scholarly analysis or material supplied specifically for the purpose of being entered and executed on a computer system, for exclusive use by the purchaser of the work. Duplication of this publication or parts thereof is permitted only under the provisions of the Copyright Law of the Publisher's location, in its current version, and permission for use must always be obtained from Springer. Permissions for use may be obtained through RightsLink at the Copyright Clearance Center. Violations are liable to prosecution under the respective Copyright Law.

The use of general descriptive names, registered names, trademarks, service marks, etc. in this publication does not imply, even in the absence of a specific statement, that such names are exempt from the relevant protective laws and regulations and therefore free for general use.

While the advice and information in this book are believed to be true and accurate at the date of publication, neither the authors nor the editors nor the publisher can accept any legal responsibility for any errors or omissions that may be made. The publisher makes no warranty, express or implied, with respect to the material contained herein.

Printed on acid-free paper

Springer is part of Springer Science+Business Media (www.springer.com)

Preface

After the publication in 2004 of *Ruthenium catalysts and fine chemistry* co-edited by Bruneau and Dixneuf (Springer-Topics in Organometallic Chemistry series no. 11), the number of innovations brought by ruthenium catalysts has considerably increased.

The design and easy preparation of new ruthenium complexes that are equipped with functionally active ligands have led to the discovery of unprecedented activation processes with useful applications in catalysis for organic synthesis, offering interfaces with energy, molecular materials and polymers. From an emerging domain using ruthenium as “an element for the connoisseur”, ruthenium catalysis is now a mature field, widely explored with increasing contributions from industry. This is due to the availability of a large number of well-defined and stable ruthenium precatalysts offering several possible oxidation states, some of them being efficient in water. They tolerate and sometimes take profit of functional groups and have revealed catalytic activities for a wide range of selective chemical transformations with atom economy. New ruthenium catalysts are able to provide unique and multiple bond activation modes and make possible selective carbon–carbon, carbon–hydrogen, carbon–heteroatom bond formation and cleavage.

In this volume, innovative aspects of ruthenium applications in their contribution to green chemistry have been included, notably formation of hydrogen, hydrogenation and hydration of polar multiple bonds, stereoselective alkene metathesis, alkyne transformations via various activation modes, sp^2C-H and sp^3C-H bond activation and functionalization, photoredox catalysis and nanoparticles in catalysis.

This monograph is not intended to provide a comprehensive view of all ruthenium-catalyzed reactions, as this metal and its numerous complexes are now involved in many useful catalytic transformations. For instance, ruthenium-catalyzed carbonylation, polymerization, enantioselective hydrogenation and cyclopropanation... have not been included in spite of their high interest in synthesis.

Ten years after the first edition and because of the tremendous novelties that have recently appeared showing the fundamental role of ruthenium in catalysis, it was the appropriate opportunity to prepare the present volume, which should be helpful to researchers, teachers and students motivated by innovative and sustainable chemistry. It might also be a source of inspiration for new and unexpected catalytic transformations. We are grateful to the authors, experts in their domain, who have contributed by writing a chapter.

We dedicate this volume to all chemists and students who have made of ruthenium chemistry and catalysis a field for the future.

Rennes, France

Christian Bruneau
Pierre H. Dixneuf

Contents

Cyclometalated Ruthenium Alkylidene Complexes: A Powerful Family of Z-Selective Olefin Metathesis Catalysts	1
Vanessa M. Marx, Lauren E. Rosebrugh, Myles B. Herbert, and Robert H. Grubbs	
Hydrogenation of Polar Bonds Catalysed by Ruthenium-Pincer Complexes	19
Ekambaram Balaraman and David Milstein	
Ruthenium-Catalyzed Hydrogen Generation from Alcohols and Formic Acid, Including Ru-Pincer-Type Complexes	45
Pamela G. Alsabeh, Dörthe Mellmann, Henrik Junge, and Matthias Beller	
Ruthenium-Catalyzed Amide-Bond Formation	81
Pascale Crochet and Victorio Cadierno	
Ruthenium(II)-Catalysed sp^2 C–H Bond Functionalization by C–C Bond Formation	119
Bin Li and Pierre H. Dixneuf	
sp^3 C–H Bond Functionalization with Ruthenium Catalysts	195
Christian Bruneau	
Catalytic Transformations of Alkynes via Ruthenium Vinylidene and Allenylidene Intermediates	237
Jesús A. Varela, Carlos González-Rodríguez, and Carlos Saá	

C–C Bond Formation on Activation of Alkynes and Alkenes with (C₅R₅)Ru Catalysts	289
Sylvie Dérien	
Organometallic Ruthenium Nanoparticles and Catalysis	319
Karine Philippot, Pascal Lignier, and Bruno Chaudret	
Visible-Light-Induced Redox Reactions by Ruthenium Photoredox Catalyst	371
Takashi Koike and Munetaka Akita	
Index	397

Cyclometalated Ruthenium Alkylidene Complexes: A Powerful Family of Z-Selective Olefin Metathesis Catalysts

Vanessa M. Marx, Lauren E. Rosebrugh, Myles B. Herbert,
and Robert H. Grubbs

Abstract The past 5 years have witnessed an enormous growth in the field of Z-selective olefin metathesis. The development of a new class of cyclometalated ruthenium-based catalysts has extended the utility of olefin metathesis to the synthesis of useful Z-olefin-containing small molecules, polymers, and natural products. This review highlights the recent advances in the area of Z-selective olefin metathesis employing cyclometalated ruthenium alkylidene catalysts, with particular focus on its applications and mechanistic basis. A deeper understanding of structure–activity relationships should aid in the future design of even more active and selective olefin metathesis catalysts.

Keywords Alkylidenes · C=C bond formation · Carbenes · Diastereoselectivity · Metathesis · Olefins · Ruthenium · Z-selective

Contents

1	Introduction	2
2	Catalyst Development	3
2.1	Original Strategy for the Design of Z-Selective Ruthenium-Based Catalysts	3
2.2	Model for Z-Selectivity of Cyclometalated Ruthenium-Based Catalysts	5
2.3	Evolution of Ruthenium-Based Cyclometalated Catalyst Systems	6
2.4	General Trends in Ruthenium-Based Cyclometalated Catalyst Systems	8
3	Applications in Z-Selective Olefin Metathesis Transformations	9
3.1	Cross Metathesis	9
3.2	Asymmetric Ring Opening Cross Metathesis	10
3.3	Macrocyclic Ring Closing Metathesis	10
3.4	Ring Opening Metathesis Polymerization	11

3.5 Z-Selective Ethenolysis	12
4 Applications in the Synthesis of Natural Products	13
5 Conclusions and Future Outlook	15
References	15

Abbreviations

Adm	Adamantyl
AROCCM	Asymmetric ring opening/cross metathesis
CM	Cross metathesis
Dipp	2,6-Diisopropylphenyl
EPA	Environmental Protection Agency
Mes	Mesityl
mRCM	Macrocyclic ring closing metathesis
NHC	<i>N</i> -heterocyclic carbene
NMR	Nuclear magnetic resonance
Piv	Pivaloyl
RCAM	Ring closing alkyne metathesis
RCM	Ring closing metathesis
ROMP	Ring opening metathesis polymerization
TON	Turnover number

1 Introduction

Initially a poorly understood catalytic process, olefin metathesis has evolved into one of the most prevailing methods for the synthesis of carbon–carbon bonds [1–10]. Seminal work in the 1970s identified early transition metal carbene complexes are able to catalyze olefin metathesis reactions [11]. This initial discovery led to the development of a number of well-defined systems that enabled thorough mechanistic investigations, including elucidation of the factors affecting catalyst activity and selectivity. Capitalizing on these results, many present-day metathesis catalysts are straightforward to use, air- and moisture-tolerant, and highly active across a broad range of substrates. Furthermore, through judicious choice of the metal and ligand, a catalyst can be readily tailored to specific applications or classes of substrates, and many are now either readily accessible or commercially available. As a result, olefin metathesis continues to see great success in a variety of fields, including organic synthesis, polymer chemistry, and chemical biology [11–16].

An ongoing challenge in the field of olefin metathesis has been the control of the *E/Z* diastereoselectivity of the reaction [17–19]. Due to the frequently reversible nature of this transformation, product distributions generally reflect thermodynamic energy differences between olefin isomers, resulting in the predominant formation of *E*-olefins (ca. 90% *E*-selectivity). Many relevant natural products and bioactive

molecules, on the other hand, contain functionality derived from *Z*-olefins. Moreover, the activity and properties of such molecules often depend heavily on the alkene geometry and can be adversely affected by even minute amounts of stereoisomeric impurities. While mixtures of *E*- and *Z*-isomers may be separated by chromatography or crystallization in most cases, this often requires extensive optimization and is not economical. Thus, it is highly desirable to develop catalyst systems that are not only kinetically selective for the formation of *Z*-olefins but are also capable of producing *stereopure Z*- or *E*-olefins. Although indirect methods have been developed, including alkyne metathesis followed by semi-reduction [20, 21], or substrate-controlled mRCM of vinylsiloxanes followed by desilylation [22, 23], the scope of these transformations is limited.

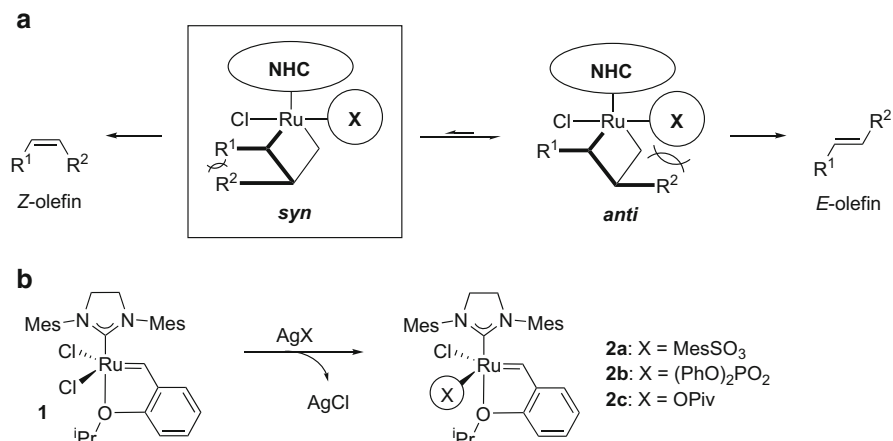
Accordingly, considerable effort has been dedicated to the development of olefin metathesis catalysts exhibiting kinetic selectivity. As a result, a number of *Z*-selective tungsten-, molybdenum-, and ruthenium-based olefin metathesis catalysts have been recently developed (For Mo- and W-based *Z*-selective catalysts: [24–41], For Ru-based *Z*-selective catalysts: [42–45], For cyclometalated Ru-based *Z*-selective catalysts: [46–58]). Many of these systems exhibit consistently high levels of activity and selectivity across a broad range of substrates. Herein, we will focus specifically on the cyclometalated ruthenium-based catalysts developed in our laboratory [46–58]. This chapter is intended to provide a comprehensive summary of the evolution of these cyclometalated ruthenium catalysts, from their initial serendipitous discovery to their recent applications in *Z*-selective olefin metathesis transformations. Current mechanistic hypotheses and limitations, as well as future directions, will also be discussed.

2 Catalyst Development

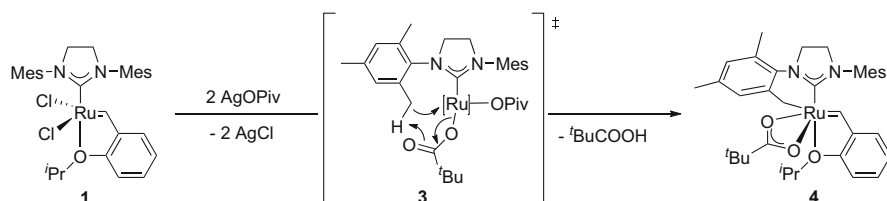
2.1 *Original Strategy for the Design of Z-Selective Ruthenium-Based Catalysts*

The selectivity exhibited by an olefin metathesis catalyst for the production of *E*-olefins or *Z*-olefins is a result of both kinetic and thermodynamic factors. Kinetic selectivity results from preferential formation of either *syn*- or *anti*-metallacyclobutanes following olefin binding: *syn*-metallacycles will undergo a cycloreversion to produce *Z*-olefins, whereas *E*-olefins are derived from *anti*-metallacycles. Thermodynamic selectivity arises as a result of secondary metathesis processes, in which the product olefins continue to react with the propagating catalyst.

A series of elegant NMR experiments have suggested that for many ruthenacyclobutanes, the NHC ligand and metallacycle are situated in the equatorial plane whereas the chloride ligands are located in apical positions, resulting in the so-called bottom-bound metallacycles (Scheme 1a) [59–67]. Thus, it was hypothesized that



Scheme 1

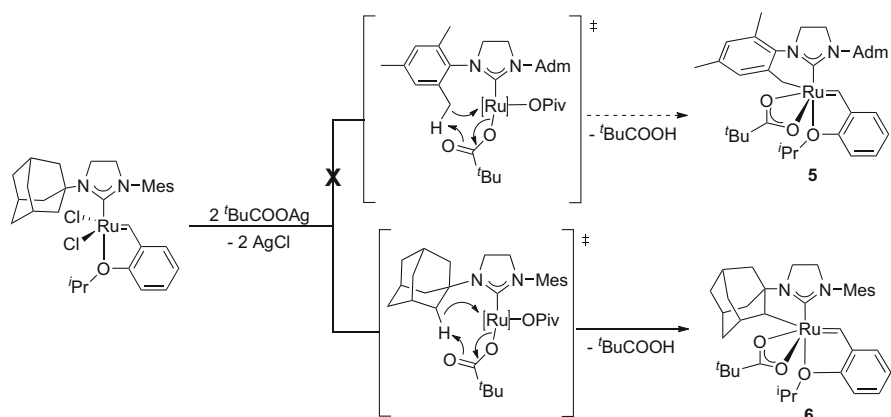


Scheme 2

Z-selectivity could be enhanced by substitution of one of the anionic chloride ligands of **1** with a bulkier ligand such as a phosphonate (**2a**) or a sulfonate (**2b**) (Scheme 1b). *Anti*-metallacycles would experience substantial steric interactions with the larger anionic ligand; as a result, this substitution might increase the preference for *syn*-metallacycles (Scheme 1a). [68]

Although complexes **2a** and **2b** did exhibit slightly increased Z-selectivity (16–25% Z) when compared to **1** (8% Z) in the CM of allylbenzene and *cis*-1,4-diacetoxybutene, **2a** and **2b** were still selective for the formation of *E*-olefins. Computational models suggested that the use of an anionic pivalate ligand (as in **2c**) might dramatically increase Z-selectivity. However, **2c** could not be synthesized under the original reaction conditions. Instead, treatment of **1** with silver pivalate led to the formation of cyclometalated complex **4**, which presumably resulted from C–H bond insertion of **3** (Scheme 2) [46]. Cyclometalated complexes derived from previous generations of ruthenium metathesis catalysts have been reported as products of catalyst decomposition; notably, no examples have been previously disclosed in which the ruthenium alkylidene remained intact [69, 70].

Interestingly, catalyst **4** not only demonstrated catalytic activity in the CM of allylbenzene and *cis*-1,4-diacetoxybutene but also provided the most promising Z-selectivity (41% Z) observed using a ruthenium-based metathesis catalyst. It was



Scheme 3

postulated that increasing the steric bulk of the non-cyclometalated substituent on the NHC would result in a more *Z*-selective catalyst; accordingly, the synthesis of **5**, containing an *N*-adamantyl group, was attempted (Scheme 3). However, the resulting cyclometalated complex was identified as **6**, which results from an unanticipated C-H insertion at the adamantyl group. Remarkably, the new cyclometalated complex **6** was found to be highly *Z*-selective (91% *Z*) in the standard CM reaction of allylbenzene and *cis*-1,4-diacetoxybutene [46].

2.2 Model for *Z*-Selectivity of Cyclometalated Ruthenium-Based Catalysts

Computational studies have provided a valuable working hypothesis for the *Z*-selectivity exhibited by cyclometalated catalyst **6** [31, 71, 72]. In contrast to the “bottom-bound” metallacycles observed with previous generations of ruthenium metathesis catalysts (cf. Sect. 2.1), it is proposed that ruthenacycles derived from **4** and **6** adopt a “side-bound” conformation (**7a**). The rationale for the preferential formation of “side-bound” ruthenacycles is twofold (Fig. 1): first, there are significant steric interactions present between the developing metallacyclobutane and the adamantyl moiety in the “bottom-bound” conformation (**7b**) that are alleviated in the “side-bound” conformation. Moreover, the “bottom-bound” conformation is destabilized as it requires back-donation from the same ruthenium d-orbital that is back-donating into the NHC; this competition is alleviated in the “side-bound” conformation, as two separate metal d-orbitals are now available for back-donation into both the NHC and alkylidene carbon p-orbitals (Fig. 1) [71].

In “side-bound” ruthenacyclobutane **7a**, the metallacycle is positioned directly underneath the *N*-aryl substituent of the NHC. It is this close proximity to the *N*-aryl

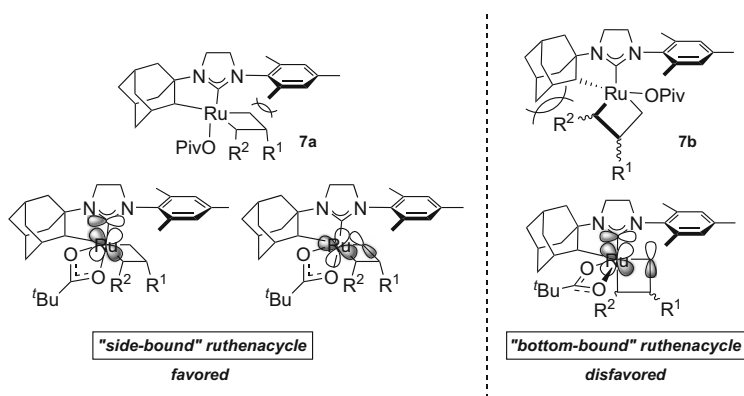
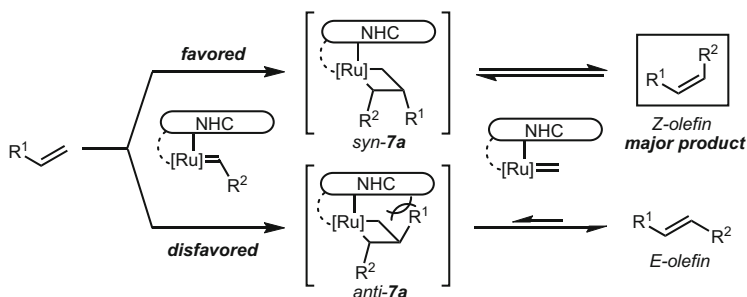


Fig. 1 Proposed steric and electronic interactions for various ruthenacycle conformations

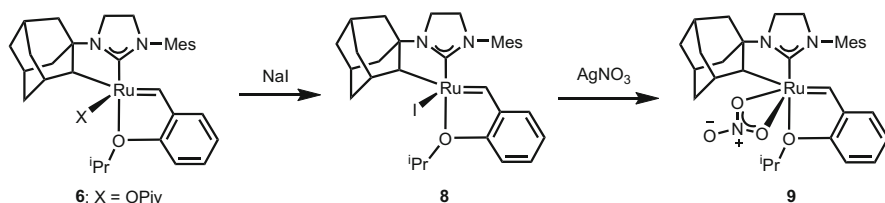


Scheme 4

substituent that is proposed to result in the selective formation of *Z*-olefins, via preferential formation of *syn-7a* (Scheme 4). *Anti-7a*, which would lead to *E*-olefins, presumably exhibits significant steric interactions with the *N*-aryl substituent. Indeed, *anti*-metallacycles derived from **6** have been computed to be much higher in energy [53, 71, 72]. Trisubstituted metallacycles are even more sterically congested; as a result, it is hypothesized that the rate of *Z*-degradation by **6** via secondary metathesis events is slow. Therefore, coupled with the inherent kinetic selectivity of **6** for *Z*-olefins, *Z*-selectivity generally remains high at high conversions (cf. Sect. 3.5) [53].

2.3 Evolution of Ruthenium-Based Cyclometalated Catalyst Systems

Following the promising results obtained with **6** in preliminary *Z*-selective olefin metathesis assays [46, 47], a variety of new cyclometalated complexes were



Scheme 5

synthesized. In order to develop structure–activity relationships and improve catalyst activity and stability, three key structural elements of the catalyst were varied: the X-type ligand, the *N*-aryl group, and the cyclometalated substituent [48, 52, 55].

New cyclometalated catalysts were initially accessed through variation of the X-type ligand (Scheme 5) [48]. Derivatives of 6 substituted with monodentate (κ^1) ligands such as iodo-complex 8 were prepared by the treatment of catalyst 6 with sodium or potassium salts. Alternatively, derivatives of 6 featuring bidentate (κ^2) ligands such as nitrate-complex 9 could be accessed from 8 by facile anion exchange with the corresponding silver (I) salt. Although a number of complexes containing a variety of X-type ligands were screened in preliminary olefin metathesis assays, all were outperformed by nitrate-catalyst 9, which demonstrated greater than 500 turnovers and ca. 90% *Z*-selectivity for a variety of CM reactions [48]. In contrast to catalyst 6 which decomposed within 2 h in solution upon exposure to air, catalyst 9 exhibited a marked improvement in stability and required up to 12 h for complete decomposition in solution. Furthermore, catalyst 9 remained bench-top stable in the solid-state for a minimum of 10 days.

Initial attempts to introduce other cyclometalated substituents or bulkier *ortho*-substituents on the *N*-aryl group only led to decomposition of the catalyst [48, 73]. Fortunately, replacement of silver pivalate with sodium pivalate allowed for a milder protocol to prepare previously inaccessible catalysts (e.g., 10 and 11) [52, 55]. With the exception of catalysts lacking *ortho*-substitution on the *N*-aryl ring (e.g., 13) [73], a variety of *N*-aryl and cyclometalated substituents were accommodated (Fig. 2). When these new catalysts were assayed in homo-CM reactions, a dramatic improvement was noted for catalyst 10, which exhibited TONs approaching 7,400 and near perfect *Z*-selectivity (>95%) [52]. This represents the highest catalytic efficiency exhibited by a *Z*-selective olefin metathesis catalyst reported to date. Catalyst 10 maintained remarkable activity and *Z*-selectivity in a variety of homodimerization reactions, as well as a selection of more complicated RCM and CM reactions (cf. Sect. 3).

It is also noteworthy to mention that the *N*-adamantyl group forms a particularly stable chelate with these cyclometalated complexes. Catalysts bearing smaller substituents were found to be much more sensitive to air, moisture, and even temperature in comparison with 6. For example, catalyst 12 could not be isolated under the standard purification conditions, and catalyst 11 required storage under inert atmosphere below room temperature (-30°C) [55].

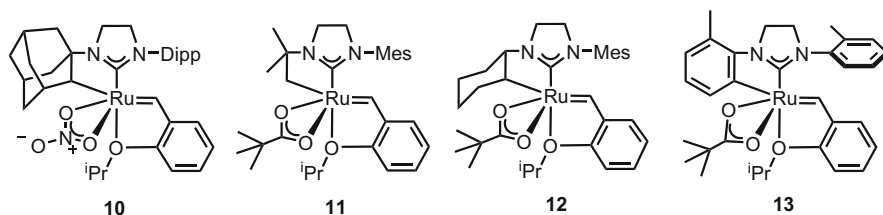


Fig. 2 Additional examples of cyclometalated ruthenium-based catalysts

2.4 General Trends in Ruthenium-Based Cyclometalated Catalyst Systems

All isolable ruthenium-based cyclometalated catalysts were evaluated for activity in two ways: by measurement of their initiation rates via reaction with *n*-butyl vinyl ether, and by investigation of their performance in simple homo-CM reactions [46–48, 52, 55, 57]. Although a more detailed account of the activity and selectivity of selected catalysts in various olefin metathesis transformations is detailed in Sect. 3, general reactivity trends with respect to substituent and ligand effects were found to be as follows:

1. A large *increase* in activity, stability, and selectivity was observed when the pivalate ligand (e.g., **6**) is exchanged for a nitrate ligand (e.g., **9**). For example, while **6** catalyzed the homo-CM of 10-methyl undecenoate with 160 turnovers and 90% *Z*-selectivity, **9** catalyzed the same transformation with 850 turnovers and >95% *Z*-selectivity. Similar TONs and selectivities were seen in a variety of other homo-CM reactions. Furthermore, **9** could be manipulated on the benchtop, as opposed to its air-sensitive predecessor **6**.
2. A large *decrease* in activity, stability, and selectivity was seen when the pivalate ligand (e.g., **6**) was exchanged for a monodentate (κ^1) ligand such as iodide (e.g., **8**). These types of catalysts were slow to initiate, often catalyzed olefin migration reactions instead of undergoing productive metathesis events, and exhibited a finite shelf life even when stored at low temperatures (-30°C) under an inert atmosphere.
3. A large *increase* in activity and selectivity was seen when one of the *ortho*-methyl substituents on the *N*-aryl ring (e.g., **9**) was replaced with larger substituents such as isopropyl groups (e.g., **10**). For example, **10** exhibited TONs approaching 7,400, as well as near perfect *Z*-selectivity (>95%), in a variety of olefin metathesis transformations such as homo-CM, hetero-CM, and mRCM.
4. A large *decrease* in activity and stability was observed when the adamantyl substituent (e.g., **6**) was replaced with a smaller substituent such as a *tert*-butyl group (e.g., **11**). For example, while **6** maintained relatively high activity in homo-CM, hetero-CM, RCM, and ROMP, **11** decomposed in the presence of terminal olefins and was thus limited to ROMP.

CM product	Catalyst	Yield	Z (%)	Ref	CM product	Catalyst	Yield	Z (%)	Ref
	9 10	91 >95	92 >95	48 52		10	70	>95	54
	9 10	85 >95	91 >95	48 52		10	66	>95	54
	9 10	67 77	81 >95	48 52		10	83	>95	58
	10	68	>95	54		10	40	>95	58

Fig. 3 Representative products produced via Z-selective CM

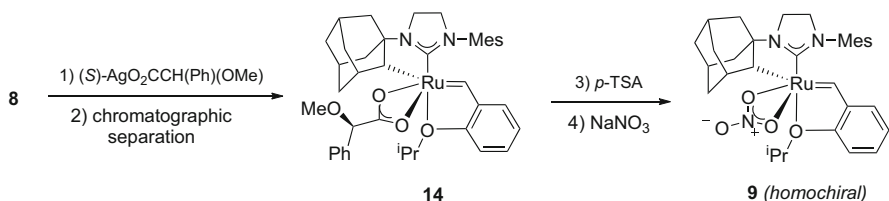
3 Applications in Z-Selective Olefin Metathesis Transformations

The abovementioned cyclometalated ruthenium catalysts have been applied in a number of Z-selective olefin metathesis reactions [46–58]. Of these catalysts, **10** remains the state of the art with respect to a general Z-selective catalyst for CM (Sect. 3.1) and mRCM (Sect. 3.3). The potential of **10** remains to be fully evaluated in more specialized transformations such as AROCM (Sect. 3.2), Z-selective ethenolysis (Sect. 3.5), or ROMP (Sect. 3.4).

3.1 Cross Metathesis

Catalysts **9** and **10** mediate a number of Z-selective CM reactions (Fig. 3); however, catalyst **10** generally outperformed catalyst **9** in terms of yield and selectivity. Near-perfect Z-selectivity (>95%) was consistently maintained for a diverse array of substrates, including those possessing amine, boronic ester, and aldehyde functional groups [46–58]. Notably, α -substituted terminal olefins were also tolerated [58]. The chemoselectivity of CM reactions was also investigated, and it was found that substrates containing internal E-olefins or 1,1-disubstituted terminal olefins did not react with catalysts **9** and **10**. Thus, CM products featuring unconjugated dienes could also be formed with high selectivity [50].

Lower catalyst loadings could be employed with **10** (0.1 mol%) than with **9** (1 mol%), with a minimal impact on yield [48, 52]. Although reactions could be run at 25°C, good yields and selectivities were also obtained at 35°C, but in decreased reaction time [48, 50, 52, 58]. For hetero-CM, conversions were generally optimal when one of the substrates was employed in excess; moreover, the choice of limiting substrate generally did not affect the outcome of the reaction [50, 54, 58]. Although it was demonstrated that a variety of solvents (including methanol, dichloromethane, benzene, acetonitrile, and dimethylformamide) could be utilized



Scheme 6

with little detriment to *Z*-selectivity, tetrahydrofuran generally provided optimal yields in the shortest reaction times.

3.2 Asymmetric Ring Opening Cross Metathesis

The generation of chiral centers through metathesis transformations is of high interest to the synthetic community. One particular reaction that has been extensively explored is AROCM, in which an olefin reacts with a norbornene derivative to produce chiral-substituted cyclopentanes. Previously reported asymmetric olefin metathesis methodologies employing enantiopure chiral catalysts have proven remarkably useful in the synthesis of natural products and other bioactive molecules that contain *E*-olefins [74]. It was expected that the development of the complementary, homochiral *Z*-selective catalysts would enable formation of enantioenriched *Z*-olefins. To this end, homochiral **9** was synthesized by resolution of racemic iodide **8** (Scheme 6) [56]. Carboxylate **14** was initially derived from **8** in a 1:1 mixture with its diastereomer; separation was achieved using silica gel chromatography, yielding **14** in >95:5 *dr*. Subsequent anion exchange mediated by *p*-TSA/NaNO₃ resulted in enantioenriched **9**.

Interestingly, although **14** exhibited low enantioselectivity in the AROCM of norbornenes, homochiral **9** was found to catalyze this reaction with a variety of terminal olefin substrates in moderate yield (40–65%), excellent *Z*-selectivity (ca. 95%), and good *ee* (60–95%) (Fig. 4) [56].

3.3 Macrocyclic Ring Closing Metathesis

Macrocycles are prevalent in a large number of natural products, pharmaceuticals, and musk fragrances. In general, the formation of large rings by mRCM of acyclic diene starting materials is a more difficult transformation compared to intermolecular CM or RCM of small rings [1]. In order to prevent oligomerization of the acyclic diene starting material, the reactions must be run at low concentration; consequently, higher catalyst loadings are typically necessary. Additionally, for

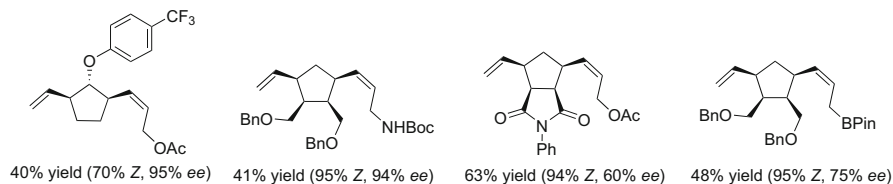


Fig. 4 Representative products produced via *Z*-selective AROCM

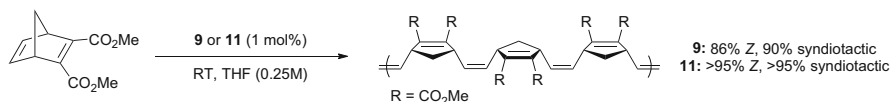
mRCM product	Catalyst	Yield	Z (%)	Ref	mRCM product	Catalyst	Yield	Z (%)	Ref
	9	56	65	51		9	83	59	52
	10	45	>95	52					
	9	50	68	51		9	21	81	54
	10	36	>95	52					

Fig. 5 Representative products produced via *Z*-selective mRCM

medium- to large-sized ring systems in which both *E*- and *Z*-isomers are accessible, it is difficult to control or predict the olefin geometry of the products. Following the discovery of the cyclometalated ruthenium alkylidene catalysts, the synthesis of a number of *Z*-macrocycles with a variety of ring sizes (13–20 atoms) containing various functional groups (ester, ketone, alcohol, protected amide) was demonstrated (Fig. 5) [51]. In general mRCM proceeded in moderate to good yields (50–75%) and with generally high *Z*-selectivity (75–94%) using catalyst **9**. Presently, it is necessary to employ a static vacuum as well as high dilution conditions in order to favor the formation of mRCM products over oligomerization of the diene starting materials. Interestingly, macrocycles containing alcohol or ketone functionality showed increased levels of *Z*-content degradation (as low as 50% *Z* after 24 h). When catalyst **10** was evaluated for mRCM, macrocyclic products were obtained with very high *Z*-selectivity (>95%), albeit in diminished yields (Fig. 5) [52].

3.4 Ring Opening Metathesis Polymerization

The exact control of polymer microstructures (e.g., tacticity and double-bond configuration) resulting from the ROMP of substituted norbornenes and norbornadienes is essential for the development of polymers with well-defined physical properties. Norbornene and norbornadiene-derived polymers could be accessed with



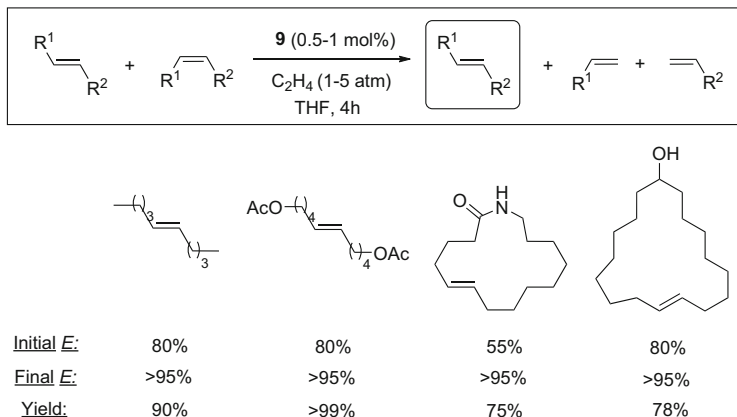
Scheme 7

consistently high syndioselectivity (ca. 90%) using catalyst **9** (Scheme 7). However, Z-selectivity depended significantly on monomer selection, and *cis* contents ranging from ca. 50–90% were observed [49, 75]. In contrast, polymers produced by catalyst **11** were consistently highly *cis* (>95% in many cases) and syndiotactic (>95% in all cases) [55]. These studies have demonstrated for the first time that polymers with a singular *cis*, syndiotactic microstructure could be produced with a ruthenium metathesis catalyst. More detailed investigations probing the exact mechanism of Z-selectivity and tacticity in ROMP exhibited by **9**, **11**, and other cyclometalated ruthenium-based initiators are currently underway [75].

3.5 Z-Selective Ethenolysis

Given that the aforementioned catalysts are highly selective for Z-olefin-containing products, it was envisioned that these catalysts could selectively react with such substrates in the reverse ethenolysis reaction (e.g., Scheme 4). Specifically, it was hypothesized that an *E/Z* mixture of olefin isomers would undergo Z-selective ethenolysis upon exposure to **9** in the presence of ethylene gas, to deliver isomerically pure *E*-olefins (Scheme 8). While a metathesis catalyst that kinetically forms an *E*-olefin as the exclusive product has not been discovered, Z-selective ethenolysis is emerging as a powerful tool to enrich the *E*-olefin content of stereoisomeric mixtures of *E*- and Z-olefins [29]. For natural products and pharmaceuticals, even minute amounts of stereoisomeric impurities can affect their physical or biological properties. Given that the separation of olefin isomers using distillation, chromatography, or crystallization can be tedious and difficult to perform, it is envisioned that Z-selective ethenolysis could serve as a practical tool for the purification of *E*-olefins. Moreover, the terminal olefins formed as by-products in the reaction can be recycled in subsequent metathesis transformations.

Cyclometalated catalyst **9** was shown to be effective in the Z-selective ethenolysis of internal olefins (Scheme 8) at relatively low catalyst loadings (0.5 mol%) and ethylene pressures (1–5 atm) [51, 53]. *E/Z*-olefin mixtures were successfully enriched to the pure *E*-isomer products, with accompanying formation of terminal olefins derived from the Z-isomer. This process was demonstrated to be effective for both linear and cyclic olefins and was found to be tolerant of a number of functional groups including esters, alcohols, amines, and ketones. Reactions were generally conducted at 35°C, which was found to provide an optimal balance with respect to yield and reaction time. Although the reaction is more rapid at



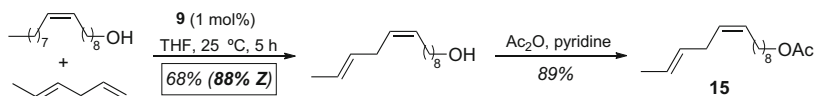
Scheme 8

higher temperatures, the overall yield decreases due to competitive ethenolysis of the *E*-isomer.

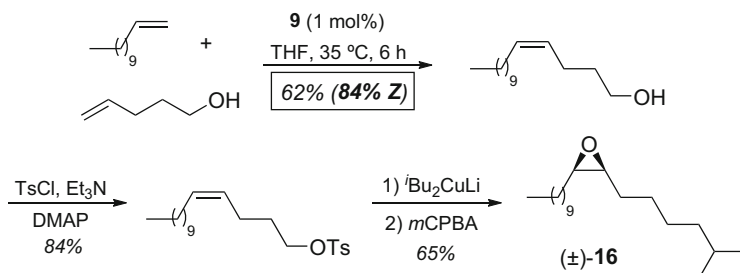
Our extensive studies in the realm of *Z*-selective ethenolysis reactions have important mechanistic implications for CM and mRCM reactions catalyzed by cyclometalated ruthenium alkyldiene complexes. For example, it was observed that the CM of two internal double bonds only proceeded in the presence of ethylene, and when both olefins were of the *Z*-configuration [53]. When an equimolar mixture of an *E*-olefin and a *Z*-olefin was reacted in the presence of ethylene, no crossover products were observed. This suggests that all internal olefins must undergo ethenolysis before they can form CM products, and that productive CM reactions only proceed through terminal olefins.

4 Applications in the Synthesis of Natural Products

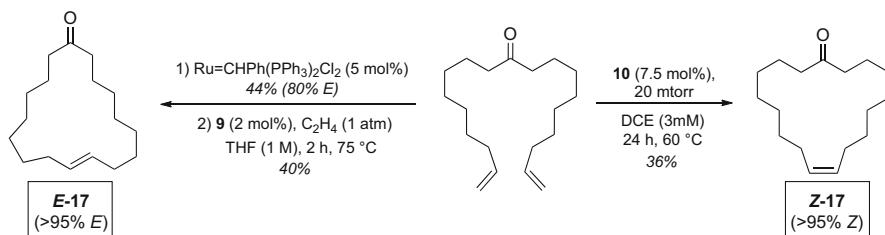
Traditionally, ruthenium olefin metathesis catalysts have been widely used in both the academic and industrial setting; therefore, although only very recently developed, it is unsurprising that the cyclometalated ruthenium-based *Z*-selective catalysts have already demonstrated potential in similar applications. For example, although the synthesis of *E*-olefin-containing pheromones utilizing olefin metathesis has been accomplished [76], the efficient synthesis of *Z*-pheromones has remained a challenge. Using catalyst **9**, nine insect pheromones approved by the EPA as pest control agents were formed in moderate to good yield (40–77%) and with high *Z*-selectivity (76–88%) [50]. Pheromone **15**, for instance, was accessed in only two steps, the shortest sequence to date, via the *Z*-selective CM of 1,4-hexadiene and oleyl alcohol (Scheme 9).



Scheme 9



Scheme 10

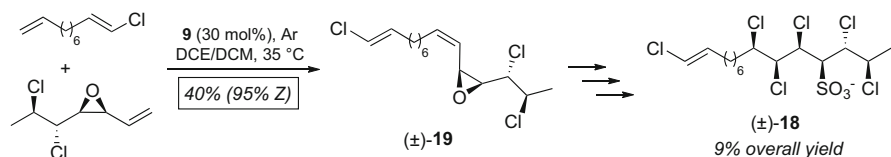


Scheme 11

Catalyst **9** has also been applied in the shortest total synthesis of (±)-**16**, a pheromone used to mitigate deforestation caused by the gypsy moth (Scheme 10) [50]. The *cis*-epoxide of **16** was derived from a *cis*-olefin, which was in turn installed via *Z*-selective CM of 4-pentenol and 1-dodecene. Recently, catalyst **10** has been utilized *in lieu* of **9** to access compounds closely related to **15** and **16**, in order to produce the *Z*-isomer exclusively (>95% *Z*) [52, 54].

As previously stated, mRCM is an important method for the synthesis of large rings (Sect. 3.3). Using cyclometalated catalysts, we are now able to exclusively prepare *Z*-macrocycles using catalyst **10** via mRCM (>95% *Z*) [52]. Alternatively, by *Z*-selective ethenolysis, we are able to form the corresponding *E*-isomer with catalyst **9** (>95% *E*). This was showcased in the synthesis of both *E*- and *Z*-civetone (**17**) (Scheme 11), as well as several other macrocyclic musk compounds [51].

This methodology has also been applied in the synthesis of more complex natural products. For example, Vanderwal and coworkers have recently reported a total synthesis of the chlorosulfolipid mytilipin A (**19**) using a highly *Z*-selective CM, mediated by catalyst **9**, in order to access the key intermediate **18** via a convergent olefination (Scheme 12) [77].



Scheme 12

5 Conclusions and Future Outlook

The discovery of isolable cyclometalated ruthenium alkylidene complexes has resulted in the development of ruthenium-based *Z*-selective metathesis catalysts, which have been implemented in the synthesis of a variety of products containing *Z*-olefins. As a complementary method to *Z*-selective CM and mRCM, the same catalysts can also be employed in the *Z*-selective ethenolysis of *E/Z* mixtures, for obtaining stereopure *E*-olefins. Alteration of the NHC substituents and X-type ligand has yielded significant insights into the stability, activity, and selectivity of these catalysts and has enabled the development of improved catalysts that can achieve >95% *Z*-selectivity with TONs reaching up to 7,400. We expect that continued research into structure–activity relationships will result in the development of even more active *Z*-selective catalysts that will display even higher levels of stability to air, moisture, and diverse functionality. The continued evolution of this versatile family of catalysts is expected to provide synthetic chemists with an ever-increasing toolset to tackle a wide range of challenging and high-value targets, derived from *Z*-olefins. Moreover, it is conceivable that an increased understanding of the mode-of-action of these catalysts will aid in the future design of a catalyst system that is kinetically selective for *E*-olefin formation.

Acknowledgments Financial support was provided by the NIH (R01-GM031332), the NSF (CHE-1212767), the NDSEG (graduate fellowship to LER), and the NSERC of Canada (postdoctoral fellowship to VMM). We are grateful to Dr. Jeff Cannon, Dr. John Hartung, Dr. Raul Navarro, and Brendan Quigley for helpful discussions associated with the drafting of this manuscript.

References

1. Fürstner A (2000) *Angew Chem Int Ed* 39:3013
2. Trnka TM, Grubbs RH (2001) *Acc Chem Res* 34:18
3. Schrock RR (2002) *Chem Rev* 102:145
4. Schrock RR, Hoveyda AH (2003) *Angew Chem Int Ed* 42:4592
5. Grubbs RH (2003) (ed) *Handbook of metathesis*, vol 2. Wiley-VCH, Weinheim
6. Nicolaou KC, Bulger PG, Sarlah D (2005) *Angew Chem Int Ed* 44:4490
7. Vougioukalakis G, Grubbs RH (2010) *Chem Rev* 110:1746
8. Samojłowicz C, Bieniek M, Grela K (2009) *Chem Rev* 109:3708
9. Lozano-Vila AM, Monsaert S, Bajek A, Verpoort F (2010) *Chem Rev* 110:4865

10. Cossy J, Arseniyadis S, Meyer C (2010) (eds) *Metathesis in Natural Product Synthesis*. Wiley-VCH, Weinheim
11. Casey CP, Burkhardt TJ (1974) *J Am Chem Soc* 96:7808
12. Khosravi E, Szymanska-Buzar T (2002) (eds) *Ring Opening Metathesis Polymerisation and Related Chemistry*. Kluwer Academic Publishers, Dordrecht
13. Mol JC (2004) *J Mol Catal A* 213:39
14. Prunet J (2005) *Curr Top Med Chem* 5:1559
15. Binder JB, Raines RT (2008) *Curr Opin Chem Biol* 12:767
16. Schrock RR (2011) *Dalton Trans* 40:7484
17. Gottumukkala AL, Madduri AVR, Minnaard AJ (2012) *ChemCatChem* 4:462
18. Fürstner A (2013) *Science* 341:1357
19. Shahane S, Bruneau C, Fischmeister C (2013) *ChemCatChem* 5:3436
20. Fürstner A, Davies PW (2005) *Chem Commun* 2307
21. Zhang W, Moore JS (2007) *Adv Synth Catal* 349:93
22. Wang Y, Jimenez M, Hansen AS, Raiber E-A, Schreiber SL, Young DW (2011) *J Am Chem Soc* 133:9196
23. Fürstner A, Gallenkamp D (2011) *J Am Chem Soc* 133:9232
24. Flook MM, Jiang AJ, Schrock RR, Müller P, Hoveyda AH (2009) *J Am Chem Soc* 131:7962
25. Ibrahim I, Yu M, Schrock RR, Hoveyda AH (2009) *J Am Chem Soc* 131:3844
26. Jiang AJ, Zhao Y, Schrock RR, Hoveyda AH (2009) *J Am Chem Soc* 131:16630
27. Hoveyda AH, Malcolmson SJ, Meek SJ, Zhugrlin AR (2010) *Angew Chem Int Ed* 49:34
28. Meek SJ, O'Brien RV, Llaveria J, Schrock RR, Hoveyda AH (2011) *Nature* 471:461
29. Marinescu SC, Levine DS, Zhao Y, Schrock RR, Hoveyda AH (2011) *J Am Chem Soc* 133:11512
30. Peryshkov DV, Schrock RR, Takase MK, Müller P, Hoveyda AH (2011) *J Am Chem Soc* 133:20754
31. Marinescu SC, Schrock RR, Müller P, Takase MK, Hoveyda AH (2011) *Organometallics* 30:1780
32. Flook MM, Ng VWL, Schrock RR (2011) *J Am Chem Soc* 133:1784
33. Yu M, Wang C, Kyle AF, Jakubec P, Dixon DJ, Schrock RR, Hoveyda AH (2011) *Nature* 479:88
34. Yu M, Ibrahim I, Hasegawa M, Schrock RR, Hoveyda AH (2012) *J Am Chem Soc* 134:2788
35. Flook MM, Borner J, Kilyanek S, Gerber LCH, Schrock RR (2012) *Organometallics* 31:6231
36. Townsend EM, Schrock RR, Hoveyda AH (2012) *J Am Chem Soc* 134:11334
37. Wang C, Yu M, Kyle AF, Jakubec P, Dixon DJ, Schrock RR, Hoveyda AH (2013) *Chem Eur J* 19:2726
38. Keisewetter ET, O'Brien RV, Yu EC, Meek SJ, Schrock RR, Hoveyda AH (2013) *J Am Chem Soc* 135:6026
39. Wang C, Haeffner RR, Schrock RR, Hoveyda AH (2013) *Angew Chem Int Ed* 52:1939
40. Yuan J, Schrock RR, Gerber LCH, Müller P, Smith S (2013) *Organometallics* 32:2983
41. Mann TJ, Speed AWH, Schrock RR, Hoveyda AH (2013) *Angew Chem Int Ed* 52:10052
42. Khan RKM, O'Brien RV, Torker S, Li B, Hoveyda AH (2012) *J Am Chem Soc* 134:12774
43. Khan RKM, Zhugrulin AR, Torker S, O'Brien RV, Lombardi PJ, Hoveyda AH (2012) *J Am Chem Soc* 134:12438
44. Khan RKM, Torker S, Hoveyda AH (2013) *J Am Chem Soc* 135:10258
45. Occhipinti G, Hansen FR, Törnroos KW, Jensen VR (2013) *J Am Chem Soc* 135:3331
46. Endo K, Grubbs RH (2011) *J Am Chem Soc* 133:8525
47. Keitz BK, Endo K, Herbert MB, Grubbs RH (2011) *J Am Chem Soc* 133:9686
48. Keitz BK, Endo K, Patel PR, Herbert MB, Grubbs RH (2012) *J Am Chem Soc* 134:693
49. Keitz BK, Federov A, Grubbs RH (2012) *J Am Chem Soc* 134:2040
50. Herbert MB, Marx VM, Pederson RL, Grubbs RH (2013) *Angew Chem Int Ed* 52:310
51. Marx VM, Herbert MB, Keitz BK, Grubbs RH (2013) *J Am Chem Soc* 135:94

52. Rosebrugh LE, Herbert MB, Marx VM, Keitz BK, Grubbs RH (2013) *J Am Chem Soc* 135:1276
53. Miyazaki H, Herbert MB, Liu P, Dong X, Xu X, Keitz BK, Ung T, Mkrtumyan G, Houk KN, Grubbs RH (2013) *J Am Chem Soc* 135:5848
54. Cannon JS, Grubbs RH (2013) *Angew Chem Int Ed* 52:9001
55. Rosebrugh LE, Marx VM, Keitz BK, Grubbs RH (2013) *J Am Chem Soc* 135:10032
56. Hartung J, Grubbs RH (2013) *J Am Chem Soc* 135:10183
57. Endo K, Herbert M, Grubbs RH (2013) *Organometallics* 32:5128
58. Quigley BL, Grubbs RH (2014) *Chem Sci* 5:501
59. Romero PE, Piers WE, McDonald R (2004) *Angew Chem Int Ed* 43:6161
60. Wenzel AG, Grubbs RH (2006) *J Am Chem Soc* 128:16048
61. Romero PE, Piers WE (2007) *J Am Chem Soc* 129:1698
62. Rowley CN, van der Eide EF, Piers WE, Woo TK (2008) *Organometallics* 27:6043
63. van der Eide EF, Romero PE, Piers WE (2008) *J Am Chem Soc* 130:4485
64. Leitao EM, van der Eide EF, Romero PE, Piers WE, McDonald R (2010) *J Am Chem Soc* 132:2784
65. van der Eide EF, Piers WE (2010) *Nat Chem* 2:571
66. Wenzel AG, Blake G, VanderVelde DG, Grubbs RH (2011) *J Am Chem Soc* 133:6249
67. Keitz BK, Grubbs RH (2011) *J Am Chem Soc* 133:16277
68. Teo P, Grubbs RH (2010) *Organometallics* 29:6045
69. Trnka TM, Morgan JP, Sanford MS, Wilhelm TE, Scholl M, Choi T-L, Ding S, Day MW, Grubbs RH (2003) *J Am Chem Soc* 125:2546
70. Leitao EM, Dubberley SR, Piers WE, Wu Q, McDonald R (2008) *Chem Eur J* 14:11565
71. Liu P, Xu X, Dong X, Keitz BK, Herbert MB, Grubbs RH, Houk KN (2012) *J Am Chem Soc* 134:1464
72. Dang Y, Wang Z-X, Wang X (2012) *Organometallics* 31:7222
73. Herbert MB, Lan Y, Keitz BK, Liu P, Endo K, Day MW, Houk KN, Grubbs RH (2012) *J Am Chem Soc* 134:7861
74. Hoveyda AH, Malcolmson SJ, Meek AR, Zhugralin AR (2010) *Angew Chem Int Ed* 49:34; Kress S, Blechert S (2012). *Chem Soc Rev* 41:4381
75. Marx VM, Rosebrugh LE, Hartung J, Ahmed TS, Grubbs RH. Manuscript in preparation
76. Pederson RL, Fellows IM, Ung TA, Ishihara H, Hajela SP (2002) *Adv Synth Catal* 344:728
77. Chung W-J, Carlson JS, Bedke DK, Vanderwal CD (2013) *Angew Chem Int Ed* 52:10052

Hydrogenation of Polar Bonds Catalysed by Ruthenium-Pincer Complexes

Ekambaram Balaraman and David Milstein

Abstract Catalytic hydrogenation of polar bonds using molecular hydrogen is an important, atom-economical synthetic reaction. Classical reduction methods of polar bond often require reactive metal-hydride reagents in stoichiometric amount and produce copious waste. Hydrogenation of carbonyl compounds in particular provides ‘green’ approaches to synthetically important building blocks, such as alcohols and amines. We have designed and synthesized several ruthenium-based pincer catalysts for unprecedented hydrogenation reactions including: (1) amides to alcohols and amines, (2) biomass-derived di-esters to 1,2-diols and (3) CO₂ and CO derivatives to methanol. These atom-economical reactions operate under neutral, homogeneous conditions, at mild temperatures, mild hydrogen pressures, and can operate in absence of solvent with no generation of waste. The postulated mechanisms involve metal–ligand cooperation (MLC) by aromatization–dearomatization of the heteroaromatic pincer core.

Keywords Amides · Carbon dioxide · Esters · Hydrogen · Hydrogenation · Metal–ligand cooperation · Pincer complexes · Ruthenium

Contents

1	Introduction and Background	20
2	Synthesis of H-Ru(II)pincer Complexes and Activation of Dihydrogen via Metal–Ligand Cooperation Approach	21

E. Balaraman (✉)
Catalysis Division, CSIR-National Chemical Laboratory, Dr. Homi Bhabha Road, Pashan,
Pune 411008, India
e-mail: eb.raman@ncl.res.in

D. Milstein
Department of Organic Chemistry, Weizmann Institute of Science, Rehovot 76100, Israel
e-mail: david.milstein@weizmann.ac.il

3	Catalytic Hydrogenation of Carbonyl Groups	25
3.1	Efficient Hydrogenation Esters and Related Compounds	25
3.2	Selective Hydrogenation of Amides to Alcohols and Amines	30
3.3	Hydrogenation of CO ₂ Derivatives to Methanol	33
4	Direct Hydrogenation of CO ₂	37
5	Conclusion	40
	References	41

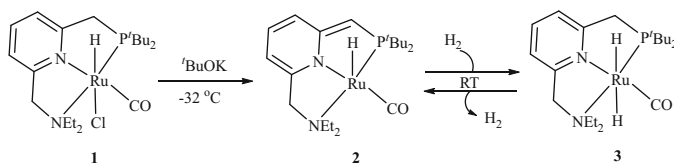
1 Introduction and Background

Design of new catalytic reactions for selective organic transformations is essential for the development of ‘green’ approaches to industrially important processes, which traditionally employ stoichiometric reagents and/or harsh conditions. Among organic transformations that are frequently used in industries, the reduction of compounds bearing polar carbonyl groups, such as esters and amides, is one of the most important reactions [1, 2]. Traditionally reduction of polar bonds is carried out by the use of toxic, reactive metal-hydride reagents in stoichiometric amounts, which produces copious waste and employs tedious procedures, making these methods problematic environmentally and economically [3–5].

In contrast, hydrogenation of polar bonds with gaseous hydrogen under mild conditions provides an atom-economical, environmentally benign and operationally simple synthetic process [6–10]. Noyori’s well-defined catalysts for hydrogenation of carbonyl compounds gave a new dimension to the homogeneous hydrogenation catalysts [11–13]. On the other hand, the hydrogenation of unreactive carbonyl compounds, particularly carboxylic acid derivatives such as esters and amides, as well as carbonic acid derivatives such as dialkyl carbonates and carbamates, as well as urea derivatives, is still challenging.

In recent years, pincer ligands which bind to metal centres in a tri-dentate, meridional fashion have drawn much attention and serve as excellent ligands, due to stability and variability of the generated metal–ligand framework [14–17]. The donor/acceptor ability at both the central and adjacent side-arm positions of the pincer ligands can be controllable. And both the electronic and steric environment around the metal centre can also be tuneable.

We have developed several unique reactions catalysed by PNN and PNP Ru(II) pincer complexes based on pyridine, bipyridine and acridine backbones. These complexes show a new mode of metal–ligand cooperation (MLC) [18] based on ligand aromatization–dearomatization, which has led to a number of bond activation processes [19–22]. Deprotonation of a methylenic side-arm proton of pyridyl- and bipyridyl-based pincer complexes leads to the corresponding dearomatized, coordinatively unsaturated 16 electron complexes. The dearomatized complex, which activates the dihydrogen by cooperation between the Ru-metal centre and the ligand, leads to *trans*-dihydride complex, thereby regaining aromatization (Scheme 1). This aromatization–dearomatization process is reversible and it can form the basis for efficient catalytic systems of both dehydrogenation of O–H



Scheme 1 Preparation of dearomatized PNN-Ru(II) complex and its reactivity towards H₂

bonds and selective hydrogenation of polar carbonyl compounds, including very challenging and less studied compounds. In this chapter we describe straightforward hydrogenation of various carbonyl compounds, in particular, carboxylic and carbonic acid derivatives catalysed by Ru(II)-pincer complexes. We have also reported Fe(II)-pincer catalysed hydrogenation of ketones and CO₂ under very mild conditions [23–25].

2 Synthesis of H-Ru(II)pincer Complexes and Activation of Dihydrogen via Metal–Ligand Cooperation Approach

Our approach towards activation of molecular hydrogen and hydrogenation reactions is based on the metal–ligand cooperation concept (MLC). In this section we describe the synthesis of Ru(II)-H pincer complexes prepared by our group and their activity towards activation of dihydrogen.

Dihydrogen addition to the bulky, electron-rich dearomatized pyridine-based Ru(II)PNN-complex **2** results in heterolytic dihydrogen cleavage (a hydride added to the metal centre and a ‘proton’ to the ligand), to form the coordinatively saturated, *trans*-dihydride complex **3** via MLC. It is important to note that the bond activation process does not involve a change in the formal oxidation state of the metal [26, 27]. Formation of *trans*-dihydride is a key step in the catalytic hydrogenation of polar bonds in our systems. The magnetically equivalent *trans*-dihydride resonates as a doublet at -4.08 ppm ($J_{\text{PH}} = 17.1$ Hz) in complex **3**. The complex slowly loses an H₂ molecule at room temperature to regenerate complex **2**. A single-crystal X-ray diffraction study of **3** (Fig. 1) reveals a distorted octahedral geometry around the ruthenium(II) centre, with the CO ligand coordinated *trans* to the pyridyl nitrogen atom.

Selected bond distances (Å): Ru1-N1 2.101 (3), Ru1-N2 2.251 (3), Ru1-P3 2.252 (1), Ru1-C1 1.821 (4), H1A-Ru1 1.71(4) Å, (H1B-Ru1 was not refined).

Selected bond angles (deg.): N1-Ru1-C1 175.0 (2), N1-Ru1-P3 82.6 (1), N1-Ru1-N2 78.0 (1), N2-Ru1-P3 160.6 (1), N2-Ru1-C1 104.8 (2), C1-Ru1-P3 94.6 (1).

The electron-rich bipyridine-based Ru(II)-PNN pincer complex **4** was synthesized by the reaction of the tridentate ligand, BPy-^{*t*}BuPNN (**5**) with [RuHCl(PPh₃)₃(CO)] in THF at 65°C (Scheme 2). The single-crystal X-ray structure of

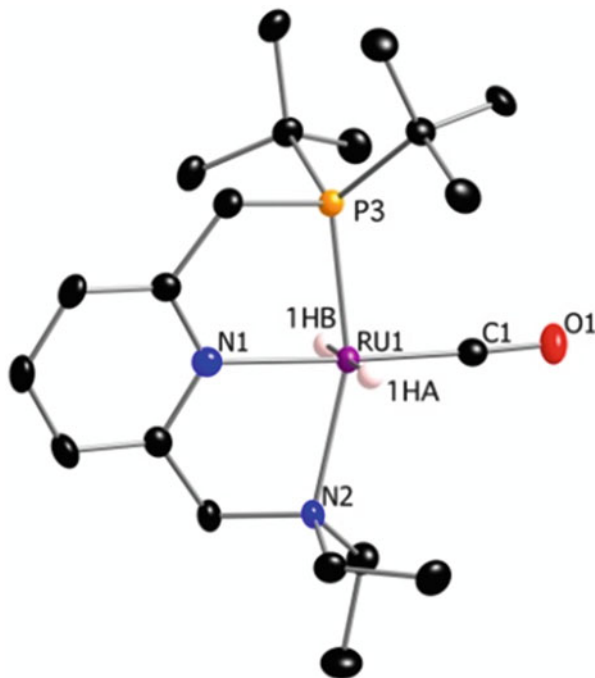
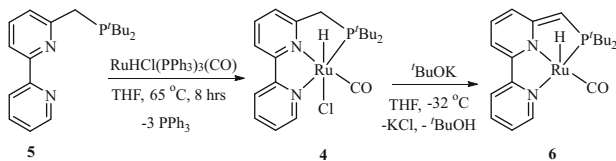


Fig. 1 X-ray structure of complex **3** (50% probability level). Hydrogen atoms (except hydrides) are omitted for clarity



Scheme 2 Synthesis of bipyridine-based H-Ru(II) Pincer complexes (**4** and **6**)

4 (Fig. 2) reveals a distorted octahedral geometry around the ruthenium centre, with the CO ligand coordinated *trans* to the central nitrogen atom of the pincer system, and the hydride *trans* to the chloride ligand [28]. Deprotonation of complex **4** with KO^tBu at -32°C gave the dearomatized, coordinatively unsaturated complex **6** in good yield. The fully characterized **6** gives rise to doublet at -20.93 ppm ($^2J_{\text{PH}} = 25.0$ Hz) in the ^1H NMR spectrum. The “arm” vinylic proton appears as singlet at 3.36 ppm and a doublet at 66.56 ($J_{\text{PC}} = 48.8$ Hz) in $^{13}\text{C}\{^1\text{H}\}$ NMR spectrum, indicating formation of an anionic PNN system.

Selected bond distances (Å): Ru1–N1 2.124(2), Ru1–N2 2.086(2), Ru1–P1 2.2859(7), Ru1–C20 1.861(3).

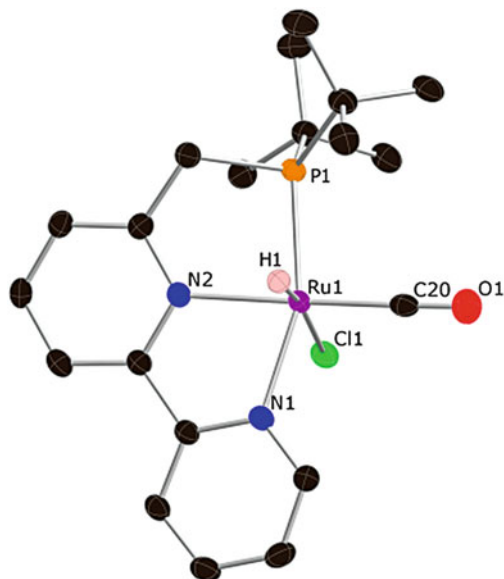
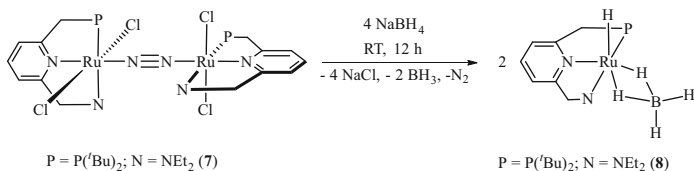


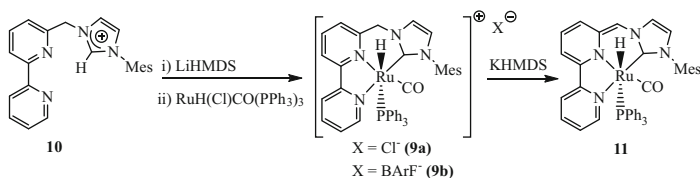
Fig. 2 X-ray structure of complex **4** (50% probability level). Hydrogen atoms (except hydride) are omitted for clarity



Scheme 3 Synthesis of ruthenium(II) hydrido borohydride complex **8**

Selected angles (deg): N2–Ru1–C20 173.34(10), N2–Ru1–H1 86.4(9), Cl1–Ru1–H1 170.4(9), N1–Ru1–P1 159.65(6).

In analogy to the *trans*-dihydride complex **3**, the Ru(II) hydridoborohydride complex **8** was prepared from the N₂-bridged binuclear complex [(RuCl₂(^tBu-PNN))₂](η²-N₂) **7** [29]. Treatment of **7** with an excess (5 equiv.) of NaBH₄ in 2-propanol for 12 h resulted in the formation of complex **8** in excellent yield (Scheme 3). The hydride ligand of complex **8** gives rise to a doublet at –16.24 ppm with *J*_{PH} = 28.0 Hz in the ¹H NMR spectrum. The IR spectrum of **8** exhibits two strong bands in the terminal B–H region at 2,378 and 2,311 cm^{–1} and two bands in the bridging Ru–H–B region at 2,096 and 1,956 cm^{–1}, consistent with



Scheme 4 Synthesis of NHC-based H-Ru(II)-pincer complexes

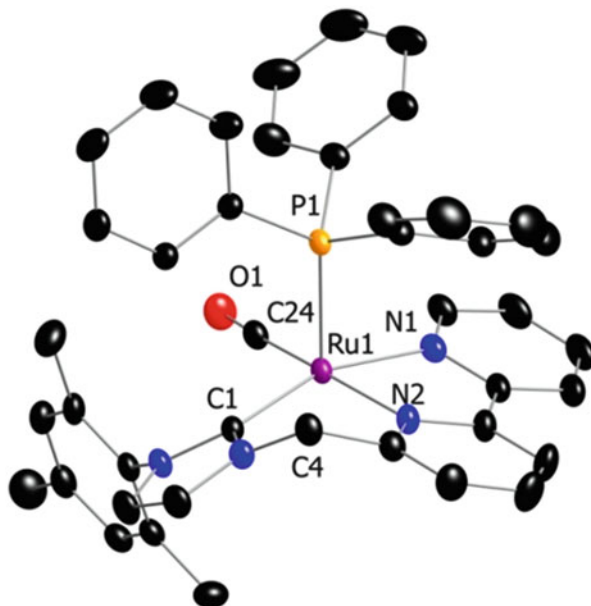


Fig. 3 ORTEP plot of complex **9b**. Hydrogen atoms and counter anion are omitted for clarity. Ellipsoids are drawn at 50% probability level

the bidentate $\eta^2\text{-BH}_4$ bonding mode. Complex **8** showed an interesting fluxional behaviour of the BH_4^- ligand [30].

The NHC analogue (**9a**) of the bipyridine-based Ru(II)-PNN pincer complex **4** was prepared by treatment of the in situ generated free NHC ligand (**10**) with $\text{RuH(Cl)CO(PPh}_3\text{)}_3$ (Scheme 4) [31]. Complex **9a** gives rise to a doublet at -7.96 ppm ($J_{\text{PH}} = 106$ Hz) in the ^1H NMR for the hydride ligand. The counter anion was exchanged with BARF^- (tetrakis[(3,5-trifluoromethyl)phenyl]borate) and crystals of **9b** suitable for X-ray diffraction were grown from a pentane-ether solution. The X-ray structure of **9b** (Fig. 3) exhibits the CO ligand *trans* to the central nitrogen atom of the pincer system and the location of the hydride is *trans* to the phosphine. Deprotonation of complex **9a** with KHMDS in benzene or toluene resulted in formation of the dearomatized complex **11** as the only product. The hydride ligand of complex **11** resonates a doublet at -7.13 ppm ($J_{\text{PH}} = 142.0$ Hz)

in the ^1H NMR spectrum. The “arm” vinylic proton appears as a singlet at 5.87 ppm and the corresponding carbon exhibits a singlet at 89.7 ppm in the $^{13}\text{C}\{^1\text{H}\}$ NMR spectrum. Complexes (**2**, **6**, **8** and **11**) were used as catalysts for hydrogenation of carboxylic acid derivatives under neutral, homogeneous conditions and the results are discussed in the following sections.

3 Catalytic Hydrogenation of Carbonyl Groups

Catalytic hydrogenation of carbonyl ($\text{C}=\text{O}$) groups using molecular hydrogen is a fundamentally important transformation and remains a challenging task in the context of hydrogen storage and sustainable chemistry. The order of susceptibility to nucleophilic attack by the hydride at the carbonyl carbon generally corresponds to the *hydridophilicity* of this carbon [32]. The lower *hydridophilicity* as a result of resonance effects involving alkoxy or amido group makes hydrogenation of carboxylic acid derivatives, in particular, esters, amides, and even more so, carbonic acid derivatives, such as organic carbonates, carbamates and urea derivatives, very difficult and less explored. The general trend in the ease of hydrogenation of polar carbonyl groups is $\text{RC}(\text{O})\text{H} > \text{RC}(\text{O})\text{R}' > > \text{RC}(\text{O})\text{OR}' > \text{RC}(\text{O})\text{NR}_2' >> > \text{ROC}(\text{O})\text{OR}' > \text{ROC}(\text{O})\text{NR}_2' > \text{R}_2\text{NC}(\text{O})\text{N}_2\text{R}'$ [33, 34].

3.1 Efficient Hydrogenation Esters and Related Compounds

3.1.1 Hydrogenation of Non-activated Esters to the Corresponding Alcohols

While there are many examples of Ru-catalysed hydrogenations of ketones and aldehydes [7, 11], and recently Fe-catalysed hydrogenation of ketones was also reported [35–39], including our system based on pincer-iron complexes [24, 25], catalytic hydrogenation of esters, particularly non-activated ones, under mild conditions is a challenging task [6, 7, 9, 10, 40, 41]. In pioneering work by Elsevier et al. various aromatic and aliphatic esters were hydrogenated in fluorinated solvent using in situ prepared ruthenium complexes bearing P,P,P ligands at high pressure of dihydrogen under basic conditions [42]. In 2006, we originally reported hydrogenation of non-activated esters to corresponding alcohols under mild, neutral conditions, catalysed by well-defined Ru(II) pincer complex **2** under low hydrogen pressure (5.3 atm) [27]. The reaction is general, both aliphatic and aromatic esters were hydrogenated to corresponding alcohols under very mild conditions without the use of any additives (Fig. 4). The reaction provides an environmentally benign protocol for the synthesis of alcohols from esters, without the need of traditionally used classical approaches (reduction of esters using toxic, reactive aluminium hydrides and the Bouveault–Blanc reduction of esters with alkali metals in ethanol).

$$\text{R}-\overset{\text{O}}{\parallel}{\text{C}}-\text{O}-\text{R}^1 + 2 \text{H}_2 \xrightarrow[\text{1,4-dioxane, 115 }^\circ\text{C}]{\text{Cat. 2 (1 mol\%)} (5.3 \text{ atm})} \text{R}-\text{CH}_2\text{OH} + \text{R}^1-\text{OH}$$

Entry	Ester	Time (hrs)	Conv. (%)	Yield (%)		
				RCH ₂ OH	R'-OH	
1		R ² = -CH ₃	4	100	(97)	CH ₃ OH (100)
		R ² = -CH ₂ CH ₃	4	99	(96)	CH ₃ CH ₂ OH (99)
		R ² = -CH ₂ Ph	7	99	(98)	
2		5	100	(97)	2 CH ₃ OH (100)	
3		R ³ = -CH ₂ CH ₂ CH ₃	4	100	(98)	CH ₃ CH ₂ OH (99)
		R ³ = -CH ₃	12	86	CH ₃ CH ₂ OH (86)	CH ₃ CH ₂ OH
4		5	83	(83)		

Fig. 4 Hydrogenation of esters to alcohols catalysed by Ru(II)PNN pincer complex (**2**)

The conventional reduction methods encounter very serious drawbacks such as the use of hazardous reagents, challenging work-up procedures, safety, and crucially, generation of large amounts of waste [3, 43].

Typical Hydrogenation Procedure:

A 90 mL Fischer–Porter tube was charged under nitrogen with the catalyst **2** (0.02 mmol), an ester (2 mmol) and 1,4-dioxane (2 mL) followed by filled with H₂ (5.3 atm). The solution was heated at 115°C (actual solution temperature) with stirring for the specified period. After cooling to room temperature, excess H₂ was vented carefully and the product yields were determined by GC.

Other catalysts (in Sect. 2) prepared in our laboratory were also employed for the hydrogenation of non-activated esters under mild conditions [30, 44]. The results are summarized in Fig. 5. Notably, higher turnover numbers (up to 3,284 TON) were obtained using complex **6** as a catalyst at 50 atm of dihydrogen for the hydrogenation of hexyl hexanoate (Fig. 5, entry 2).

Subsequent to our original work, several reports on hydrogenation of esters to alcohols catalysed by various Ru(II) pincer complexes appeared (Scheme 5)

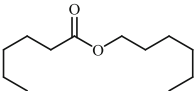
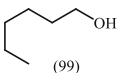
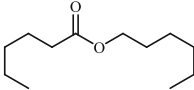
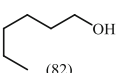
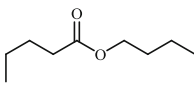
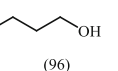
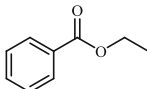
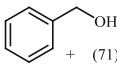
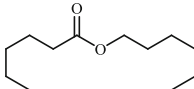
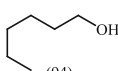
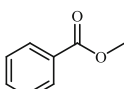
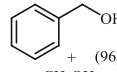
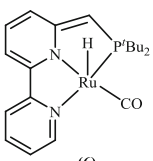
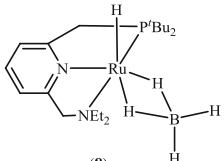
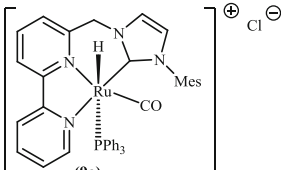
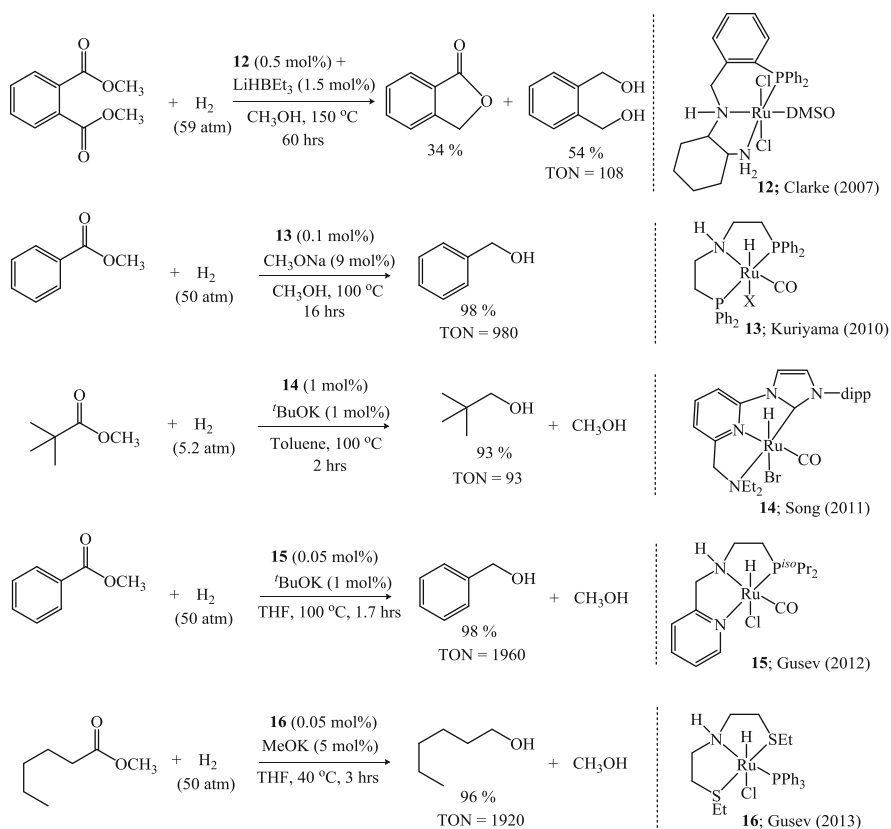
Entry	Ester	Catalyst	Reaction condition	Conv. (%)	Yield (%)	TON
1		6	6 (0.01 mmol), ester (20 mmol), $P\text{H}_2 = 50$ atm, THF (5 mL), Temp. = 110 °C, t = 16 hrs	100	 (99)	2000
2		6	6 (0.005 mmol), ester (20 mmol), $P\text{H}_2 = 50$ atm, THF (5 mL), Temp. = 110 °C, t = 16 hrs	82	 (82)	3284
3		9a	9a + ^t BuOK (each 0.01 mmol), ester (1 mmol), $P\text{H}_2 = 5.4$ atm, Toluene (2 mL), Temp. = 135 °C, t = 2 hrs	96	 (96)	96
4		9a	9a + ^t BuOK (each 0.025 mmol), ester (1 mmol), $P\text{H}_2 = 5.4$ atm, Toluene (2 mL), Temp. = 135 °C, t = 2 hrs	72	 + (71) $\text{CH}_3\text{CH}_2\text{OH}$ (69)	2840
5		8	8 (0.01 mmol), ester (2 mmol), $P\text{H}_2 = 10$ atm, THF (2 mL), Temp. = 110 °C, t = 12 hrs	94	 (94)	188
6		8	8 (0.01 mmol), ester (2 mmol), $P\text{H}_2 = 10$ atm, THF (2 mL), Temp. = 110 °C, t = 12 hrs	97	 + (96) CH_3OH (93)	194
Catalysts:						
						

Fig. 5 Catalytic hydrogenation of non-activated esters to alcohols

[45–51]. Very recently, Ikariya et al. reported the selective hydrogenation of α -fluorinated esters to fluorinated alcohols and fluorohemiacetal intermediates catalysed by commercially available complex **13** under mild, homogeneous conditions [52]. For a recent review on hydrogenation of polar bonds, including esters, see [10].

3.1.2 Complete Hydrogenation of Biomass-Derived Di-esters to 1,2-diols

A selective, complete hydrogenation of cyclic di-esters, in particular the biomass-derived glycolide and lactide to the corresponding 1,2-diols was accomplished

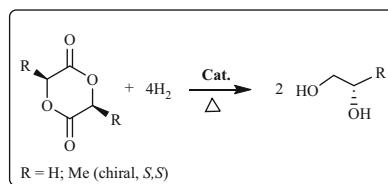


Scheme 5 Ru(II) pincer complexes for homogeneous hydrogenation of esters to alcohols

using bipyridine-based pincer complexes (**6** and **11**) [53]. This method offers an environmentally benign approach to the indirect transformation of biomass to important synthetic building blocks, ethylene glycol and propylene glycol. Significantly, no racemization took place when a chiral di-ester (L-lactide) was used (Fig. 6).

Hydrogenation Procedure:

Catalyst (0.2–1 mol%), di-esters, H₂ and dry THF (3–5 mL) were heated in a Fischer–Porter tube or a high-pressure reactor at 110°C (oil bath temperature) and the yields of 1,2-diols were analysed by GC. In the case of complex **9a**, 1 equiv. (relative to Ru) of KO^tBu was used for the in-situ generation of the dearomatized catalyst.

Fig. 6 Hydrogenation of cyclic di-esters to 1,2-diols

Entry	Cat.	Ester R	$P(H_2)$ atm	Yield	TON
1	6	R = H	10	93	93
2	6	R = H	50	85	425
3	9a	R = H	50	58	290
4	6	R = Me (chiral, <i>S,S</i>)	10	82	82
5	6	R = Me (chiral, <i>S,S</i>)	50	91	455
6	9a	R = Me (chiral, <i>S,S</i>)	50	67	335

3.1.3 Straightforward Hydrogenation of Organic Formates to Methanol

The selective hydrogenation of methyl formate to methanol, catalysed by the Ru(II)-PNN complexes **2–3** and **6**, proceeds efficiently under mild, neutral conditions using low hydrogen pressure, and low temperature, without generation of any waste or by-products and in high turnover numbers was reported by us [54]. The reaction proceeds very well also under neat conditions without using any solvents, representing an ultimate “green” hydrogenation reaction (Fig. 7). The reaction is general and other alkyl formate esters are also hydrogenated efficiently leading to methanol and the corresponding alcohols (ethyl formate to methanol and ethanol and butylformate to methanol and *n*-butanol, respectively) in excellent yields without formation of CO [55–57].

Reaction Conditions:

Catalyst, methyl formate, H_2 and dry THF (3–5 mL) were heated in a Fischer–Porter tube or a high-pressure reactor at specified temperature and the yields of methanol were quantified on GC.

A possible mechanism for general ester hydrogenation to alcohols is depicted in Fig. 8. Initially, reaction of coordinatively unsaturated dearomatized complex **2** with H_2 leads to the fully characterized *trans*-dihydride (**3**) via metal–ligand cooperation (MLC). Decoordination of the hemilabile amine ‘arm’ can provide a site for ester to coordinate with ruthenium centre, and forming intermediate **A**. Hydride transfer to the ester carbonyl gives hemiacetoxy intermediate **B**. Subsequent coordination of amine arm followed by dearomatization of the pincer core regenerate the original complex **2** with elimination of a hemiacetal, which is in

Entry	Cat.	Solvent	Temp. (°C)	P_{H_2} (atm)	Time (hrs)	Conv. (%)	Yield (%)	TON
1	2	THF	110	10	48	78	77	1155
2	3	THF	110	10	48	84	81	1215
3	6	THF	110	10	48	96	96	1440
4	6	THF	110	50	14	94	94	4700
5	6	Neat	80	10	8	~99	98	980

Fig. 7 Hydrogenation of methyl formate to methanol

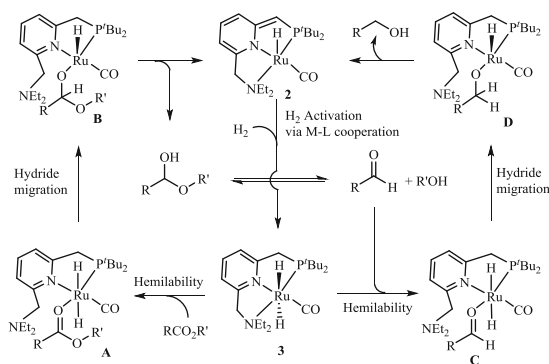
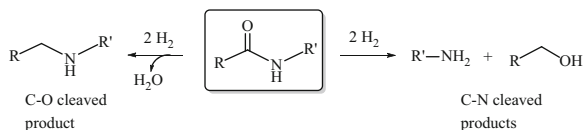


Fig. 8 Proposed catalytic cycle for the hydrogenation of esters to alcohols by complex **2**

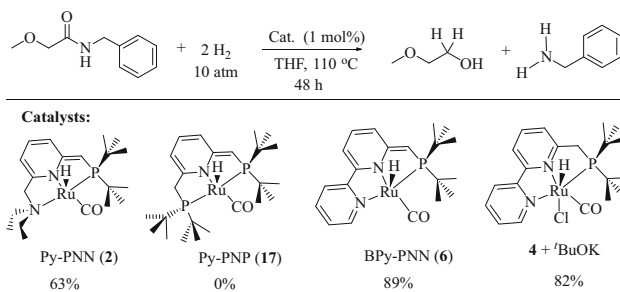
equilibrium with the aldehyde. In general, aldehydes are more susceptible to undergo hydrogenation much faster than esters and thus following the similar catalytic cycle (involving the intermediates **C** and **D**) to lead to the corresponding alcohol. The direct attack of the *trans*-dihydride on the ester carbonyl group, without prior coordination, is also possible. Based on DFT calculations, Hasanayn and his co-workers reported a metathesis-type mechanism [58], in which a hydride transfer from Ru-H to esters can directly lead to aldehyde and Ru-alkoxide in the hydrogenation of esters catalysed complex **2**. This approach can give a new dimension to an active catalyst design for future directions.

3.2 Selective Hydrogenation of Amides to Alcohols and Amines

Among the carboxylic acid derivatives amides, bearing a less electrophilic (hydridophilic) carbonyl group, are the most challenging substrates to hydrogenate



Scheme 6 Possible pathways for the hydrogenation of amides



Scheme 7 Hydrogenation of amides using various pincer catalysts

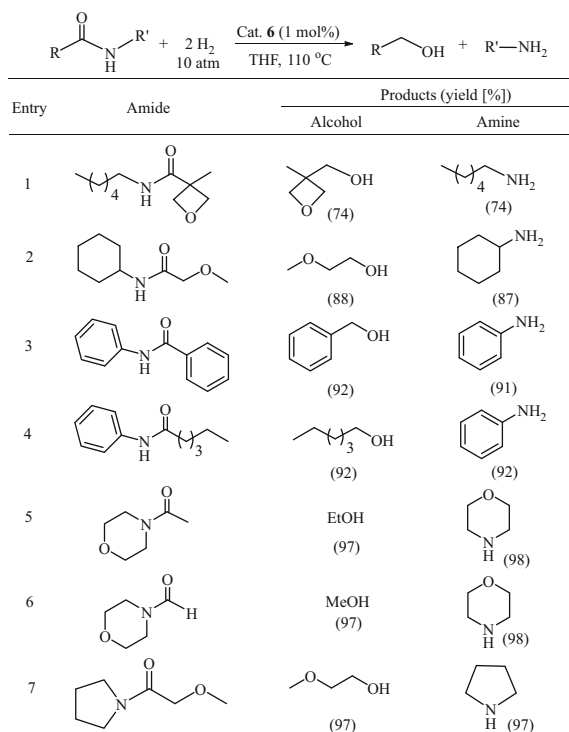
[59, 60]. Possible pathways for the hydrogenation of amides are shown in Scheme 6. A few cases of reductive cleavage of the C=O bond with the formation of a secondary amine were reported [61–65].

The (unprecedented at the time) selective hydrogenation of amides (both aliphatic and aromatic) to the corresponding alcohols and amines in excellent yields, involving C–N bond cleavage was selectively catalysed by **2** and **6** under mild hydrogen pressure and temperature [28], the expected products of C–O cleavage not being formed. Initial screening (Scheme 7; Fig. 9) showed that the bipyridyl-based Ru(II)-pincer complex (**6**) was a more effective catalyst than the pyridyl-based PNN-Ru(II) pincer complex (**2**). Later, other reports on the hydrogenation of amides to alcohols and amines were reported [34, 66–68].

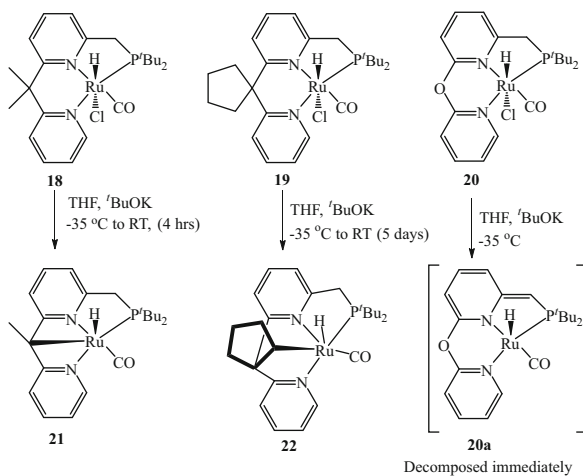
Like in the case of **2**, the bipyridine-based Ru(II)-PNN pincer complex **6** plausibly displays a novel type of metal–ligand cooperative activity through aromatization–dearomatization processes. Recently, a DFT calculation on classical C–O cleavage *vs* our newly reported C–N bond breaking in the amide hydrogenation reaction was reported by Cantillo [69].

In continuation of our research on design of novel catalysts for selective organic transformations, we have synthesized more flexible, expanded PNN-type pincer ruthenium complexes (**18–20**). However, only modest catalytic activity and selectivity was observed with these bridged-bipyridine-based PNN-Ru(II) complexes in amide hydrogenation (25–65% yields) and other reactions [70]. This is likely a result of cyclometalation of the active species **21** and **22**, which is detrimental to the catalysis (Scheme 8; Fig. 10). The low stability of the expected dearomatized complex (**20a**) formed by deprotonation of **20** was also detrimental to catalysis.

Fig. 9 Selective hydrogenation of amides to the corresponding alcohols and amines catalysed by complex **6**



Scheme 8 Cyclometalated Ru(II)-pincer complexes



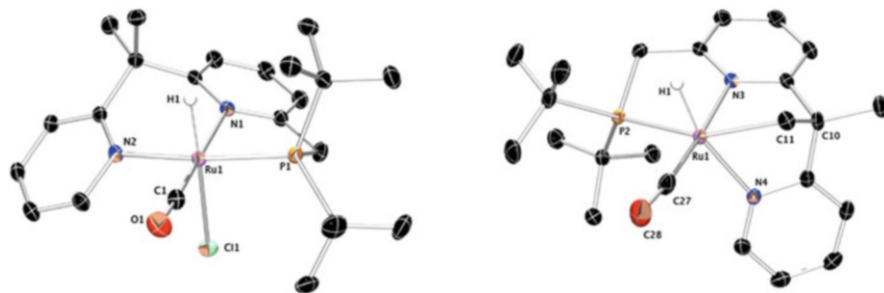


Fig. 10 ORTEP drawing at 50% of probability of Ru(II) complexes **18** and **21**. Hydrogen atoms (except hydride) are omitted for clarity

3.3 Hydrogenation of CO_2 Derivatives to Methanol

3.3.1 Selective Hydrogenation of Organic Carbonates (e.g., DMC) to Methanol

In continuation of our research aimed at sustainable catalytic hydrogenation of various demanding substrates, we reported yet another unprecedented hydrogenation of extremely challenging polar carbonyl compounds, including organic carbonates, carbamates and urea derivatives selectively to methanol, which can serve as an efficient energy storage chemical and a convenient fuel-substitute in the foreseeable future. Catalytic hydrogenation of these important families of compounds under very mild operational conditions is of significant interest, since these compounds can be produced from CO_2 and CO, and their selective hydrogenation would ultimately represent an indirect approach to transformation of C1 sources (CO_2 and CO) to fuel, which is of intense current interest with regard to “methanol economy” [71–74].

The simplest organic carbonate, dimethyl carbonate (DMC), serves as a stable and ‘green’ solvent [75], and is even used as an inert solvent for hydrogenation reactions under extremely harsh conditions with regard to temperature and pressure. In industry, DMC is produced from CO or CO_2 either by oxidative carbonylation of methanol or by straightforward synthesis from CO_2 and methanol, respectively [76–79]. The hydrogenation of DMC to methanol under mild conditions (either by heterogeneous or homogeneous) has not previously been achieved, prior to our report [54].

Dimethyl carbonate was quantitatively hydrogenated into methanol under mild, neutral conditions, catalysed by the Ru(II)-pincer complexes **2–3** and **6** under low hydrogen pressure and relatively low temperature with high TON (up to 4,400 after 14 h). Moreover, the hydrogenation of dimethyl carbonate proceeds smoothly under *solvent free* conditions in case of catalyst **2** and TON more than 990 were achieved after 8 h.

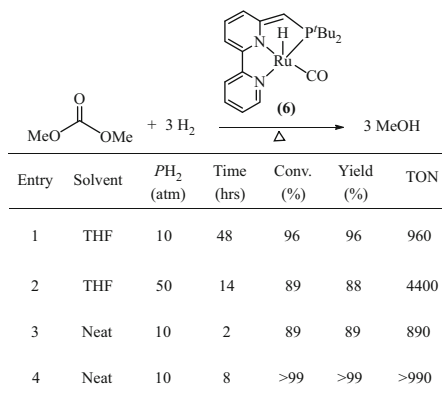


Fig. 11 Hydrogenation of dimethyl carbonate to methanol catalysed by BPy-PNN Ru(II) (**6**)

The attractive characteristics of DMC hydrogenation to methanol, namely solvent free, waste-free, atom-economical, mild pressure and temperature, high turnover numbers (TON), and high selectivity, represent an ultimate green process and make this catalytic transformation an attractive technology for methanol synthesis [80–82]. Some representative examples catalysed by complex **6** are presented in Fig. 11 (vide supra).

Based on model stoichiometric experiments and known metal–ligand cooperation by aromatization–dearomatization of the pincer complex **2**, a mechanism for the selective hydrogenation of dimethyl carbonate to methanol is proposed (Fig. 12). A possible catalytic cycle is as follows: (1) formation of the *trans*-dihydride complex **3** via metal–ligand cooperation (MLC), (2) hydride transfer from the *trans*-dihydride complex to dimethyl carbonate may lead to intermediate **A** which forms methanol by deprotonation of the pincer ligand, generating the methyl formato-dearomatized complex **B**, (3) hydrogen addition and hydride transfer to the coordinated formato moiety forming intermediate **C**, followed by proton abstraction from the pincer ligand leads to methanol and the formaldehyde complex **D**. Addition of hydrogen to form complex **23**, followed by methanol elimination regenerated the dearomatized complex **2** and completes the catalytic cycle.

Recently, density functional computation on hydrogenation of dimethyl carbonate to methanol, catalysed by Ru(II)-PNN catalyst **2** supported a stepwise hydrogenation mechanism (Fig. 13) [83, 84]. A hydride/methoxide metathesis-based mechanism was suggested by DFT [85].

Ding and co-workers demonstrated the hydrogenation of cyclic carbonates selectively to methanol and corresponding diols [86] in good yields catalysed by complex **13** using 0.05 mol% and catalytic amount of base under 50 atm of hydrogen pressure and at 140°C (Scheme 9).

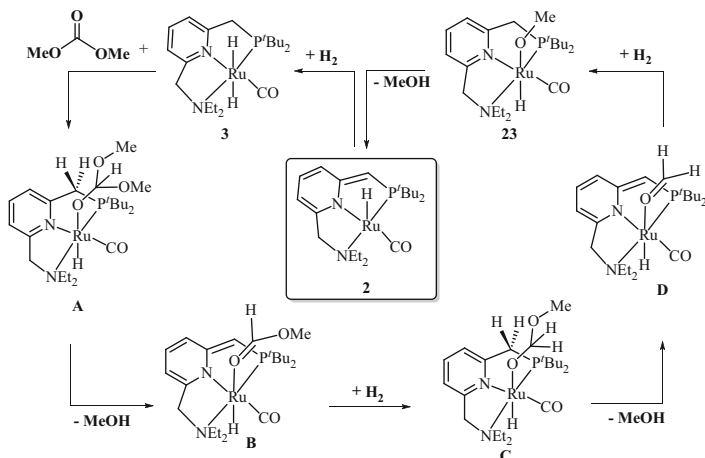


Fig. 12 Postulated mechanism for the selective hydrogenation of DMC to methanol catalysed by **2**

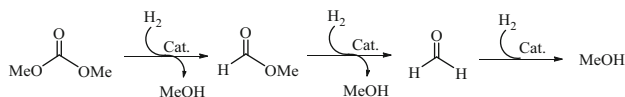
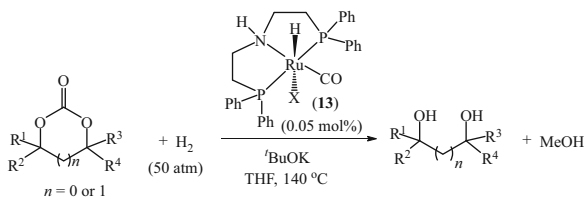


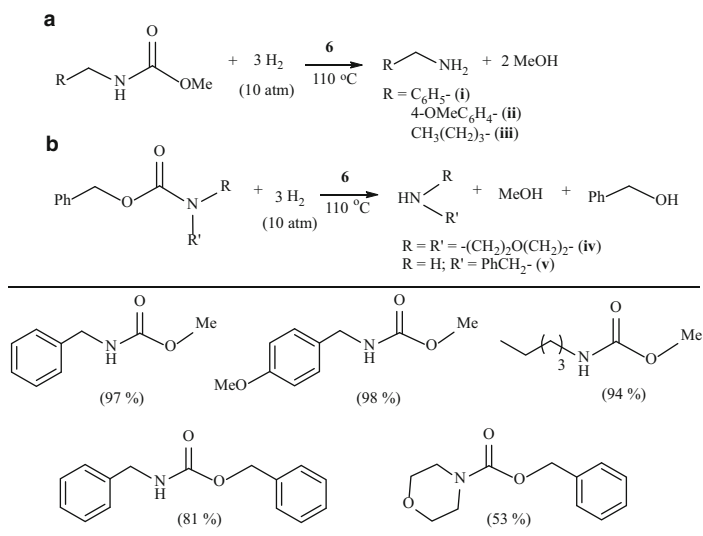
Fig. 13 Catalytic stepwise hydrogenation of DMC to methanol



Scheme 9 Hydrogenation of cyclic carbonates to methanol and diols [86]

3.3.2 Catalytic Hydrogenation of Carbamates by BPy-PNN Ru(II) Pincer Complex (**6**)

We have reported the first example of catalytic hydrogenation of carbamates to selectively form methanol and the corresponding amines and alcohols, without cleavage of the arylalkyl-O bond under mild hydrogen pressure and neutral conditions, with no generation of waste, using catalyst **6** (Scheme 10, yields are based on methanol) [54]. The reaction proceeds well with 1 mol% of complex **6**. In contrast to the well-known hydrogenation of benzyl carbamates by heterogeneous catalysts (e.g. Pd/C), in which the carbonyl group is not reduced, forming CO₂, amine and

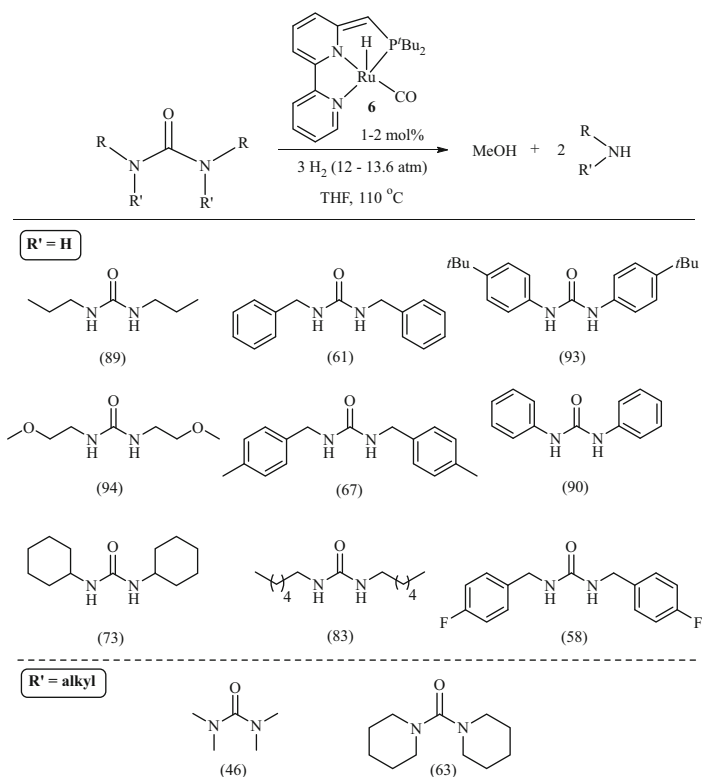


Scheme 10 Catalytic hydrogenation of (a) methyl and (b) benzyl carbonates to methanol

hydrocarbon, with no methanol formation [87], the Ru(II) pincer complex **6** catalyses hydrogenation of the carbonyl group, forming methanol, together with the corresponding alcohols and amines. Notably, carbamates are derivatives of CO₂ and synthetic methods for their formation are well established [78, 88, 89].

3.3.3 Hydrogenation of Urea Derivatives to Methanol and Amines

Among carbonyl compounds, hydrogenation of urea derivatives is the most challenging due to the low electrophilicity of the carbonyl group as a result of the resonance effect. Notably, alkyl urea compounds have been used as ‘green’ solvents in catalytic hydrogenation reactions of other compounds and as ‘green’ solvents in metal-mediated organic transformations [90, 91]. Unprecedented hydrogenation of urea derivatives was achieved with complex **6** as catalyst. In this process, cleavage of two strong C–N bonds takes place, using various alkyl- and aryl- urea derivatives, selectively producing methanol and the respective amines in high yield under mild reaction conditions, namely 110°C and 13.6 atm H₂ pressure [92]. Traces of formamides were observed in several cases, confirming the stepwise hydrogenation mechanism (urea to formamide to methanol) like in the case of dimethyl carbonate hydrogenation (Scheme 11; GC yields are based on methanol). Since alkyl- and aryl-urea derivatives are readily obtained from CO₂ and amines [93], their hydrogenation offers an environmentally benign, mild, atom-economical approach to the indirect transformation of CO₂ to methanol [81].

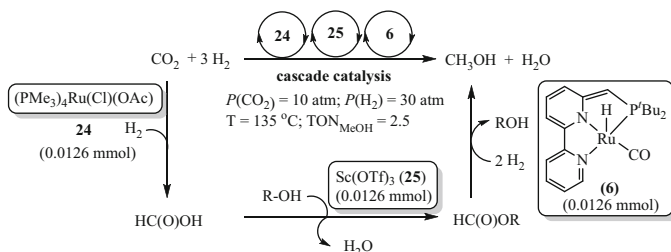


Scheme 11 Unprecedented hydrogenation of urea derivatives to methanol and amines catalysed by **6**

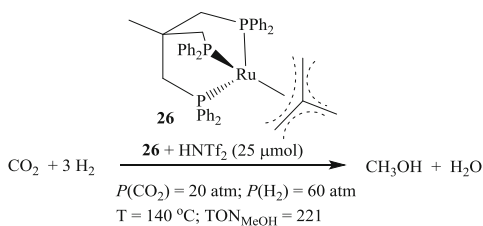
4 Direct Hydrogenation of CO₂

Sanford et al. recently demonstrated “cascade catalysis” aimed at the direct hydrogenation of CO₂ to methanol by using a (PMe₃)₄Ru(Cl)(CO) **24**/ Sc(OTf)₃ **25**/ (BPy-PNN⁻)RuH(CO) **6** homogeneous catalyst combination to effect the stepwise (CO₂ to HC(O)OCH₃ [via HC(O)OH] to CH₃OH) hydrogenation with low TON (2.5) [94]. The cascade direct hydrogenation of CO₂ to methanol involves three steps, (1) conversion of CO₂ to formic acid affected by Jessop’s catalyst (**24**), (2) Lewis-acid catalysed esterification of formic acid with methanol to provide methyl formate and (3) effective methyl formate hydrogenation by (BPy-PNN⁻)RuH(CO) **6** to liberate 2 equiv. of CH₃OH (Scheme 12).

Direct hydrogenation of CO₂ to methanol was recently reported by Klankermayer and Leitner using a non-pincer catalytic system, comprised of a ruthenium(II)-complex [(triphos)Ru-(TMM)] **26** (TMM = trimethylenemethane), and an acid, achieving turnover numbers up to 221 [95]. Catalytic *N*-methylation of secondary and primary aromatic amines using CO₂ as C1 source and molecular



Scheme 12 Triple catalyst cascade hydrogenation of CO_2 to methanol [94]



Scheme 13 Ru(II) catalysed direct hydrogenation of CO_2 to methanol [95]

hydrogen directly as reducing agent was also reported by Klankermayer and Leitner using the Ru(II)-complex **26** and an acid (HNTf_2) (Scheme 13) [96].

Sanford and co-workers subjected our catalyst (**2**) for highly efficient catalytic hydrogenation of CO_2 to formate salts [97] and displays similar activity to known Nozaki's Ir(III) pincer catalyst **27** ($\text{TON} = 3,500,000$ and $\text{TOF} = 150,000 \text{ h}^{-1}$ for CO_2 to $\text{HC}(\text{O})\text{OK}$) [98, 99]. Heating a diglyme solution of complex **2**, base (K_2CO_3), carbon dioxide, and hydrogen resulted in the formation of potassium formate with excellent TON of 23,000 and TOF of up to $2,200 \text{ h}^{-1}$. The postulated mechanism for the hydrogenation of CO_2 by **2** is shown in Fig. 14. Hydrogenation of carbon dioxide catalysed by ruthenium(II)-PNP pincer (**17**) was reported by Pidko et al. indicating that CO_2 binding to the deprotonated pincer arm inhibits the reaction, whereas faddition of water restores reactivity [100].

Efficient hydrogenation of CO_2 using an iron-based catalyst is an important goal. Beller and co-workers reported hydrogenation of bicarbonates and carbon dioxide to formates and formamides catalysed by well-defined Fe(II) complexes [101, 102]. Thus, heating a methanol solution of $\text{Fe}(\text{BF}_4)_2 \cdot 6\text{H}_2\text{O}$ and the ligand **28** (in situ generated complex **29**), HNMe_2 (80 mmol), carbon dioxide (30 atm), and hydrogen (30 atm) resulted in the formation of DMF (74%) and formic acid (7.7%) with TON of 5,104 (Scheme 14).

Recently, we reported an efficient hydrogenation of carbon dioxide and sodium bicarbonate to formate salt catalysed by the dihydride Fe(II)-pincer complex **30**. Carbon dioxide and sodium bicarbonate are economically hydrogenated in aqueous media at 80°C under remarkably low pressures (6–10 bar), with TON up to 788 (Scheme 15) [23].

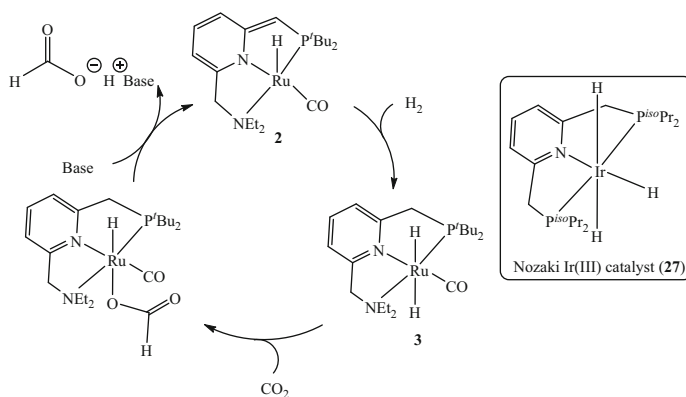
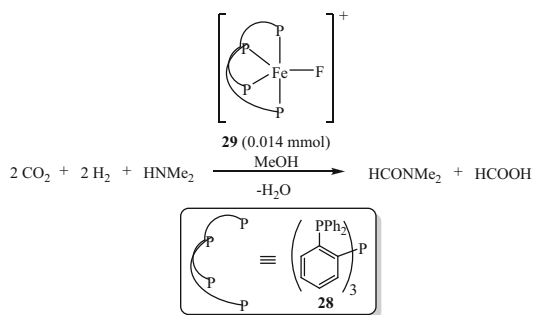
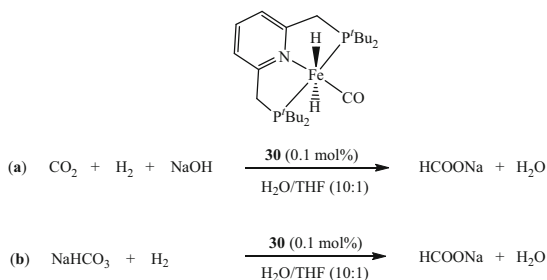


Fig. 14 Proposed catalytic cycle for the hydrogenation of CO₂ by **2**



Scheme 14 Catalytic hydrogenation of CO₂ to formamide and formic acid by iron complex **29** (in situ generated)



Scheme 15 Iron pincer complex (**30**) catalysed hydrogenation of (a) CO₂ and (b) bicarbonate to formate salt

A possible catalytic cycle for the hydrogenation of CO₂ to formate catalysed by the iron pincer complex **30** is as follows (Fig. 15): (1) Formation of the hydridoformato complex **31** by direct electrophilic attack of CO₂ on the *trans*-dihydride **30**,

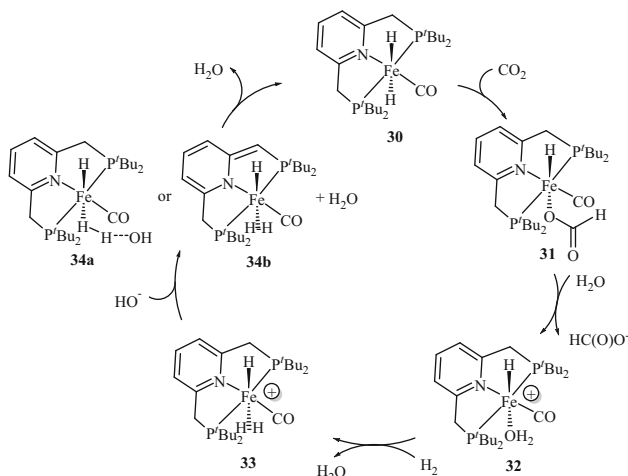


Fig. 15 Proposed mechanism for the hydrogenation of CO₂ to formate salt catalysed by the iron pincer complex **30**

(2) displacement of the formate ligand (as a formate salt) by a water molecule, forming complex **32**, (3) formation of the dihydrogen intermediate **33** under hydrogen pressure, followed by regeneration of the *trans*-dihydride **30** either by heterolytic cleavage of the coordinated H₂ by ⁻OH (**34a**) or by dearomatization and subsequent proton migration (**34b**). Based on DFT calculations, similar catalytic cycles were postulated for iridium, cobalt and iron pincer complexes [103–105].

5 Conclusion

In this chapter, we have discussed hydrogenation of carbonyl compounds, in particular, esters, amides, and the CO₂-derived formates, carbonates, carbamates and ureas to fundamentally important building blocks, catalysed by pincer-based Ru(II) complexes. These efficient, atom-economical reactions operate under very mild low hydrogen pressure, produce no waste and provide alternative, environmentally benign approaches to traditional reduction methods, which often produce copious waste. The metal–ligand cooperation approach (MLC) significantly contributes to the reactivity and selectivity in the hydrogenation reactions. Still there is room to improve the catalytic reactivity and selectivity (e.g. in direct, efficient hydrogenation of CO₂ to methanol). The development of efficient catalysts based on iron pincer complexes is an important challenge; promising results in the hydrogenation of ketones and CO₂ were already obtained [23–25].

Acknowledgements Supported by the European Research Council (ERC) under the FP7 framework (No. 246837), Kimmel Center for Molecular Design and CSIR-NCL (start-up grant to E.B, MLP028726). D.M. is the Israel Matz Professorial Chair of Organic Chemistry.

References

1. Constable DJC, Dunn PJ, Hayler JD, Humphrey GR, Leazer HL, Linderman RJ Jr, Lorenz K, Manley J, Pearlman BA, Wells A, Zaks A, Zhang TY (2007) *Green Chem* 9:411
2. Aldridge S (2008) *Pharm Technol Eur* 20:15
3. Seyden-Penne J (1997) *Reductions by alumino- and borohydrides in organic synthesis*. Wiley, New York
4. Gribble GW (1998) *Chem Soc Rev* 27:395
5. Rothenberg G (2008) *Catalysis: Concepts and Green Applications*. Wiley-VCH, Weinheim
6. Clapham SE, Hadzovic A, Morris RH (2004) *Coord Chem Rev* 248:2201
7. Ito M, Ikariya T (2007) *Chem Commun* 5134
8. Kubas GJ (2007) *Chem Rev* 107:4152
9. Wylie WNO, Lough AJ, Morris RH (2010) *Chem Commun* 46:8240
10. Dub PA, Ikariya T (2012) *ACS Catal* 2:1718
11. Noyori R (2002) *Angew Chem Int Ed* 41:2008
12. Ohkuma T, Ooka H, Hashiguchi S, Ikariya T, Noyori R (1995) *J Am Chem Soc* 117:2675
13. Ohkuma T, Noyori R (2001) *Angew Chem Int Ed* 40:40
14. Albrecht M, Van Koten G (2001) *Angew Chem Int Ed* 40:3750
15. van der Boom ME, Milstein D (2003) *Chem Rev* 103:1759
16. Morales-Morales D, Jensen CM (eds) (2007) *The chemistry of pincer compounds*. Elsevier, Amsterdam
17. van Koten G, Milstein D (eds) (2013) *Organometallic pincer chemistry*. Springer-Verlag Berlin Heidelberg
18. Kanai M, Ikariya T, Ooi T, Ding K, Milstein D (2013) Recent topics in cooperative catalysis: asymmetric catalysis, polymerization, hydrogen activation, and water splitting. In: Ding K, Dai L-X (eds) *Organic chemistry- breakthroughs and perspectives*. Wiley-VCH, Weinheim, pp 385–412
19. Milstein D (2010) *Top Catal* 53:915
20. Gunanathan C, Milstein D (2011) *Top Organomet Chem* 37:55
21. Gunanathan C, Milstein D (2011) *Acc Chem Res* 44:588
22. Gunanathan C, Milstein D (2013) *Science* 341:249
23. Langer R, Diskin-Posner Y, Leitus G, Shimon LJW, Ben-David Y, Milstein D (2011) *Angew Chem Int Ed* 50:9948
24. Langer R, Leitus G, Ben-David Y, Milstein D (2011) *Angew Chem Int Ed* 50:2120
25. Langer R, Iron MA, Konstantinovski L, Diskin-Posner Y, Leitus G, Ben-David Y, Milstein D (2012) *Chem Eur J* 18:7196
26. Zhang J, Leitus G, Ben-David Y, Milstein D (2005) *J Am Chem Soc* 127:12429
27. Zhang J, Leitus G, Ben-David Y, Milstein D (2006) *Angew Chem Int Ed* 45:1113
28. Balaraman E, Gnanaprakasam B, Shimon LJW, Milstein D (2010) *J Am Chem Soc* 132:16756
29. Zhang J, Gandelman M, Shimon LJW, Milstein D (2007) *J Chem Soc Dalton Trans* 107
30. Zhang J, Balaraman E, Leitus G, Milstein D (2011) *Organometallics* 30:5716
31. Fogler E, Balaraman E, Ben-David Y, Leitus G, Shimon LJW, Milstein D (2011) *Organometallics* 30:3826
32. Carey FA, Sundberg RJ (2000) *Advanced Organic Chemistry*. Kluwer Academic/Plenum, New York
33. McAlees AJ, McCrindle R (1969) *J Chem Soc* 2425
34. Ito M, Ootsuka T, Watari R, Shiibashi A, Himizu A, Ikariya T (2011) *J Am Chem Soc* 133:4240
35. Casey CP, Guan H (2007) *J Am Chem Soc* 129:5816
36. Bullock RA (2007) *Angew Chem Int Ed* 46:7360
37. Morris RH (2009) *Chem Soc Rev* 38:2282
38. Bauer G, Kirchner KA (2011) *Angew Chem Int Ed* 50:5798

39. Junge K, Schröder K, Beller M (2011) *Chem Commun* 47:4849
40. Grey RA, Pez GP, Wallo A (1981) *J Am Chem Soc* 103:7536
41. Clarke ML (2012) *Catal Sci Technol* 2:2418
42. Teunissen HT, Elsevier CJ (1998) *Chem Commun* 1367
43. Vogt P, Bodnar B (2009) *Spec Chem Mag* 29/7:22
44. Milstein D, Balaraman E, Gunanathan C, Gnanaprakasam B, Zhang J (2012) *WO 2012/052996A2*
45. Clarke ML, Diaz-Valenzuela MB, Slawin AMZ (2007) *Organometallics* 26:16
46. Clarke ML, Roff GJ (2007) in *Handbook of Homogeneous Hydrogenation* 1:413; de Vries JG, Elsevier CJ (eds) Wiley, New York
47. Kuriyama W, Matsumoto T, Ino Y, Ogata O (2011) Takasago International Corporation, Japan *WO2011048727A1*
48. Kuriyama W, Matsumoto T, Ogata O, Ino Y, Aoki K, Tanaka S, Ishida K, Kobayashi T, Sayo N, Saito T (2012) *Org Process Res Dev* 16:166
49. Sun YS, Koehler C, Tan RY, Annibale VT, Song DT (2011) *Chem Commun* 47:8349
50. Spasyuk D, Smith S, Gusev DG (2012) *Angew Chem Int Ed* 51:2772
51. Spasyuk D, Smith S, Gusev DG (2013) *Angew Chem Int Ed* 52:2538
52. Otsuka T, Ishii A, Dub PA, Ikariya T (2013) *J Am Chem Soc* 135:9600
53. Balaraman E, Fogler E, Milstein D (2012) *Chem Commun* 48:1111
54. Balaraman E, Gunanathan C, Zhang J, Shimon LJW, Milstein D (2011) *Nature Chem* 3:609
55. Gormley RJ, Rao VUS, Soong Y (1992) *Appl Catal A* 87:81
56. Iwasa N, Terashita M, Arai M, Takezawa N (2001) *React Kinet Catal Lett* 74:93
57. Monti DM, Kohler MA, Wainwright MS, Trimm DL, Cant NW (1986) *Appl Catal* 22:123
58. Hasanayn F, Baroudi A (2013) *Organometallics* 32:2493
59. Robin MB, Bovey FA, Basch, H (1970) in *The Chemistry of Amides* (ed: Zabicky, J), Interscience, New York
60. Hartwig J (2010) *Organotransition Metal Chemistry*; University Science Books: Sausalito, CA
61. NuñezMagro AA, Eastham GR, Cole-Hamilton DJ (2007) *Chem Commun* 3154
62. Beamson G, Papworth AJ, Philipps C, Smith AM, Whyman R (2010) *Adv Synth Catal* 352:869
63. Stein M, Breit B (2013) *Angew Chem Int Ed* 52:2231
64. Coetzee J, Deborah L, Dodds DL, Klankermayer J, Brosinski S, Leitner W, Slawin AMZ, Cole-Hamilton DJ (2013) *Chem Eur J* 19:11039
65. Coetzee J, Manyar HG, Hardacre C, Cole-Hamilton DJ (2013) *ChemCatChem* 5:2843
66. John JM, Bergens SH (2011) *Angew Chem Int Ed* 50:10377
67. John JM, Bergens SH (2012) *Angew Chem Int Ed* 51:2533
68. Miura T, Held IE, Oishi S, Naruto M, Saito S (2013) *Tetrahedron Lett* 54:2674
69. Cantillo D (2011) *Eur J InorgChem* 3008
70. Barrios-Francisco R, Balaraman E, Diskin-Posner Y, Leitner G, Shimon LJW, Milstein D (2013) *Organometallics* 32:2973
71. Olah GA, Goeppert A, Prakash GKS (2006) *Beyond Oil and Gas: The Methanol Economy*. Wiley-VCH, Weinheim
72. Olah GA (2005) *Angew Chem Int Ed* 44:2636
73. Olah GA, Goeppert A, Prakash GKS (2009) *J Org Chem* 74:487
74. Cokoja M, Bruckmeier C, Rieger B, Herrmann WA, Kühn FE (2011) *Angew Chem Int Ed* 50:8510
75. Schaffner B, Schaffner F, Verevkin SP, Borner (2010) *Chem Rev* 110:4554
76. Delledonne D, Rivetti F, Romano U (1995) *J Organomet Chem* 448:C15
77. Delledonne D, Rivetti F, Romano U (2001) *Appl Catal A* 221:241
78. Sakakura T, Kohno K (2009) *Chem Commun* 45:1312
79. Sakakura T, Choi JC, Yasuda H (2007) *Chem Rev* 107:2365
80. Dixneuf PH (2011) *Nature Chem* 3:578

81. Choudhury J (2012) *ChemCatChem* 4:609
82. Li Y, Junge K, Beller M (2013) *ChemCatChem* 5:1072
83. Li H, Wen M, Wang Z-X (2012) *Inorg Chem* 51:5716
84. Yang X (2012) *ACS Catal* 2:964
85. Hasanayn F, Baroudi A, Bengali AA, Goldman AS (2013) *Organometallics* 32:6969
86. Han Z, Rong L, Wu J, Zhang L, Wang Z, Ding K (2012) *Angew Chem Int Ed* 51:13041
87. Kocienski PJ (2005) *Protecting Groups*, Thieme
88. Abla M, Choi JC, Sakakura T (2001) *Chem Commun* 37:2238
89. Abla M, Choi JC, Sakakura T (2004) *Green Chem* 6:524
90. Ohgomori Y, Mori S, Yoshida S, Watanabe Y (1987) *J Mol Catal* 40:223
91. Imperato G, Höger S, Lenoir D, König B (2006) *Green Chem* 8:1051
92. Balaraman E, Ben-David Y, Milstein D (2011) *Angew Chem Int Ed* 50:11702
93. Wu C, Cheng H, Liu R, Wang Q, Hao Y, Yu Y, Zhao F (2010) *Green Chem* 12:1811
94. Huff CA, Sanford MS (2011) *J Am Chem Soc* 133:18122
95. Wesselbaum S, vom Stein T, Klankermayer J, Leitner W (2012) *Angew Chem Int Ed* 51:7499
96. Beydoun K, vom Stein T, Klankermayer J, Leitner W (2013) *Angew Chem Int Ed* 52:9554
97. Huff CA, Sanford MS (2013) *ACS Catal* 3:2412
98. Tanaka R, Yamashita M, Nozaki K (2009) *J Am Chem Soc* 131:14168
99. Federsel C, Jackstell R, Beller M (2010) *Angew Chem Int Ed* 49:6254
100. Filonenko GA, Conley MP, Copéret C, Lutz M, Hensen EJM, Pidko EA (2013) *ACS Catal* 3:2522
101. Federsel C, Boddien A, Jackstell R, Jennerjahn R, Dyson PJ, Scopelliti R, Laurenczy G, Beller M (2010) *Angew Chem Int Ed* 49:9777
102. Ziebart C, Federsel C, Anbarasan P, Jackstell R, Baumann W, Spannenberg A, Beller M (2012) *J Am Chem Soc* 134:20701
103. Schmeier TJ, Dobereiner GE, Crabtree RH, Hazari N (2011) *J Am Chem Soc* 133:9274
104. Ahlquist MSG (2010) *J Mol Catal A* 324:3
105. Yang X (2011) *ACS Catal* 1:849

Ruthenium-Catalyzed Hydrogen Generation from Alcohols and Formic Acid, Including Ru-Pincer-Type Complexes

Pamela G. Alsabeh, Dörthe Mellmann, Henrik Junge, and Matthias Beller

Abstract The current feedstock for global energy demands is fossil fuels, which are not renewable and therefore have a limited lifetime as an energy supply. Renewable feedstocks such as biologically derived substrates, formic acid, and alcohols have been proposed as alternative energy sources, which can be used to produce hydrogen gas as one of the most simple chemical energy carriers. The dehydrogenation reaction is thus a necessary key step to establish a potential “hydrogen economy.” The following review chapter highlights recent advances in the areas of alcohol and formic acid dehydrogenation focusing on ruthenium-catalyzed processes. Although alcohol dehydrogenation has been studied extensively for its organic synthetic aspects, significantly fewer systems have directed efforts towards efficient hydrogen generation; those examples detailing TON and TOF values for gas evolution are described. Not only are ruthenium complexes bearing simple monodentate ligands successful as catalysts for conversion of challenging alcohols, but also those featuring pincer-type ligands. In addition, various ruthenium-catalyzed formic acid dehydrogenation methods have been developed. These protocols are performed mainly in the presence of amine or base to generate hydrogen but also include the absence of base, use of ionic liquids, continuous flow systems as well as hydrogen storage processes. In all of the abovementioned examples, ruthenium catalysts demonstrate high activity at relatively low loadings as well as long-term stability.

Keywords Alcohols · Catalysis · Dehydrogenation · Formic acid · Ruthenium

Pamela G. Alsabeh and Dörthe Mellmann contributed to this work equally.

P.G. Alsabeh, D. Mellmann, H. Junge, and M. Beller (✉)
Leibniz-Institut für Katalyse e.V. an der Universität Rostock, Albert-Einstein-Straße 29a,
18059 Rostock, Germany
e-mail: matthias.beller@catalysis.de

Contents

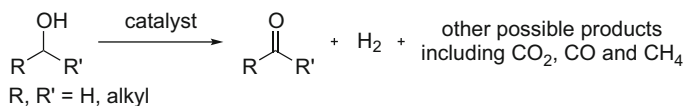
1	Introduction	46
2	Hydrogen Generation from Alcohols	49
2.1	Pioneering Contributions	49
2.2	Current Developments in Alcohol Dehydrogenation (2005 to Present)	50
2.3	Methods for the Aqueous-Phase Reforming of Methanol	54
3	Dehydrogenation of Formic Acid	58
3.1	Dehydrogenation from Aqueous FA/Formate	58
3.2	Dehydrogenation of Formic Acid/Amine Mixtures (FAA)	62
3.3	Dehydrogenation Without Base	64
3.4	Ionic Liquid-Assisted Hydrogen Evolution	65
3.5	Continuous Flow Methods	68
3.6	Progress Towards Hydrogen Storage Devices	71
4	Conclusions	73
	References	74

Abbreviations

dppe	1,2-bis(diphenylphosphino)ethane
dppm	1,1-bis(diphenylphosphino)methane
DH	Dehydrogenation
DMF	<i>N,N</i> -dimethylformamide
DMOA	Dimethyloctylamine
DMSO	Dimethylsulfoxide
FA	Formic acid
FAA	Formic acid/amine
IL	Ionic liquid
PEM	Proton exchange membrane fuel cell
TMEDA	<i>N,N,N',N'</i> -tetramethylethylenediamine
TOF	Turnover frequency
TON	Turnover number

1 Introduction

It is well known that current energy for the entire world population stems from fossil fuels (i.e. coal, oil and gas). The reservoirs of these fuels are continuously being depleted and will eventually be exhausted to the point that they are no longer in reliable quantities. There are also environmental concerns with the combustion of such resources, in that they produce large amounts of CO₂, which inevitably contribute to greenhouse gas emissions [1]. Thus, it is of utmost importance to discover cleaner alternatives and renewable fuel sources that would sustain the



Scheme 1 Typical reaction scheme for acceptorless alcohol dehydrogenation

global energy demand. One solution proposed to address this issue is the use of hydrogen gas, due to its high gravimetric energy content (33.3 kWh kg^{-1}) and clean combustibility properties (forming only water and heat) [2]. The use of hydrogen gas to produce energy for transportation and electricity has led to the idea of a potential “hydrogen economy” [3–5]. Central to this effort is the implementation of fuel cells, which convert the chemical energy of hydrogen gas to electrical energy by use of electrochemical processes; proton exchange membrane (PEM) fuel cells, for example, operate using hydrogen and air and are currently tested as a highly efficient alternative to combustion engines in vehicles [1]. Since hydrogen is currently almost entirely generated from fossil fuels (>95%), it would act as a secondary energy carrier initially being produced from a primary fuel source such as water, biomass, or other renewable resources. In recent years, significant efforts have been directed towards the use of formic acid and alcohols for hydrogen generation, both of which can be more easily handled and stored, and also produced from biological feedstocks.

Acceptorless dehydrogenation of alcohols is a topic that has gained a lot of attention as an environmentally relevant means to generate hydrogen. The products of these processes are typically an aldehyde or ketone (from a primary or secondary alcohol, respectively) and hydrogen gas (Scheme 1), where one molecule of H_2 is produced for every OH group present. In comparison with formic acid (vide infra), alcohols can possess relatively higher gravimetric hydrogen contents, particularly those of low molecular weights such as methanol (12.6%) and ethanol (13.2%), both of which are low-boiling liquids at standard temperatures and pressures allowing for easy handling and storage.

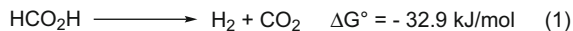
The obvious choice for a renewable hydrogen feedstock would be bioethanol, a mixture of water and ethanol produced from biological fermentation processes, and the use of which can result in a complete carbon cycle, thereby reducing harmful emissions [6]. Thus, alcohols have been investigated for their utility in hydrogen generation since the 1960s when Charman first reported the use of rhodium complexes for the dehydrogenation of isopropanol [7, 8]. Robinson then introduced ruthenium-catalyzed processes in the 1970s, incorporating both primary and secondary alcohols [9, 10]. Currently, ruthenium-based complexes are prominent catalysts among alcohol dehydrogenation procedures but other platinum group metals, primarily iridium [11–13] and osmium [14–17], are also applicable to this chemistry. Most recently, non-noble metal systems of iron and cobalt have demonstrated promising catalytic activity [18–20]. With respect to the scope of alcohols, secondary and/or longer chain alcohols were initial challenges earlier on that have since been addressed and more recent breakthroughs include even more

difficult small primary alcohols, ethanol and methanol (*vide infra*). Nevertheless, there is still significant progress to be made towards sustainable hydrogen generation.

The majority of recent contributions to the field of alcohol dehydrogenation have focused on the synthetic utility of these methods, including but not limited to the formation of ketones and aldehydes [21–24], esters [25–29], amides [30–35] as well as some heterocycles [36–38], from alcohols. These procedures are thoroughly described in several recent reviews [39–41] and thus are not included in the present chapter. As described earlier, hydrogen production is of significant interest for energy applications and the utility of the aforementioned synthetic protocols would gain further importance if they were to concentrate on hydrogen evolution in addition to the organic products. In this context, the following sections discuss those reports in which efforts are directed towards ruthenium-catalyzed dehydrogenation of alcoholic solutions, where turnover number (TON) and turnover frequency (TOF) correspond to hydrogen evolution.

Formic acid (HCO_2H) is a relatively nontoxic (in dilute quantities) yet corrosive liquid at room temperature that can be stored and transported for energy use. It is produced in industrial processes [42, 43] and via biological pathways including fermentation of biomass [44]. Given the desired target hydrogen content by the U.S. Department of Energy of 5.5 wt%, formic acid falls just short of this value at 4.4 wt% [45]. Based on the gravimetric energy content of hydrogen (33.3 kWh kg^{-1}), 1.43 kWh kg^{-1} of energy can thus be generated from the hydrogen contained in formic acid. In terms of formic acid decomposition, there are two possible routes: dehydrogenation or decarbonylation, where the former process forms H_2 and CO_2 and the latter results in CO and H_2O (Scheme 2). Although the hydrogen generation pathway is energetically more favorable, formic acid undergoes decarbonylation at elevated temperatures ($>78^\circ\text{C}$) in the absence of a suitable catalyst [46]. Thus, current efforts are directed towards the design of catalysts to suppress this undesired reaction and selectively dehydrogenate formic acid under mild conditions. Notably, proton exchange membrane fuel cells (PEM) can tolerate mixtures of H_2 and CO_2 gas to generate electrical energy but the presence of CO has been shown to irreversibly inhibit the performance of such devices [47].

Since the first reports of hydrogen production from formic acid in the early twentieth century [48, 49], there has been significant progress highlighted in several reviews [41, 50–55]. Depending on the catalyst employed, these reactions can be performed under aqueous acidic or basic conditions as well as under the influence of light, which has been shown to promote catalytic activity [56]. With respect to the mechanism, common catalytic intermediates generally include hydride, formate, and dihydrogen species as well as carbonyl-containing complexes [41, 50, 52, 57–59]. In addition to ruthenium-catalyzed methods (*vide infra*), other noble-metal systems have been successful including iridium [51, 60–62], molybdenum [63], palladium [64], platinum [65–67], and rhodium [57, 68–70] as well as hetero-bimetallic catalysts [71, 72]. Also noteworthy are non-noble metal catalysts including iron-based systems, which have displayed significant activities [73–75]. This



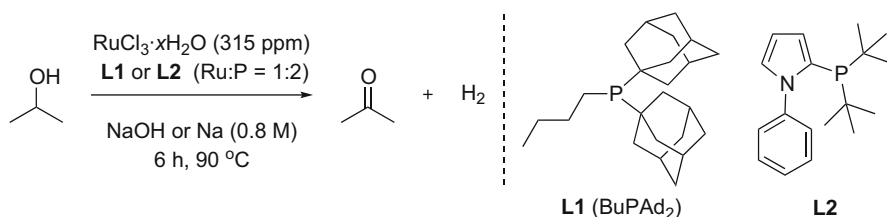
Scheme 2 Thermodynamic data for the decomposition pathways of formic acid [50]

review chapter will discuss ruthenium-catalyzed formic acid dehydrogenation comprising the period from late 2010 to early 2014. Additional information with respect to formic acid as well as alcohols can be found in previous review papers [39, 41, 50, 52, 54, 76–81].

2 Hydrogen Generation from Alcohols

2.1 Pioneering Contributions

The pioneering work of alcohol dehydrogenation began with initial reports by Robinson, who demonstrated the catalytic utility of ruthenium complex $[\text{Ru}(\text{OCOCF}_3)_2(\text{CO})(\text{PPh}_3)_2]$ in the presence of trifluoroacetic acid to dehydrogenate various primary and secondary alcohols [9, 10]. Higher TOFs were achieved for higher boiling alcohols ($8,172 \text{ h}^{-1}$ for benzyl alcohol, 27 h^{-1} for ethanol) corresponding to the designated reaction temperature. Garrou contributed to these early examples by employing chelate-modified ruthenium catalysts for the dehydrogenation of cyclohexanol with up to 500 TONs [82]; primary alcohols were not tolerant substrates in this case. Shinoda and Saito [83–85] were able to dehydrogenate methanol for the first time utilizing mono- and dinuclear ruthenium species albeit at low TOFs up to 0.96 h^{-1} . Saito then optimized this process by combining $\text{RuCl}_3 \cdot \text{H}_2\text{O}$ catalyst with sub-stoichiometric amounts of either sodium methoxide, which gave only a slightly increased TOF for methanol (1.68 h^{-1}), or sodium ethoxide, which allowed for the more efficient ethanol dehydrogenation (TOF 28 h^{-1}). Some final early contributions also came from Cole-Hamilton [86, 87], who was successful in using ruthenium catalysts with light to produce hydrogen at substantial TOFs from several primary alcohols, including methanol (TOF up to 37 h^{-1}) and ethanol (TOF up to 210 h^{-1}). Although these accounts highlight hydrogen evolution, other groups have influenced the development of ruthenium-catalyzed alcohol dehydrogenation through a synthetic organic focus [88–91].

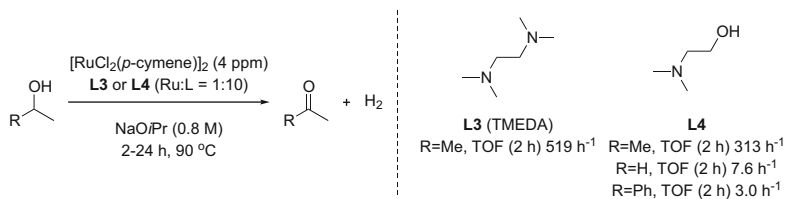


Scheme 3 Ruthenium-catalyzed dehydrogenation of isopropanol under mild conditions

2.2 Current Developments in Alcohol Dehydrogenation (2005 to Present)

Recent publications in this ruthenium-catalyzed area of hydrogen generation from renewable resources have directed efforts towards the development of catalysts that work under milder reaction conditions (i.e., lower temperatures and catalyst loadings) with increased catalytic activity. Beller and coworkers have been active contributors in this regard with an initial report describing dehydrogenation of isopropanol by use of $\text{RuCl}_3 \cdot x\text{H}_2\text{O}/\text{PR}_3$ catalytic mixtures (Scheme 3) [92]. Screening of several different Ru catalyst precursors revealed that 315 ppm of $\text{RuCl}_3 \cdot x\text{H}_2\text{O}$ in combination with PCy_3 and NaOH (0.8 M) as base at 90°C generated more than 70 mL of hydrogen gas from 5 mL of *i*-PrOH after a 2 h reaction time (78 h^{-1} TOF) and nearly 150 mL at 6 h (54 h^{-1}). In testing various base concentrations, similar TOFs were observed for 0.1–0.8 M NaOH, although a lack of base resulted in slow hydrogen evolution (TOF_{2h}, 11 h^{-1}) and an excess (1.5 M) proved to be detrimental to the reaction with a TOF_{2h} of 34 h^{-1} . Utilizing different tertiary phosphine ligands showed that either the use of trialkyl variant diadamant-1-yl-butylphosphine (BuPAD₂, **L1**) with NaOH or 2-di-*tert*-butylphosphinyl-1-phenyl-1*H*-pyrrole (**L2**) with Na allowed for the highest TOFs of 104 and 155 h^{-1} (2 h), respectively. Notably, these results are a significant improvement from the earlier discussed work considering the very low quantities of catalyst employed as well as mild temperatures ($<100^\circ\text{C}$). It is worth mentioning that under modified conditions (2.5 ppm Ru, $-\text{PAD}_2$ variant of **L2**, 10 mL *i*PrOH, 0.8 M NaOiPr), TOF values of 727 and 473 h^{-1} could be achieved at 2 and 6 h, respectively (Junge H, Beller M, unpublished results).

Subsequently, this method was further modified in a later report by Beller to exploit nitrogen- rather than phosphine-containing ligands in this chemistry (due to the increased stability of N vs P compounds) [93]. A variety of ligands featuring one, two, or three *N*-donor sites were screened for their catalytic utility in combination with ppm amounts of $[\text{RuCl}_2(p\text{-cymene})]_2$ (N:Ru = 1, 2 or 3) in the presence of 0.8 M NaOiPr with respect to 10 mL *i*PrOH. These ligands demonstrated improved catalytic activity in comparison with the use of “ligandless” $[\text{RuCl}_2(p\text{-cymene})]_2$ (TOFs of 192 and 120 h^{-1} at 2 and 6 h, respectively) (Scheme 4). Primary and secondary amines, such as 2-aminomethylpyridine,



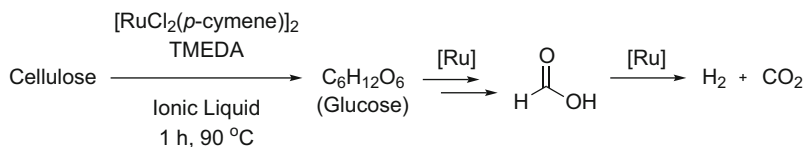
Scheme 4 Improved catalyst system featuring nitrogen ligands for alcohol dehydrogenation under mild conditions

were inferior to either tertiary amine tridentate ligands TMEDA (**L3**) or 2-dimethylaminoethanol (**L4**), which gave promising TOFs at 2 h of 309 and 373 h⁻¹, respectively. As a result of catalytic inhibitory effects of the dehydrogenation products in solution, including acetone as well as minor products from aldol condensations and Guerbet processes [94, 95], there was an evident decrease in the TOF at 6 h (**L3**: 190 h⁻¹, **L4**: 236 h⁻¹) and more so at 24 h.

With variation of the catalyst loading, volume of isopropanol and metal:ligand ratio, 4 ppm of the Ru precursor with 10 equiv. of TMEDA (Ru:N = 1:20) in 40 mL of *i*PrOH resulted in the highest TOF for this process below 100°C reported to date, that is 519 h⁻¹. Even with a decrease in catalytic activity over time, this particular system was shown to maintain activity after 11 days (268 h) with a total TON of 17,215 (71 mmol H₂ generated) corresponding to a potential electric energy of 4.8 W for the conversion of H₂ to H₂O in a fuel cell. The Ru-**L4** catalyst was also used for hydrogen generation from 1-phenylethanol and ethanol, though the activity for these substrates (TOF_{2h} < 10 h⁻¹) was significantly lower than that for isopropanol (66 h⁻¹). Notably, the dehydrogenation of ethanol resulted in acetaldehyde, which was further converted to high molecular weight alcohols, and also traces of methane gas.

Glucose, as well as its polymer, cellulose have been applied to dehydrogenation conditions as a means to employ direct biological feedstocks for hydrogen evolution (Scheme 5). Wasserscheid and coworkers described the use of ionic liquids (ILs) for this process due to the ability of ILs to dissolve carbohydrates and the low solubility of hydrogen gas in ILs (to prevent further reactivity with hydrogen and thus unwanted by-products) [96]. Combining C₆H₁₂O₆ · H₂O as the glucose source with the previously reported Beller catalyst system [RuCl₂(*p*-cymene)]₂/TMEDA (**L3**) [93] at 180°C, imidazolium-based ILs were shown to be unstable under the reaction conditions and even produced hydrogen in the absence of glucose.

Phosphonium ILs were more stable to the reaction conditions and allowed for the dehydrogenation of glucose up to 72 turnovers in 1 h and cellulose with a TON of 26. Based on ¹³C NMR experiments, it was found that formic acid is formed as an intermediate in these reactions which then produces hydrogen. Thus, for every mole of glucose consumed, one mole of formic acid followed by one mole of hydrogen is produced. The above turnover values for glucose and cellulose correspond to hydrogen yields of 31 and 12%, respectively. Although these values are low, this method represents the first example of cellulose conversion directly to hydrogen



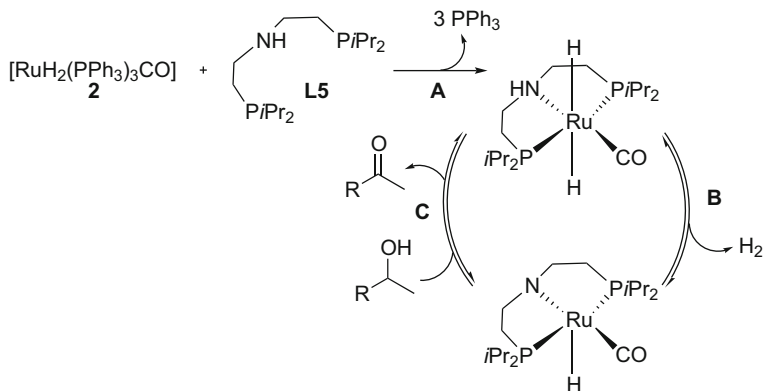
Scheme 5 Hydrogen production from carbohydrates via formic acid as an intermediate

Table 1 Summary of improved alcohol dehydrogenation under mild conditions

R	[Ru]/L (1:1)	NaO <i>i</i> Pr (equiv.)	TOF _{2h} (h ⁻¹)
Me	1 , 32 ppm	1.3	1,231
Me	2/L5 , 4 ppm [RuH ₂ (PPh ₃) ₃ CO]	0	8,382
H	2/L5 , 3.1 ppm	0	1,483

without any initial treatment; cellulose is first depolymerized to glucose under the catalytic conditions leading to formic acid and finally hydrogen.

In 2011, Beller and coworkers extended their initial work on acceptorless alcohol dehydrogenation with a report on hydrogen production from alcohols under increasingly mild conditions [97]. Ruthenium complexes featuring PNP pincer-type ligands were synthesized and tested at 32 ppm catalyst loading in the dehydrogenation of isopropanol. Under refluxing conditions in isopropanol (10 mL) using stoichiometric amounts of NaO*i*Pr (up to 2,000 equiv. with respect to the catalyst loading) as base, a ruthenium complex bearing an HPNP^{Ph} ligand (**1**; Table 1) initially provided high TOFs at 2 h (1,231 h⁻¹) and at 6 h (644 h⁻¹). Further catalyst screening of Ru precursors/ligand mixtures demonstrated that a highly active catalyst was formed from the 1:1 combination of [RuH₂(PPh₃)₃(CO)] and HPNP^{*i*Pr} ligand (**2** and **L5**, respectively; Table 1). Without the need for added base, **2/L5** mixtures allowed for a significant improvement in TOF values to 2,048 h⁻¹ (2 h) and 1,109 h⁻¹ (6 h). The authors suggest that inferior results obtained in the presence of base may be attributable to catalyst inhibition by the isopropoxide anion. Increased steric bulk on the phosphine ligand arms with *tert*-butyl groups (HPNP^{*t*Bu}) also proved to be detrimental to the catalytic activity



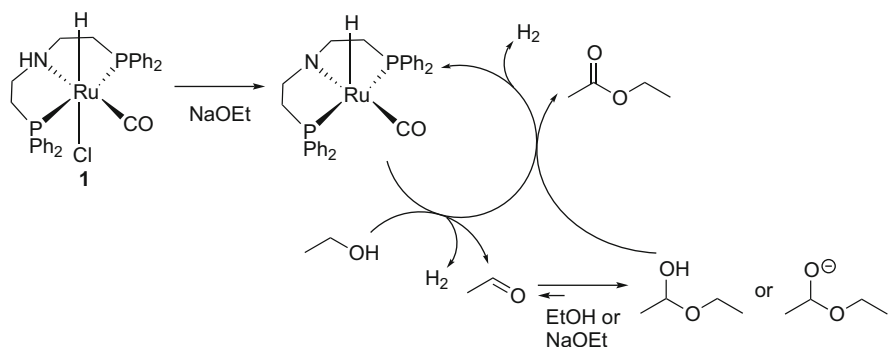
Scheme 6 Proposed mechanism for alcohol dehydrogenation catalyzed by **2/L5** mixtures

($100 \text{ h}^{-1} \text{ TOF}_{2\text{h}}$). Decreasing the catalyst loading from 32 to 4 ppm demonstrated a further increase of the $\text{TOF}_{2\text{h}}$ to $8,382 \text{ h}^{-1}$ and TON of 40,000 at 12 h, which exceeds the earlier Beller results (TON 17,215, 11 days; [93]).

New TOFs for ethanol were also obtained using 3.1 ppm catalyst ($\text{Ru:L} = 1:1$) without base; $1,483 \text{ h}^{-1}$ at 2 h became the highest TOF to date for dehydrogenation of this primary alcohol. The authors also propose a mechanism (Scheme 6), which suggests an outer-sphere process for the dehydrogenative step (step C) of the catalytic cycle, whereby a Ru-amide intermediate undergoes H–H addition across the Ru–N bond.

A more recent study from the Beller group focussed on dehydrogenation methods of ethanol to generate ethyl acetate for potential applications on large-scale [98, 99]. This report also featured ruthenium-pincer-based catalysts **1** and **2/L5** as the most active systems (25 ppm loading; $\text{TOF}_{2\text{h}}$: 1,134 and $1,107 \text{ h}^{-1}$, respectively) to generate ethyl acetate and hydrogen from ethanol (10 mL, 171.3 mmol) in the presence of catalytic amounts of NaOEt (0.3–3.2 mol%). Although 500 ppm of **1** allowed for 81% yield of ethyl acetate when gas evolution had stopped (6 h), corresponding to a TON of 1,620, reducing the catalyst loading to 50 ppm led to a significant increase in activity with a TON of 15,400 after 46 h and a comparable ethyl acetate yield of 77%. The TOF at 2 h nearly doubled to 934 h^{-1} with this tenfold decrease in the catalyst loading, and even at 10 h, the TOF was still quite high (730 h^{-1}). In contrast to earlier discussed reports with isopropanol where dehydrogenation products caused catalyst inhibition, ethyl acetate in this case did not interfere with the progress of the reaction.

In place of ethanol, 1-octanol, as a representative substrate, was subjected to the reaction conditions employing 500 ppm of **1** and 1 mol% NaOEt to form the corresponding ester, octyl octanoate with a $\text{TOF}_{2\text{h}}$ of 330 h^{-1} ; the authors attribute this lower frequency to the increased carbon chain length in comparison to ethanol. In the presence of an aldehyde, octanal, the reaction of ethanol was inhibited



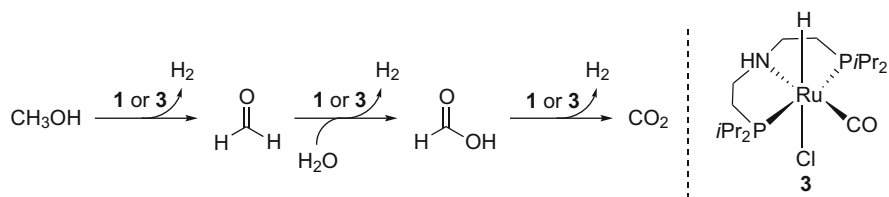
Scheme 7 Putative mechanism for the dehydrogenative ethyl acetate formation from ethanol

resulting in no conversion and no hydrogen production, which suggests that formation of free acetaldehyde during the catalytic cycle is minimal. These observations led to a proposed mechanism shown in Scheme 7, which is similar to that shown in Scheme 6 but involves a second ethanol molecule and a β -hydride elimination to form ethyl acetate.

2.3 Methods for the Aqueous-Phase Reforming of Methanol

The process in which water is used to convert a hydrocarbon to hydrogen and carbon dioxide is known as steam reforming. This two-step method first involves the substrate reacting with water to generate hydrogen and CO, the latter of which then undergoes the water–gas shift reaction to produce CO₂ and additional hydrogen [100, 101]. Notably, this protocol employs heterogeneous catalysts that operate under very harsh conditions (>700 K). Liquid- or aqueous-phase reforming of methanol, as a potential hydrogen source, was initially reported by Dumesic et al., who utilized a Pt/Al₂O₃ catalyst at still high temperatures (ca. 500 K) to achieve TOFs up to 564 h⁻¹ [102, 103]. Considering the use of a heterogeneous catalyst system under these harsh conditions, an improved method is needed for aqueous-phase reforming to be applicable to renewable hydrogen generation.

Efforts in the Beller group were then directed toward the use of methanol as a renewable resource for hydrogen production. An aqueous-phase reforming method was utilized to dehydrogenate methanol forming hydrogen and carbon dioxide [104] employing a molecularly defined catalyst under comparatively mild conditions. Initial catalyst screening conditions involved a mixture of methanol and water (10–40 mL, 4:1 ratio) in the presence of 0.5 M NaOH with heating at 72°C. This revealed that complexes 1 or 3 could be used to produce very pure volumes of hydrogen gas with TOFs (3 h) of 121 and 48 h⁻¹, respectively. Notably, three molecules of hydrogen and one molecule of CO₂ could be generated for every



Scheme 8 Aqueous-phase reforming of methanol involving three dehydrogenation steps

Table 2 Ruthenium-catalyzed aqueous-phase methanol dehydrogenation^a

Entry	Catalyst amount (μmol , ppm)	Reaction temperature ($^{\circ}\text{C}$)	MeOH:H ₂ O	TOF 3 h (h^{-1})
1	1 (4.18, 21)	89	4:1	860
2	1 (4.18, 19)	91	9:1	1,093
3	3 (1.58, 1.8)	91	9:1	2,670
4	3 (1.58, 16)	95	1:9	201
5	3 (1.58, 1.6)	95	10:0 (neat MeOH)	4,734

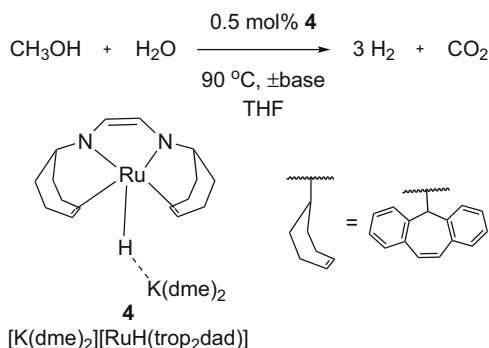
^aReaction conditions: catalyst loadings of **1** or **3** given in μmol and $\mu\text{mol mol}^{-1}$ of MeOH (ppm); 10–40 mL solution of MeOH/H₂O; 8.0 M KOH (based on MeOH/H₂O volume)

reaction (Scheme 8) or three catalyst turnovers; thus, production of one H₂ molecule corresponds to one catalytic turnover.

Optimization of the initial conditions showed that the choice of base and its concentration significantly influenced catalyst performance; use of 8.0 M KOH gave an improved TOF (3 h) of 860 h^{-1} (Table 2, entry 1). Furthermore, an increase in the reaction temperature caused by the high base concentration (due to the salt effect) also contributed to the superior catalyst activity. Detailed investigations of the amount of base versus temperature further validated the beneficial effect of both factors on catalyst activity.

Although a larger ratio of methanol to water gave higher turnover frequencies (Table 2, entries 2–3), a very small ratio of 1:9 containing mostly water also demonstrated considerable hydrogen evolution (entry 4). The complete lack of water proved to further increase the turnover frequency substantially to 4,734 h^{-1} (entry 5). Notably, complex **3** is more active than **1** in this study. In performing a long-term experiment using 0.88 μmol (1 ppm) of **3** for a 40-mL solution of 9:1 methanol: water, catalyst stability was maintained for 23 days with a total TON of 350,000, a final TOF of 200 h^{-1} and an overall hydrogen yield of 27% (with respect to water). Increasing the catalyst loading for this experiment to 150 ppm of **3** achieved the same yield after only 90 min, but then improved further to 59% yield (relative to water) within 24 h reaction time. Additionally, under modified conditions (0.1 M NaOH, 4:1 MeOH/H₂O, 250 ppm **1**), the production of a true 3:1 H₂/CO₂ gas composition ratio was demonstrated and maintained after 5–6 h. The proposed catalytic cycle based on in situ NMR experiments involves concerted outer-sphere processes for generation of the first two hydrogen molecules and H–H elimination from the Ru–N bond for the third molecule. It is important to note that ligand participation (via the N donor atom)

Scheme 9 Hydrogen production from methanol-water mixtures using a chelated ruthenium catalyst



is a significant factor in the mechanism. Overall, this process has become the new state-of-the-art for hydrogen production from methanol, although catalytic activity has a strong dependence on the presence of base.

Concomitantly to this report, the groups of Trincado and Grützmacher published a similar study on the development of (bis)olefin diazene-chelated ruthenium complexes as catalysts for hydrogen production from methanol-water mixtures [105]. Although the main focus of the publication is the synthesis and characterization of the catalyst featuring a redox-active ligand as well as key catalytic intermediates, the authors do discuss hydrogen evolution from MeOH-water-tetrahydrofuran mixtures (1:1.3 MeOH/H₂O) in the presence and absence of base. Up to 90% conversion of methanol and 84% yield of gas (3:1 H₂/CO₂) could be obtained using 0.5 mol% catalyst loading of $[\text{K}(\text{dme})_2][\text{RuH}(\text{trop}_2\text{dad})]$ (**4**) at 90°C for 10 h when the reaction was performed in an open system (Scheme 9). These optimal results, without the use of base, correspond to a TOF of 50 h⁻¹ for hydrogen evolution (based on 75% H₂ content of the evolved gas). Alternatively, in a closed system with one equiv. each of NEt₃ and Ba(OH)₂ added to the reaction resulted in only ~25% conversion of methanol. Interestingly, the hydrogen generated from the open system conditions was of adequate purity to directly power an H₂/O₂ fuel cell. Thus, the authors further demonstrate the applicability of Ru catalysis in alcohol dehydrogenation and are able to generate hydrogen from methanol without the requirement for base. The stoichiometric experiments incorporated in this study reveal the “non-innocent” nature of the redox-active trop₂dad ligand as it is proposed to undergo hydrogenation and dehydrogenation sequences in the catalytic cycle.

Most recently, a method for methanol dehydrogenation, which does not require the use of base, has been disclosed by Beller and coworkers [106]. Preliminary experiments in the presence of 8.0 M KOH showed either Ru-pincer complexes **1** or **5**, which features an η¹-borohydride ligand in place of the chloride (see Table 3), were suitable catalysts for effecting the dehydrogenation of methanol/water (9:1, 10 mL) mixtures (>2,000 TON_{3h}). However, in the absence of base, catalyst activity significantly decreased to <80 TON_{3h}, although the catalyst loading had been raised from 5 to 95 μmol. Considering **5** demonstrated higher activity in the initial studies, **1** was not utilized for further optimization. Addition of a second catalyst was then investigated in combination with **5** or other relevant complexes to

Table 3 Bi-catalytic systems for base-free dehydrogenation of methanol^a

$$\text{CH}_3\text{OH} + \text{H}_2\text{O} \xrightarrow[\text{triglyme}]{[\text{Ru}]_A/[\text{Ru}]_B (1:1)} 3 \text{H}_2 + \text{CO}_2$$

93.5 °C

Entry	[Ru] _A	[Ru] _B	Gas evolution rate over first 3 h (mL h ⁻¹)	TOF _{1h} (h ⁻¹) ^b	TOF _{3h} (h ⁻¹) ^b	TOF _{7h} (h ⁻¹) ^b
1	5	6	60	239	138	83
2	5	7	30	87	94	93
3	8	7	26	80	79	77
4	9	7	25	76	76	–
5	5	–	1.7	–	–	32
6	–	7	9.1	–	–	30

^aReaction conditions: 10 mL solution of MeOH/H₂O (9:1), triglyme (4 mL), [Ru]_A (5 μmol), [Ru]_B (5 μmol), *T*_{set} = 93.5 °C

^bTOFs were calculated based on the theoretical value of 75% H₂ content in the gas phase

achieve fast dehydrogenation of formic acid, an intermediate believed to be inhibiting the catalyst. Employing a 1:1 mixture of two catalysts (5 μmol each) initially showed that **5** and **6** provided a high TOF at 1 h of 239 h⁻¹, but this system proved to deactivate over time (Table 3, entry 1). A consistent gas evolution rate over a 7-hour period was then achieved via co-catalysis between **5** and **7** with an average TOF of 93 h⁻¹ (Table 3, entry 2). Comparable rates could also be obtained with the combination of **8** or **9** with **7** (Table 3, entries 3–4).

Additional studies of the **5/7** system demonstrated that individually these catalysts are poor for methanol dehydrogenation (Table 3, entries 5–6) but together they produced enhanced activity. An experiment performed over 10 days produced 1,400 mL of gas corresponding to a TON of 4,286 and a hydrogen yield of 26% (relative to H₂O), thus establishing the long-term stability of this bi-catalytic system. In situ IR spectroscopy investigations provide evidence that the mechanism proceeds through formaldehyde and formic acid intermediates

3 Dehydrogenation of Formic Acid

3.1 Dehydrogenation from Aqueous FA/Formate

Catalysis in water offers several advantages as an alternative to the use of organic solvents [107]. Water is ubiquitous in nature, environmentally benign, and a clean product of energy production using H₂/O₂ PEM fuel cells [108–110]. In the case of formic acid, pH-controlled catalysis is possible in diluted FA/water mixtures due to the acid–base equilibria of FA/formate and CO₂/HCO₃[−]/CO₃^{2−} [68, 76]. While the hydrogenation of CO₂ is thermodynamically favored in the presence of base [55, 111], such as amine, the dehydrogenation reaction is usually feasible under acidic conditions. However, there are only a few examples reported on transition metal-catalyzed H₂ formation from FA without the use of any additives [75, 112–114]. Instead, the addition of base, such as formate or amine (Sect. 3.2), proved to be beneficial for enhanced activity of iridium, rhodium, and ruthenium organometallic complexes [41, 50, 53, 77, 111]. Choosing the appropriate reaction conditions is not trivial since the stability of in situ catalytic intermediates (e.g., hydrides and dihydrogen complexes) depends on the pH [115–117]. For example, the presence of base can create free coordination sites by halide abstraction from the metal center while a lower pH can facilitate the protonation of hydrides for subsequent H₂ evolution [57]. Advantageously, deuterated water can be utilized for efficient D₂ generation from FA/D₂O solutions that can be further used for (transfer) deuterio-hydrogenation reactions [72, 118]. Typically, water-soluble metal complexes (e.g., Ru chlorides) and ligands (e.g., *mtppts/mtppds*) [53, 119–121] are applied. In the recent past, the use of proton-responsive ligands coordinated to Ir, Rh, and Ru have also gained appreciable attention both in the dehydrogenation of FA [51, 57, 72, 122–124] and hydrogenation of CO₂/HCO₃[−] [125–127].

In 2011, Himeda et al. reported on the use of water-soluble metal half-sandwich complexes of the type [(L1)Cp*M(L2)(4-dhbp)]ⁿ⁺ (M = Ru, Ir [123], Rh; L1 = Cp*, C₆Me₆); L2 = H₂O, Cl] for the dehydrogenation of HCO₂H [68]. These complexes bear a proton-switchable 4-dhbp (4dhbp = 4,4'-dihydroxy-2,2'-bipyridine) ligand with a hydroxyl group (−OH) that can be reversibly deprotonated to the oxyanion (−O[−]) in dependence of the pH of the catalyst solution. Interestingly, such and similar complexes [77, 122, 124, 128, 129] can be used for reversible hydrogen storage because in the presence of the (de)protonated catalyst one or the other half reaction is preferred. At 60°C, the [(C₆Me₆)RuCl(4-dhbp)]Cl (Fig. 1, R = OH) complex exhibited a 2.9-fold higher dehydrogenation rate of FA than the non-substituted bipyridine complex indicating the electronic effect of the hydroxyl group for H₂ evolution. In contrast, the electronic effect was more pronounced in the hydrogenation of CO₂ (65-fold increase). For all different substituted bipyridine complexes, both the proton shifts and the initial turnover frequency (TOF) could be correlated with the Hammett substitution constant. Full conversion of FA to a clean 1:1 H₂/CO₂ mixture without concomitant CO production was observed with the Ru transition metal complexes [68].

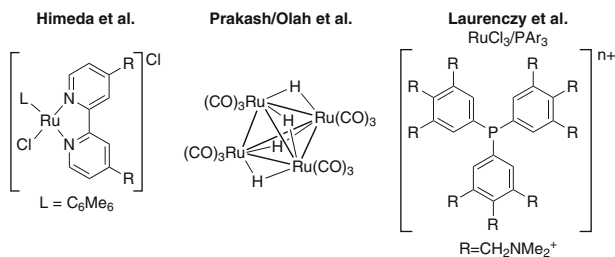


Fig. 1 Selected catalyst/ligand systems used by Himeda [68], Prakash/Olah [58], and Laurency [131] for hydrogen generation from aqueous FA/formate solutions

One year later, Himeda reported on the efficient generation of deuterated hydrogen gas (HD , D_2) from $\text{HCO}_2\text{H}/\text{D}_2\text{O}$, $\text{DCO}_2\text{D}/\text{H}_2\text{O}$, or $\text{DCO}_2\text{D}/\text{D}_2\text{O}$ solutions and its use for (transfer) deuterio-hydrogenation of α,β -unsaturated carboxylic acids [118]. Iridium, rhodium, and ruthenium dhbp complexes catalyzed the decomposition in the presence of formate with different activities and selectivities. In contrast to the Ir-(Cp*) and Rh-(Cp*) analogues, $[(\text{C}_6\text{Me}_6)\text{Ru}(\text{H}_2\text{O})(4\text{-dhbp})]^{2+}$ catalyzes the decomposition of $\text{HCO}_2\text{H}/\text{HCO}_2\text{Na}$ (9:1) and $\text{DCO}_2\text{D}/\text{DCO}_2\text{Na}$ (9:1) in H_2O or D_2O slowly (TOF: $36\text{--}80\text{ h}^{-1}$ at 60°C). The authors revealed that the selectivity depends greatly on the nature of the metal hydride (M–H), i.e. its acidity and hydricity and thus its proneness towards an exchange reaction with the deuteron (D^+) of the solvent to form a metal deuteride (M–D). This “umpolung” reaction is the key step for beneficial D_2 production from $\text{HCO}_2\text{H}/\text{D}_2\text{O}$ solutions. The rate-determining step in this Ru-catalyzed reaction is the formation of the metal hydride complex via β -hydride elimination of a coordinated formate. Further indication is given by the KIE values. The transfer deuterio-hydrogenation based on catalytic decomposition of FA in the presence of the cheap deuterium source D_2O is attractive due to time- and cost-savings and provides access to widely used deuterated chemical compounds [118].

Prakash and Olah et al. [58] studied hydrogen generation from aqueous FA/NaHCO_2 (9:1) solution with simple RuCl_3 salts in a closed reactor by measuring the pressure increase. A reaction rate of $22.882 \times 10^{-5}\text{ M s}^{-1}$ and substantial CO formation was observed (0.21% CO, $\sim 1:1\text{ H}_2/\text{CO}_2$). The absence of formate leads to significantly lower activity of more than one order of magnitude ($4.854 \times 10^{-5}\text{ M s}^{-1}$ at 100°C) which was observed also by Laurency [120]. Catalyst reactivation was feasible by addition of sodium formate. A tetranuclear ruthenium $[\text{Ru}_4(\text{CO})_{12}\text{H}_4]$ (Fig. 1) was isolated as a stable complex (X-Ray). The occurrence of FA decarbonylation was demonstrated in both stoichiometric and catalytic reactions of RuCl_3 and FA. The tetranuclear complex $[\text{Ru}_4(\text{CO})_{12}\text{H}_4]$ gave a superior activity, by a factor of 5, ($122.6 \times 10^{-5}\text{ M s}^{-1}$, 109°C) compared to the in situ generated catalyst from RuCl_3 in aqueous $\text{FA}/\text{formate}$ (9:1) solution. This suggests that $[\text{Ru}_4(\text{CO})_{12}\text{H}_4]$ is either the active species or is a direct precursor for formation of the active species. Notably, FA was fully converted to a CO-free 1:1 H_2/CO_2 mixture. Therefore, the authors suggest that in the beginning of the

in situ reaction, decarbonylation of FA takes place due to the absence of active species that needs to form. As soon as sufficient active Ru carbonyl complexes are formed, the dehydrogenation of FA is catalyzed in a selective manner [58].

As an alternative to their previous work [58], where simple RuCl_3 or preformed phosphine-free catalyst $[\text{Ru}_4(\text{CO})_{12}\text{H}_4]$ were used, Czaun and Olah [130] reported the use of ruthenium with commercially available cheap ligands (e.g., PPh_3) for hydrogen generation from FA in emulsions. Instead of using sulfonated ligands (e.g., tppts) [120] for enhanced water solubility, the authors applied surfactants as a solubility mediator in aqueous solution. The surfactant, sodium dodecyl sulfate (SDS) proved to be more suitable than tetrabutylammonium bromide (TBAB) and trimethylammonium bromide (MitMAB). The catalytic dehydrogenation of FA was initiated by heating (90–117°C) a mixture of an aqueous solution of $\text{RuCl}_3/\text{FA}/\text{formate}$ (9:1) and a prepared $\text{PPh}_3/\text{toluene}/\text{SDS}$ solution. The superior decomposition rate of the second run ($20.0 \times 10^{-6} \text{ M s}^{-1}$) compared to that of the first run ($16.9 \times 10^{-6} \text{ M s}^{-1}$) indicates the formation of the active species during the initial cycle [53, 131]. However, in the second run that was initiated by FA addition, the CO selectivity decreased (0.25 vol.%, GC). $[\text{Ru}(\text{CO})_3(\text{PPh}_3)_2]$ [132, 133], $[\text{Ru}(\text{HCO}_2)_2(\text{CO})_2(\text{PPh}_3)_2]$ [132, 133], and a dimeric carbonyl formate complex $[\text{Ru}_2(\text{HCO}_2)_2(\text{CO})_4(\text{PPh}_3)_2]$ [134] could be isolated from the reaction mixture and characterized by NMR, FTIR, and X-Ray. In the dehydrogenation experiment, $[\text{Ru}_2(\text{HCO}_2)_2(\text{CO})_4(\text{PPh}_3)_2]$ is less stable and less active ($0.7 \times 10^{-6} \text{ M s}^{-1}$, 115°C, 8.6 vol.% CO) than the mononuclear $[\text{Ru}(\text{CO})_3(\text{PPh}_3)_2]$ ($2.1 \times 10^{-6} \text{ M s}^{-1}$, 115°C, 1.74 vol.% CO) and bis-formate species $[\text{Ru}(\text{HCO}_2)_2(\text{CO})_2(\text{PPh}_3)_2]$ ($1.2 \times 10^{-6} \text{ M s}^{-1}$, 115°C, 2.72 vol.% CO). Notably, the formation of intermediate $[\text{Ru}(\text{HCO}_2)_2(\text{CO})_2(\text{PPh}_3)_2]$ during catalysis reveals both the carbonylating and reducing features of FA. The reaction rate and selectivity drops significantly in the absence of catalyst ($0.4 \times 10^{-6} \text{ M s}^{-1}$, 117°C, 10.1 vol.% CO) and toluene/surfactant ($9.9 \times 10^{-6} \text{ M s}^{-1}$, 100°C, 0.3 vol.% CO) compared to the use of the surfactant SDS in the system ($69.1 \times 10^{-6} \text{ M s}^{-1}$, 100°C, no CO). This underlines the suitability of biphasic (aqueous/organic) reaction systems for accelerated and more selective catalysis [135, 136].

Recently, Papp and Joo [137] provide profound insights into the formation of ruthenium(II)-hydrides during the hydrogenation of water-soluble dimeric $[\text{RuCl}_2(\text{mtppps})_2]_2$ (*mtppps* = *meta*-monosulfonated triphenylphosphine) in aqueous solution with excess *mtppps*. Due to the reversibility of the hydrogenation reaction, this study is of importance also for the dehydrogenation reaction that was catalyzed by in situ ruthenium chlorides in the presence of phosphines [41, 50, 53, 58, 111, 138]. Through variation of the reaction conditions (pH, H_2 pressure, substrate concentration) the following ruthenium complexes could be observed in the hydrogenation of $[\text{RuCl}_2(\text{mtppps})_2]_2$: (1) $[\text{RuHCl}(\text{mtppps})_3]$ and $[\text{RuHCl}(\text{mtppps})_2]_2$ (acidic solution, 1 bar H_2), (2) *trans*- $[\text{RuH}_2(\text{mtppps})_4]$ (pH 3, 5 bar H_2), (3) *cis-fac*- $[\text{RuH}_2(\text{H}_2\text{O})(\text{mtppps})_3]$ (pH 10, 1 bar H_2), and (4) $[\text{RuH}_2(\eta^2\text{-H}_2)(\text{mtppps})_3]$ (pH 10, 5 bar H_2). In the presence of 2 M NaBr and NaI solutions, $[\text{RuHX}(\text{mtppps})_3]$ (X = Br, I) were formed in acidic solutions at atmospheric hydrogen pressure (1 bar). By variation of the formate concentration,

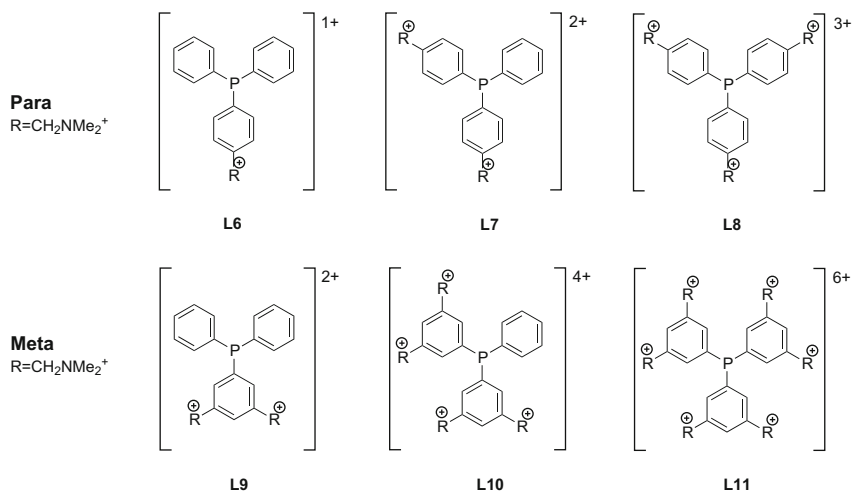


Fig. 2 New class of ammoniomethyl substituted cationic phosphine ligands used to form in situ catalysts with RuCl₃ [131]

trans-[RuH₂(HCOO)(*mtppps*)₃][−] (high conc.) and *trans*-[RuH₂(H₂O)(*mtppps*)₃] (very low conc.) were identified. All classical and non-classical phosphine-Ru(II)-hydrides were characterized using NMR techniques (¹H, ¹³C, ³¹P). The findings about the stability and interconversion of such ruthenium species are required for the understanding of the catalytic mechanism and tailored design of catalysts for both (transfer) hydrogenation and dehydrogenation processes [137].

Ruthenium in combination with hydrophilic ligands that contain anionic sulfonate groups (e.g., *mtppps* or *mtppts*) proved to be active and stable catalysts for hydrogen generation from aqueous FA/formate solutions [53, 119–121, 139]. Recently, immobilization of the homogeneous water-soluble Ru(II)/*mtppts* complex (*mtppts* = *m*-trisulfonated triphenylphosphine) in a hydrophilic silica support led to excellent selective hydrogen formation from FA and marks a step towards mobile applications [140]. In another work, Laurenczy et al. [131] report on tailoring oligocationic triarylphosphine ligands. These types of phosphines bear an ammoniomethyl-group [141, 142] and showed appreciable activity as a ligand in other catalytic reactions [142–145]. Tailored functionalization of the ligands is feasible by introducing different numbers of cationic ammoniomethyl moieties in different positions (*meta*- or *para*) on the triaryl backbone (Fig. 2). Thus, the hydrophilicity, steric demand (**L6** < **L7** < **L8**, **L9** < **L10** < **L11**), and electronic properties of the ligand can be tuned. Consequently, the in situ formation of the active catalyst with the metal precursor as well as the stability and activity of the catalyst can be improved. The electron-donating properties of the ligands were derived from the determined ¹J_{P-Se} coupling constant (³¹P NMR) of the respective phosphine selenides. *Para*-substituted ammoniomethyl-substituted ligands are

better σ -donors than those which are *meta*-substituted. Notably, the *para*-tricationic ligand **L8** inherits similar electronic properties to those of the anionic *mt*ppts ligand.

The precursor $\text{RuCl}_3 \cdot \text{H}_2\text{O}$ was then investigated in situ with two equivalents of the triarylphosphine tetrafluoroborate ($[\text{BF}_4]^-$) salts (**L6–L11**) (Fig. 2) in the dehydrogenation of aqueous formic acid/formate (9:1) solutions at 90°C [131]. The active Ru(II) catalyst species is formed after the second catalyst cycle and formic acid could be converted up to 95% to a CO-free (<3 ppm, FTIR) H_2/CO_2 mixture. Except for ligands **L10** and **L11**, all types of cationic triarylphosphines formed more active catalysts with ruthenium than did hydrophilic air-stable anionic (*mt*ppts and *mt*ppds) and neutral (PTA, 1,3,5-triaza-7-phosphaadamantane) ligands (see Fig. 5). The in situ generated catalyst from Ru/**L9** (TOF $1,430\text{ h}^{-1}$) exhibited 50% higher activity than the catalyst formed from Ru/*m*-tppts (TOF 600 h^{-1}). Ru(III) in combination with ligands **L10**, **L11**, or PTA showed one order of magnitude less activity (TOF $80\text{--}130\text{ h}^{-1}$). According to the authors, Ru complexes bearing ligands **L6–L9** facilitate catalysis due to coulombic interactions [146] of the positively charged ligands with the negatively charged substrates (HCO_2^- and others). Contrastively, in situ applied Ru(III) in combination with ligands **L10** or **L11** likely suffers from inhibited substrate coordination (steric demand), and using PTA as the ligand can result in undesired protonation. The authors also considered that hydrophobic effects and coulombic repulsion, which were not studied in this work, could cause lower catalytic activity. The influence of the initial pH, the reaction temperature as well as the catalyst concentration and ligand-to-catalyst ratio were also reported. Under optimized conditions, the in situ catalyst formed from Ru/**L8** $[\text{BF}_4]_3$ showed very high dehydrogenation activity (TOF of $1,950\text{ h}^{-1}$ at 120°C) and excellent productivity during 30 recycle experiments (TON 10,000 at 90°C) even under pressure (1–100 bar). An intermediate Ru species (as observed by use of coupled and decoupled ^1H NMR) with one axially coordinated hydride and three phosphines (two *cis*, one *trans* to H) was suggested. The elucidation of the structure–activity relationship of oligocationic ammoniomethyl-substituted phosphines in Ru catalysis marks a milestone on the way to novel tailored catalyst design for (continuous) H_2 generation but also reversible hydrogen storage [131].

3.2 Dehydrogenation of Formic Acid/Amine Mixtures (FAA)

Apart from the use of formate as a basic additive, amines are also employed as valuable co-catalysts and solvents for the catalytic decomposition of FA [50]. At certain FA/amine ratios, stable azeotropes can be formed, such as from (triethylamine) mixtures [147]. In such adducts, the FA is experimentally preformed as the more reactive formate ($[\text{HCO}_2^-][\text{HN}^+\text{R}_3]$). With respect to reversible CO_2 -neutral hydrogen storage [138, 148], the use of amine might help to “capture” CO_2 by polar interactions. For decades, FAAs were appreciated hydrogen reservoirs for transfer hydrogenation reactions (especially Rh, Ru

catalysts). In the hydrogenation of CO_2 , the addition of amine helps to form stable formic acid-amine adducts [149–155]. Co-catalysts are usually employed in substoichiometric amounts and they do not decompose under the reaction conditions. However, the addition of further liquid compounds to the hydrogen storage system should be avoided since the overall hydrogen density is decreased (2.3 wt% for 5:2 FA/NEt) in contrast to pure FA (4.4 wt%). Furthermore, there is the risk of amine and/or FA discharge in continuous hydrogen generation (vide infra) that can poison connected fuel cells [156, 157]. In 1998, Puddephat observed accelerated H_2 rates upon addition of amine to a solution of FA and Ru catalyst [113, 114]. Since 2008, Beller and coworkers have reported on the versatility of different FAAs, especially for Ru-catalyzed hydrogen generation from FA [41, 50, 158]. The active catalyst was generated in situ by use of a variety of Ru(II)/Ru(III) precursors in the presence of phosphine ligands, solvent, additives [159], different amines, and also light [50, 56]. For instance, H_2 formation catalyzed by $[\text{RuCl}_2(\text{benzene})]_2/\text{dppe}$ occurs at one order of magnitude higher rate in the presence of light than the non-photoassisted reaction. For the first time the connection between the hydrogen generation system and a low temperature H_2/O_2 fuel cell could be established [160]. In 2009, Wills et al. reported on efficient phosphine-free Ru-catalyzed dehydrogenation that proceeds with a *TOF* of $18,000 \text{ h}^{-1}$ at 120°C [134]. As catalysts, both Ru(II) and Ru(III) compounds were applied, including $[\text{Ru}_2\text{Cl}_2(\text{DMSO})_4]$, $[\text{RuCl}_2(\text{NH}_3)_6]$, and $[\text{RuCl}_3]$. One drawback is the low hydrogen selectivity ($\text{CO} > 200 \text{ ppm}$) generates hydrogen gas of insufficient purity for use in a fuel cell.

In 2011, Schaub and Paciello observed the formation of ruthenium carbonyl and formate complexes in the catalytic reaction of electron-rich complex $[\text{Ru}(\text{H})_2(\text{P}n\text{Bu}_3)_4]$ with FA in the presence of trihexylamine (NHex_3) [161]. $[\text{Ru}(\text{CO})(\text{H})_2(\text{P}n\text{Bu}_3)_3]$ and $[\text{Ru}(\text{CO})(\text{H})(\text{HCOO})(\text{P}n\text{Bu}_3)_3]$ were identified in the dehydrogenation of ammonium formate $[\text{HNNH}_3][\text{HCOO}]$ (in 2-methyl-1,3-propanediol) catalyzed by $[\text{Ru}(\text{H})_2(\text{P}n\text{Bu}_3)_4]$ (in NHex_3) at 70°C . These investigations clearly provide evidence for the carbonylating properties of FA and ammonium formates [161].

While predominantly mono- and bidentate phosphines were used in Ru-catalyzed FA dehydrogenation, as of yet, multidentate phosphines are considered less so despite their beneficial ligating properties in other catalytic reactions due to enhanced stabilization of corresponding transition metal complexes [75, 116, 162–172]. In 2012, Peruzzini and Gonsalvi and coworkers in cooperation with Beller explored the versatility of tripodal phosphine ligands, such as triphos (1,1,1-tris-(diphenylphosphinomethyl)ethane) and NP_3 (tris-[2-diphenylphosphino]ethyl)-amine) in the presence of a Ru(III)-precursor or in preformed Ru complexes for H_2 generation from FAA mixtures [173]. The combination of tridentate triphos and the tetradentate NP_3 with the precursor $\text{Ru}(\text{acac})_3$ did not allow the formation of an active catalyst from 5:2 ratio of an FA/ NEt_3 solution at 40°C . At higher temperature (80°C), an active catalyst was formed in situ and allowed for full conversion of FA/DMOA (11:10) to a CO-free H_2/CO_2 mixture. In contrast, preformed $[\text{Ru}(\kappa^3\text{-triphos})(\text{MeCN})_3](\text{OTf})_2$ [174] and $[\text{Ru}(\kappa^4\text{-NP}_3)\text{Cl}_2]$ [175]

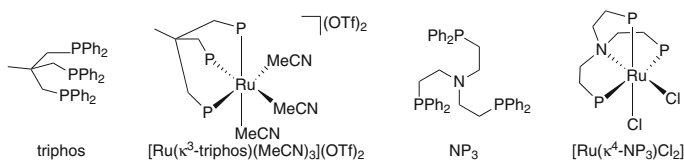


Fig. 3 Triphos and NP₃ ligands investigated via in situ catalysis with Ru or preformed complexes [Ru(κ³-triphos)(MeCN)₃](OTf)₂ and [Ru(κ⁴-NP₃)Cl₂] [173]

(Fig. 3) were active catalysts at 40°C for selective H₂ generation (CO < 10 ppm) from a 5:2 FA/NEt₃ mixture with TONs of 487 (18 h) and 604 (45 h), respectively. During in situ catalysis applying Ru/triphos, crystalline [Ru(κ³-triphos)(CO)(H)₂] [176] was formed, as observed by NMR, that was suggested to be a catalytic intermediate. [Ru(κ³-triphos)(CO)(H)₂] exhibited the same catalytic activity for FAAs as the in situ formed catalyst from Ru/triphos. [Ru(κ³-triphos)(MeCN)₃](OTf)₂ could be recycled up to eight times at 80°C by addition of more FA. Full and selective conversion was achieved but the catalyst performance clearly decreased after 1 h. Variable temperature (VT) NMR measurements (233–313 K) and FT-IR suggest the formation of a putative [Ru(κ³-triphos)(η¹-OOCH)(η²-OOCH)] probably via [Ru(κ³-triphos)(MeCN)(η¹-OOCH)]⁺, which was formed in the stoichiometric reaction of FA/NEt₃ (1:1) with the hexafluorophosphate ruthenium complex [Ru(κ³-triphos)(MeCN)₃](PF₆)₂. DFT studies suggest that formate activation occurs via a ligand-centered outer-sphere mechanism where the formation of Ru hydride is not essential for catalysis [177]. In contrast to [Ru(κ³-triphos)(MeCN)₃](PF₆)₂, [Ru(κ⁴-NP₃)Cl₂] catalyzes H₂ formation via an inner-sphere catalytic mechanism (NMR and DFT [177]) with [Ru(κ⁴-NP₃)Cl(H)] as the central species. In the first cycle, the hydrido-chloride complex is formed from [Ru(κ⁴-NP₃)Cl₂] upon formate coordination and chloride dissociation followed by subsequent β-hydride elimination and CO₂ evolution. Protonation of [Ru(κ⁴-NP₃)(H)Cl] recovers the starting complex via [Ru(κ⁴-NP₃)Cl(η²-H₂)]⁺. In addition, formate activation by [Ru(κ⁴-NP₃)(H)Cl] via (unobserved) [Ru(κ⁴-NP₃)H(η¹-OOCH)] was considered in a second cycle. These new insights are expected to encourage catalysis using polydentate ligands [173].

3.3 Dehydrogenation Without Base

While most of the promising state-of-the-art catalysts require the presence of additives, to date there are only scarce examples of hydrogen generation from formic acid without base or from pure FA without addition of solvent. This might be due to the use of mainly organometallic transition metal complexes that exhibited superior activity over simple Ru salts. In 1995, the DH of aqueous FA catalyzed by Ir, Rh, Ru, and Pd chlorides as well as the promoting ability of nitrites for Rh catalysis was reported [178]. Three years later, Puddephat

et al. presented a now pioneering binuclear ruthenium phosphine complex $[\text{Ru}_2(\mu\text{-CO})(\text{CO})_4(\mu\text{-dppm})_2]$ capable of selective base-free H_2 generation (initial *TOF* of 500 h^{-1} at 25°C) and hydrogenation of CO_2 [41, 111, 113]. Despite this excellent performance, the beneficial role of base additives (formates, amines) for accelerated catalysis was demonstrated. A related publication revealed efficient iron-catalyzed base-free H_2 evolution from an FA/propylene carbonate solution [75]. In recent years, the use of functional ligands bearing Brønsted bases gained attention since they allow metal-ligand cooperative catalysis [14, 16, 98, 179–181]. This section will highlight one representative example in H_2 generation from FA without external base.

The groups of Trincado and Grützmacher recently developed a ruthenium complex bearing a chelating bis(olefin)diazadiene ligand for the DH of 1:1 MeOH/ H_2O mixtures via FA to CO_2 and H_2 under metal-ligand cooperativity [105]. As discussed in Sect. 2.3, the catalyst $[\text{K}(\text{dme})_2][\text{RuH}(\text{trop}_2\text{dad})]$ (4) bears the so-called redox “non-innocent” [182–185] ligand 1,4-bis(5*H*-dibenzo[*a,d*]cyclohepten-5-yl)-1,4-diazabuta-1,3-diene (trop_2dad) (Scheme 9, Sect. 2.3) and allows full conversion of FA (1 M, 1 mmol) in dioxane solution at 90°C within a few minutes. A high initial *TOF* of $24,000 \text{ h}^{-1}$ was observed at low catalyst loadings (0.01 mol%). Notably, this is the highest activity reported to date for the DH of FA without further additives [105].

3.4 Ionic Liquid-Assisted Hydrogen Evolution

En route to practical applications, it is highly desirable to avoid the use of (substantial) amounts of additives, such as liquid amines or solvents. One reason is the risk of liquid discharge for large-scale hydrogen production that can cause the collapse of the catalyst system (vide infra, see Sect. 3.5). Furthermore, additional gas purification is required in order to protect downstream applications (e.g., fuel cells). Alternatively, ionic liquids (ILs) provide beneficial properties since they can act as excellent solvents [186–189] and bases simultaneously and they possess low volatility [190, 191] and recyclability properties [111, 192]. Overall, ILs are attractive because they not only allow for efficient catalysis and CO_2 dissolution [52, 193], due to their base and solvent functions, but also thermal FA separation from low vapor pressure ILs is possible, which enhances the applicability of an FA/IL-based storage system. In 2009, the use of ILs as beneficial solvents in Ru-catalyzed H_2 generation was reported [50]. As far as we know, only Ru-catalyzed H_2 generation and storage using FA was investigated in the presence of IL. The work of representative research groups among Shi/Deng, Klein, Nakahara, Dupont, and Wasserscheid will be presented below.

In 2010, Shi/Deng and coworkers explored the versatility of commercially available $[\text{RuCl}_2(p\text{-cymene})]_2$ in combination with ILs (BMimCl, BMimBF₄) and amine (*i*Pr₂NEt) for H_2 generation from FA/formate solutions in a temperature range of $40\text{--}60^\circ\text{C}$ [194]. The catalytic activity of $[\text{RuCl}_2(p\text{-cymene})]_2$ is only low

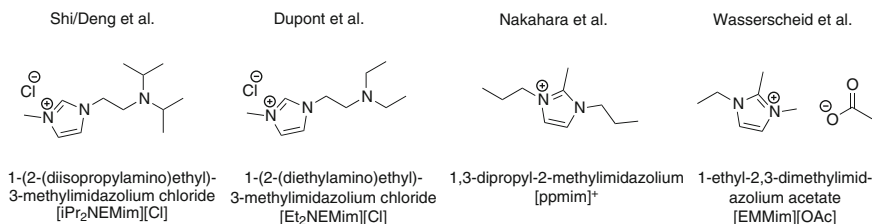


Fig. 4 Selected ILs that were investigated in Ru-catalyzed dehydrogenation of FA by the groups of Shi/Deng [194], Dupont [195], Nakahara [198], and Wasserscheid [199]

in the presence of either inorganic (formate) or organic (amine) base but can be accelerated significantly in the presence of suitable ILs. Further improvement is possible by employing both bases together with the IL. To avoid amine volatility issues and thus, contaminants in the evolved hydrogen gas, amine-functionalized ILs were synthesized. Among the functionalized ligands tested, *i*Pr₂NEMimCl gave the best results with a TON_{2h} up to 1,267 at 60°C (Fig. 4). Additionally, hydrogen could be evolved constantly over 11 h applying 10 mmol *i*Pr₂NEMimCl and 31 mmol [RuCl₂(*p*-cymene)]₂. However, the amount of FA converted was limited to the moles of IL applied and catalyst deactivation was observed upon addition of FA to restart experiments. Notably, [Et₂NEMim]Cl, [iPr₂NEMim]BF₄, [iPr₂NEMim]OTf, and [iPr₂NEMim]NTf₂ were poor catalysts. From these results, the future potential for applications is vague since there is no comment on the CO selectivity of the released gas mixture [194].

One year later, Dupont et al. examined in parallel the use of the same ruthenium catalyst [RuCl₂(*p*-cymene)]₂ with an IL that contains an ethyl-substituted amine functionality [195]. [Et₂NEMim]Cl (Fig. 4) proved to be a very active catalyst for hydrogen production (TOF 1,540 h⁻¹) at 80°C, notably in the absence of formate. This is in contrast to the previous work [194] where Ru/[Et₂NEMim]Cl exhibited very low activity compared to Ru/[iPr₂NEMim]Cl. Most likely, the IL is subjected to side-reactions in the presence of base, such as deprotonation of the imidazolium [196] or the decomposition of the IL by Hoffmann elimination [197]. The presence of water reduces the catalytic activity, which can be attributed to coordination effects. Up to a certain concentration, ILs stabilize the catalyst and promote catalysis whereas very high IL concentrations have a detrimental effect on catalysis; similar observations were made with phosphines [120]. Also the influence of temperature, catalyst, and substrate loadings is reported. The optimized [RuCl₂(*p*-cymene)]₂/[iPr₂NEMim]Cl catalyst system could convert FA selectively (CO < 10 ppm) and completely in five consecutive recharge cycles. The presence of dimeric formic acid was revealed by the determined reaction order of FA (2.00 ± 0.17). During catalysis dimeric Ru hydride ionic species [{Ru(*p*-cymene)}₂{(H)μ-(H)-μ-(HCO₂)}]⁺ and [{Ru(*p*-cymene)}₂{(H)μ-(Cl)μ-(HCO₂)}]⁺ were formed (ESI-MS). The activation energy (69.1 ± 7.6 kJ mol⁻¹) is comparable with known (non)-noble metal-based homogeneous catalyst systems [195].

In another work, Nakahara et al. [198] studied the chemical equilibrium between IL-solubilized FA and the gases H_2 and CO_2 for reversible hydrogen storage. As the catalyst, $[RuCl_2(PPh_3)_4]/[ppmim^+]$ was employed ($[ppmim^+] = 1,3$ -dipropyl-2-methylimidazolium) that forms $[ppmim^+][HCOO^-]$ salts in the presence of FA (Fig. 4). The equilibrium between FA and H_2/CO_2 was studied and compared in the gas phase, in the presence of water as well as in the IL ($K_{vacuum} > K_{water} > K_{IL}$). The presence of IL allows for the hydrogenation of CO_2 at lower hydrogen pressures (factor of 100) than required in water as solvent.

A more recent report by Wasserscheid et al. [199] involved dehydrogenation of FA in the presence of $RuCl_3$ and the ionic cations 1-ethyl-3-methylimidazolium (EMim) and 1-ethyl-2,3-dimethylimidazolium (EMMim). A significant influence of the IL counter-anions, such as $[OAc]^-$, $[PF_6]^-$, $[OTf]^-$, $[N(CN)_2]^-$, $[EtSO_4]^-$ and $[NTf_2]^-$ was revealed. The catalytic experiments were carried out in a pressurized reaction vessel at $80^\circ C$ from solutions containing FA (10 mmol), $RuCl_3$ (10 μ mol), the IL and $NaHCO_2$ as base additive (1 mmol). $Ru/[EMim][PF_6]$ preferably catalyzes the dehydration (9.6 vol.% CO) instead of the dehydrogenation (5.2 vol.% $H_2/4.0$ vol.% CO_2) pathway. The lower CO_2 concentration is attributed to its dissolution in the IL phase. The catalytic performance of Ru(III) was increased in the presence of the ILs $[EMim][NTf_2]$, $[EMim][OAc]$, and $[EMMim][OAc]$ in comparison with the IL salts of $[EMim]^+/[PF_6]^-$, $[OTf]^-$, $[N(CN)_2]^-$, $[EtSO_4]^-$. In the first case, FA was almost fully converted to a CO-free H_2/CO_2 mixture ($CO < 10$ ppm) in the presence of $[EMMim][OAc]$ (91%) (Fig. 4). Recycling experiments with $RuCl_3/[EMim][NTf_2]$ failed since it deactivated upon FA addition, possibly due to the formation of Ru nanoparticles (3–5 nm) (TEM). $RuCl_3/[EMMim][OAc]$ formed an active Ru(II) species [120] during the first catalytic cycle and allowed for stable hydrogen generation during three following catalyst recycle reactions. FA could be fully converted during nine recycle runs and demonstrated good stability. The $RuCl_3/[EMMim][OAc]$ system gave TOF's of 150 and 850 h^{-1} at 80 and $120^\circ C$, respectively. The active catalyst species was proposed to be Ru(II) based on dehydrogenation experiments with Ru(0), Ru(II), and Ru(III) precursors in the presence of $[EMMim][OAc]$. Despite the high conversions of FA, the activities of this Ru/IL system are quite low in comparison with the state-of-the-art catalyst systems [199].

Klein et al. revealed a new catalytic mechanism of FA decomposition in the presence of IL 1,3-dimethylimidazolium ([mmim]) performing a Born-Oppenheimer molecular dynamics (BO-MD)[200, 201] simulation at an elevated temperature of 3,000 K. It was shown that formate (HCO_2^-) dissociates into hydride (H^-) and carbon dioxide (CO_2), which was proposed to be the rate-determining step. This decomposition pathway can be explained by the stabilization of the hydride in the strong electrostatic field (cation and anion shells) of the IL. Calculated radial distribution functions (RDF) shed light on the solvation of the formate in the ionic liquid 1,3-dimethylimidazolium formate $[mmim][HCOO]$ [202].

3.5 Continuous Flow Methods

Many of the Ru compounds presented thus far have proved to be suitable catalysts for selective H₂ release, i.e. without concomitant CO production. Advantageously, this reaction is often feasible over a broad temperature range below 100°C, which makes this H₂ source very attractive for energy applications, such as stationary or mobile appliances, using low-temperature fuel cells. However, as of yet this has not been realized probably as a result of high demands imposed on the (de)hydrogenation catalysts. Energy conversion in a H₂/O₂ low-temperature fuel cell requires a sufficient, constant, and clean gas flow from the H₂ generator. Therefore, the catalyst should possess the following criteria: (1) sufficient activity, (2) selectivity, and (3) long-term stability for large-scale conditions at the desired reaction temperature. However, the flow of the liquid reactor components, such as substrate or additives (solvent, amine) can lead to the breakdown of the catalyst system or poisoning of the fuel cell. In order to circumvent this problem, the development of either alternative base-free catalyst systems or engineering solutions is necessary for the separation of the spray particles from the gas flow and the feedback of the essential reaction components. Another aspect is the need for a simple and safe reaction system as well as control by monitoring parameters, such as pH, pressure, temperature, and dosage.

Already in 2009, Beller et al. [203] had reported on continuous H₂ generation from FAA mixtures in glass apparatuses. An in situ generated catalyst from a [RuCl₂(benzene)]₂/dppe mixture could release CO-free H₂/CO₂ gas over 11 days with a TON of 260,000 at room temperature. In the same year, the group of Wills [134] described a highly active [RuCl₂(DMSO)₄] catalyst that reached a TOF of 18,000 h⁻¹ from 5:2 mixture of FA/Et₃N at 120°C, although the selectivity was not sufficient. Other noble metal catalyst systems (vide supra) were examined in catalyst-recycling experiments in batch mode [51, 68, 131, 173, 194, 199], by addition of a defined amount of FA. Unfortunately, these approaches did not demonstrate real long-term stable hydrogen production and FA was not dosed continuously. Thus, the following section highlights three examples of conceptualized continuous hydrogen production.

In 2010, Kendall and Wills reported on a control concept for continuous H₂ formation from FA in the presence of amines [157]. In preliminary experiments, various high-boiling aliphatic and aromatic amines were examined as alternative co-catalysts to the commonly used Et₃N. Under optimized conditions, a maximum H₂-evolution rate of 150 mL min⁻¹ could be observed in the presence of previously used [RuCl₂(DMSO)₄] [134] in a 5:2 FA/DMOA solution at 120°C in batch mode. A test mini-plant was setup for continuous hydrogen generation that consisted of a 2 L reaction flask, a pump for FA dosage, condensers (-7°C), and a downstream gas flow meter. The continuous hydrogen generation could be controlled by either temperature or impedance measurements. All physical parameters were monitored with a LabView program. Temperature control was achieved by addition of FA to the amine solution causing a decrease in the desired temperature; the reaction

temperature was then maintained due to the exothermic reaction between the acid and base. In this way, continuous H₂ generation from an FA/DMOA solution could be demonstrated at 120°C. On the first day, H₂-evolution rates up to 2.5 L min⁻¹ could be reached that decreased to 0.8 L min⁻¹ on the sixth day. The same catalyst was used over 6 days and was subjected to several start/stop cycles, thus proving to be a robust in situ catalyst. However, the dehydrogenation was accompanied by CO-formation that exceeded 100 ppm, resulting in hydrogen gas of insufficient purity and preventing the direct connection of the hydrogen generator to a fuel cell. Also, reaction control proved somewhat difficult due to the delay in temperature reading response.

Therefore, impedance-based reaction control was evaluated as an alternative method. It is based on the electrolytic and dielectric nature of the formate salts and amines. In analogy to the temperature-feedback method, a value of impedance was fixed (80 Ω) for the start of FA dosage. Similar to the temperature-controlled continuous H₂ generation using [RuCl₂(DMSO)₄] and an FA/DMOA mixture, an initial first-day high rate (>1.5 L min⁻¹) could be maintained that decreased over the following days. Beneficially, the reaction temperature remained constant and oscillation of the measured impedance increased only slightly during the test days. The elevated CO concentrations in the gas mixture (70–350 ppm) necessitate gas purification prior to its use in a low-temperature PEM fuel cell [157].

Recently, Beller and coworkers described the development of large-scale and long-term H₂ production from FA in a mini-plant [156]. It is known that the combination of a simple Ru(II) precursor and bidentate phosphines (dppm, dppe) forms very active catalysts for the DH of FA from FAA mixtures but also for reversible hydrogen storage, notably with high selectivity and activity under ambient conditions [50, 203–205]. In their previous work [204], high catalyst stability with 800,000 turnovers was observed in a long-term experiment that was executed in glassware. In order to scale up the reaction [203], a pressure stable mini-plant made of stainless steel was constructed for safe continuous H₂ production. The plant consists of an FA storage tank connected to a pressure stable autoclave and downstream purification unit (condenser, carbon column). Connected gas and liquid flow meters allowed for monitoring the FA dosage and the resulting gas flow. Temperature and pressure sensors helped to survey and maintain constant reaction conditions. The use of a pressure-stable autoclave allows for the application of pressure during the dehydrogenation reaction and also for the storage of released gas. In preliminary tests, batch reactions were performed in a sealed autoclave with 10 μmol of the preformed catalyst [RuH₂(dppe)₂] [203] and 10 mL of a 5:2 FA/Et₃N mixture to check the influence of reaction parameters, such as (1) stirring rate, (2) temperature, and (3) choice of amine. In addition to common aliphatic amines (Me₂NHex, Me₂NOct, Me₂NDec), high-boiling oligomeric/polymeric (Lupasol FG) and solid amines (Urotropin) were also used (Fig. 5). Unfortunately, the latter two gave very low activity (TON_{3h} < 31 at 25°C), and only two liquid aliphatic amines (Me₂NHex and Me₂NOct) provided the best results (TON_{3h} 2,090 and 2,007 at 25°C). DMOA (Me₂NOct) was selected as the amine of choice due to its higher boiling point (195°C). To note, preformed

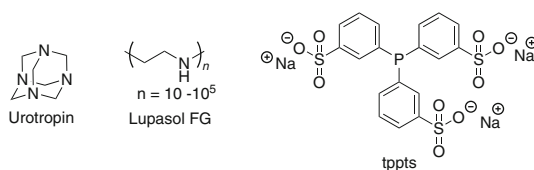


Fig. 5 Ligands used by Beller (amines, [156]) and Laurency (tppts, [52]) for Ru-catalyzed FA dehydrogenation

$[\text{RuH}_2(\text{dppe})_2]$ and $[\text{RuH}_2(\text{dppm})_2]$ catalyze H_2 release from FA under ambient conditions [203, 204], but for continuous mode, the more stable ligand dppe was applied in situ with the commercially available $[\text{RuCl}_2(\text{benzene})]_2$ at a Ru:dppe ratio of 1:6.

In order to test the long-term stability of the catalyst at room temperature, FA was fed into ($13 \mu\text{L min}^{-1}$) the autoclave, which contained 10 μmol Ru dimer/6 equiv. dppe in 20 mL DMOA. FA decomposed selectively to a 1:1 H_2/CO_2 mixture ($\text{CO} < 2$ ppm) at an average rate of 15 mL min^{-1} (1:1 H_2/CO_2) for 45 days, thereby reaching 1,000,000 catalytic turnovers. In an approach to increase the H_2 -evolution rate, the FA flow was increased step-wise from 500 to 1,300 $\mu\text{L min}^{-1}$. A constant gas evolution rate was achieved in the presence 6.5 bar of pressure. A gas flow of up to 1,300 mL min^{-1} (H_2 flow of 650 mL) was observed corresponding to a TOF of $16,000 \text{ h}^{-1}$. However, the catalyst deactivated after 7 h, which was attributed to an acidified catalyst solution and thus catalyst drowning. At a moderate FA dosage ($200 \mu\text{L min}^{-1}$) and 60°C , the influence of amine and catalyst concentration on the durability of the catalyst system was studied. Application of a slight pressure (6.5 bar) increased the lifetime of the catalysts since the discharge of amine is reduced. Also, higher catalyst (40 μmol) and amine (40 mL) loadings could prolong the catalyst's long-term stability. It turned out that amine discharge is limiting catalyst lifetime since the catalyst solution becomes too acidic and therefore deactivates the active ruthenium hydride species. Finally, in the presence of 6.5 bar of pressure and 200 μmol Ru, 18 L of H_2 per hour could be generated from FA (0.5 mL min^{-1}) over 54 h. Even at higher FA dosage (1.3 mL min^{-1}), the catalyst was capable of producing 47 L of H_2/h for 6 h which corresponds to 70 W of electrical power supply including 50% fuel cell efficiency (H_2/O_2 fuel cell) and 20 W energy loss to peripheral devices (pumps, heaters). Although using more amine extended catalyst lifetime, there is the need to either suppress amine discharge with filters and use solid amines or recycle the amine in order to maintain catalyst activity [156].

The group of Laurency [52, 206] designed and developed a mini-plant for the generation of 1 kW of electrical energy. Utilizing a homogeneous Ru/tppts catalyst previously reported by the Laurency group [53, 119, 120] (Fig. 5), H_2 generation from an aqueous FA/formate solution was demonstrated in a 5 L tank. The plant consists of FA, a pump for dosage, the 5 L reactor as well as downstream liquid/gas separation units and a mass flow meter. A constant power output of 30 L/min

H₂/CO₂ corresponding to 1 kW of electrical power was achieved in the presence of 12 g of RuCl₃ · 3H₂O/Na₃tppts (1:2 ratio) in 1.5 L of a 1 M formate solution. Remarkably, the catalyst was stable and useable over a 1-year period. In contrast to the catalyst systems for continuous H₂ generation described earlier, an amine co-catalyst is not essential in this case. Liquid entrainment into the gas phase (FA, water) must also be considered due to the high temperature and gas evolution. Therefore, separator/recycle units for the condensate as well as heat exchanger units were also included in the plant. Detailed data, such as reaction temperature, were not included in this report since the project is still in the developmental stages, as the authors state. This continuous H₂ generation system is very promising since not only was high activity and robustness of the catalyst shown under large-scale reaction conditions but also engineering solutions were found for efficient heating and condensate separation/recycling.

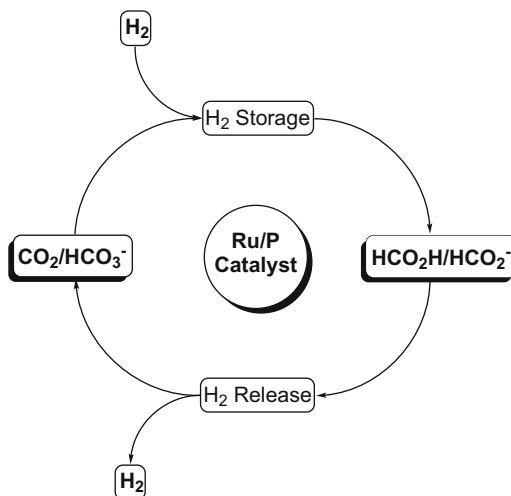
3.6 Progress Towards Hydrogen Storage Devices

Great improvements have been made towards the development of stable and active catalysts for the DH of FA/formates and the hydrogenation of carbon dioxide or (bi) carbonates. In order to use FA as a CO₂-neutral H₂-storage material, there is the need to successfully combine both half-reactions [54, 81, 207–209]. Notably, reversible hydrogen storage using FA has been considered utilizing other precious metals [61, 68, 76, 77, 81, 129, 210]. Also, in principle, the dehydrogenation of FA [73, 75] and hydrogenation of CO₂/HCO₃⁻ [211–213] can be accessed by non-noble metal catalysts (Fe, Co). However, no real consecutive (de)hydrogenation cycles have been shown to date. Instead, promising examples of applicable hydrogen storage systems based on the use of Ru/phosphine catalysts have been recently reported. Thus, H₂ (possibly generated from renewable resources) and CO₂ can be stored as FA or formate and converted back on demand in a selective fashion to an H₂/CO₂ mixture (Scheme 10). Consecutive discharge and charge cycles have been demonstrated in both aqueous and FAA solutions.

As discussed in Sect. 3.2, Schaub and Paciello proposed the use of a biphasic amine-diol system for the production of FA [161]. They demonstrated that [Ru(H)₂(P*n*Bu₃)₄] is a viable catalyst for the hydrogenation of CO₂ in the presence of amine (NHex₃) but also for the selective DH of ammonium formate. FAA salts are soluble in diols but not miscible with the free amine, thus allowing for catalyst (soluble in free amine) and product separation (soluble in diol) as well as FA removal by distillation. In addition to their investigations of the interactions of FA and amine, the authors reveal the presence of active catalytic species in both the hydrogenation and DH reactions (*vide supra*). Nevertheless, reversible hydrogen storage was not demonstrated.

In the same year, Papp and Joo [214] employed water-soluble catalyst [RuCl(*m*TPPMS)₂]₂ developed by Laurenczy [53] for the hydrogen charge and discharge of sodium bicarbonate (NaHCO₃) and sodium formate (NaHCO₂) solutions.

Scheme 10 Schematic representation of Ru-catalyzed hydrogen storage based on the use of FA or formates



Advantageously, no additives or organic solvents were used and the reversibility of the reaction could be tuned by pressure changes in the reactor. While formate was obtained at elevated hydrogen pressure (100 bar), bicarbonate could be formed under reduced pressure with selective H_2 release ($\text{CO} < 10$ ppm). The hydrogenation of ^{13}C -enriched hydrogen carbonate yielded 90% $\text{H}^{13}\text{CO}_2\text{Na}$ (^{13}C NMR) after 200 min at 83°C . Pressure reduction to ambient pressure led to 40–50% conversion of $\text{H}^{13}\text{CO}_2\text{Na}$ to $\text{H}^{13}\text{CO}_3\text{Na}$, corresponding to 40–50% of hydrogen capacity used. Over 2.5 days, three reversible hydrogenation and dehydrogenation sequences were demonstrated. In addition, hydrogen generation was also feasible up to 6.2 bar of pressure.

Concurrently, Beller et al. investigated H_2 uptake by bicarbonates and subsequent hydrogen release from aqueous formate solutions using $[\text{RuCl}_2(\text{benzene})_2]_2/\text{dppm}$ [205]. The goal was to combine both half-reactions with the same catalyst under ambient conditions and to trap CO_2 evolved from the dehydrogenation reaction under basic conditions. The catalytic performance of the in situ applied catalyst was examined in individual experiments for the hydrogenation ($\text{Ru}:\text{P} = 1:4$) and dehydrogenation ($\text{Ru}:\text{P} = 1:6$) reactions in THF/ H_2O and DMF solution, respectively. Based on these preliminary investigations, commercial NaHCO_2 and NaHCO_3 were subjected to a dehydrogenation/hydrogenation sequence in separate experiments after product isolation. In the first case, sodium formate could be dehydrogenated by in situ applied Ru/dppm with 90% conversion at 30°C and hydrogenated (80 bar) back in 80% yield. However, the consecutive conversions required solvent removal and the yield dropped significantly for the second step. Likewise, commercial sodium carbonate could be hydrogenated (95% yield) to formate and dehydrogenated to recover the starting material (80% yield). Despite some economic drawbacks (solvent removal), CO_2 -neutral hydrogen storage could be realized in a proof-of-principle method under ambient conditions [205].

Following this report, a selective and reversible hydrogen storage procedure was published using FAA mixtures and organic solvents [204]. Continuing efforts in this area, Beller and coworkers demonstrated that (de)hydrogenation reactions could be catalyzed by in situ applied system $[\text{RuCl}_2(\text{benzene})]_2/\text{bisphosphine}$ ($\text{Ru}:\text{L} = 1:6$, where $\text{L} = \text{dppe}, \text{dppm}$). Optimal hydrogenation yields were obtained using DMF as solvent and NEt_3 as the amine, which is in agreement with related methods of other research groups [161]. Hydrogenation of CO_2 under moderate pressures (30 bar $\text{H}_2 + 30$ bar CO_2) yielded high $\text{FA}:\text{NEt}_3$ ratios (2.69) at 100°C . The preformed catalyst $[\text{Ru}(\text{H})_2(\text{dppm})_2]$ also allowed for high conversion giving high FAA ratios (2.33) at room temperature. In a proof-of-principle experiment, eight reversible hydrogen charge and discharge cycles were executed in the presence of the defined catalyst $[\text{Ru}(\text{H})_2(\text{dppm})_2]$ and NEt_3 in an autoclave at room temperature. During the hydrogenation reaction, the initial pressure (60 bar) was reduced to 45 bar. Between 1.6 and 2.2 L of gas ($\text{H}_2 + \text{CO}_2$) were produced selectively (that is, no CO formation) upon pressure release. To a minor extent, catalyst deterioration occurred after the eight consecutive cycles. Despite the overall reduced hydrogen content due to the use of amine and solvent, this is a viable example of a hydrogen battery.

4 Conclusions

The dehydrogenation of formic acid and alcohols employing ruthenium catalysts has become a well-established research endeavor for clean and renewable hydrogen production. Since the early work in alcohol dehydrogenation by Robinson, Cole-Hamilton, and others, significant progress has been made to develop increasingly active catalysts that operate under milder conditions ($<100^\circ\text{C}$) with very low catalyst loadings (ppm quantities). The scope of alcoholic substrates has progressed from high boiling and long chain secondary alcohols such as cyclohexanol and isopropanol, which currently undergo facile dehydrogenation, to more challenging short chain congeners like ethanol and methanol. Efforts have also extended to direct products of biomass like glucose and cellulose using ILs. Ruthenium catalysts featuring chelating and pincer-type ligands have generally allowed for an increase in catalytic activity corresponding to very high TON and TOF values. Although catalytic activity is generally high, conversion of alcohols and the corresponding yield of hydrogen are still quite poor in most cases, thus requiring further improvement. The mechanistic details briefly discussed combined with recent studies on related catalytic systems provide further evidence for the “non-innocent” nature of pincer ligands [11, 179, 215–217].

With respect to hydrogen production from formic acid, the described studies demonstrate the progress concerning improvement of reaction conditions, selectivity and dehydrogenation rates in different media, i.e. presence of water, additives (formate, amines), or ILs. Important insights into the mechanism of activation of FA by metal, metal-ligand cooperativity as well as IL-assisted catalysis were

gained. Ligand effects in catalysis were also examined in situ as well as in the respective metal complexes and could allow for a more tailored ligand design in the future. The continuous hydrogen generation systems constitute important progress in the development of practical hydrogen generation from formic acid-amine mixtures. Feasible concepts for controlled H₂ generation by dosage, temperature, and impedance as well as outstanding long-term stability of the in situ generated catalysts were shown for a broad temperature range. Despite some limitations, both continuous hydrogen generation and reversible hydrogen storage have been significantly improved, which is an important step towards practical applications of ruthenium-catalyzed hydrogen-storage systems.

Although the scope of this book chapter encompasses Ru-based catalysts, recent reports have also proceeded in a more biologically relevant direction with the implementation of environmentally benign, inexpensive, and more abundant metals, such as iron and cobalt, for dehydrogenation processes of alcohols [18–20, 75] and formic acid [73–75, 211–213]. In summary, the reports discussed in this review chapter have demonstrated the capabilities of ruthenium catalysis with respect to dehydrogenation, where alcohols still require further development for sufficient hydrogen yields but formic acid is significantly closer to a renewable and reversible solution.

References

1. Olah GA, Goepfert A, Prakash GKS (2009) Beyond oil and gas: the methanol economy. Wiley-VCH, Weinheim, 143
2. Amaroli N, Balzani V (2011) ChemSusChem 4:21
3. Blagojevic VA, Minic DM, Minic DG, Novakovic JG (2012) Hydrogen economy: modern concepts, challenges and perspectives. In: Minic D (ed) Hydrogen energy - challenges and perspectives, ISBN: 978-953-51-0812-2, InTech. doi:10.5772/46098
4. Moriarty P, Honnery D (2010) Int J Hydrogen Energy 35:12374
5. Turner JA (2004) Science 305:972
6. Alonso DM, Bond JQ, Dumesic JA (2010) Green Chem 12:1493
7. Charman HB (1970) J Chem Soc B 584
8. Charman HB (1967) J Chem Soc B 629
9. Dobson A, Robinson SD (1977) Inorg Chem 16:137
10. Dobson A, Robinson SD (1975) J Organomet Chem 87:C52
11. Zeng G, Sakaki S, Fujita K-I, Sano H, Yamaguchi R (2014) ACS Catal 4:1010
12. Polukeev AV, Petrovskii PV, Peregudov AS, Ezernitskaya MG, Koridze AA (2013) Organometallics 32:1000
13. Kawahara R, Fujita K-I, Yamaguchi R (2012) J Am Chem Soc 134:3643
14. Spasyuk D, Smith S, Gusev DG (2012) Angew Chem Int Ed 51:2772
15. Putignano E, Bossi G, Rigo P, Baratta W (2012) Organometallics 31:1133
16. Bertoli M, Choualeb A, Lough AJ, Moore B, Spasyuk D, Gusev DG (2011) Organometallics 30:3479
17. Baratta W, Bossi G, Putignano E, Rigo P (2011) Chem Eur J 17:3474
18. Zhang G, Vasudevan KV, Scott BL, Hanson SK (2013) J Am Chem Soc 135:8668
19. Zhang G, Hanson SK (2013) Org Lett 15:650

20. Alberico E, Sponholz P, Cordes C, Nielsen M, Drexler H-J, Baumann W, Junge H, Beller M (2013) *Angew Chem Int Ed* 52:14162
21. Naziruddin AR, Zhuang C-S, Lin W-J, Hwang W-S (2014) *Dalton Trans* 43:5335
22. Delgado-Rebollo M, Canseco-Gonzalez D, Hollering M, Mueller-Bunz H, Albrecht M (2014) *Dalton Trans* 43:4462
23. Yuan J, Sun Y, Yu G-A, Zhao C, She N-F, Mao S-L, Huang P-S, Han Z-J, Yin J, Liu S-H (2012) *Dalton Trans* 41:10309
24. Shahane S, Fischmeister C, Bruneau C (2012) *Catal Sci Technol* 2:1425
25. Makarov IS, Madsen R (2013) *J Org Chem* 78:6593
26. Langer R, Fuchs I, Vogt M, Balaraman E, Diskin-Posner Y, Shimon LJW, Ben-David Y, Milstein D (2013) *Chem Eur J* 19:3407
27. Srimani D, Balaraman E, Gnanaprakasam B, Ben-David Y, Milstein D (2012) *Adv Synth Catal* 354:2403
28. Prechtl MHG, Wobser K, Theyssen N, Ben-David Y, Milstein D, Leitner W (2012) *Catal Sci Technol* 2:2039
29. Sølvhøj A, Madsen R (2011) *Organometallics* 30:6044
30. Saha B, Sengupta G, Sarbajna A, Dutta I, Bera JK (2014) *J Organomet Chem.* doi:10.1016/j.jorganchem.2013.12.051
31. Srimani D, Balaraman E, Hu P, Ben-David Y, Milstein D (2013) *Adv Synth Catal* 355:2525
32. Ortega N, Richter C, Glorius F (2013) *Org Lett* 15:1776
33. Makarov IS, Fristrup P, Madsen R (2012) *Chem Eur J* 18:15683
34. Gnanaprakasam B, Balaraman E, Gunanathan C, Milstein D (2012) *J Polym Sci A Polym Chem* 50:1755
35. Fu Z, Lee J, Kang B, Hong SH (2012) *Org Lett* 14:6028
36. Tseng K-NT, Kampf JW, Szymczak NK (2013) *Organometallics* 32:2046
37. Srimani D, Ben-David Y, Milstein D (2013) *Angew Chem Int Ed* 52:4012
38. Srimani D, Ben-David Y, Milstein D (2013) *Chem Commun* 49:6632
39. Gunanathan C, Milstein D (2013) *Science* 341. doi:10.1126/science.1229712
40. Boddien A, Gärtner F, Nielsen M, Losse S, Junge H (2013) In: Reedijk J, Poepplmeier K (eds) *Comprehensive inorganic chemistry II*, 2nd edn. Elsevier, Amsterdam, p 587
41. Johnson TC, Morris DJ, Wills M (2010) *Chem Soc Rev* 39:81
42. Aguilo A, Horlenko T (1980) *Hydrocarbon process. Int Ed* 59:120
43. Leonard JD (1979) EP0005998
44. Crable BR, Plugge CM, McInerney MJ, Stams AJ (2011) *Enzyme Res* 2011:532536
45. Satyapal S, Petrovic J, Read C, Thomas G, Ordaz G (2007) *Catal Today* 120:246
46. King RB, King A Jr, Bhattacharyya N (1995) *Trans Met Chem* 20:321
47. Tingelöf T, Hedström L, Holmström N, Alvfors P, Lindbergh G (2008) *Int J Hydrogen Energy* 33:2064
48. Hinshelwood CN, Topley B (1923) *J Chem Soc Trans* 123:1333
49. Sabatier P, Mailhe A (1912) *Compt Rend* 152:1212
50. Loges B, Boddien A, Gärtner F, Junge H, Beller M (2010) *Top Catal* 53:902
51. Oldenhof S, de Bruin B, Lutz M, Siegler MA, Patureau FW, van der Vlugt JI, Reek JN (2013) *Chem Eur J* 19:11507
52. Grasemann M, Laurency G (2012) *Energy Environ Sci* 5:8171
53. Laurency G (2011) *Chimia* 65:663
54. Enthaler S, von Langermann J, Schmidt T (2010) *Energy Environ Sci* 3:1207
55. Jessop PG (2007) In: Vries JGD, Elsevier CJ (eds) *The handbook of homogeneous hydrogenation*. Wiley-VCH, Weinheim, p 489
56. Loges B, Boddien A, Junge H, Noyes JR, Baumann W, Beller M (2009) *Chem Commun* 4185
57. Fukuzumi S, Kobayashi T, Suenobu T (2008) *ChemSusChem* 1:827
58. Czaun M, Goepfert A, May R, Haiges R, Prakash GKS, Olah GA (2011) *ChemSusChem* 4:1241
59. Ogo S, Nishida H, Hayashi H, Murata Y, Fukuzumi S (2005) *Organometallics* 24:4816

60. Barnard JH, Wang C, Berry NG, Xiao J (2013) *Chem Sci* 4:1234
61. Maenaka Y, Suenobu T, Fukuzumi S (2012) *Energy Environ Sci* 5:7360
62. Choi J, MacArthur AHR, Brookhart M, Goldman AS (2011) *Chem Rev* 111:1761
63. Shin JH, Churchill DG, Parkin G (2002) *J Organomet Chem* 642:9
64. Wiener H, Sasson Y, Blum J (1986) *J Mol Catal* 35:277
65. Rieckborn TP, Huber E, Karakoc E, Prosenc MH (2010) *Eur J Inorg Chem* 2010:4757
66. Paonessa RS, Troglor WC (1982) *J Am Chem Soc* 104:3529
67. Yoshida T, Ueda Y, Otsuka S (1978) *J Am Chem Soc* 100:3941
68. Himeda Y, Miyazawa S, Hirose T (2011) *ChemSusChem* 4:487
69. Strauss SH, Whitmire KH, Shriver DF (1979) *J Organomet Chem* 174:C59
70. Forster D, Beck GR (1971) *J Chem Soc D* 1072
71. Fukuzumi S, Yamada Y, Suenobu T, Ohkubo K, Kotani H (2011) *Energy Environ Sci* 4:2754
72. Fukuzumi S, Kobayashi T, Suenobu T (2010) *J Am Chem Soc* 132:1496
73. Zell T, Butschke B, Ben-David Y, Milstein D (2013) *Chem Eur J* 19:8068
74. Boddien A, Loges B, Gärtner F, Torborg C, Fumino K, Junge H, Ludwig R, Beller M (2010) *J Am Chem Soc* 132:8924
75. Boddien A, Mellmann D, Gärtner F, Jackstell R, Junge H, Dyson PJ, Laurenczy G, Ludwig R, Beller M (2011) *Science* 333:1733
76. Fujita E, Muckerman JT, Himeda Y (2013) *Biochim Biophys Acta* 1827:1031
77. Fukuzumi S, Suenobu T (2013) *Dalton Trans* 42:18
78. Jiang H-L, Singh SK, Yan J-M, Zhang X-B, Xu Q (2010) *ChemSusChem* 3:541
79. Dobereiner GE, Crabtree RH (2009) *Chem Rev* 110:681
80. Friedrich A, Schneider S (2009) *ChemCatChem* 1:72
81. Fukuzumi S (2008) *Eur J Inorg Chem* 2008:1351
82. Jung CW, Garrou PE (1982) *Organometallics* 1:658
83. Shinoda S, Itagaki H, Saito Y (1985) *J Chem Soc Chem Commun* 860
84. Fujii T, Saito Y (1991) *J Mol Catal* 67:185
85. Yang L-C, Ishida T, Yamakawa T, Shinoda S (1996) *J Mol Catal A Chem* 108:87
86. Morton D, Cole-Hamilton DJ, Utuk ID, Paneque-Sosa M, Lopez-Poveda M (1989) *J Chem Soc Dalton Trans* 489
87. Morton D, Cole-Hamilton DJ (1988) *J Chem Soc Chem Commun* 1154
88. Murahashi S, Naota T, Ito K, Maeda Y, Taki H (1987) *J Org Chem* 52:4319
89. Blum Y, Shvo Y (1985) *J Organomet Chem* 282:C7
90. Tomioka H, Takai K, Oshima K, Nozaki H (1981) *Tetrahedron Lett* 22:1605
91. Murahashi S-I, Ito K-I, Naota T, Maeda Y (1981) *Tetrahedron Lett* 22:5327
92. Junge H, Beller M (2005) *Tetrahedron Lett* 46:1031
93. Junge H, Loges B, Beller M (2007) *Chem Commun* 522
94. Veibel S, Nielsen JI (1967) *Tetrahedron* 23:1723
95. Dowson GRM, Haddow MF, Lee J, Wingad RL, Wass DF (2013) *Angew Chem Int Ed* 52:9005
96. Taccardi N, Assenbaum D, Berger MEM, Bosmann A, Enzenberger F, Wolfel R, Neuendorf S, Goeke V, Schodel N, Maass HJ, Kistenmacher H, Wasserscheid P (2010) *Green Chem* 12:1150
97. Nielsen M, Kammer A, Cozzula D, Junge H, Gladiali S, Beller M (2011) *Angew Chem Int Ed* 50:9593
98. Nielsen M, Junge H, Kammer A, Beller M (2012) *Angew Chem Int Ed* 51:5711
99. Nielsen M, Kammer A, Junge H, Beller M (2013) *International Patent* WO2013079659A1
100. Navarro RM, Peña MA, Fierro JLG (2007) *Chem Rev* 107:3952
101. Palo DR, Dagle RA, Holladay JD (2007) *Chem Rev* 107:3992
102. Shabaker JW, Davda RR, Huber GW, Cortright RD, Dumesic JA (2003) *J Catal* 215:344
103. Cortright RD, Davda RR, Dumesic JA (2002) *Nature* 418:964
104. Nielsen M, Alberico E, Baumann W, Drexler H-J, Junge H, Gladiali S, Beller M (2013) *Nature* 495:85

105. Rodríguez-Lugo RE, Trincado M, Vogt M, Tewes F, Santiso-Quinones G, Grützmacher H (2013) *Nat Chem* 5:342
106. Monney A, Barsch E, Sponholz P, Junge H, Ludwig R, Beller M (2014) *Chem Commun* 50:707
107. Sinou D (1999) In: Knochel P (ed) *Modern solvents in organic synthesis*. Springer, Berlin/Heidelberg, p 41
108. de Bruijn FA, Rietveld B, van den Brink RW (2007) *Catalysis for renewables*. Wiley-VCH, Weinheim, p 299
109. Zhang H, Shen PK (2012) *Chem Rev* 112:2780
110. Pourbaba M, Zirakkar S (2011) *Procedia Eng* 21:1088
111. Boddien A, Gärtner F, Nielsen M, Losse S, Junge H (2013) In: Reedijk J, Poeppelmeier K (eds) *Comprehensive inorganic chemistry II*. Elsevier, Oxford, p 587
112. Coffey RS (1967) *Chem Commun* 18:923a
113. Gao Y, Kuncheria J, Puddephatt RJ, Yap GPA (1998) *Chem Commun* 2365
114. Gao Y, Kuncheria JK, Jenkins HA, Puddephatt RJ, Yap GPA (2000) *J Chem Soc Dalton Trans* 18:3212
115. Esteruelas MA, Oro LA (1998) *Chem Rev* 98:577
116. Bianchini C, Peruzzini M (2001) In: Peruzzini M, Poli R (eds) *Recent advances in hydride chemistry*. Elsevier, Amsterdam, p 271
117. Besora M, Lledos A, Maseras F (2009) *Chem Soc Rev* 38:957
118. Wang W-H, Hull JF, Muckerman JT, Fujita E, Hirose T, Himeda Y (2012) *Chem Eur J* 18:9397
119. Gan W, Fellay C, Dyson PJ, Laurency G (2010) *J Coord Chem* 63:2685
120. Fellay C, Yan N, Dyson PJ, Laurency G (2009) *Chem Eur J* 15:3752
121. Fellay C, Dyson PJ, Laurency G (2008) *Angew Chem Int Ed* 47:3966
122. Hayashi H, Ogo S, Fukuzumi S (2004) *Chem Commun* 2714
123. Himeda Y (2009) *Green Chem* 11:2018
124. Ogo S, Kabe R, Hayashi H, Harada R, Fukuzumi S (2006) *Dalton Trans* 4657
125. Himeda Y (2007) *Eur J Inorg Chem* 2007:3927
126. Himeda Y, Onozawa-Komatsuzaki N, Sugihara H, Arakawa H, Kasuga K (2004) *Organometallics* 23:1480
127. Himeda Y, Onozawa-Komatsuzaki N, Sugihara H, Kasuga K (2007) *Organometallics* 26:702
128. Hayashi H, Ogo S, Abura T, Fukuzumi S (2003) *J Am Chem Soc* 125:14266
129. Hull JF, Himeda Y, Wang WH, Hashiguchi B, Periana R, Szalda DJ, Muckerman JT, Fujita E (2012) *Nat Chem* 4:383
130. Czaun M, Goeppert A, Kothandaraman J, May RB, Haiges R, Prakash GKS, Olah GA (2013) *ACS Catal* 4:311
131. Gan W, Snelders DJM, Dyson PJ, Laurency G (2013) *ChemCatChem* 5:1126
132. Johnson BFG, Johnston RD, Lewis J, Williams IG (1971) *J Chem Soc A* 689
133. Collman JP, Roper WR (1965) *J Am Chem Soc* 87:4008
134. Morris DJ, Clarkson GJ, Wills M (2009) *Organometallics* 28:4133
135. Jung Y, Marcus RA (2007) *J Am Chem Soc* 129:5492
136. Beattie JK, McErlean CSP, Phippen CBW (2010) *Chem Eur J* 16:8972
137. Papp G, Horvath H, Laurency G, Szatmari I, Katho A, Joo F (2013) *Dalton Trans* 42:521
138. Boddien A, Gärtner F, Mellmann D, Sponholz P, Junge H, Laurency G, Beller M (2011) *Chimia* 65:214
139. Elek J, Nádasdi L, Papp G, Laurency G, Joó F (2003) *Appl Catal A* 255:59
140. Gan WJ, Dyson PJ, Laurency G (2013) *ChemCatChem* 5:3124
141. Kreiter R, Klein Gebbink RJM, van Koten G (2003) *Tetrahedron* 59:3989
142. Snelders DJM, van der Burg C, Lutz M, Spek AL, van Koten G, Klein Gebbink RJM (2010) *ChemCatChem* 2:1425
143. Snelders DJM, Kreiter R, Firet JJ, van Koten G, Klein Gebbink RJM (2008) *Adv Synth Catal* 350:262

144. Snelders DJM, van Koten G, Klein Gebbink RJM (2009) *J Am Chem Soc* 131:11407
145. Snelders DJM, Kunna K, Müller C, Vogt D, Koten GV, Klein Gebbink RJM (2010) *Tetrahedron Asymmetry* 21:1411
146. Snelders DJM, van Koten G, Klein Gebbink RJM (2011) *Chem Eur J* 17:42
147. Wagner K (1970) *Angew Chem Int Ed* 9:50
148. Yu C-H, Huang C-H, Tan C-S (2012) *Aerosol Air Qual Res* 12:745
149. Malacea R, Poli R, Manoury E (2010) *Coord Chem Rev* 254:729
150. Gladiali S, Alberico E (2006) *Chem Soc Rev* 35:226
151. Bartoszewicz A, Ahlsten N, Martín-Matute B (2013) *Chem Eur J* 19:7274
152. Clapham SE, Hadzovic A, Morris RH (2004) *Coord Chem Rev* 248:2201
153. Fujii A, Hashiguchi S, Uematsu N, Ikariya T, Noyori R (1996) *J Am Chem Soc* 118:2521
154. Bianchini C, Glendenning L (1997) *Chemtracts Inorg Chem* 10:333
155. Gladiali S, Alberico E (2004) *Transition metals for organic synthesis*, 2nd edn. Wiley-VCH, Weinheim, 145
156. Sponholz P, Mellmann D, Junge H, Beller M (2013) *ChemSusChem* 6:1172
157. Majewski A, Morris DJ, Kendall K, Wills M (2010) *ChemSusChem* 3:431
158. Boddien A, Loges B, Junge H, Beller M (2008) *ChemSusChem* 1:751
159. Junge H, Boddien A, Capitta F, Loges B, Noyes JR, Gladiali S, Beller M (2009) *Tetrahedron Lett* 50:1603
160. Loges B, Boddien A, Junge H, Beller M (2008) *Angew Chem Int Ed* 47:3962
161. Schaub T, Paciello RA (2011) *Angew Chem Int Ed* 50:7278
162. Bianchini C, Peruzzini M, Polo A, Vacca A, Zanobini F (1991) *Gazz Chim Ital* 121:543
163. Siegl WO, Lapporte SJ, Collman JP (1973) *Inorg Chem* 12:674
164. Bianchini C, Meli A, Peruzzini M, Vizza F, Zanobini F (1992) *Coord Chem Rev* 120:193
165. Cotton FA, Hong B (1992) In: Lippard SJ (ed) *Progress in inorganic chemistry*. Wiley, Weinheim, p 179
166. Mayer HA, Kaska WC (1994) *Chem Rev* 94:1239
167. Teunissen HT, Elsevier CJ (1997) *Chem Commun* 667
168. Teunissen HT (1998) *Chem Commun* 1367
169. van Engelen MC, Teunissen HT, de Vries JG, Elsevier CJ (2003) *J Mol Catal A Chem* 206:185
170. Geilen FMA, Engendahl B, Harwardt A, Marquardt W, Klankermayer J, Leitner W (2010) *Angew Chem Int Ed* 49:5510
171. Rosi L, Frediani M, Frediani P (2010) *J Organomet Chem* 695:1314
172. Furst MRL, Goff RL, Quinzler D, Mecking S, Botting CH, Cole-Hamilton DJ (2012) *Green Chem* 14:472
173. Mellone I, Peruzzini M, Rosi L, Mellmann D, Junge H, Beller M, Gonsalvi L (2013) *Dalton Trans* 42:2495
174. Rhodes LF, Sorato C, Venanzi LM, Bachechi F (1988) *Inorg Chem* 27:604
175. Dahlenburg L, Frosin KM, Kerstan S, Werner D (1991) *J Organomet Chem* 407:115
176. Bakhmutov VI, Bakhmutova EV, Belkova NV, Bianchini C, Epstein LM, Masi D, Peruzzini M, Shubina ES, Vorontsov EV, Zanobini F (2001) *Can J Chem* 79:479
177. Manca G, Mellone I, Bertini F, Peruzzini M, Rosi L, Mellmann D, Junge H, Beller M, Ienco A, Gonsalvi L (2013) *Organometallics* 32:7053
178. King RB, Bhattacharyya NK (1995) *Inorg Chim Acta* 237:65
179. Gunanathan C, Milstein D (2011) *Acc Chem Res* 44:588
180. Friedrich A, Drees M, Schmedt auf der Günne J, Schneider S (2009) *J Am Chem Soc* 131:17552
181. Käb M, Friedrich A, Drees M, Schneider S (2009) *Angew Chem Int Ed* 48:905
182. Kaim W, Sieger M, Greulich S, Sarkar B, Fiedler J, Zális S (2010) *J Organomet Chem* 695:1052
183. Chirik PJ, Wieghardt K (2010) *Science* 327:794
184. Lyaskovskyy V, de Bruin B (2012) *ACS Catal* 2:270

185. Caulton KG (2012) *Eur J Inorg Chem* 2012:435
186. Ingram JA, Moog RS, Ito N, Biswas R, Maroncelli M (2003) *J Phys Chem B* 107:5926
187. Jin H, Baker GA, Arzhantsev S, Dong J, Maroncelli M (2007) *J Phys Chem B* 111:7291
188. Yasaka Y, Wakai C, Matubayasi N, Nakahara M (2007) *J Phys Chem A* 111:541
189. Yasaka Y, Wakai C, Matubayasi N, Nakahara M (2007) *J Chem Phys* 127:104506
190. Wasserscheid P, Welton T (2008) *Ionic liquids in synthesis II*. Wiley-VCH, Weinheim
191. Welton T (1999) *Chem Rev* 99:2071
192. Sahler S, Prechtl MHG (2012) Application of ionic liquids in hydrogen storage systems. In: Liu J (ed) *Hydrogen storage*, ISBN: 978-953-51-0731-6, InTech. doi:10.5772/50154
193. Bates ED, Mayton RD, Ntai I, Davis JH (2002) *J Am Chem Soc* 124:926
194. Li X, Ma X, Shi F, Deng Y (2010) *ChemSusChem* 3:71
195. Scholten JD, Prechtl MHG, Dupont J (2010) *ChemCatChem* 2:1265
196. Scholten JD, Dupont J (2008) *Organometallics* 27:4439
197. Dullius JEL, Suarez PAZ, Einloft S, de Souza RF, Dupont J, Fischer J, De Cian A (1998) *Organometallics* 17:815
198. Yasaka Y, Wakai C, Matubayasi N, Nakahara M (2010) *J Phys Chem A* 114:3510
199. Berger MEM, Assenbaum D, Taccardi N, Spiecker E, Wasserscheid P (2011) *Green Chem* 13:1411
200. Geissler PL, Dellago C, Chandler D, Hutter J, Parrinello M (2001) *Science* 291:2121
201. Kirchner B, Dio P, Hutter J (2012) In: Kirchner B, Vrabec J (eds) *Multiscale molecular methods in applied chemistry*. Springer, Berlin/Heidelberg, p 109
202. Bhargava BL, Yasaka Y, Klein ML (2011) *J Phys Chem B* 115:14136
203. Boddien A, Loges B, Junge H, Gärtner F, Noyes JR, Beller M (2009) *Adv Synth Catal* 351:2517
204. Boddien A, Federsel C, Sponholz P, Mellmann D, Jackstell R, Junge H, Laurency G, Beller M (2012) *Energy Environ Sci* 5:8907
205. Boddien A, Gärtner F, Federsel C, Sponholz P, Mellmann D, Jackstell R, Junge H, Beller M (2011) *Angew Chem Int Ed* 50:6411
206. Laurency GG, Grasemann M, Lorent B, Raspail P (2011) *Electrosuisse Bull* 7:33
207. Joó F (2008) *ChemSusChem* 1:805
208. Enthaler S (2008) *ChemSusChem* 1:801
209. Sordakis K, Beller M, Laurency G (2014) *ChemCatChem* 6:96
210. Tanaka R, Yamashita M, Chung LW, Morokuma K, Nozaki K (2011) *Organometallics* 30:6742
211. Ziebart C, Federsel C, Anbarasan P, Jackstell R, Baumann W, Spannenberg A, Beller M (2012) *J Am Chem Soc* 134:20701
212. Federsel C, Ziebart C, Jackstell R, Baumann W, Beller M (2011) *Chem Eur J* 18:72
213. Federsel C, Boddien A, Jackstell R, Jennerjahn R, Dyson PJ, Scopelliti R, Laurency G, Beller M (2010) *Angew Chem Int Ed* 49:9777
214. Papp G, Csorba J, Laurency G, Joó F (2011) *Angew Chem Int Ed* 50:10433
215. Yang XZ (2013) *ACS Catal* 3:2684
216. Li H, Hall MB (2013) *J Am Chem Soc* 136:383
217. Cho D, Ko KC, Lee JY (2013) *Organometallics* 32:4571

Ruthenium-Catalyzed Amide-Bond Formation

Pascale Crochet and Victorio Cadierno

Abstract The amide functionality is one of the most important functional groups in organic and biological chemistry. Classical synthetic strategies of amides involve the stoichiometric, and poor atom efficient, reaction of amines with carboxylic acid derivatives. Transition-metal-catalyzed reactions have emerged in recent years as more atom-economical and powerful tools for preparing amides, opening previously unavailable routes from substrates other than the carboxylic acids and their derivatives. Ruthenium-based catalysts have been at the heart of these advances, and this chapter pretends to give an overview of the field. Among others, the following ruthenium-catalyzed synthetic approaches of amides will be discussed: the hydration of nitriles, the hydrolytic amidation of nitriles with amines, the rearrangement of aldoximes, the coupling of aldehydes with hydroxylamine, and the dehydrogenative amidation of alcohols, aldehydes, and esters.

Keywords Amide-bond formation · Dehydrogenative amidation · Hydrolytic amidation · Nitrile hydration · Rearrangements · Ruthenium catalysts

Contents

1	Introduction	83
2	Ruthenium-Catalyzed Hydration of Nitriles	84
3	Ruthenium-Catalyzed Hydrolytic Amidation of Nitriles with Amines	93
4	Ruthenium-Catalyzed Rearrangement of Aldoximes	95

P. Crochet and V. Cadierno (✉)

Laboratorio de Compuestos Organometálicos y Catálisis (Unidad Asociada al CSIC), Red ORFEO-CINQA – Centro de Innovación en Química Avanzada, Departamento de Química Orgánica e Inorgánica, Facultad de Química, Instituto Universitario de Química Organometálica “Enrique Moles”, Universidad de Oviedo, Julián Clavería 8, 33006 Oviedo, Spain
e-mail: vcm@uniovi.es

5	Ruthenium-Catalyzed Dehydrogenative Amidations	98
5.1	Starting from Alcohols	98
5.2	Starting from Aldehydes	105
5.3	Starting from Esters	107
6	Other Ruthenium-Catalyzed Amide-Bond Forming Reactions	108
7	Conclusion	111
	References	111

Abbreviations

Ac	Acetyl
acac	Acetylacetonate
Bn	Benzyl
cod	1,5-Cyclooctadiene
cot	1,3,5,7-Cyclooctatetraene
Cy	Cyclohexyl
Da	Dalton
DCE	1,2-Dichloroethane
DFT	Density functional theory
DME	1,2-Dimethoxyethane
DMSO	Dimethyl sulfoxide
DNA	Deoxyribonucleic acid
dppb	1,4-Bis(diphenylphosphino)butane
dppe	1,2-Bis(diphenylphosphino)ethane
dppm	Bis(diphenylphosphino)methane
equiv.	Equivalent(s)
Et	Ethyl
h	Hour(s)
<i>i</i> -Bu	<i>iso</i> -Butyl
<i>li</i> Pr	1,3-Diisopropylimidazol-2-ylidene
<i>i</i> -Pr	<i>iso</i> -Propyl
Me	Methyl
min	Minute(s)
mol	Mole(s)
Ms	Mesyl, methanesulfonyl
MW	Microwave
<i>n</i> -Bu	Butyl
NHC	<i>N</i> -heterocyclic carbene
NSAIDs	Non-steroidal anti-inflammatory drugs
PCyp ₃	Tricyclopentylphosphine
Pent	Pentyl
Ph	Phenyl
PPh ₂ (py-4-NMe ₂)	2-Diphenylphosphino-4-pyridyl(dimethyl)amine
PPh ₂ py	2-(Diphenylphosphino)pyridine
Pr	Propyl

PTA	1,3,5-Triaza-7-phosphaadamantane
PVP	Polyvinylpyrrolidone
py	Pyridine
rt	Room temperature
<i>s</i> -Bu	<i>sec</i> -Butyl
<i>t</i> -Bu	<i>tert</i> -Butyl
terpy	2,2':6',2''-Terpyridine
TOF	Turnover frequency
TON	Turnover number
Tp	Hydrotris(pyrazolyl)borate
Ts	Tosyl, 4-toluenesulfonyl

1 Introduction

The amide bond is one of the most important linkages in organic chemistry, and also plays a major role in the composition of biological systems since it constitutes a *leit motiv* unit in the structure of peptides and proteins. Amides are versatile synthetic intermediates used in the manufacture of several pharmacological and biological active products, polymers, detergents, lubricants, and drug stabilizers. They are also key structural motifs in multitude of natural products [1, 2]. Studies carried out by leading pharmaceutical companies have pointed out that amide-bond forming reactions are among the most executed chemical transformations in their laboratories [3, 4]. Indeed, an in-depth analysis of medicinal chemistry databases revealed that the amide group is present in more than 25% of the drugs currently known [5]. All these facts clearly show the importance and prevalence of amides in synthetic organic chemistry.

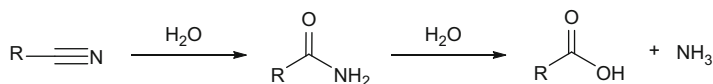
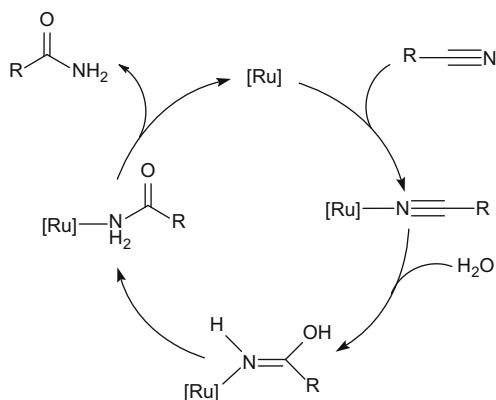
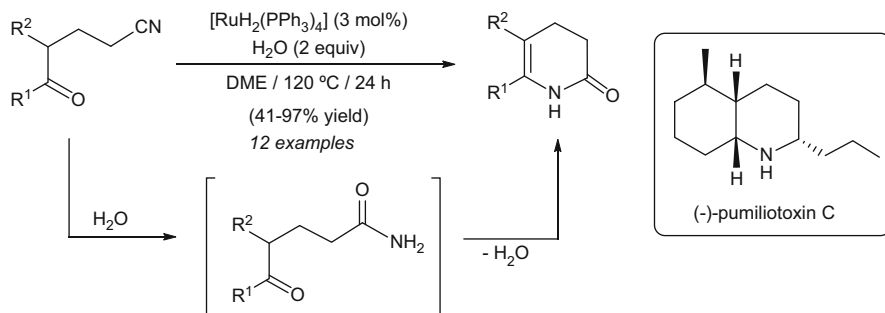
In general, traditional approaches for amide synthesis rely on the use of activated carboxylic acid derivatives and amines, processes which often require stoichiometric amounts of coupling reagents and suffer from the inherent drawback of producing large amounts of waste products along with the desired amide [1, 2, 6, 7]. In this sense, a recent report by the ACS GCIPR (American Chemical Society Green Chemistry Institute Pharmaceutical Roundtable) has identified amide formation avoiding poor atom economy reagents as a priority area of research for the pharmaceutical industry [8]. In the search of improved synthetic methods, metal-catalyzed transformations have emerged in recent years as the most promising alternatives for the atom-economical and cost-effective synthesis of amides. The use of metal catalysts has also opened previously unavailable routes starting from substrates other than carboxylic acids and their derivatives [9–14]. Ruthenium-based catalysts have been at the heart of these recent advances and, herein, an overview of the ruthenium-catalyzed amide-bond forming reactions reported to date in the literature is presented. Both homogeneous and heterogeneous systems will be discussed. Transformations in which the amide functionality already exists in the molecule, and a ruthenium catalyst is employed to promote further structural modifications, are considered to be out of the scope of this chapter.

2 Ruthenium-Catalyzed Hydration of Nitriles

Addition of water to the $C\equiv N$ bond of nitriles is probably the simplest route that one can imagine to generate primary amides in an atom-economical manner. This reaction is currently employed in industry for the large-scale production of acrylamide, nicotinamide, 5-cyanovaleramide, and the antiepileptic drug levetiracetam through biocatalytic transformations [15–18]. More conventional methods to hydrate nitriles involve the use of strong acids and bases under harsh conditions. However, these classical methods are not compatible with many functional groups, and they are usually unable to control hydrolysis to the corresponding carboxylic acids (Scheme 1) or the competing formation of polymeric side products [19, and references cited therein]. Transition-metal complexes are able to facilitate the hydration reaction by activating the nitrile substrate, the water nucleophile, or both upon coordination. Accordingly, a variety of metal catalysts, showing a high selectivity towards the amide under milder conditions to those employed with strong acids or bases, have been described in the literature [20–22]. In this context, ruthenium complexes are among the most versatile nitrile hydration catalysts discovered with regard to activity, selectivity, and tolerance to functional groups.

Pioneering work in the field was reported by Murahashi and co-workers in 1992 employing the ruthenium(II)-dihydride complex $[RuH_2(PPh_3)_4]$ [23–26]. Hydration of several organonitriles proceeded smoothly with 3 mol% of $[RuH_2(PPh_3)_4]$ upon treatment with 1–2 equiv. of water in DME at 120°C, leading to the corresponding primary amides in high yields (TOF up to 2 h^{-1}). A catalytic cycle involving the initial coordination of the nitrile to ruthenium, followed by intermolecular nucleophilic attack of water to generate an iminol that tautomerizes into the amide, was proposed (Scheme 2) [24]. As shown in Scheme 3, when δ -keto nitriles were used as the starting materials ene-lactams were selectively formed, via a ruthenium-catalyzed tandem hydration/cyclocondensation sequence [23, 24]. Such a process was applied by Murahashi and co-workers in the total synthesis of (–)-pumiliotoxin C, a naturally occurring alkaloid [24].

In addition to $[RuH_2(PPh_3)_4]$, other hydrido-ruthenium(II) complexes $[RuH(\eta^5-C_9H_7)(dppm)]$ [27], $[RuH(Tp)(PPh_3)(NCMe)]$ [28, 29], $[RuH\{tmeP_2N(NH)\}]$ (**1** in Fig. 1) [30], and $[\{(PCy_3)(CO)RuH\}_4(\mu_4-O)(\mu_3-OH)(\mu_2-OH)]$ (**2** in Fig. 1) [31] proved to be also able to promote the selective hydration of nitriles to primary amides. Among them, the indenyl derivative $[RuH(\eta^5-C_9H_7)(dppm)]$ merits to be highlighted since it is able to operate directly in water at relatively high rates [27]. For example, TOF and TON values of 11 h^{-1} and 800, respectively, were reached in the hydration of benzonitrile with 0.1 mol% of $[RuH(\eta^5-C_9H_7)(dppm)]$ at 120°C. This hydrido-ruthenium(II) complex is also interesting from a mechanistic point of view, because it belongs to a particular class of catalysts that activate the nucleophilic water molecule through an outer sphere mechanism. Thus, DFT calculations confirmed that, in the rate-limiting step of the reaction, the nucleophilic attack of water on the coordinated nitrile is assisted by the hydride ligand,

**Scheme 1** The nitrile hydration and amide hydrolysis reactions**Scheme 2** Catalytic cycle for the hydration of nitriles promoted by $[\text{RuH}_2(\text{PPh}_3)_4]$ **Scheme 3** Catalytic synthesis of ene-lactams using $[\text{RuH}_2(\text{PPh}_3)_4]$ and structure of the alkaloid (-)-pumiliotoxin C

which activates the water molecule through a $\text{Ru}-\text{H} \cdots \text{H}-\text{OH}$ hydrogen-bond interaction (Scheme 4).

A related intramolecular activation of water by the pyridinic nitrogen of the auxiliary 2-(diphenylphosphino)pyridine ligand was proposed by Oshiki and co-workers to explain the high reactivity shown by the octahedral ruthenium (II) complex *cis*- $[\text{Ru}(\text{acac})_2(\text{PPh}_2\text{py})_2]$ [32–34]. As shown in Scheme 5, performing the reactions in DME at 180 °C with a small amount of water, this catalyst (0.2–0.4 mol%) was able to transform a large variety of nitriles into the corresponding amides in high yields and short times. An impressive TOF value of 20,900 h^{-1} , the highest reported to date for this catalytic transformation, could be

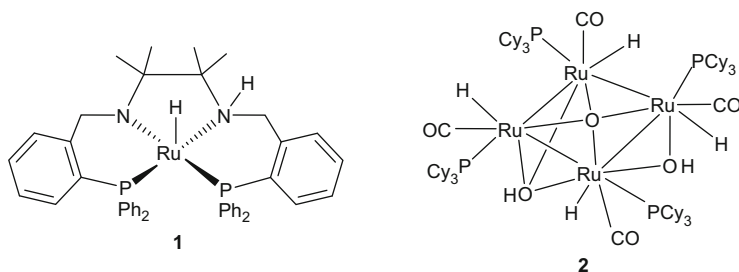
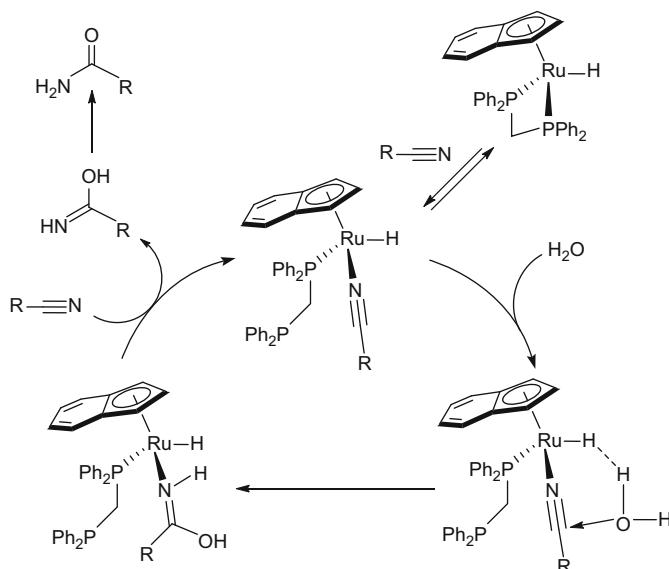
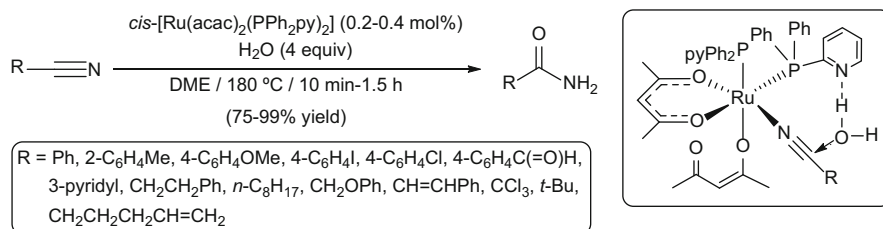


Fig. 1 Structure of the hydrido-ruthenium(II) catalysts 1–2



Scheme 4 Catalytic cycle for the hydration of nitriles promoted by $[\text{RuH}(\eta^5\text{-C}_9\text{H}_7)(\text{dppm})]$



Scheme 5 Catalytic hydration of nitriles using $\text{cis-}[\text{Ru}(\text{acac})_2(\text{PPh}_2\text{py})_2]$

reached in the hydration of benzonitrile employing 0.024 mol% of $\text{cis-}[\text{Ru}(\text{acac})_2(\text{PPh}_2\text{py})_2]$ (85% conversion after 10 min). The cooperative effect exerted by the pyridyl-phosphine ligand in $\text{cis-}[\text{Ru}(\text{acac})_2(\text{PPh}_2\text{py})_2]$ was supported by the

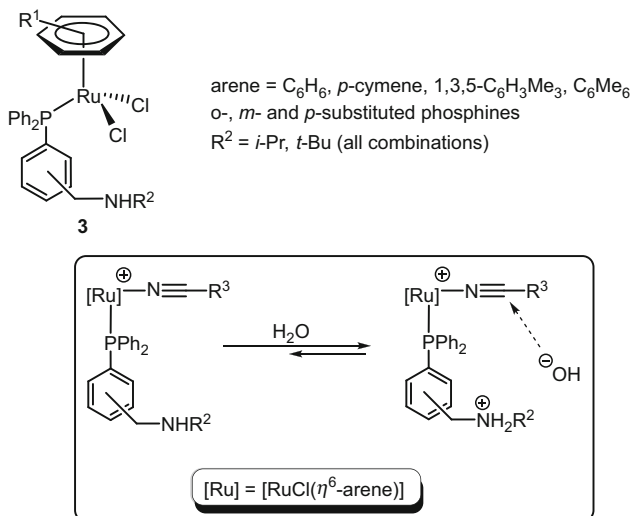


Fig. 2 Structure and activating effect of the arene-ruthenium(II) complexes [RuCl₂(η⁶-arene)(Ph₂PC₆H₄CH₂NHR)] (**3**)

fact that replacement of PPh₂py by PPh₃, PMe₃ or P(*n*-Bu)₃ led to much less active catalysts [32–34]. The same group also described the hydration of several organonitriles under milder reaction conditions, i.e. in DME at 80°C, employing the bis(allyl)-ruthenium(II) complex [Ru(η³-2-C₃H₄Me)₂(cod)] (0.5 mol%) in combination with the dimethylamino-substituted pyridyl-phosphine PPh₂(py-4-NMe₂) (1.5 mol%) [35, 36]. However, we must note that longer reaction times (48 h; TOF up to 5 h⁻¹) were in this case needed to generate the amides in high yields, and that incomplete conversions were in some cases observed. Inspired by these works, other groups have studied the catalytic behavior of different ruthenium(II) and ruthenium(IV) complexes bearing pyridyl-phosphine ligands, but none of the described systems enabled to improve the results obtained by Oshiki [37, 38]. The tendency of the ligands to adopt a chelating coordination was, in some cases, responsible for the low catalytic activity observed [38].

Activation of water by the ancillary phosphine ligands was also evidenced when arene-ruthenium(II) complexes of general composition [RuCl₂(η⁶-arene)(Ph₂PC₆H₄CH₂NHR)] (**3** in Fig. 2) were employed as catalysts [39]. Although the activity shown by these complexes was only moderate (TOF up to 3 h⁻¹ at 100°C), the hydration reactions proceeded significantly faster than those using the analogous triphenylphosphine derivatives [RuCl₂(η⁶-arene)(PPh₃)] under identical experimental conditions (TOF up to 0.1 h⁻¹). However, when free amine PhCH₂NHR (R = *n*-Bu or *i*-Pr) was added to the [RuCl₂(η⁶-arene)(PPh₃)]-catalyzed reactions the hydration rates increased, becoming similar to those observed with complexes **3** [39]. This fact suggested that the higher activity of [RuCl₂(η⁶-arene)(Ph₂PC₆H₄CH₂NHR)] (**3**) vs [RuCl₂(η⁶-arene)(PPh₃)] is not due to a ligand-assisted activation of water by hydrogen-bonding. More likely, the

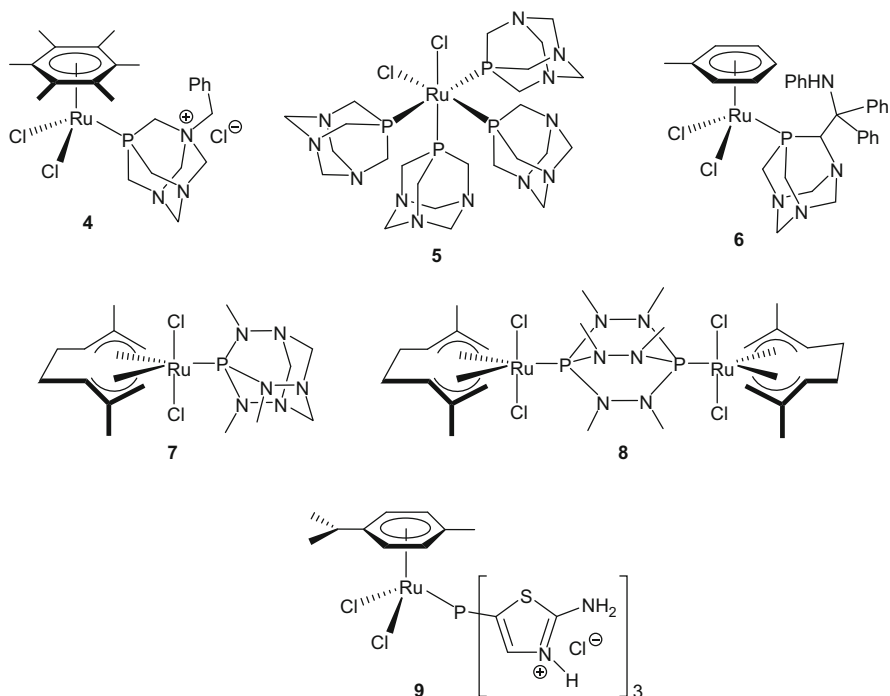
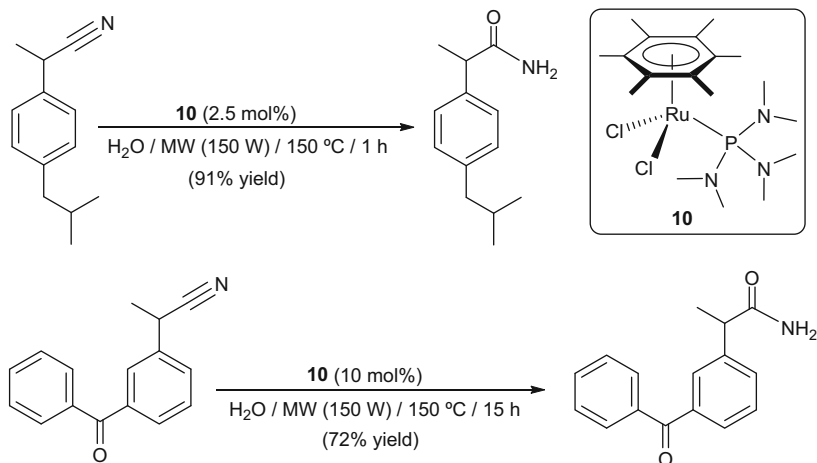


Fig. 3 Structure of the water-soluble ruthenium catalysts 4–9

intrinsic basic nature of the pendant amino group of the aryl-phosphines would increase the concentration of the more nucleophilic hydroxide anion in the solution, thus accelerating the hydration process (Fig. 2).

The use of auxiliary ligands derived from the aminophosphine PTA (1,3,5-triaza-7-phosphaadamantane) and related water-soluble “cage-like” phosphines has led in recent years to highly efficient ruthenium catalysts for nitrile hydration in pure water [40–44]. Complexes 4–8 are the most representative examples (Fig. 3). Almost quantitative conversions of a wide variety of aromatic, heteroaromatic, α,β -unsaturated, and aliphatic nitriles into the corresponding amides were achieved at 100–150°C (classical oil-bath or MW heating) employing 5 mol% of these complexes (TOF values in the range 30–285 h⁻¹). Common functional groups such as halides, nitro, hydroxy, ethers, thioethers, amino, ketones, aldehydes, esters, or alkynes were in general tolerated. The high efficiencies of 4–8 were attributed to the ability of the nitrogenated phosphines to serve as hydrogen bond acceptors to activate the nucleophilic water molecules. Interestingly, performing the catalytic hydration of benzonitrile with only 0.001 mol% of complexes 5 and 6 turnover numbers of 22,000 and 97,000, respectively, could be attained. However, very long reaction times of 97 (5) [42] and 14 (6) [44] days were needed to achieve such a high productivity. It is also noteworthy that, after selective crystallization of the final amides, recycling of the aqueous phase containing

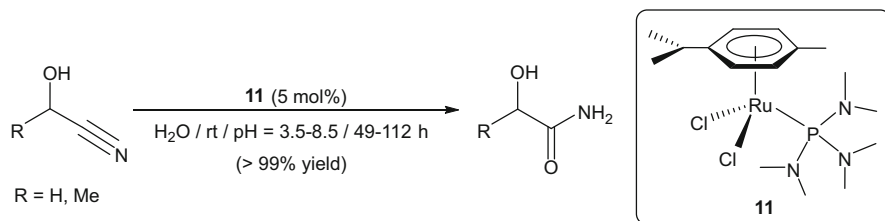


Scheme 6 Synthesis of the NSAIDs ibuprofenamide and ketoprofenamide by catalytic hydration

complexes **4** (2 times) [40] and **5** (6 times) [42] was possible. The arene-ruthenium(II) complex **9**, bearing the water-soluble and potentially H-bond acceptor ligand tris(5-(2-aminothiazolyl))-phosphine trihydrochloride (Fig. 3), featured also a high activity (TOF up to 66 h⁻¹), productivity (TON up to 9800), substrate scope and functional group tolerance, combined with an effective recycling (up to five consecutive runs) [45].

Selective conversion of nitriles to amides, in water under neutral conditions, was also described employing complexes [RuCl₂(η⁶-arene){P(NMe₂)₃}] (arene = C₆H₆, *p*-cymene, 1,3,5-C₆H₃Me₃, C₆Me₆) as catalysts. These compounds make use of the commercially available and inexpensive tris(dimethylamino)phosphine ligand, making them much more attractive for practical applications than the examples discussed above containing rather elaborated water-soluble phosphines. In particular, the hexamethylbenzene derivative [RuCl₂(η⁶-C₆Me₆){P(NMe₂)₃}] (**10**) proved to be highly efficient, providing the desired amides from a wide range of organonitriles in excellent yields and short times [46, 47]. TOF values up to 11,400 h⁻¹, the highest reported to date for this catalytic transformation in pure water, were reached with complex **10** by performing the catalytic reactions at 150 °C under MW irradiation. Remarkably, taking advantage of the outstanding performance of [RuCl₂(η⁶-C₆Me₆){P(NMe₂)₃}] (**10**), unprecedented synthetic routes for the preparation of the non-steroidal anti-inflammatory drugs ibuprofenamide and ketoprofenamide, by catalytic hydration of 2-(4-isobutylphenyl)propionitrile and 2-(3-benzoylphenyl)propionitrile, respectively, were developed (Scheme 6) [46, 47].

The synthetic utility of complexes [RuCl₂(η⁶-arene){P(NMe₂)₃}] was further demonstrated in the challenging hydration of cyanohydrins (α-hydroxynitriles), substrates usually difficult to hydrate because they degrade to produce cyanide which poisons the catalysts. As shown in Scheme 7, using 5 mol% of the *p*-cymene complex [RuCl₂(η⁶-*p*-cymene){P(NMe₂)₃}] (**11**), and performing the catalytic



Scheme 7 Cyanohydrins hydration using $[\text{RuCl}_2(\eta^6\text{-}p\text{-cymene})\{\text{P}(\text{NMe}_2)_3\}]$ (**11**) as catalyst

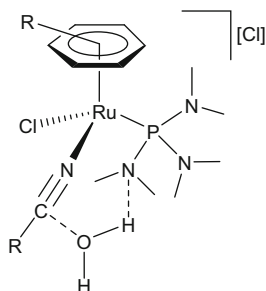


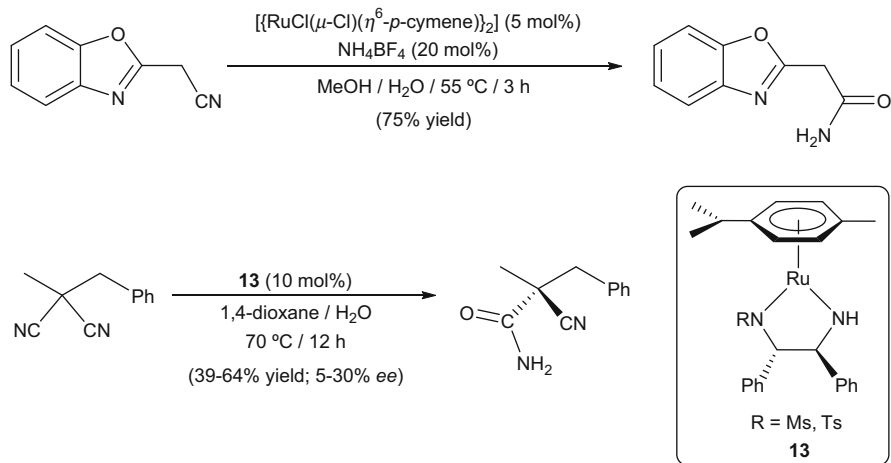
Fig. 4 The cooperative effect of the tris(dimethylamino)phosphine ligand

reactions at room temperature within the pH range 3.5–8.5 to minimize the decomposition of the substrates into the corresponding aldehydes and HCN, glycolonitrile and lactonitrile could be completely transformed into the corresponding α -hydroxyamides [48, 49].

The H-bond accepting properties of tris(dimethylamino)phosphine were again evoked to explain the excellent catalytic activities observed, a cooperative effect that was supported by DFT calculations (Fig. 4) [49]. Secondary coordination sphere activation of water, via hydrogen-bonding with the OH group of the ligand, also explains the outstanding performances of the related phosphinite-ruthenium(II) complex $[\text{RuCl}_2(\eta^6\text{-}p\text{-cymene})\{\text{PMe}_2(\text{OH})\}]$ (**12**), which was also able to hydrate cyanohydrins [50, 51]. Although other catalytic systems for the selective hydration of organonitriles in water have been described [52–57], none of them presented an activity and scope comparable to those of the bifunctional catalysts **4–12**.

Additional examples of nitrile hydration reactions catalyzed by homogeneous ruthenium catalysts in organic media are (Scheme 8): (1) The hydration of benzoxazolylacetonitrile by the arene-ruthenium(II) dimer $[\{\text{RuCl}(\mu\text{-Cl})(\eta^6\text{-}p\text{-cymene})\}_2]$, which led to benzoxazolylacetamide in high yield [58], and (2) the asymmetric hydration of α -benzyl- α -methylmalononitrile by the chiral catalysts **13** [59]. Modest yields and low enantiomeric excesses were obtained in this latter reaction. However, we must note that this is the first example of a nonenzymatic asymmetric nitrile hydration process reported to date in the literature.

On the other hand, different heterogeneous ruthenium-based systems able to promote the selective hydration of nitriles to amides have also been developed.

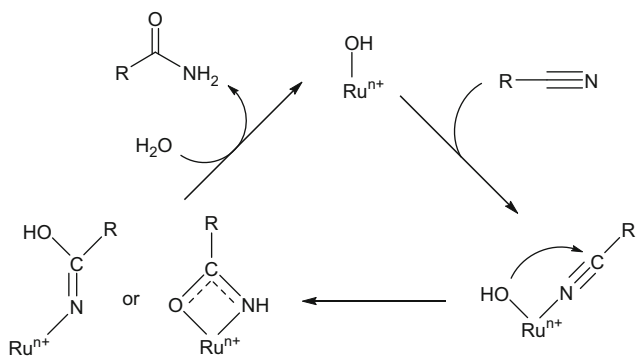


Scheme 8 Some nitrile hydrations catalyzed by ruthenium(II) complexes

A benchmark in the field was described by Mizuno and co-workers in 2004 employing ruthenium hydroxide supported on alumina ($\text{Ru}(\text{OH})_x/\text{Al}_2\text{O}_3$) as catalyst [60]. This system was able to operate directly in water, showed a great substrate scope, and led to TOF and TON values of up to 13 h^{-1} and 234, respectively, at 140°C . Notably, the use of organic solvents was not needed during work-up since the solid catalyst could be separated from the reaction mixture by hot filtration at 90°C , and the amides crystallized in pure form from the filtrate upon cooling at 0°C . In addition, the heterogeneous $\text{Ru}(\text{OH})_x/\text{Al}_2\text{O}_3$ system could be reused two times without significant loss of catalytic activity. A mechanism involving the coordination of the nitrile to ruthenium on the surface of $\text{Ru}(\text{OH})_x/\text{Al}_2\text{O}_3$, followed by attack of a ruthenium hydroxide species on the coordinated nitrile, was proposed (Scheme 9).

Related organic solvents-free protocols were described employing as catalysts ruthenium hydroxide supported on dopamine-functionalized Fe_3O_4 nanoparticles **14** [61, 62], $\text{Ru}(\text{OH})_x$ nanoparticles supported on silica-coated Fe_3O_4 nanoparticles **15** [63], and the arene-ruthenium(II) complex supported on silica-coated Fe_3O_4 nanoparticles **16** [64] (Fig. 5). All these nanocatalysts showed excellent activities (TOFs up to 170 h^{-1}) and selectivities for a broad range of activated and inactivated benzonitriles, as well as heteroaromatic, aliphatic, and α,β -unsaturated nitriles, leading to the corresponding primary amides in high yields (70–95%) after 0.5–7 h of MW irradiation at $100\text{--}150^\circ\text{C}$ in pure water. The magnetic nature of the nano-ferrites-based supports enabled an easy catalyst/product separation just by applying an external magnet. The recovered catalysts could be reused three (**14–15**) or six (**16**) times, and the amides isolated by simple crystallization from the aqueous solutions.

Ruthenium-substituted hydroxyapatite ($(\text{RuCl})_2\text{Ca}_8(\text{PO}_4)_6(\text{OH})_2$) [65], the modified nafion resin **17** (Fig. 6) [66] and a series of ruthenium nanoparticles supported



Scheme 9 Proposed mechanism for the catalytic hydration of nitriles promoted by $\text{Ru}(\text{OH})_x/\text{Al}_2\text{O}_3$

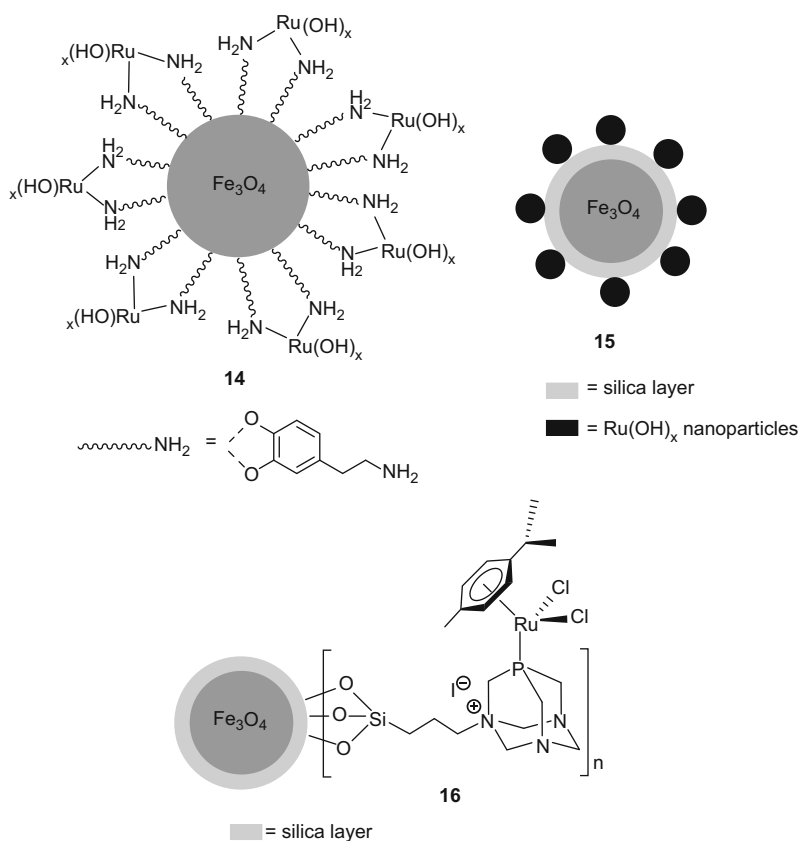
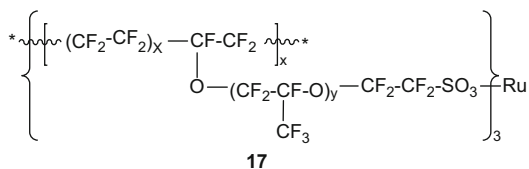


Fig. 5 Structure of the heterogeneous ruthenium catalysts 14–16

Fig. 6 Structure of the nafion-Ru resin **17**



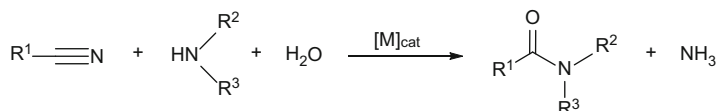
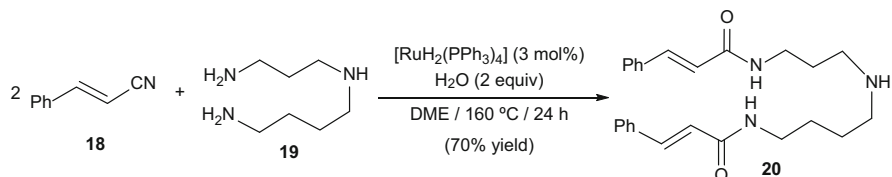
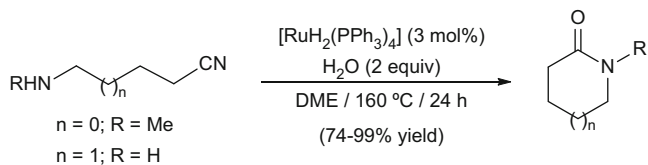
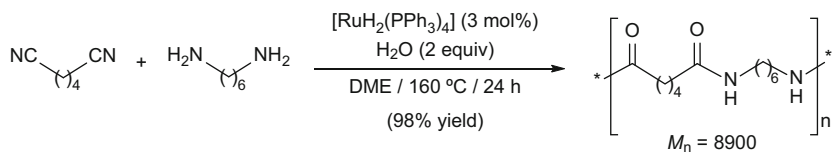
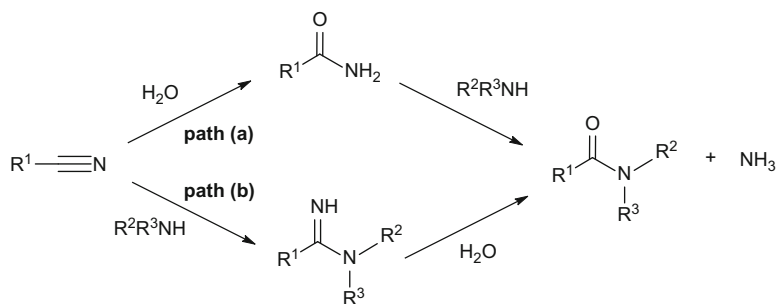
on carbon [67], alumina [68], polyvinylpyrrolidone (PVP) [69] and the ion exchange polystyrene resin Amberlite IRA 900 chloride [70] are other heterogeneous ruthenium-based nitrile hydration catalysts described in the literature. All of them were active in pure water and recoverable by filtration. However, their activities and substrate scope were, in general, comparatively lower with regard to those of the magnetic nanocatalysts **14–16**.

3 Ruthenium-Catalyzed Hydrolytic Amidation of Nitriles with Amines

Despite the great advances reached in the catalytic nitrile hydration, reactions to form *N*-substituted amides from nitriles have few precedents. In this context, although little studied, the catalytic amidation of nitriles with amines in the presence of water has emerged in recent years as a useful tool for the straightforward generation of secondary and tertiary amides (Scheme 10) [71–77].

This amidation reaction was reported for the first time by Murahashi and co-workers in 1986 using the unique ruthenium catalyst described so far for this catalytic transformation [78]. Thus, they were able to synthesize a large variety of *N*-substituted amides from different nitrile/amine combinations by performing the catalytic reactions in DME at 160°C with 3 mol% of the ruthenium(II)-dihydride complex [RuH₂(PPh₃)₄] and 2 equiv. of water [25, 26, 78]. The synthesis with high yield of the maytenine alkaloid **20**, by coupling of cinnamonitrile **18** with the triamine **19**, is an illustrative example of the synthetic utility of this amide-bond forming process (Scheme 11). As shown in Scheme 12, the intramolecular version of the reaction provided an efficient method for the catalytic synthesis of lactams [78]. Murahashi and co-workers also demonstrated the utility of this catalytic transformation for the preparation of industrially relevant polyamides, as exemplified in the reaction of adiponitrile with 1,6-hexanediamine to give the nylon-6,6 polymer (Scheme 13) [78].

Mechanistic studies by Duchateau and co-workers, employing the [RuH₂(PPh₃)₄]-catalyzed hydrolytic amidation of pentanenitrile with *n*-hexylamine as model reaction, pointed out that the process proceeds through the initial hydration of the nitrile to form an intermediate primary amide, which subsequently reacts with the amine to give the final *N*-substituted amide product (path (a) in Scheme 14) [79]. This reaction pathway contrasts with that commonly proposed for other

**Scheme 10** The hydrolytic amidation of nitriles with amines**Scheme 11** Ruthenium-catalyzed synthesis of maytenine**Scheme 12** Ruthenium-catalyzed synthesis of lactams by intramolecular hydrolytic amidation**Scheme 13** Ruthenium-catalyzed synthesis of the polymer nylon-6,6**Scheme 14** Possible reaction pathways for the catalytic amidations of nitriles with amines

homogeneous metal catalysts (Pt-, Cu- Zn-, or Fe-based systems) where an amidine intermediate, which evolves into the final amide product by hydrolysis, is initially formed (path (b) in Scheme 14) [71, 73, 75–77].

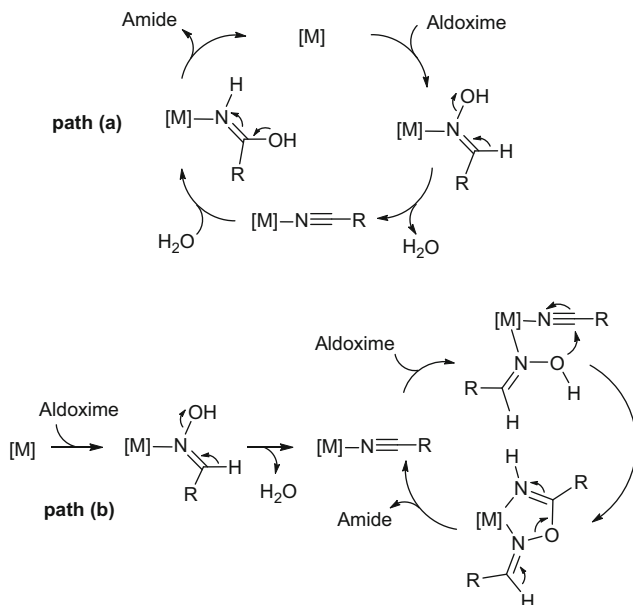
4 Ruthenium-Catalyzed Rearrangement of Aldoximes

Although the first report on metal-catalyzed rearrangement of aldoximes dates back to the early 1960s [80], only in recent years this transformation appeared to be an attractive method for synthesizing primary amides [81]. The main advantages of this reaction stem from its total atom economy and the availability of the starting materials, which are easily accessible by condensation of an aldehyde with hydroxylamine. From a mechanistic point of view, two main reaction pathways have been proposed. The first one consists of the initial dehydration of the aldoxime to form a nitrile, which is further rehydrated by the water molecule released in the previous step (Scheme 15, path (a)). The second mechanism also starts with the dehydration of the aldoxime into a nitrile, which now reacts with a second molecule of aldoxime, acting as a water surrogate, to deliver the free amide and regenerate the active metal-nitrile species (Scheme 15, path (b)). Remarkably, although pathway (a) has been the generally accepted mechanism, a recent study of Williams and co-workers using ^{18}O -labeled substrates revealed that most of the catalytic systems reported to date operate indeed through the pathway (b) [82].

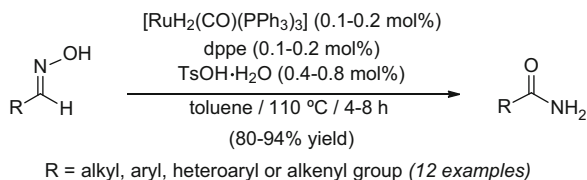
The first examples of the rearrangement of aldoximes into primary amides involving a ruthenium catalyst, namely $[\text{Ru}(\text{cod})(\text{py})_4][\text{BPh}_4]_2$, were reported by Kiji and co-workers in 1982 [83]. However, efficient and general ruthenium-based protocols did not appear till 2007, when Williams and co-workers described the activity of the ruthenium-dihydride complex $[\text{RuH}_2(\text{CO})(\text{PPh}_3)_3]$ associated with different bidentate ligands [84]. The best performances were obtained with 1,2-bis(diphenylphosphino)ethane (dppe) (Scheme 16). Moreover, the addition of 4 equiv. of *p*-toluenesulfonic acid per ruthenium to the reaction medium was required to achieve good rates and selectivities. Under these optimal conditions, both aromatic and aliphatic aldoximes, as well as α,β -unsaturated ones, could be converted into the corresponding primary amides in excellent yields.

A more convenient additive-free protocol was developed a couple of years later using 1 mol% of the octahedral ruthenium complex $[\text{RuCl}_2(\text{PPh}_3)(\text{terpy})]$ [85]. Aldoximes with both *syn* and *anti* conformation could be employed, with no difference in the rate of the isomerization process. This catalytic system proved to be also useful for the rearrangement of aldoximes generated in situ from the corresponding aldehydes. Thus, as shown in Scheme 17, the heating of a 1:1:1 mixture of the aldehyde, hydroxylammonium chloride, and NaHCO_3 , in the presence of $[\text{RuCl}_2(\text{PPh}_3)(\text{terpy})]$ (1 mol%), selectively led to the desired primary amides in good yields.

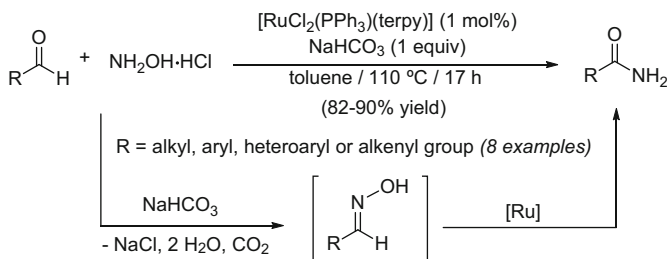
Since then, different octahedral ruthenium(II) complexes (1 mol%) have been employed to generate primary amides through the direct rearrangement of isolated



Scheme 15 Proposed mechanisms for the metal-catalyzed rearrangement of aldoximes



Scheme 16 Ruthenium-catalyzed rearrangement of aldoximes into primary amides



Scheme 17 Ru-catalyzed rearrangement of aldoximes generated in situ from aldehydes

aldoximes (**21** in Fig. 7), or through the one-pot coupling of aldehydes with hydroxylammonium salts (**22–24** in Fig. 7) [86–89]. Both processes were also catalyzed by $[\text{RuCl}_2(\text{DMSO})_4]$, albeit a higher metal loading (5 mol%) was in this case needed [90].

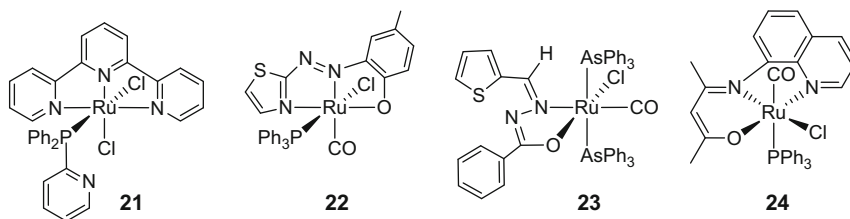


Fig. 7 Structure of the ruthenium(II) complexes 21–24

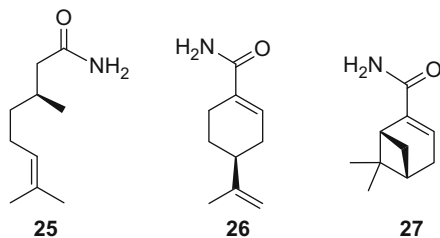
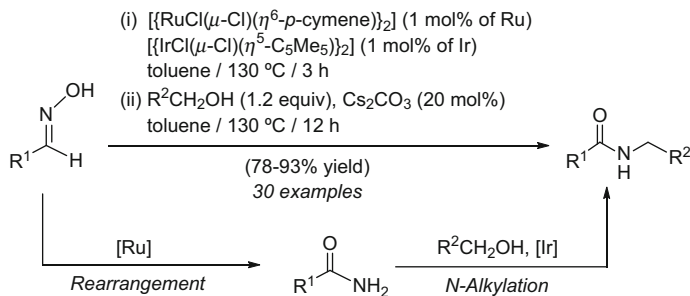


Fig. 8 Structure of the optically active amides 25–27

Interestingly, using 5 mol% of the arene-ruthenium(II) complex $[\text{RuCl}_2(\eta^6\text{-C}_6\text{Me}_6)\{\text{P}(\text{NMe}_2)_3\}]$ (**10** in Scheme 6), the rearrangement of aldoximes could be successfully performed in aqueous medium at 100°C [91]. Kinetic studies and experiments in ^{18}O -labeled water indicated that, for this particular catalyst, the reaction proceeds simultaneously through the two mechanisms depicted in Scheme 15, albeit pathway (b) showed to be predominant. This aqueous methodology was applicable to a wide range of aromatic, heteroaromatic, aliphatic, and α,β -unsaturated aldoximes (39 examples). The synthetic utility of complex **10** was fully demonstrated in the preparation of the chiral amides (*S*)-(-)-citronellamide (**25**), (*S*)-(-)-perillamide (**26**), and (*1R*)-(-)-myrtenamide (**27**), compounds of relevance in the fragrance industry (Fig. 8).

Complex $[\text{RuCl}_2(\eta^6\text{-C}_6\text{Me}_6)\{\text{P}(\text{NMe}_2)_3\}]$ (**10**) also resulted operative in the one-pot synthesis of amides from aldehydes in water [92]. Interestingly, besides the classical source of the NH_2 group, i.e. the $\text{NH}_2\text{OH}\cdot\text{HCl}$ salt associated with NaHCO_3 , commercially available hydroxylamine solution (50 wt% in H_2O) could also be employed, improving notably the atom economy of the overall process since only water was generated as by-product. More recently, the highly water-soluble complex **9** (Fig. 3), which contains a thiazolyl-phosphine hydrochloride salt as ligand, was also found active in the synthesis of primary amides from aldoximes and aldehydes using water as solvent [45].

On the other hand, the preparation of secondary amides from aldoximes has been recently achieved through the one-pot sequential rearrangement/*N*-alkylation process depicted in Scheme 18 [93]. The reactions were carried out heating a toluene solution of the aldoxime with a mixture of dimers $[\{\text{RuCl}(\mu\text{-Cl})(\eta^6\text{-}p\text{-cymene})\}_2]$



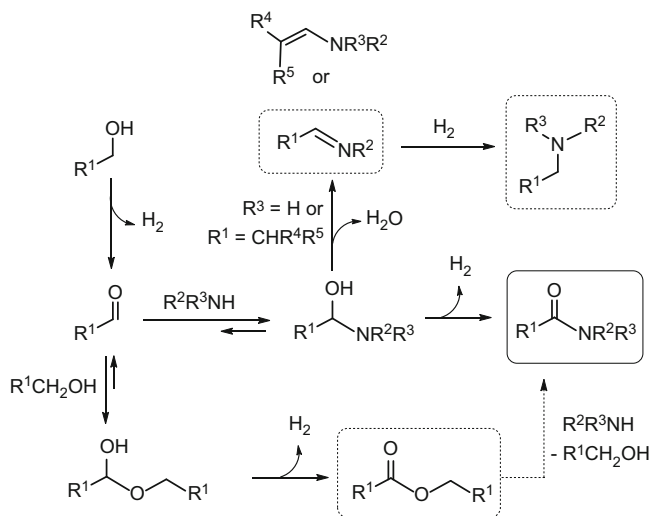
Scheme 18 Synthesis of secondary amides from aldoximes through sequential rearrangement/*N*-alkylation reactions

and $[\{\text{IrCl}(\mu\text{-Cl})(\eta^5\text{-C}_5\text{Me}_5)\}_2]$, followed by the addition of an alcohol and Cs_2CO_3 to the medium. Under these conditions selective formation of *N*-monoalkylated amides occurred, primary or *N,N*-dialkylated ones being not detected at the end of the reactions. Although the two steps involved in the process could be promoted by both ruthenium and iridium species alone, the initial rearrangement of the aldoxime was particularly favored in the presence of Ru, while the *N*-alkylation of the resulting primary amide was more effective with Ir. Therefore, the combination of the two metals resulted more advantageous than their use separately. The methodology proved to be general and it was successfully applied to a variety of aromatic, heteroaromatic, and aliphatic aldoximes. Benzyl or alkyl primary alcohols were satisfactorily involved in the *N*-alkylation step, but the secondary and tertiary ones, much more hindered, were not tolerated.

5 Ruthenium-Catalyzed Dehydrogenative Amidations

5.1 Starting from Alcohols

The catalytic oxidative dehydrogenation of primary alcohols in the presence of amines has emerged in recent years as an attractive alternative for the synthesis of amides [94, 95]. The reaction is assumed to take place through the initial dehydrogenation of the alcohol into the corresponding aldehyde, followed by nucleophilic attack of the amine and subsequent dehydrogenation of the resulting hemiaminal (Scheme 19). In these dehydrogenative processes, esters [95, 96], imines [97], and amines [95, 96, 98] can also be generated through competing reaction pathways (Scheme 19). The selectivity towards amides strongly depends on the nature of substrates and catalysts, as well as on the experimental conditions employed, but, despite the great advances reached in this area during the last years, the factors that govern the outcome of the reaction are still little understood. Actually, the number of catalytic systems active in dehydrogenative amidation processes, most based on



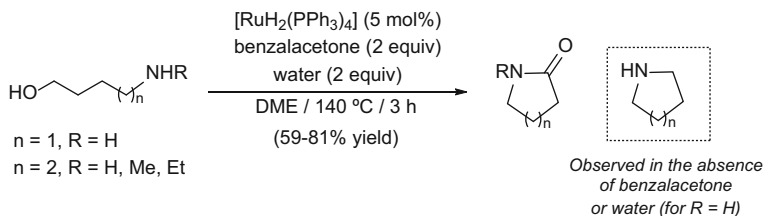
Scheme 19 Dehydrogenative amidation of primary alcohols and competing processes

ruthenium complexes, is by far smaller than those able to promote the formation of amines or esters [95, 96, 98].

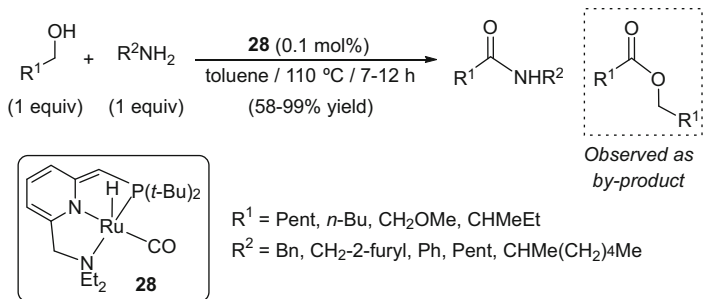
Pioneering work in the field was reported by Murahashi and co-workers in 1991 [99]. They discovered that 1,4- and 1,5-amino-alcohols can be selectively converted into lactams, through an intramolecular coupling, in the presence of catalytic amounts of the ruthenium-dihydride derivative $[\text{RuH}_2(\text{PPh}_3)_4]$ (Scheme 20). With this system, the use of at least 2 equiv. of a hydrogen acceptor, such as benzalacetone, was needed to achieve high conversions and selectivities in the desired cyclic amides. Moreover, the substrates bearing a primary amino group ($\text{R} = \text{H}$, in Scheme 20) required a two-fold excess of water in order to prevent the competing formation of a cyclic amine, the latter resulting from the dehydration of the hemiaminal intermediate and subsequent hydrogenation of the resulting imine.

This amidation process, poorly exploited till 2007 [100], regained popularity after Milstein's report on a highly efficient and atom-economical procedure that did not require a sacrificial hydrogen acceptor, the oxidations of the alcohol and the hemiaminal proceeding with formation of hydrogen gas as the only by-product [101]. The catalytic system, based on the PNN-pincer ruthenium derivative **28**, was successfully applied to the highly selective synthesis of a variety of secondary amides from 1:1 mixtures of primary alcohols and amines (Scheme 21). However, when amines with only a moderate nucleophilic character were employed as substrates, small amounts of esters were also formed as by-products.

The efficient removal of H_2 during the course of the reaction appeared to be crucial. In this sense, high yields in the amides were obtained when the reactions were performed in refluxing toluene under a flow of argon, while lower conversions and selectivities were reached in a closed system. Alternatively, the catalytic reactions could be performed in the presence of the related air-stable hydrochloride



Scheme 20 Synthesis of lactams promoted by $[\text{RuH}_2(\text{PPh}_3)_4]$



Scheme 21 Acceptorless-protocol to generate secondary amides from alcohols and amines

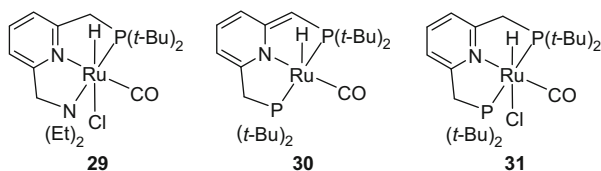
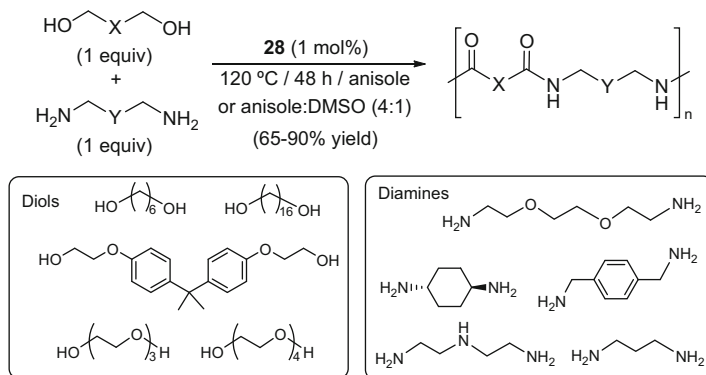


Fig. 9 Structure of the PNN- and PNP-pincer complexes **29–31**

complex $[\text{RuClH}(\text{CO})(\text{PNN})]$ (**29** in Fig. 9) associated with one equivalent (per Ru) of base [102]. Under these basic conditions, **29** is quantitatively converted into **28** through the deprotonation of the tridentate ligand backbone [103]. The high efficiency of **28** and **29** is ascribed to the cooperation of the PNN-pincer ligand in the different H-atom transfers involved in the reaction, through reversible aromatization/dearomatization processes of the pyridine-based core [102–107]. Surprisingly, under similar experimental conditions, the analogous PNP-pincer derivatives **30** and **31** (Fig. 9), susceptible to undergo related aromatization/dearomatization processes of the ligand, produced imines selectively instead of amides [97, 103]. The authors attributed this different chemical behavior to the lack of a hemilabile group in the catalysts' structure (i.e., absence of the CH_2NEt_2 arm). However, we must note that later DFT calculations suggested that electronic properties rather govern the outcome of the reaction [105–107].

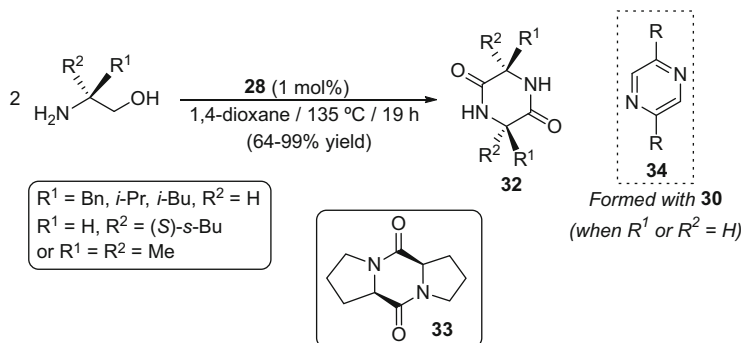


Scheme 22 Synthesis of polyamides through dehydrogenative processes

The catalytic protocol based on complex **28** proved to be also suitable for the bis-acylation of diamines with simple alcohols [101]. In addition, polyamines with both primary and secondary groups reacted with complete chemoselectivity at the NH_2 positions keeping untouched the NH functions, without the need of a protection/deprotection strategy. The methodology was extended, separately by Guan [108] and Milstein [109, 110], to the synthesis of polyamides starting from diols and diamines (representative examples are given in Scheme 22). The replacement of toluene by a more solubilizing solvent (i.e., anisole, anisole:DMSO or 1,4-dioxane) proved to be crucial to obtain high molecular weight polymers (up to 28.4 kDa).

The formation of polyamides also occurred in the self-coupling of sterically non-hindered 1,2-amino-alcohols [111]. However, when substrates with large substituents in α -position with respect to the amino group were employed, diketopiperazines **32** were instead selectively obtained (Scheme 23). Interestingly, the transformation of chiral amino-alcohols took place without epimerization, affording the cyclic dipeptides **32** in optically pure form. This methodology was also operative with the cyclic secondary amino-alcohol (*S*)-prolinol, thus allowing the preparation of the tricyclic product **33**. Once again, a striking difference in reactivity was observed when using complex **30** as catalyst, pyrazines **34** being in this case the major reaction products [111].

In addition to the PNN-pincer derivative **28**, other transition metal catalysts, associated or not with a hydrogen acceptor, have been developed for the dehydrogenative amidation of alcohols with amines. Ruthenium complexes, and especially NHC-compounds, have been the most widely studied [94], albeit highly efficient processes promoted by rhodium or silver have also been described [112, 113]. In regard to ruthenium, both in-situ-generated catalytic systems (Table 1) [114–123] and well-defined catalysts **38–44** (Fig. 10) [124–131] have been reported. In most of the cases, high metal loadings (usually 5 mol%) and an excess of a strong base (10–40 mol% of NaH or KO-*t*-Bu) were required to achieve satisfactory yields in the amides. In general, the reactions showed to be strongly sensitive to the steric hindrance of the substrates. Thus, branched primary alcohols



Scheme 23 Synthesis of 3,6-disubstituted-piperazine-2,5-diones promoted by complex **28**

Table 1 Examples of ruthenium-based catalytic systems generated in situ

Catalytic system ^a	References
 $\text{R} = i\text{-Pr, X} = \text{Cl}$ (35a) $\text{R} = i\text{-Pr, X} = \text{Br}$ (35b)	[114]
 36	[115]
 37	[116]
$[\text{RuCl}_2(\text{cod})]_n$ (5 mol% Ru), 35a (5 mol%), $\text{PCy}_3 \cdot \text{HBF}_4$ (5 mol%), $\text{KO-}t\text{-Bu}$ (20 mol%)	[114]
$[\{\text{RuCl}(\mu\text{-Cl})(\eta^6\text{-C}_6\text{H}_6)\}_2]$ (5 mol% Ru), 35b (5 mol%), MeCN (5 mol%), NaH (15 mol%), 36 h	[115]
RuCl_3 (5 mol%), 35b (5 mol%), pyridine (5 mol%), NaH (40 mol%)	[116]
$[\text{RuCl}_2(\text{LiPr})(\eta^6\text{-}p\text{-cymene})]$ (5 mol%), PCy_3 (5 mol%), $\text{KO-}t\text{-Bu}$ (10 mol%)	[117]
$[\text{RuH}_2(\text{PPh}_3)_4]$ (5 mol%), 35b (5 mol%), MeCN (5 mol%), NaH (20 mol%)	[118, 119]
$[\text{RuCl}_2(\text{LiPr})(\eta^6\text{-}p\text{-cymene})]$ (5 mol%), $\text{PCy}_3 \cdot \text{HBF}_4$ (5 mol%), $\text{KO-}t\text{-Bu}$ (15 mol%) ^b	[120]
$[\text{Ru}(\eta^3\text{-C}_3\text{H}_4\text{Me})_2(\text{cod})]$ (0.2–1 mol%), 36 (0.26–1.3 mol%), 20 h	[121]
$[\text{Ru}_3(\text{CO})_{12}]$ (1.5 mol% Ru), 37 (3 mol%), in cyclohexane at 140 °C for 21 h	[122]
$[\{\text{RuCl}(\mu\text{-Cl})(\eta^6\text{-}p\text{-cymene})\}_2]$ (5 mol% Ru), dppb (5 mol%), Cs_2CO_3 (10 mol%), 3-methyl-2-butanone (2.5 equiv.) as H_2 -acceptor, in $t\text{-BuOH}$ at reflux for 24 h	[123]

^aReactions performed in toluene at 110 °C for 24 h, unless otherwise indicated

^bLiPr = 1,3-diisopropylimidazol-2-ylidene

and amines, such as 2,2-dimethylpropanol, 2-methylbutanol or 2-heptanamine, gave rise to lower conversions than the linear ones [101, 115, 116, 119, 124, 125, 129]. In the same line, cyclic secondary amines (e.g., morpholine, piperidine, or *N*-methylpiperazine) provided the corresponding tertiary amides in good yields, while the non-cyclic ones, more sterically hindered, resulted poorly reactive or even totally inactive [114, 115]. For these latter substrates, some yield improvements have been recently achieved using less sterically congested catalysts. For example, modest to good yields were obtained with the ruthenium complex **39** (Fig. 10) bearing diphenylphosphino- and pyridyl-fragments, whereas the related compounds **28** and **29**, with bigger (*t*-Bu)₂P and NEt₂ groups resulted inoperative under the same reaction conditions [129].

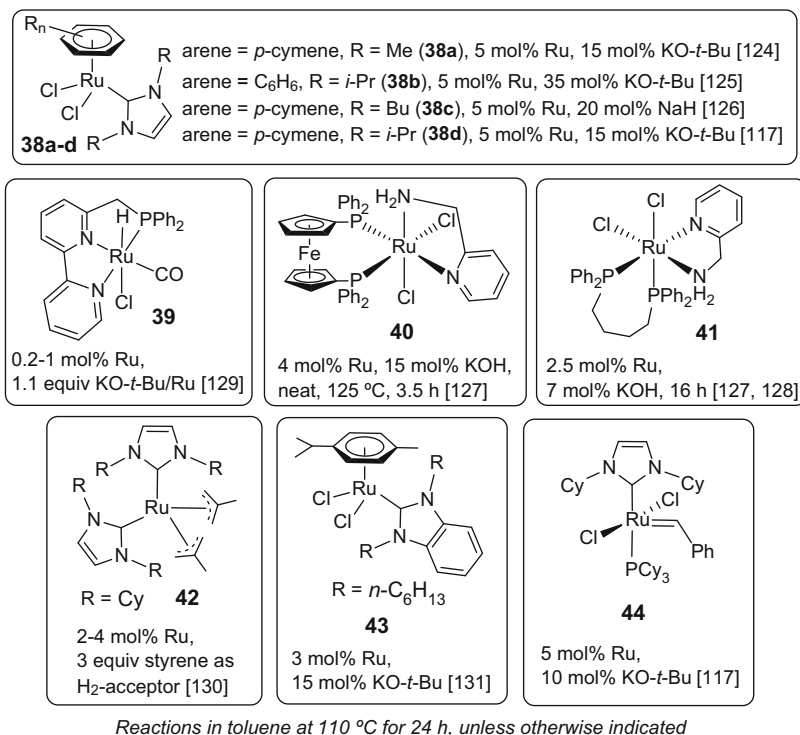
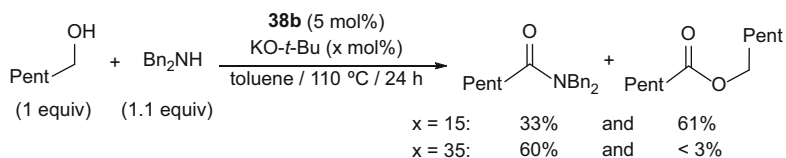
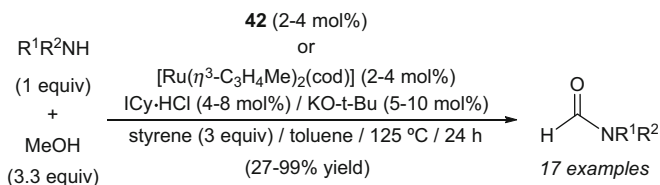


Fig. 10 Structure of well-defined ruthenium catalysts employed in the dehydrogenative amidation of alcohols and experimental conditions



Scheme 24 Effect of the base loading on the synthesis of tertiary amides

High base loadings also showed to favor the dehydrogenative coupling of alcohols with hindered secondary amines [125]. Thus, reactions promoted by complex [RuCl₂(η⁶-C₆H₆)(*i*Pr)] (**38b**) in combination with 35 mol% of KO-*t*-Bu led to the desired tertiary amides, while the use of only 15 mol% of KO-*t*-Bu resulted in the major formation of esters (Scheme 24). The authors suggested that, in this case, the synthesis of amides takes place through the initial formation of the esters, which further react with the amines (Scheme 19). Accordingly, they evidenced that the direct transformation of esters into amides promoted by **38b** was clearly accelerated by adding large amounts of a base to the reaction medium (see Sect. 5.3).



Scheme 25 Ruthenium-catalyzed *N*-formylation of primary and secondary amines

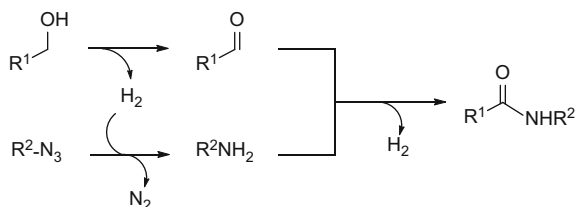
On the other hand, the dehydrogenative amidation proved to be also sensitive to the electronic properties of the amines. Thus, with electron-poor amines, which display a low nucleophilic character, the formation of the hemiaminal intermediate is disfavored. As a consequence, substrates like anilines usually lead to low or moderate conversions, even at elevated temperatures or after long reaction periods, and large amounts of the corresponding esters by-products are formed. In this context, the ruthenium catalysts have conducted, in general, to quite disappointing results [114, 115, 117, 124]. In fact, only gold nanoparticles have proven to be useful with this type of amines [132].

Methanol also represents a challenging substrate for dehydrogenative amidations due to its high energy activation barrier. Till now, only one ruthenium-based catalytic system, developed by Glorius and co-workers, proved to be suitable for the amidation of methanol [130]. Thus, using 2–4 mol% of the preformed or in-situ generated complex **42**, a variety of primary and secondary amines could be cleanly converted into the corresponding formamides (Scheme 25). Although catalyst **42** could operate without a hydrogen acceptor, highest conversions were reached in the presence of 3 equiv. of styrene.

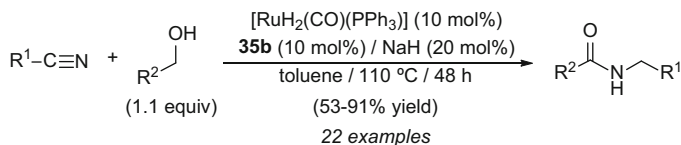
Gold- and rhodium-catalyzed acylations of ammonia have been reported [112, 132], but similar transformations promoted by homogeneous ruthenium catalysts still remain unknown. Such a reaction could only be performed employing a heterogeneous ruthenium-based system under aerobic conditions. However, a completely different mechanism operates in this case (see Sect. 6) [133].

Interestingly, Hong and co-workers have also demonstrated that the amidation of alcohols can be satisfactorily performed using azides instead of amines as the nitrogen source [134]. The reactions were carried out with 5 mol% of the ruthenium-dihydride complex $[\text{RuH}_2(\text{PPh}_3)_4]$ associated with 1,3-diisopropylimidazolium bromide (**35b** in Table 1; 5 mol%), acetonitrile (5 mol%), and NaH (20 mol%) in refluxing toluene for 48 h. The proposed mechanism involves again the initial dehydrogenation of the primary alcohol into an aldehyde. The hydrogen released in this step reduces the azide, thus generating in situ the corresponding amine (Scheme 26). Interestingly, this methodology offered an easy entry to ^{15}N -labeled amides starting from ^{15}N -azides, which are readily accessible from alkyl halides and commercially available ^{15}N -labeled NaN_3 [134].

More recently, the same authors have extended their studies to the synthesis of amides from alcohols and nitriles, via formation of a transient hemiaminal intermediate (Scheme 27) [135]. Among the different catalysts tested, the best



Scheme 26 Proposed mechanism for the dehydrogenative amidation of alcohols with azides



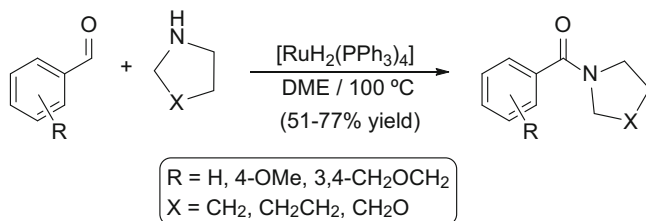
Scheme 27 Ruthenium-catalyzed synthesis of amides from alcohols and nitriles

performances were reached with the dihydride-ruthenium derivative $[\text{RuH}_2(\text{CO})(\text{PPh}_3)_3]$. This synthetic methodology also offered an easy access to ^{13}C - and ^{15}N -labeled amides from isotopically enriched nitriles.

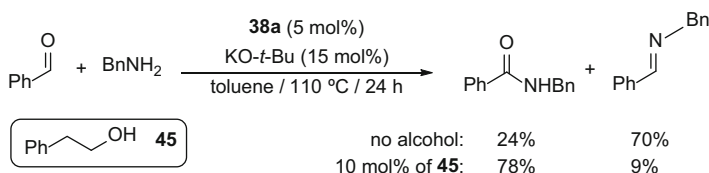
5.2 Starting from Aldehydes

Since formation of an aldehyde intermediate constitutes the first step in the dehydrogenative amidation of alcohols, one might anticipate that similar processes would also readily take place starting directly from aldehydes. However, most of the ruthenium catalysts described in the previous section showed limited or no activity in the amidation of aldehydes. This discrepancy suggests that, in the amidation of alcohols, the aldehyde intermediate remains coordinated to the ruthenium center during the catalytic cycle. In addition, starting from aldehydes, imines are usually the major reaction products observed, evidencing that the dehydration of the hemiaminal intermediate prevails towards the dehydrogenation (Scheme 19). However, selective formation of amides occurs when the own structure of the substrates precludes the generation of imine or enamine derivatives (i.e., when $\text{R}^3 \neq \text{H}$ or $\text{R}^1 \neq \text{CHR}^4\text{R}^5$ in Scheme 19). Thus, in 1991, Murahashi and co-workers reported the synthesis of different benzamides by coupling benzaldehydes with secondary amines [99]. The process, promoted by $[\text{RuH}_2(\text{PPh}_3)_4]$, afforded the corresponding tertiary benzamides in moderate to good yields (Scheme 28).

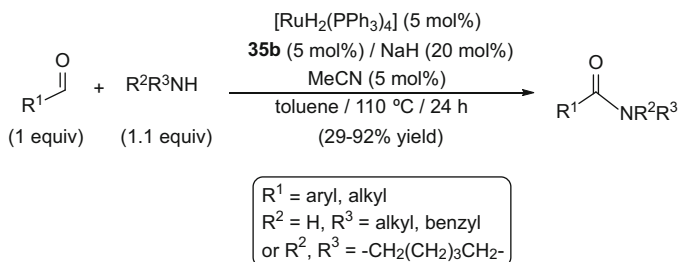
Interestingly, Hong and co-workers evidenced that the selectivity of the coupling between aldehydes and amines can be modified by adding small amounts of an alcohol to the reaction medium (Scheme 29) [124]. Thus, with the same catalytic system, imine formation was favored in absence of alcohol, whereas amide was



Scheme 28 Dehydrogenative amidation of aldehydes promoted by $[\text{RuH}_2(\text{PPh}_3)_4]$



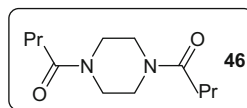
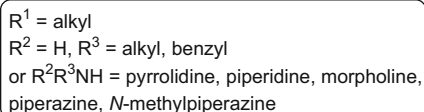
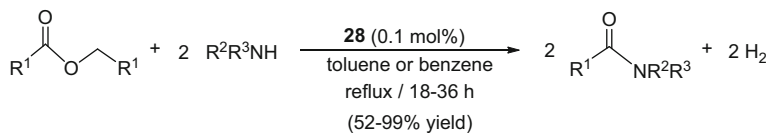
Scheme 29 Influence of an alcohol on the selectivity of the aldehyde amidation processes



Scheme 30 $[\text{RuH}_2(\text{PPh}_3)_4]$ -promoted synthesis of amides from aldehydes

predominantly formed in the presence of 10% of 2-phenylethanol **45**. Under the basic conditions employed, the alcohol presumably generates a metal-hydride via initial formation of an alkoxide-ruthenium complex and subsequent β -elimination. The authors assumed that this hydrido-derivative favors the dehydrogenation of the hemiaminal intermediate in detriment of the dehydration, thus giving rise to the desired amides as the major reaction products.

On this basis, the same authors subsequently developed an effective protocol for synthesizing amides from aldehydes using $[\text{RuH}_2(\text{PPh}_3)_4]$ [119]. In combination with the imidazolium salt **35b** (see Table 1), sodium hydride and acetonitrile, this complex readily converted a variety of aliphatic and aromatic aldehydes into amides (Scheme 30). Further studies on the stoichiometric reactivity of $[\text{RuH}_2(\text{PPh}_3)_4]$ with NaH at 110 °C suggested the formation of ruthenium(0) species during the catalytic events. This proposal was also supported by fact that the ruthenium(0) complexes $[\text{Ru}_3(\text{CO})_{12}]$ and $[\text{Ru}(\text{cod})(\text{cot})]$, associated with **35b**



Scheme 31 Ruthenium-catalyzed synthesis of amides from esters

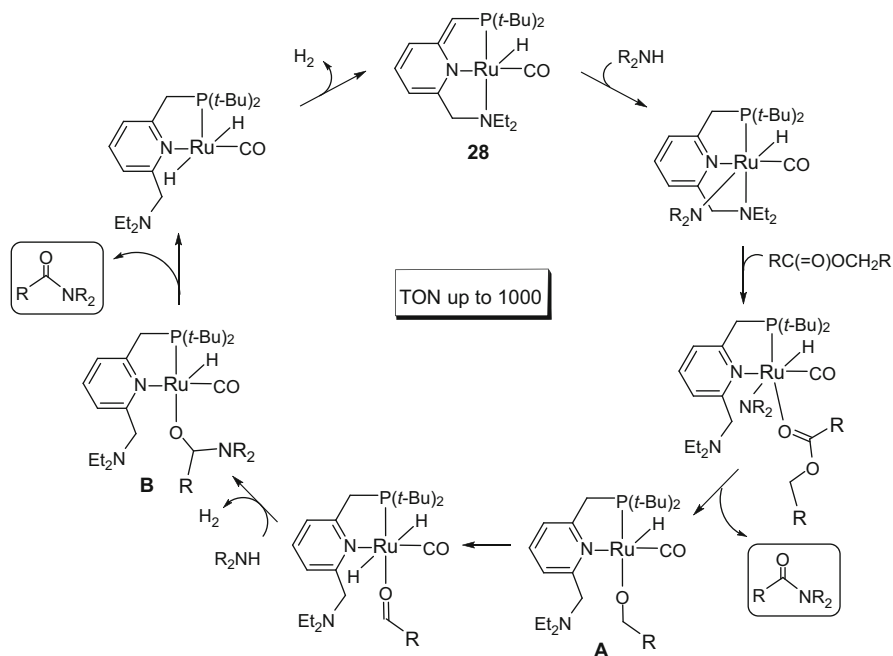
and NaH, proved to be also active in the process. However, using $[\text{Ru}_3(\text{CO})_{12}]$ and $[\text{Ru}(\text{cod})(\text{cot})]$ a large quantity of NaH (40 mol%), more than that required for the generation of the NHC ligand, was needed to achieve good conversions and the reason for this still remains unclear.

5.3 Starting from Esters

The direct conversion of esters into amides is a synthetically useful transformation. However, most of the methodologies developed till now usually require harsh reaction conditions, are poorly compatible with sensitive substrates, and present a low atom economy [136, and references cited therein]. Very recently, Milstein and co-workers demonstrated that esters can be selectively converted into amides generating molecular hydrogen as the only by-product (Scheme 31) [137]. The catalytic reactions were carried out with 2 equiv. of amine per ester in toluene or benzene at reflux in the presence of 0.1 mol% of the dearomatized PNN-pincer ruthenium complex $[\text{RuH}(\text{CO})(\text{PNN})]$ (**28**) (see Scheme 21). Strikingly, both the acyl and the alkoxy units of the starting ester are involved in the amide production. Hence, to avoid mixtures of products, the process was only applied to symmetrical esters. The catalytic protocol was effective for both primary and secondary cyclic amines. In addition, the coupling of piperazine and butylbutyrate provided compound **46**, which results from the bis-acylation of the diamine (Scheme 31).

The proposed mechanism for this transformation involves the initial activation of the N–H bond of the amine assisted by the dearomatized PNN-ligand (Scheme 32). Subsequent coordination of the ester with ruthenium, and coupling with the amido ligand, leads to the alkoxy intermediate **A** with concomitant release of 1 equiv. of amide. Subsequent β -elimination and further nucleophilic attack of the amine to the resulting aldehyde give rise to the hemiaminal **B**, which evolves releasing a second equivalent of the amide. The active species is then regenerated, via deprotonation of the PNN-ligand, with H_2 liberation.

Shortly afterward, Hong and co-workers reported another ruthenium-based catalytic system able to promote the transformation of esters into amides

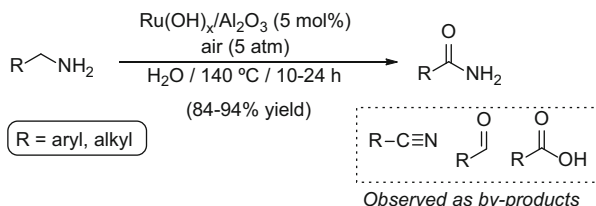


Scheme 32 Proposed mechanism for the ruthenium-catalyzed dehydrogenative amidation of esters

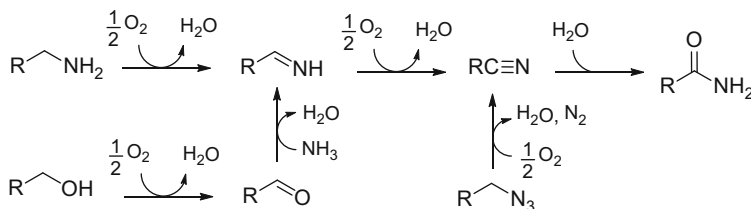
[125]. Their study, which was focused on the reaction of the hexylhexanoate with the dibenzylamine, evidenced that the presence of a large amount of base favors the generation of the amide. Thus, while the use of 5 mol% of $[\text{RuCl}_2(\eta^6\text{-C}_6\text{H}_6)(\text{I}i\text{Pr})]$ (**38b**) and 20 mol% of $\text{KO}-t\text{-Bu}$ produced the corresponding amide in only 6% yield, an increase of the base loading to 40 mol% resulted in a considerable improvement of the efficiency, giving rise to a conversion of 59%.

6 Other Ruthenium-Catalyzed Amide-Bond Forming Reactions

Although amides have occasionally been reported as by-products during oxidation processes involving amines, this synthetic route remains extremely challenging [138, 139]. The oxyfunctionalization of the α -methylene group of amines RCH_2NH_2 usually requires the use of stoichiometric amounts of a strong oxidant, which renders mandatory the protection of the NH_2 group. In this context, Mizuno and co-workers have developed a more attractive protocol based on the direct oxidation of CH_2 group using air as the sole oxidant (Scheme 33) [140]. The process, performed in water under air pressure (5 atm) at 140°C , could be catalyzed



Scheme 33 Direct oxidation of primary amines into amides

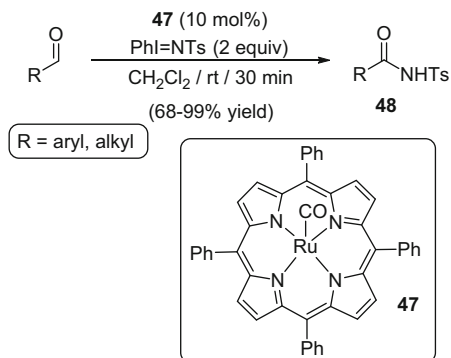


Scheme 34 Proposed pathways for amide formation through oxidative processes involving amines, azides and alcohols

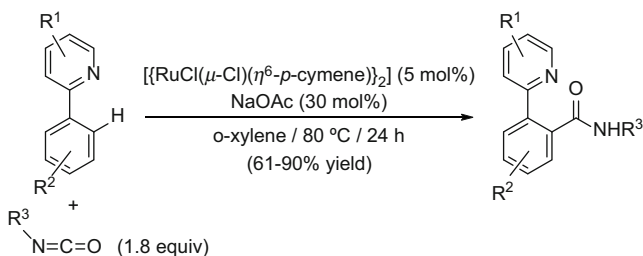
by different ruthenium compounds such as RuCl_3 , $[\text{Ru}(\text{acac})_3]$, $[\text{RuCl}_2(\text{PPh}_3)_3]$, $[\{\text{RuCl}(\mu\text{-Cl})(\eta^6\text{-}p\text{-cymene})\}_2]$, and $[\text{Ru}_3(\text{CO})_{12}]$, but much higher selectivities were achieved with the heterogeneous system $\text{Ru}(\text{OH})_x/\text{Al}_2\text{O}_3$. Under optimal conditions, several benzyl- or alkyl-amines produced predominantly the corresponding primary amides, with traces of the nitriles, aldehydes, and carboxylic acids being formed as by-products. Interestingly, the catalytic system could be separated by simple filtration and reused without significant loss in activity. A reaction pathway involving the successive oxidative dehydrogenation of the amine into the corresponding imine and nitrile, which is subsequently hydrated, was proposed by the authors (Scheme 34) [139, 140]. A related one-pot sequential process has also been described using the ruthenium-substituted hydroxyapatite $((\text{RuCl})_2\text{Ca}_8(\text{PO}_4)_6(\text{OH})_2)$ as catalyst [65].

As the amines, benzylic and aliphatic azides could also be transformed into the corresponding primary amides through aerobic oxidation in water by means of $\text{Ru}(\text{OH})_x/\text{Al}_2\text{O}_3$ [141]. Once again, the process proceeded via the formation of a nitrile intermediate (Scheme 34), with concomitant release of water and nitrogen gas. Primary amides were also synthesized from benzylic alcohols and ammonia using $\text{Ru}(\text{OH})_x/\text{Al}_2\text{O}_3$ under air pressure [133]. In this case, the proposed mechanism is based on the following steps: (1) the dehydrogenation of the alcohol into an aldehyde, (2) the condensation of the aldehyde with NH_3 , (3) oxidation of the resulting imine to generate a nitrile, and (4) final hydration of the nitrile to generate the corresponding primary amide (Scheme 34).

On the other hand, unprecedented amidations of aldehydes involving nitrogen-atom transfer reactions to the acyl $\text{C}(\text{sp}^2)\text{-H}$ bond have been reported by Chan and co-workers [142]. As shown in Scheme 35, the treatment of aliphatic and aromatic



Scheme 35 Catalytic synthesis of amides through the activation of the acyl C-H bond of aldehydes

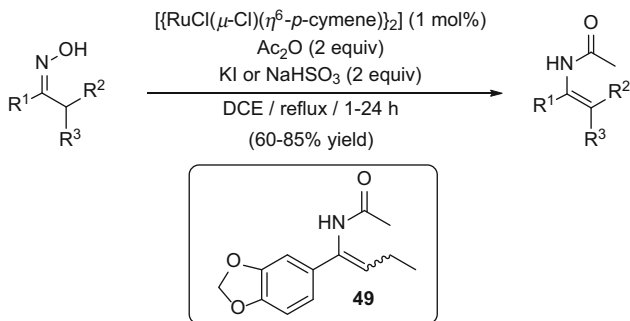


Scheme 36 Catalytic formation of amides by isocyanate insertion into C-H bonds

aldehydes with two-fold excess of PhI=NTs, in the presence of 10 mol% of the porphyrin-ruthenium(II) complex **47**, readily afforded the corresponding acylsulfonamides **48** in high yield. Remarkably, chemoselective processes were observed even for aldehydes containing benzylic C-H or C=C bonds, known to be reactive against PhI=NTs.

C-H bond activation was also involved in the reactions of 2-arylpyridines with isocyanates promoted by the dimeric precursor $[\{\text{RuCl}(\mu\text{-Cl})(\eta^6\text{-}p\text{-cymene})\}_2]$ (Scheme 36) [143]. The process was satisfactorily applied to the synthesis of a wide range (22 examples) of pyridyl-functionalized benzamides. Arylpyridines with both electron-donating and electron-withdrawing substituents were suitable substrates, and classical organic functional groups such as ether, halogen, aldehyde, or cyano were tolerated. Notably, when the aryl ring presented an unsymmetrical substitution pattern, the C-H activation took place at the less hindered position selectively.

Metal-catalyzed reductive acylation reactions of ketoximes into *N*-acetyl enamides are known for long time [144, and references cited therein]. Recently, an example promoted by the ruthenium dimer $[\{\text{RuCl}(\mu\text{-Cl})(\eta^6\text{-}p\text{-cymene})\}_2]$ has been described (Scheme 37) [145]. Remarkably, the process was successfully applied to the synthesis of **49**, a key intermediate in the preparation of leukocyte elastase inhibitor DMP 777.



Scheme 37 Ruthenium-catalyzed reductive acylation of ketoximes

7 Conclusion

In the last years there has been an increasing interest in applying catalytic methods for amide formation since, compared to classical amide couplings involving carboxylic acids and their derivatives with amines, they are more environmentally sustainable and cost effective. Ruthenium catalysts have played a key role in advancing this field, and in many cases have led to pioneer transformations. Throughout this chapter we have tried to highlight the utility and the huge potential of these catalysts. The range of methods currently available allows synthetic chemists choosing from a wide variety of starting materials for the construction of amide bonds (nitriles, aldoximes, primary alcohols, aldehydes, esters, etc.). Obviously the field remains open and hopefully more active catalysts for known processes, as well as new innovative transformations, will see the light in the coming years. We hope that reading this chapter serves as a catalyst and inspires future developments.

Acknowledgments Our research in the field of amide-bond forming reactions was supported by MINECO of Spain (projects CTQ2006-08485/BQU, CTQ2010-14796/BQU and CSD2007-00006). We heartily wish to thank our co-workers Dr. Javier Francos and Dr. Rocío García-Álvarez for their strong commitment to this chemistry.

References

1. Zabicky J (1970) The chemistry of amides. Wiley, New York
2. Greenberg A, Breneman CM, Liebman (2000) The amide linkage: structural significance in chemistry, biochemistry and materials science. Wiley, New York
3. Dugger RW, Ragan JA, Ripin DHB (2005) Survey of GMP bulk reactions run in a research facility between 1985 and 2002. *Org Process Res Dev* 9:253
4. Carey JS, Laffan D, Thomson C, Williams TM (2006) Analysis of the reactions used for the preparation of drug candidate molecules. *Org Biomol Chem* 4:2337

5. Ghose AK, Viswanadhan VN, Wendoloski JJ (1999) A knowledge-based approach in designing combinatorial or medicinal chemistry libraries for drug discovery. 1. A qualitative and quantitative characterization of known drug databases. *J Comb Chem* 1:55
6. Montalbetti CAGN, Falque V (2005) Amide bond formation and peptide coupling. *Tetrahedron* 61:10827
7. Valeur E, Bradley M (2009) Amide bond formation: beyond the myth of coupling reagents. *Chem Soc Rev* 38:606
8. Constable DJC, Dunn PJ, Hayler JD, Humphrey GR, Leazer JL, Linderman RJ, Lorenz K, Manley J, Pearlman BA, Wells A, Zaks A, Zhang TY (2007) Key green chemistry research areas – a perspective from pharmaceutical manufacturers. *Green Chem* 9:411
9. Allen CL, Williams MJM (2011) Metal-catalysed approaches to amide bond formation. *Chem Soc Rev* 40:3405
10. Pattabiraman VR, Bode JW (2011) Rethinking amide bond synthesis. *Nature* 480:471
11. Roy S, Roy S, Gribble GW (2012) Metal-catalyzed amidation. *Tetrahedron* 68:9867
12. García-Álvarez R, Crochet P, Cadierno V (2013) Metal-catalyzed amide bond forming reactions in an environmentally friendly aqueous medium: Nitrile hydrations and beyond. *Green Chem* 15:46
13. Bode JW (2013) Reinventing amide bond formation. *Top Organomet Chem* 44:13
14. Singh C, Kumar V, Sharma U, Kumar N, Singh B (2013) Emerging catalytic methods for amide synthesis. *Curr Org Synth* 10:241
15. Yamada H, Kobayashi M (1996) Nitrile hydratase and its application to industrial production of acrylamide. *Biosci Biotech Biochem* 60:1391
16. Tao J, Xu JH (2009) Biocatalysis in development of green pharmaceutical processes. *Curr Opin Chem Biol* 13:45
17. Sanchez S, Demain AL (2011) Enzymes and bioconversions of industrial, pharmaceutical, and biotechnological significance. *Org Process Res Dev* 15:224
18. Li B, Su J, Tao J (2011) Enzyme and process development for production of nicotinamide. *Org Process Res Dev* 15:291
19. Kopylovich MN, Kukushkin VY, Haukka M, Fraústo da Silva JJR, Pombeiro AJL (2002) Zinc(II)/ketoxime system as a simple and efficient catalyst for hydrolysis of organonitriles. *Inorg Chem* 41:4789
20. Kukushkin VY, Pombeiro AJL (2002) Additions to metal-activated organonitriles. *Chem Rev* 102:1771
21. Kukushkin VY, Pombeiro AJL (2005) Metal-mediated and metal-catalyzed hydrolysis of nitriles. *Inorg Chim Acta* 358:1
22. Ahmed TJ, Knapp SMM, Tyler DR (2011) Frontiers in catalytic nitrile hydration: nitrile and cyanohydrin hydration catalyzed by homogeneous organometallic complexes. *Coord Chem Rev* 255:949
23. Murahashi SI, Sasao S, Saito E, Naota T (1992) Ruthenium-catalyzed hydration of nitriles and transformation of δ -keto nitriles to ene-lactams. *J Org Chem* 57:2521
24. Murahashi SI, Sasao S, Saito E, Naota T (1993) Ruthenium-catalyzed hydration of nitriles and transformation of δ -keto nitriles to ene-lactams: Total synthesis of (–)-pumiliotoxin C. *Tetrahedron* 49:8805
25. Murahashi SI, Naota T (1996) A new way for efficient catalysis by using low valent ruthenium complexes as redox Lewis acid and base catalysts. *Bull Chem Soc Jpn* 69:1805
26. Murahashi SI, Takaya H (2000) Low-valent ruthenium and iridium hydride complexes as alternatives to Lewis acid and base catalysts. *Acc Chem Res* 33:225
27. Fung WK, Huang X, Man ML, Ng SM, Hung MY, Lin Z, Lau CP (2003) Dihydrogen-bond-promoted catalysis: Catalytic hydration of nitriles with the indenylruthenium hydride complex (η^5 -C₉H₇)Ru(dppm)H (dppm = bis(diphenylphosphino)methane). *J Am Chem Soc* 125:11539
28. Leung CW, Zheng W, Wang D, Ng SM, Yeung CH, Zhou Z, Lin Z, Lau CP (2007) Catalytic H/D exchange between organic compounds and D₂O with TpRu(PPh₃)(CH₃CN)H

- (Tp = hydro(trispyrazolyl)borate). Reaction of $\text{TpRu}(\text{PPh}_3)(\text{CH}_3\text{CN})\text{H}$ with water to form acetamido complex $\text{TpRu}(\text{PPh}_3)(\text{H}_2\text{O})(\text{NHC}(\text{O})\text{CH}_3)$. *Organometallics* 26:1924
29. Leung CW, Zheng W, Zhou Z, Lin Z, Lau CP (2008) Mechanism of catalytic hydration of nitriles with hydrotris(pyrazolyl)borato (Tp) ruthenium complexes. *Organometallics* 27:4957
 30. Li T, Bergner I, Haque FN, Zimmer-De Iulius M, Song D, Morris RH (2007) Hydrogenation of benzonitrile to benzylamine catalyzed by ruthenium hydride complexes with P-NH-NH-P tetradentate ligands: evidence for a hydridic-protonic outer sphere mechanism. *Organometallics* 26:5940
 31. Yi CS, Zeczycki TN, Lindeman SV (2008) Kinetic, spectroscopic, and X-ray crystallographic evidence for the cooperative mechanism of the hydration of nitriles catalyzed by a tetranuclear ruthenium- μ -oxo- μ -hydroxo complex. *Organometallics* 27:2030
 32. Utsunomiya M, Takahashi K, Oshiki T, Takai K (2004) New ruthenium complex, method for producing the same and method for producing amide compound using the same. *Jpn Kokai Tokkyo Koho JP 2004269522*
 33. Oshiki T, Yamashita H, Sawada K, Utsunomiya M, Takahashi K, Takai K (2005) Dramatic rate acceleration by a diphenyl-2-pyridylphosphine ligand in the hydration of nitriles catalyzed by $\text{Ru}(\text{acac})_2$ complexes. *Organometallics* 24:6287
 34. Oshiki T, Hyodo I, Ishizuka A (2005) Highly reactive bifunctional chemical catalysts for the hydration of nitriles. *J Synth Org Chem Jpn* 68:41
 35. Oshiki T, Takai K (2008) Method for producing amide compound and catalyst used for the same method. *Jpn Kokai Tokkyo Koho JP 2008088153*
 36. Muranaka M, Hyodo I, Okumura W, Oshiki T (2011) 2-Diphenylphosphanyl-4-pyridyl (dimethyl)amine as an effective ligand for the ruthenium(II) complex catalyzed homogeneous hydration of nitriles under neutral conditions. *Catal Today* 164:552
 37. Šmejkal T, Breit B (2007) Self-assembled bidentate ligands for ruthenium-catalyzed hydration of nitriles. *Organometallics* 26:2461
 38. García-Álvarez R, García-Garrido, SE, Díez J, Crochet P, Cadierno V (2012) Arene-ruthenium (II) and bis(allyl)-ruthenium(IV) complexes containing 2-(diphenylphosphanyl)pyridine ligands: Potential catalysts for nitrile hydration reactions? *Eur J Inorg Chem* 4218
 39. García-Álvarez R, Díez J, Crochet P, Cadierno V (2010) Arene-ruthenium(II) complexes containing amino-phosphine ligands as catalysts for nitrile hydration reactions. *Organometallics* 29:3955
 40. Cadierno V, Francos J, Gimeno J (2008) Selective ruthenium-catalyzed hydration of nitriles to amides in pure aqueous medium under neutral conditions. *Chem Eur J* 14:6601
 41. Cadierno V, Díez J, Francos J, Gimeno J (2010) Bis(allyl)ruthenium(IV) complexes containing water-soluble phosphane ligands: Synthesis, structure, and application as catalysts in the selective hydration of organonitriles into amides. *Chem Eur J* 16:9808
 42. Lee WC, Frost BJ (2012) Aqueous and biphasic nitrile hydration catalyzed by a recyclable Ru(II) complex under atmospheric conditions. *Green Chem* 14:62
 43. Frost BJ, Lee WC (2013) Nitrile hydration catalyzed by recyclable ruthenium complexes. *US Pat Appl US2013/0,096,344*
 44. Lee WC, Sears JM, Enow RA, Eads K, Krogstad DA, Frost BJ (2013) Hemilabile β -aminophosphine ligands derived from 1,3,5-triaza-7-phosphaadamantane: Application in aqueous ruthenium catalyzed nitrile hydration. *Inorg Chem* 52:1737
 45. García-Álvarez R, Zablocka M, Crochet P, Duhayon C, Majoral JP, Cadierno V (2013) Thiazolyl-phosphine hydrochloride salts: effective auxiliary ligands for ruthenium-catalyzed nitrile hydration reactions and related amide bond forming processes in water. *Green Chem* 15:2447
 46. García-Álvarez R, Francos J, Crochet P, Cadierno V (2011) Ibuprofenamide: A convenient method of synthesis by catalytic hydration of 2-(4-isobutylphenyl)propionitrile in pure aqueous medium. *Tetrahedron Lett* 52:4218

47. García-Álvarez R, Díez J, Crochet P, Cadierno V (2011) Arene-ruthenium(II) complexes containing inexpensive tris(dimethylamino)phosphine: Highly efficient catalysts for the selective hydration of nitriles to amides. *Organometallics* 30:5442
48. Knapp SMM, Sherbow TJ, Juliette JJ, Tyler DR (2012) Cyanohydrin hydration with $[\text{Ru}(\eta^6\text{-}p\text{-cymene})\text{Cl}_2\text{PR}_3]$ complexes. *Organometallics* 31:2941
49. Knapp SMM, Sherbow TJ, Yelle RB, Zakharov LN, Juliette JJ, Tyler DR (2013) Mechanistic investigations and secondary coordination sphere effects in the hydration of nitriles with $[\text{Ru}(\eta^6\text{-arene})\text{Cl}_2\text{PR}_3]$ complexes. *Organometallics* 32:824
50. Knapp SMM, Sherbow TJ, Yelle RB, Juliette JJ, Tyler DR (2013) Catalytic nitrile hydration with $[\text{Ru}(\eta^6\text{-}p\text{-cymene})\text{Cl}_2(\text{PR}_2\text{R}')]]$ complexes: Secondary coordination sphere effects with phosphine oxide and phosphinite ligands. *Organometallics* 32:3744
51. Oshiki T, Muranaka M (2012) Metal complex compound and amide production method that utilizes said metal complex compound. PCT Int Appl WO2012/017966
52. Ashraf SM, Berger I, Nazarov AA, Hartinger CG, Koroteev MP, Nifantev EE, Keppler BK (2008) Phosphite-derivatized ruthenium-carbohydrate complexes in the catalytic hydration of nitriles. *Chem Biodiversity* 5:1640
53. Ashraf SM, Kandioller W, Mendoza-Ferri MG, Nazarov AA, Hartinger CG, Keppler BK (2008) The hydration of chloroacetonitriles catalyzed by mono- and dinuclear Ru^{II} - and Os^{II} -arene complexes. *Chem Biodiversity* 5:2060
54. Martín M, Horváth H, Sola E, Kathó Á, Joó F (2009) Water-soluble triisopropylphosphine complexes of ruthenium(II): synthesis, equilibria, and acetonitrile hydration. *Organometallics* 28:561
55. Cavarzan A, Scarso A, Strukul G (2010) Efficient nitrile hydration mediated by Ru^{II} catalysts in micellar media. *Green Chem* 12:790
56. Ferrer Í, Rich J, Fontrodona X, Rodríguez M, Romero I (2013) Ru(II) complexes containing dmsol and pyrazolyl ligands as catalysts for nitrile hydration in environmentally friendly media. *Dalton Trans* 42:13461
57. Kumar D, Masitas CA, Nguyen TN, Grapperhaus GA (2013) Bioinspired catalytic nitrile hydration by dithiolato, sulfinato/thiolato, and sulfenato/sulfinato ruthenium complexes. *Chem Commun* 49:294
58. Ammar HB, Miao X, Fischmeister C, Toupet L, Dixneuf PH (2010) Bidentate oxazoline-imine ruthenium(II) complexes: Intermediates in the methanolysis/hydration of nitrile groups. *Organometallics* 29:4234
59. Kamezaki S, Akiyama S, Kayaki Y, Kuwata S, Ikariya T (2010) Asymmetric nitrile-hydration with bifunctional ruthenium catalysts bearing chiral *N*-sulfonyldiamine ligands. *Tetrahedron Asymmetry* 21:1169
60. Yamaguchi K, Matsushita M, Mizuno N (2004) Efficient hydration of nitriles to amides in water, catalyzed by ruthenium hydroxide supported on alumina. *Angew Chem Int Ed* 43:1576
61. Polshettiwar V, Varma RS (2009) Nanoparticle-supported and magnetically recoverable ruthenium hydroxide catalyst: Efficient hydration of nitriles to amides in aqueous medium. *Chem Eur J* 15:1582
62. Baig RBN, Varma RS (2013) Organic synthesis *via* magnetic attraction: Benign and sustainable protocols using magnetic nanoferrites. *Green Chem* 15:398
63. Baig RBN, Varma RS (2012) A facile one-pot synthesis of ruthenium hydroxide nanoparticles on magnetic silica: Aqueous hydration of nitriles to amides. *Chem Commun* 48:6220
64. García-Garrido SE, Francos J, Cadierno V, Basset JM, Polshettiwar V (2011) Chemistry by nanocatalysis: First example of a solid-supported RAPTA complex for organic reactions in aqueous medium. *ChemSusChem* 4:104
65. Mori K, Yamaguchi K, Mizugaki T, Ebitani K, Kaneda K (2001) Catalysis of a hydroxyapatite-bound Ru complex: efficient heterogeneous oxidation of primary amines to nitriles in the presence of molecular oxygen. *Chem Commun* 461

66. Prakash GKS, Munoz SB, Papp A, Masood K, Bychinskaya I, Mathew T, Olah GA (2012) Nafion-Ru: A sustainable catalyst for selective hydration of nitriles to amides. *Asian J Org Chem* 1:146
67. Kurata T, Tamaru A, Murata Y, Nagashima S, Okano T, Ohfucchi K (1973) Unsaturated amides. *Jpn Kokai Tokkyo Koho JP 48054021*
68. Mizuno T (2005) Method for producing amide compounds by hydration reaction of nitrile compounds. *Jpn Kokai Tokkyo Koho JP 2005170821*
69. Oshiki T, Ishizuka A (2009) Method for producing amide compound and catalyst to be used therein. *Jpn Kokai Tokkyo Koho JP 2009214099*
70. Kumar S, Das P (2013) Solid-supported ruthenium(0): An efficient heterogeneous catalyst for hydration of nitriles to amides under microwave irradiation. *New J Chem* 37:2987
71. Cogley CJ, van den Heuvel M, Abbadi A, de Vries JG (2000) Platinum catalysed hydrolytic amidation of unactivated nitriles. *Tetrahedron Lett* 41:2467
72. van Dijk AJM, Duchateau R, Hensen EJM, Meuldijk J, Koning CE (2007) Polyamide synthesis from 6-aminocapronitrile, part 2: Heterogeneously catalyzed nitrile hydrolysis with consecutive amine amidation. *Chem Eur J* 13:7673
73. Allen CL, Lapkin AA, Williams MJM (2009) An iron-catalysed synthesis of amides from nitriles and amines. *Tetrahedron Lett* 50:4262
74. Tamura M, Tonomura T, Shimizu KI, Satsuma A (2012) CeO₂-catalyzed one-pot selective synthesis of *N*-alkyl amides from nitriles, amines and water. *Appl Catal A Gen* 417–418:6
75. Davulcu S, Allen CL, Milne K, Williams MJM (2013) Catalytic conversion of nitriles into secondary- and tertiary amides. *ChemCatChem* 5:435
76. Li X, Li Z, Deng H, Zhou X (2013) An efficient protocol for the preparation of amides by copper-catalyzed reactions between nitriles and amines in water. *Tetrahedron Lett* 54:2212
77. Ghodsinia SSE, Akhlaghinia B, Safaei E, Eshghi H (2013) Green and selective synthesis of *N*-substituted amides using water-soluble porphyrinato copper(II) catalyst. *J Braz Chem Soc* 24:895
78. Murahashi SI, Naota T, Saito E (1986) Ruthenium-catalyzed amidation of nitriles with amines. A novel, facile route to amides and polyamides. *J Am Chem Soc* 108:7846
79. van Dijk AJM, Heyligen T, Duchateau R, Meuldijk J, Koning CE (2007) Polyamide synthesis from 6-aminocapronitrile, part 1: *N*-alkyl amide formation by amine amidation of a hydrolyzed nitrile. *Chem Eur J* 13:7664
80. Field L, Hughmark PB, Shumaker SH, Marshall WS (1961) Isomerization of aldoximes to amides under substantially neutral conditions. *J Am Chem Soc* 83:1983
81. Park S, Choi Y, Han H, Yang SH, Chang S (2003) Rh-catalyzed one-pot and practical transformation of aldoximes to amides. *Chem Commun* 1936
82. Allen CL, Lawrence R, Emmett L, Williams MJM (2011) Mechanistic studies into metal-catalyzed aldoxime to amide rearrangement. *Adv Synth Catal* 353:3262
83. Okano T, Fujiwara K, Konishi H, Kiji J (1982) Application of the water-gas shift reaction. III. Reduction of oxidized nitrogen compounds with CO and H₂O catalyzed by [Ru(cod)py₄] (BPh₄)₂. *Bull Chem Soc Jpn* 55:1975
84. Owston NA, Parker AJ, Williams MJM (2007) Highly efficient ruthenium-catalyzed oxime to amide rearrangement. *Org Lett* 9:3599
85. Gnanamgari D, Crabtree RH (2009) Terpyridine ruthenium-catalyzed one-pot conversion of aldehydes into amides. *Organometallics* 28:922
86. Kumar P, Singh AK, Pandey R, Pandey DS (2011) Bio-catalysts and catalysts based on ruthenium(II) polypyridyl complexes imparting diphenyl-(2-pyridyl)-phosphine as a co-ligand. *J Organomet Chem* 696:3454
87. Raja N, Raja MU, Ramesh R (2012) Ruthenium(II) NNO pincer type catalyst for the conversion of aldehydes to amides. *Inorg Chem Commun* 19:51
88. Prabhu RN, Ramesh R (2012) Ruthenium(II) carbonyl complexes containing benzhydrazone ligands: Synthesis, structure and facile one-pot conversion of aldehydes to amides. *RSC Adv* 2:4515

89. Manikandan R, Prakash G, Kathirvel R, Viswanathamurthi P (2013) Ruthenium(II) carbonyl complexes bearing quinoline-based NNO tridentate ligands as catalyst for one-pot conversion of aldehydes to amides and *O*-allylation of phenols. *Spectrochim Acta A* 116:501
90. Hull JF, Hilton ST, Crabtree RH (2010) A simple Ru catalyst for the conversion of aldehydes or oximes to primary amides. *Inorg Chim Acta* 363:1243
91. García-Álvarez R, Díaz-Álvarez AE, Borge J, Crochet P, Cadierno V (2012) Ruthenium-catalyzed rearrangement of aldoximes to primary amides in water. *Organometallics* 31:6482
92. García-Álvarez R, Díaz-Álvarez AE, Crochet P, Cadierno V (2013) Ruthenium-catalyzed one-pot synthesis of primary amides from aldehydes in water. *RSC Adv* 3:5889
93. Li F, Qu P, Ma J, Zou X, Sun C (2013) Tandem synthesis of *N*-alkylated amides from aldoximes and alcohols by using a Ru/Ir dual-catalyst system. *ChemCatChem* 5:2178
94. Chen C, Hong SH (2011) Oxidative amide synthesis directly from alcohols with amines. *Org Biomol Chem* 9:20
95. Gunanathan C, Milstein D (2013) Applications of acceptorless dehydrogenation and related transformations in chemical synthesis. *Science* 341:249
96. Dobreiner GE, Crabtree RH (2010) Dehydrogenation as a substrate-activating strategy in homogeneous transition-metal catalysis. *Chem Rev* 110:681
97. Gnanaprakasam B, Zhang J, Milstein D (2010) Direct synthesis of imines from alcohols and amines with liberation of H₂. *Angew Chem Int Ed* 49:1468
98. Marr AC (2012) Organometallic hydrogen transfer and dehydrogenation catalysts for the conversion of bio-renewable alcohols. *Catal Sci Technol* 2:279
99. Naota T, Murahashi SI (1991) Ruthenium-catalyzed transformations of amino alcohols to lactams. *Synlett* 693
100. Fujita K-I, Takahashi Y, Owaki M, Yamamoto K, Yamaguchi R (2004) Synthesis of five-, six-, and seven-membered ring lactams by Cp*Rh complex-catalyzed oxidative *N*-heterocyclization of amino alcohols. *Org Lett* 6:2785
101. Gunanathan C, Ben-David Y, Milstein D (2007) Direct synthesis of amides from alcohols and amines with liberation of H₂. *Science* 317:790
102. Gunanathan C, Milstein D (2011) Bond activation by metal-ligand cooperation: Design of “green” catalytic reactions based on aromatization-dearomatization of pincer complexes. *Top Organomet Chem* 37:55
103. Gunanathan C, Milstein D (2011) Metal-ligand cooperation by aromatization-dearomatization: a new paradigm in bond activation and “green” catalysis. *Acc Chem Res* 44:588
104. Milstein D (2010) Discovery of environmentally benign catalytic reactions of alcohols catalyzed by pyridine-based pincer Ru complexes, based on metal-ligand cooperation. *Top Catal* 53:915
105. Li H, Wang X, Huang F, Lu G, Jiang J, Wang ZX (2011) Computational study on the catalytic role of pincer ruthenium(II)-PNN complex in directly synthesizing amide from alcohol and amine: the origin of selectivity of amide over ester and imine. *Organometallics* 30:5233
106. Zeng G, Li S (2011) Insights into dehydrogenative coupling of alcohols and amines catalyzed by a (PNN)-Ru(II) hydride complex: unusual metal-ligand cooperation. *Inorg Chem* 50:10572
107. Cho D, Ko KC, Lee JY (2013) Catalytic mechanism for the ruthenium-complex-catalyzed synthesis of amides from alcohols and amines: a DFT study. *Organometallics* 32:4571
108. Zeng H, Guan Z (2011) Direct synthesis of polyamides via catalytic dehydrogenation of diols and diamines. *J Am Chem Soc* 133:1159
109. Gnanaprakasam B, Balaraman E, Gunanathan C, Milstein D (2012) Synthesis of polyamides from diols and diamines with liberation of H₂. *J Poly Sci Part A Polymer Chem* 50:1755
110. Milstein D, Balaraman E, Gunanathan C, Gnanaprakasam B, Zhang J (2012) Novel ruthenium complexes and their uses in processes for formation and/or hydrogenation of esters, amides and derivatives thereof. *PCT Int Appl WO* 2012052996

111. Gnanaprakasam B, Balaraman E, Ben-David Y, Milstein D (2011) Synthesis of peptides and pyrazines from β -amino alcohols through extrusion of H_2 catalyzed by ruthenium pincer complexes: Ligands-controlled selectivity. *Angew Chem Int Ed* 50:12240
112. Zweifel T, Naubron JV, Grützmacher H (2009) Catalyzed dehydrogenative coupling of primary alcohols with water, methanol, or amines. *Angew Chem Int Ed* 48:559
113. Shimizu KI, Ohshima K, Satsuma A (2009) Direct dehydrogenative amide synthesis from alcohols and amines catalyzed by γ -alumina supported silver cluster. *Chem Eur J* 15:9977
114. Nordstrøm LU, Vogt H, Madsen R (2008) Amide synthesis from alcohols and amines by the extrusion of dihydrogen. *J Am Chem Soc* 130:17672
115. Ghosh SC, Muthaiah S, Zhang Y, Xu X, Hong SH (2009) Direct amide synthesis from alcohols and amines by phosphine-free ruthenium catalyst systems. *Adv Synth Catal* 351:2643
116. Ghosh SC, Hong SH (2010) Simple $RuCl_3$ -catalyzed amide synthesis from alcohols and amines. *Eur J Org Chem* 4266
117. Dam JH, Osztrovsky G, Nordstrøm LU, Madsen R (2010) Amide synthesis from alcohols and amines catalyzed by ruthenium *N*-heterocyclic carbene complexes. *Chem Eur J* 16:6820
118. Zhang J, Senthilkumar M, Ghosh SC, Hong SH (2010) Synthesis of cyclic imides from simple diols. *Angew Chem Int Ed* 49:6391
119. Muthaiah S, Ghosh SC, Jee JE, Chen C, Zhang J, Hong SH (2010) Direct amides synthesis from either alcohols or aldehydes with amines: activity of Ru(II) hydride and Ru(0) complexes. *J Org Chem* 75:3002
120. Makarov IS, Frstrup P, Madsen R (2012) Mechanistic investigation of ruthenium-*N*-heterocyclic-carbene-catalyzed amidation of amines with alcohols. *Chem Eur J* 18:15683
121. Prechtl MHG, Wobser K, Theyssen N, Ben-David Y, Milstein D, Leitner W (2012) Direct coupling of alcohols to form esters and amides with evolution of H_2 using in situ formed ruthenium catalysts. *Catal Sci Technol* 2:2039
122. Pingen D, Vogt D (2014) Amino-alcohols cyclization: Selective synthesis of lactams and cyclic amines from amino-alcohols. *Catal Sci Technol* 4:47
123. Watson AJA, Maxwell AC, Williams MJM (2009) Ruthenium-catalyzed oxidation of alcohols into amides. *Org Lett* 11:2667
124. Zhang Y, Chen C, Ghosh SC, Li Y, Hong SH (2010) Well-defined *N*-heterocyclic carbene based ruthenium catalysts for direct amide synthesis from alcohols and amines. *Organometallics* 29:1374
125. Chen C, Zhang Y, Hongs H (2011) *N*-heterocyclic carbene based ruthenium-catalyzed direct amide synthesis from alcohols and secondary amines: involvement of esters. *J Org Chem* 76:10005
126. Prades A, Peris E, Albrecht M (2011) Oxidations and oxidative couplings catalyzed by triazolylidene ruthenium complexes. *Organometallics* 30:1162
127. Schley N, Dobereiner GE, Crabtree RH (2011) Oxidative synthesis of amides and pyrroles via dehydrogenative alcohol oxidation by ruthenium diphosphine diamine complexes. *Organometallics* 30:4174
128. Nova A, Balcells D, Schley ND, Dobereiner GE, Crabtree RH, Eisenstein O (2010) An experimental-theoretical study of the factors that affect the switch between ruthenium-catalyzed dehydrogenative amide formation versus amine alkylation. *Organometallics* 29:6548
129. Srimani D, Balaraman E, Hu P, Ben-David Y, Milstein D (2013) Formation of tertiary amides and dihydrogen by dehydrogenative coupling of primary alcohols with secondary amines catalyzed by ruthenium bipyridine-based pincer complexes. *Adv Synth Catal* 355:2525
130. Ortega N, Richter C, Glorius F (2013) *N*-formylation of amines by methanol activation. *Org Lett* 15:1776
131. Malineni J, Merckens C, Keul H, Möller M (2013) An efficient *N*-heterocyclic carbene based ruthenium-catalyst: application towards the synthesis of esters and amides. *Catal Commun* 40:80

132. Wang Y, Zhu D, Tang L, Wang S, Wang Z (2011) Highly efficient amide synthesis from alcohols and amines by virtue of a water-soluble gold/DNA catalyst. *Angew Chem Int Ed* 50:8917
133. Oishi T, Yamaguchi K, Mizuno N (2010) An efficient one-pot synthesis of nitriles from alcohols or aldehydes with NH_3 catalyzed by a supported ruthenium hydroxide. *Top Catal* 53:479
134. Fu Z, Lee J, Kang B, Hong SH (2012) Dehydrogenative amide synthesis: azide as a nitrogen source. *Org Lett* 14:6028
135. Kang B, Fu Z, Hong SH (2013) Ruthenium-catalyzed redox-neutral and single-step amide synthesis from alcohol and nitrile with complete atom economy. *J Am Chem Soc* 135:11704
136. Varma RS, Naicker KP (1999) Solvent-free synthesis of amides from non-enolizable esters and amines using microwave irradiation. *Tetrahedron Lett* 40:6177
137. Gnanaprakasam B, Milstein D (2011) Synthesis of amides from esters and amines with liberation of H_2 under neutral conditions. *J Am Chem Soc* 133:1682
138. Yamaguchi K, Mizuno N (2010) Green functional group transformations by supported ruthenium hydroxide catalysts. *Synlett* 2365
139. Schümperli MT, Hammond C, Hermans I (2012) Developments in the aerobic oxidation of amines. *ACS Catal* 2:1108
140. Kim JW, Yamaguchi K, Mizuno N (2008) Heterogeneously catalyzed efficient oxygenation of primary amines to amides by a supported ruthenium hydroxide catalyst. *Angew Chem Int Ed* 47:9249
141. He J, Yamaguchi K, Mizuno N (2011) Aerobic oxidative transformation of primary azides to nitriles by ruthenium hydroxide catalyst. *J Org Chem* 76:4606
142. Chang JWW, Chan PWH (2008) Highly efficient ruthenium(II) porphyrin catalyzed amidation of aldehydes. *Angew Chem Int Ed* 47:1138
143. Muralirajan K, Parthasarathy K, Cheng CH (2012) Ru(II)-catalyzed amidation of 2-arylpyridines with isocyanates via C-H activation. *Org Lett* 14:4262
144. Tang W, Capacci A, Sarvestani M, Wei X, Yee NK, Senanayake CH (2009) A facile and practical synthesis of *N*-acetyl enamides. *J Org Chem* 74:9528
145. Murugan K, Huang DW, Chien YT, Liu ST (2013) An efficient preparation of *N*-acetyl enamides catalyzed by Ru(II) complexes. *Tetrahedron* 69:268

Ruthenium(II)-Catalysed sp^2 C–H Bond Functionalization by C–C Bond Formation

Bin Li and Pierre H. Dixneuf

Abstract The selective catalytic activation/functionalization of sp^2 C–H bonds is expected to improve synthesis methods by better step number and atom economy. This chapter describes the recent achievements of ruthenium(II) catalysed transformations of sp^2 C–H bonds for cross-coupled C–C bond formation. First arylation and heteroarylation with aromatic halides of a variety of (hetero)arenes, that are directed at *ortho* position by heterocycle or imine groups, are presented. The role of carboxylate partners is shown for Ru(II) catalysts that are able to operate profitably in water and to selectively produce diarylated or monoarylated products. The alkylation of (hetero)arenes with primary and secondary alkylhalides, and by hydroarylation of alkene C=C bonds is presented. The recent access to functional alkenes via oxidative dehydrogenative functionalization of C–H bonds with alkenes first, and then with alkynes, is shown to be catalysed by a Ru(II) species associated with a silver salt in the presence of an oxidant such as $Cu(OAc)_2$. Finally the catalytic oxidative annulations with alkynes to rapidly form a variety of heterocycles are described by initial activation of C–H followed by that of N–H or O–H bonds and by formation of a second C–C bond on reaction with C=O, C=N, and sp^3 C–H bonds. Most catalytic cycles leading from C–H to C–C bond are discussed.

B. Li

School of Chemical and Environmental Engineering, Wuyi University, Jiangmen, 529020 Guangdong Province, P.R. China

Institut Sciences Chimiques de Rennes, UMR 6226 CNRS-Université de Rennes, “Organometallics: Materials and Catalysis” Centre for Catalysis and Green Chemistry, Campus de Beaulieu, 35042 Rennes, France

P.H. Dixneuf (✉)

Institut Sciences Chimiques de Rennes, UMR 6226 CNRS-Université de Rennes, “Organometallics: Materials and Catalysis” Centre for Catalysis and Green Chemistry, Campus de Beaulieu, 35042 Rennes, France
e-mail: Pierre.dixneuf@univ-rennes1.fr

Keywords Alkene hydroarylation · Alkenylation · Alkylation · Alkyne hydroarylation · Annulations · Arylation · C–C bond cross-couplings · Heteroarylation · Ruthenium(II) catalysis · sp^2 C–H bond activation

Contents

1	Introduction	120
2	Ruthenium (II)-Catalysed Arylation of Arenes and Heteroarenes via sp^2 C–H Bond Activation	122
2.1	Arylation of Functional (Hetero)arenes with (Hetero)arylhalides	122
2.2	Arylation with Aryl Tosylates and Phenols	140
2.3	Arylation with Boronic Acids	141
3	Ruthenium(II)-Catalysed Alkylation of Alkenes and (Hetero)arenes	142
3.1	Alkylation of (Hetero)arenes with Alkylhalides	142
3.2	Hydroarylation of Alkenes	145
3.3	Alkylation of (Hetero)arenes and Alkenes with Alcohols	149
4	Electrophilic Substitutions of Arenes with Ruthenium(II) and C–H Bond Activation ...	151
5	Synthesis of Alkenylated (Hetero)arenes with Ruthenium(II) Catalysts	153
5.1	Ruthenium-Catalysed Alkenylation of sp^2 C–H Bonds with Functional Alkenes ..	153
5.2	Hydroarylation of Alkynes	170
5.3	Prenylation of Heteroarenes with Allyl Derivatives	172
6	Ruthenium(II)-Catalysed Annulations with Alkynes	174
6.1	Annulation with Alkynes and C–H Bond Activation: Formation of C–C and C–N Bonds	174
6.2	Annulation with Alkynes and C–H Bond Activation: Formation of C–C and C–O Bonds	181
6.3	Annulation with Alkynes and C–H Bond Activation: Formation of Two C–C Bonds	183
7	Conclusion	188
	References	189

1 Introduction

The metal activation of sp^2 C–H bonds is offering a high potential for direct catalytic cross-couplings of C–C bonds that have already found many applications in the building of complex molecules for medicine, natural product synthesis, and for access to molecular materials especially for the creation or modification of optical properties. The C–C bond cross-couplings from C–H bonds have the potential to replace, with better atom and energy economy, the classical, very useful catalytic cross-couplings between a stoichiometric amount of an organometallic RM (M: Li, MgX, ZnX, BR₂, SnR₃, SiR₃...) and with an organic halide. Initiated in 1972 and progressively improved during the last four decades, the Tamao–Kumada–Corriu coupling, first based on nickel(0) and then on palladium(0) catalysts [1, 2], but also the Negishi [3], Sonogashira [4], Stille [5], Miyaura–Suzuki [6], and Hiyama [7] coupling reactions have brought a revolution in organic synthesis. However, they require the preliminary preparation of one and often 2 equiv. of organometallic compounds. On the contrary, the C–C bond cross-couplings from

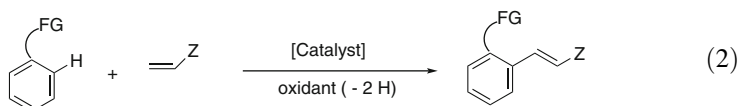
C–H bonds only require the addition of a base to neutralize the generated acid HX, thus constitute more environment-friendly and atom economy processes.

Initially palladium [8–15] and rhodium [15–23] catalysts have tremendously contributed to C–C bond cross-couplings from C–H bonds, under mild conditions and with excellent regioselectivity when an inert to metal functional group, thus becoming a directing group, was present in the substrate. Several reviews have presented the first discoveries and the high potential of these fast developing synthetic methods [24–35]. Various metal catalysts are now contributing to this field [11, 35], including ruthenium(0) catalysts [36–41], that are lower cost catalysts, have been shown by the Murai group since 1993 [36], to generate sp^2 C–Ru–H reactive species offering a variety of new catalytic functionalization of arenes, heteroarenes or olefin C–H bonds [36–41].

During the last decade, following the pioneer discoveries by Oi and Inoue starting in 2001 [42, 43], easy to prepare ruthenium(II) catalysts have been shown to promote sp^2 C–H bond catalytic transformations. Ruthenium(II)-catalysed arylation, heteroarylation, even alkylation of a variety of sp^2 C–H bonds have been performed within the last decade initially by Ackermann in 2005 [44, 45], Bruneau and Dixneuf in 2008 [46], recently joined by a variety of research groups worldwide and presented in reviews [47, 48]. The success of ruthenium(II) catalysts for C–H bond transformation is due to the easy formation of cyclometallated intermediate on coordination of a functional group and C–H bond deprotonation by ligand or external base [49] [(Eq. 1)] and to the possibility, arising from the tolerance of some ruthenium(II) catalysts by water, to perform such reactions in water as safe solvent [50, 51].



In order to find alternative routes to functional olefins via the very useful Heck reaction [52] oxidative dehydrogenative cross-coupling of sp^2 C–H bonds with (alkene) C–H bond was first discovered using Pd(II) catalyst and an oxidant, by Moritani and Fujiwara [25, 53]. This oxidative alkenylation of aromatic C–H bonds profitably performed using cheap and stable ruthenium(II) catalysts was shown for the first time in 2011 successively by the groups of Satoh and Miura [54], Ackermann [55], Bruneau and Dixneuf [56], and Jeganmohan [57] [(Eq. 2)]. This Ru(II)-catalysed alkenylation reaction offers a potential to reach a large variety of functional alkenes at low cost and has been extended to annulation reactions with alkynes for a fast access to heterocycles.



The objective of this chapter is to show the recent contributions of ruthenium (II) catalysts for the arylation, heteroarylation, alkylation, and alkenylation of sp^2

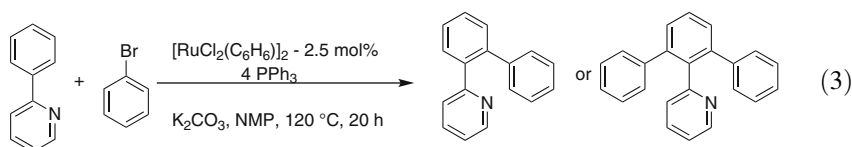
C–H bonds for C–C cross-couplings and annulation reactions. These ruthenium (II) catalysed cross-coupling reactions from C–H bonds have been recently presented in reviews [47, 48, 58]. Consequently, after a short presentation of the original examples this chapter will describe recent ruthenium(II) catalysed functionalization of sp^2 C–H bonds and C–C bond formations, including the examples reported till the end of 2013, and discuss some catalytic mechanism aspects.

2 Ruthenium (II)-Catalysed Arylation of Arenes and Heteroarenes via sp^2 C–H Bond Activation

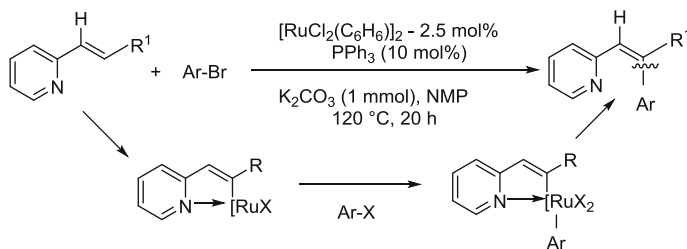
2.1 Arylation of Functional (Hetero)arenes with (Hetero) arylhalides

2.1.1 The First Examples of Direct Arylations with Ruthenium (II) Catalysts

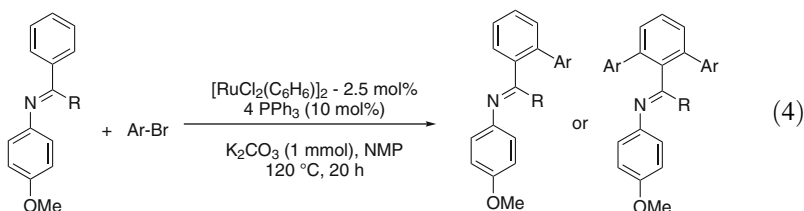
The direct catalytic arylation of functional arenes and heteroarenes with (hetero) arylhalides by transformation of a sp^2 C–H bond into a C–C bond has become one of the most efficient methods leading to useful bi-aryl and aryl-heteroaryl derivatives. Although the alkylation of heteroarenes with primary alcohols was performed with $[RuCl_2(arene)]_2$ catalysts in 1986 [59], it is only in 2001 that Oi and Inoue showed the first direct *ortho*-arylation of phenylpyridine with phenyl bromide using a ruthenium(II) catalyst $[RuCl_2(p\text{-cymene})]_2/4 PPh_3$ and could reach a good selectivity in mono and in diarylation in organic solvent NMP [(Eq. 3)] [42]. $RuCl_2(PPh_3)_3$ led to similar catalyst activity and the sequence for easiness of arylation corresponded to the sequence $PhBr > PhI > PhOTf >> PhCl$.



Using the same type of ruthenium(II) catalyst and conditions, Oi and Inoue succeeded the direct *ortho* monoarylation and diarylation of imines arising from aniline derivatives. Aldimines led preferentially to diarylated products. These reactions showed that the aryl imines were stable and that the imine nitrogen could direct the activation of *ortho* C–H bonds [(Eq. 4)] [43].

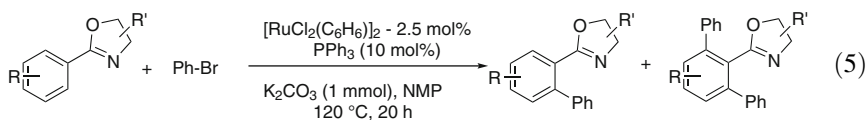


Scheme 1 Ru(II)-catalysed arylation of 2-pyridyl alkenes with aryl bromides



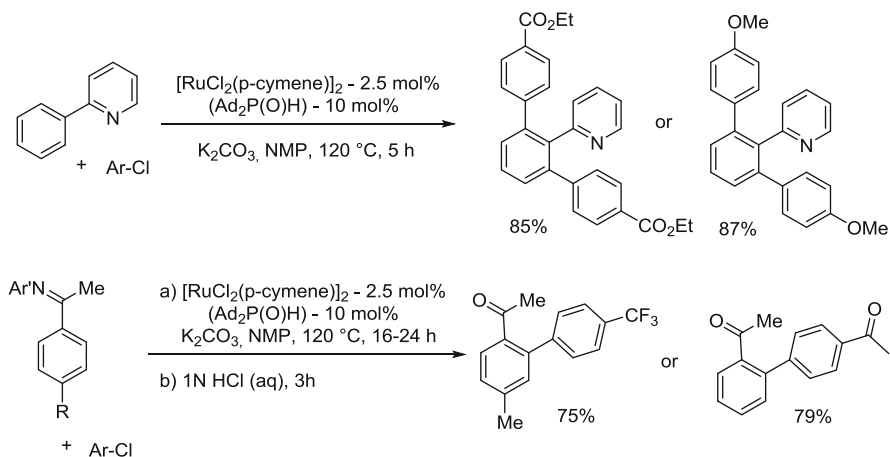
Oi and Inoue demonstrated that similar ruthenium(II) catalysts could catalyse the arylation of sp^2 C–H bond of 2-alkenyl pyridine without Heck type reaction to produce arylated alkenes. The alkene C–H bond facing the pyridine nitrogen was stereoselectively arylated suggesting a cyclometallated ruthenium(II) intermediate (Scheme 1) [60].

2-Oxazoline was shown to be an efficient directing group for arylation of arene derivatives with Ru(II) catalyst [(Eq. 5)] [61]. *N*-Acylimidazole was also shown to be a directing group promoting *ortho* monoarylation of arene. *Ortho*-alkenylation of 2-phenyl oxazoline with alkenylbromide was performed using the same ruthenium(II) catalyst [61].



The *ortho*-heteroarylation of 2-phenylpyridine and 2-phenyloxazoline with thiophenyl-, furanyl-, thiazolylbromides can also be promoted by $[\text{RuCl}_2(\text{C}_6\text{H}_6)]_2/4 \text{ PPh}_3$ catalyst, and an excess of heteroaryl bromide easily leads to the diheteroarylated product [62]. Imidazoles and thiazoles can be used as directing groups for the selective *ortho*-arylation of their 2-aryl derivatives with $[\text{RuCl}_2(\text{C}_6\text{H}_6)]_2/4 \text{ PPh}_3$ catalyst [63].

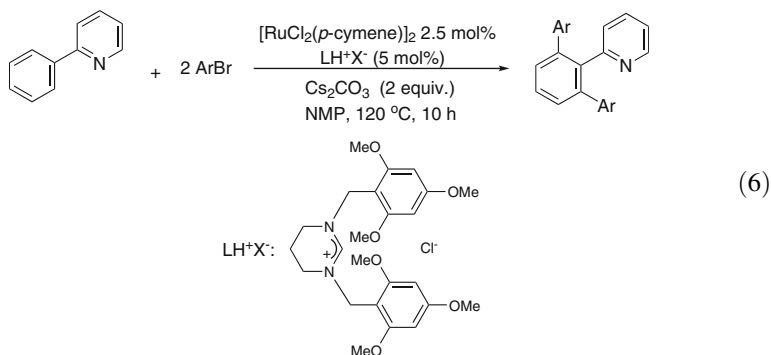
Ackermann showed in 2005 that phosphine oxide $\text{R}_2\text{P}(\text{O})\text{H}$ additives efficiently activate the ruthenium(II) catalyst, which allowed the direct C–H bond arylation with the less reactive but readily available arylchlorides, such as (adamantyl) $_2$ - $\text{P}(\text{O})\text{H}$ ($\text{Ad}_2\text{P}(\text{O})\text{H}$) associated with $[\text{RuCl}_2(p\text{-cymene})]_2$ (Scheme 2) [44]. This catalytic system was used for the monoarylation with arylchlorides of ketimines to



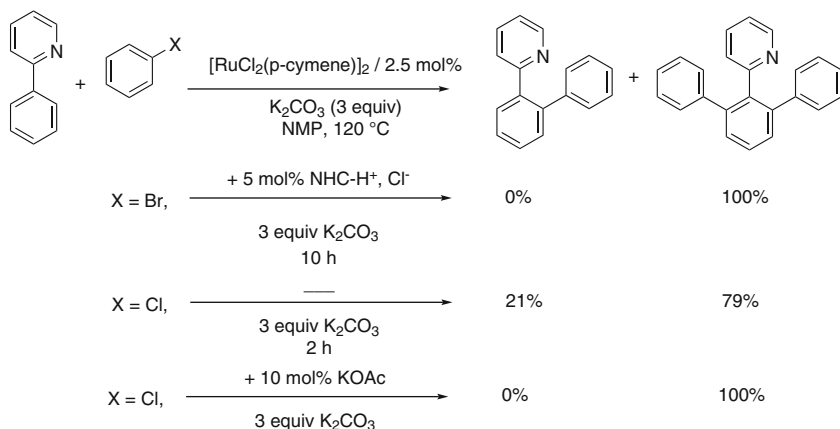
Scheme 2 Improved Ru(II)-catalyzed arylation with arylchlorides and $\text{R}_2\text{P}(\text{O})\text{H}$ additive

give the corresponding ketones after subsequent acid hydrolysis [44]. The anion $\text{R}_2\text{P}(\text{O})^-$ generated in basic medium may actually assist the deprotonation of C–H bond on its interaction with Ru(II) centre to afford the ruthenacycle intermediate [49].

The *ortho*-diarylation of phenylpyridine with arylbromides was also performed with $\text{RuCl}_2(\text{NHC})(p\text{-cymene})$ catalysts preferably with respect to phosphine containing catalysts. They were in situ generated from $[\text{RuCl}_2(p\text{-cymene})]_2$ on reaction with imidazolium salts, but preferably with pyrimidinium salts and carbonate as a base [(Eq. 6)] [46].

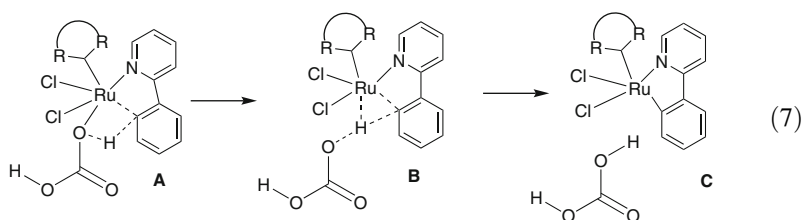


The crucial role of carbonate that can coordinate to Ru(II) sites [64] was shown to be responsible for the initial intramolecular C–H bond deprotonation leading to ruthenacycle intermediate **C**, as supported by DFT calculations [(Eq. 7)] [46]. This observation led later to discover better catalysts for arylation of C–H bonds



Scheme 3 Compared influence of acetate, carbonate, and NHC ligands on arylation of phenylpyridine

associating Ru(II) sites with carbonate or/and carboxylate without additional phosphorus or NHC ligands [65].



Few early examples of sp^2 C–H bond functionalization with ruthenium (II) catalysts were revealed in allylation and homocoupling reactions with $[RuCl_2(COD)]_n/PPH_3$ [66, 67] and $[Cp^*Ru(SR)X]_2$ [68] catalysts and even with Grubbs $[RuCl_2(=CHPh)(PCy_3)_2]$ olefin metathesis catalyst [69].

2.1.2 Carboxylate as Ruthenium(II) Partner for Direct Arylations of sp^2 C–H Bonds

The influence of both carbonate and acetate ligands on ruthenium(II) catalysts was evaluated and compared to the influence of phosphine or NHC ligands. The catalytic arylation of phenylpyridine under conditions to reach a complete conversion of phenylpyridine was performed by association of $[RuCl_2(p\text{-cymene})]_2$ with K_2CO_3 and KOAc [65].

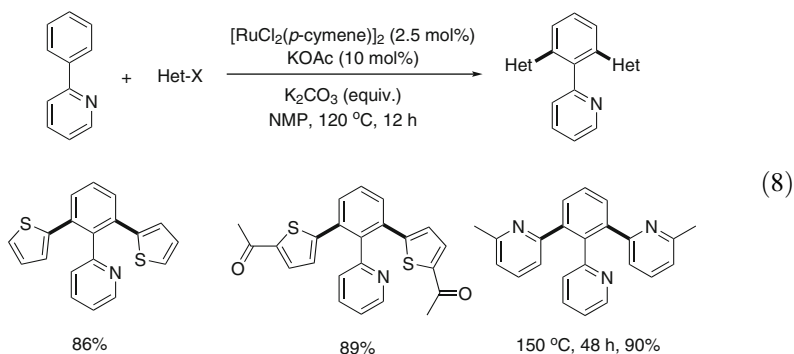
In the presence of imidazolium salt $NHC-H^+Cl^-$, the NHC (N-HeterocyclicCarbene) precursor, 100% of diarylation in the presence of PhBr was reached but after 10 h at 120 °C ([Eq. 6], Scheme 3) [65, 70]. More importantly

using the less reactive PhCl, in the presence of K_2CO_3 (3 equiv.), without phosphine or NHC ligand, 100% of conversion was obtained in NMP at $120^\circ C$ in only 2 h, but 21% of monoarylated product still remained (Scheme 3) [65]. Thus, K_2CO_3 alone promotes more efficiently the C–H activation and arylation than catalytic amount of other ligands such as phosphine, $R_2P(O)H$ or even NHCarene [46].

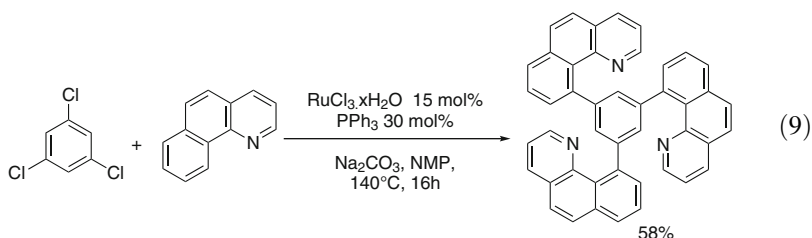
Surprisingly after addition of only 10 mol% of KOAc (2 KOAc per Ru atom), with 3 equiv. of K_2CO_3 , complete conversion and diarylation with PhCl were reached in only 1 h at $120^\circ C$ (Scheme 3) [65]. The in situ prepared catalyst $Ru(OAc)_2(p\text{-cymene})$ under these conditions is the best promoter of the C–H bond activation/arylation with the less reactive PhCl, demonstrating that ruthenium-carboxylate catalysts play a crucial role for C–H bond functionalization [65, 71].

The in situ prepared catalyst $Ru(OAc)_2(p\text{-cymene})$ in the presence of the K_2CO_3 was almost as active as the isolated complex and was preferentially used [65]. This catalytic system was selected for the efficient preparation of a variety of polyheterocyclic compounds or tridentate ligands such as the tripodal tris-1,2,3-(heteroaryl)benzene [(Eq. 8)] [65]. The same type of diarylated derivatives and polyheterocyclic compounds can now be preferentially prepared in diethyl carbonate, a non-toxic solvent, instead of NMP even if the reaction is slower [71].

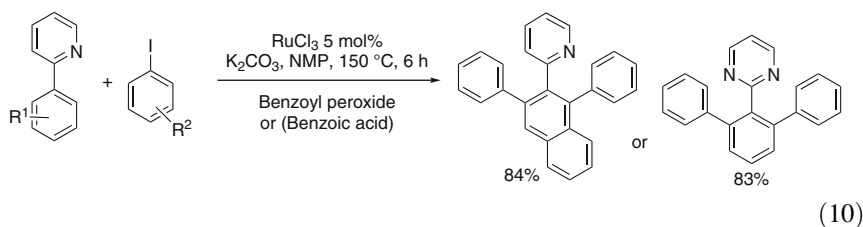
Due to the reversibility of the *ortho* C–H bond activation/cleavage the $RuCl_2(NHC)(\text{arene})/2\text{ KOAc}$ catalyst was shown to be efficient for the deuteration of *ortho* C–H bonds of a variety of functional arenes in $MeOH-d_4$ [72].



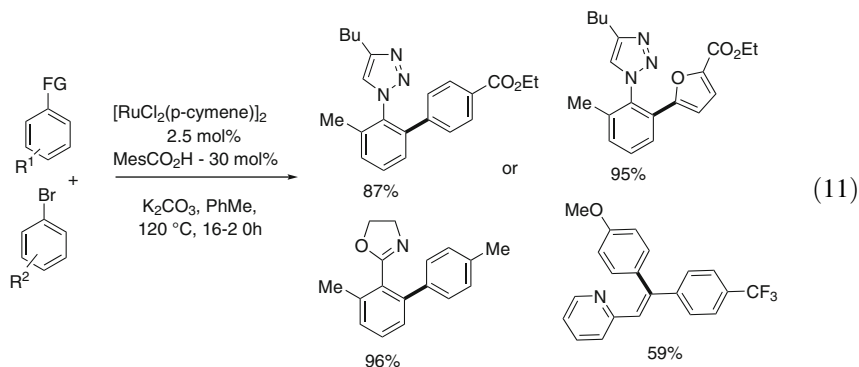
Several examples of simple catalytic systems based on inexpensive $RuCl_{3 \cdot x}H_2O$ associated with only carbonate were reported for direct arylation of functional arenes with arylhalides, with K_2CO_3 in NMP at $120^\circ C$ for 20 h by Ackermann et al. [73, 74]. On addition of 2 equiv. per Ru atom of PPh_3 to $RuCl_{3 \cdot x}H_2O$, but associated with a more efficient base in that case Na_2CO_3 , the direct arylation of arenes or benzoquinoline with aryl chlorides at $140^\circ C$ in NMP was reported by Zhengkun Yu who applied these conditions to the synthesis of the tris benzoquinoline derivatives [(Eq. 9)] [75].



Yuhong Zhang demonstrated the regioselective arylation of 2-phenylpyridine with aryl iodides with 5 mol% of the same easily available RuCl_3 catalyst with K_2CO_3 in NMP at 150°C for a shorter time of 6 h but in the presence of benzoyl peroxide additive or benzoic acid additive that may play the same profitable role as acetate [(Eq. 10)] [76].



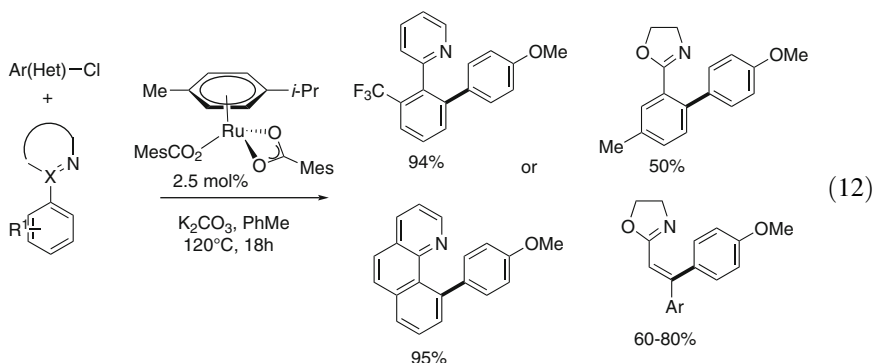
In 2008, Ackermann and co-workers demonstrated that the addition of 30 mol% of a carboxylic acid MeCO_2H tremendously improved the catalytic system $[\text{RuCl}_2(p\text{-cymene})]_2/\text{K}_2\text{CO}_3$ for the selective arylation of phenyl triazoles with arylbromides in toluene at 120°C . This catalytic system was shown to be efficient even for arylation with arylchlorides of aryl-oxazolines, pyrazoles and alkenes. The catalytic efficiency was attributed to a ruthenation via concerted metalation and deprotonation [(Eq. 11)] [77].



The monoarylation of aryl-triazoles with arylchlorides can be achieved with $[\text{RuCl}_2(p\text{-cymene})]_2$ catalyst with large excess of PCy_3 in more drastic conditions, $120\text{--}135^\circ\text{C}$ for 20 h, than with carboxylic acid additive, whereas arylbromides

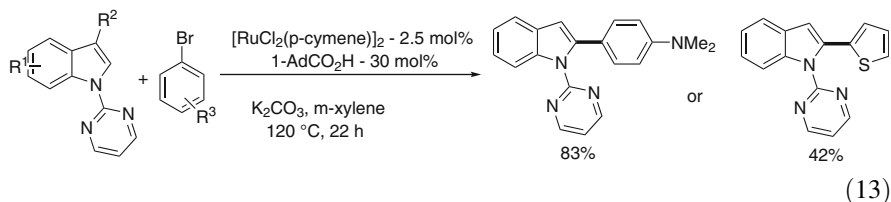
provide the diarylated products selectively under the same conditions [78]. The direct arylation of triazolyl-arenes with arylhalides in the presence of Ru (II) catalyst associated with MesCO₂H in toluene at 120°C was largely improved as the diarylated products were selectively obtained [79]. When the reaction was performed in the presence of *ortho* substituted arylchlorides such as *ortho*-trifluoromethylchlorobenzene, acting as a sacrificial oxidant, homocoupling took place at the *ortho* carbon of the arene linked to pyridine, pyrazole or triazole directing group [79].

By contrast the well-defined Ru(O₂CMes)₂(arene) catalyst was efficient to perform *ortho* mono(hetero)arylation of arenes containing a nitrogen directing group (pyridine, oxazoline, pyrazole, benzoquinoline...), when the second *ortho* C–H bond was protected, but also of alkenes [(Eq. 12)] [80].

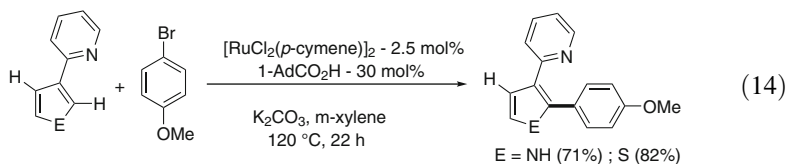


With Ru(O₂CMes)₂(*p*-cymene) catalyst, competitive experiments revealed that the electron-deficient arylhalides reacted preferentially as oxidative addition is favoured, whatever the nature of the solvent but that surprisingly arylchlorides were more reactive than arylbromides [80].

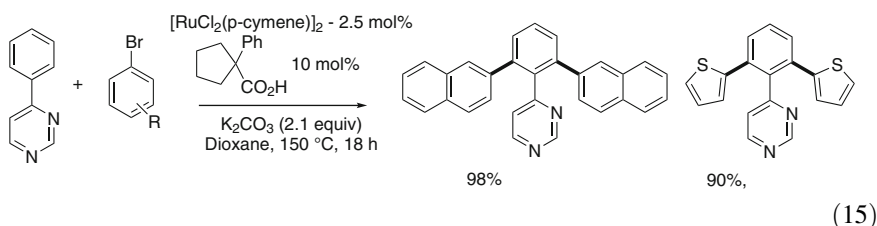
The reaction of 2-pyrimidylindole, thus containing a strong N-chelating group, with aryl or heteroaryl bromides with the catalyst [RuCl₂(*p*-cymene)]₂/AdCO₂H in xylene led to the selective C₂ arylation, with a broad scope [(Eq. 13)] [81].



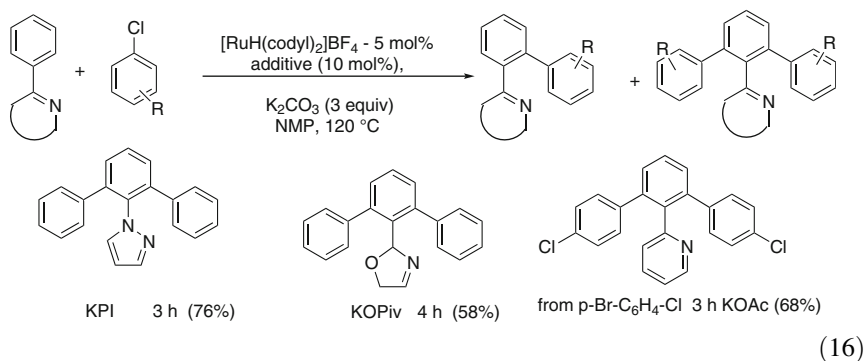
Unprotected pyrrole and thiophene, containing a coordinating 2-pyridyl group at C₃, can be arylated with arylbromide regioselectively at C₂ in the presence of the same catalytic system [(Eq. 14)] [81].



A sterically hindered carboxylic acid the 1-phenyl-1-cyclopentanecarboxylic acid has been shown to be an efficient partner of ruthenium(II) catalyst by Pozgan and co-workers [(Eq. 15)] [82]. They have reported the C–H bond functionalization of 2- and 4-phenylpyrimidine with arylhalides, at 150°C, affording the mono- or the disubstituted products and the heteroarylation with 2-bromothiophene and 3-bromopyridine proceeded very well.



The search for efficient ruthenium catalysts has led to explore the use of the ruthenium(IV) stable system $[\text{RuH}(\text{cyclooctadienyl})_2]\text{BF}_4$. This Ru(IV) precursor is deprotonated into Ru(II) species in the presence of a base. Carboxylate salts KOAc, KOiv, and potassium phthalimide (KPI) are able to completely promote diarylation of 2-phenylpyridine with chlorobenzene in 1 h at 120°C. The efficiency of the catalytic system was the best in the presence of KPI with chlorobenzene. For 2-chlorotoluene, 2-chlorothiophene, 6-methyl-2-bromopyridine the best yields were obtained with $[\text{RuH}(\text{cyclooctadienyl})_2]\text{BF}_4$. and KOAc in NMP, and from $p\text{-Br-C}_6\text{H}_4\text{-Cl}$ the dichloro derivatives could be obtained [(Eq. 16)] [83].



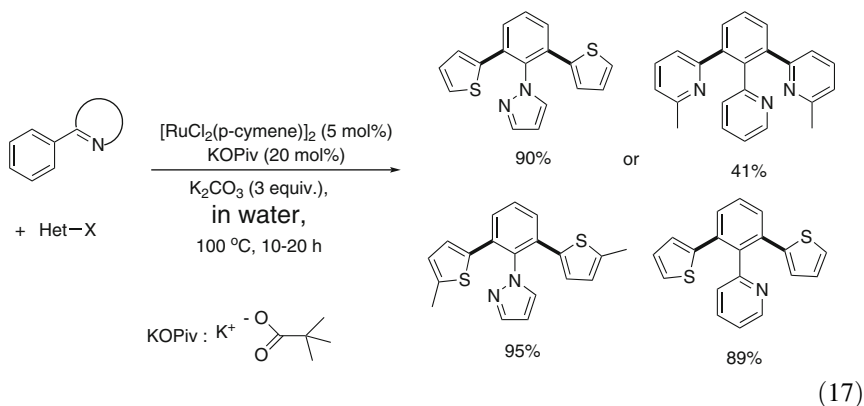
These *ortho* (hetero)arylation examples show that the combination of a simple ruthenium(II) catalyst in the presence of a carboxylate as a co-catalyst and with carbonate as the base leads to an excellent system for arylation of arenes containing

a coordinating nitrogen atom included in a heterocycle directing group. However it cannot be applied yet to weak coordinating functional groups for arylation, and milder conditions in greener solvents have to be found.

2.1.3 Arylation with Ruthenium(II)-Carboxylate Catalysts in Water

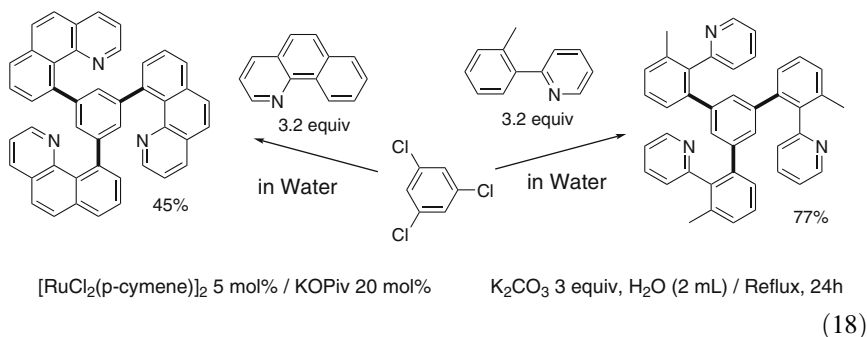
Most arylations with (hetero)arylhalides of sp^2 C–H bonds were initially performed in organic solvents such as toluene or NMP. Then attempts of arylation were made in environment-tolerant, non-toxic solvents: *the dialkyl carbonates*. The arylation with arylchlorides of phenylpyridine in the presence of Ru(II)/2 KOPiv catalyst was successfully and completely performed in diethyl carbonate. The reaction at 120°C was slower than in NMP, but it was significantly improved with pivalamide additive (2 h) [71].

Among the environment-tolerant solvents water is a candidate of choice as a non-toxic, non-flammable, inexpensive solvent, and catalytic C–H bond functionalization with Ru(II) catalyst could be successfully performed in water. It was first shown that water in NMP (1:2) did not inhibit the arylation of phenylpyridine with PhCl with a Ru(II)/Ad₂P(O)H catalyst; however, the pure NMP solvent allowed to reach higher yields than in NMP-water [44]. More importantly it was demonstrated that *ruthenium(II)/pivalate catalysts allowed arylation in pure water, in the absence of surfactants, and that the catalyst system was more active than in organic solvents* [50]. Thus with [RuCl₂(*p*-cymene)]₂/4 KOPiv catalyst in water diarylation of phenyl-nitrogen containing heterocycles was performed in good yields and even allowed the access to a variety of polyheterocycles that can be used as tridentate ligands [(Eq. 17)] [50]. For instance, 1,2,3-tris(2-pyridyl)benzene was prepared from 2-phenylpyridine. In addition it was shown that the favourable sequence of bases was K₂CO₃ > KHCO₃ > K₃PO₄ and that of arylhalides, due to their solubility in water, was PhCl > PhBr > PhI [50].

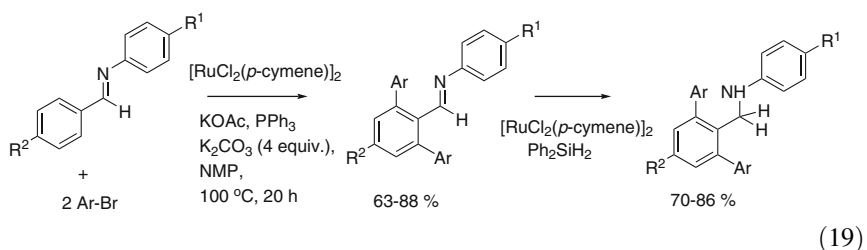


Tridentate ligands were easily prepared in water using the same type of Ru(II)/KOPiv catalyst at 100°C by arylation with the 1,3,5-trichlorobenzene and thus a

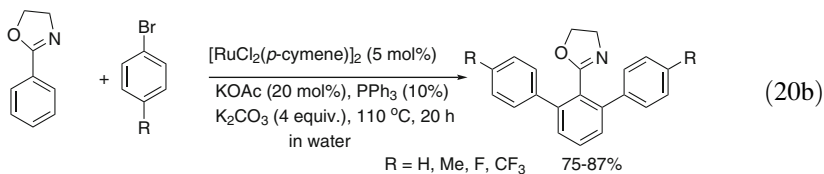
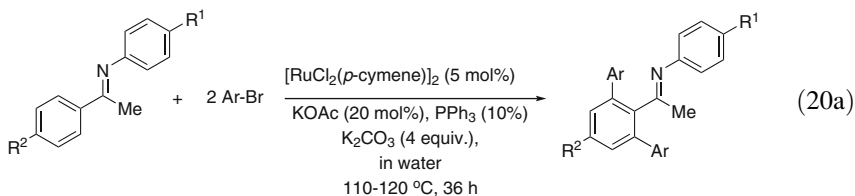
trispyridine ligand and a trisbenzoquinoline ligand were obtained in 77% and 45%, respectively, in better yield than in NMP at 120°C [(Eq. 18)] [50].



Following the pioneering discovery by Oi and Inoue on the diarylation of imines [43], improved diarylation of imines was reached in NMP using a Ru(II)/KOAc/ PPh_3 catalytic system for aldimines and Ru(II)/2 KOAc without PPh_3 but for longer time for ketimines. The diarylated imines could be reduced into bulky amines by catalytic hydrosilylation with the same Ru(II) catalyst. Thus the overall reaction could be performed in two steps via sequential Ru(II) catalysed C–H bond functionalization/hydrosilylation [(Eq. 19)] [84].



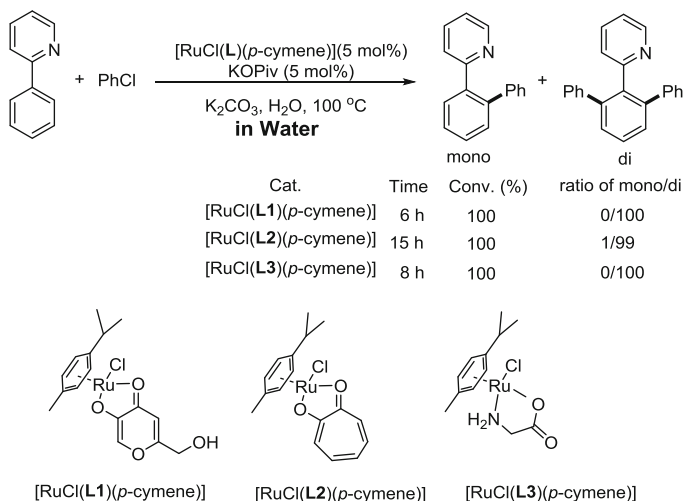
More importantly it was found that the ketimines could be more easily diarylated in water in basic medium (K_2CO_3) than in NMP using the Ru(II)/2KOAc/1 PPh_3 catalytic system [(Eq. 20a)] [85]. As ketones do not direct *ortho* C–H bond activation followed by arylation, this arylation of aldimines and ketimes can be used for the access to diarylated aldehydes and ketones that are thus obtained by acidification of their aqueous solution. Oxazoline can also efficiently direct *ortho*-arylation of aryl groups [(Eq. 20b)] [85].



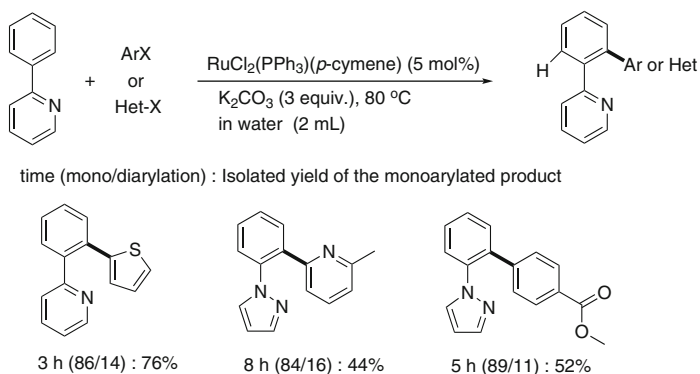
Very recently, Singh and Dixneuf evaluated some novel ruthenium (II) complexes, containing a O[^]O or O[^]N chelated ligand, synthesized from kojic acid, tropolone, and glycine. The water soluble ruthenium(II) complexes [RuCl(L₁)(*p*-cymene)] (L₁ = 5-hydroxy-2-(hydroxymethyl)-4-pyronate and [RuCl(L₃)(*p*-cymene)] (L₃ = glycinate) were found to be effective catalysts for direct sp² C–H bond diarylation of heteroarenes with (Hetero)aryl halides in water in the presence of KOⁱPr co-catalyst and base K₂CO₃ (Scheme 4) [86]. The glycinate and kojic acid ruthenium(II) complexes appeared to offer the best catalyst activity in water, whereas in NMP the catalyst containing L₂ is more active than that containing L₁.

From Easy Diarylations to Selective Monoarylations of (Heteroarenes)

During arylation or heteroarylation of (hetero)arenes at non-protected *ortho* C–H bonds with ruthenium(II) catalysts in organic solvents, the diarylated products were easier to produce selectively than the monoarylated ones, as the rate of monoarylation was quite similar to that of diarylation. Consequently, it appeared difficult to produce selectively mono (hetero)arylated products when two non-protected aromatic C–H bonds were present in order to generate later disymmetrically substituted molecules. A possible reason was that after fast monoarylation, the second C–H bond activation and diarylation starts immediately without decoordination of the functional group (heterocycle) from the Ru (II) centre. It was observed in some examples that water decreased the rate of diarylation [50] and that the use of bulky phosphine favoured monoarylation [42, 43, 87, 88]. Thus the Rennes team found that by combining these two factors of influence, water solvent and PR₃ ligand, selective monoarylation of functional arenes could be obtained [89]. The sequence of phosphine favouring monoarylation appeared to be: PPh₃ > PCy₃ > P(*i*Pr)₃ > P(*o*-Me-C₆H₄)₃. The RuCl₂(PPh₃)(*p*-cymene) catalyst operating in water at 80 °C can lead to selective monoarylation of 2-phenylpyridine and *N*-phenylpyrazole. (Scheme 5) [89].



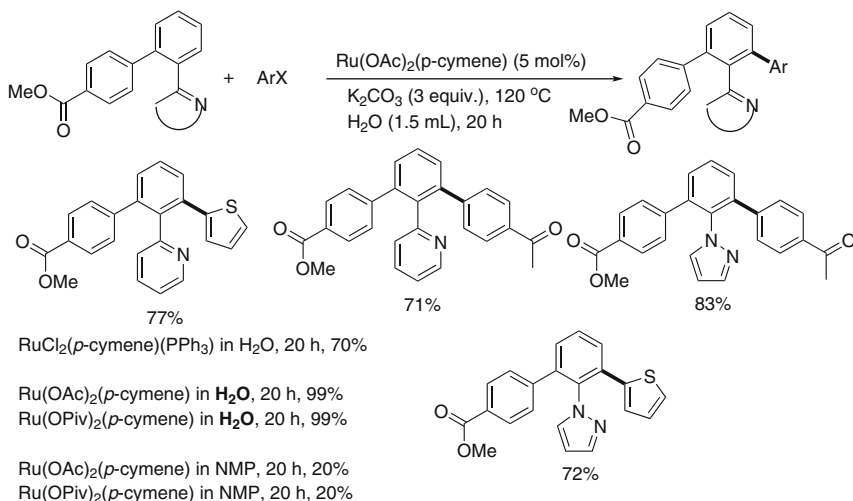
Scheme 4 Arylation with Ru(II)-O[^]O and -O[^]N bidentate ligand catalyst in water



Scheme 5 Selective monoarylation of *ortho* C–H bonds with Ru(II)-PPh₃ catalyst in water

It is noteworthy that these monoarylated products with a free *ortho* C–H bond adjacent to the functional group could be arylated with a different aryl or heteroarylchloride using Ru(OAc)₂(*p*-cymene) or Ru(OPiv)₂(*p*-cymene) *in water* leading to unsymmetrically diarylated trifunctional (hetero)aryl derivatives in 70–83% isolated yields (Scheme 6) [89].

It was especially observed that the second arylation or heteroarylation can be performed only in water as the use of Ru(OAc)₂(*p*-cymene) in NMP for 20 h leads only to 20% of conversion of the monoarylated product into the mixed diarylated product, whereas the direct homodiarlylation of the same 2-phenylpyridine with thienylchloride with the same catalyst in NMP needed only 12 h at 120°C to reach complete diheteroarylation [65]. These results show that in NMP the second direct

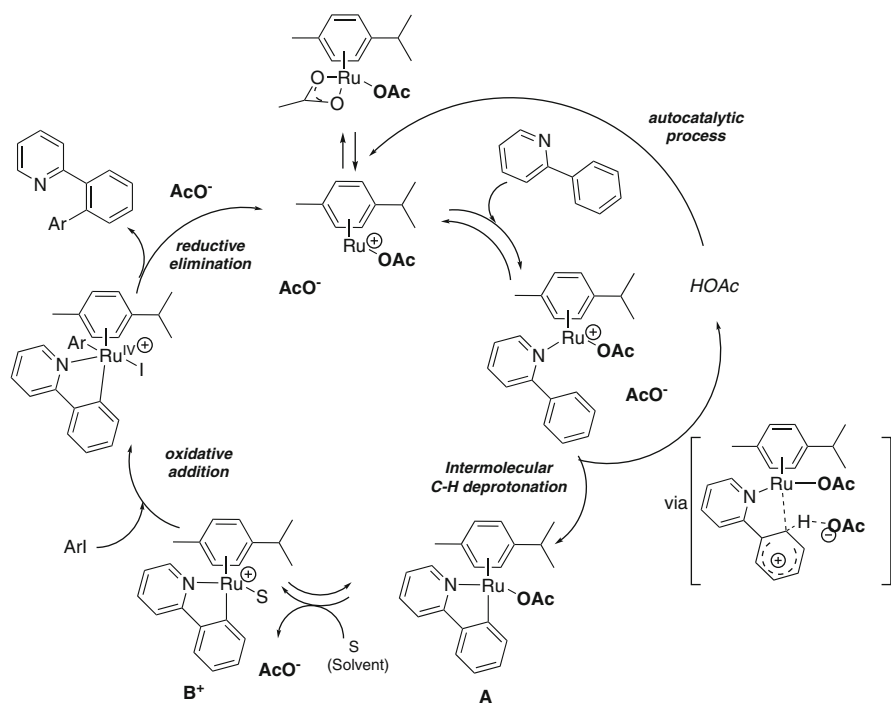


Scheme 6 Second *ortho* C–H bond arylation with $\text{Ru}(\text{OAc})_2(\text{arene})$ catalyst in water

arylation is faster than from isolated monoarylated product. This is likely due to a second arylation taking place in NMP without decoordination of the pyridine directing group. These results show that water drastically favours the second arylation with respect to NMP.

2.1.4 Mechanism of C–H Bond Activation/Arylation with Carboxylate-Ruthenium(II) Catalyst: An Autocatalytic Process

The profitable role of carboxylate co-catalysts and base carbonate on the ruthenium (II) sp^2 C–H bond activation was well established in the previous examples and motivated the mechanism investigation. First with K_2CO_3 only, it was established by DFT calculations that carbonate coordinated to the Ru(II) site and, after coordination of the substrate directing group, intramolecularly deprotonated the *ortho* C–H bond with the help of the interaction of the Ru(II) with this C–H carbon atom [46]. To explain the tremendous rate increasing with the carboxylate partner a kinetic study was performed by A. Jutand [49] on the arylation with phenylhalide of phenylpyridine with isolated $\text{Ru}(\text{OAc})_2(p\text{-cymene})$ catalyst. The kinetics performed in CH_3CN at 27 °C showed first the formation of the cyclometallated derivative **A** but surprisingly that the freed AcOH accelerated this reaction via an autocatalysed process. (Scheme 7) [49]. This was consistent with a dissociation of the weak Ru–OAc bond, assisted by AcOH and, after coordination of PyPh, deprotonation of the C–H bond by the external AcO^- anion acting as a proton shuttle toward the carbonate. This room temperature C–H bond deprotonation is likely favoured by electrophilic interaction of the Ru(II) site with arene electrons and *ortho* carbon atom.



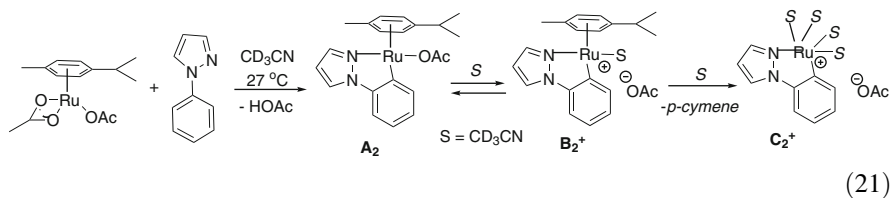
Scheme 7 Mechanism for Ru(II)-OAc-assisted C–H bond activation and arylation

The formation of cyclometallate **A** is accelerated by additional KOAc supporting that the deprotonation of C–H bond by AcO[−] is intermolecular. Pivalic acid accelerates the formation of analogous **A** intermediate but not as much as AcOH and the addition of a small amount of water, increasing the acidity of both acids, favours the process and also explains the positive role of water as solvent in catalysis.

It is shown that the oxidative addition of PhI does not take place with the 18 electron intermediate **A** but with the cation **B⁺** and is rate-determining. It requires higher temperature than the C–H bond cleavage step. This is also consistent with a weak Ru(II)-OAc bond observed in the formation and stability of related ruthenacycles [90].

A kinetic study performed on 1-phenylpyrazole and 2-phenyl-2-oxazoline in the presence of Ru(OAc)₂(*p*-cymene) revealed that they also lead to room temperature formation of ruthenacycles of type **A** [Eq. 21] and that the reactivity order is 2-phenylpyridine > 2-phenyl-2-oxazoline > 1-phenylpyrazole [91]. The process acceleration by AcOH reveals an autocatalytic process and by AcO[−] reveals an acetate intermolecular C–H bond deprotonation process. By contrast, the base carbonate is shown in these three examples to slow down the C–H bond activation

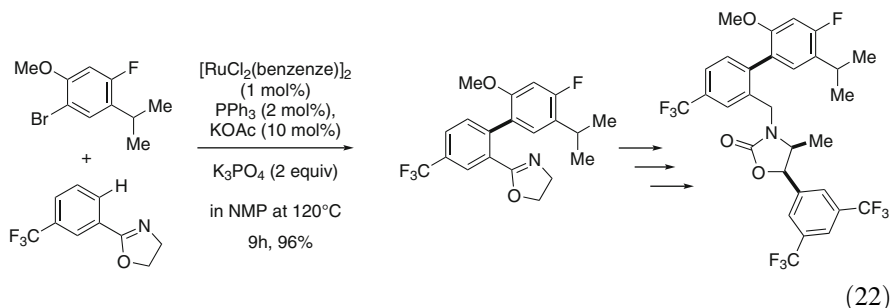
process, as expected by the deprotonation of the freed AcOH, but is required for HX elimination.



The C–H bond activation process by $\text{Ru}(\text{OAc})_2(p\text{-cymene})$ and $\text{Pd}(\text{OAc})_2$ can be compared by kinetic study of their reaction with phenylpyridine leading in both cases to a cyclometallate complex. Although the reaction with $\text{Pd}(\text{OAc})_2$ is faster than with the ruthenium(II) catalyst, it is not affected by addition of acetic acid or acetate, thus the reaction with $\text{Pd}(\text{OAc})_2$ proceeds – to the difference of $\text{Ru}(\text{OAc})_2L_n$ – via an intramolecular non-autocatalysed Concerted Metallation-Deprotonation (CMD) mechanism [91].

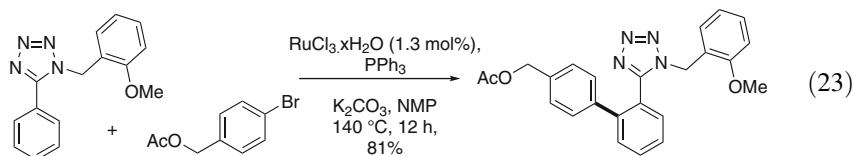
2.1.5 Recent Novel Monoarylations and Synthesis of Biorelevant Biaryl Derivatives

The first key intermediate in the synthesis of Anacetrapib (MK-0859) a protein inhibitor has been synthesized at a kilogram scale via controlled monoarylation with ruthenium(II) catalyst of a phenyloxazoline derivative with a fluorinated arylbromide [(Eq. 22)] [92]. This successful catalytic reaction was due to the combination of $[\text{RuCl}_2(\text{benzene})]_2$ with 10 KOAc in the presence of K_3PO_4 . The further addition of 1 equiv. of PPh_3 per Ru atom favoured the oxidative addition of ArBr to the ruthenacycle intermediate and also decreased the diarylation rate.

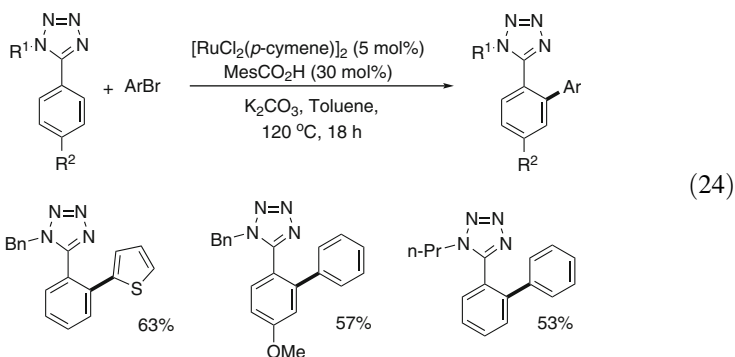


In 2011, Seki reported a $\text{RuCl}_3 \cdot x\text{H}_2\text{O}/\text{PPh}_3$ catalysed monoarylation of a phenyl tetrazole with arylbromide to generate a functional biaryl as a key step in the synthesis of the Angiotensin II receptor blockers (ARBs) derivatives, which emerged as an efficient antihypertensive drug and is produced in more than

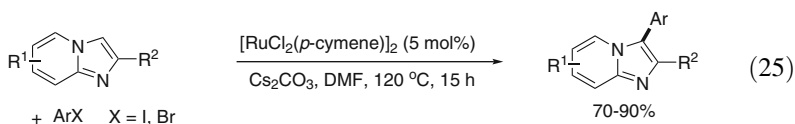
1,000 tons/year for clinical treatment worldwide [(Eq. 23)] [93]. The catalysis does not require carboxylate but the presence of both K_2CO_3 and PPh_3 to decrease the rate of diarylation. This catalyst $RuCl_3 \cdot xH_2O/PPh_3$ appeared more efficient than the $Ru(II)$ catalysts $[RuCl_2(COD)]_2$ and $[RuCl_2(arene)]_2$ [94].



Recently, to synthesize a key intermediate for the access to ARBs derivatives via direct arylation of phenyltetrazoles, Ackermann's group developed a catalyst based on in situ generated bis carboxylate ruthenium(II) that was found to display a more efficient catalytic activity than $RuCl_3/PPh_3$ [(Eq. 24)] [95]. Various 5-aryltetrazoles were formed as mono-arylated products with $[RuCl_2(p\text{-cymene})]_2$ (5 mol%)/ $MesCO_2H$ (30 mol%)/ K_2CO_3 catalytic system. The H/D exchange at the *ortho*-C–H bonds of aryl tetrazole revealed a reversible cyclometallation reaction.



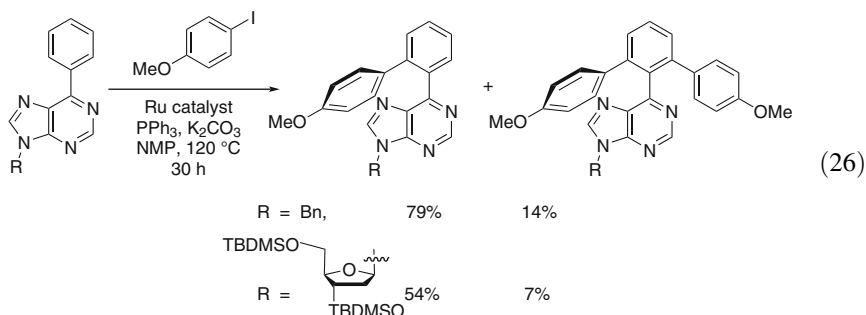
Direct arylation of imidazo[1,2-a]pyridines with arylhalides using $[RuCl_2(p\text{-cymene})]_2/Cs_2CO_3$ catalyst was explored by Yi and co-workers [(Eq. 25)] [96]. Arylation took place only at the imidazole C–H bond and arylated products at C-3 position were isolated in higher yields with aryl iodides (80–93%) than with aryl bromides (70–86%).



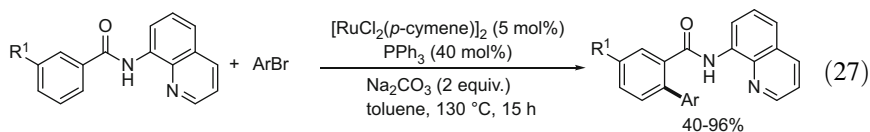
Another ruthenium catalytic system based on $[RuCl_2(\eta^6\text{-benzene})MOTPP]$ (5 mol%) [$MOTPP = \text{tris}(4\text{-methoxyphenyl})\text{phosphane}$] and acetamide (20 mol%) as additive was applied in direct arylation of 2-phenylpyridine with arylchlorides in the presence of K_2CO_3 (3 equiv.) in 1,4-dioxane at $101^\circ C$

[97]. After 15 h, quantitative yields of arylated products were produced, but in a mixture of mono and diarylated products. However catalysts such as $[\text{RuCl}_2(p\text{-cymene})]_2$ (2.5 mol%)/KOAc (10 mol%) were used for efficient arylation with arylchlorides affording 100% conversion in NMP at 120°C for only 1 h [65].

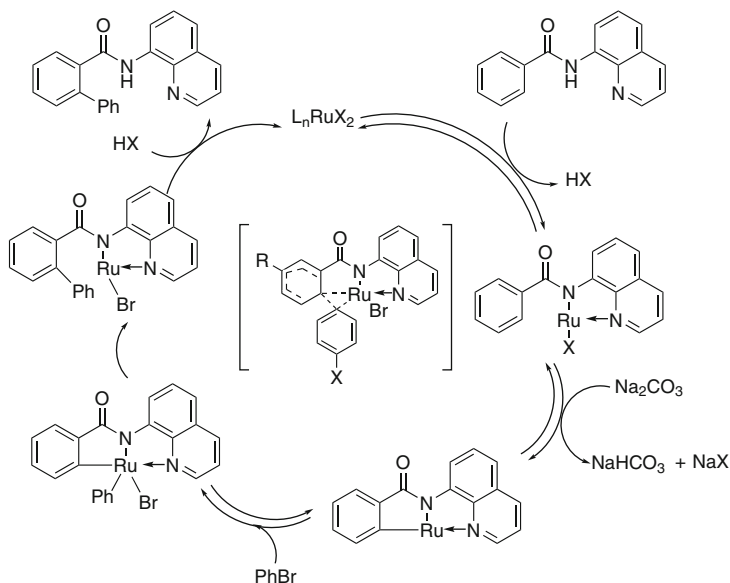
The purine derivative (R=Bn) was shown, on action of both aryl iodides and bromides with $[\text{RuCl}_2(\text{benzene})]_2/8 \text{ PPh}_3$ catalyst, to preferentially generate monoarylated compounds, in the presence of K_2CO_3 in NMP at 120°C [(Eq. 26)] [98]. The monoarylated derivative of 3',5'-di-*O*-silyl-6-arylpurine was preferentially prepared but in drastic conditions (120°C , 30 h) as no carboxylate was associated with the Ru(II) catalyst.



Chatani developed the use of *N,N*-bidentate directing group first in Ru(0)-catalysed carbonylation [99] and recently he used such a bidentate directing group combined with aromatic amides for Ru(II)-catalysed *ortho*-arylation [100]. This reaction was performed with catalyst $[\text{RuCl}_2(p\text{-cymene})]_2/\text{PPh}_3$, with Na_2CO_3 (3 equiv.) in toluene at 140°C [(Eq. 27)]. In that case the addition of Na_2CO_3 as a base was more effective than that K_2CO_3 and Cs_2CO_3 . The aromatic amides containing various functional groups R^1 , such as dimethylamino, methoxy, ester, trifluoromethyl, ketone groups at *meta*-position reacted with heteroaromatic bromides and led to the monoarylated compounds due to the protection of one *ortho* C–H bond by the substituent R^1 at *meta*-position.



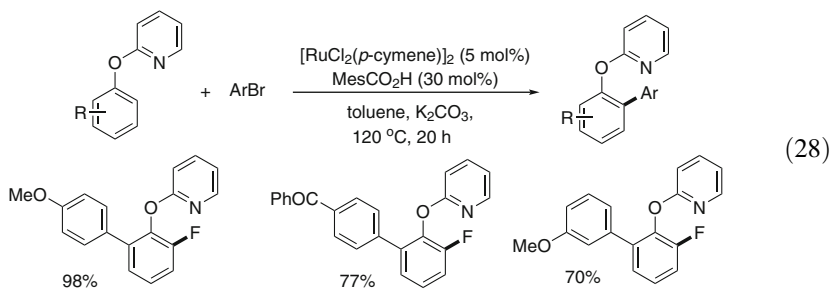
The competition experiments revealed that (1) electron-withdrawing groups of *meta*-substituted aromatic amides facilitate the reaction; (2) the electronic nature of the substituent in the aromatic amide is a dominant factor; (3) the electron-donating groups (OMe and NMe_2) favour this reaction, and that the electron-withdrawing nature of the substituent (COMe or CO_2Me) in the aryl bromides also accelerated the oxidative addition step. The Hammett plots show two lines in V shape. In addition, the H/D experiments indicated that the deprotonation of C–H bond is a



Scheme 8 Proposed mechanism for the arylation with N,N -bidentate directing system

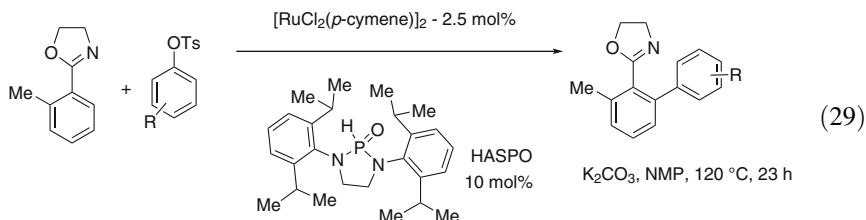
reversible and rapid step and is not the rate-determining one. The proposed mechanism suggests a concerted metallation-deprotonation (CMD) mechanism followed by an oxidative addition step of aryl bromides. However when aryl bromide contains an electron-withdrawing COMe or CO_2Me group, a nucleophilic substitution mechanism of the arylhalide by the Ru(II) centre is proposed (Scheme 8) [100].

The ruthenium(II) carboxylate catalysed direct arylation of phenols protected by a removal directing pyridine group in 2-phenoxy pyridine with arylhalides was recently demonstrated by Ackermann for the access to arylated phenols [101]. The reaction takes place in toluene at $120^\circ C$ for 20 h affording 66% of mono- and 24% di-arylated products – thus under more drastic conditions with respect to previous diarylation of 2-phenyl pyridine [65]. However the reaction can be performed in water to generate 50% of mono- and 31% di-arylated products. When the reaction involved *ortho* substituted 2-aryloxy pyridines, moderate to excellent yields of monoarylated products were thus obtained [(Eq. 28)] [101]. The electron-deficient arenes provided higher yields than electron-rich arenes. Monoarylated phenols could be produced by the further treatment of the arylated 2-aryloxy pyridine with MeOTf in toluene at $100^\circ C$, followed by reaction with sodium in MeOH. It is noteworthy that in this example the key intermediate is a *six-membered ruthenacycle* generated by deprotonation and cyclometallation and it is not so easily generated as the previous five-membered ruthenacycle intermediates.

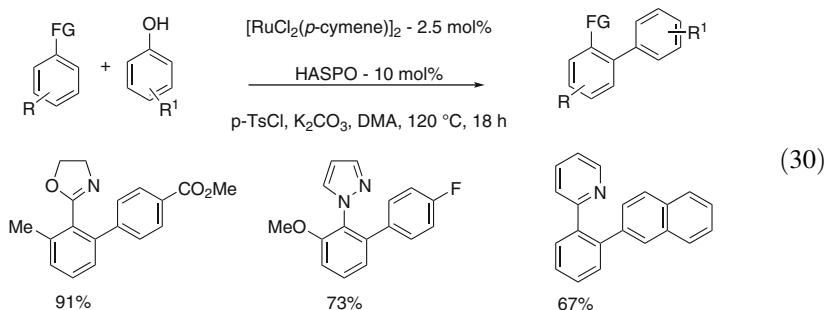


2.2 Arylation with Aryl Tosylates and Phenols

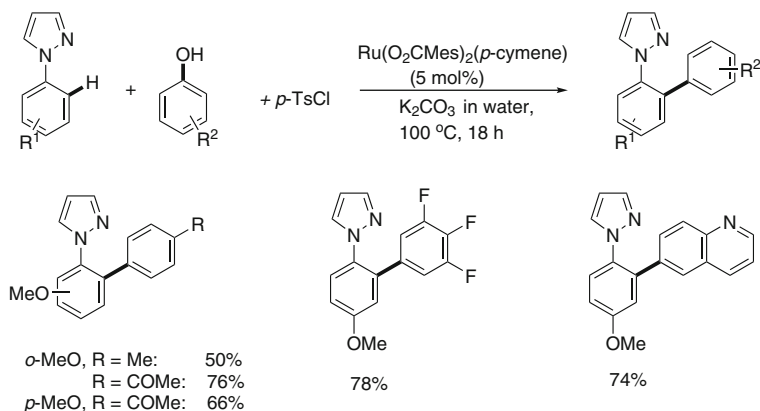
Ackermann previously showed that a ruthenium(II) catalyst, associated with the secondary phosphine oxide (HASPO), promoted the arylation of 2-aryloxazolines with *aryl tosylates* containing a large variety of functional groups, although they are not as reactive as the arylchlorides under the same conditions [(Eq. 29)] [45].



A more direct approach involves now the arylation with in situ generated tosylate from the reaction of phenol in the presence of *p*-tolylsulfonylchloride. The reaction is performed with $[\text{RuCl}_2(p\text{-cymene})]_2$ and 10 mol% of HASPO ligand [(Eq. 30)] [102]. The catalytic system tolerates other heterocycle directing groups such as pyridine and pyrazole.



The arylation of functional arenes with phenols in the presence of tosylchlorides can take place in water using $\text{Ru}(\text{O}_2\text{CMes})_2(p\text{-cymene})$ catalyst in the functionalization of *N*-arylpiprazole. Thus the arylation with aryl tosylates is faster than the

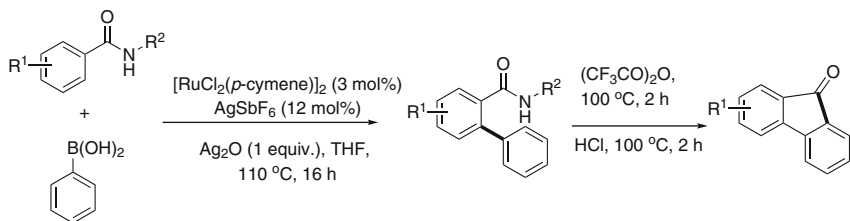


Scheme 9 Ru(II) catalysed arylation of *N*-phenyl pyrazole with phenols in water

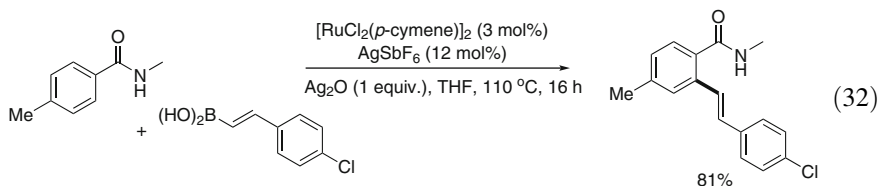
tosylchloride hydrolysis under these conditions and the reaction tolerates a variety of nitrogen containing functional groups (Scheme 9) [103].

2.3 Arylation with Boronic Acids

Organoboron reagents are highly attractive for C–C bond cross-coupling reactions due to their large variety and availability, air and moisture stability, and low toxicity [104]. They have already wide applications in Suzuki cross-coupling reactions. Direct sp^2 C–H bond arylation using organoboron reagents had not been well explored previously. Recently, Jeganmohan developed the *ortho*-arylation of *N*-alkylbenzamides with aromatic boronic acids in the presence of $[\text{RuCl}_2(p\text{-cymene})]_2/\text{AgSbF}_6$ catalyst, with 1 equiv. of Ag_2O in THF. Moreover, the arylated products react with $(\text{CF}_3\text{CO})_2\text{O}$ followed by HCl hydrolysis, leading to fluorenone compounds in high yields [(Eq. 31)] [105].



(31)



Jeganmohan and his group have also demonstrated that alkenylboronic acids can transform arylamides under similar conditions and lead to C–C bond cross-coupling and that the alkenylation occurred at the amide *ortho* position [(Eq. 32)] [105]. Ag_2O plays a significant role to accelerate the transmetalation step of boronic acid to the five-membered Ru(II) cyclometallated intermediate.

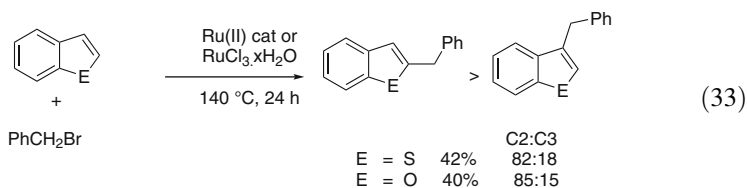
At the end of this part 2 it can be pointed out that the direct arylation of functional arenes and heteroarenes with aryl halides can now be easily promoted by Ru(II) catalysts: (1) Ru(II) species with carboxylate as co-catalyst can accomplish arylation at *ortho* position of functional group even with arylchlorides, (2) these arylations against expectation can be achieved more easily in water as solvent, without surfactants, and (3) selective monoarylations can be reached with R(II)- PR_3 catalyst in water and it offers access to mixed diarylated derivatives. However at the moment only strongly coordinating functional groups such as N-containing heterocycles or imines can direct this ruthenium(II)-catalysed cross-coupling reaction.

3 Ruthenium(II)-Catalysed Alkylation of Alkenes and (Hetero)arenes

3.1 Alkylation of (Hetero)arenes with Alkylhalides

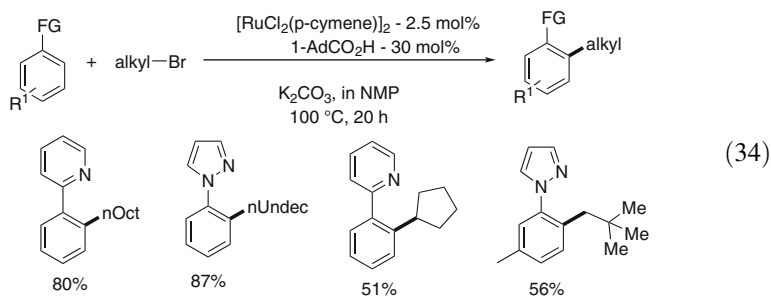
The C–C bond cross-coupling reaction of sp^2 C–H bond with alkylhalides following the ruthenium(II) catalysed C–H bond activation process has not been well explored in comparison with arylations with arylhalides, especially for the secondary alkylhalides which are more sterically demanding and electron-rich thus leading to the oxidative addition step with difficulty [106].

The alkylation of benzofuran and benzothiophene, catalysed by ruthenium (II) catalysts, was first performed with benzylbromide. $\text{RuCl}_3 \cdot x\text{H}_2\text{O}$ appeared a better catalyst in pentane or under neat conditions and led to preferential 2-benylation with respect to 3-benylation [(Eq. 33)] [107].

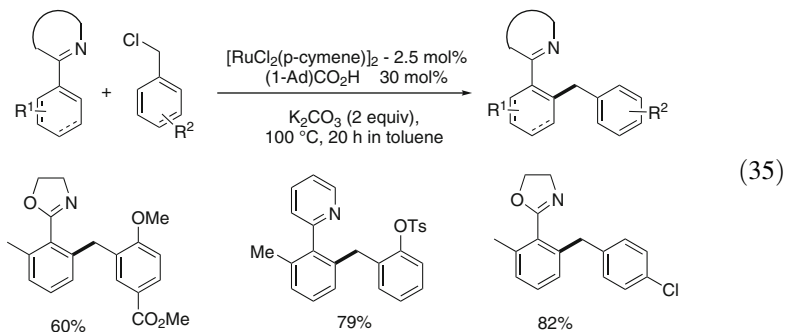


The previous alkylation with benzylbromide does not allow a β -elimination process. Ackermann has then shown some examples of monoalkylation with alkylbromides demonstrating that reductive elimination was faster than β -elimination of the transmetallated alkyl-ruthenium(II) $\text{Ru}(\text{Ar})(\text{CH}_2\text{CH}_2\text{R})$ moiety [108] and that the reaction could even be performed for some examples in water [109].

The alkylation of arylpyridine derivatives with unactivated alkylhalides bearing β -hydrogen was carried out with the $[\text{RuCl}_2(p\text{-cymene})]_2/1\text{-AdCO}_2\text{H}$ catalyst in NMP and produced only the monoalkylated products [Eq. 34] [108]. The alkylation of phenylpyridine and pyrazole with both primary and cyclic secondary alkyl halides led to regioselective intermolecular *ortho* monoalkylation.

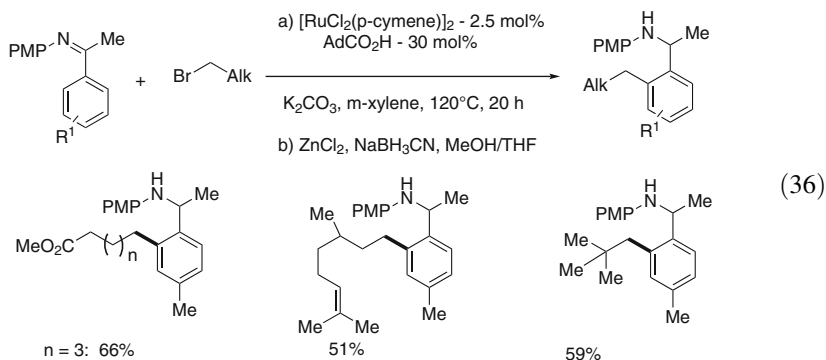


The alkylation of 2-arylpyridine and 2-aryloxazoline derivatives with benzylhalides leads to regioselective *ortho*-monoalkylations under similar conditions and to the formation of diarylmethane compounds. However this reaction revealed the surprising higher efficiency of benzylchlorides compared to benzylbromides [(Eq. 35)] [110].



The monoalkylation of protected aromatic imines with alkylbromides in the presence of $[\text{RuCl}_2(p\text{-cymene})]_2$ catalyst with AdCO_2H , preferentially to AcOK , as

co-catalyst was operating in *m*-xylene at 120°C. With β -hydrogen with respect to the bromide no β -elimination was observed illustrating a fast reductive elimination in the C–C bond formation. The reaction could be followed by reduction into *ortho*-alkylated amines using the ZnCl₂/NaBH₃CN/MeOH-THF stoichiometric reagent [(Eq. 36)]. PMP=*p*-methoxyphenyl [108, 109].

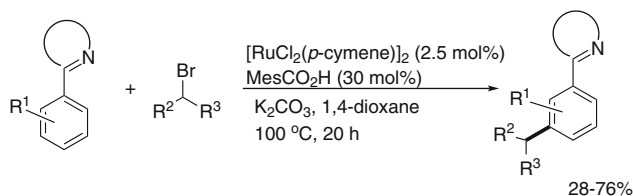
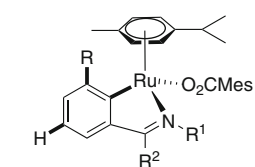


The alkylation of *meta*-substituted arylketimines shows that *meta* substituents protect the neighbouring *ortho* C–H bond by steric hindrance. By contrast, if this *meta* group is an electron-withdrawing group such as fluorine its neighbouring *ortho* C–H bond is preferentially activated and then alkylated [109].

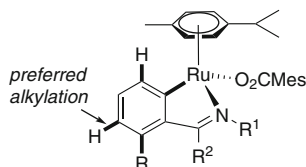
The alkylation of *p*-methoxyphenylpyridine is not inhibited by water as solvent but water slightly modifies the regioselectivity of alkylation as a small amount of alkylation at *meta*-position is observed beside the major alkylation at *ortho*-position [109].

Site selectivity in intermolecular C–H bond transformations favouring *meta* with respect to *ortho* position is a challenging topic and is attracting wide interest. In the field of ruthenium catalysed C–H bond activation, Frost et al. demonstrated first that ruthenium-catalysed electrophilic sulfonation with sulfonyl chlorides of phenylpyridine led to *meta*-selective sulfonation [111]. Recently, Ackermann's group reported the carboxylate-assisted ruthenium-catalysed *meta*-selective C–H bond alkylation with secondary alkylhalides of arenes containing heterocycle directing group [112]. Pyridyl-, pyrimidyl-, pyrazolyl-, imidazolyl-, and benzimidazolyl-substituted arenes reacted with secondary alkylhalides affording the *meta*-alkylated products in moderate to good yields by using [RuCl₂(*p*-cymene)]₂/MesCO₂H catalytic system (Scheme 10).

Based on the support of mechanistic studies, a reversible cyclometallation and electrophilic-type substitution are proposed in the catalytic cycle. Electron-rich groups on the arene ring favour this reaction. The electron-rich ruthenium (II) moiety in the metallacycle intermediate orientates electrophilic substitution at its *para*-position thus at the *meta*-position of functional group (Scheme 10b) [112].

(a) *Meta*-substituted arene

steric interaction: reduced efficacy

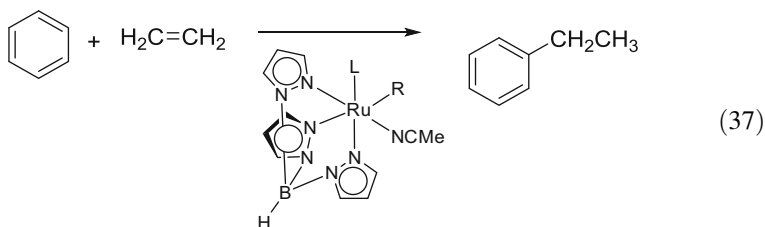
(b) *Ortho*-substituted arene

mainly C-3 alkylation

Scheme 10 Ru(II)-*meta*-selective alkylation of arenes with secondary alkylhalides. (a) *Meta*-substituted arene; (b) *Ortho*-substituted arene

3.2 Hydroarylation of Alkenes

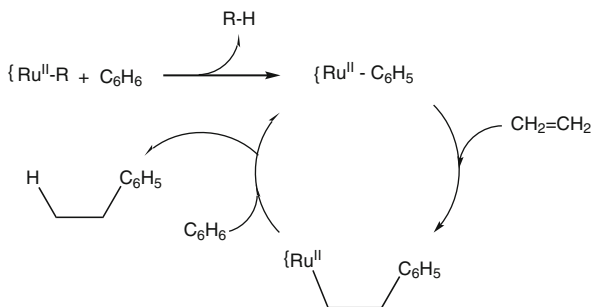
Hydroarylation of alkenes offers a more atom-economical process of catalytic C–H bond alkylation. It involves the transition-metal catalysed formal addition of the arene C–H bond onto C=C bonds. Especially T. B. Gunnoe and his group have shown that ruthenium(II) catalysts favour the addition of aromatic C–H bonds to an olefin C=C bond. They have used ruthenium(II) catalysts of type $TpRu-R(L)$ (NCMe) (Tp =hydrotris(pyrazolyl)borate) and demonstrated the efficiency of the formation of ethylbenzene via catalytic addition of benzene to ethylene [(Eq. 37)] [113–118]. Analogously the same type of catalyst $TpRu-R(L)$ (NCMe) promotes the alkylation by ethylene at C2 position of furan and thiophene [119].



(37)

The proposed mechanism based on kinetic studies and calculations involves the initial reversible coordination of benzene and the formation of a key Ru(II)-C₆H₅ bond with alkane R–H elimination without formation of a Ru(IV) intermediate

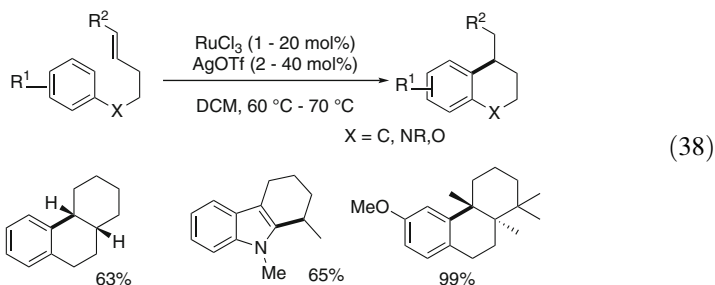
Scheme 11 Proposed mechanism for the Ru(II)-catalysed hydroarylation of ethylene



species. The ethylene inserts into the Ru(II)-C₆H₅ bond to give an alkyl-Ru(II) species that reacts with benzene to regenerate the Ru(II)-C₆H₅ and to produce the ethylbenzene (Scheme 11) [113–118, 120].

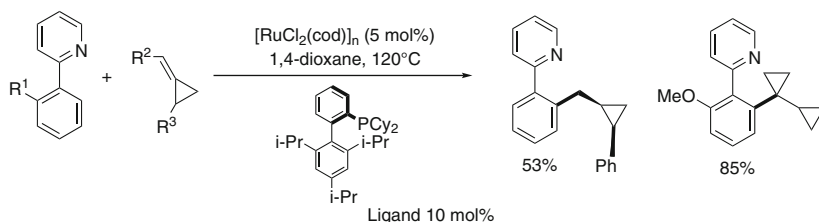
The C–H bond activation of coordinated benzene is the rate-determining step and is favoured by electron-donating ligands L. By contrast the withdrawing ligand L=CO provides a more efficient catalyst for hydroarylation of ethylene, by decreasing the energy barrier of the olefin insertion [120].

Another formal hydroarylation of alkenes corresponds to the electrophilic substitution of arenes with alkenes assisted by an electrophile. Sames and co-workers have demonstrated that the catalytic system RuCl₃/AgOTf transformed selectively arenes containing an alkene chain via the intramolecular hydroarylation of the distant C=C bond leading to the formation of a cycle [(Eq. 38)] [121]. A variety of bicyclic compounds such as tetrahydroquinoline, indolo-cyclohexane or cyclopentane, chromane, tetralin, and dihydrocoumarin have thus been obtained. The catalyst tolerates functional groups of substituted homoallylic aryl ethers such as phenol and protected amine. Polyene chains can lead to terpenoids in good yield with low catalyst loading. This reaction likely proceeds via electrophilic activation of the double bond with dehalogenated Ru(III) cationic species, electrophilic substitution of arene with C–C bond formation, and protonation of the remaining C–Ru intermediate, rather than involving a C–H bond activation.



Under conditions of ruthenium(II) catalysed sp² C–H bond activation of phenyl pyridine Ackermann has shown the direct intermolecular hydroarylation of highly

strained methylenecyclopropanes. The $[\text{RuCl}_2(\text{cod})]_n$ catalyst with an excess of bulky electron-rich monophosphine was successfully used. The hydroarylation of bicyclopropylidene with *ortho* C–H bond of phenylpyridine was performed. The hydroarylation of substituted methylenecyclopropanes leads to the formation of *cis*-adducts [(Eq. 39)] [122].

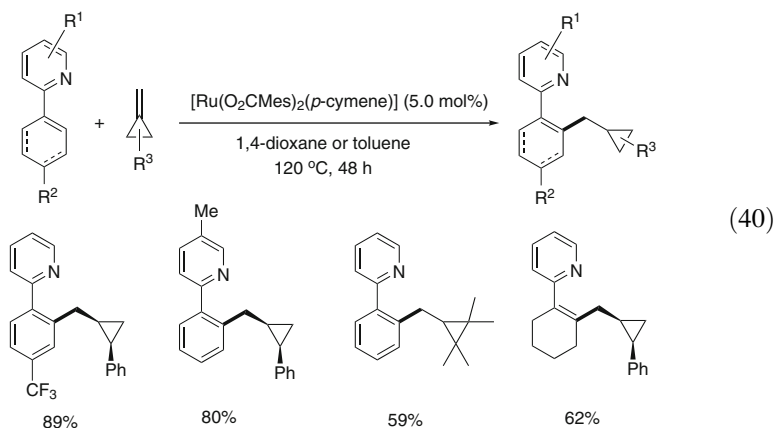


(39)

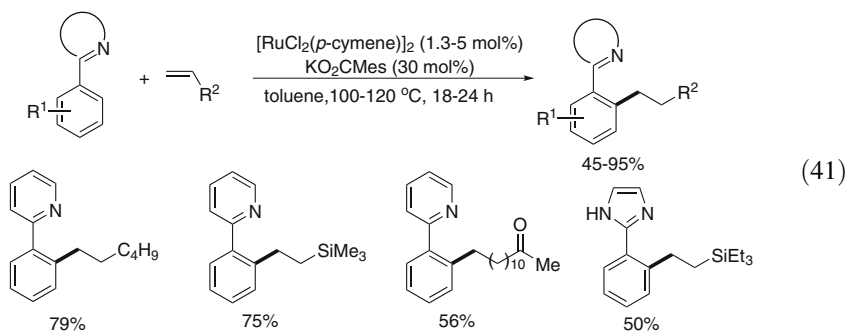
Recently, Ackermann extended this ruthenium(II) catalysed alkylation with methylenecyclopropanes at *ortho*-position of a variety of nitrogen containing 2-arylheterocycles using $[\text{RuCl}_2(\text{cod})]_2$ catalyst with basic and bulky phosphine (X-Phos). In some examples an *anti*-Markovnikov addition was observed, but in some examples ring opening occurred and *ortho*-dialkylated product could be formed [123].

The use of C_6D_5 -Py showed a partial deuterium retention in the resulting alkyl group. Thus the authors suggested that the reaction occurs via the formal insertion of the ruthenium(II) into the *ortho* C–H bond, alkene insertion into the Ru–H bond and reductive elimination with C–C bond formation similarly to a Ru(0) catalysed Murai type reaction [36, 39]. However this possible mechanism needs to be demonstrated as it may also result from a classical Ru(II) C–H bond activation, cyclometallation and insertion of the C=C bond into the Ru–C bond. The later process corresponds to the addition of the Ru–C bond to the less hindered face of the alkene (opposite to the Ph substituent). The last step involves a protonation of the Ru–C bond after alkene insertion [122, 123].

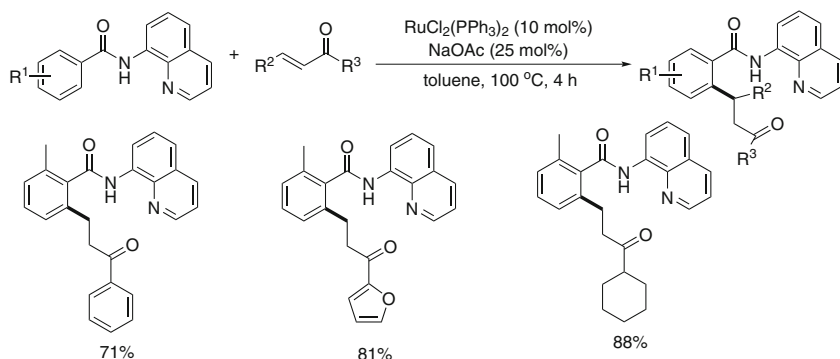
It has now been found that the well-defined catalyst containing carboxylate ligands $\text{Ru}(\text{O}_2\text{CMes})_2(p\text{-cymene})$ appears as a more efficient catalyst than $[\text{RuCl}_2(\text{cod})]_2$ catalyst without additional phosphine and the reaction occurs without ring opening [(Eq. 40)] [124]. A high regioselectivity and stereoselectivity of the hydroarylation are observed.



With the modified carboxylate-Ru(II) catalyst $\text{Ru}(\text{O}_2\text{CMes})_2(p\text{-cymene})$, the hydroarylation of non-activated and unstrained alkenes was strongly improved in toluene, even in H_2O . Various unactivated alkenes including ether, ketone, hydroxyl, ester, and fluorine functionalized alkenes led to monoalkylated products in moderate to high yields [(Eq. 41)] [125]. This alkylation method could also be applied directly to heterocycles such as indole and thiophene derivatives and proceeded in site-selective manner.



α,β -Unsaturated acceptors have already been used for the sp^2 C–H bond alkylation of functional arenes by Ackermann [123, 125]. However, in 2013 Chatani developed a new C–H bond *ortho*-alkylation of aromatic amides, using this time an 8-aminoquinoline bidentate directing group, with various α,β -unsaturated ketones in the presence of $\text{RuCl}_2(\text{PPh}_3)_3/\text{NaOAc}$ catalytic system via the expected C–H bond deprotonation followed by 1,4-addition process [(Eq. 42)] [126].

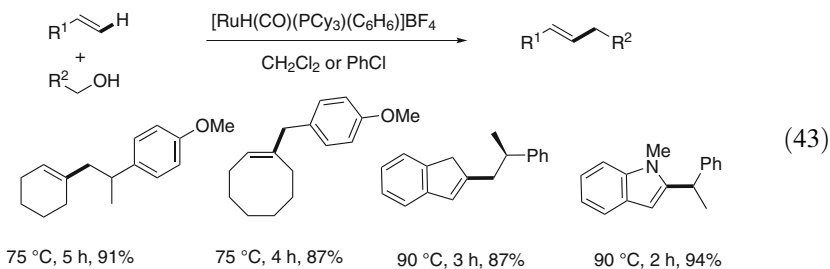


(42)

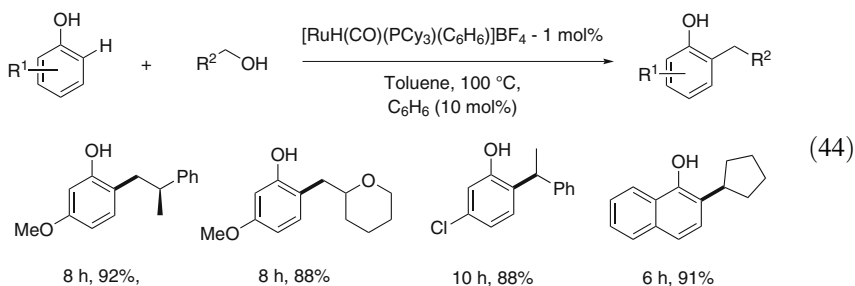
The reaction of 2-substituted aromatic amides afforded monoalkylated products, whereas the formation of dialkylated compounds was preferred in the case of 4-substituted aromatic amides. Furthermore, the 3-substituted group on the aromatic ring led to a mixture of mono- and di-alkylated amides. It is noteworthy that electron-withdrawing C=O group conjugated with olefins plays an important role to facilitate this reaction, as styrene and 1-hexene disfavoured this reaction. The H/D exchange occurred in the cleavage of the N–H bond indicating that the N–H bond is involved in the reaction.

3.3 Alkylation of (Hetero)arenes and Alkenes with Alcohols

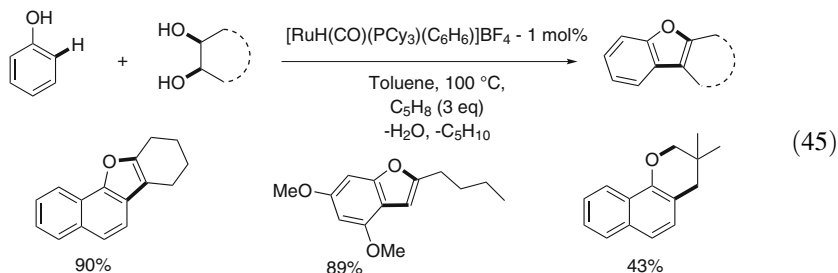
Primary alcohols are currently used as alkylating reagents with ruthenium (II) catalysts, in hydrogen borrowing reactions, via the formation of aldehydes, their condensation and rehydrogenation [59, 127, 128]. The first alkylation of heterocycle C–H bonds with ethanol was promoted with $[\text{RuCl}_2(p\text{-cymene})_2]$ [59]. Chae S. Yi has now succeeded using the ionic ruthenium(II) catalyst $[\text{RuH}(\text{CO})(\text{PCy}_3)(\text{C}_6\text{H}_6)]\text{BF}_4$ to alkylate alkenes simply with primary alcohols [(Eq. 43)] [129]. The reaction takes place with various terminal alkenes, cyclic olefins, indene or heterocycles with aliphatic and benzylic alcohols with high regioselectivity, high TON, and yield. Thus the intramolecular alkylation of geraniol generates *para*-cymene. Although the mechanism is not demonstrated, it is established that the rate-limiting step for this alkylation is the C–C bond formation, consistent with the $^{12}\text{C}/^{13}\text{C}$ kinetic isotope effects. The authors suggest the initial formation of a Ru-alkenyl bond from the alkene and the Ru-H species. However a hydrogen borrowing type reaction cannot be excluded via reaction of alkenyl-ruthenium species with the generated aldehyde.



The same $\text{RuH}(\text{CO})(\text{PCy}_3)(\text{C}_6\text{H}_6)]\text{BF}_4$ catalyst precursor has been used for the *ortho* sp^2 C–H bond monoalkylation of phenols with both primary and secondary alcohols, in which the hydroxyl phenol group is a directing group for C–H bond activation [(Eq. 44)] [130]. The alkylation with chiral (R)-PhCH(Me)CH₂OH occurs without racemization.



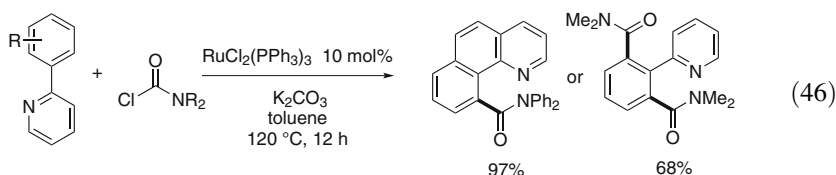
The $\text{RuH}(\text{CO})(\text{PCy}_3)(\text{C}_6\text{H}_6)]\text{BF}_4$ catalyst was used for the alkylation of phenol derivatives with 1,2-diols and the transformation affords selectively benzofurans via alkylation of *ortho* C–H bond of phenols and ether formation [(Eq. 45)] [130].



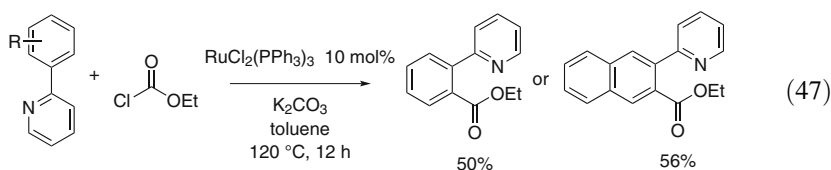
The proposed mechanism suggests the initial *ortho* aryl C–H bond deprotonation of phenols with ruthenium(II), although phenols were not shown to lead to a ruthenacycle intermediate, followed by electrophilic activation of alcohols on coordination to the ruthenium species followed by C–C bond formation [130].

4 Electrophilic Substitutions of Arenes with Ruthenium (II) and C–H Bond Activation

Ruthenium(II) catalysts have been shown recently and only in a few examples to allow Friedel–Crafts type reactions, via cross-coupled C–C bond formation involving a functional group, but without the addition of a traditional Lewis acid. An early example was reported by Kakiuchi et al. for the aminocarbonylation of phenylpyridine using $\text{RuCl}_2(\text{PPh}_3)_3$ catalyst in toluene [(Eq. 46)] [131]. The reaction with *N,N*-dialkylcarbamoyl chlorides R_2NCOCl led to diaminocarbonylation of the phenyl at *ortho*-position of the heterocyclic directing group and some dicarbonylation products could also be selectively obtained.

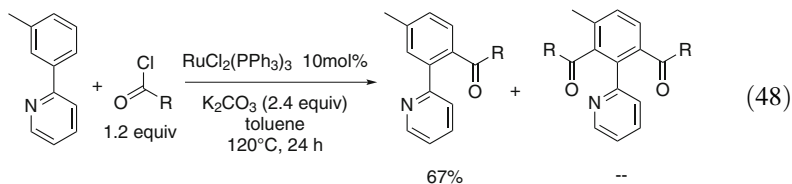


Usually Friedel–Crafts reactions are not possible with chloroformate reagents as decarboxylation takes place, but by using the same ruthenium(II) catalyst the reaction of phenylpyridine with alkyl chloroformate led to mono alkoxy carbonylation at the aryl *ortho* carbon atom showing that the ruthenium(II) catalyst tolerates ester groups [(Eq. 47)] [131]. These reactions require the presence of a strongly coordinating directing group such as pyridine. The same reactions with benzoquinoline led to monoaminocarbonylation and alkoxy carbonylation at C_{10} position.

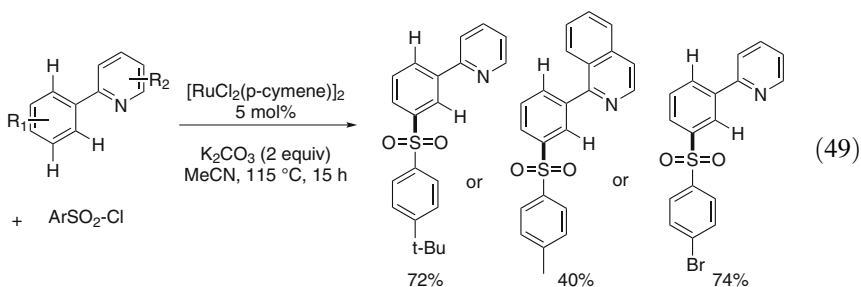


It is observed that the presence of a CF_3 group at the arene *meta*-position leads to a fast reaction likely by increasing the acidity of the *ortho* C–H bond thus favouring the ruthenacycle intermediate formation. The proposed mechanism, as for direct arylation of phenyl pyridine C–H bonds, involves initial cyclometalation, via carbonate-assisted C–H bond deprotonation, successive oxidative addition of ClCO_2R or ClCONR_2 and reductive elimination forming a C–CONu bond.

The $\text{RuCl}_2(\text{PPh}_3)_3$ catalyst can perform selective *ortho* acylation with arylchlorides of arylpyridines without addition of stoichiometric amount of a Lewis acid [(Eq. 48)] [132].



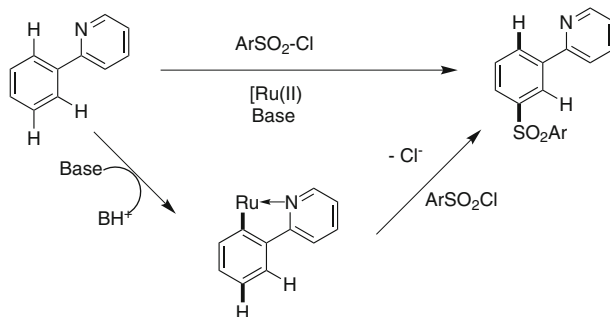
Whereas the previous arene electrophilic substitutions take place at *ortho* position of pyridine coordinating group, the sulfonation with arylsulfonyl chloride of phenylpyridines but in the presence of a ruthenium(II) catalyst $[\text{RuCl}_2(p\text{-cymene})]_2$ surprisingly led Frost et al. to observe for the first time an unexpected regioselective sulfonation at *meta*-position of the directing 2-pyridyl group [(Eq. 49)] [111].



The authors explained the surprising regioselectivity via the formation of the expected ruthenacycle arising from *ortho* C–H bond deprotonation followed by a $\text{S}_{\text{E}}\text{Ar}$ electrophilic substitution at the *para*-position with respect to the electron releasing ruthenium atom, thus at the *meta*-position of the 2-pyridyl directing group (Scheme 12) [111].

Actually for the arene alkylation of a variety of arylheterocycles with secondary alkylhalides, using the $[\text{RuCl}_2(p\text{-cymene})]_2/\text{MesCO}_2\text{H}$ catalytic system, which also afforded the *meta*-alkylated products, Ackermann also proposed an electrophilic substitution at the *para*-position of the ruthenium atom in the ruthenacycle intermediate (Scheme 10) [112].

The above examples demonstrate that Friedel–Crafts type reactions of functional arenes can be profitably performed using ruthenium(II) catalysts without Lewis acid addition. Whereas only *ortho* transformations of C–H bonds were observed before, the sulfonation reaction and the alkylation with secondary alkyl halides offer a challenging modification of the regioselectivity that is starting to occur at the *meta*-position of the functional groups and illustrate the specific positive role of the ruthenium atom in the metallacycle intermediate.



Scheme 12 Proposed mechanism for Ru(II)-assisted *meta* sulfonation

5 Synthesis of Alkenylated (Hetero)arenes with Ruthenium (II) Catalysts

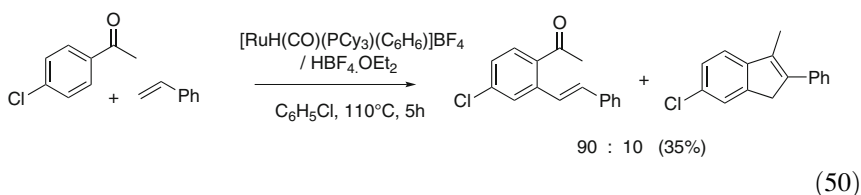
5.1 Ruthenium-Catalysed Alkenylation of sp^2 C–H Bonds with Functional Alkenes

5.1.1 First Examples of Ruthenium(II) Catalysed Alkenylation of C–H Bonds

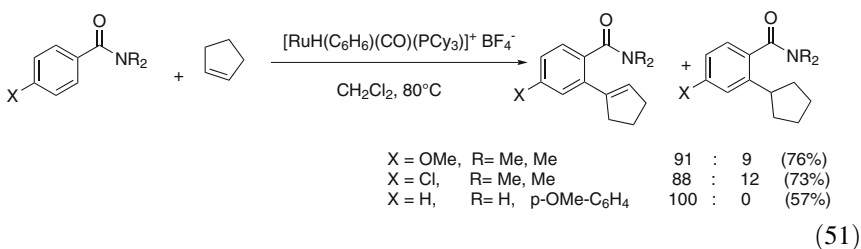
The Mizoroki–Heck type reaction is one of the most important processes for the cross C–C bond formation and for the useful synthesis of functional alkenes [52, 133, 134]. Recently, the oxidative Fujiwara–Moritani alkenylation [53], the first oxidative dehydrogenative C–C cross-coupling reaction between an alkene C–H and a different C–H bonds, initially performed with Pd(II) catalyst, has attracted a tremendous interest as an atom-economical way to form cross-coupled C–C bonds and functional alkenes [25]. This reaction was first reported by using palladium [53, 135] and then rhodium [17] catalysts. However, the less expensive ruthenium-catalysed oxidative alkenylation has not developed so fast. After a few rare previous examples a general method of ruthenium(II) catalysed alkenylation has been developed only since 2011, successively by Satoh and Miura [54], Ackermann [55], Bruneau and Dixneuf [56], and Jeganmohan [57]. The previous examples of alkenylation of C–H bonds with ruthenium(II) catalysts involved the use of alkenylboronic acids. They were first demonstrated by J. M. Brown using the $[RuCl_2(p\text{-cymene})]_2$ catalyst with $Cu(OAc)_2$ as stoichiometric oxidant at room temperature [136, 137]. Recently Jeganmohan has applied this reaction to the alkenylation of arylamides using the $[RuCl_2(p\text{-cymene})]_2/AgSbF_6$ catalyst with AgO as oxidant [(Eq. 32)] [105]. The first real oxidative alkenylation of arene with alkene catalysed by ruthenium was reported by Milstein in 2001. He performed the alkenylation of benzene with acrylate using $RuCl_3 \cdot xH_2O$, $[RuCl_2(CO)_3]_2$ and $[RuCl_2(C_6H_6)]_2$ catalyst precursors. The production was moderate but was

disfavoured by the absence of directing coordinating group and was improved by operating under carbon monoxide atmosphere [138].

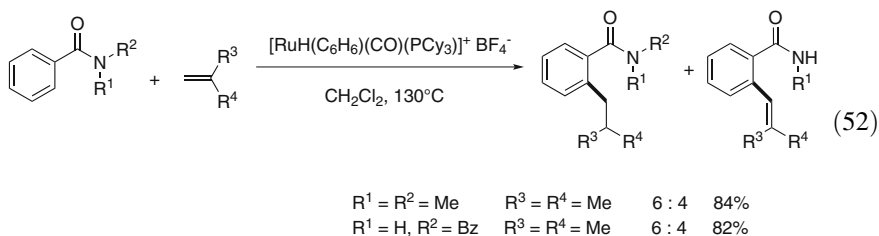
Alkenylation of aromatic C–H bonds was initially observed in several examples by Chae S. Yi using $[\text{RuH}(\text{CO})(\text{PCy}_3)(\text{C}_6\text{H}_6)]\text{BF}_4$ as catalyst precursor with a strong acid $\text{HBF}_4 \cdot \text{OEt}_2$ as catalyst precursor. The reaction of the naphthylketone with styrene led preferentially to the *ortho*-alkenylation product with low yield (35%) [(Eq. 50)] [139].



Chae S. Yi also reported the reaction of excess of cyclopentene with arylamides in the presence of $[\text{RuH}(\text{CO})(\text{PCy}_3)(\text{C}_6\text{H}_6)]\text{BF}_4$ catalyst which predominantly led to the *ortho*-alkenylation with a small amount of the alkylated product corresponding to the alkene insertion into the *ortho* C–H bond [(Eq. 51)] [140].



The use of 1,1-disubstituted terminal alkenes with the same catalyst and amides afforded the products with better yields but with a lower ratio in oxidative dehydrogenative coupling to the profit of the *ortho*-alkylated products [(Eq. 52)] [140].



These examples demonstrate that a ruthenium(II) catalyst precursor can lead to alkenylation of arenes at *ortho* position of ketone and amide functions without oxidant beside an acid. Whereas ketones did not allow the arylation at their *ortho*

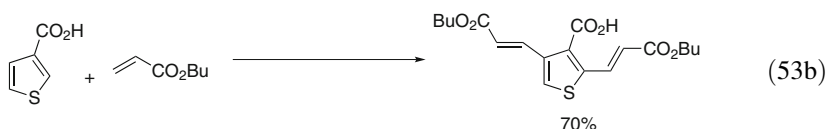
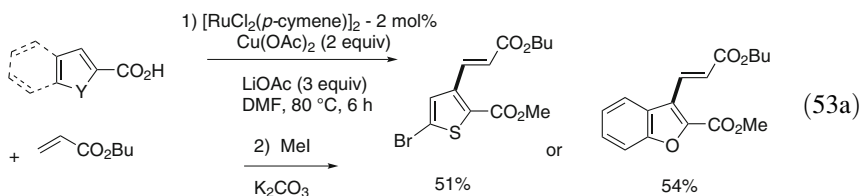
position these weakly coordinating functional groups play for the first time the role of directing group for both C–H bond activation and alkenylation.

5.1.2 A New Method of Alkenylation of Arenes with Ruthenium (II) and Copper(II)

The first general method for ruthenium(II)-catalysed oxidative dehydrogenative alkenylation of functional arenes showed successively the ability of carboxylate, heterocycle, ketone, aldehyde, amides, esters, and carbamates to behave as directing groups for C–H bond alkenylation and could also be applied to alkenes, ferrocenes, heterocycles, and protected phenols.

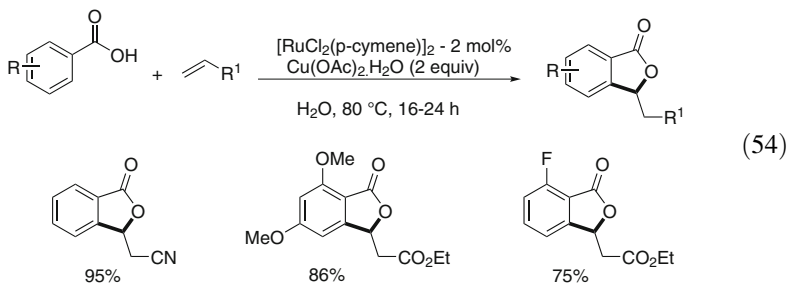
Carboxylate Directing Group

In 2011 Satoh and Miura reported a general method for the alkenylation of heterocycles containing a carboxylic acid function using ruthenium(II) catalyst. They showed that the dehydrogenative alkenylation by acrylates, with $[\text{RuCl}_2(p\text{-cymene})]_2$ catalyst and a stoichiometric amount of $\text{Cu}(\text{OAc})_2 \cdot \text{H}_2\text{O}$ as oxidant, was directed by the carboxylate group but took place without decarboxylation [Eq. 53a] [54]. The obvious advantage was that previous alkenylations with palladium(II) catalysts of heterocycles containing a carboxylic acid directing group took place with decarboxylation [141].



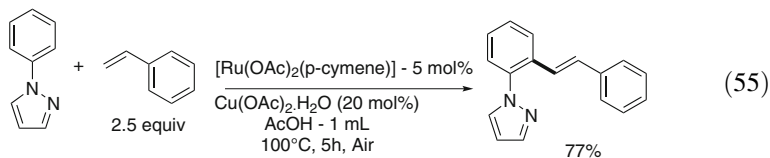
The directing ability of the carboxylic group was demonstrated by the alkenylation of the thiophene-3-carboxylic acid under the same conditions that led to the dialkenylation at both neighbouring C2 and C4 positions of the carboxylate [Eq. 53b] [54].

Ackermann reported the second general example of oxidative alkenylation with Ru(II) catalyst by reaction of benzoic acid derivatives with acrylonitrile or alkyl acrylates. The alkenylation this time was performed *in water* under mild conditions. Further oxa-Michael reaction occurred leading to lactones in good yields [(Eq. 54)] [55].

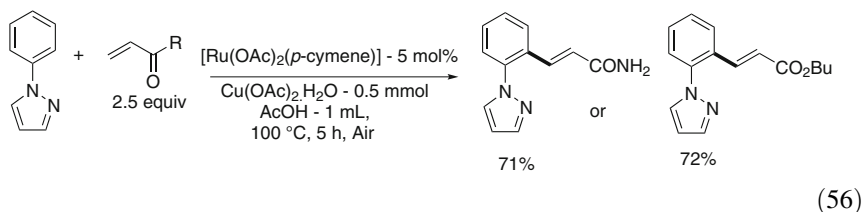


Heterocycle Directing Group

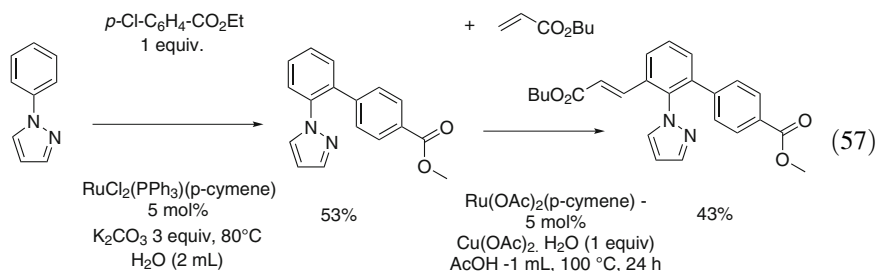
Oxidative monoalkenylation of functional arenes containing a *heterocycle as directing group* has been shown in parallel with a non-activated alkene by the Rennes group. The reaction of *N*-arylpyrazoles with styrene was promoted by Ru(OAc)₂(*p*-cymene) catalyst, with catalytic amount of Cu(OAc)₂.H₂O (20 mol %) in air at 100 °C [(Eq. 55)] [56]. The success was due to the use of acetic acid as solvent favouring the autocatalysed C–H bond activation of functional arenes by Ru (II)-OAc catalyst [49].



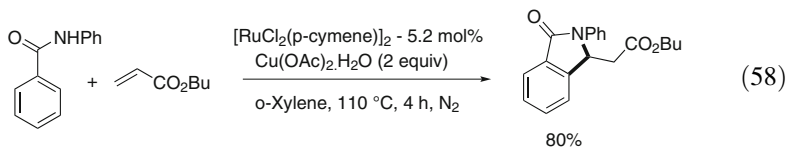
This alkenylation of pyrazoles with electrophilic alkenes such as alkyl acrylates or acryl amide with Ru(OAc)₂(*p*-cymene) catalyst is possible but is slower than with styrene. However it takes place almost quantitatively with stoichiometric amount of Cu(OAc)₂.H₂O in acetic acid [(Eq. 56)] [56]. With *N*-*p*-methoxy-substituted arylpyrazoles, the *ortho*-alkenylation with acrylates can take place using stoichiometric amount of Cu(OAc)₂.H₂O [56].



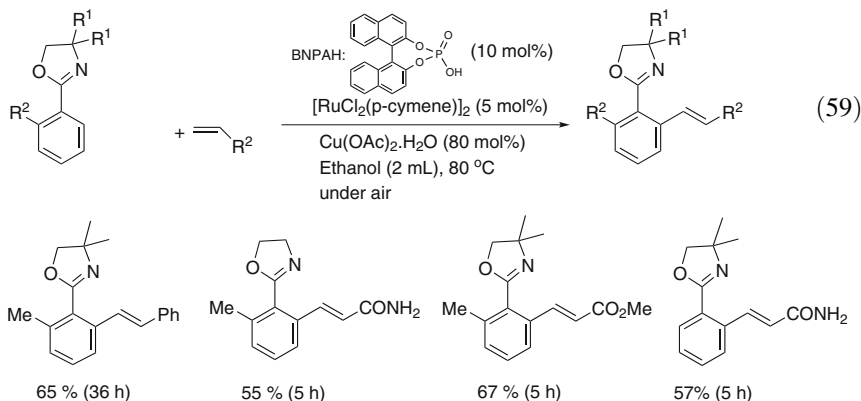
Alkenylation directed by pyrazole has been used to introduce different functions at arene *ortho* position. First selective monoarylation of *N*-phenylpyrazole was achieved using $\text{RuCl}_2(\text{PPh}_3)(p\text{-cymene})$ catalyst but in water [(Eq. 57)] [89]. The alkenylation of monoarylated phenylpyrazole with *n*-butyl acrylate was attempted in the presence of $[\text{RuCl}_2(p\text{-cymene})]_2/\text{AgSbF}_6$ catalyst with $\text{Cu}(\text{OAc})_2 \cdot \text{H}_2\text{O}$ but this catalytic system did not provide any conversion. However the second *ortho* C–H bond was successfully alkenylated with carboxylate-ruthenium(II) $\text{Ru}(\text{OAc})_2(p\text{-cymene})$ as catalyst with $\text{Cu}(\text{OAc})_2 \cdot \text{H}_2\text{O}$ as oxidant and in acetic acid [(Eq. 57)] [89].



The *ortho*-alkenylation of arylpyrazoles with acrylates has also been performed by Miura et al. with $[\text{RuCl}_2(p\text{-cymene})]_2$ catalyst and 2 equiv. of $\text{Cu}(\text{OAc})_2 \cdot \text{H}_2\text{O}$ in DMF under nitrogen atmosphere [142]. They also found that under the same conditions benzylanilide reacts with *n*-butyl acrylate in *o*-xylene on activation with Ru(II) catalyst and the reaction further led to intramolecular nucleophilic addition to the double C=C bond and to the corresponding lactam [(Eq. 58)] [142].

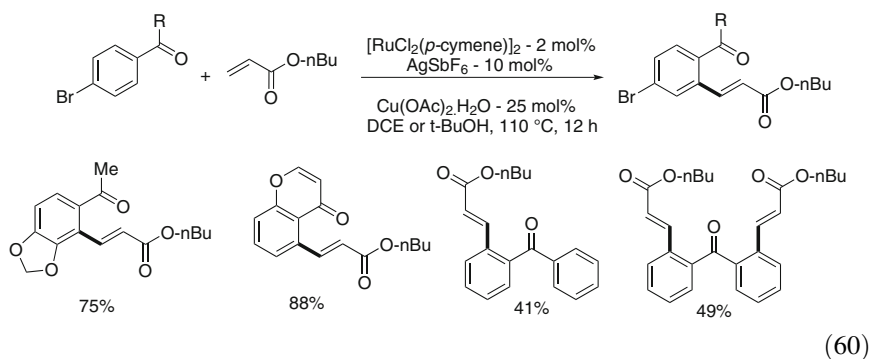


The oxazoline group has been used profitably to direct the *ortho*-alkenylation with acrylates of the linked phenyl group. The reaction occurs under mild conditions using the 1,1'-binaphthyl-2,2'-diyl hydrogenphosphonate (HMPAH) in methanol preferably to KOAc or $\text{K}_2\text{O}_2\text{CPh}$. The reaction requires less than 1 equiv. of $\text{Cu}(\text{OAc})_2 \cdot \text{H}_2\text{O}$ but under air [(Eq. 59)] [143]. The selective mono alkenylations with acrylates, styrenes, and acrylamide could be made.



Ketone Directing Group

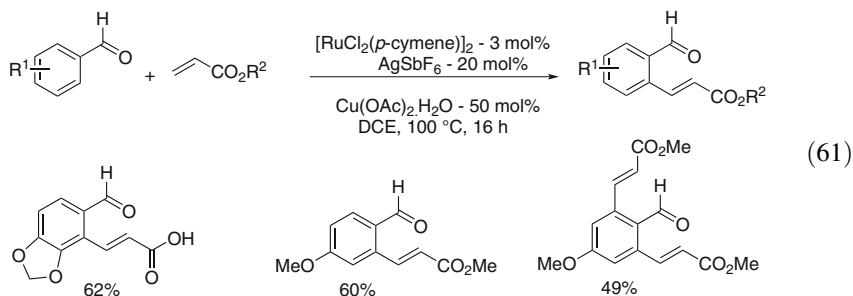
At the end of 2011 Jeganmohan reported for the first time the general ruthenium(II)-catalysed functionalization of aryl C–H bonds at the *ortho*-position of a ketone directing group, which was not possible previously for direct arylation by contrast to the corresponding imines [43, 44, 84, 85]. Jeganmohan used the ruthenium (II) catalyst $[\text{RuCl}_2(p\text{-cymene})]_2$ with AgSbF_6 to abstract the chlorides from the ruthenium(II) complex and, in the presence of $\text{Cu}(\text{OAc})_2 \cdot \text{H}_2\text{O}$ as oxidant succeeded for the first time with Ru(II) catalyst to achieve the *ortho*-*E*-alkenylation of arenes bearing a directing ketone group. Under similar conditions benzophenone led to *ortho* mono and dialkenylated products [(Eq. 60)] [57]. This Jeganmohan catalytic system is now currently used in alkenylation reactions.



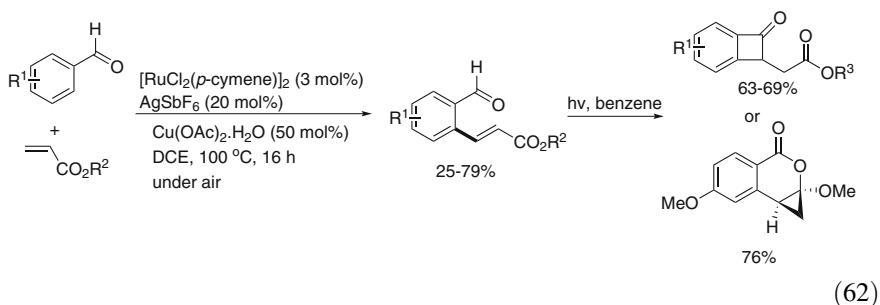
After abstraction of chlorides affording a cationic ruthenium(II) species the mechanism is thought to generate the 5-membered cyclometalated complex via C–H bond deprotonation, followed by regioselective alkene insertion and β -elimination [57]. The in situ formation of $\text{Ru}(\text{OAc})_2(\text{arene})$ is postulated.

Formyl Directing Group

Using a similar catalytic system $\text{RuCl}_2(p\text{-cymene})_2/\text{AgSbF}_6$ with $\text{Cu}(\text{OAc})_2 \cdot \text{H}_2\text{O}$ under open atmosphere Jeganmohan showed in 2012 that the formyl group, a weakly coordinating group, directed the alkenylation at their *ortho*-position of aromatic aldehydes. Electron-rich substituents on the aromatic ring such as dioxole, OMe, Me, and NMe_2 gave higher yields than electron-withdrawing substituents such as Cl, CN, and CO_2Me [(Eq. 61)] [144].

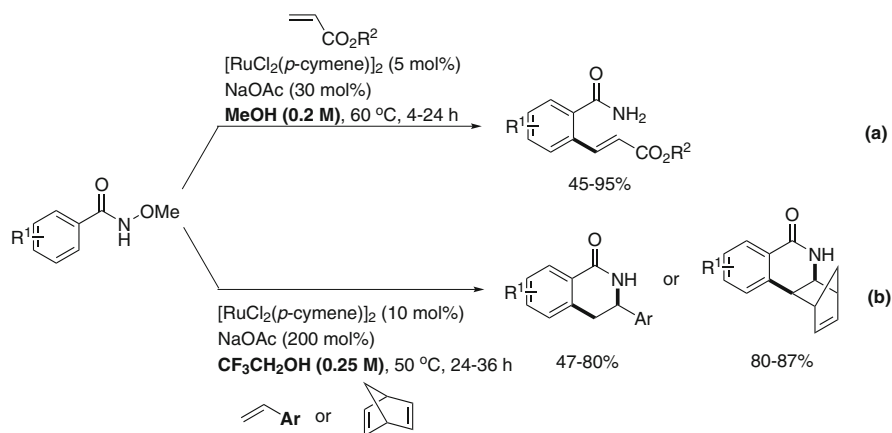


Interestingly, the *ortho*-alkenylation of aromatic aldehydes allowed the access to four-membered cyclic ketones and to polysubstituted isochromanone derivatives by an irradiation in benzene of the alkenylated product [(Eq. 62)] [144].



Amide Directing Group

Just after one first example of alkenylation directed by an amide by Miura [(Eq. 53)] [142] Bin Li and Baiquan Wang, in the beginning of 2012, reported the $[\text{RuCl}_2(p\text{-cymene})_2]$ catalysed oxidative alkenylation with acrylates of *N*-methoxybenzamides but this time without $\text{Cu}(\text{OAc})_2 \cdot \text{H}_2\text{O}$ using the CONH(OMe) group as an oxidizing and directing group (Scheme 13a) [145]. The reaction is performed in the presence of NaOAc (30 mol%) in methanol at 60°C. The alkenylation is reached with acrylates, but less active styrene and norbornadiene

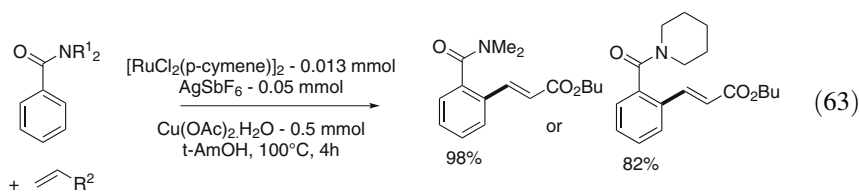


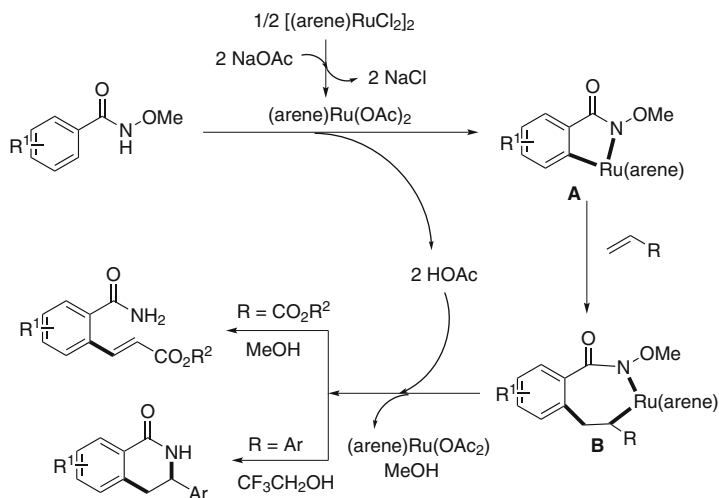
Scheme 13 Alkenylation of *N*-methoxybenzamides with acrylate in MeOH and styrene in CF₃CH₂OH

can not afford the desired product. However, *N*-methoxybenzamides react with styrene and norbornadiene in the presence of 10 mol% of catalyst but in solvent CF₃CH₂OH and the alkenylation is followed by nucleophilic intramolecular addition to the formed C=C bond and 3,4-dihydroisoquinolinone derivatives were isolated in 47–87% yields (Scheme 13b) [145].

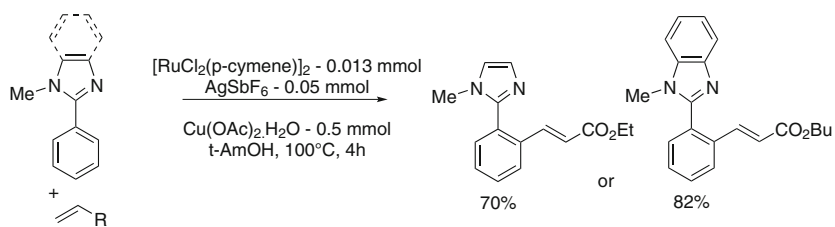
The H/D experiment studies show that the acetate-assisted C–H bond metallation is an irreversible step. A proposed mechanism is shown in Scheme 14 [145]. The cyclometallated intermediate **A** is expected to be formed from *N*-methoxybenzamide with in situ generated Ru(OAc)₂(*p*-cymene) catalyst. The regioselective insertion of the alkene leads to the intermediate **B**. The alkenylated product is produced via β-elimination from the intermediate **B** in the case of acrylate in methanol, whereas with styrene or norbornadiene in CF₃CH₂OH alkyl and aryl group in **B** favour reductive elimination. These last processes lead to the release of MeOH with the regeneration of the Ru(OAc)₂(*p*-cymene) catalyst.

Using a similar [RuCl₂(*p*-cymene)]₂/AgSbF₆ catalytic system and Cu(OAc)₂·H₂O but in *t*-AmOH at 100 °C under nitrogen, Miura and co-workers reported the regioselective *ortho*-alkenylation with alkyl acrylates of *N,N*-dialkylbenzamides [(Eq. 63)] and phenylazoles [(Eq. 64)] [146].



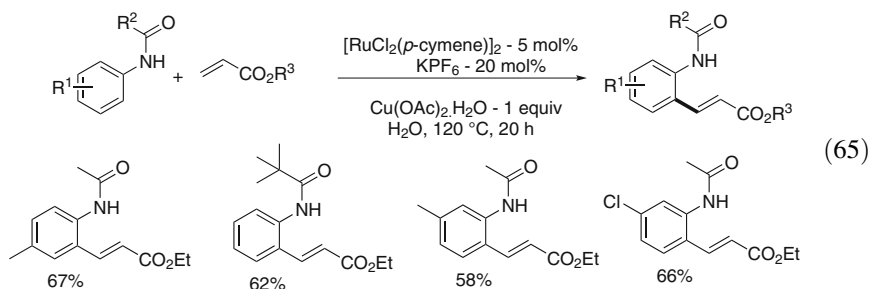


Scheme 14 Proposed mechanism for alkenylation of *N*-methoxybenzamides

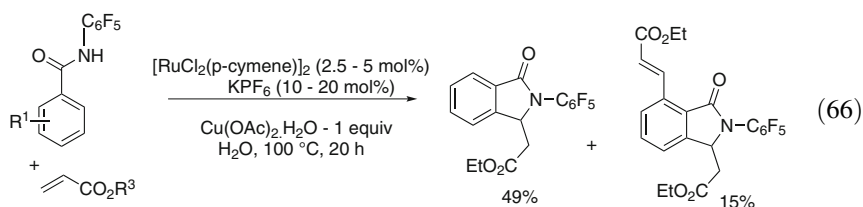


(64)

The above ruthenium(II)-catalysed cross-dehydrogenative alkenylation of benzamides and anilides with ruthenium(II) catalyst was performed in organic solvent. Ackermann's group succeeded to perform this catalytic monoalkenylation reaction in water using the non-coordinating salt KPF₆ (20 mol%) in the presence of Cu(OAc)₂.H₂O as the oxidant. It is noteworthy that this catalytic system is more active in water than in DMF, NMP, *t*-AmOH and the reaction is favoured by electron-rich anilides [(Eq. 65)] [147]. For *N*-benzoyl anilines the C–H bond alkenylation of the aromatic ring linked to the amide carbonyl was observed. It is consistent with the activation of the more acidic C–H bond of the phenyl linked to the carbonyl group and with the preferred NH coordinating directing group leading to a N–Ru bond in the 5-membered cyclometallate intermediate.

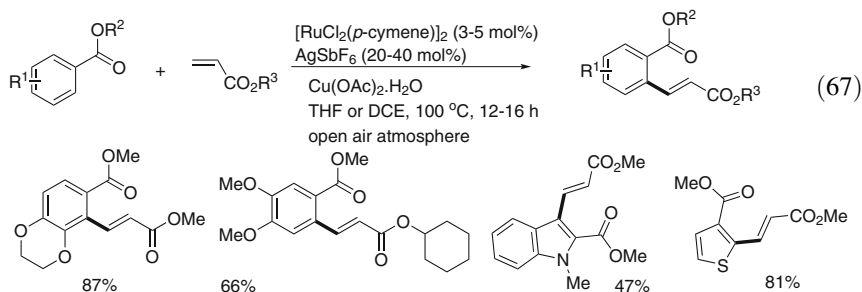


The same reaction in water applied to *N*-pentafluorophenyl benzamides led to the mono alkenylation of benzamides followed by intramolecular aza-Michael addition and formation of lactams [(Eq. 66)] [147].



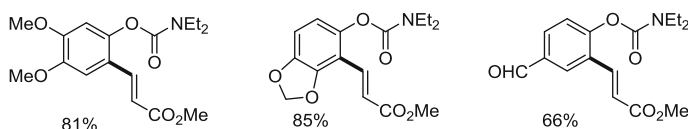
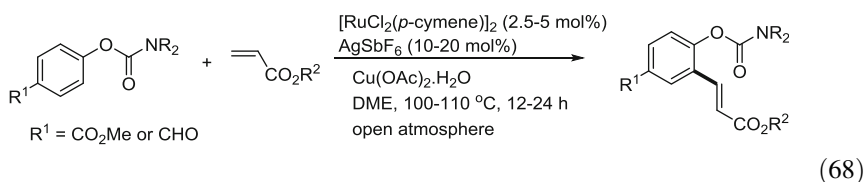
Ester Directing Group

A similar catalyst $[\text{RuCl}_2(p\text{-cymene})]_2/\text{AgSbF}_6$ was used first by Jegannathan [148], and soon after by Ackermann [149], to show that aromatic and heteroaromatic esters could be alkenylated by acrylates with the help of $\text{Cu}(\text{OAc})_2 \cdot \text{H}_2\text{O}$ under an open air atmosphere in 1,2-dichloroethane [(Eq. 67)]. Thus ester groups are tolerated and direct C–H activation at *ortho* position. The reaction appears quite general and can be applied to thiophene, furan, and indol derivatives but an electron-withdrawing group on aromatic esters disfavours this cross-coupling reaction [(Eq. 67)] [148, 149].



Carbamate Directing Group

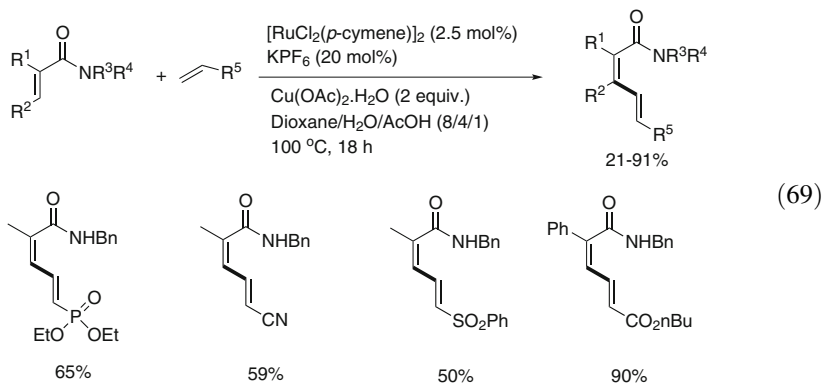
Carbamates are very useful compounds in organic synthesis and protecting groups of phenol, thus aryl carbamates have been explored as directing groups for alkenylation by Ackermann first [150] and then by Jeganmohan [(Eq. 68)] [151]. They showed the mono *ortho*-alkenylation of aryl carbamates with acrylates but also with unreactive alkenes such as phenyl vinyl sulfone, acrylonitrile, and less reactive styrenes, using catalyst $[\text{RuCl}_2(p\text{-cymene})]_2/\text{AgSbF}_6$ in 1,2-dimethoxyethane [(Eq. 68)] [151]. It is noteworthy that both electron-donating and electron-withdrawing groups are suitable for this cross-coupling reaction. It was shown that carbamate groups are more efficient directing groups than CO_2Me or CHO groups, as when R^1 is CO_2Me or CHO group alkenylation took place only at the *ortho* position of the carbamate group [(Eq. 68)] [151].



The carbamate directing group is easily removed and led to substituted phenol using 10–20 equiv. of NaOH in EtOH at 80°C [150, 152] or using 5 equiv. of LiOH. H₂O in THF/MeOH/H₂O (4:1:1) solvent at 80°C [151].

5.1.3 Alkenylation of Alkenes, Ferrocenes, Heterocycles, and Phenol Derivatives with Ru(II) and Cu(II) Partners

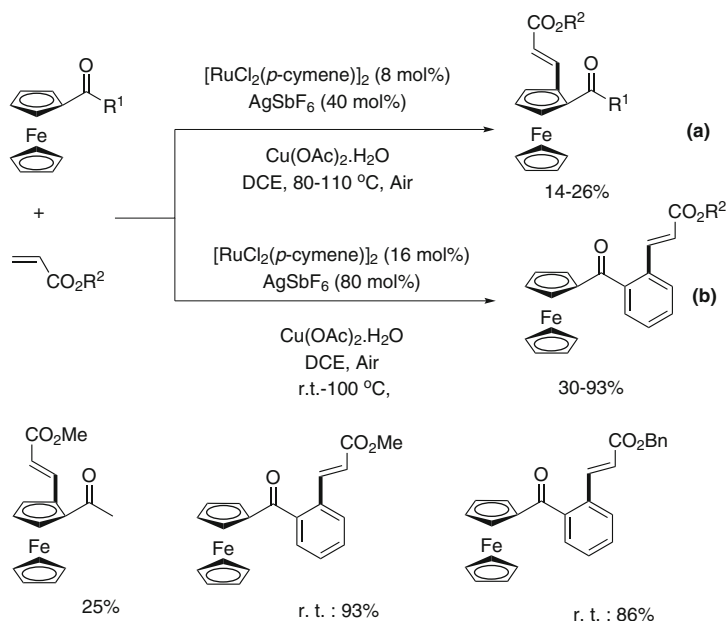
The ruthenium(II) alkenylation of functional alkenes was first performed by Loh [153]. Thus (*Z,E*)-dienamides were successfully produced via the Ru(II)-catalysed alkenylation of acrylamides with electron-deficient alkenes. This reaction was performed in the presence of 2.5 mol% of $[\text{RuCl}_2(p\text{-cymene})]_2$, 20 mol% of KPF_6 , with oxidant $\text{Cu}(\text{OAc})_2 \cdot \text{H}_2\text{O}$. Various functional alkenes containing the CO_2R , CONHBn , $\text{PO}(\text{OEt})_2$, CN , SO_2Ph , or 4-Cl phenyl group led to the (*Z,E*)-dienamides in moderate to good yields. The reaction *N*-aryl methacrylamides with acrylate gave the desired products in 31–39% yield [(Eq. 69)] [153].



Functional ferrocene derivatives offer wide applications as ligands in catalysis, optical materials and polymers, due to their sandwich structure. The catalytic ferrocene C–H bond functionalization remains a challenge to synthesize new ferrocene derivatives with planar chirality. Although the direct arylation of ferrocene derivatives with aryl halides has not been performed yet with ruthenium catalysts, Singh and Dixneuf have reported the catalytic alkenylation of ferrocenyl ketones via C–H bond activation using ruthenium(II) catalyst. The ferrocenyl alkyl ketones were alkenylated with alkyl acrylates under conditions close to that of Jeganmohan for aromatic ketones [(Eq. 60)] [57], in the presence of 8 mol% of $[\text{RuCl}_2(p\text{-cymene})]_2$, 40 mol% of AgSbF_6 and 2 equiv. of $\text{Cu(OAc)}_2 \cdot \text{H}_2\text{O}$ in DCE under aerobic conditions at 80–110°C, but in low to moderate yields (<30 %) (Scheme 15a) [154]. However this reaction shows that the ketone group on ferrocene directs alkenylation at ferrocene position 2 only, thus affording a planar chiral derivative.

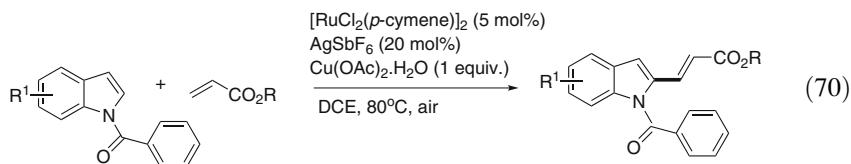
This reaction was performed with ferrocenyl phenyl ketone to explore the competition between (Fc)C–H and (Ph)C–H bonds. Surprisingly the reaction took place *at room temperature* and quantitative yields of the phenyl monoalkenylated products were obtained (Scheme 15b) [154]. These reactions show the regioselective *ortho*-alkenylation of the phenyl C–H bond closed to the carbonyl group and that the phenyl group is alkenylated much faster than the electron-rich ferrocenyl group.

The previous oxidative alkenylations were mostly performed by initial ruthenium(II) C–H bond activation of arenes involving a 5-membered metallacycle intermediate. Recently Prabhu performed this reaction with heterocycles attached to a directing group using the now classical catalyst based on Ru(II)/ AgSbF_6 system with $\text{Cu(OAc)}_2 \cdot \text{H}_2\text{O}$ as oxidant. The alkenylation with alkyl acrylates of indoles containing a *N*-benzoyl directing group led to the functionalization of indole C2 carbon exclusively, not at the phenyl of the benzoyl group [(Eq. 70)] [155]. This

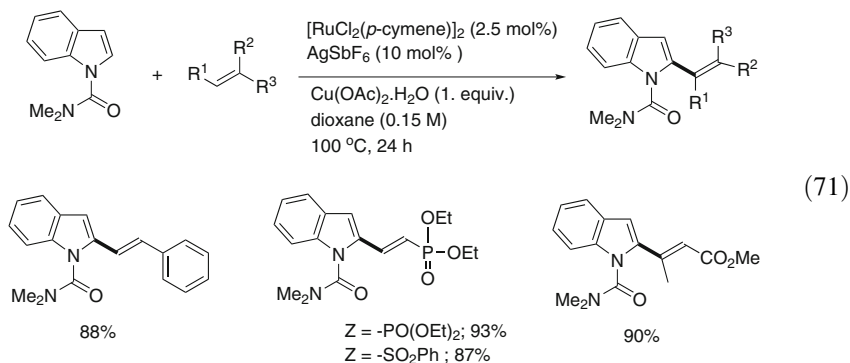


Scheme 15 Ru(II)-catalysed alkenylation of ferrocenyl ketones

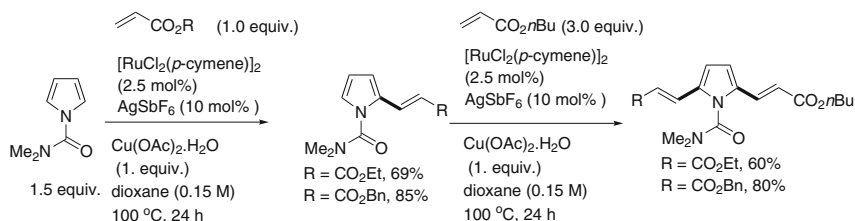
contrasts with the alkenylation of the same indoles with palladium(II) catalysts leading to alkenylation at the indole C3 carbon and shows the complementary benefit brought by ruthenium(II) catalysts [155].



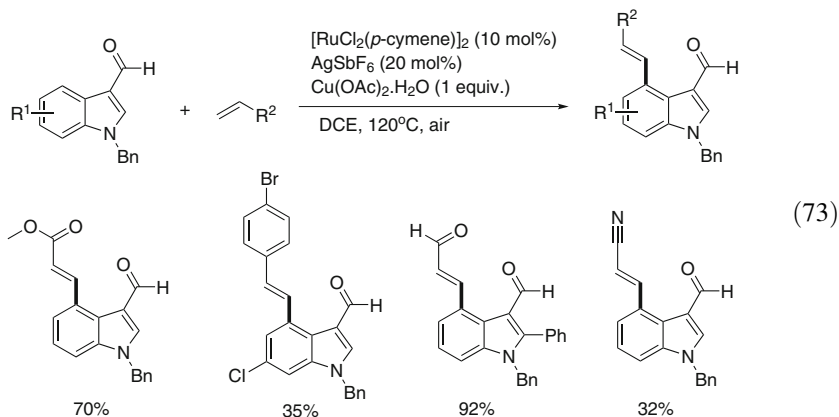
Li and Wang using Ru(II)/ $AgSbF_6$ system with $Cu(OAc)_2 \cdot H_2O$ as oxidant showed in parallel the selective oxidative alkenylation of indoles, containing an easily removable N-protecting dialkylamide group with acrylates and styrene. The alkenylation selectively occurred at C2 position and showed the directing ability of the N-amide. A large variety of functional alkenes were profitably used including cyclopentenone, methyl methacrylate, and *E*-methyl crotonate [(Eq. 71)] [156].



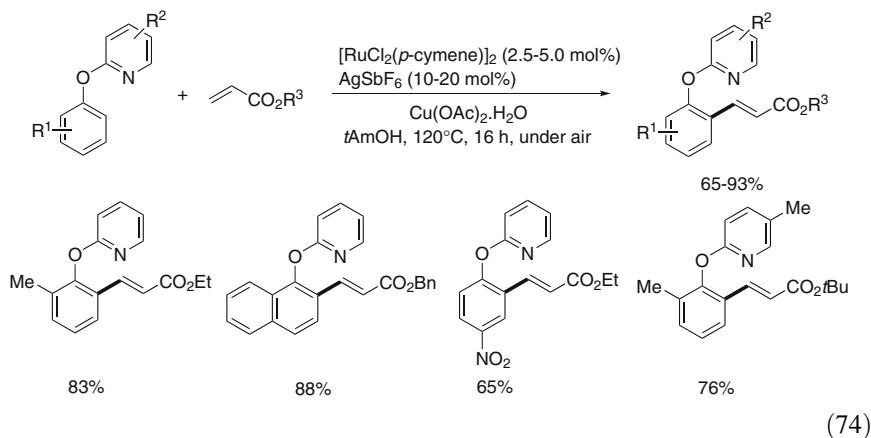
The alkenylations of amide N-protected pyrrole with an excess of acrylate led to dialkenylation at C2 and C5 positions of pyrrole. The successive alkenylation of pyrrole at C2 and C5 positions led to unsymmetrical substituted pyrroles [(Eq. 72)] [156].



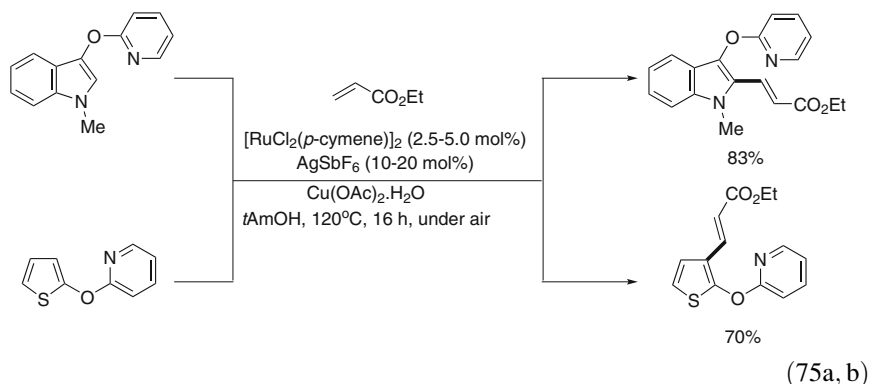
Prabhu recently showed that a formyl group at C3 position of N-protected indoles allowed the selective functionalization of the C4-H bond. Using the Ru (II)/AgSbF₆ catalytic system with Cu(OAc)₂.H₂O as oxidant they demonstrated that surprisingly the formyl group directed the alkenylation with acrylates at the C4 not at C2 position of N-benzylindoles. This result demonstrates that in the previous alkenylation of indole [(Eq. 71)] the N-amide was a directing group for transformation of C2-H bond. Acrylonitrile and styrenes led to alkenylation, however the product yields were lower than with acrylates [(Eq. 73)] [157]. In this reaction the formyl group favours alkenylation, as a cross experiment between the C3-formyl N-amide-indole and the previous N-benzoyl indole [(Eq. 70)] afforded the C4-alkenyl C3-formyl indole in large excess [157].



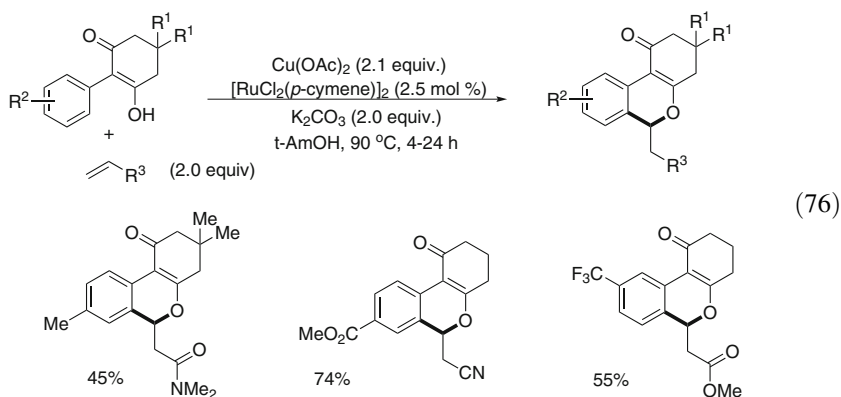
The Ru(II) catalysed arylation of *O*-protected phenols by 2-pyridyl group was already performed under efficient conditions [(Eq. 28)] [101]. Ackermann has now succeeded to perform their oxidative alkenylation with alkyl acrylates and Ru(II)/AgSbF₆ catalytic system with Cu(OAc)₂·H₂O as oxidant in aerobic atmosphere at *ortho*-position of the *O*-Py group [(Eq. 74)] [158]. The *ortho* C–H bond activation of these substrates is providing a 6-membered metallacycle intermediate by contrast to all the previous examples of alkenylation taking place via a 5-membered metallacycle. The phenol can be obtained from the alkenylated *O*-2-Py product by successive treatment with MeOTf and sodium in methanol without transformation of the alkenyl ester group and with tolerance of *p*-Cl, *p*-COR, *p*-CO₂R, or *p*-NO₂ arene substituent.



The same reaction process was applied to heterocycles such as *N*-methylindole containing a *O*-(2-pyridyl) group at C3 and led to the alkenylation at C2 only [(Eq. 75a)] [158]. The reaction of thiophene with a *O*-(2-pyridyl) group at C2 led to selective alkenylation at C3 position showing the strong directing power of the *O*-Py group [(Eq. 75b)] [158].

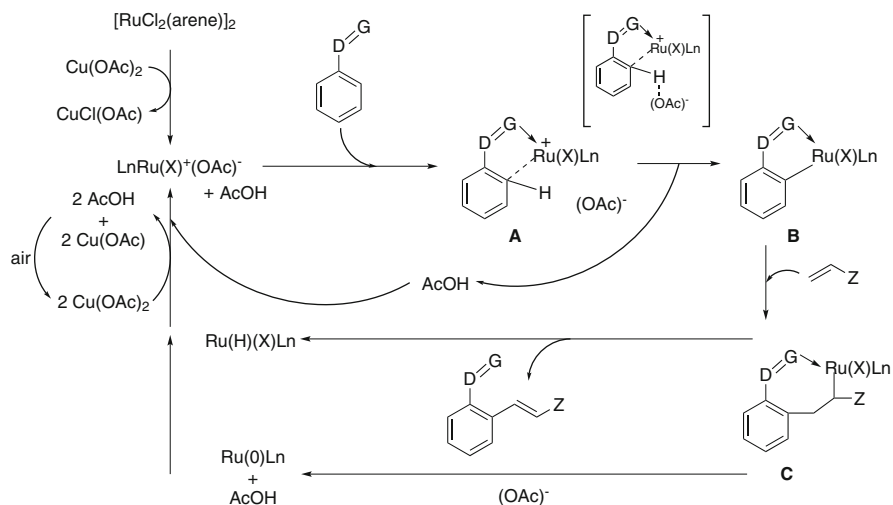


The synthesis of benzopyrans has been described by Lam via the alkenylation of 2-aryl-3-hydroxy-2-cyclohexenones followed by oxa-Michael type addition of the enol oxygen atom to the alkenylated intermediate. The reaction requires 2 equiv. of $\text{Cu}(\text{OAc})_2 \cdot \text{H}_2\text{O}$ in addition to the catalyst $[\text{RuCl}_2(p\text{-cymene})]_2$ [(Eq. 76)] [159]. The similar reaction using $\text{Pd}(\text{OAc})_2$ with $\text{Cu}(\text{OAc})_2 \cdot \text{H}_2\text{O}$ could be performed for methylvinylketone and phenyl vinyl sulfone [159].



5.1.4 Mechanism for Ru(II) Catalysed Alkenylation of sp^2 C–H Bonds with $\text{Cu}(\text{OAc})_2$

Most of the above oxidative alkenylations take place with 2–5 mol% of a Ru (II) species and excess of silver salt, usually 20 mol%, and 1 equiv of Cu(II) unless the reaction can be performed in air. As $[\text{RuCl}_2(p\text{-cymene})]_2$ leads to partial formation of $\text{Ru}(\text{OAc})_2(p\text{-cymene})$ with $\text{Cu}(\text{OAc})_2 \cdot \text{H}_2\text{O}$ [160], AgSbF_6 by abstracting the chlorides is expected to increase the formation of $\text{Ru}(\text{OAc})_2(p\text{-cymene})$. The Ru–OAc bond of the latter dissociates easily [49, 91] to allow the coordination of the heterocycle Directing Group (D=G) to the Ru (II) centre (Scheme 16). The interaction of the Ru(II) site with the *ortho* carbon atom (A) is expected to favour the deprotonation of its C–H bond by the external



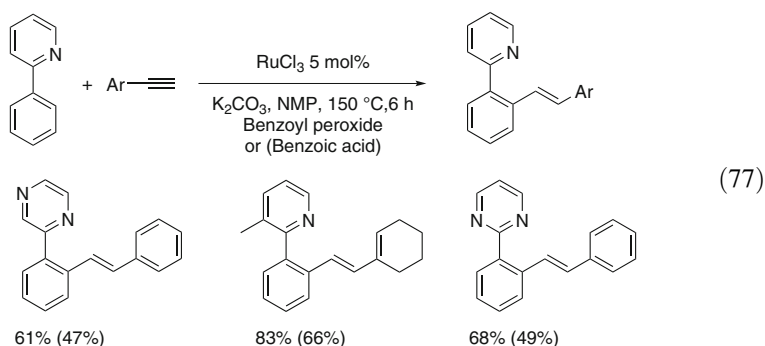
Scheme 16 Proposed mechanism for directed *ortho*-alkenylation of arenes and heterocycles

acetate, to generate the cyclometallate intermediate **B** that can be isolated in some examples [49, 90]. The regioselective insertion of the alkene into the Ru–C bond leads directly to the 7-membered cyclometallate **C**. The intermediate **C** could lead to β elimination to afford the *ortho*-alkenylated product and $Ru(H)(OAc)Ln$ species [90, 143]. However this process is not favoured as β elimination requires that the Ru–C–C–H bonds are coplanar and with Ru–C and C–H in syn position which is not possible due to the rigidity of the Ru–CH(Z)–CH₂–C bridge in intermediate **C**. Thus the C=C bond formation may result from the alkyl group deprotonation at the β position of the Ru atom by external acetate to generate the alkenylated product and $Ru(0)Ln + AcOH = RuH(OAc)Ln$. $Cu(OAc)_2 \cdot H_2O$ in the presence of $AcOH$ is expected to regenerate the catalyst precursor $Ru(OAc)_2Ln$ via reoxidation of the $Ru(0)Ln$ species or transformation of the $RuH(OAc)Ln$ species. In favourable media the presence of air is known to reoxidize the $Cu(I)$ into $Cu(II)$ species (Scheme 16) [143].

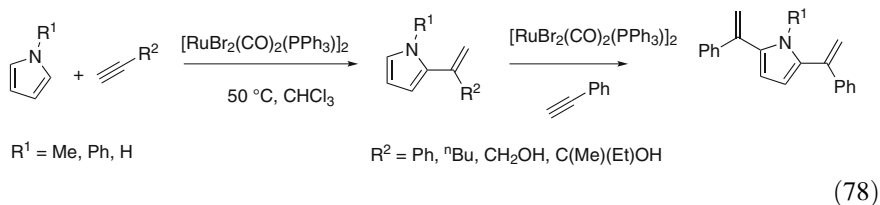
The oxidative dehydrogenative alkenylations with ruthenium(II) catalysts are now possible for functional arenes, alkenes, ferrocenes, heterocycles, and phenol derivatives. Very often the $Ru(II)$ catalyst is associated with a silver salt as chloride abstractor and in the presence of copper(II) oxidant able to regenerate the $Ru(II)$ species in air. More importantly these above results have shown that the successive C–H bond activation and alkenylation are directed by weak coordinating groups such as carboxylate, ketone, formyl, ester, amide, and carbamate groups. Most of the examples involve a 5-membered metallacycle intermediate; however, it is possible that for 6-membered metallacycle intermediate formation a stronger coordinating group is required. This alkenylation has become a general reaction, that has already been discussed in reviews [48, 58], and shows the profit brought by ruthenium(II) catalysts with respect to other more expensive catalysts.

5.2 Hydroarylation of Alkynes

Catalytic hydroarylation of alkynes is another efficient way to synthesize alkenylarenes. As early as 2008 Yuhong Zhang and co-workers were the first to regioselectively insert internal alkynes, using a ruthenium catalyst, into the *ortho* C–H bond of phenylpyrimidine and arylpyridines. This new alkenylation of functional arenes using the simple RuCl_3 catalyst required carbonate as a base with benzoyl peroxide or benzoic acid as additive in NMP, and offered high stereoselectivity towards (*E*)-stereoisomers [Eq. 77] [161]. The mechanism appears to involve the formation of a 5-membered cyclometallated intermediate via deprotonation of C–H bond, regioselective insertion of alkyne and protonation of the resulting Ru–C bond with the proton just taken at the *ortho*-position. However internal alkynes were inactive at that time. Actually the peroxide improves the reaction but benzoic acid alone allows the reaction with lower yield, although due to recent studies the benzoate likely favours the cyclometallation [49].

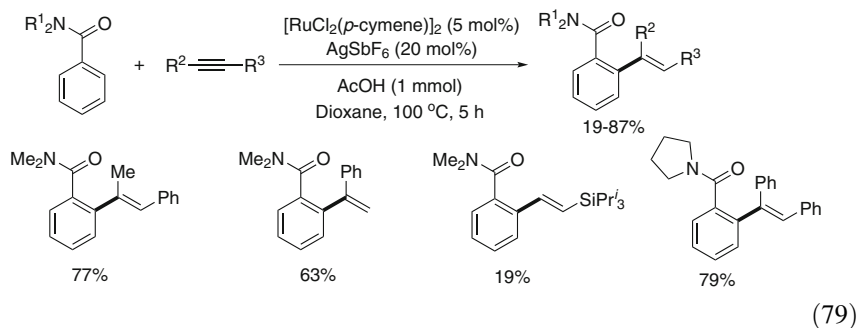


Using the binuclear ruthenium(II) catalyst $[\text{RuBr}_2(\text{CO})_2(\text{PPh}_3)]_2$ Wai Yip Fan succeeded to achieve the alkenylation of pyrroles with terminal alkynes under mild conditions at 50°C. This catalyst leads to the reverse regioselectivity for hydroheteroarylation of alkynes and the dialkenylation of pyrrole can be controlled. The mechanism likely involves an electrophilic activation of the alkyne by the Ru (II) species favouring the nucleophilic Markovnikov addition of pyrrole to the alkyne internal carbon [Eq. 78] [162].



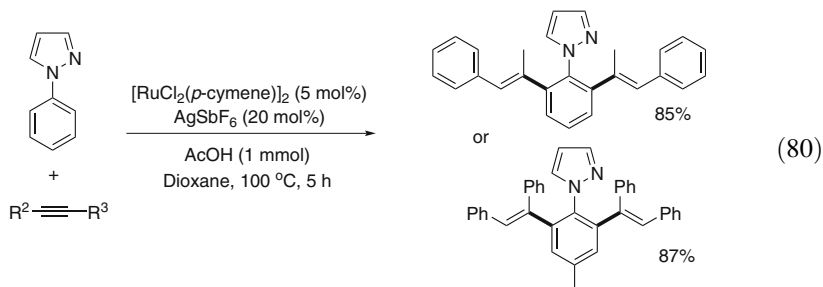
Recently, Miura and co-workers developed a ruthenium-catalysed regioselective monohydroarylation of alkynes with benzamides and dihydroarylation of alkynes

with phenylpyrazoles using the catalytic system $[\text{RuCl}_2(p\text{-cymene})]_2/\text{AgSbF}_6$. This reaction requires 1 equiv. of AcOH and applies now to disubstituted alkynes [(Eq. 79)] [163, 164]. The role of AcOH likely favours the C–H bond activation via an autocatalytic process [49, 91] and the Ru–C bond protonolysis.



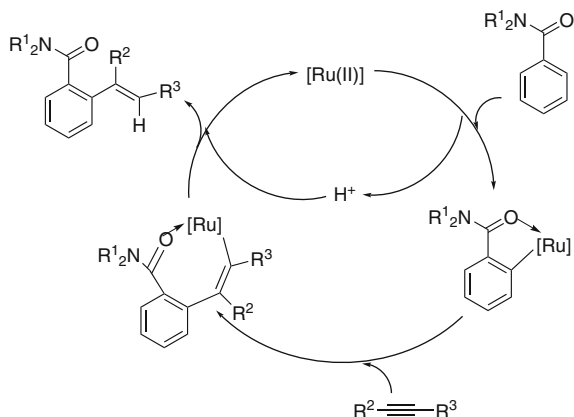
The competitive experiments and KIE reactions show that C–H bond cleavage is a rate-determining step and leads to a $S_{\text{E}}\text{Ar}$ -like metallation. A five-membered ruthenacycle intermediate was proposed via an *ortho* C–H deprotonation directed by the carbonyl group with ruthenium catalyst by analogy to the alkenylation mechanism (Scheme 16). Then alkyne insertion into the resulting Ru–C bond gave a seven-membered intermediate, and the hydroarylated product was produced by protonolysis of the Ru–C bond (Scheme 17) [163, 164].

When these conditions were applied to alkenylation of phenylpyrazoles the dihydroarylated products were easily synthesized in good yield in the presence of AcOH [(Eq. 80)] [163, 164]. In contrast, hydroarylation of alkynes with substituted phenylimidazole led selectively to monohydroarylated products likely due to sterical effects. The initial cyclometallation via *ortho* C–H bond deprotonation, insertion of alkyne into C–Ru bond, and protonolysis of the Ru–C bond are the key steps of the reaction (Scheme 17).

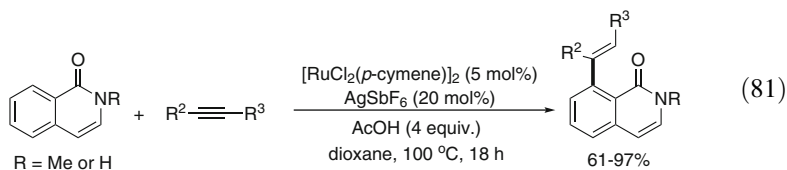


The previous ruthenium(II) catalytic system was successfully applied to the hydroarylation of aryl- and alkyl-substituted non-symmetrical alkynes with isoquinolone and *N*-protected isoquinolones, but using 4 equiv. of HOAc at 100°C. Notably, the electron-rich alkynes gave lower yields than the electron-

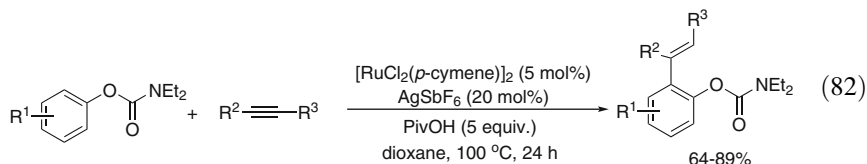
Scheme 17 Proposed mechanism for Ru(II)-catalysed hydroarylation of alkynes



deficient ones. In another hand, *N*-protected isoquinolones were more reactive than isoquinolone [(Eq. 81)] [165].



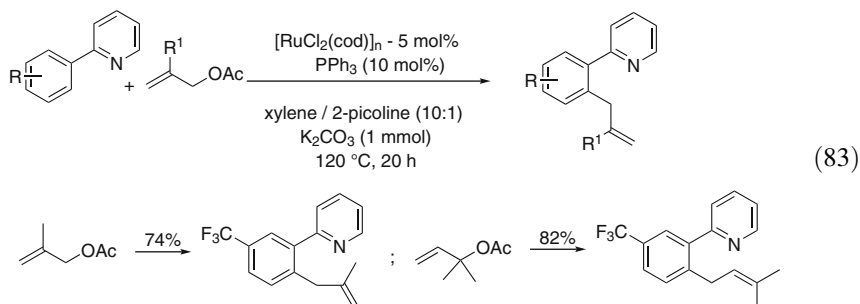
Various functional alkenes were similarly synthesized with high regio and *E*-stereoselective manner via $[\text{RuCl}_2(p\text{-cymene})]_2/\text{AgSbF}_6$ catalysed hydroarylation of phenyl or ester substituted alkynes with aromatic carbamates. The addition of 5 equiv. of pivalic acid improves the reaction in 1,4-dioxane. The alkenyl ester is converted into carboxylic acid by using 2 equiv. of LiOH, whereas phenol derivatives were deprotected by addition of 10 equiv. of LiOH [(Eq. 82)] [166].



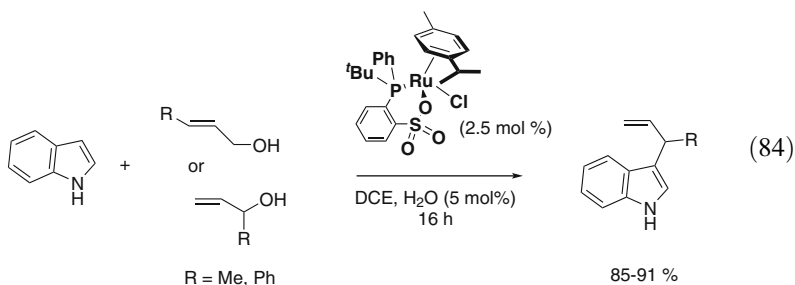
5.3 Prenylation of Heteroarenes with Allyl Derivatives

The allylation of C–H bonds promoted by ruthenium(II) catalyst was first performed on phenylpyridine with allyl acetates by Oi and Inoue and led to the *ortho*-allylation of the phenyl ring. This catalyst is known to easily give the cyclometallate via C–H bond deprotonation and, as the branched allyl acetates

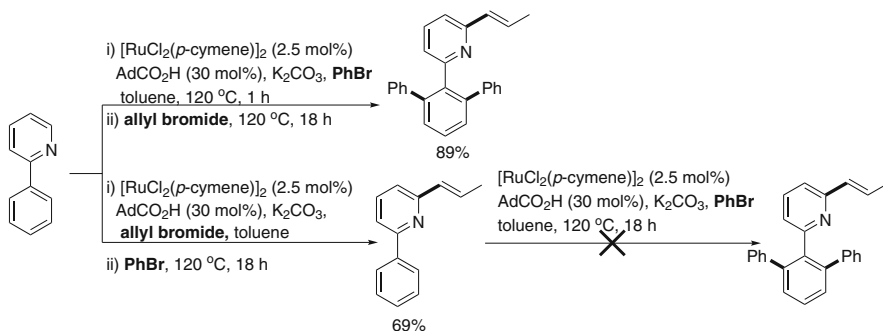
afforded linear products exclusively, the reaction is expected to proceed by oxidative allylation of the metallacycle followed by reductive elimination [(Eq. 83)] [66, 67].



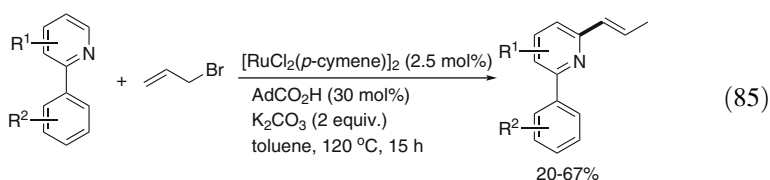
The direct ruthenium catalysed allylation with allylic alcohol derivatives of various aromatic compounds and heterocycles such as furans and thiophenes was performed by Nishibayashi with cationic thiolate-bridged diruthenium(III, II) catalysts. The reaction is consistent with an electrophilic aromatic substitution by the electrophilically activated allyl moiety [68]. Allylation also takes place with the alkene metathesis Grubbs catalyst [69]. More importantly using (phosphine-sulfonate)ruthenium(II) catalyst Bruneau et al. have recently shown that allyl alcohols are activated generating an allyl-ruthenium(IV) intermediate leading to C3-allylation of indole with high regioselectivity in favour of the branched allyl derivative [(Eq. 84)] [167].



By contrast Ramana et al. [168] demonstrated that the attempt to propenylate phenylpyridine with allylchloride with the $\text{RuCl}_2(p\text{-cymene})_2/\text{AdCO}_2\text{H}$ catalyst actually allowed the alkenylation at carbon C6 of the pyridine ring, leading directly to the 2-aryl-6-alkenyl pyridines [(Eq. 85)]. This direct regioselective C–H bond propenylation led to a wide range of propenylated pyridine derivatives with allylbromide preferentially to allyliodide and allylchloride. However, *ortho*-C–H propenylation of the phenyl group was observed in the presence of allyl acetate as reagent [168].



Scheme 18 Sequential Ru(II)-catalysed prenylation and arylation of 2-phenylpyridine

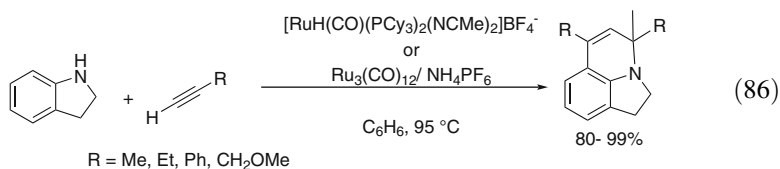


A one pot sequential *ortho*-arylation and C(6) propenylation was found with the same $[\text{RuCl}_2(p\text{-cymene})]_2/\text{AdCO}_2\text{H}$ catalyst in toluene. The order of addition of reactants is crucial: when the arylbromide was added first, followed by the addition of allylbromide, the diarylated and C(6) propenylated pyridine derivative was produced. Surprisingly, only C(6) propenylated product was obtained with the reversed substrate addition order showing that the alkenylated group inhibited the arylation (Scheme 18) [168].

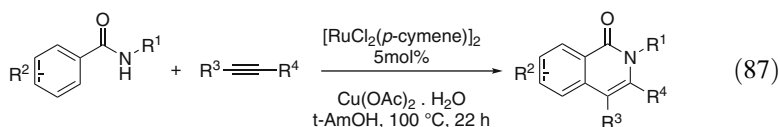
6 Ruthenium(II)-Catalysed Annulations with Alkynes

6.1 Annulation with Alkynes and C–H Bond Activation: Formation of C–C and C–N Bonds

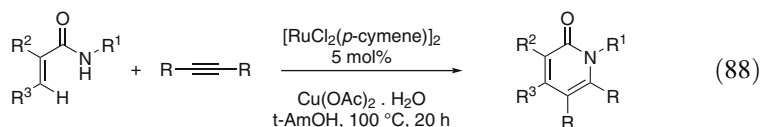
Oxidative annulations reaction of alkynes is one of the important methods to synthesize fused polycyclic heteroarenes [169–173]. Whereas the above examples show easy ruthenium catalysed insertions of alkynes into aromatic sp^2 C–H bonds efforts have been made with related catalysts to perform the double insertion of alkynes into C–H and heteroatom–hydrogen bonds as a route to a variety of heterocycles. Chae S. Yi, has first shown, using ruthenium(II) catalyst precursors $[\text{RuH}(\text{CO})(\text{PCy}_3)_2(\text{NCMe})_2]\text{BF}_4$ and preferably $\text{Ru}_3(\text{CO})_{12}/\text{NH}_4\text{PF}_6$, the alkenylation and double insertions of alkynes into C–H and N–H bonds for the transformation of indolines with terminal alkynes into quinoline derivatives [Eq. 86] [174, 175].



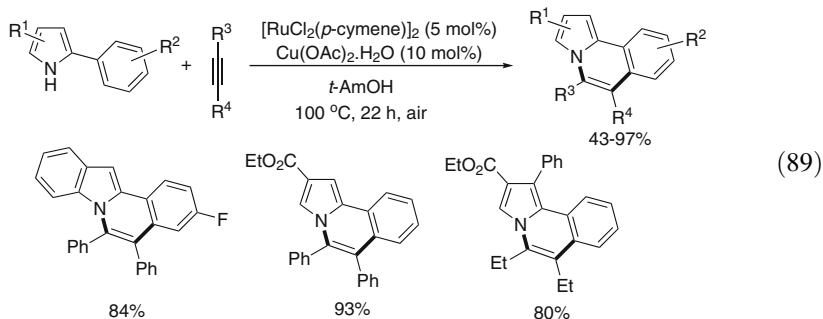
Ackermann's group reported the oxidative annulations of alkynes with benzamides with a ruthenium(II) catalyst in 2011 with the use of an oxidant $\text{Cu}(\text{OAc})_2 \cdot \text{H}_2\text{O}$, under conditions of C–H bond activation. This dehydrogenative annulation of benzamides via transformation of both *ortho* C–H and amide N–H bonds selectively produced isoquinolones [(Eq. 87)] [176]. Diphenylacetylene is shown to be much more reactive than diethylacetylene, and electron-deficient alkynes preferentially react with benzamides to give isoquinolones.



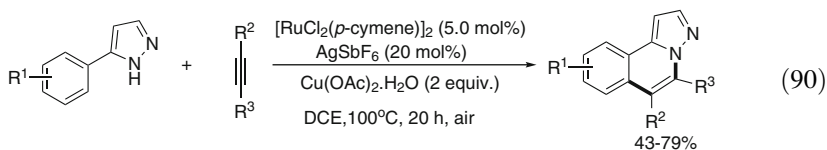
The same ruthenium(II) catalytic system with 1 equiv. of $\text{Cu}(\text{OAc})_2 \cdot \text{H}_2\text{O}$ oxidant was used to generate 2-pyridones directly from acrylamides by C–H and N–H bond functionalization and annulation with alkynes. This reaction offers improved substrate scope with respect to the similar reaction reported with rhodium catalyst [(Eq. 88)] [177]. The reaction is applicable to dialkylacetylenes. Alkylphenylacetylenes lead to regioselective annulation with an (aryl)C–N linkage formation, consistent with the coupling of the electron-deficient alkyne carbon with the electron-rich carbon of the Ru–C bond.



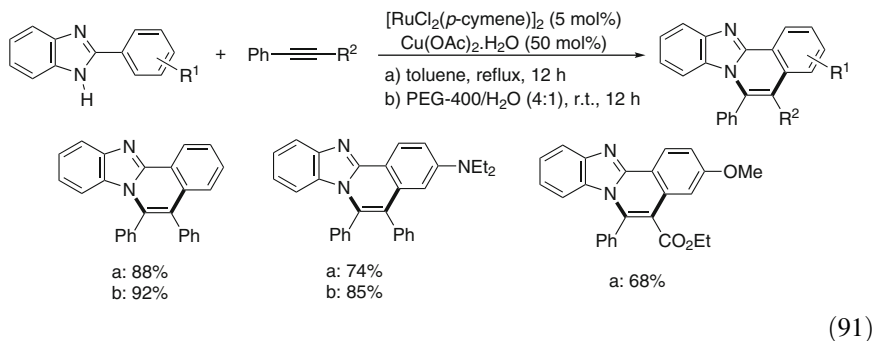
The aerobic dehydrogenative annulation of 2-aryl-substituted pyrroles and indoles for a variety of alkynes, using the system ruthenium(II) catalyst with oxidant $\text{Cu}(\text{OAc})_2 \cdot \text{H}_2\text{O}$, was then reported. The reaction was now performed under ambient air as the ideal sacrificial oxidant, thus only 10 mol% of $\text{Cu}(\text{OAc})_2 \cdot \text{H}_2\text{O}$ could be used for efficient transformations of indoles [(Eq. 89)] [178]. This method could also be applied to synthesize pyrrolo[2,1-a]isoquinolines from 2-arylpyrroles with dialkyl-, diaryl-, or alkylarylacetylenes with an excellent regioselectivity. The competition experiments showed that an electron-deficient alkyne favours this reaction and that the more acidic C–H bond activation is favoured [(Eq. 89)] [178].



1H-pyrazoles appeared also suitable substrates for the oxidative annulation with aryl- and alkyl- alkynes with good chemo- and regioselectivities. This reaction was carried out using 5 mol% of $[\text{RuCl}_2(p\text{-cymene})]_2$, 20 mol% of AgSbF_6 , 1 equiv. of $\text{Cu}(\text{OAc})_2 \cdot \text{H}_2\text{O}$ as the oxidant. The H/D experiments indicate a reversible C–H bond metallation step with the Ru(II)/ AgSbF_6 catalytic system in DCE/ D_2O (9:1) [(Eq. 90)] [179].

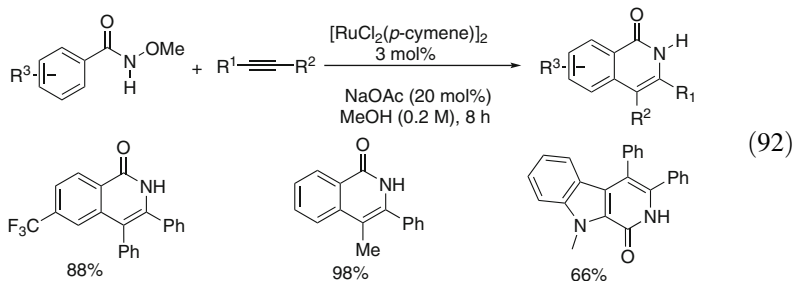


The previous catalysts were adapted for the ruthenium-catalysed benzimidazoi-quinoline synthesis via oxidative coupling of 2-arylbenzimidazoles with alkynes. Thus $[\text{RuCl}_2(p\text{-cymene})]_2$, with 0.5–2 equiv. of $\text{Cu}(\text{OAc})_2 \cdot \text{H}_2\text{O}$ in toluene at reflux produced a variety of benzimidazoiquinolines. Unsymmetrical alkynes such as phenylpropionate led to the regioselective insertion with (Ph)C–C bond formation [(Eq. 91)] [180]. As an attempt to recover the catalyst, reactions were performed in PEG-400 as a solvent medium and the products were obtained in similar yields as in toluene and the catalyst could be recycled a few times [(Eq. 91)].

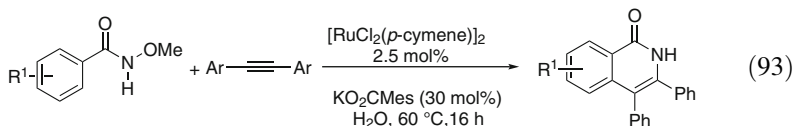


The ruthenium(II) catalytic annulations of benzamides with alkynes leading to isoquinolones were performed under much milder conditions by the introduction of

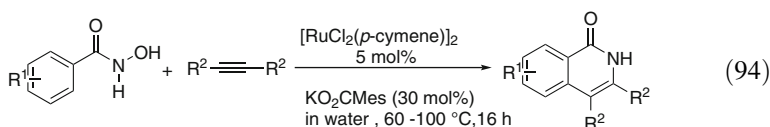
an oxidizing N-methoxy group by Li and Wang. This room temperature reaction in methanol using [RuCl₂(*p*-cymene)]₂ catalyst does not require oxidant such as Cu(OAc)₂·H₂O. The reaction can be extended to heteroarylcarboxamides, free hydroxamic acid, and indole [(Eq. 92)] [181].



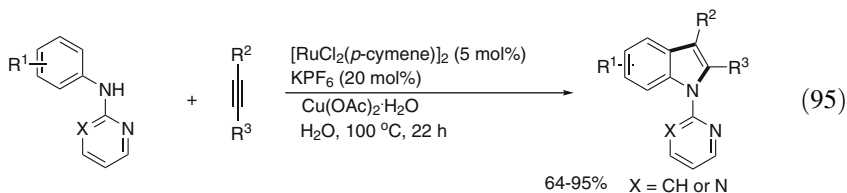
The previous synthesis can also be performed in *water* from both *N*-methoxybenzamides and free hydroxamic acid. In water the best catalytic system was found to be [RuCl₂(*p*-cymene)]₂ associated with KO₂CMes (30 mol%) and the reaction takes place at 60 °C [(Eq. 93)] [182].



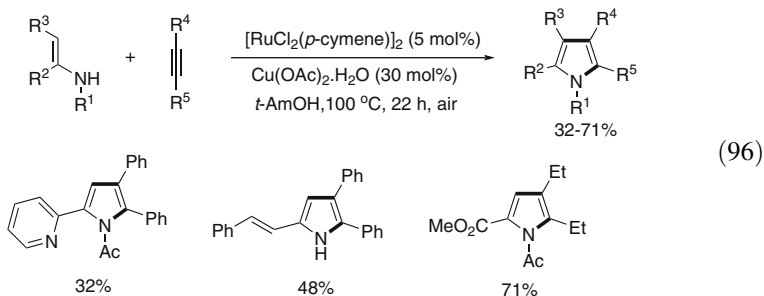
The C–H bonds that are not sterically hindered by a neighbouring substituent in *meta*-position, unless they are electron-withdrawing groups, provide better reactivity. This reaction applied to free hydroxamic acid leads to isoquinolones but under slightly more drastic conditions at 60–100 °C [(Eq. 94)] [182].



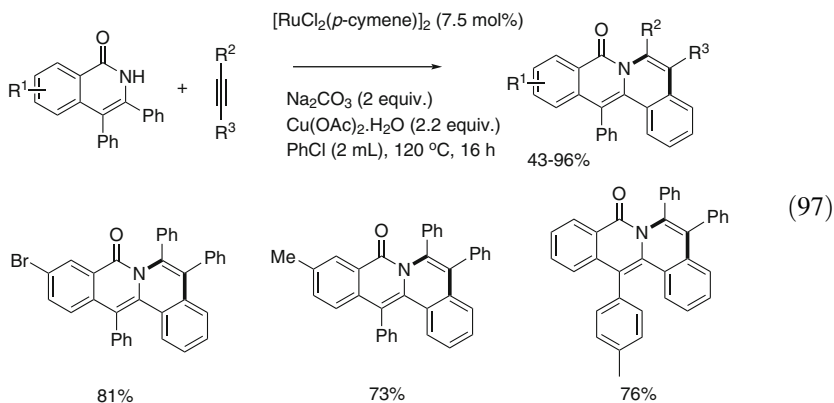
The synthesis of indoles from *N*-protected anilines and bearing a 2-pyridyl or a pyrimidyl group was performed with [RuCl₂(*p*-cymene)]₂/4 KPF₆ catalytic system. This bidentate strong coordinating group is essential for the reaction to take place. The reaction requires the use of Cu(OAc)₂·H₂O as the oxidant but is adapted to be operative *in water*. This oxidative dehydrogenative process produced a large variety of indole derivatives that were deprotected by treatment with NaOEt in DMSO [(Eq. 95)] [183]. The reaction is faster with diarylacetylenes than with dialkylacetylenes, and is regioselective with alkylarylacetylenes, as the nitrogen atom selectively binds to the alkyne carbon linked to the aryl group. The reaction is favoured by electron-donating groups (*p*-OMe versus *p*-F).



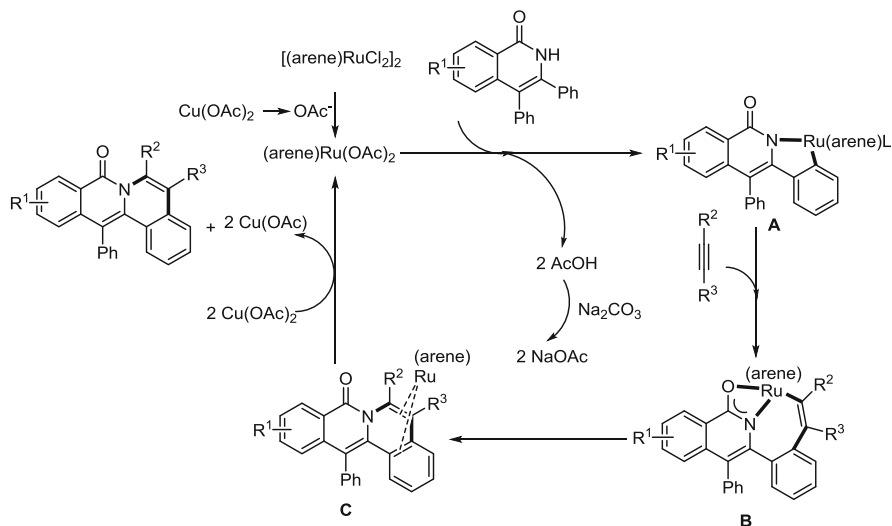
Various pyrroles were synthesized through the ruthenium(II)-catalysed oxidative annulation of enamines with aryl- and alkyl-alkynes in *t*-AmOH with only 30 mol% of $\text{Cu}(\text{OAc})_2 \cdot \text{H}_2\text{O}$ under ambient air conditions. Numerous functional groups including ester, vinyl, bromo, nitro substituents and heteroaromatic were tolerated in this catalytic system [(Eq. 96)] [184].



More recently, Wang and Li demonstrated a highly regioselective $[\text{RuCl}_2(p\text{-cymene})]_2$ catalysed oxidative annulation of isoquinolones with alkynes. A wide range of dibenzo[a,g]quinolizin-8-one derivatives were isolated with $[\text{RuCl}_2(p\text{-cymene})]_2$ (7.5 mol%) catalyst and $\text{Cu}(\text{OAc})_2 \cdot \text{H}_2\text{O}$ (2.2 equiv.) as an oxidant together with 2 equiv. of Na_2CO_3 . Notably, 3,4-diphenylisoquinolones bearing electron-withdrawing groups favour the reaction (81–96%) with respect to those bearing electron-donating groups (64–81%) [(Eq. 97)] [185].



A detailed study of the mechanism of the Ru(II) catalysed annulation of isoquinolone with alkynes was proposed. Noteworthy, all of the key intermediates

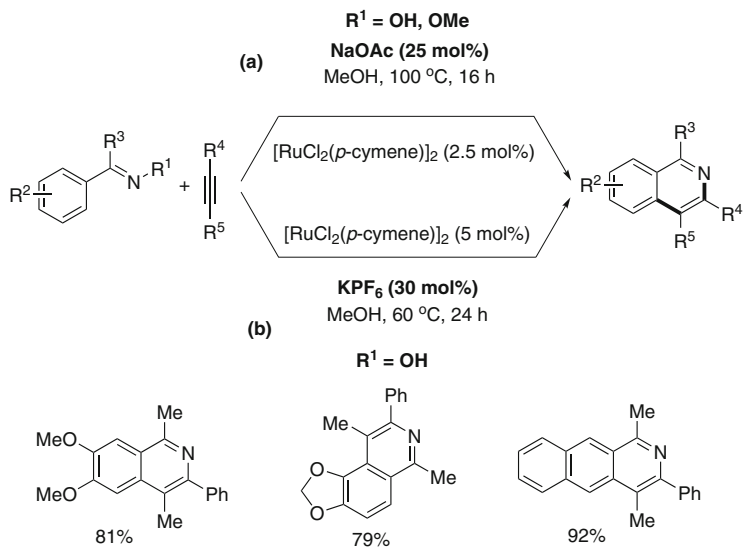


Scheme 19 Proposed mechanism for Ru(II)-catalysed annulation of isoquinolones with alkynes

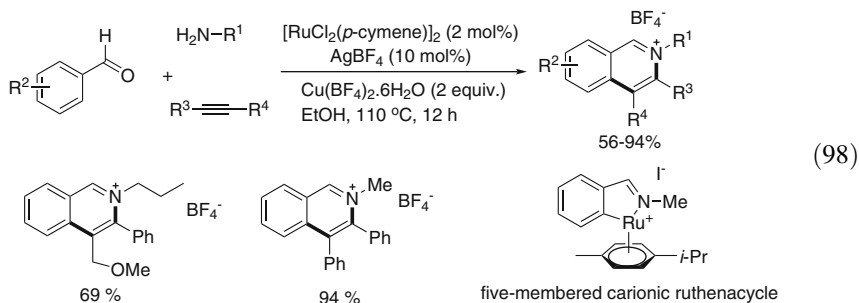
A, **B**, and **C** were isolated and their structure confirmed by X-ray crystallographic analysis of their single crystals. First, the in situ generated ruthenium acetate catalyst reacts with isoquinolone to form the five-membered ruthenacycle **A** by an acetate-assisted deprotonation mechanism. Then, the alkyne insertion into the Ru–C bond affords a seven-membered ruthenacycle intermediate **B**. After the reductive elimination from **B** forming the C–N bond, a $\text{Ru}(0)$ intermediate **C** was generated. Finally, the desired product was obtained from the decooordination of a $\text{Ru}(0)$ species which regenerated the active $\text{Ru}(\text{OAc})_2(p\text{-cymene})$ initial complex on oxidation with copper acetate (Scheme 19) [185].

Recently, Jegannathan et al. developed a method to synthesize substituted isoquinolines through the annulation of aromatic and heteroaromatic ketoximes with alkynes using 2.5 mol% of $[\text{RuCl}_2(p\text{-cymene})]_2$ and 25 mol% NaOAc in MeOH (Scheme 20a) [186]. Then Ackermann explored this reaction by modifying the co-catalyst KPF_6 instead of NaOAc to operate at 60°C but with a higher catalyst loading (5 mol%) and longer reaction time (24 h) (Scheme 20b) [187]. The five-membered ruthenacycle key intermediate was isolated from the stoichiometric reaction of $[\text{RuCl}_2(p\text{-cymene})]_2$, and NaOAc in MeOH at 100°C for 16 h. [186].

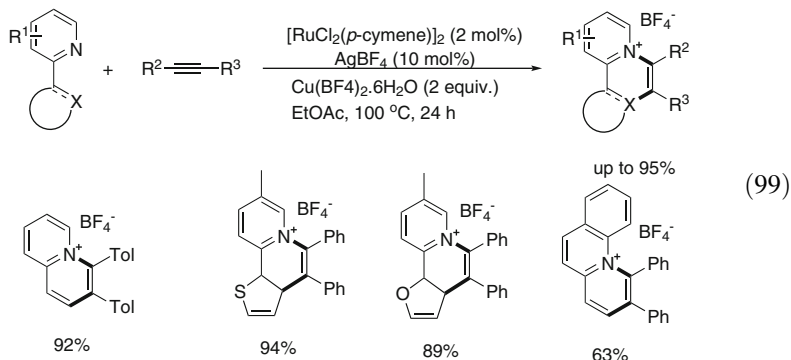
Cheng recently explored an efficient method to synthesize substituted isoquinolinium salts from the one pot ruthenium-catalysed annulation with alkynes of in situ generated aldimines, from benzaldehydes and amines. $[\text{RuCl}_2(p\text{-cymene})]_2/\text{AgBF}_4$ catalyst associated with the oxidant $\text{Cu}(\text{BF}_4)_2 \cdot 6\text{H}_2\text{O}$ (2 equiv.) at 110°C , led to isoquinolinium salts. The postulated five-membered cationic ruthenacycle intermediate was isolated in that case [(Eq. 98)] [188].



Scheme 20 Ru(II)-catalysed annulation of imines with alkynes



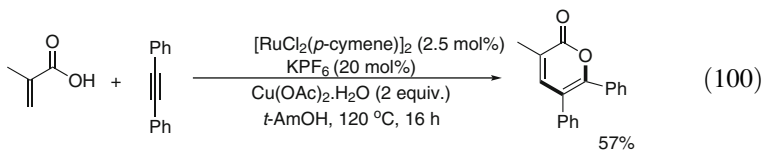
This Ru(II) catalysed reaction has been adapted by Cheng for the annulation with alkynes of 2-vinylpyridines for the quantitative production of quinolinizinium salts. The use of $[\text{RuCl}_2(p\text{-cymene})]_2/\text{AgBF}_4$ catalyst with $\text{Cu}(\text{BF}_4)_2 \cdot 6\text{H}_2\text{O}$ (2 equiv.) allowed the heterocyclic annulation of a variety of vinylpyridines but also of 2-heteroaryl pyridines bearing a $=\text{C}-\text{H}$ bond at the 4-position with respect to the nitrogen atom [(Eq. 99) [189]. The Ru(II) catalytic system can be compared to the $[\text{RhCl}_2\text{Cp}^*]_2$ catalyst with $\text{Cu}(\text{BF}_4)_2 \cdot 6\text{H}_2\text{O}$ (0.5 equiv.) under air [189]. The Rh(III) catalyst in some cases is more active than the less expensive Ru(II) catalytic system which offers complementary reactivity.



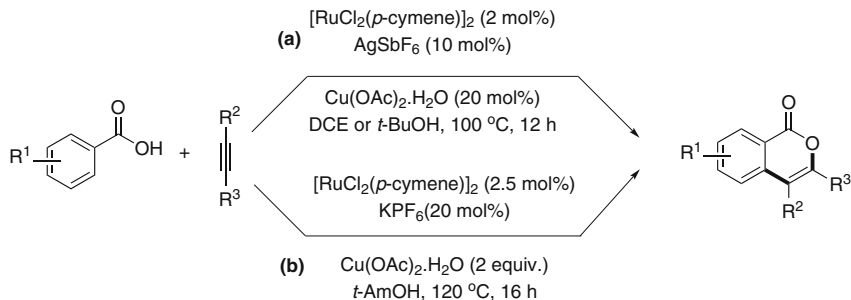
6.2 Annulation with Alkynes and C–H Bond Activation: Formation of C–C and C–O Bonds

The synthesis of isocoumarins from carboxylic acids and alkynes via $[\text{RuCl}_2(p\text{-cymene})]_2$ catalysed oxidative annulations in the presence of catalytic amount of AgSbF_6 and $\text{Cu}(\text{OAc})_2 \cdot \text{H}_2\text{O}$ in DCE at 100°C for 12 h was first reported by Jeganmohan [190]. (Scheme 21a). Ackermann's group also showed a similar reaction but with catalytic amount of KPF_6 and $\text{Cu}(\text{OAc})_2 \cdot \text{H}_2\text{O}$ in *t*-AmOH at 120°C for 16 h [191, 192]. (Scheme 21b) The role of AgSbF_6 or KPF_6 is to avoid the coordination of Cl^- to the Ru(II) site, and in situ generate the cationic ruthenium(II) complex $[\text{Ru}(\text{OAc})(p\text{-cymene})]^+[\text{SbF}_6]^-$ or $[\text{PF}_6]^-$ with $\text{Cu}(\text{OAc})_2 \cdot \text{H}_2\text{O}$. The five-membered ruthenacycle intermediate was formed on *ortho*-C–H bond deprotonation. The desired isocoumarin product was produced by the alkyne insertion into the Ru–C bond, followed with a reductive elimination.

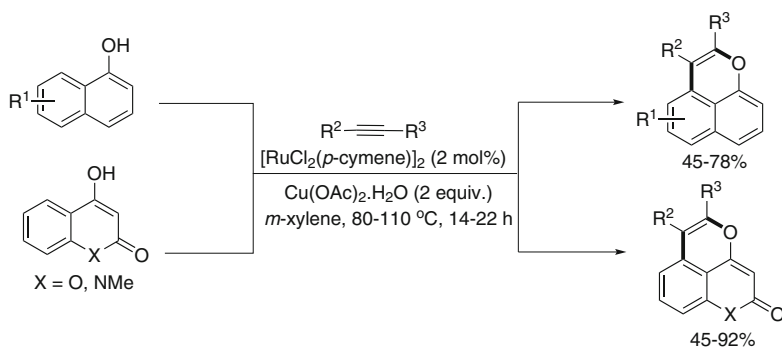
It is noteworthy that based on this reaction α -pyrone could be synthesized from the oxidative annulation with alkynes of acrylic acid derivative with $[\text{RuCl}_2(p\text{-cymene})]_2/\text{KPF}_6$ catalytic system [(Eq. 100)] [191]



Hydroxy directing groups such as in naphthols, 4-hydroxycoumarin and 4-hydroxy-substituted quinolin-2-one were found to promote the formation of fluorescent pyrans via ruthenium(II) catalysed annulation with alkynes by addition of 2 equiv. of $\text{Cu}(\text{OAc})_2 \cdot \text{H}_2\text{O}$ as the oxidant. The competition results revealed that electron-deficient alkynes favour this reaction (Scheme 22) [193].

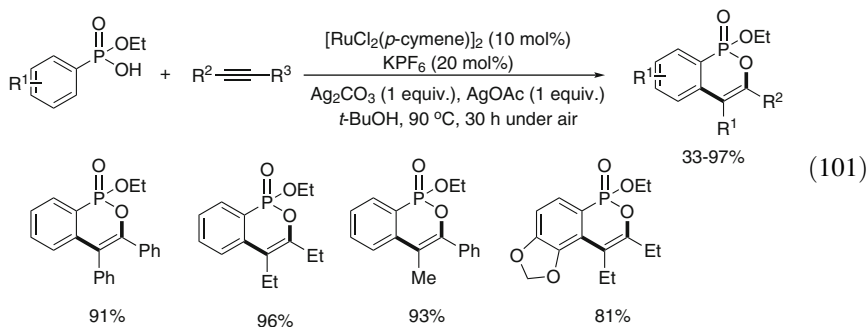


Scheme 21 Ru(II)-catalysed annulation of carboxylic acids with alkynes



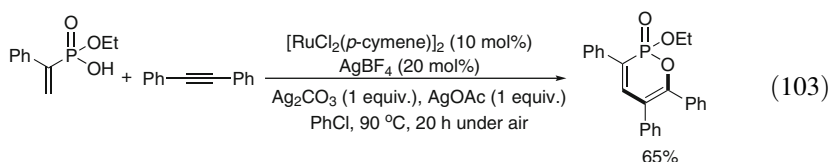
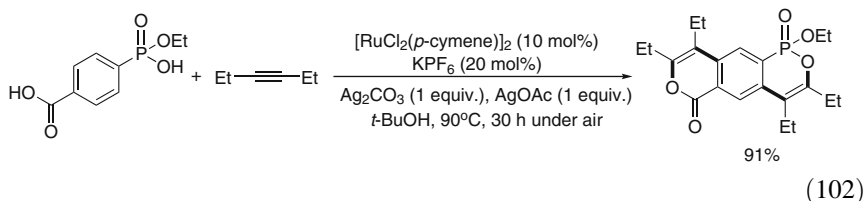
Scheme 22 Ru(II)-catalysed annulation of hydroxy-substituted quinoline-2-ones with alkynes

Another example of ruthenium(II)-catalysed double insertion of alkynes into C–H and O–H bonds was reported by Lee. The C–H bond oxidative cyclizations of phosphonic acid monoesters or phosphinic acids with alkynes lead to a wide range of phosphaisocoumarins with excellent yields up to 97%. The catalyst was prepared from $[\text{RuCl}_2(p\text{-cymene})]_2/\text{KPF}_6$, with 1 equiv. of Ag_2CO_3 and of AgOAc in *t*-BuOH, under aerobic conditions [(Eq. 101)] [194].



It is noteworthy that these oxidative cyclizations were not affected by the electronic effects of alkynes as shown by the competition experiments between

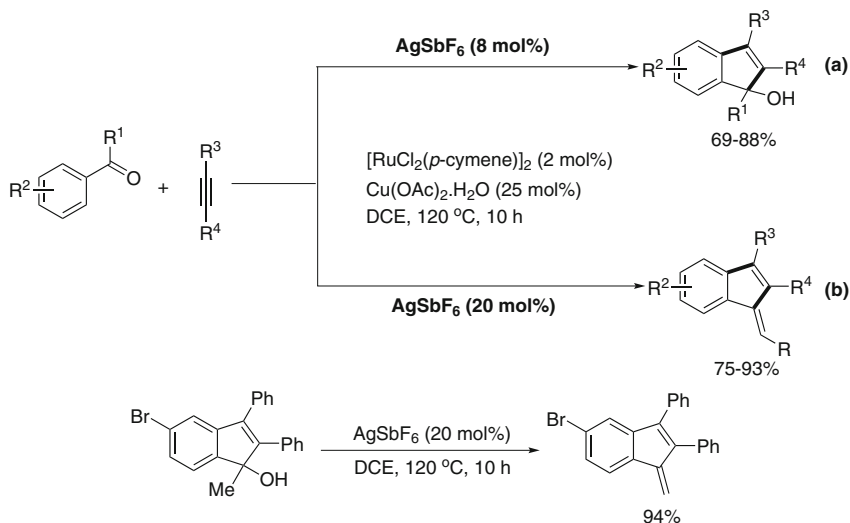
diaryl- and dialkyl alkynes and between diarylacetylenes having *p*-methoxy and *p*-chloro groups. Furthermore, the mechanistic studies revealed that C–H bond cleavage at the 2-position of phosphinic acid and phosphonic monoester is the rate-limiting step. The aryl derivative containing both a benzoic acid and a phosphinic monoester functions led to double insertion of hex-3-yne into C–H and O–H bonds [(Eq. 102)]. Analogously a vinyl phosphinic monoester with diphenylacetylene produced a phosphorous 2-pyrone by insertion of the alkyne into vinyl C–H and O–H bonds [(Eq. 103)] [194].



6.3 Annulation with Alkynes and C–H Bond Activation: Formation of Two C–C Bonds

With the use of halide free ruthenium(II) catalysts Jegannathan has previously shown that a ketone group could direct C–H bond activation [57]. He has now developed the oxidative annulation of aromatic ketones with alkynes using $[RuCl_2(p\text{-cymene})]_2/4$ $AgSbF_6$ (8 mol%) catalytic system to synthesize indenols and benzofulvenes via insertion of alkyne into *ortho* C–H and coupling with the carbonyl carbon. 69–88% yields of indenols were isolated after 10 h at 120°C in DCE (Scheme 23a) [195]. With alkylarylacetylene the reaction is regioselective. The alkyne insertion corresponds to the preferred addition of the Ru(II) site to the alkyne aryl carbon atom.

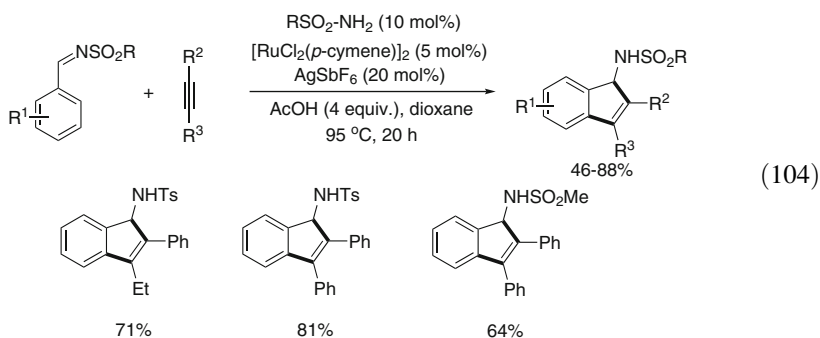
Surprisingly, when 20 mol% of $AgSbF_6$ was added to this reaction, benzofulvenes derivatives were produced as the major products by the dehydration of indenol derivatives. (Scheme 23b) [195]. It is noteworthy that the addition of silver salt plays two important roles in this reaction: (1) removal of the Cl^- to generate the active cationic ruthenium species; (2) the excess of silver salt is a good catalyst for the dehydration of indenol derivatives into benzofulvenes.



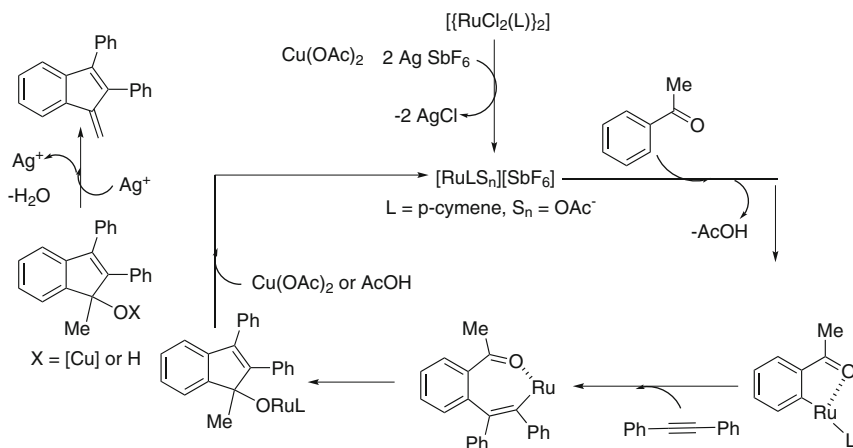
Scheme 23 Ru(II)-catalysed annulation of aromatic ketones with alkynes

The mechanism likely involves the initial formation of the ruthenacycle with regioselective insertion of alkyne into the Ru(II)–C bond with addition of the Ru(II) site to the aryl carbon atom, and insertion of the carbonyl group into the Ru(II)–C bond. The resulting intermediate gives indenols on protonation or benzofulvenes on dehydration with an excess of silver salt (Scheme 24) [195].

When the reaction of *N*-sulfonyl aryl aldimines and alkynes was carried out in the presence of 5 mol% of [RuCl₂(*p*-cymene)]₂, 20 mol% of AgSbF₆, 10 mol% TsNH₂ and 4 equiv. of AcOH in dioxane at 95 °C, after 20 h, no isoquinoline derivative was obtained as for ketimines (Scheme 20), but indenamine derivatives were obtained instead resulting from C–H bond activation, insertion of alkyne, and C–C bond formation [(Eq. 104)] [196].



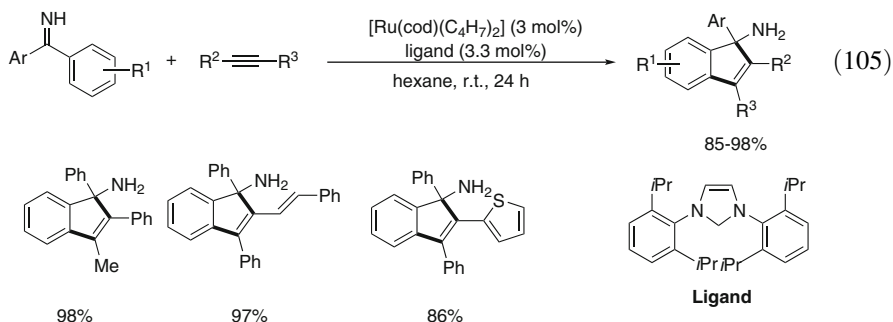
Only trace amounts of indenamine derivatives were observed without the addition of TsNH₂. Thus the primary sulfonamide plays a significant role in activating the imine substrate. The proposed mechanism involves the initial formation of



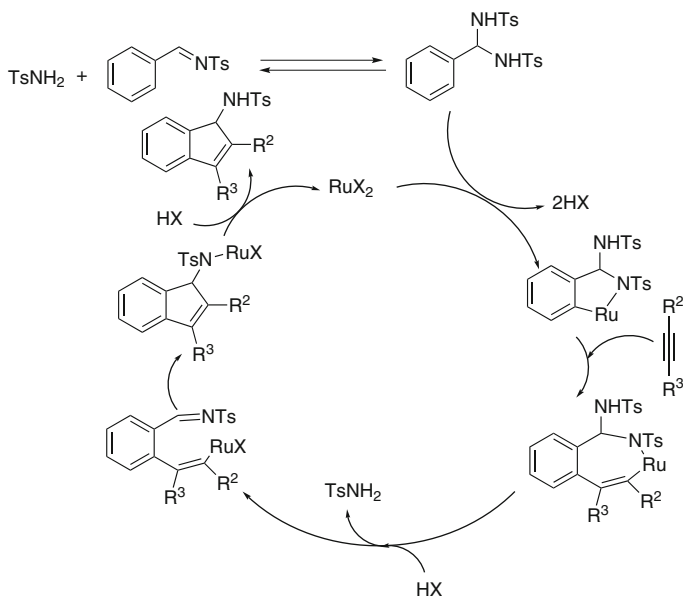
Scheme 24 Mechanism for Ru(II) catalysed synthesis of indenol and benzofulvene from arylketones

ditosyldiamine. It is noteworthy that the reversible protonolysis of the Ru–N bond can be facilitated by the acetic acid additive. The formation of cyclometallate is proposed to arise from ditosyldiamine followed by insertion of alkyne, elimination of tosylamine to generate the reactive imine for addition of Ru–C bond, and protonolysis of the N–Ru bond (Scheme 25) [196].

NHC–Ru(II) complexes have been recently shown by Pinjing Zhao to perform the catalysed [3+2]carbocyclizations of alkynes with aromatic N–H ketimines [(Eq. 105)] [197]. The ruthenium(II) catalyst is based on π -allyl precursor $[\text{cod}]\text{Ru}(\eta^3\text{-methallyl})_2$ with addition of an NHCarbene as ligand, which is necessary for the reaction to take place and to occur at room temperature. Thus this catalyst significantly decreased this [3+2] annulation temperature. It is noteworthy that the C–H bond at the more electron-deficient arene favoured this reaction in non-polar solvents.

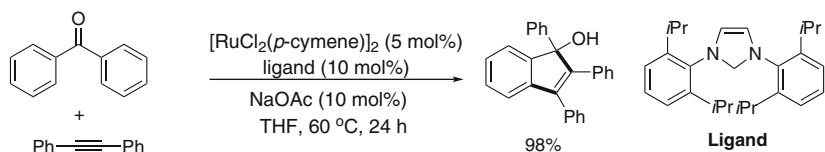


It is shown that the ruthenium complex alone promotes the double cyclometallation of arylketimine with elimination of isobutene. Thus the reaction



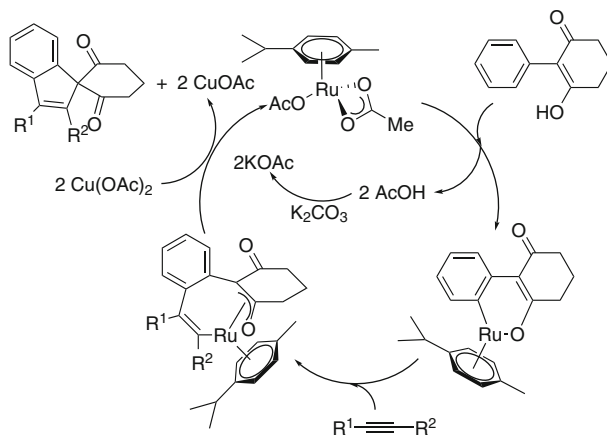
Scheme 25 Mechanism of Ru(II)-catalysed formation of indenamines from *N*-sulfonyl imines

likely involves the insertion of the alkyne into the Ru–C bond of the cyclometallate, insertion of the imine C=N bond into the new Ru–C bond followed by protonolysis via a mechanism similar to that of Jeganmohan reaction of aromatic ketone with alkyne (Scheme 23) [195]. Actually a related Ru(II) catalytic system, based on addition of the NHC ligand to $[\text{RuCl}_2(p\text{-cymene})]_2$, promotes this addition of alkyne to aromatic ketone under mild condition at 60°C [(Eq. 106)] [197].



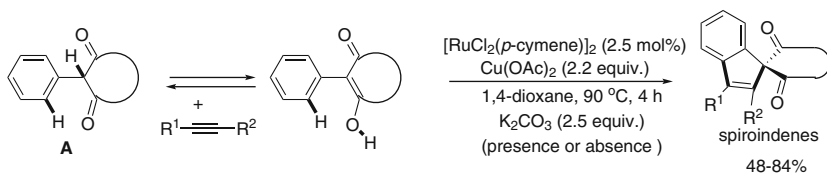
(106)

The direct oxidative annulations with alkynes by $\text{Csp}^3\text{-H}/\text{Csp}^2\text{-H}$ bond cleavage have not been developed yet: only two examples were described in this area using nickel(0) by Hiyama [198] and rhodium(III) by Wang [199]. With ruthenium(II) catalyst, Lam reported the first annulations with alkynes of 2-aryl-1,3-dicarbonyl compounds by $\text{Csp}^3\text{-H}$ and $\text{Csp}^2\text{-H}$ bond activation [200]. The reaction of 2-aryl-3-hydroxy-2-cyclohexenones and cyclic 2-aryl-1,3-dicarbonyl compounds with 2.5 mol% of $[\text{RuCl}_2(p\text{-cymene})]_2$ and 2.2 equiv. of $\text{Cu}(\text{OAc})_2$ was performed in 1,4-dioxane at 90°C, and led to spiroindene derivatives in 50–84%



Scheme 26 Proposed mechanism for Ru(II)-catalysed annulations of alkynes with 2-aryl-1,3-dicarbonyl compounds

isolated yields [(Eq. 107)] [200]. In some cases, the addition of K_2CO_3 (2.5 equiv.) increased the yields. Terminal alkynes were not suitable for this annulation.



(107)

In the catalytic cycle, in situ generated $Ru(OAc)_2(p\text{-cymene})$ is expected to react with 2-aryl-3-hydroxy-2-cyclohexenones to form first the six-membered ruthenacycles. After alkyne insertion into the Ru–C bond and reductive elimination, spiroindene is produced. $Cu(OAc)_2$ promoted the reductive elimination or the oxidation of Ru(0) into $Ru(OAc)_2Ln$. (Scheme 26) [200].

The above reports demonstrate that ruthenium(II) catalysed annulations with alkynes, involving as a first step a sp^2 C–H bond activation by deprotonation, constitute a low-cost and efficient method to produce a variety of heterocycles. The catalyst is a simple association of $RuCl_2Ln$ complex and an oxidant usually $Cu(OAc)_2$ that allows the oxidative dehydrogenative coupling of alkyne carbons with a (C–H) carbon and a nitrogen or oxygen atom. The formation of two C–C bonds, by coupling of alkyne carbons with a (C–H) carbon and the carbon of ketone carbonyl, imine C=N bond and enolate sp^3 C–H bond, is an emerging field.

7 Conclusion

Ruthenium(II) catalyst precursors and sometimes even simple RuCl_3 derivatives are allowing easy activation of sp^2 C–H bonds of functional arenes, heterocycles, alkenes, and further catalytic functionalization. These low-cost ruthenium (II) catalysts offer the advantages of their facility of preparation, stability even often in the presence of water or as a solvent. The sp^2 C–H bond activation with Ru (II) catalyst usually occurs at room temperature, via deprotonation of the C–H bond affording a metallacycle. However the further functionalization of the (CH) carbon usually requires more energy.

Arylation and heteroarylation of functional arenes, heteroarenes, alkenes with (hetero)aryl bromides and chlorides with ruthenium(II) catalysts in the presence of a base, usually carbonate, are now well developed. The profitable role of carboxylate as a co-catalyst forming weak Ru(II)- O_2CR bonds is well demonstrated and favours C–H bond deprotonation by concerted action of the Ru(II) centre and external carboxylate to form a ruthenacycle. A few examples of arylation with tosylates have also been described. The diarylations at *ortho*-positions of the functional group are easier to reach than selective monoarylations, with strongly bonding functional groups such as nitrogen-containing heterocycles or imines. The ruthenium(II) arylation are now commonly used for the design of polyheterocycles and polydentate ligands. Most importantly Ru(II)-catalysed direct arylation with arylchlorides can be performed profitably in water as solvent without additional surfactants.

The monoarylation of non-protected *ortho* C–H is now controlled both by using Ru(II)- PR_3 precursor and by operating in water. Thus mixed diarylations are now possible.

The weakest point is that up to now and using mostly $[\text{RuCl}_2(\text{arene})]_2$ or $\text{RuCl}_2(\text{PR}_3)_{3,4}$ precursors weakly coordinated functional groups such as ketones, esters, amides do not direct the *ortho* C–H bond activation and arylation of arenes and heterocycles.

Simple ruthenium(II) catalysts can now perform heterocycle directed alkylation and Friedel–Crafts type reactions at *ortho*-positions of arenes and heteroarenes. The former reaction takes place without β elimination and the latter reaction takes place without addition of Lewis acid to form arenes containing a ketone, amide, or ester functionality. Hydroarylation of strained alkenes can be performed to obtain *ortho* alkyl (hetero)arenes and alkylation of sp^2 C–H bond can be observed using alcohol as a precursor.

Since 2011, the ruthenium(II) catalysed alkenylation of arenes, alkenes, heterocycles, ferrocenes has been established as a catalytic method to produce a large variety of functional alkenes. The reaction requires a Ru(II) catalyst associated with an oxidant such as $\text{Cu}(\text{OAc})_2 \cdot \text{H}_2\text{O}$. More importantly using usually $[\text{RuCl}_2(\text{arene})]_2$ catalyst with a slight excess of silver salt in the presence of an oxidant $\text{Cu}(\text{OAc})_2$ under air the alkenylation of (hetero)arenes and alkenes can be directed by weakly coordinating groups such as ketone, aldehydes, amides, carbamates, and esters.

Ruthenium(II)/AgSbF₆ catalyst, without oxidant but with carboxylic acid, can perform the *ortho*-alkenylation of (hetero)arenes with alkynes as an atom economy reaction.

A tremendous recent innovation brought by ruthenium(II) catalysts deals with the oxidative annulations with alkynes and activation of both C–H and N–H or O–H bonds to form very easily a large variety of heterocycles. Ruthenium(II) activation of C–H bond in the presence of alkynes can be tamed to form two C–C bonds from C–H bond activation and, after alkyne insertion, on addition of C–Ru bond to a ketone or imine group.

Ruthenium(II)-catalysed activation of C–H bond offers many challenges to overcome. One of the first deals with regioselectivity, especially for the activation of *para* and *meta* C–H bonds of (hetero)arenes instead of the *ortho* C–H bonds. A few examples have already appeared in the selective sulfonation and alkylation with secondary alkylhalides of arenes. New efforts will probably lead to fill this gap.

Simple RuCl₂L_{*n*} and Ru(O₂CR)XL_{*n*} have shown the first innovations in catalytic sp^2 C–H bond functionalization and new C–C bond formation. In the near future, no doubt that other more efficient ruthenium catalysts for C–H bond functionalization, and tolerating new functional groups to direct C–H bond activation, will be discovered and successfully applied.

Whereas this chapter has concentrated on C–C bond cross-couplings from sp^2 C–H bonds, there are already several excellent examples of Ru(II)-catalysed selective transformations of sp^2 C–H bonds into C–O and C–N bonds and no doubt that this field will be developed soon. Future development and investigation of ruthenium(II)-catalysed activation of C–H bond will deal with the catalytic functionalization of sp^3 C–H bonds with cheap ruthenium catalysts and the first contributions to solve some challenges in this area will be presented by Bruneau in the following chapter.

References

1. Tamao K, Sumitani K, Kumada M (1972) *J Am Chem Soc* 94:4374
2. Corriu RJP, Masse JP (1972) *J Chem Soc Chem Commun* 144
3. King AO, Okukado N, Negishi EI (1977) *J Chem Soc Chem Commun* 683
4. Sonogashira K, Tohda Y, Hagihara N (1975) *Tetrahedron Lett* 16:4467
5. Milstein D, Stille JK (1978) *J Am Chem Soc* 100:3636
6. Miyaura N, Yamada K, Suzuki A (1979) *Tetrahedron Lett* 20:3437
7. Hatanaka Y, Hiyama T (1988) *J Org Chem* 53:918
8. Campeau LC, Fagnou K (2006) *Chem Commun* 1253
9. Daugulis O, Zaitsev VG, Shabashov D, Pham QN, Lazareva A (2006) *Synlett* 3382
10. Chen X, Engle KM, Wang DH, Yu JQ (2009) *Angew Chem Int Ed* 48:5094
11. Lyons TW, Sanford MS (2010) *Chem Rev* 110:1147
12. Beck EM, Gaunt MJ (2010) *Top Curr Chem* 292:85
13. Ackermann L (2011) *Chem Rev* 111:1315
14. Engle KM, Mei TS, Wasa M, Yu JQ (2011) *Acc Chem Res* 45:788

15. Li BJ, Shi ZJ (2012) *Chem Soc Rev* 41:5588
16. Davies HML, Beckwith REJ (2003) *Chem Rev* 103:2861
17. Berman AM, Lewis JC, Bergman RG, Ellman JA (2008) *J Am Chem Soc* 130:14926
18. Satoh T, Miura M (2010) *Chem Eur J* 16:11212
19. Lewis JC, Bergman RG, Ellman JA (2008) *Acc Chem Res* 41:1013
20. Colby DA, Bergman RG, Ellman JA (2010) *Chem Rev* 110:624
21. Wencel-Delord J, Droge T, Liu F, Glorius F (2011) *Chem Soc Rev* 40:4740
22. Song G, Wang F, Li X (2012) *Chem Soc Rev* 41:3651
23. Colby DA, Tsai AS, Bergman RG, Ellman JA (2012) *Acc Chem Res* 45:814
24. Sen A (1998) *Acc Chem Res* 31:550
25. Jia C, Kitamura T, Fujiwara Y (2001) *Acc Chem Res* 34:633
26. Ritleng V, Sirlin C, Pfeffer M (2002) *Chem Rev* 102:1731
27. Labinger JA, Bercaw JE (2002) *Nature* 417:507
28. Fagnou K, Lautens M (2003) *Chem Rev* 103:169
29. Godula K, Sames D (2006) *Science* 312:67
30. Bergman RG (2007) *Nature* 446:391
31. Alberico D, Scott ME, Lautens M (2007) *Chem Rev* 107:174
32. Seregin IV, Gevorgyan V (2007) *Chem Soc Rev* 36:1173
33. Kulkarni AA, Daugulis O (2009) *Synthesis* 4087
34. Mkhaliid IAI, Barnard JH, Marder TB, Murphy JM, Hartwig JF (2010) *Chem Rev* 110:890
35. Choi J, MacArthur AHR, Brookhart M, Goldman AS (2011) *Chem Rev* 111:1761
36. Murai S, Kakiuchi F, Sekine S, Tanaka Y, Kamatani A, Sonoda M, Chatani N (1993) *Nature* 366:529
37. Kakiuchi F, Tanaka Y, Sato T, Chatani N, Murai S (1995) *Chem Lett* 679
38. Kakiuchi F, Murai S (2002) *Acc Chem Res* 35:826
39. Kakiuchi F, Chatani N (2003) *Adv Synth Catal* 345:1077
40. Kakiuchi F, Chatani N (2004) In: Bruneau C, Dixneuf PH (eds) *Ruthenium catalysts and fine chemistry*, vol 11. Springer, Heidelberg, p 45
41. Kakiuchi F, Kochi T (2008) *Synthesis* 3013
42. Oi S, Fukita S, Hirata N, Watanuki N, Miyano S, Inoue Y (2001) *Org Lett* 3:2579
43. Oi S, Ogino Y, Fukita S, Inoue Y (2002) *Org Lett* 4:1783
44. Ackermann L (2005) *Org Lett* 7:3123
45. Ackermann L, Althammer A, Born R (2006) *Angew Chem Int Ed* 45:2619
46. Özdemir I, Demir S, Cetinkaya B, Gourlaouen C, Maseras F, Bruneau C, Dixneuf PH (2008) *J Am Chem Soc* 130:1156
47. Ackermann L (2010) *Chem Commun* 46:4866
48. Arockiam PB, Bruneau C, Dixneuf PH (2012) *Chem Rev* 112:5879
49. Ferrer-Flegeau EF, Bruneau C, Dixneuf PH, Jutand A (2011) *J Am Chem Soc* 133:10161
50. Arockiam PB, Fischmeister C, Bruneau C, Dixneuf PH (2010) *Angew Chem Int Ed* 49:6629
51. Li B, Dixneuf PH (2013) *Chem Soc Rev* 42:5744
52. Heck RF, Nolley JP (1972) *J Org Chem* 37:2320
53. Fujiwara Y, Moritani I, Matsuda M, Teranishi S (1968) *Tetrahedron Lett* 633
54. Ueyama T, Mochida S, Fukutani T, Hirano K, Satoh T, Miura M (2011) *Org Lett* 13:706
55. Ackermann L, Pospech J (2011) *Org Lett* 13:4153
56. Arockiam PB, Fischmeister C, Bruneau C, Dixneuf PH (2011) *Green Chem* 13:3075
57. Padala K, Jeganmohan M (2011) *Org Lett* 13:6144
58. Kozhushkov SI, Ackermann L (2013) *Chem Sci* 4:886
59. Jaouhari R, Guenot P, Dixneuf PH (1986) *J Chem Soc Chem Commun* 1255
60. Oi S, Sakai K, Inoue Y (2005) *Org Lett* 7:4009
61. Oi S, Aizawa E, Ogino Y, Inoue Y (2005) *J Org Chem* 70:3113
62. Oi S, Funayama R, Hattori T, Inoue Y (2008) *Tetrahedron* 64:6051
63. Oi S, Sasamoto H, Funayama R, Inoue Y (2008) *Chem Lett* 37:994

64. Demerseman B, Diagne Mbaye M, Semeril D, Toupet L, Bruneau C, Dixneuf PH (2006) *Eur J Inorg Chem* 1174
65. Pozgan F, Dixneuf PH (2009) *Adv Synth Catal* 351:1737
66. Oi S, Tanaka Y, Inoue Y (2006) *Organometallics* 25:4773
67. Oi S, Sato H, Sugawara S, Inoue Y (2008) *Org Lett* 10:1823
68. Onodera G, Imajima H, Yamanashi M, Nishibayashi Y, Hidai M, Uemura S (2004) *Organometallics* 23:5841
69. Ackermann L, Born R, Alvarez-Bercedo P (2007) *Angew Chem Int Ed* 46:6364
70. Yaşar S, Dogan Ö, Özdemir I, Çetinkaya B (2008) *Appl Organomet Chem* 22:314
71. Arockiam P, Poirier V, Fischmeister C, Bruneau C, Dixneuf PH (2009) *Green Chem* 11:1871
72. Prades A, Poyatos M, Peris E (2010) *Adv Synth Catal* 352:1155
73. Ackermann L, Althammer A, Born R (2008) *Tetrahedron* 64:6115
74. Ackermann L, Althammer A, Born R (2007) *Synlett* 2833
75. Luo N, Yu ZK (2010) *Chem Eur J* 16:787
76. Cheng K, Zhang YH, Zhao JL, Xie CS (2008) *Synlett* 1325
77. Ackermann L, Vicente R, Althammer A (2008) *Org Lett* 10:2299
78. Ackermann L, Born R, Vicente R (2009) *ChemSusChem* 2:546
79. Ackermann L, Novak P, Vicente R, Pirovano V, Potukuchi HK (2010) *Synthesis* 2245
80. Ackermann L, Vicente R, Potukuchi HK, Pirovano V (2010) *Org Lett* 12:5032
81. Ackermann L, Lygin AV (2011) *Org Lett* 13:3332
82. Stefane B, Fabris J, Pozgan F (2011) *Eur J Org Chem* 3474
83. Li WB, Arockiam PB, Fischmeister C, Bruneau C, Dixneuf PH (2011) *Green Chem* 13:2315
84. Li B, Bheeter CB, Darcel C, Dixneuf PH (2011) *ACS Catalysis* 1:1221
85. Li B, Devaraj K, Darcel C, Dixneuf PH (2012) *Tetrahedron* 68:5179
86. Singh KS, Dixneuf PH (2013) *ChemCatChem* 5:1313
87. Yu BR, Yan XY, Wang S, Tang N, Xi CJ (2010) *Organometallics* 29:3222
88. Doherty S, Knight JG, Addyman CR, Smyth CH, Ward NAB, Harrington RW (2011) *Organometallics* 30:6010
89. Arockiam PB, Fischmeister C, Bruneau C, Dixneuf PH (2013) *Green Chem* 15:67
90. Li B, Roisnel T, Darcel C, Dixneuf PH (2012) *Dalton Trans* 41:10934
91. Fabre I, von Wolff N, Le Duc G, Ferrer Flegeau E, Bruneau C, Dixneuf PH, Jutand A (2013) *Chem Eur J* 19:7595
92. Ouellet SG, Roy A, Molinaro C, Angelaud R, Marcoux JF, O'Shea PD, Davies IW (2011) *J Org Chem* 76:1436
93. Seki M (2011) *ACS Catal* 607
94. Seki M, Nagahama M (2011) *J Org Chem* 76:10198
95. Diers E, Kumar NYP, Mejuch T, Marek I, Ackermann L (2013) *Tetrahedron* 69:4445
96. Yang H, Yang L, Li Y, Zhang F, Liu H, Yi B (2012) *Catal Commun* 26:11
97. Zhang J, Yang Q, Zhu Z, Yuan ML, Fu HY, Zheng XL, Chen H, Li RX (2012) *Eur J Org Chem* 6702
98. Lakshman MK, Deb AC, Chamala RR, Pradhan P, Pratap R (2011) *Angew Chem Int Ed* 50:11400
99. Inoue S, Shiota H, Fukumoto Y, Chatani N (2009) *J Am Chem Soc* 131:6898
100. Shiota H, Ano Y, Aihara Y, Fukumoto Y, Chatani N (2011) *J Am Chem Soc* 133:14952
101. Ackermann L, Diers E, Manvar A (2012) *Org Lett* 14:1154
102. Ackermann L, Mulzer M (2008) *Org Lett* 10:5043
103. Ackermann L, Pospech J, Potukuchi HK (2012) *Org Lett* 14:2146
104. Miyaura N, Suzuki A (1995) *Chem Rev* 95:2457
105. Chinnagolla RK, Jeganmohan M (2012) *Org Lett* 14:5246
106. Rudolph A, Lautens M (2009) *Angew Chem Int Ed* 48:2656
107. Jaouhari R, Dixneuf PH (1988) *Inorg Chim Acta* 145:179
108. Ackermann L, Novak P, Vicente R, Hofmann N (2009) *Angew Chem Int Ed* 48:6045
109. Ackermann L, Hofmann N, Vicente R (2011) *Org Lett* 13:1875

110. Ackermann L, Novak P (2009) *Org Lett* 11:4966
111. Saidi O, Marafie J, Ledger AEW, Liu PM, Mahon MF, Kociok-Kohn G, Whittlesey MK, Frost CG (2011) *J Am Chem Soc* 133:19298
112. Hofmann N, Ackermann L (2013) *J Am Chem Soc* 135:5877
113. Lail M, Arrowood BN, Gunnoe TB (2003) *J Am Chem Soc* 125:7506
114. Lail M, Bell CM, Conner D, Cundari TR, Gunnoe TB, Petersen JL (2004) *Organometallics* 23:5007
115. Foley NA, Lail M, Lee JP, Gunnoe TB, Cundari TR, Petersen JL (2007) *J Am Chem Soc* 129:6765
116. Foley NA, Ke Z, Gunnoe TB, Cundari TR, Petersen JL (2008) *Organometallics* 27:3007
117. Foley NA, Lee JP, Ke Z, Gunnoe TB, Cundari TR (2009) *Acc Chem Res* 42:585
118. Andreatta JR, McKeown BA, Gunnoe TB (2011) *J Organomet Chem* 696:305
119. Pittard KA, Lee JP, Cundari TR, Gunnoe TB, Petersen JL (2004) *Organometallics* 23:5514
120. Oxgaard J, Periana RA, Goddard WA (2004) *J Am Chem Soc* 126:11658
121. Youn SW, Pastine SJ, Sames D (2004) *Org Lett* 6:581
122. Kozhushkov SI, Yufit DS, Ackermann L (2008) *Org Lett* 10:3409
123. Ackermann L, Kozhushkov SI, Yufit DS (2012) *Chem Eur J* 18:12068
124. Schinkel M, Wallbaum J, Kozhushkov SI, Marek I, Ackermann L (2013) *Org Lett* 15:4482
125. Schinkel M, Marek I, Ackermann L (2013) *Angew Chem Int Ed* 52:3977
126. Rouquet G, Chatani N (2013) *Chem Sci* 4:2201
127. Hamid MHSA, Slatford PA, Williams MJM (2007) *Adv Synth Catal* 349:1555
128. Moran J, Krische MJ (2012) *Pure Appl Chem* 84:1729
129. Lee DH, Kwon KH, Yi CS (2011) *Science* 333:1613
130. Lee DH, Kwon KH, Yi CS (2012) *J Am Chem Soc* 134:7325
131. Kochi T, Urano S, Seki H, Mizushima E, Sato M, Kakiuchi F (2009) *J Am Chem Soc* 131:2792
132. Kochi T, Tazawa A, Honda K, Kakiuchi F (2011) *Chem Lett* 40:1018
133. Bräse S, de Meijere A (2004) In: de Meijere A, Diederich F (eds) *Metal-catalyzed cross-coupling reactions*. Wiley-VCH, New York, Chapter 5
134. Oestreich M (2009) *The Mizoroki–Heck reaction*. Wiley, Chichester
135. Bayardon J, Holz J, Schäffner B, Andrushko V, Verevkin S, Preetz A, Börner A (2007) *Angew Chem Int Ed* 46:5971
136. Farrington EJ, Brown JM, Barnard CFJ, Rowsell E (2002) *Angew Chem Int Ed* 41:169
137. Farrington EJ, Barnard CFJ, Rowsell E, Brown JM (2005) *Adv Synth Catal* 347:185
138. Weissman H, Song XP, Milstein D (2001) *J Am Chem Soc* 123:337
139. Yi CS, Lee DW (2009) *Organometallics* 28:4266
140. Kwon KH, Lee DW, Yi CS (2010) *Organometallics* 29:5748
141. Yamashita M, Hirano K, Satoh T, Miura M (2010) *Org Lett* 12:592
142. Hashimoto Y, Ueyama T, Fukutani T, Hirano K, Satoh T, Miura M (2011) *Chem Lett* 40:1165
143. Li B, Devaraj K, Darcel C, Dixneuf PH (2012) *Green Chem* 14:2706
144. Padala K, Jeganmohan M (2012) *Org Lett* 14:1134
145. Li B, Ma JF, Wang NC, Feng HL, Xu SS, Wang B (2012) *Org Lett* 14:736
146. Hashimoto Y, Orloff T, Hirano K, Satoh T, Bolm C, Miura M (2012) *Chem Lett* 41:151
147. Ackermann L, Wang L, Wolfram R, Lygin AV (2012) *Org Lett* 14:728
148. Padala K, Pimparkar S, Madasamy P, Jeganmohan M (2012) *Chem Commun* 48:7140
149. Graczyk K, Ma W, Ackermann L (2012) *Org Lett* 14:4110
150. Li J, Kornhaaf C, Ackermann L (2012) *Chem Commun* 48:11343
151. Reddy MC, Jeganmohan M (2013) *Eur J Org Chem* 1150
152. Li B, Ma J, Liang Y, Wang N, Xu S, Song H, Wang B (2013) *Eur J Org Chem* 1950
153. Zhang J, Loh TP (2012) *Chem Commun* 48:11232
154. Singh KS, Dixneuf PH (2012) *Organometallics* 31:7320
155. Lanke V, Prabhu KR (2013) *Org Lett* 15:2818

156. Li B, Ma J, Xie W, Song H, Xu S, Wang B (2013) *J Org Chem* 78:9345
157. Lanke V, Prabhu KR (2013) *Org Lett* 15:6262
158. Ma W, Ackermann L (2013) *Chem Eur J* 19:13925
159. Chidipudi SR, Wiczysty MD, Khan I, Lam HW (2013) *Org Lett* 15:570
160. Li B, Darcel C, Dixneuf PH (2014) *Chem Commun* 50:5970
161. Cheng K, Yao BB, Zhao JL, Zhang YH (2008) *Org Lett* 10:5309
162. Tan ST, Teo YC, Fan WY (2012) *J Organomet Chem* 58:708
163. Hashimoto Y, Hirano K, Satoh T, Kakiuchi F, Miura M (2012) *Org Lett* 14:2058
164. Hashimoto Y, Hirano K, Satoh T, Kakiuchi F, Miura M (2013) *J Org Chem* 78:638
165. Zhao P, Niu R, Wang F, Han K, Li X (2012) *Org Lett* 14:4166
166. Reddy MC, Jeganmohan M (2013) *Chem Commun* 49:481
167. Sundararaju B, Achard M, Demerseman B, Toupet L, Sharma GVM, Bruneau C (2010) *Angew Chem Int Ed* 49:2782
168. Goriya Y, Ramana CV (2012) *Chem Eur J* 18:13288
169. Cho SH, Kim JY, Kwak J, Chang S (2011) *Chem Soc Rev* 40:5068
170. Yeung S, Dong VM (2011) *Chem Rev* 111:1215
171. Liu C, Zhang H, Shi HW, Lei A (2011) *Chem Rev* 111:1780
172. Yoo WJ, Li CJ (2010) *Top Curr Chem* 292:281
173. Ueura K, Satoh T, Miura M (2007) *Org Lett* 9:1407
174. Yi CS, Yun SY, Guzei IA (2005) *J Am Chem Soc* 127:5782
175. Yi CS, Yun SY (2005) *J Am Chem Soc* 127:17000
176. Ackermann L, Lygin AV, Hofmann N (2011) *Angew Chem Int Ed* 50:6379
177. Ackermann L, Lygin AV, Hofmann N (2011) *Org Lett* 13:3278
178. Ackermann L, Wang L, Lygin AV (2012) *Chem Sci* 3:177
179. Ma W, Graczyk K, Ackermann L (2012) *Org Lett* 14:6318
180. Kavitha N, Sukumar G, Kumar VP, Mainkar PS, Chandrasekhar S (2013) *Tetrahedron Lett* 54:4198
181. Li B, Feng HL, Xu SS, Wang BQ (2011) *Chem Eur J* 17:12573
182. Ackermann L, Fenner S (2011) *Org Lett* 13:6548
183. Ackermann L, Lygin AV (2012) *Org Lett* 14:764
184. Wang L, Ackermann L (2013) *Org Lett* 15:176
185. Li B, Feng H, Wang N, Ma J, Song H, Xu S, Wang B (2012) *Chem Eur J* 18:12873
186. Chinnagolla RK, Pimparkar S, Jeganmohan M (2012) *Org Lett* 14:3032
187. Kornhaaß C, Li J, Ackermann L (2012) *J Org Chem* 77:9190
188. Parthasarathy K, Senthilkumar N, Jayakumar J, Cheng CH (2012) *Org Lett* 14:3478
189. Luo CZ, Gandeepan P, Cheng CH (2013) *Chem Commun* 49:8528
190. Chinnagolla RK, Jeganmohan M (2012) *Chem Commun* 48:2030
191. Ackermann L, Pospech J, Graczyk K, Rauch K (2012) *Org Lett* 14:930
192. Deponti M, Kozhushkov S, Yufit DS, Ackermann L (2013) *Org Biomol Chem* 11:142
193. Thirunavukkarasu VS, Donati M, Ackermann L (2012) *Org Lett* 14:3416
194. Park Y, Jeon I, Shin S, Min J, Lee PH (2013) *J Org Chem* 78:10209
195. Chinnagolla RK, Jeganmohan M (2012) *Eur J Org Chem* 417
196. Zhao P, Wang F, Han K, Li X (2012) *Org Lett* 14:5506
197. Zhang J, Ugrinov A, Zhao P (2013) *Angew Chem Int Ed* 52:6681
198. Nakao Y, Morita E, Idei H, Hiyama T (2011) *J Am Chem Soc* 133:3264
199. Tan X, Liu B, Li X, Li B, Xu S, Song H, Wang B (2012) *J Am Chem Soc* 134:16131
200. Chidipudi SR, Khan I, Lam HW (2012) *Angew Chem Int Ed* 51:12115

sp^3 C–H Bond Functionalization with Ruthenium Catalysts

Christian Bruneau

Abstract The selective formation of carbon–carbon bond by functionalization of an sp^3 C–H bond is still a challenge in organic synthesis. There are already examples involving transition metal catalysis. In this chapter we review the use of ruthenium (0) and ruthenium(II) catalysts for the formation of carbon–carbon bonds based on creation of reactive sites by sp^3 C–H bond activation. We show that in most cases, regioselective sp^3 C–H bond activation is induced either from functional substrates bearing a directing group, which strongly coordinates the metal centre, or by selective C–H bond activation at the α -carbon of a heteroatom accompanied by hydrogen transfer processes and transient creation of reactive functional groups.

Keywords Carbon–carbon bond formation · Ruthenium catalysis · sp^3 C–H activation

Contents

1	Introduction	196
2	Catalytic Activation with Ruthenium(0) Catalysts	196
2.1	Insertion of Alkenes into sp^3 C–H Bonds with Ru(0) Catalysts	196
2.2	Carbonylation of sp^3 C–H Bonds with Ru(0) Catalysts	202
2.3	Arylation of sp^3 C–H Bonds with Arylboronates	205
3	Catalytic Functionalization of sp^3 C–H Bonds with Ruthenium(II) Catalysts	211
3.1	Directed sp^3 C–H Bond Arylation	211
3.2	Functionalization of Non-benzylic Aliphatic Amines	212
3.3	sp^3 C– sp^3 C Bond Formation Involving Alcohol α - sp^3 C–H Bond Activation and Hydrogen Borrowing	217

C. Bruneau (✉)

UMR 6226, CNRS-Université de Rennes 1, Institut des Sciences Chimiques de Rennes –
Centre for Catalysis and Green Chemistry, Campus de Beaulieu, 35042 Rennes,
Cedex, France
e-mail: christian.bruneau@univ-rennes1.fr

3.4	Miscellaneous Reactions Involving Carbon–Carbon Bond Formation via sp^3C-H Bond Activation	231
4	Conclusion	234
	References	234

1 Introduction

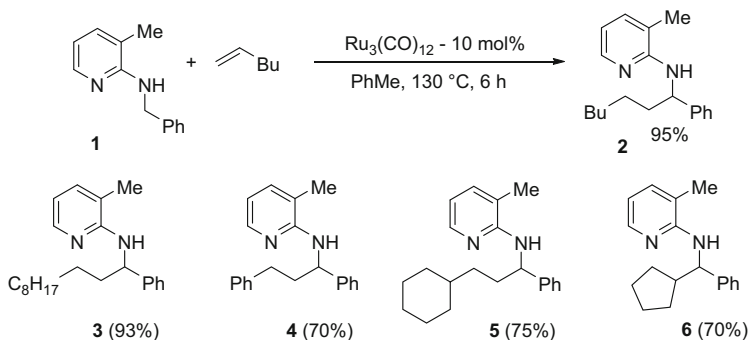
Modern chemistry requires synthetic methods able to perform transformations with high efficiency and selectivity. For cost and environment issues these processes have also to be as clean as possible and must therefore offer the possibility of performing transformations with atom economy. Even though catalytic reactions promoted by transition metal complexes are able to fulfil these criteria, selective creation of carbon–carbon single bonds via metal-catalysed sp^3C-H bond activation/functionalization is still a challenge for organic synthesis. Among the group 8 transition metals, ruthenium(0) and ruthenium(II) catalysts have attracted much attention during the last decade to achieve such transformations. Indeed, ruthenium catalysts promote carbon–carbon bond formation via greener processes than the well-established cross coupling reactions of organohalides (or pseudohalides) with organometallic substrates. This chapter specifically reports on sp^3C-H bond activation with subsequent formation of carbon–carbon bonds, formation of carbon–heteroatom bonds being excluded.

2 Catalytic Activation with Ruthenium(0) Catalysts

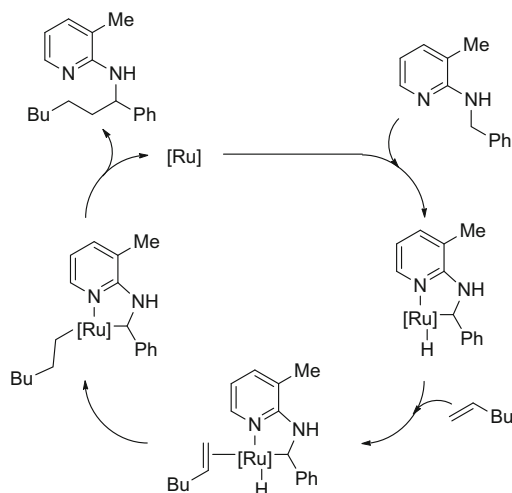
2.1 Insertion of Alkenes into sp^3C-H Bonds with Ru(0) Catalysts

A few examples of directed sp^3C-H bond activation in the presence of ruthenium(0) catalyst precursors with formal insertion of a carbon–carbon double bond into a transient ruthenium–hydride bond have been reported. In particular, $Ru_3(CO)_{12}$ catalysed the alkylation at sp^3 carbons by terminal olefins with the assistance of pyridine chelation. In 1998, Jun was the first to show the insertion of an alkene into the sp^3C-H bond of a benzyl group using a ruthenium(0) catalyst [1]. The strongly chelating pyridine-containing benzylamine **1** in the presence of a large excess of hex-1-ene at 130°C with 10 mol% of $Ru_3(CO)_{12}$ led to the formal insertion of the alkene into one benzyl sp^3C-H bond and thus to the alkylation of an sp^3C-H bond to give the alkylated benzylic amine **2** (Scheme 1).

The suggested mechanism is shown in Scheme 2: it involves the initial coordination of the pyridine that directs oxidative addition of one benzylic sp^3C-H bond to the Ru(0) centre, followed by insertion of the alkene into the Ru-H bond, and



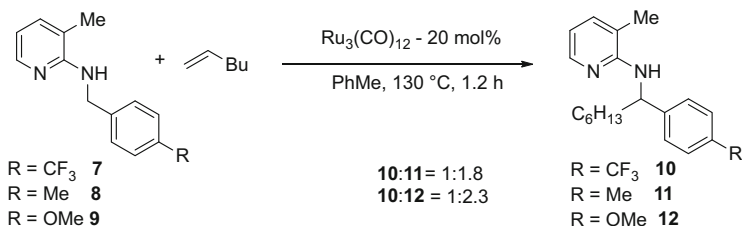
Scheme 1 First chelation-assisted ruthenium-catalysed alkylation of benzyl amine derivatives



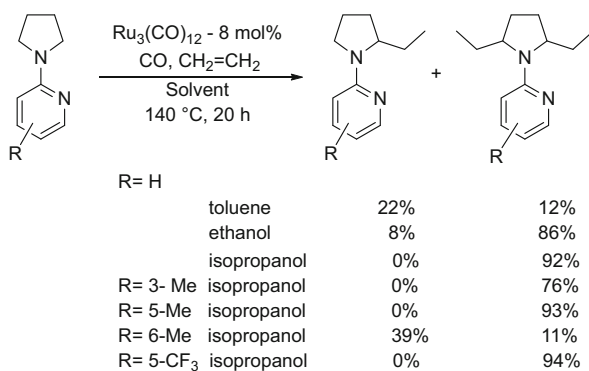
Scheme 2 Proposed catalytic cycle for sp^3C –H alkylation with alkenes

reductive elimination of the formed alkyl ligands leading to sp^3C – sp^3C bond formation. This mechanism is analogous to that of Murai's reaction involving sp^2C – H bond and alkenes [2]. The success of this reaction is likely due to the strongly chelating pyridine group at the proximity of the sp^3C – H bond and to the easy sp^3C – H bond activation adjacent to the amino group.

It is noteworthy that when the internal alkenes hex-2-ene and hex-3-ene were used the same product **2** was obtained with good 85 and 81% yield, respectively, showing that the isomerization of 2- or 3-hexyl into 1-hexyl ligand was faster than the reductive elimination step. The easiness of the reaction depended on the arene substituent nature. When a 1:1 mixture of **7** ($\text{R}=\text{CF}_3$) and **8** ($\text{R}=\text{Me}$) was reacted with hex-1-ene a mixture of **10** and **11** in a 1:1.8 ratio was obtained. Analogously a 1:1 mixture of **7** and **9** led to a **10/12** mixture in a 1:2.3 ratio (Scheme 3). Thus, the most electron-donating the substituent, the faster the sp^3C – H bond alkylation.



Scheme 3 Compared reactivities of various benzylic amines with alkenes



Scheme 4 $\text{Ru}_3(\text{CO})_{12}$ -catalysed α -alkylation of cyclic amines with ethylene

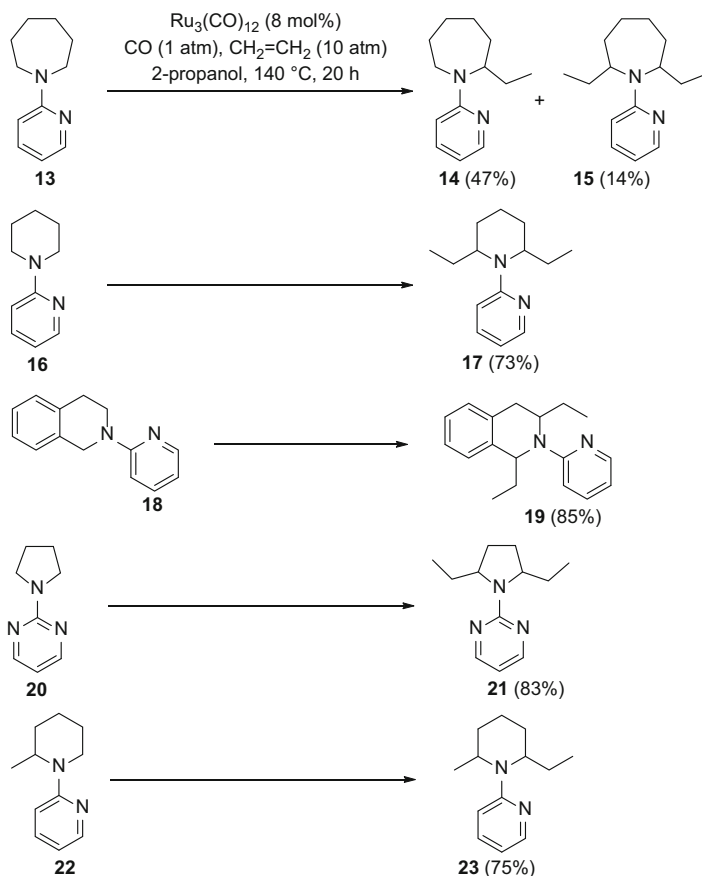
Whereas the above reaction is limited to pyridine-containing benzylamines, Murai and coll. succeeded to extend this alkylation reaction to a variety of cyclic alkylamines N-protected by a 2-pyridyl group as a chelating and directing group using the same catalyst $\text{Ru}_3(\text{CO})_{12}$ [3].

When 2-(1-pyrrolidinyl)pyridine was reacted with ethylene (10 atm initial pressure) in the presence of CO (1 atm initial pressure) at 140 °C in toluene for 20 h with $\text{Ru}_3(\text{CO})_{12}$ as catalyst, 22% of monoalkylated pyrrolidine was obtained along with 12% of dialkylated pyrrolidine but no carbonylation was observed (Scheme 4) [3].

The nature of the solvent was crucial as 86 and 92% of the dialkylated product were obtained in ethanol and isopropanol, respectively. It is noteworthy that the use of CO was not essential but allowed to reach better yields, likely avoiding the decomposition of the catalyst. Thus, the dialkylated pyrrolidine in isopropanol was obtained in 77% instead of 92% yield when carbon monoxide was replaced by nitrogen.

It is noteworthy that other ruthenium *catalysts* such as $\text{RuH}_2(\text{CO})(\text{PPh}_3)_3$ and $\text{Ru}(\text{acac})_3$ showed no activity whereas $\text{RuCl}_3 \cdot 3\text{H}_2\text{O}$ and $\text{RuCl}_2(\text{PPh}_3)_3$ presented some activity but not as high as $\text{Ru}_3(\text{CO})_{12}$ [3]. Electronic properties and position of substituents on the pyridine ring played a crucial role on reactivity (Scheme 4).

Other protecting groups (CN, COR, CO₂R, CH=NR) linked to the cyclic amine N-atom instead of pyridine did not lead to the alkylation of pyrrolidine, thus showing that a Ru(0) strongly binding group is required.

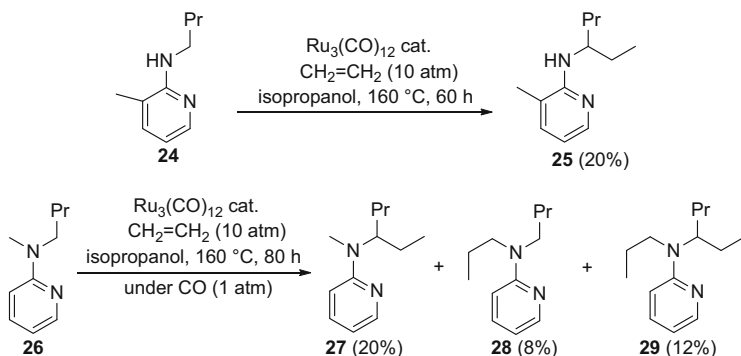


Scheme 5 $\text{Ru}_3(\text{CO})_{12}$ -catalysed alkylation of cyclic amines with ethylene

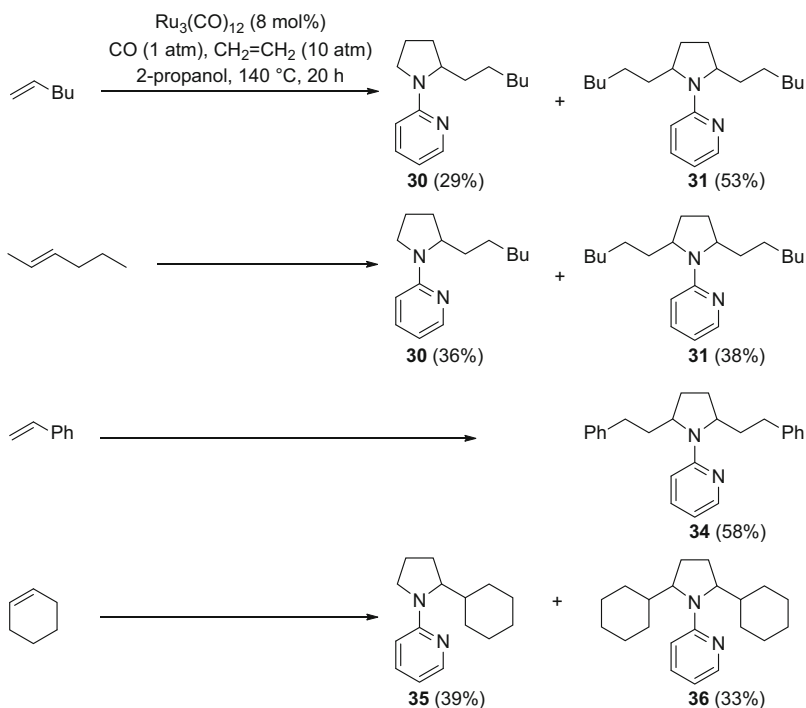
This alkylation reaction has been applied to other 2-pyridyl- and 2-pyrimidinyl-protected saturated cyclic amines and good yields of α, α' -dialkylated cyclic amines were obtained. The monoalkylated derivatives were obtained only when one adjacent position of the amine N-atom was already substituted (Scheme 5) [3].

With secondary acyclic alkylamines (Scheme 6) the alkylation was performed without CO, as under the previous experimental conditions, the reaction preferentially led to the carbonylation of the N–H bond and the formation of formamide. The alkylation of secondary amines with ethylene in isopropanol led to monoalkylation of the benzylic sp³C–H bond. Alkylation of the tertiary dialkylamine **26** took place under carbon monoxide but was not selective leading to a mixture of mono- and dialkylated products **27–29** (Scheme 6).

The alkylation was extended to a variety of alkenes such as hexene, styrene, *tert*-butylethylene and cyclohexene (Scheme 7). Under typical conditions a large excess of the alkene (10 equiv.) was reacted at 140 °C for 40–60 h in the presence of 8 mol

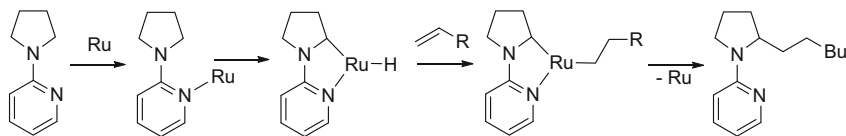


Scheme 6 $\text{Ru}_3(\text{CO})_{12}$ -catalysed alkylation of secondary benzylic amines with ethylene

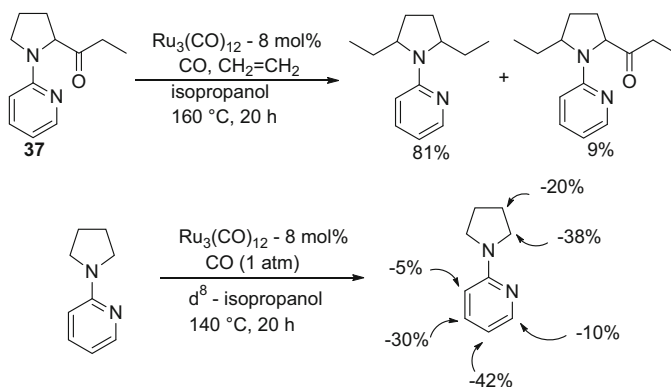


Scheme 7 $\text{Ru}_3(\text{CO})_{12}$ -catalysed α -alkylation of *N*-(2-pyridyl)pyrrolidine with alkenes

% of $\text{Ru}_3(\text{CO})_{12}$ without carbon monoxide. It is noteworthy that with 2-hexene its pyrrolidine derivatives **30** and **31** containing 1-hexyl substituents were formed, as it was also observed by Jun [1]. On the other hand, functional olefins such as acrylonitrile and butyl vinyl ether were not reactive.



Scheme 8 Proposed mechanism for ruthenium(0)-catalysed sp³C–H alkylation with alkenes



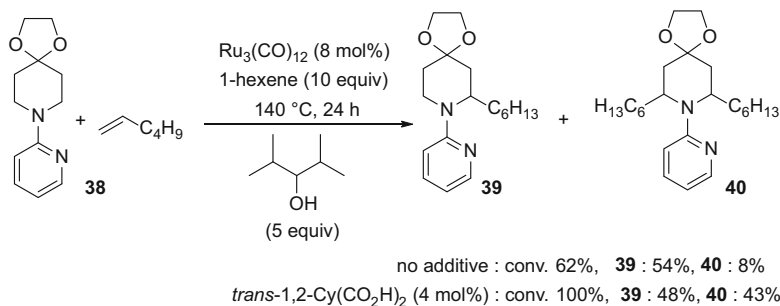
Scheme 9 Decarbonylation of acylpyrrolidine **37** and H/D exchange experiments

The proposed mechanism (Scheme 8) involves initial coordination of the pyridine to direct sp³C–H bond oxidative addition to the Ru(0) centre followed by alkene insertion into a Ru–H bond and reductive elimination as for the Murai reaction involving sp²C–H bond alkylation [3].

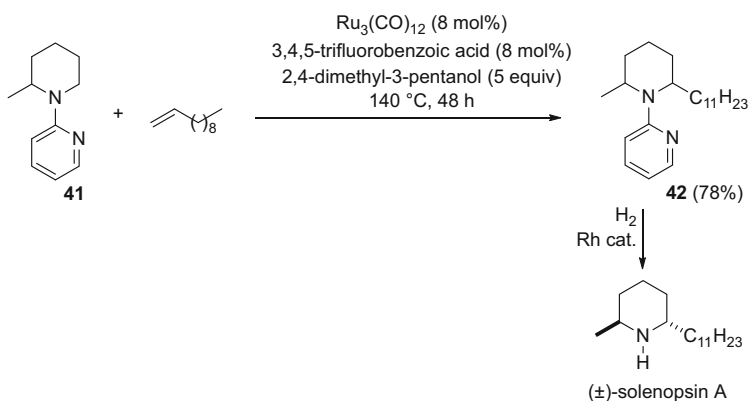
However a hydride transfer from the N adjacent carbon, to form an iminium cation as in the Murahashi [4] oxidative functionalization of tertiary amines is also discussed. In the absence of any oxidant, this process seems less realistic.

It is noteworthy that the pyrrolidine **37**, containing an acyl group at the N-adjacent carbon, under the catalytic reaction conditions surprisingly led to decarbonylation giving the dialkylated product as a major product, thus showing the reversibility of a possible acyl intermediate in the general reaction under carbon monoxide (Scheme 9). Under conditions of H/D exchange with d⁸-isopropanol and under the catalytic conditions without ethylene, the deuterium incorporation at carbon atoms C₂ (38%) and more surprisingly C₃ (20%) of the pyrrolidine ring and to a lesser extent to all C–H positions of the pyridine ring were observed (Scheme 9).

It has been shown that the presence of catalytic amounts of carboxylic acid such as *trans*-1,2-cyclohexyldicarboxylic or 3,4,5-trifluorobenzoic acid improved the ruthenium-catalysed sp³C–H bond alkylation of cyclic amines by terminal olefins and allowed reaching full conversion of less reactive *N*-pyridylpiperidine derivatives. Thus, in the absence of CO but in the presence of *trans*-1,2-cyclohexyldicarboxylic acid, the *N*-pyridylpiperidine **38** was efficiently hexylated into mono- **39** and dialkylated **40** piperidine derivatives, whereas in the absence of carboxylic acid



Scheme 10 Influence of carboxylic acid additive in $\text{Ru}_3(\text{CO})_{12}$ -catalysed alkylation of cyclic amines



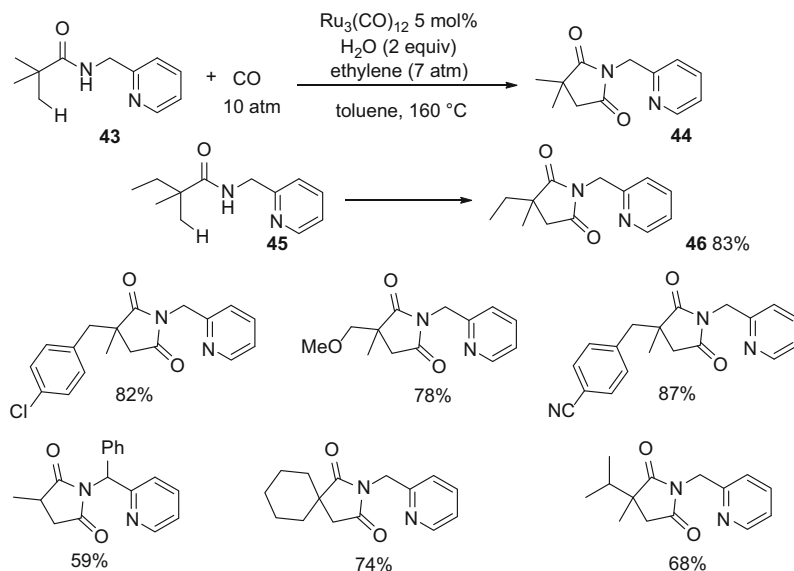
Scheme 11 Synthesis of (±)-solenopsin A intermediate **42**

under otherwise identical conditions, the conversion was lower leading to the monoalkylated **39** as the major product (Scheme 10) [5].

The utility of this alkylation reaction was exemplified by the preparation of the piperidine derivative **42** from **41**, an intermediate in the synthesis of *trans*-2-methyl-6-undecylpiperidine, (±)-solenopsin A (Scheme 11).

2.2 Carbonylation of $\text{sp}^3\text{C-H}$ Bonds with $\text{Ru}(0)$ Catalysts

Initially, carbonylation of unactivated alkanes $\text{sp}^3\text{C-H}$ bonds to produce aldehydes has been performed by Tanaka in the presence of rhodium catalyst under photochemical irradiation [6]. The Chatani–Kakiuchi–Murai group also performed the rhodium-catalysed monocarbonylation of $\text{sp}^3\text{C-H}$ bond adjacent to the nitrogen atom of cyclic amines and directed by a pyridine group in the presence of ethylene to produce α -propanoyl amines [7]. It is only very recently in 2011 that Chatani has



Scheme 12 Carbonylation of unactivated sp³C–H bonds

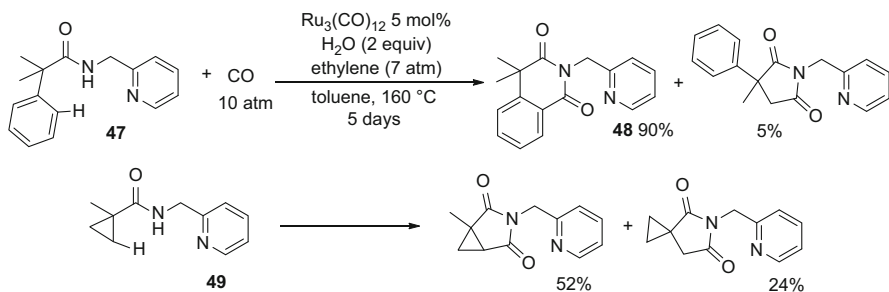
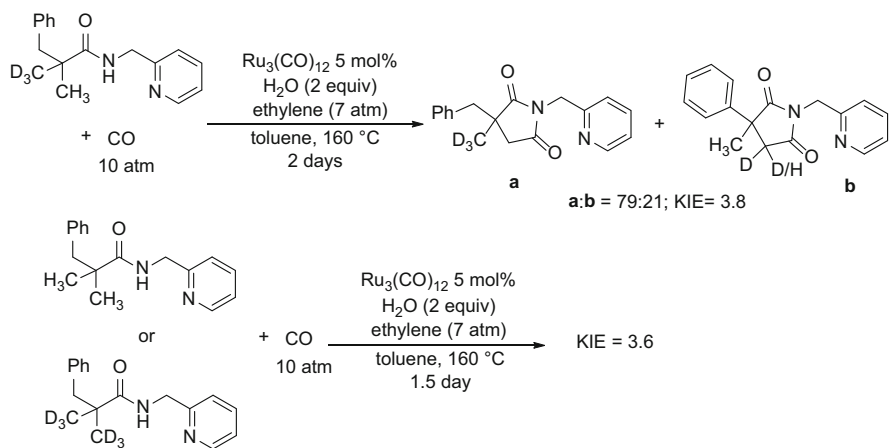
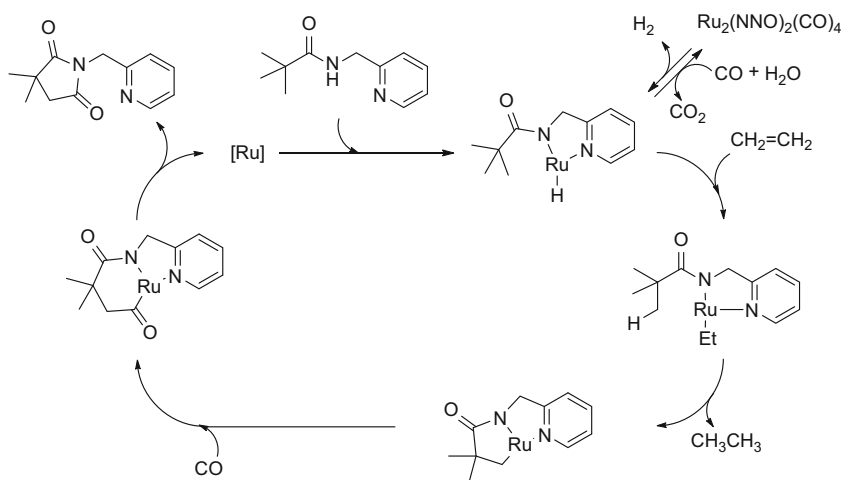
reported the catalytic carbonylation of sp³C–H bond of amides, containing a strongly chelating pyridyl group, catalysed by $\text{Ru}_3(\text{CO})_{12}$ (Scheme 12) [8].

The reaction of **43** took place under 10 atm of CO at 160 °C for 5 days but the presence of ethylene (7 atm) was required as well as small amount of water, to get 79% of the succinimide **44**. The carbonylation of methyl C–H bond was regioselective as no carbonylation of methylene C–H bond was observed (Scheme 12). When a competition was offered between a methyl and an ethyl group as in **45**, carbonylation selectively took place at the methyl group to give **46** in 83% yield. The reaction tolerated a variety of functional groups attached to a neighbouring benzylic group (CN, CF₃, Br, MeO ...).

The reaction of **47** mainly led to the sp²C–H carbonylation and formation of **48** (90%) with 5% only of sp³C–H bond carbonylation showing that sp²C–H bond activation and carbonylation was favoured (Scheme 13). The carbonylation of compound **49** showed that the activation of the cyclopropyl methylene C–H bond was favoured with respect to the methyl one (Scheme 13).

Labelled H/D experiments showed that the C–H bond activation/cleavage was irreversible. It was also shown by comparative reaction of substrates containing CH₃ and/or CD₃ groups (Scheme 14) that the reaction took place with a large kinetic isotope effect of 3.8 within the same molecule and of 3.6 in the intermolecular competition experiment. This is consistent with a rate-determining step for the cleavage of the C–H bond.

The proposed mechanism is given in Scheme 15. It suggests first the Ru(0) insertion into the N–H amide bond followed by insertion of ethylene into the Ru–H bond and elimination of the ethyl ligand with one methyl hydrogen atom to give the

**Scheme 13** Competitive carbonylation reactions**Scheme 14** Isotope effect studied by deuterium labelling experiments**Scheme 15** Proposed mechanism for intramolecular carbonylation of amides via $\text{sp}^3\text{C-H}$ activation

cyclometallated intermediate. The latter can insert CO into the Ru–C bond before reductive elimination. The crucial point for this catalytic reaction is the formation of an *N,N*-bidentate ligand as no carbonylation took place from benzylamides [8, 9].

The role of water is assumed to help the reduction of the inactive, isolable binuclear complex Ru₂(NNO)₂(CO)₄ to generate a mononuclear species, which can enter the catalytic cycle.

2.3 Arylation of sp³C–H Bonds with Arylboronates

Following the directed arylation of aromatic substrates by arylboronates in the presence of ruthenium(0) active species generated from RuH₂(CO)(PPh₃)₃ [10], the amidine-directed arylation of saturated cyclic amines via sp³C–H bond activation was reported by Sames [11]. Starting from a mono 2-substituted pyrrolidine, Ru₃(CO)₁₂ was the best catalyst among other mono- and binuclear ruthenium complexes and gave 5-arylated pyrrolidine derivatives at 150°C in good yields with the *trans*-product as the major diastereomer in the presence of 5 equiv. of *tert*-butylmethylketone, which played a critical role in the reaction (Scheme 16) [11].

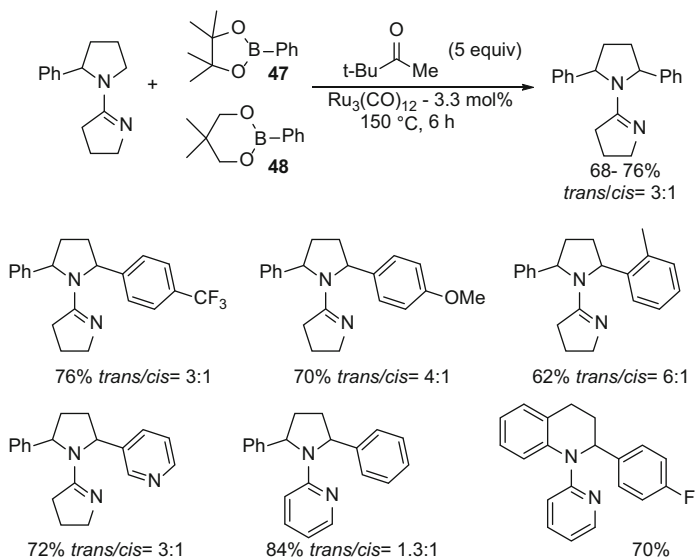
This catalytic reaction was compatible with a large variety of substituted arylboronates including indole- and pyridine-containing boronate esters. The reaction was extended to protected piperidine and tetrahydroquinoline as saturated cyclic substrates. This arylation was applied to pyrrolidines containing either a pyridine or a pyrimidine group as N-protecting/directing group but required higher catalyst loading (10 mol%). With these directing groups, the arylated products were obtained as a mixture of diastereoisomers with low stereoselectivity, which was attributed to a fast isomerization with respect to arylation under the reaction conditions [11].

The proposed mechanism (Scheme 17) involves the initial sp³C–H bond oxidative addition to ruthenium(0) followed by aryl transmetalation and reductive elimination. It was suggested by Sames [11] that the role of the ketone was to insert into the Ru–H bond to favour *trans*-arylation with the phenylboronate ester. Later on it was shown by Maes that pinacolyl alcohol was formed via Ru-catalysed hydrogenation of pinacolone rather than through a Ru-alkoxide intermediate [12].

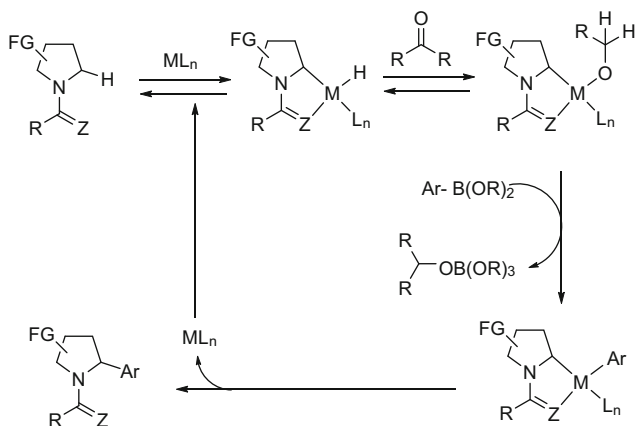
It was shown on some examples that the deprotection of the 2,5-diarylated amidines to give 2,5-disubstituted pyrrolidines was easily performed by treatment with H₂NNH₂/CF₃CO₂H (Scheme 18) [11].

It must be noted that when the saturated cyclic amine was protected in 2-position by an ester group (proline derivative), sp³C–H bond activation did not operate at C5 but a decarboxylative arylation took place in the absence of pinacolone leading to monoarylated pyrroline products (Scheme 19) [13].

Shortly after, Maes proposed another catalytic system also based on ruthenium (0) catalyst, which allowed the direct arylation of the less reactive N-protected piperidines [12]. Improvements came from the use of 2-pyridine as a directing group, that is also an efficient chelating group to the Ru(0) centre. It was shown that



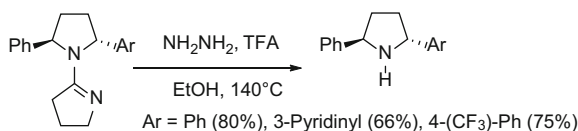
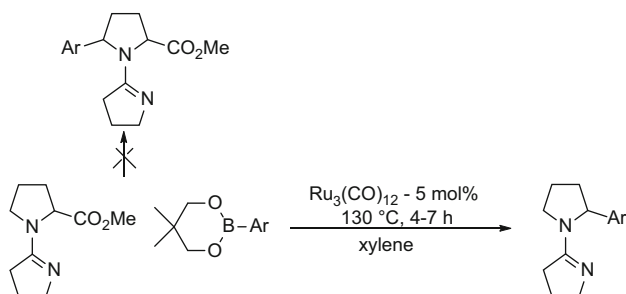
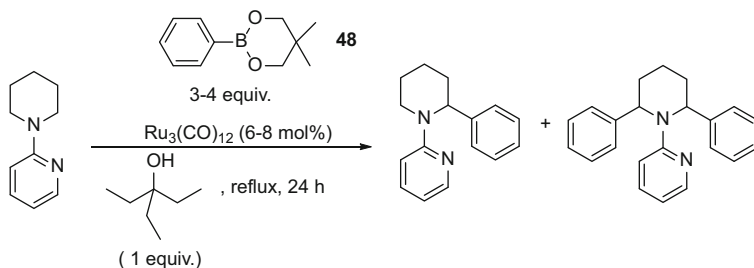
Scheme 16 $\text{Ru}_3(\text{CO})_{12}$ -catalysed $\text{sp}^3\text{C-H}$ bond arylation with arylboronates



Scheme 17 A mechanistic proposal for $\text{sp}^3\text{C-H}$ bond arylation with arylboronates and $\text{Ru}(0)$ catalysts

the ketone was not advantageous with respect to an alcohol as solvent ($t\text{BuOH}$ or Et_3COH) (Scheme 20).

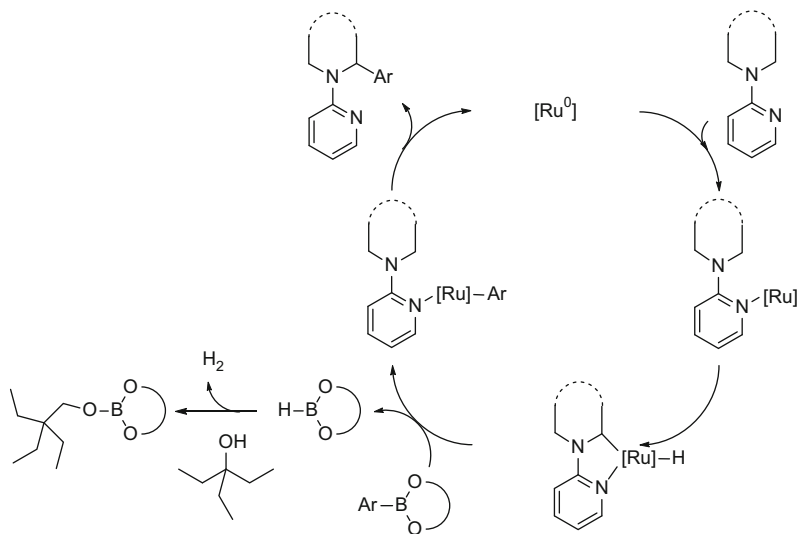
These observations led to the catalytic cycle proposed in Scheme 21. The innovation deals with the direct transarylation on the Ru-H species and formation of the pinacolborane that is scavenged by the tertiary alcohol with formation of hydrogen.

**Scheme 18** Deprotection of 2,5-disubstituted amidines**Scheme 19** Decarboxylative arylation of proline derivatives**Scheme 20** sp³C(2)-H mono and diarylation of *N*-(2-pyridinyl)piperidine

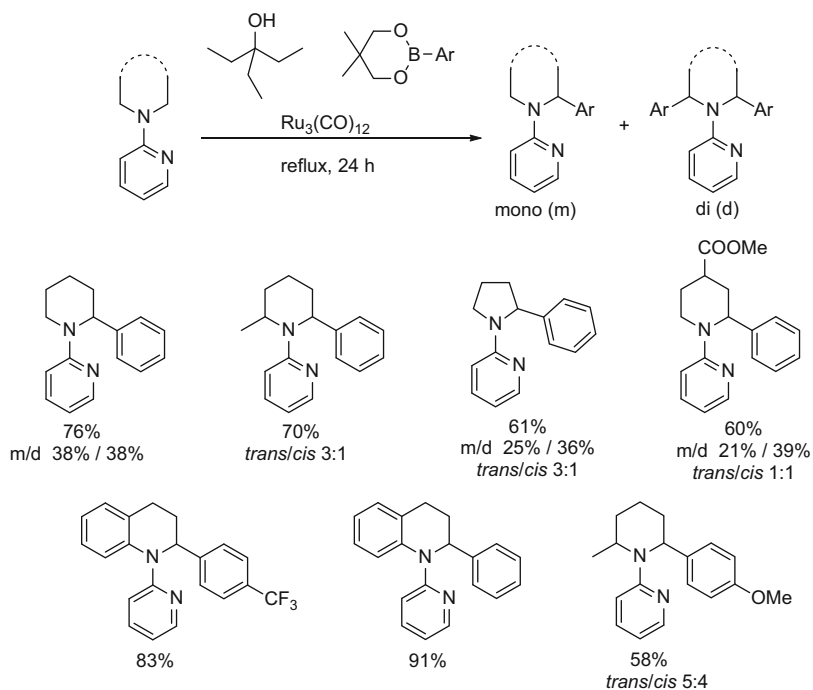
The reaction usually requires 3 equiv. of phenylboronic acid neopentylglycol ester **48** with 6 mol% of Ru₃(CO)₁₂ in 3-ethylpentan-3-ol (1 equiv.) at reflux for 24 h (Scheme 22). Some less reactive substrates required 8 mol% of catalyst and 4 equiv. of arylboronate **48**.

The reaction was then extended to α-(hetero)arylation of various *N*-(2-pyridinyl) saturated cyclic amines under similar catalytic conditions [14]. The deprotection of the cyclic amine can be obtained selectively by sequential catalytic hydrogenation on Pd/C followed by reaction with H₂NNH₂/AcOH/^{*i*}PrOH (Scheme 23) [12, 15] or by quaternization by MeOTf followed by reduction with NaBH₄ [15].

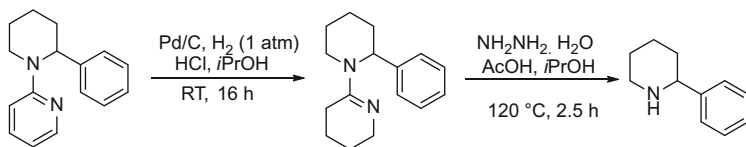
The first selective monoarylation of (*N*-pyridin-2-yl)piperidine was made possible by introduction of a trifluoromethyl substituent at the 3-position of the pyridin-2-yl directing group (Scheme 24) [16]. The steric hindrance brought by this substituent favoured the sole formation of monoarylated piperidines. A beneficial effect of metal salt additives to the Ru₃(CO)₁₂-based catalyst was observed on



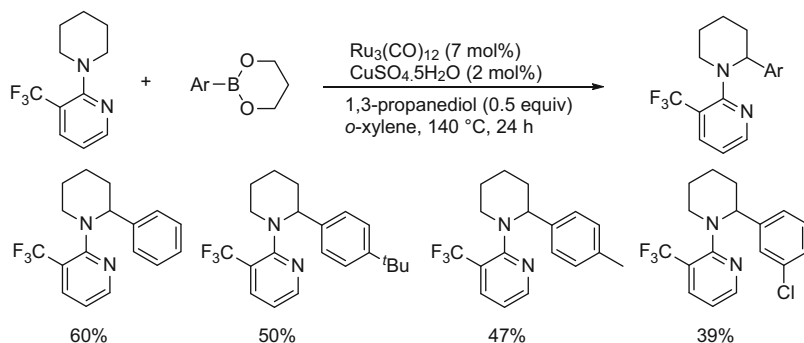
Scheme 21 Proposed mechanism for the $\text{sp}^3\text{C}(2)\text{-H}$ arylation of cyclic amines



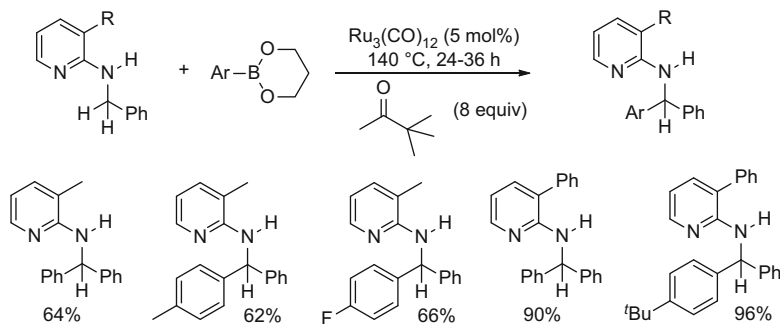
Scheme 22 $\text{sp}^3\text{C-H}$ arylation of various saturated cyclic N -(2-pyridinyl)amines with arylboronates



Scheme 23 One route for removal of the pyridine directing group from piperidine derivatives



Scheme 24 Monoarylation of *N*-(3-(trifluoromethyl)pyridin-2-yl)piperidine with arylboronates

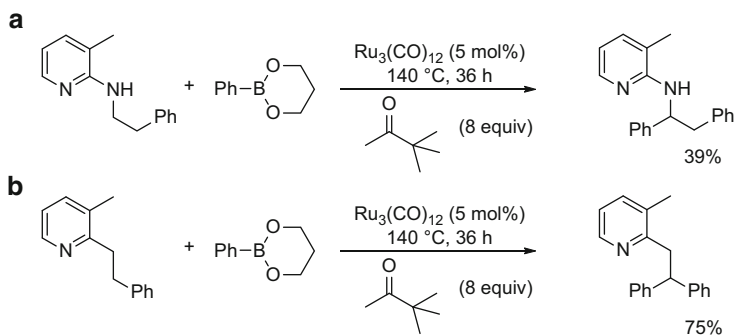


Scheme 25 Directed cross coupling at the benzylic position of benzyl amine

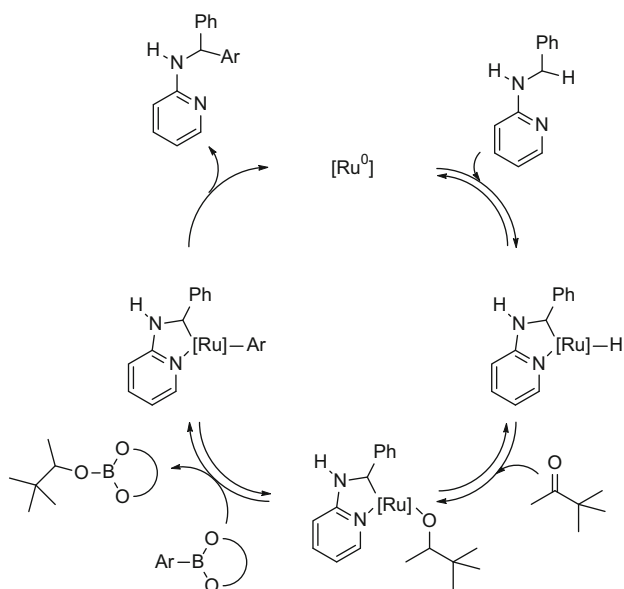
conversion of the substrates. $\text{Cu}(\text{SO}_4)\cdot 5\text{H}_2\text{O}$ provided the best results when the reactions were performed at 140°C in *o*-xylene in the presence of 0.5 equiv. of 1,3-propanediol.

Arylboronate reagents have also been used for the cross coupling at the sp³C–H bond of benzylic amines in the presence of $\text{Ru}_3(\text{CO})_{12}$ and pinacolone as solvent. The reaction was not only directed by a pyridine substituent but also required substitution of this pyridyl group at the 3-position [17, 18].

The preferred substituents at this position were the methyl, trifluoromethyl and phenyl groups (Scheme 25). The arylation worked better with six-membered 2-aryl-1,3,2-dioxaborinane reagents and with pinacolone as solvent of choice, a ketone that



Scheme 26 sp^3C-H arylation at non-benzylic position (**a**) and without adjacent N-H group (**b**)



Scheme 27 Proposed catalytic cycle for ruthenium(0) activation of benzylic sp^3C-H bonds

worked as hydrogen and boron scavenger simultaneously. Many substituents were tolerated on the aryl group, except the coordinating 4-CN and 4-NO₂, which led to complete inhibition of the arylation reaction [17, 18]. Arylboronates containing a coordinating aryl group such as 3-pyridyl or 2-thienyl were also unreactive [17, 18]. It is noteworthy that the reaction also took place with non-benzylic sp^3C-H bonds as exemplified by the arylation by phenylboronate of 3-methyl-*N*-(2-phenylethyl)-2-pyridineamine in 39% yield, and with 3-methyl-2-(2-phenylethyl)pyridine in 75% yield suggesting that an adjacent NH has a lower activating influence on the CH₂ group activation than an adjacent phenyl group (Scheme 26) [18].

A mechanism was proposed where the initial step is coordination of pyridine nitrogen to the ruthenium(0) centre, followed by oxidative addition to give the

cyclometalated intermediate. Insertion of the carbonyl group of the ketone into the Ru–H bond leads to the formation of a ruthenium alkoxide, which facilitates the transmetalation with the arylboronate. Finally, reductive elimination delivers the arylated benzylamine derivative (Scheme 27).

3 Catalytic Functionalization of sp³C–H Bonds with Ruthenium(II) Catalysts

3.1 Directed sp³C–H Bond Arylation

3.1.1 sp³C–H Bond Arylation of Benzylic Amines

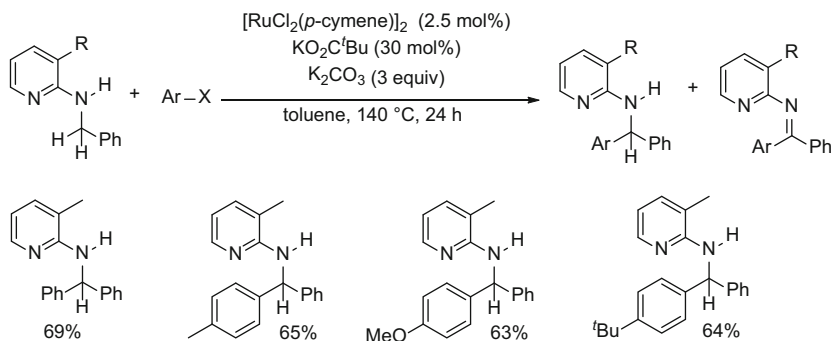
Recently, the same type of arylation of benzylamine derivatives equipped with a 2-pyridinyl directing group was carried out with aryl halides but with the ruthenium(II) catalyst precursor ([RuCl₂(*p*-cymene)]₂) in the presence of potassium pivalate [19, 20] or directly with Ru(carboxylate)₂(*p*-cymene) [21]. Both catalytic systems operate at 140°C for 24 h in toluene or *o*-xylene in the presence of 2.5–5 mol% catalyst loading and a carbonate as a base. The advantage of using the well-defined ruthenium(II)bis(carboxylate) complex is that it does not require an excess of carboxylate as it is the case with the in situ generated catalytic system.

Some selected examples with the two catalytic systems are presented in Schemes 28 and 29 [20, 21].

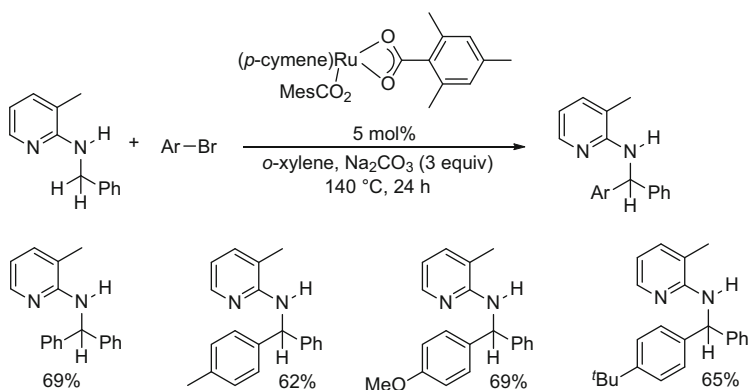
With the system generated from the ruthenium dimer, a ketimine was detected as by-product resulting from either dehydrogenation of the formed product or arylation of the sp²C–H bond obtained by dehydrogenation of the substrate (Scheme 28). This imine was formed in variable amounts depending on the nature of the additive incorporated in the Ru(II) catalytic system and the starting aryl halide. In the case of well-defined catalysts, Ru(O₂CMes)₂(*p*-cymene) was more active than Ru(O₂C^{*t*}Bu)₂(*p*-cymene), and Na₂CO₃ led to better results than K₂CO₃, KOAc and K₃PO₄ as a base in *o*-xylene as solvent. The mechanism [18] is directly related to the concerted metalation deprotonation mechanism, which is operative in sp²C–H bond activation with ruthenium(II) carboxylate catalytic systems (Scheme 30).

3.1.2 Directed Arylation of sp³C–H Bond of Non Functional Cycloalkanes

A ruthenium(II)-catalysed oxidative cross-coupling of phenylpyridine substrates with cycloalkanes has been reported (Scheme 31) [22]. The proposed mechanism involves directed metalation of phenylpyridine and formation of a ruthenium alkyl species in the presence of *tert*-butyl peroxide as an oxidizing reagent. The reaction required an excess of oxidizing reagent (4 equiv. with respect to phenylpyridine) as



Scheme 28 $\text{sp}^3\text{C-H}$ bond arylation with in situ generated ruthenium(II) catalyst



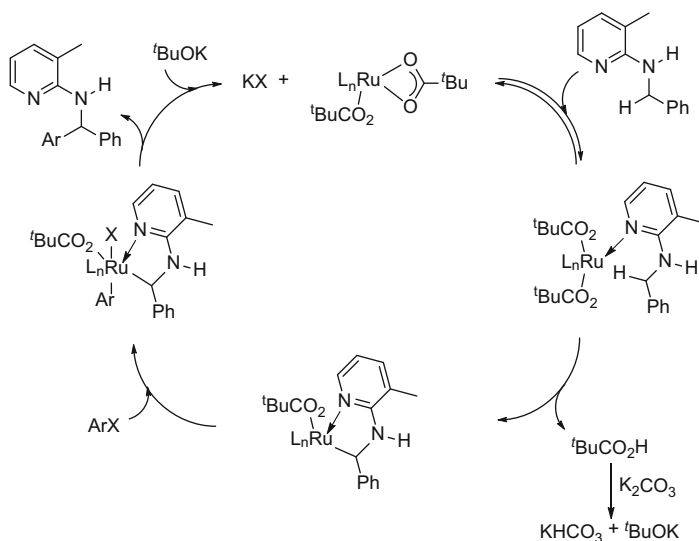
Scheme 29 $\text{sp}^3\text{C-H}$ bond arylation with arylhalides in the presence of (ruthenium)bis(carboxylate) catalyst

well as an excess of cycloalkane. Unsubstituted phenylpyridine led to almost equimolecular amounts of mono- and disubstituted phenylpyridine products, whereas selective monoalkylation was observed with *meta*-substituted phenylpyridines. Cyclohexane, cycloheptane and cyclooctane reacted similarly to regioselectively afford the mono- and disubstituted expected products [20].

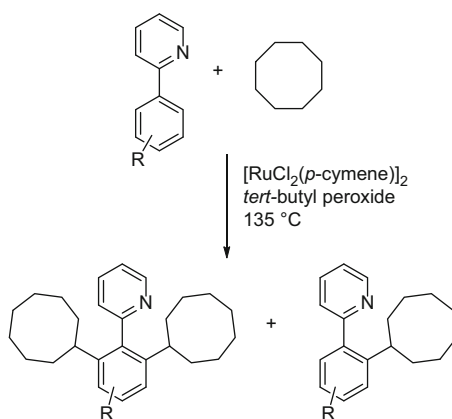
3.2 Functionalization of Non-benzylic Aliphatic Amines

3.2.1 Carbon–Carbon Bond Formation via $\text{sp}^3\text{C-H}$ Oxidative Activation at C(2) Carbon of Saturated Amines

Murahashi first showed that $\text{RuCl}_2(\text{PPh}_3)_3$ catalysed the $\text{sp}^3\text{C-H}$ bond oxidation of tertiary amine with *tert*-butyl hydroperoxide at an α -carbon of the nitrogen atom leading to a peroxide that can generate a reactive iminium salt intermediate upon



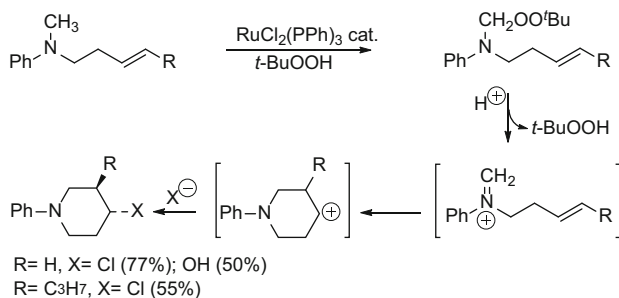
Scheme 30 Proposed mechanism for the ruthenium(II)-catalysed sp³C–H bond activation



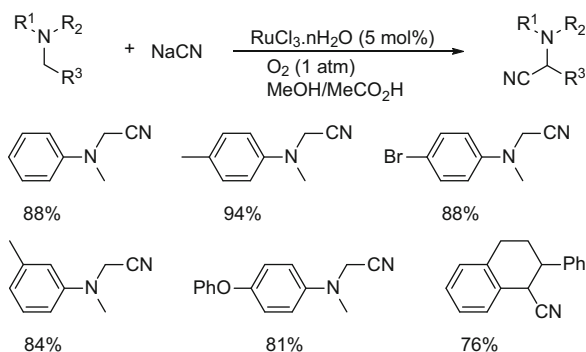
Scheme 31 Ruthenium-catalysed oxidative cross-coupling of chelating arenes with cycloalkanes

protonation. Then, cyclization resulting from intramolecular nucleophilic attack of an alkene followed by reaction with a nucleophile (halide, hydroxide) led to new cyclic amines via selective formation of a carbon–carbon bond (Scheme 32) [23].

The above oxidation protocol was adapted to the formation C_α–CN bond of tertiary amines using RuCl₃·nH₂O as the ruthenium catalyst and oxygen in the presence of acetic acid as the oxidant at 60 °C in a 3:1 methanol/acid acetic media (Scheme 33) [24]. Other ruthenium complexes were tested and RuCl₃, K₂[RuCl₅(H₂O)] and Ru₂(OAc)₄Cl were found to be excellent catalysts for the



Scheme 32 Ruthenium-catalysed formation of cyclic amines via reactive iminium intermediates



Scheme 33 Oxidative cyanation of tertiary amines with sodium cyanide with RuCl₃/oxygen

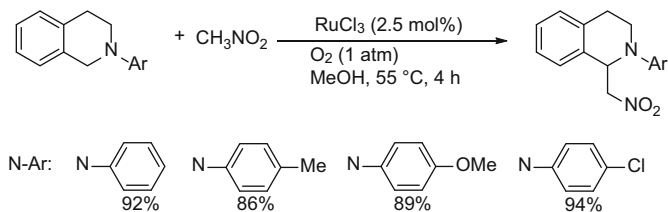
aerobic oxidative cyanation of dimethylaniline selected as model substrate [25]. It was also shown that aqueous solution of hydrogen peroxide could be used to perform this cyanation reaction [25].

This general synthesis of α -aminonitriles is explained by the iminium salt formation, via the formal hydride abstraction with the ruthenium catalyst, and addition of cyanide. The oxidant has the role of reoxidizing intermediate ruthenium species formed during the catalytic cycle. Slightly different catalytic steps have been proposed for the reaction using oxygen or hydrogen peroxide as oxidant [25, 26].

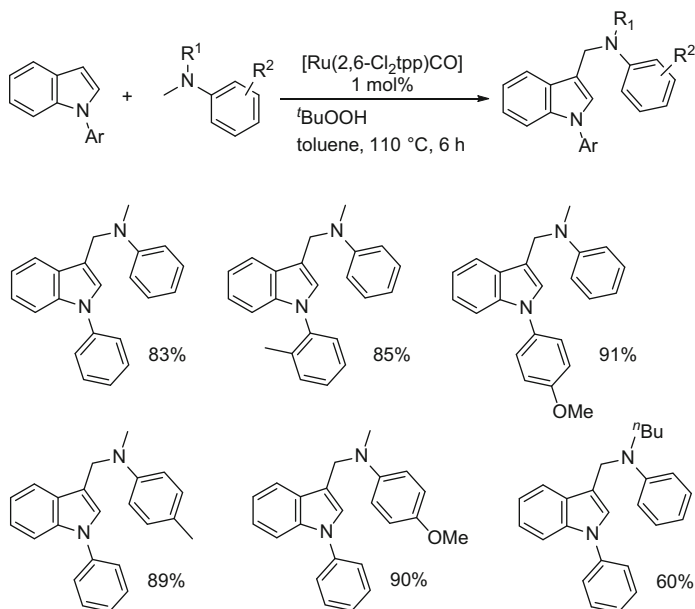
Other carbonucleophiles such as nitromethane [27] and indoles [28] have been used under similar oxidative conditions to produce sp^3 - sp^3 and sp^2 - sp^3 carbon-carbon bonds, respectively.

A selection of aromatic amines derived from tetrahydroisoquinolines is shown in Scheme 34. It is noteworthy that the products result only from sp^3 - sp^3 carbon-carbon bond formation at the benzylic position of the substrates. The reaction was also carried out with dialkyl (or cycloalkyl) anilines as tertiary amines, and nitroethane and diethyl malonate as substrates [27].

The oxidative coupling of tertiary amines with indoles has been successfully achieved with RuCl₃ and ruthenium porphyrin complexes such as [Ru(2,6-Cl₂tpp)



Scheme 34 Selected α -nitromethyl tetrahydroisoquinolines obtained via cross dehydrogenative coupling with nitromethane



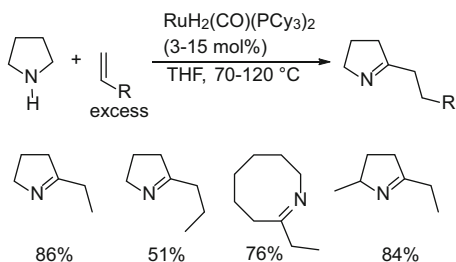
Scheme 35 Ruthenium-catalysed alkylation of indoles with tertiary methyl amines

CO] (tpp=tetraphenylporphyrinato) [28]. *tert*-Butyl hydroperoxide was used as oxidant and the reactions were carried out in toluene at 110 °C for 6 h. Excellent yields of 3-substituted indoles were obtained whatever the nature of the electronic effects of the substituents of each substrate (Scheme 35).

3.2.2 Formation of C(2)-Substituted Imines from Cyclic Secondary Amines and Alkenes

A ruthenium(II)-catalysed dehydrogenative coupling of saturated cyclic amines with an olefin has been reported using $\text{RuH}_2(\text{CO})(\text{PCy}_3)_2$ as catalyst under neutral conditions in THF at 70–120 °C (Scheme 36) [29].

Scheme 36 Coupling of pyrrolidine with olefins with ruthenium dihydride catalyst



Imines were preferentially formed and the carbon–carbon bond was selectively formed at the C(2) position of the cyclic amine. With ethylene and propene, only imines were formed but with more bulky olefins and 7-membered cyclic amines, reduction to 2-alkyl cyclic amine took place, and N-alkylation was also observed from bicyclic amine.

On the other hand, the reaction with triethoxyvinylsilane exclusively formed the N-silylated product. It has been suggested that the C-alkylation reaction proceeded via both C–H and N–H bond activation as shown in the proposed mechanism, Scheme 37.

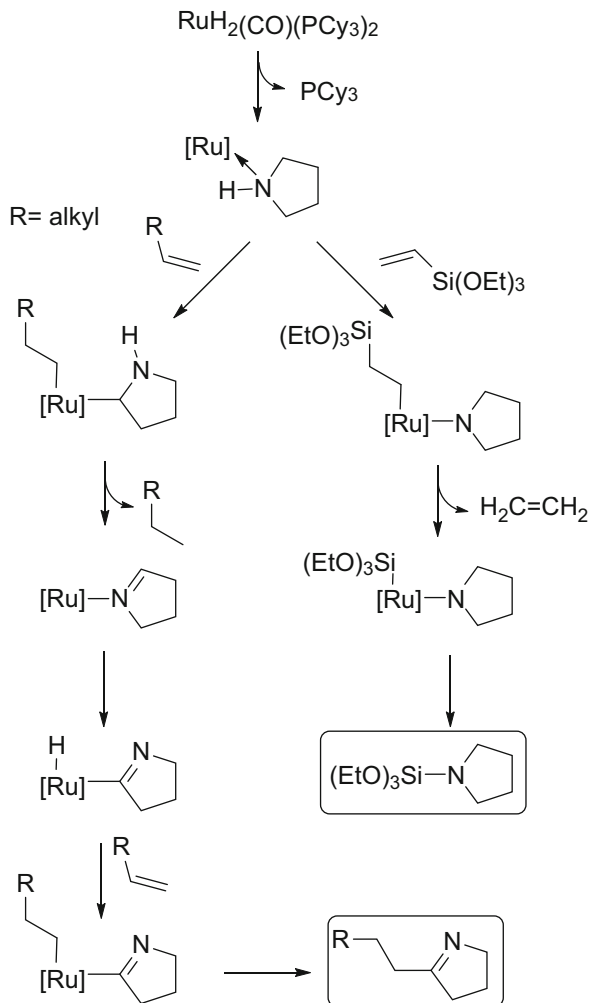
3.2.3 C(3)-Alkylation of $\text{sp}^3\text{C-H}$ Bond via Dehydrogenation of Saturated Cyclic Amines

The dehydrogenation of saturated amines to form enamines involving $\text{sp}^3\text{C-H}$ bond activation has been reported with iridium [30] and cobalt [31, 32] catalysts in the presence of a hydrogen acceptor. Using $\text{RuCl}(\text{o-tert-butylphenylphosphinobenzene-sulfonate})(\textit{p-cymene})$ as ruthenium catalyst, the dehydrogenation of *N*-protected cyclic amines leading to intermediate cyclic enamines was performed at 140°C in toluene, and further alkylation at a β -carbon of the cyclic amine in the presence of an electrophile took place. Indeed, in the presence of camphorsulfonic acid (CSA), the regioselective condensation with aldehyde provided a conjugated azadiene that was reduced under hydrogen transfer conditions [33]. Thus, the overall catalytic reaction consists in the regioselective alkylation at carbon C(3) of saturated cyclic amines (Scheme 38). This reaction requires 2 equiv. of saturated amine, but it can also be efficiently performed by addition of formic acid as an extra hydrogen donor at the end of the reaction.

The scope of the reaction is very large as it applied to saturated 5-, 6- and 7-membered cyclic amine and tetrahydroquinoline derivatives on the amine side and to a variety of functional aromatic aldehydes including heterocyclic ones and aliphatic aldehydes (Scheme 39) [33, 34]. The reaction has found useful applications in the preparation of new alkaloids consisting of cyclic amines substituted at the N and C(3) positions by terpene motives including chiral ones (Scheme 40) [35].

Starting directly from unprotected amines and alcohols, N- and C(3)-dialkylation took place. This overall transformation resulted from dehydrogenation of the alcohol via hydrogen transfer followed by a mechanism similar to the previous one involving borrowing hydrogen processes (Scheme 41) [36].

Scheme 37 Proposed mechanism for imine formation with ruthenium(II) dihydride catalyst

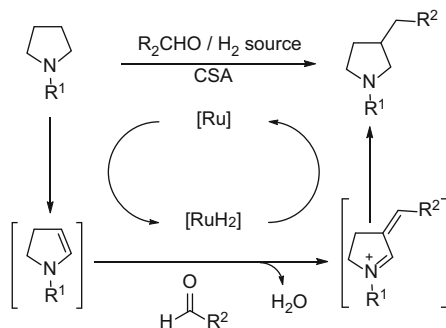


Aromatic alcohols reacted better than aliphatic ones, and this cascade transformation led to cyclic amine derivatives in good yields with identical substituents at the N and C(3) positions.

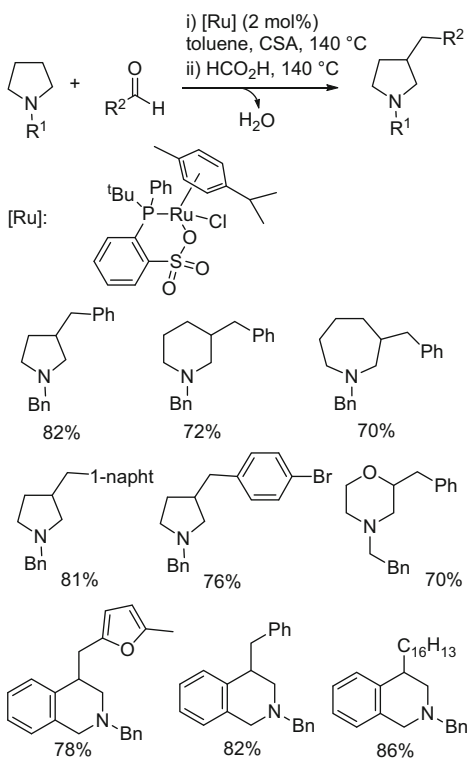
3.3 *sp*³C–*sp*³C Bond Formation Involving Alcohol α -*sp*³C–H Bond Activation and Hydrogen Borrowing

Another strategy for the functionalization of *sp*³C–H bonds of primary and secondary alcohols is based on ruthenium-catalysed hydrogen transfer reactions in tandem transformations involving a sequence of first dehydrogenation of alcohol with

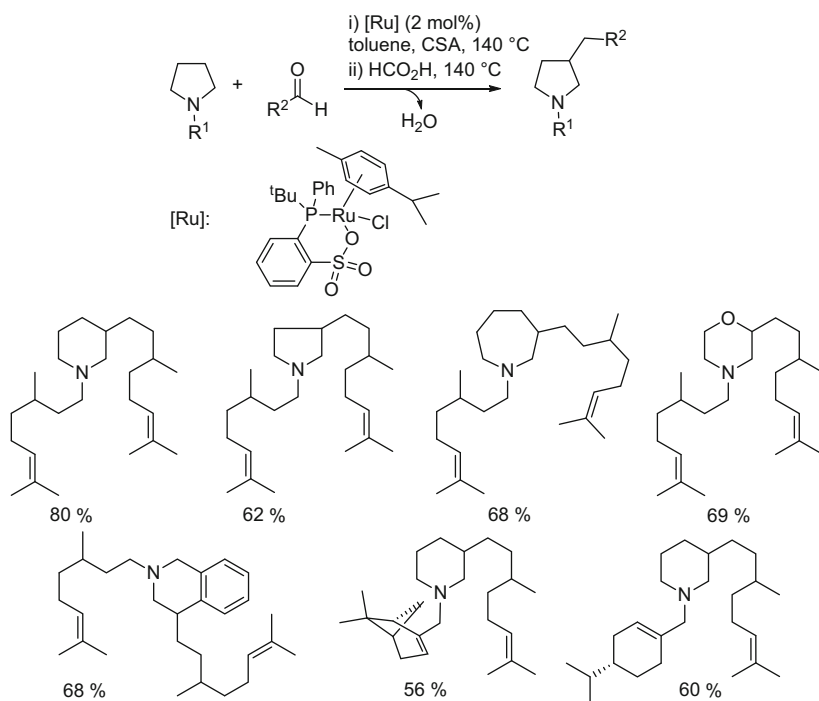
Scheme 38 Simplified catalytic cycle for C–C bond formation from cyclic amine and aldehyde



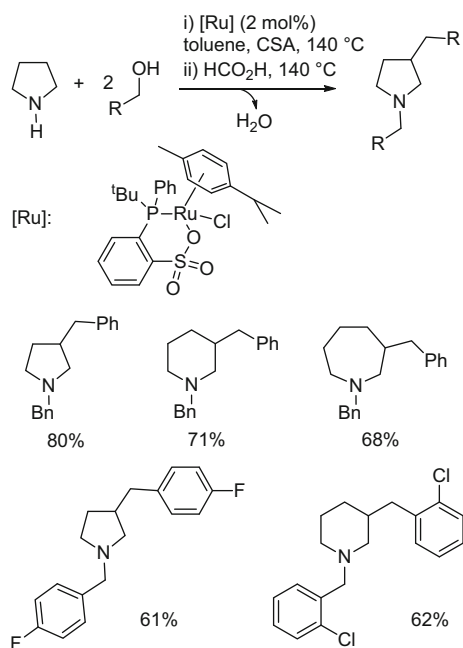
Scheme 39 Scope of the selective C(3)-alkylation of cyclic amines with aldehydes



formation of metal-hydride species, reaction with a second substrate forming unsaturated intermediates, and final reduction with the help of the initially formed ruthenium hydride. This is illustrated in Scheme 42 with reactions starting from primary alcohols [37]. This methodology is now accepted as borrowing hydrogen chemistry or hydrogen auto-transfer process and involves the formation of carbonyl compound (ketone or aldehyde) from alcohol without oxidant. In this chapter we only report on carbon–carbon bond formation reactions based on this synthetic method, which has rapidly become a powerful tool in organic synthesis.

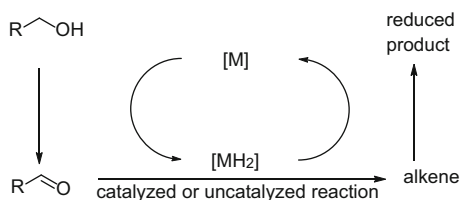


Scheme 40 Preparation of alkaloids based on alkylation with terpene derivatives

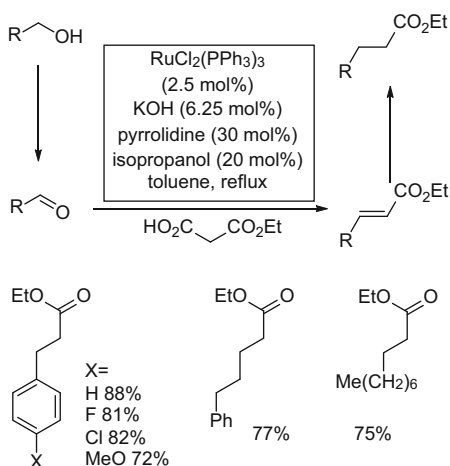


Scheme 41 N,C(3)-dialkylation of cyclic saturated amines with primary alcohols

Scheme 42 General scheme for hydrogen borrowing sequence



Scheme 43 C–C coupling from malonate derivatives



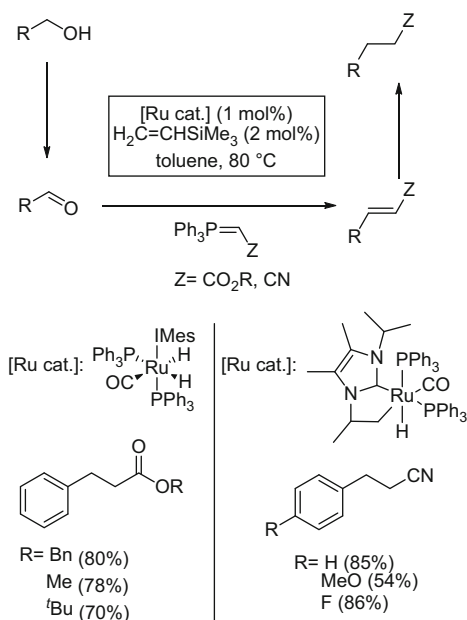
3.3.1 Reaction of Primary Alcohols with Malonate Derivatives

This strategy allowed the alkylation of malonate half esters with decarboxylation via borrowing hydrogen pathway catalysed by $\text{RuCl}_2(\text{PPh}_3)_3$ in the presence of KOH (Scheme 43) [38]. In this reaction pyrrolidine was used to catalyse the decarboxylative Knoevenagel reaction. Satisfactory results were obtained from benzylic alcohols but aliphatic alcohols required higher catalyst loading. It is noteworthy that in the presence of a hydrogen acceptor such as crotonitrile, the final reduction did not take place and alkenes were selectively formed from primary alcohols and malonic half esters and nitroalkanes [39].

The association of $\text{RuH}_2(\text{CO})(\text{PPh}_3)_3$ (0.5 mol%) with Xantphos ligand (0.5 mol%) led to the formation of the $\text{RuH}_2(\text{CO})(\text{diphosphine})(\text{PPh}_3)$ complex, which had a positive effect on the reactivity of the ruthenium catalyst for alkylation of activated methylene substrates including malonates, ketonitriles and ester nitriles [40].

3.3.2 Reaction of Primary Alcohols with Phosphorane Ester or Nitrile Ylides

Another example of hydrogen transfer from alcohols to alkenes is illustrated by the Wittig reaction operating with an aldehyde generated in situ via oxidation of a

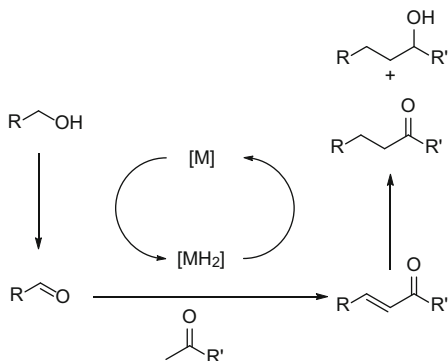
Scheme 44 C–C coupling from ylides with alcohols

primary alcohol and a phosphorane ester or nitrile ylide. $\text{RuH}_2(\text{CO})(\text{PPh}_3)_3$ was reasonably active but ruthenium(II) complexes featuring hydride and N-heterocyclic carbene ligands were more efficient for this reaction. Trimethylsilylene was used to facilitate the initial dehydrogenation of the catalyst (Scheme 44) [41, 42].

3.3.3 Reaction of Primary Alcohols with Ketones

Aldol condensation of ketones with aldehydes resulting from hydrogen transfer from primary alcohols has been efficiently carried out in the presence of various ruthenium catalysts and a base (Scheme 45). $\text{RuCl}_2(\text{PPh}_3)_3$ was efficient in the presence of 1-dodecene as hydrogen acceptor, KOH as a base and dioxane as hydrogen donor solvent and made possible the condensation of aromatic and aliphatic ketones with benzylic alcohols [43]. With this ruthenium precursor, it was shown that in the absence of 1-dodecene, reduction of the final ketone to alcohol took place in very good yields [44]. $\text{RuCl}_2(\text{DMSO})_4$ (2 mol%) was also found to be an efficient catalyst for the transformation of equimolar amounts of ketone and alcohol into ketones in the presence of KOH in dioxane at 80°C. Tuning the catalyst activity was possible by using an excess of alcohol and the presence of PPh_3 as additive (2 mol%) to favour the selective formation of the alcohols [45, 46].

Scheme 45 Aldol reactions via initial activation of primary alcohol



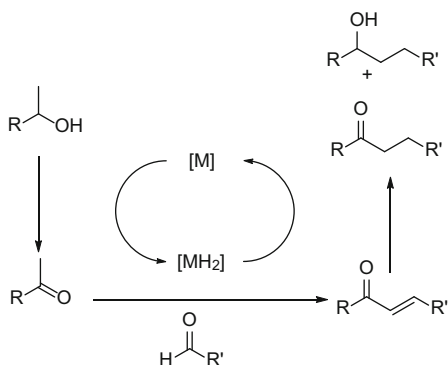
3.3.4 Reaction of Primary and Secondary Alcohols

Very recently, the reverse strategy has been successfully investigated, allowing the aldol condensation between an aldehyde and a ketone generated in situ via hydrogen transfer (Scheme 46) [47]. In the presence of 1-dodecene, $\text{RuCl}_2(\text{PPh}_3)_3$ (2 mol%) and KOH (2 mol%) in dioxane at 80°C provided a good catalytic system to produce ketones, whereas with a 3-fold excess of secondary alcohol and in the absence of 1-dodecene as hydrogen acceptor, the formation of alcohols was highly favoured.

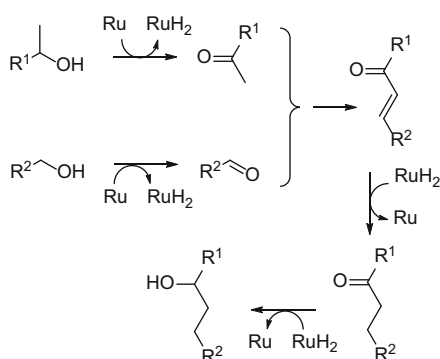
The use of the borrowing hydrogen methodology has then been applied directly starting from one primary and one secondary alcohol with the objective of generating aldehyde and ketone upon catalytic oxidation via hydrogen transfer (Scheme 47). The aldol reaction can take place in situ and the subsequent reduction of the carbon-carbon double bond and eventually the ketone with the help of the ruthenium hydrides intermediates is possible. $\text{RuCl}_2(\text{PPh}_3)_3$ and KOH with 1-dodecene as sacrificial hydrogen acceptor catalysed the selective formation of alcohols in dioxane at 80°C in the presence of an excess of primary alcohol. The reaction was more efficient starting from aromatic secondary alcohols [48]. In the presence of KOH, other ruthenium(II) precatalysts such as $\text{RuCl}_2(\text{DMSO})_4$ [49], $\text{RuCl}_2(\text{NHC})(\text{arene})$ [50, 51], $[\text{RuCl}_2(p\text{-cymene})]_2$ and even the metathesis catalyst $\text{RuCl}_2(=\text{CHPh})(\text{PCy}_3)_2$ [52] were efficient to perform the cascade reaction leading to alcohols as major products. The deshydrogenative self-coupling of secondary alcohols to selectively form ketones has been achieved in the presence of a $\text{RuCl}_2(\text{NHC})(\text{arene})$ (2 mol%), $\text{PCy}_3 \cdot \text{HBF}_4$ (2 mol%), and KOH (106 mol%) in toluene at 110°C [53].

Another type of C-C coupling reaction between tertiary and primary alcohols has been carried out with $\text{RuCl}_2(\text{PPh}_3)_3$ as ruthenium catalyst and $\text{BF}_3 \cdot \text{OEt}_2$ as Lewis acid promoter (Scheme 48) [54]. Secondary alcohols were formed in very good yields, especially when the quaternary centre of the tertiary alcohol was connected to two aromatic groups. In many cases almost perfect diastereoselectivity in favour of the *syn*-stereoisomer was obtained. The proposed mechanism is based on dehydration of the tertiary alcohol and formation of a carbon-centred

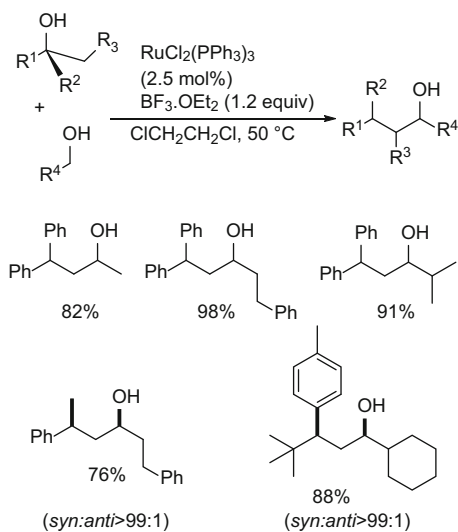
Scheme 46 Aldol reactions via initial activation of secondary alcohol

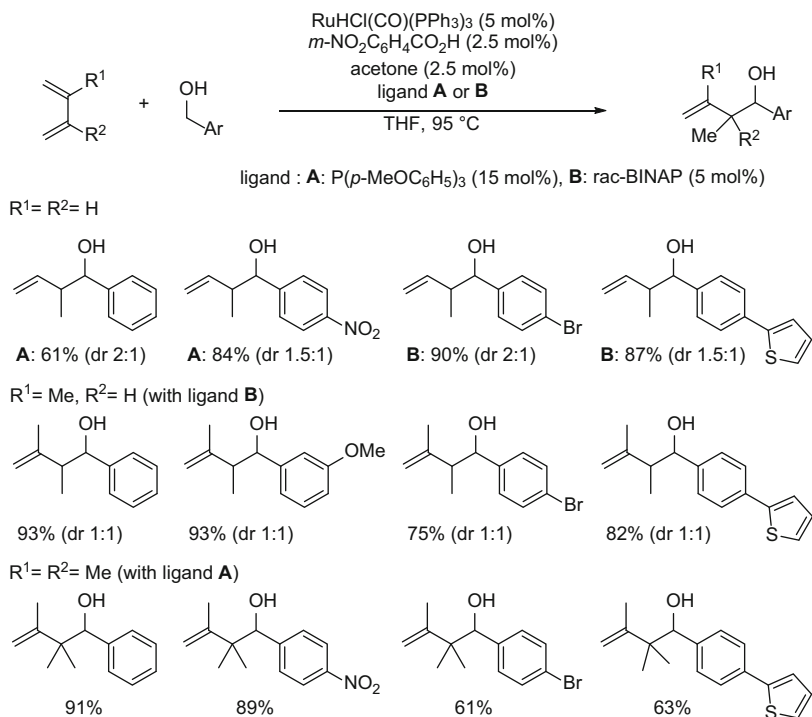


Scheme 47 Alkylation of secondary alcohols with primary alcohols via hydrogen transfer reactions



Scheme 48 Ruthenium/Lewis acid-catalysed C–C coupling of aliphatic alcohols



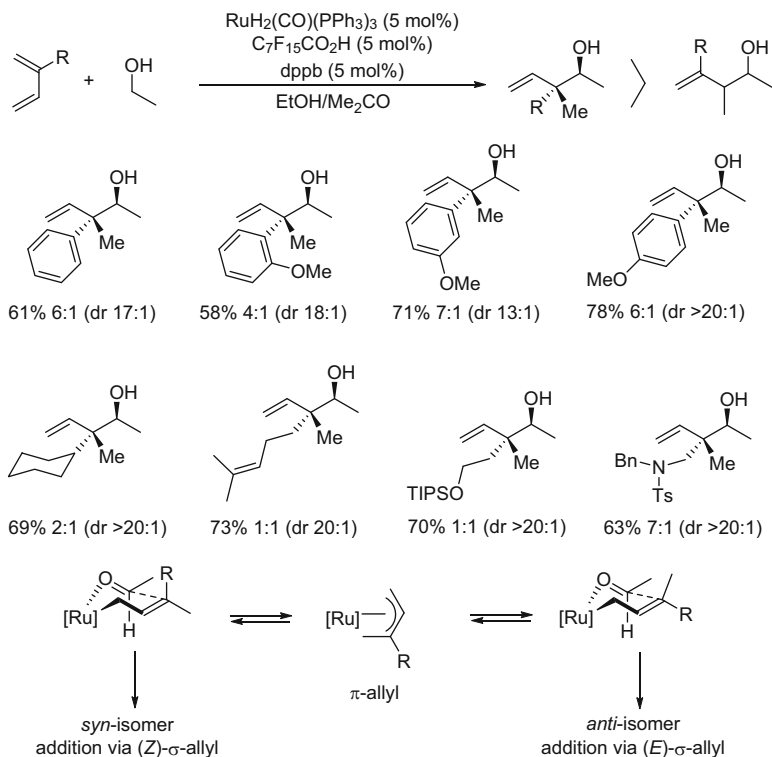


Scheme 49 Coupling of acyclic 1,3-dienes with primary aromatic alcohols

radical from the primary alcohol assisted by both the ruthenium species and the Lewis acid. Then, this radical adds to the carbon–carbon double bond and abstracts a hydrogen atom from a [Ru–H] radical to give the final alcohol.

3.3.5 Reaction of Primary Alcohols with Dienes

In 2008, Krische reported an unprecedented C–C bond coupling under ruthenium-catalysed transfer hydrogenation conditions. Conjugated 1,3-dienes, namely 1,3-butadiene, isoprene and 2,3-dimethylbutadiene reacted with benzylic alcohols in the presence of catalytic amounts of $\text{RuHCl}(\text{CO})(\text{PPh}_3)_3$ as catalyst precursor, *m*-nitrobenzoic acid and acetone at 95 °C in THF to give homoallylic alcohols in high yields (Scheme 49) [55]. Aliphatic alcohols and more efficiently allylic alcohols also coupled with butadienes under these conditions. The key step of the catalytic cycle is the insertion of a double bond into a ruthenium hydride bond arising from alcohol oxidation via hydrogen transfer. Then the in situ formed aldehyde adds to the allyl metal species to form the carbon–carbon bond. It can be noted that the same reaction was carried out starting from aldehyde but in this case required the presence of isopropanol or formic acid as hydrogen donor [55].

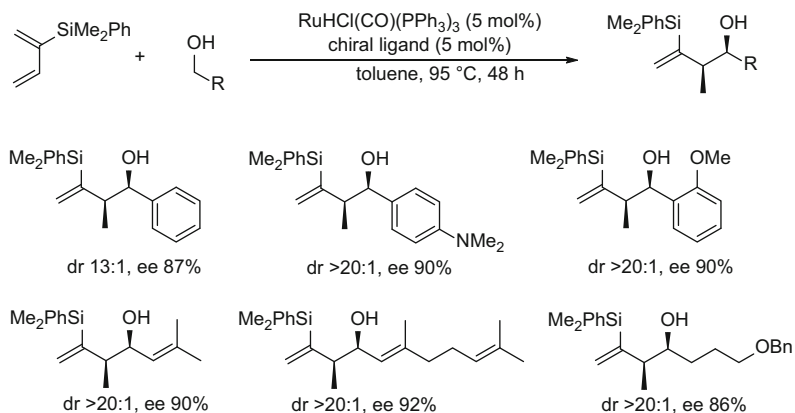


Scheme 50 Coupling of acyclic conjugated dienes with ethanol

When 2-substituted conjugated dienes were involved in this reaction with ethanol in the presence of 5 mol% of $\text{RuH}(\text{O}_2\text{CC}_7\text{F}_{15})(\text{CO})(\text{dppb})(\text{PPh}_3)$ generated in situ from $\text{RuH}_2(\text{CO})(\text{PPh}_3)_3$, $\text{C}_7\text{F}_{15}\text{CO}_2\text{H}$, and diphenylphosphinobutane (dppb) at 80–100°C in EtOH/Me₂CO as solvent, diastereoselective formation of homoallylic alcohols with a quaternary centre took place [56]. In most cases, the regioselectivity of the coupling was also high. The formation of *anti*-isomers was assumed to result from favoured addition of the aldehyde from the (E)- σ -allyl species involving *pseudo*-equatorial placement of the R group in the chairlike transition structure (Scheme 50).

A *syn*-diastereo- and enantioselective version of this reaction has been developed from 2-silylbutadienes and a variety of primary alcohols. $\text{RuHCl}(\text{CO})(\text{PPh}_3)_3$ associated with the optically pure (R)-SEGPHOS or (R)-DM-SEGPHOS (Scheme 51) provided *syn/anti* ratios higher than 20:1 and enantioselectivities in the 86–92% range [57].

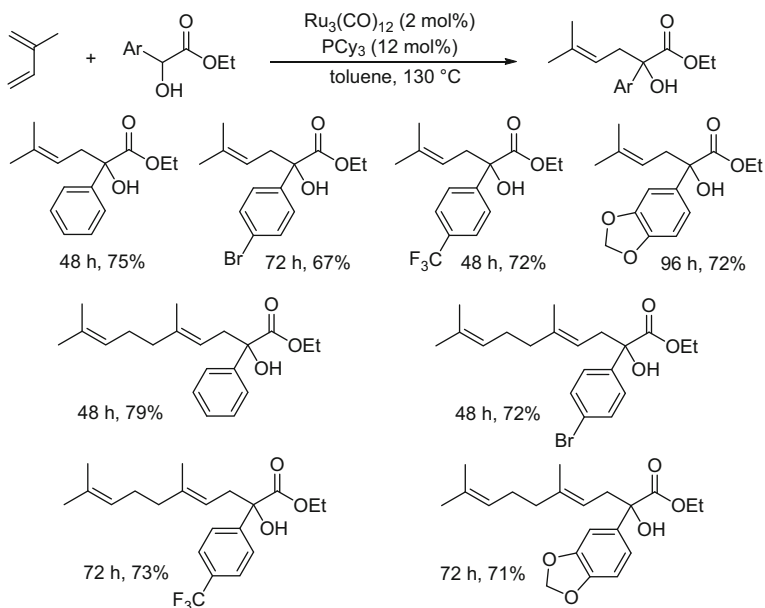
Transfer hydrogenation from secondary alcohols leads to the formation of ketones, which are less reactive than aldehydes with unsaturated reactants. However, due to the presence of a vicinal ester group, α -ketoesters are reactive with dienes. It was recently shown that the $\text{Ru}_3(\text{CO})_{12}/\text{PCy}_3$ system catalysed the



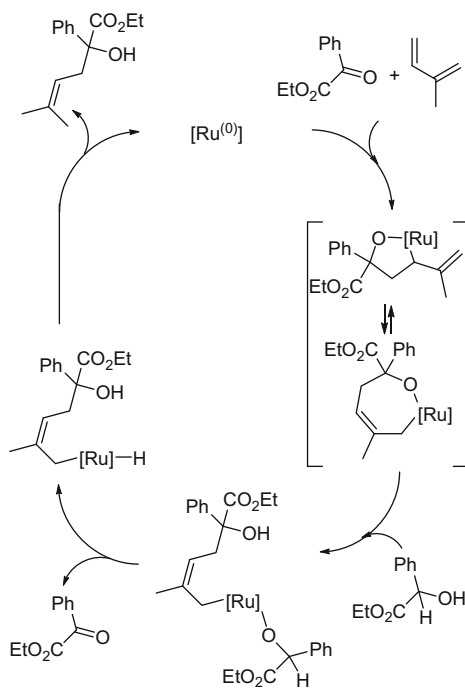
Scheme 51 Diastereoselective ruthenium-catalysed hydrohydroxylation of 2-silylbutadienes

unique regioselective formation of carbon–carbon bond from α -hydroxyesters and conjugated dienes such as isoprene and myrcene leading to prenylation and geranylation of the secondary carbinol C–H bond, respectively. These reactions required an excess of diene and long reaction times but led to the stereoselective formation of *E* isomers in the case of myrcene [58]. In contrast with the reaction from primary alcohols, which resulted in hydroxyalkylation of dienes involving formation of an allylic intermediate (Scheme 52), the mechanism of this reaction is likely based on oxidative coupling of the carbonyl ketone group in situ generated via hydrogen transfer from the alcohol function and the less substituted diene double bond to form an oxaruthenacycle (Scheme 53). The formation of the (*Z*)-stereoisomer ((*Z*)-but-2-en-1-yl substituent) from unsubstituted butadiene supports an oxidative coupling mechanism.

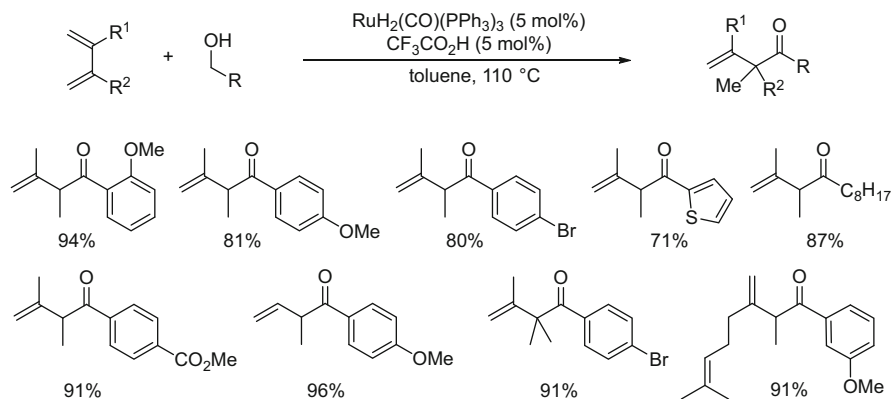
Ketones were observed as side products of this reaction. They likely resulted from β -hydride elimination from the intermediate alkoxyruthenium species, which was favoured from coordinatively unsaturated ruthenium species. Thus, β,γ -unsaturated ketones were formed when $\text{RuHCl(CO)(PPh}_3)_3$ was used in the absence of added phosphine. In the same direction, replacement of the chloride by a more labile carboxylate ligand favoured the formation of ketone. A catalytic system consisting of $\text{RuH}_2(\text{CO})(\text{PPh}_3)_3$ in the presence of trifluoroacetic acid proved to be very efficient for the formation of unsaturated ketones from dienes and alcohols involving hydrogenation transfer as the initial step (Scheme 54) [59]. A mechanism closely related to that of Scheme 53 has been proposed. Ruthenium hydride formed upon dehydrogenation of alcohol hydrometalates the less substituted double bond of the diene to form an σ -allyl ruthenium intermediate. Addition of the carbonyl group of the aldehyde generated in the first step provides an alkoxyruthenium species, which after β -hydride elimination leads to the β,γ -enone corresponding to a diene hydroacylation reaction (Scheme 55).



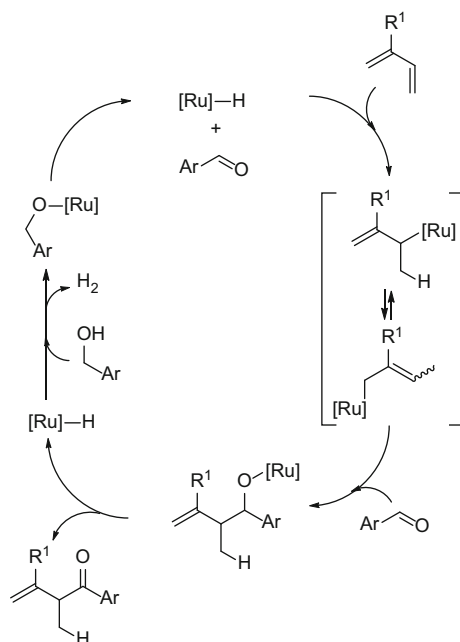
Scheme 52 Prenylation and geranylation via coupling of isoprene and myrcene with α -hydroxyesters



Scheme 53 Plausible mechanism for prenylation of ethyl mandelate



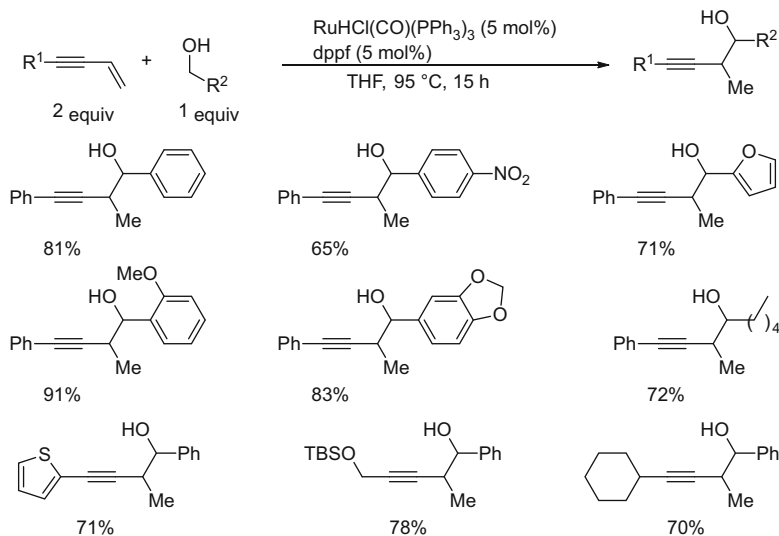
Scheme 54 Diene hydroacylation via ruthenium-catalysed C–C bond forming transfer hydrogenation



Scheme 55 Proposed catalytic cycle for ruthenium-catalysed diene hydroacylation

3.3.6 Reaction of Primary Alcohols with Enynes, Alkynes and Allenes

The formation of carbon–carbon bond leading to homopropargylic alcohols is possible from conjugated enynes and primary alcohols following the same type of



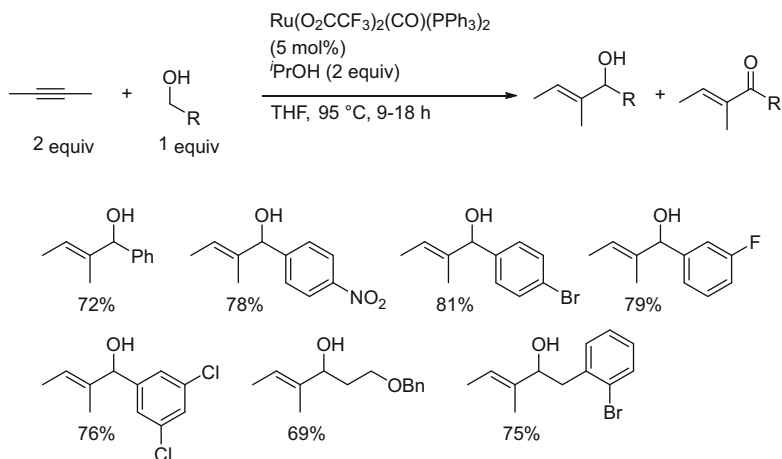
Scheme 56 Coupling of enynes and primary alcohols involving hydrogen transfer

mechanism in the presence of catalytic amounts of $\text{RuHCl(CO)(PPh}_3)_3$ associated with the 1,1'-bis(diphenylphosphino)ferrocene (dpfp) ligand (Scheme 56) [60].

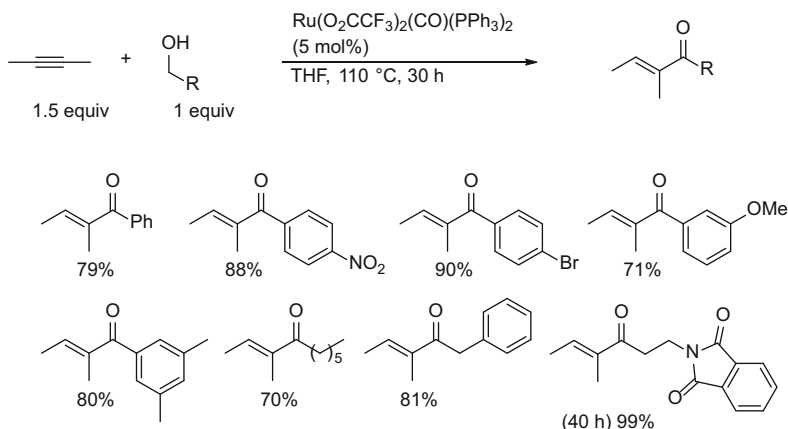
The homopropargylic alcohols, which are resistant to over-oxidation, are also obtained under similar conditions from aldehydes in the presence of isopropanol as hydrogen donor.

The C–C coupling took place regioselectively at the olefinic group in the presence of $\text{RuHCl(CO)(PPh}_3)_3/\text{dpfp}$, but in the presence of $\text{Ru(O}_2\text{CCF}_3)_2(\text{CO})(\text{PPh}_3)_2$ as catalyst the reaction was less productive leading to homopropargylic alcohol and 2-vinylallylic alcohol in equal amounts (11%) suggesting that nonconjugated alkynes could be used as substrates in direct vinylation reactions in the presence of this ruthenium catalyst [61]. Indeed, the reaction was feasible from 2-butyne and primary alcohols to give 1-substituted 2-methylbut-2-enols in high yields with only small amounts of conjugated enones as side products (less than 10%). Optimized reactions were performed using 5 mol% of $\text{Ru(O}_2\text{CCF}_3)_2(\text{CO})(\text{PPh}_3)_2$ at 95 °C in THF in the presence of 2 equiv. of isopropanol (Scheme 57) [61].

It was then shown that starting from primary alcohol, in the absence of isopropanol and at higher temperature (110 °C) for longer reaction times (30 h), the formation of conjugated enones was favoured with the same catalyst (Scheme 58) [62]. This reaction tolerated various functional groups and was not highly sensitive to electronic properties of the aromatic substituents of the benzylic alcohol. It could be also conducted with unsymmetrical internal alkynes with high regioselectivity.

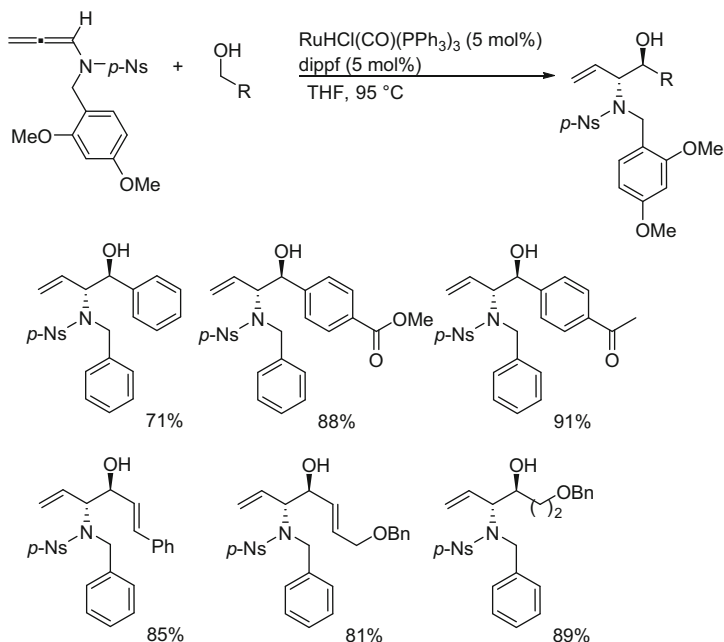


Scheme 57 Reductive coupling of alkynes and primary alcohols in the presence of a hydrogen donor



Scheme 58 Hydroacylation of 2-butyne from primary alcohols

Finally, allene derivatives were also convenient unsaturated substrates allowing carbon–carbon bond formation from benzylic alcohol via hydrogen transfer processes. With these substrates, the best catalytic systems were based on $\text{RuHCl}(\text{CO})(\text{PPh}_3)_3$ in the presence of an equimolar amount of phosphine ligand such as bis(diisopropylphosphino)ferrocene (dippf) [63], bis(dicyclohexylphosphino)ferrocene or PCyPh_2 [64]. Some examples of selective formation of homoallylic alcohols using this reaction are reported in Scheme 59.



Scheme 59 Coupling of allenamides with primary alcohols

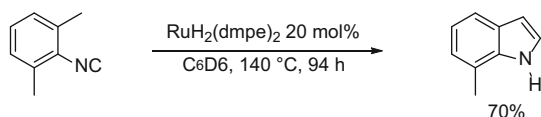
3.4 Miscellaneous Reactions Involving Carbon–Carbon Bond Formation via sp³C–H Bond Activation

3.4.1 sp³C–H Bond Insertion into an Isocyanide Bond: Synthesis of Indoles

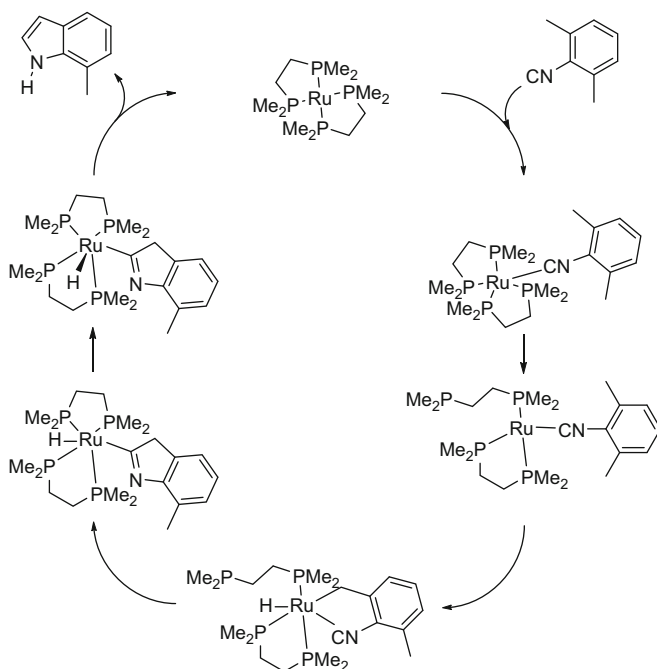
The synthesis of indoles from 2,6-xylylisocyanides involving sp³C–H bond activation has been reported as early as 1986. The catalyst precursor was the ruthenium (II) complex $\text{RuH}_2(\text{dmpe})_2$ (dmpe=1,2-dimethylphosphinoethane) and the reaction was performed at 140 °C in a sealed tube in the presence of 20 mol% of the catalyst (Scheme 60) [63]. The catalytic reaction could also be carried out in the presence of $\text{RuH}(\text{2-naphthyl})(\text{dmpe})_2$ but required the presence of hydrogen to complete the catalytic cycle, which is proposed in Scheme 61 [65, 66]. The catalytic preparation of indoles was only possible starting from 2,6-disubstituted isocyanides (2,6-dimethyl, 2-ethyl-6-methyl, 2,6-diethyl), whereas less substituted isocyanides only led to stoichiometric formation of indole ruthenium species [66].

3.4.2 Photocatalytic sp³C–H Bond Activation

This topic is detailed in the chapter “Visible-light-induced Redox Reactions by Ruthenium Photoredox Catalyst” by Akita and Koike.



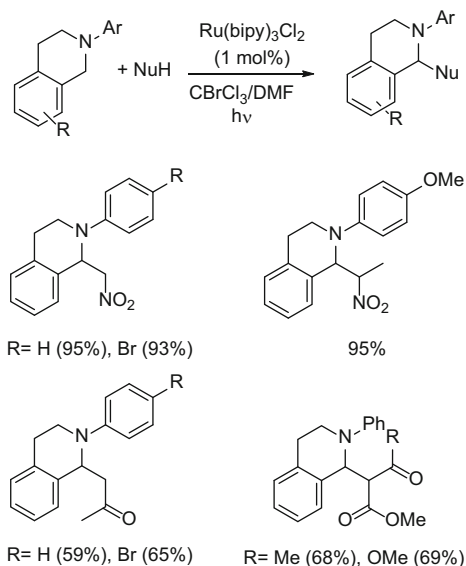
Scheme 60 Ruthenium(II)-catalysed synthesis of 7-methylindole via $\text{sp}^3\text{C-H}$ activation



Scheme 61 Proposed catalytic cycle for indole synthesis from isocyanide

Indeed, photoredox catalysis with Ru polypyridine complexes has emerged as a powerful tool for redox reactions including formation of carbon–carbon bonds based on oxidation of $\text{sp}^3\text{C-H}$ bonds via single-electron-transfer (SET) processes. Results that are closely related to those shown in Schemes 33, 34, and 35, where the carbon–carbon bond formation resulted from the benzylic $\text{sp}^3\text{C-H}$ oxidative activation in the presence of $t\text{BuOOH}$, have been recently reported for the regioselective functionalization of tetrahydroisoquinolines with cyanide and a variety of nucleophiles arising from ketones, nitroalkanes, allyltrimethylsilane, silyl enol ethers, 1,3-dicarbonyl compounds under photocatalytic conditions [67–70] as illustrated in Scheme 62 [67]. Other applications of $\text{Ru}(\text{bipy})_3\text{Cl}_2$ in photocatalytic cyclization reactions involving carbon–carbon bond formation have appeared [71, 72].

Scheme 62 Regioselective functionalization of tetrahydroisoquinolines using photoredox catalysis

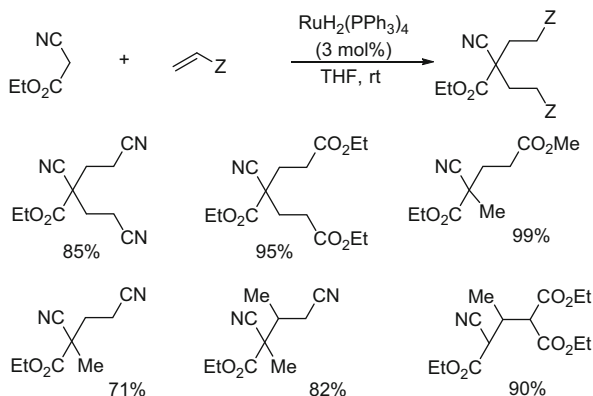


3.4.3 sp³C–H Activation from Stabilized Carbonucleophiles

It was initially shown that active methylene compounds having a nitrile group reacted with electron-deficient olefins to give an efficient Michael addition reaction in the presence of $\text{RuH}_2(\text{PPh}_3)_4$ as catalyst (Scheme 63) [73, 74]. It was assumed that the sp³C–H bond activation resulted from coordination of the nitrile leading to a hydrido(enolato)ruthenium species, which reacted with the electron deficient olefin [74]. It is noteworthy that the same catalyst made the Michael addition of 2-cyanopropionate to the electron poor triple bond of methyl propiolate [74, 75].

$\text{RuH}_2(\text{PPh}_3)_4$ showed no catalytic activity for the Michael addition with purely carbonyl substrates such as 1,3-diester, 1,3-diketones and 1,3-ketoesters in THF. On the other hand, when the reactions were carried out at 23°C in acetonitrile, a very efficient catalytic system was generated leading to very high yields of mono- and disubstituted malonates, Meldrum acid, 1,3-diketones, ... [76]. It was also possible to perform this Michael addition in the presence of $\text{Ru(H)Cp(PPh}_3)_2$ as catalyst [76]. The difference of reactivity of the two ruthenium complexes was attributed to the coordination mode of 1,3-dicarbonyl ligand that can lead to catalytically inactive bidentate (η^2 -O-enolato) from $\text{RuH}_2(\text{PPh}_3)_4$ or active (η^1 -O-enolato) from $\text{Ru(H)Cp(PPh}_3)_2$ [76–78]. The non-hydride binuclear ruthenium complex $[\text{Ru}(\text{O}_2\text{CH})(\text{CO})_2(\text{PPh}_3)]_2$ was also an active catalyst for the addition of ketoesters and diketones to but-1-en-3-one but required higher reaction temperature [79]. Starting from linear 1,3-diester and 1,3-cyanoester featuring two reactive hydrogen atoms at position 2 and an excess of butenone (2–3 equiv.), double Michael addition took place and formation of cyclic products resulting from intramolecular aldol condensation was observed.

Scheme 63 Selected examples of $\text{RuH}_2(\text{PPh}_3)_4$ -catalysed Michael addition of nitriles



4 Conclusion

From this literature survey, it appears that the first ruthenium-catalysed reaction involving $\text{sp}^3\text{C-H}$ bond activation was published in 1986 by Jones and Kosar [65]. Since that time various strategies have been put in action to achieve C-H bond activation/functionalization for the formation of carbon-carbon bonds. Regioselective insertions of olefin and/or carbon monoxide into $\text{sp}^3\text{C-H}$ bonds as well as arylation reactions involving ruthenium(0) precatalysts have been made possible using strongly chelating nitrogen-directing groups, mainly based on pyridine. The same method based on directing groups was also efficient for arylation of $\text{sp}^3\text{C-H}$ bonds in the presence of ruthenium(II) catalysts. However, the tools that can be applied with ruthenium(II) catalysts are more diverse as activation of $\text{sp}^3\text{C-H}$ bonds can also be achieved using selective oxidation, photooxidation, dehydrogenation and hydrogen borrowing strategies. During the last decade an increasing number of efficient applications have been discovered, not only with ruthenium catalysts, and the direct functionalization of reputed inert $\text{sp}^3\text{C-H}$ bonds represents the future of synthetic chemistry in perfect adequation with the principle of green chemistry. Further investigations on new ruthenium catalysts including complexes with pincer ligands should allow new types of $\text{sp}^3\text{C-H}$ bond activation.

References

1. Jun CH, Hwang DC, Na SJ (1998) Chem Commun 1405
2. Kakiuchi F, Kochi T, Mizushima E, Murai S (2010) J Am Chem Soc 132:17741
3. Chatani N, Asaumi T, Yorimitsu S, Ikeda T, Kakiuchi F, Murai S (2001) J Am Chem Soc 123:10935
4. Murahashi SI, Zhang D (2008) Chem Soc Rev 37:1490
5. Bergman SD, Storr TE, Prokopcova H, Aelvoet K, Diels G, Meerpoel L, Maes BUW (2012) Chem Eur J 18:10393

6. Sakakura T, Sodeyama T, Sasaki K, Wada K, Tanaka M (1990) *J Am Chem Soc* 112:7221
7. Chatani N, Asaumi T, Ikeda T, Yorimitsu S, Ishii Y, Kakiuchi F, Murai S (2000) *J Am Chem Soc* 122:12882
8. Hasegawa N, Charra V, Inoue S, Fukumoto Y, Chatani N (2011) *J Am Chem Soc* 133:8070
9. Hasegawa N, Shibata K, Charra V, Inoue S, Fukumoto Y, Chatani N (2013) *Tetrahedron* 69:4466
10. Kakiuchi F, Kan S, Igi K, Chatani N, Murai S (2003) *J Am Chem Soc* 125:1698
11. Pastine SJ, Gribkov DV, Sames D (2006) *J Am Chem Soc* 128:14220
12. Prokopcova H, Bergman SD, Aelvoet K, Smout V, Herrebout W, Van der Veken B, Meerpoel L, Maes BUW (2010) *Chem Eur J* 16:13063
13. Gribkov DV, Pastine SJ, Schnürch M, Sames D (2007) *J Am Chem Soc* 129:11750
14. Oeschiulli A, Smout V, Storr TE, Mitchell EA, Elias Z, Herrebout W, berthelot D, Meerpoel L, Maes BUW (2013) *Chem Eur J* 19:10378
15. Smout V, Peschiulli A, Verbeeck, S, Mitchell EA, Herrebout W, Bultinck P, Vande Velde CML, Berthelot D, Meerpoel L, Maes BUW (2013) *J Org Chem* 78:9803
16. Schwarz MC, Dastbaravardeh N, Kirchner K, Schnürch M, Mihovilovic MD (2013) *Monatsh Chem* 144:539
17. Dastbaravardeh N, Schnürch M, Mihovilovic MD (2012) *Org Lett* 14:1930
18. Dastbaravardeh N, Kirchner K, Schnürch M, Mihovilovic MD (2013) *J Org Chem* 78:658
19. Dastbaravardeh N, Schnürch M, Mihovilovic MD (2012) *Org Lett* 14:3792
20. Dastbaravardeh N, Schnürch M, Mihovilovic MD (2013) *Eur J Org Chem* 2878
21. Kumar NYP, Jeyachandran R, Ackermann L (2013) *J Org Chem* 78:4145
22. Deng G, Zhao L, Li CJ (2008) *Angew Chem Int Ed* 47:6278
23. Murahashi SI, Naota T, Yonemura K (1988) *J Am Chem Soc* 110:8256
24. Murahashi SI, Komiya N, Terai H, Nakae T (2003) *J Am Chem Soc* 125:15312
25. Murahashi SI, Nakae T, Terai H, Komiya N (2008) *J Am Chem Soc* 130:11005
26. Murahashi SI, Komiya N, Terai H (2005) *Angew Chem Int Ed* 44:6931
27. Yu A, Gu Z, Chen D, He W, Tan P, Xiang J (2009) *Catal Commun* 11:162
28. Wang MZ, Zhou CY, Wong MK, Che CM (2010) *Chem Eur J* 16:5723
29. Yi CS, Yun SY, Guzei IA (2004) *Organometallics* 23:5392
30. Zhang X, Fried A, Knapp S, Goldman AS (2003) *Chem Commun* 2060
31. Bolig AD, Brookhart M (2007) *J Am Chem Soc* 129:14544
32. Hung-Low F, Krogman JP, Tye JW, Bradley CA (2012) *Chem Commun* 48:368
33. Sundararaju B, Achard M, Sharma GVM, Bruneau C (2011) *J Am Chem Soc* 133:10340
34. Boudiar T, Sahli Z, Sundararaju B, Achard M, Kabouche Z, Doucet H, Bruneau C (2012) *J Org Chem* 77:3674
35. Sahli Z, Sundararaju B, Bruneau C, Achard M (2013) *Green Chem* 15:775
36. Sundararaju B, Tang Z, Achard M, Sharma GVM, Toupet L, Bruneau C (2010) *Adv Synth Catal* 352:3141
37. Nixon TD, Whittlesey MK, Williams JMJ (2009) *Dalton Trans* 753
38. Pridmore SJ, Williams JMJ (2008) *Tetrahedron Lett* 49:7413
39. Hall MI, Pridmore SJ, Williams JMJ (2008) *Adv Synth Catal* 350:1975
40. Slatford PA, Whittlesey MK, Williams JMJ (2006) *Tetrahedron Lett* 47:6787
41. Edwards MG, Jazzar RFR, Paine BM, Shermer DJ, Whittlesey MK, Williams JMJ, Edney DD (2004) *Chem Commun* 90
42. Burling S, Paine BM, Nama D, Brown VS, Mahon MF, Prior TJ, Pregosin PS, Whittlesey MK, Williams JMJ (2007) *J Am Chem Soc* 129:1987
43. Cho CS, Kim BT, Kim TJ, Shim SC (2002) *Tetrahedron Lett* 43:7987
44. Cho CS, Kim BT, Kim TJ, Shim SC (2001) *J Org Chem* 66:9020
45. Martinez R, Brand GJ, Ramon DJ, Yus M (2005) *Tetrahedron Lett* 46:3683
46. Martinez R, Ramon DJ, Yus M (2006) *Tetrahedron* 62:8988
47. Cho CS, Kim BT, Yoon NS (2011) *Appl Organomet Chem* 25:695
48. Cho CS, Kim BT, Kim TJ, Shim SC (2003) *Organometallics* 22:3608

49. Martinez R, Ramon DJ, Yus M (2006) *Tetrahedron* 62:8982
50. Viciano M, Sanau M, Peris E (2007) *Organometallics* 26:6050
51. Prades A, Viciano M, Sanau M, Peris E (2008) *Organometallics* 27:4254
52. Adair GRA, Williams MJ (2005) *Tetrahedron Lett* 46:8233
53. Makarov IS, Madsen R (2013) *J Org Chem* 78:6593
54. Zhang SY, Tu YQ, Fa CA, Jiang YJ, Shi L, Cao K, Zhang E (2008) *Chem Eur J* 14:10201
55. Shibahara F, Bower JF, Krische MJ (2008) *J Am Chem Soc* 130:6338
56. Han H, Krische MJ (2010) *Org Lett* 12:2844
57. Zbieg JR, Moran J, Krische MJ (2011) *J Am Chem Soc* 133:10582
58. Leung JC, Geary LM, Chen TY, Zbieg JR, Krische MJ (2012) *J Am Chem Soc* 134:15700
59. Shibahara F, Bower JF, Krische MJ (2008) *J Am Chem Soc* 130:14120
60. Patman RL, Williams VM, Bower JF, Krische MJ (2008) *Angew Chem Int Ed* 47:5220
61. Patman RL, Chaulagain MR, Williams VM, Krische MJ (2009) *J Am Chem Soc* 131:2066
62. Williams VM, Leung JC, Krische MJ (2009) *Tetrahedron* 65:5024
63. Zbieg JR, McInturff EL, Krische MJ (2010) *Org Lett* 12:2514
64. Zbieg JR, McInturff EL, Leung JC, Krische MJ (2011) *J Am Chem Soc* 133:1141
65. Jones WD, Kosar WP (1986) *J Am Chem Soc* 108:5640
66. Hsu GC, Kosar WP, Jones WD (1994) *Organometallics* 13:385
67. Freeman DB, Furst L, Condie AG, Stephenson CRJ (2012) *Org Lett* 14:94
68. Condie AG, Gonzales-Gomez JC, Stephenson CRJ (2010) *J Am Chem Soc* 132:1464
69. Zhao G, Yang C, Guo L, Sun H, Chen C, Xia W (2012) *Chem Commun* 48:2337
70. Rueping M, Vila C, Koenigs RM, Poschary K, Fabry DC (2011) *Chem Commun* 47:2360
71. Lu Z, Shen M, Yoon TP (2011) *J Am Chem Soc* 133:1162
72. Ju X, Li D, Li W, Yu W, Bian F (2012) *Adv Synth Catal* 354:3561
73. Naota T, Taki H, Mizuno M, Murahashi SI (1989) *J Am Chem Soc* 111:5954
74. Murahashi SI, Naota T, Taki H, Mizuno M, Takaya H, Komiya S, Mizuho Y, Oyasato N, Hiraoka M, Hirano M, Fukuoka A (1995) *J Am Chem Soc* 117:12436
75. Murahashi SI, Takaya H (2000) *Acc Chem Res* 33:225
76. Gomez-Bengoia E, Cuerva JM, Mateo C, Echavarren AM (1996) *J Am Chem Soc* 118:8553
77. Komiya S, Hirano M (2003) *Dalton Trans* 1439
78. Alvarez SG, Hasegawa S, Hirano M, Komiya S (1998) *Tetrahedron Lett* 39:5209
79. Picquet M, Bruneau C, Dixneuf PH (1999) *Tetrahedron* 55:3937

Catalytic Transformations of Alkynes via Ruthenium Vinylidene and Allenylidene Intermediates

Jesús A. Varela, Carlos González-Rodríguez, and Carlos Saá

Abstract Vinylidenes are high-energy tautomers of terminal alkynes and they can be stabilized by coordination with transition metals. The resulting metal-vinylidene species have interesting chemical properties that make their reactivity different to that of the free and metal π -coordinated alkynes: the carbon α to the metal is electrophilic whereas the β carbon is nucleophilic. Ruthenium is one of the most commonly used transition metals to stabilize vinylidenes and the resulting species can undergo a range of useful transformations. The most remarkable transformations are the regioselective anti-Markovnikov addition of different nucleophiles to catalytic ruthenium vinylidenes and the participation of the π system of catalytic ruthenium vinylidenes in pericyclic reactions. Ruthenium vinylidenes have also been employed as precatalysts in ring closing metathesis (RCM) or ring opening metathesis polymerization (ROMP).

Allenylidenes could be considered as divalent radicals derived from allenes. In a similar way to vinylidenes, allenylidenes can be stabilized by coordination with transition metals and again ruthenium is one of the most widely used metals. Metal-allenylidene complexes can be easily obtained from terminal propargylic alcohols by dehydration of the initially formed metal-hydroxyvinylidenes, in which the reactivity of these metal complexes is based on the electrophilic nature of $C\alpha$ and $C\gamma$, while $C\beta$ is nucleophilic. Catalytic processes based on nucleophilic additions and pericyclic reactions involving the π system of ruthenium allenylidenes afford interesting new structures with high selectivity and atom economy.

Keywords Ruthenium allenylidenes · Ruthenium catalysis · Ruthenium vinylidenes

J.A. Varela, C. González-Rodríguez, and C. Saá (✉)
Departamento de Química Orgánica y Centro Singular de Investigación en Química Biológica y Materiales Moleculares (CIQUS), Universidad de Santiago de Compostela, 15782 Santiago de Compostela, Spain
e-mail: carlos.saa@usc.es

Contents

1	Introduction	240
2	Nucleophilic Addition to Catalytic Ruthenium Vinylidenes	242
2.1	<i>O</i> - and <i>S</i> -Nucleophiles	242
2.2	<i>N</i> - and <i>P</i> -Nucleophiles	250
2.3	C-Nucleophiles	255
2.4	B-Nucleophiles	258
3	Intramolecular Cyclizations	259
4	Pericyclic Reactions	263
4.1	Electrocyclizations	263
4.2	Cycloadditions	264
4.3	[1,5] Sigmatropic Rearrangements	268
5	Vinylideneruthenium Catalysts in Metathesis	269
6	Ruthenium Allenylidenes in Catalysis	272
6.1	Nucleophilic Addition to Allenylidenes $C\gamma$	272
6.2	Nucleophilic Addition to Allenylidenes $C\alpha$	275
6.3	Pericyclic Reactions with Ruthenium Allenylidenes	276
6.4	Allenylideneruthenium Catalysts in Metathesis	280
7	Conclusion	282
	References	282

Abbreviations

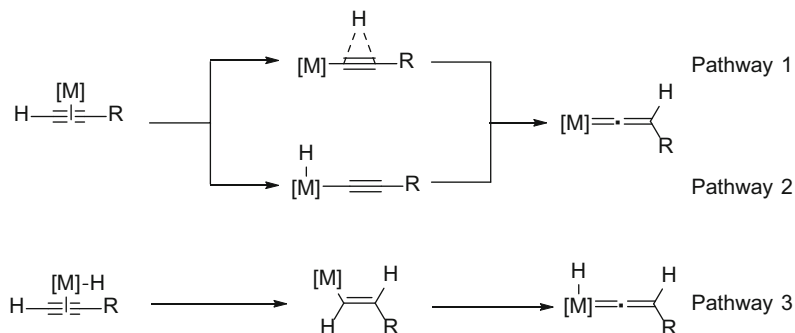
9-BBN	9-Borabicyclo[3.3.1]nonane
Ac	Acetyl
acac	Acetylacetonate
AIBN	2,2'-Azobisisobutyronitrile
anhyd	Anhydrous
Ar	Aryl
Bn	Benzyl
Boc	<i>Tert</i> -butoxycarbonyl
Bp	Boiling point
Bpy	2,2'-Bipyridyl
Bu	Butyl
Bz	Benzoyl
CAN	Ceric ammonium nitrate
cat	Catalyst
Cbz	Benzyloxycarbonyl
CIP	Cahn–Ingold–Prelog
cod	Cyclooctadiene
concd	Concentrated
cot	Cyclooctatetraene
Cp	Cyclopentadienyl
CSA	Camphorsulfonic acid
d	Day(s)

DABCO	1,4-Diazabicyclo[2.2.2]octane
DBN	1,5-Diazabicyclo[4.3.0]non-5-ene
DBU	1,8-Diazabicyclo[5.4.0]undec-7-ene
DCC	<i>N,N</i> -dicyclohexylcarbodiimide
DDQ	2,3-Dichloro-5,6-dicyano-1,4-benzoquinone
de	Diastereomeric excess (discouraged, see dr)
DEAD	Diethyl azodicarboxylate
DET	Diethyl tartrate
DIBALH	Diisobutylaluminum hydride
DIPT	Diisopropyl tartrate
DMAP	4-(Dimethylamino)pyridine
DMB	3,4-Dimethoxybenzyl
DME	1,2-Dimethoxyethane
DMF	Dimethylformamide
DMPU	1,3-Dimethyl-3,4,5,6-tetrahydro-2(1H)-pyrimidinone
DMSO	Dimethyl sulfoxide
dppe	Bis(diphenylphosphino)ethane
dppm	Bis(diphenylphosphino)methane
dr	Diastereomeric ratio
EDTA	Ethylenediaminetetraacetic acid
<i>ee</i>	Enantiomeric excess
equiv	Equivalent(s)
Et	Ethyl
Fmoc	9-Fluorenylmethoxycarbonyl
h	Hour(s)
HMPA	Hexamethylphosphoric triamide
<i>i</i> -Pr	Isopropyl
KHMDS	Potassium hexamethyldisilazide, potassium bis(trimethylsilyl)amide
L	Liter(s)
LDA	Lithium diisopropylamide
LHMDS	Lithium hexamethyldisilazide, lithium bis(trimethylsilyl)amide
LTMP	Lithium 2,2,6,6-tetramethylpiperidide
<i>m</i> -CPBA	<i>m</i> -Chloroperoxybenzoic acid
Me	Methyl
MEM	(2-Methoxyethoxy)methyl
Mes	Mesityl, 2,4,6-trimethylphenyl (not methanesulfonyl)
min	Minute(s)
mol	Mole(s)
MOM	Methoxymethyl
Ms	Methanesulfonyl (mesyl)
nbd	Norbornadiene

NBS	<i>N</i> -bromosuccinimide
NCS	<i>N</i> -chlorosuccinimide
Nu	Nucleophile
op	Optical purity (discouraged, see <i>ee</i>)
PCC	Pyridinium chlorochromate
PDC	Pyridinium dichromate
Ph	Phenyl
phth	Phthalate
PMB	4-Methoxyphenyl
PNB	4-Nitrobenzyl
PPA	Poly(phosphoric acid)
PPTS	Pyridinium <i>p</i> -toluenesulfonate
Pr	Propyl
Pv	Pivaloyl
py	Pyridine
rt	Room temperature
s	Second(s)
<i>s</i> -Bu	<i>Sec</i> -butyl
SEM	2-(Trimethylsilyl)ethoxymethyl
TBAF	Tetrabutylammonium fluoride
TBDMS	<i>Tert</i> -butyldimethylsilyl
TBDPS	<i>Tert</i> -butyldiphenylsilyl
<i>t</i> -Bu	<i>Tert</i> -butyl
TCNE	Tetracyanoethylene
Tf	Trifluoromethanesulfonyl (triflyl)
TFA	Trifluoroacetic acid
TFAA	Trifluoroacetic anhydride
thexyl	1,1,2-Trimethylpropyl
THF	Tetrahydrofuran
THP	Tetrahydropyran-2-yl
TIPDS	1,1,3,3-Tetraisopropylidisiloxane-1,3-diyl
TIPS	Triisopropylsilyl
TMEDA	<i>N,N,N',N'</i> -tetramethyl-1,2-ethylenediamine
TMS	Trimethylsilyl
Tol	4-Methylphenyl
Tr	Triphenylmethyl (trityl)
Ts	Tosyl, 4-toluenesulfonyl

1 Introduction

Free vinylidene is a high-energy tautomer of an alkyne that can be effectively stabilized by coordination with transition metals [1–5]. Since the first formation and stabilization of vinylidenes at a transition metal center reported in 1966 [6, 7], a



Scheme 1 General pathways for the formation of metal vinylidenes from terminal alkynes

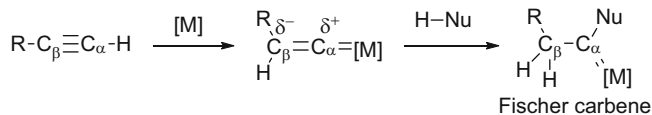
great deal of effort has been focused on both experimental and theoretical approaches to determine the mechanism for the transformation of terminal alkynes into the corresponding vinylidene complexes [8–13]. It is widely accepted that there are three general pathways through which this transformation can occur (Scheme 1) and each involves the initial formation of a complex that contains an alkyne in a η^2 -binding mode. Two alternative pathways have been proposed for concerted migration of the hydrogen atom: (1) for d^6 metal systems such as Ru(II) and Mn(I) complexes the migration proceeds by a 1,2-hydrogen shift (pathway 1, Scheme 1) [8–17]; (2) isomerization of the d^8 metal systems such as Co(I) and Rh(I) occurs by a 1,3-hydrogen shift via a hydride-alkynyl intermediate (pathway 2, Scheme 1) [8–13, 18–23]. In the specific case where the central metal bears a hydride, a new route to vinylidenes has been identified and this involves the intermediacy of a metal alkenyl ligand, which can be obtained through insertion of an alkyne into a metal hydride bond (pathway 3, Scheme 1) [8–13, 15, 24].

The conversion of internal alkynes to vinylidenes was considered an unusual process and it had only been reported for trialkylsilyl [25–40], trimethylstannane [41, 42], alkylthiol [43], and iodo [44–46] substituted alkynes. Nevertheless, it has been recently reported the migration of acyl and aryl substituents in internal alkynes, [47–54] with the following order of the migratory efficiency: $\text{CO}_2\text{Et} > p\text{-CO}_2\text{EtC}_6\text{H}_4 > p\text{-ClC}_6\text{H}_4 > \text{Ph} > p\text{-MeC}_6\text{H}_4\text{Me} > p\text{-OMeC}_6\text{H}_4$, [47–54] in which electron-withdrawing substituents on the aryl ring enhance the migratory aptitude.

The properties of vinylidene ligands are derived from the presence of an electrophilic coordinated carbon atom as well as the metal carbene character. The main processes in which metal-vinylidenes are involved that highlight their catalytic applications are:

1. Addition of nucleophiles to the electrophilic coordinated $\text{C}\alpha$.
2. Alkyl, alkenyl, or alkynyl migration from the metal center to the $\text{C}\alpha$.
3. Pericyclic reactions.

In this chapter the main applications of catalytic ruthenium vinylidenes that have been reported in the last decade are reviewed [55–65].



Scheme 2 Addition of nucleophiles to the electrophilic C α of metal vinylidenes

2 Nucleophilic Addition to Catalytic Ruthenium Vinylidenes

Due to the electrophilic nature of the C α in vinylidenes, their reactivity is dominated by the addition of nucleophiles to this position to afford Fischer-type carbenes (Scheme 2). Depending on the nature of the nucleophile and the subsequent evolution of the carbene a wide variety of compounds can be generated (aldehydes, dihydropyrans, furans, β,γ -unsaturated ketones, etc.) [55–65]. The regioselectivity of this process led to the product resulting from addition of the nucleophile to the less substituted carbon of the alkyne (anti-Markovnikov addition), which is the opposite result to that observed when the alkyne is activated by a Lewis acid (Markovnikov addition).

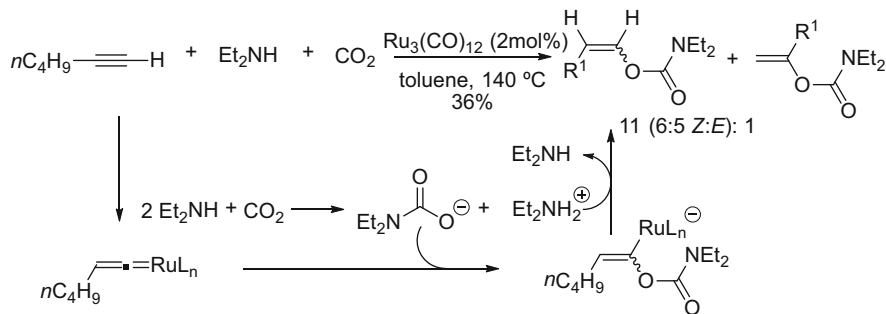
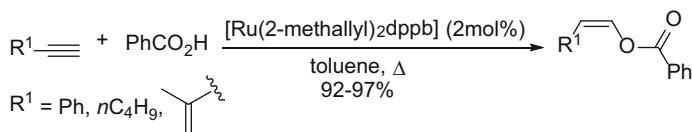
2.1 O- and S-Nucleophiles

The use of catalytic vinylidenes was first reported by Dixneuf and Sasaki for the synthesis of alkenyl carbamates by anti-Markovnikov addition of an in situ generated carbamate to alkynes (Scheme 3) [66]. Since then, several variations – including catalyst modifications – have been attempted in an effort to improve selectivities and yields [67–72].

Carboxylic acids are capable of adding to catalytic ruthenium vinylidenes to afford enol ester derivatives. The mechanism involves the formation of a ruthenium vinylidene species followed by nucleophilic attack of the benzoic acid to the electrophilic C α of the vinylidene. The [Ru(2-methallyl) $_2$ dppb] complex has proven to be a superb catalyst for this transformation (Scheme 4) [73–76].

Interestingly, modulation of the regioselectivity of the reaction from anti-Markovnikov (formation of the vinylidene) to Markovnikov (either by electrophilic activation of the alkynes or by oxidative addition of the acid to the ruthenium complex and subsequent migratory insertion and reductive elimination) was observed on using [(*p*-cymene)RuCl $_2$] $_2$ as the ruthenium catalyst and different phosphine ligands and bases (Table 1) [58, 61, 77].

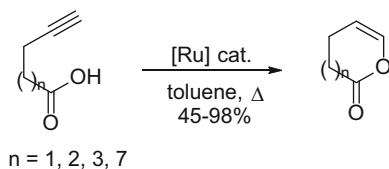
Intramolecular anti-Markovnikov addition of carboxylic acids to alkynes was also achieved using ruthenium catalysts. α,ω -Alkynoic acids afford the corresponding cycloalkene lactones by intramolecular addition of the carboxylic acid to the corresponding catalytic vinylidene species obtained by treatment of the

**Scheme 3** Synthesis of alkenyl carbamates through Ru vinylidenes**Scheme 4** Synthesis of enol esters through Ru vinylidenes**Table 1** Regioselectivity of the Ru-catalyzed addition of benzoic acids to terminal alkynes

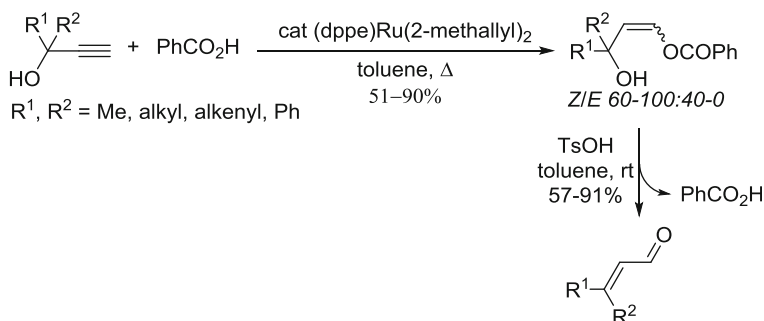
R	Cat. (mol%)	Ligand (mol%)	Base (mol%)	T (°C)	Yield (mol%)	I/II
<i>n</i> -Bu	1	P(4-Cl-C ₆ H ₄) ₃ (3)	DMAP (4)	60	89	50:1
<i>n</i> -Bu	0.4	P(furyl) ₃ (0.8)	Na ₂ CO ₃ (1.6)	50	93	1:30
Ph	1	P(4-Cl-C ₆ H ₄) ₃ (3)	DMAP (4)	60	99	50:1
Ph	0.4	P(furyl) ₃ (0.8)	Na ₂ CO ₃ (1.6)	70	88	1:1.5
<i>t</i> -Bu	1	P(4-Cl-C ₆ H ₄) ₃ (3)	DMAP (4)	80	68	50:1
<i>t</i> -Bu	0.4	P(furyl) ₃ (0.8)	Na ₂ CO ₃ (1.6)	50	88	1:10

alkyne with the complex [TpRu[C(Ph)=C(Ph)C≡CPh]PMe(*i*-Pr)₂] [78] or [RuCl_x(*p*-cymene)(triazol-5-ylidene)] (Scheme 5) [79].

The enol esters obtained in this transformation can be further modified bearing in mind that they are protected aldehydes. Treatment of propargyl alcohols with benzoic acid in the presence of complex (dppe)Ru(2-methallyl)₂ as catalyst affords the enol esters derived from the anti-Markovnikov addition of the acid to the alkyne (Scheme 6). Subsequent acid treatment gives rise to the conjugated enal, which is an isomer of the starting propargylic alcohol [80, 81].



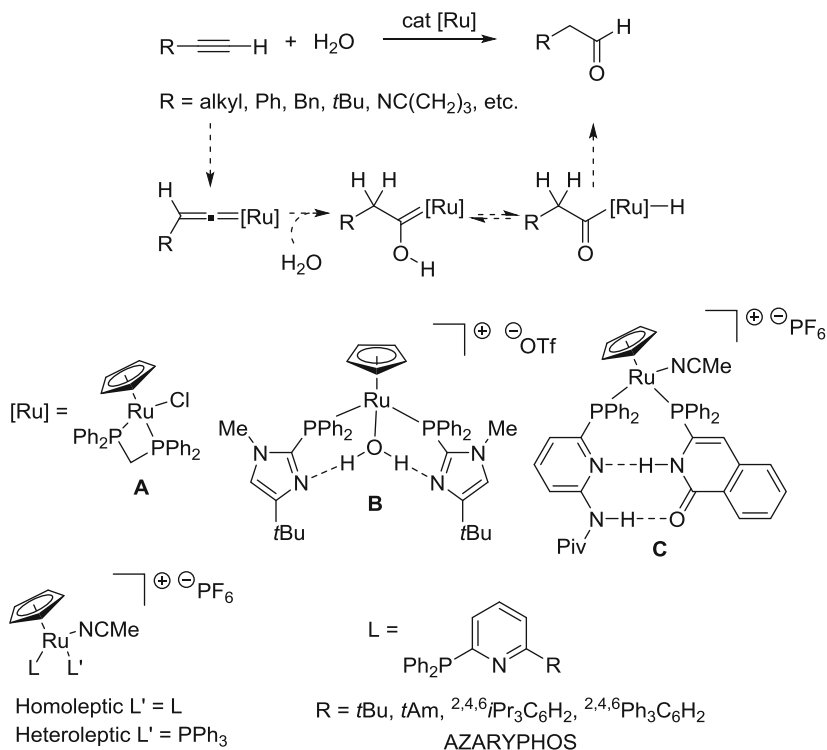
Scheme 5 Synthesis of lactones from α,ω -alkynoic acids



Scheme 6 Synthesis of conjugated enals from enol esters

The use of water as the nucleophile in the presence of a catalytic ruthenium vinylidene directly affords the aldehyde derived from the anti-Markovnikov hydration of a terminal alkyne. The first example of this reaction was reported by the group of Wakatsuki, who used $[\text{RuCl}_2(\text{C}_6\text{H}_6)]_2$ or $\text{RuCl}_2(\text{C}_6\text{H}_6)(\text{phosphine})$ with additional specific phosphine ligands $\text{PPh}_2(\text{C}_6\text{F}_5)$ or $\text{P}(3\text{-C}_6\text{H}_4\text{SO}_3\text{Na})_3$ [82]. The same research group reported that cyclopentadienylruthenium complexes of type **A** (Scheme 7) bearing bidentate phosphine ligands show much higher activity and complete selectivity to the anti-Markovnikov hydration product [15, 83]. Grotjahn and coworkers reported that other ruthenium catalysts obtained by changing the phosphine ligand for imidazolylphosphanes (type **B**, Scheme 7) [84] showed even better selectivities under milder conditions, i.e., room temperature and with lower catalytic loadings. On the other hand, Breit and coworkers showed that ruthenium catalysts bearing bidentate ligands, generated by the self-assembly of monodentate ligands through complementary hydrogen bonding of aminopyridine/isoquinoline systems, also lead to highly regioselective anti-Markovnikov hydration of terminal alkynes (type **C**, Scheme 7) [85].

Another family of phosphane ligands that contain a phosphine unit and sterically shielded nitrogen lone pairs in the ligand periphery are the so-called AZARYPHOS (aza-aryl-phosphane, L) ligands. The incorporation of these ligands into homoleptic ruthenium complexes $[\text{RuCp}(\text{L})_2(\text{MeCN})][\text{PF}_6]$, either preformed [86] or generated in situ [87], provides catalysts for the anti-Markovnikov hydration of terminal



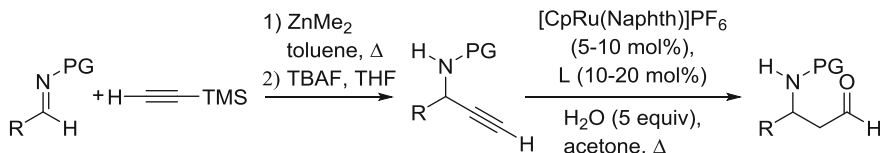
Scheme 7 Anti-Markovnikov hydration of terminal alkynes through Ru vinylidenes

alkynes with the highest known activities [88]. Recently, heteroleptic ruthenium complexes $[RuCp(L)(L')(MeCN)][PF_6]$, in which L is AZARYPHOS and L' is a suitable non-functionalized placeholder phosphane ligand such as PPh₃, have shown high catalytic activity. This result implies that only one bifunctional ligand is involved in the postulated ambifunctional reaction mechanism (Scheme 7) [89].

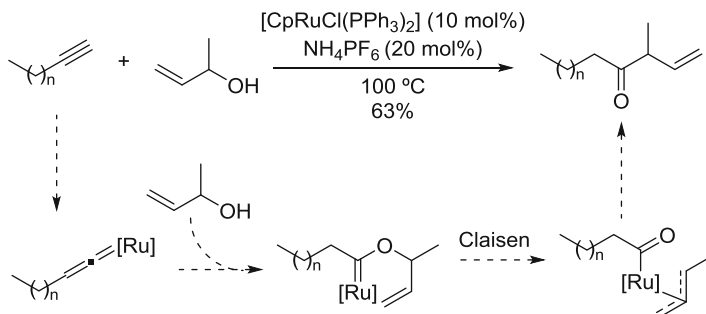
N-Protected β -amino aldehydes have been prepared from imines through a sequence that involves a Zn-mediated direct alkynylation followed by a Ru-catalyzed anti-Markovnikov alkyne hydration using a homoleptic ruthenium complex with AZARYPHOS ligands (Scheme 8) [90, 91].

Intermolecular addition of alcohols to catalytic ruthenium vinylidenes is far more difficult than the addition of water except when allylic alcohols are employed (Scheme 9) [92–96]. In this case, the reaction of an allylic alcohol with a terminal alkyne catalyzed by $CpRuCl(PPh_3)_2$ afforded a β,γ -unsaturated ketone. The initial ruthenium oxacarbene obtained by addition of the alcohol to the ruthenium vinylidene evolves through a Claisen rearrangement to a π -allyl ruthenium species. Reductive elimination then gives rise to the final unsaturated ketone.

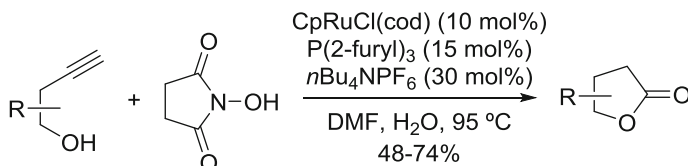
Intramolecular addition of alcohols to vinylidenes to afford oxygen-containing heterocycles has been used more widely than the intermolecular version of this reaction [97, 98]. Trost and coworkers described the cyclization of homo- and



Scheme 8 *N*-Protected β -amino aldehydes from imines and terminal alkynes



Scheme 9 β,γ -Unsaturated ketones from intermolecular addition of allylic alcohols to terminal alkynes

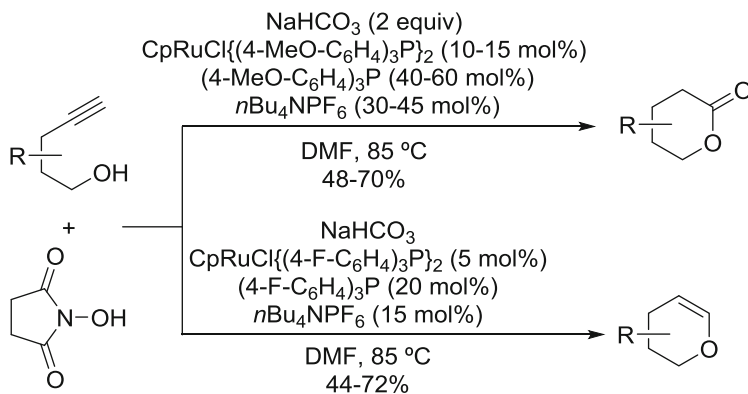


Scheme 10 γ -Butyrolactones from oxidative cyclization of homopropargyl alcohols through Ru vinylidenes

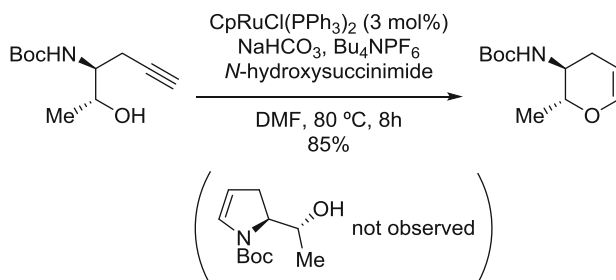
bis-homopropargyl alcohols in the presence of catalytic ruthenium vinylidenes. Cyclization of homopropargyl alcohols in the presence of catalytic amounts of CpRuCl(cod) afforded the corresponding γ -butyrolactones by a sequence that involved intramolecular addition of the hydroxy group to the ruthenium vinylidene followed by oxidation of the initially formed hemiacetal group (Scheme 10) [99].

On the other hand, cyclization of bis-homopropargyl alcohols with CpRuCl(PAr₃)₂ can be modulated depending on the electronic properties of the ligand [100]. The use of electron-donating ligands such as tris(4-methoxyphenyl) phosphine gave rise to δ -valerolactone (addition of the hydroxy group to the Ru-vinylidene followed by oxidation), while the use of the electron-withdrawing ligand tris(4-fluorophenyl)phosphine led to cycloisomerization to give dihydropyrans (addition of the hydroxy group to the Ru-vinylidene followed by β -hydride elimination) (Scheme 11).

These cycloisomerization conditions proved to be chemoselective for the *O*-cyclizations over the *N*-cyclizations. Dihydropyrans were the products obtained when aminoalcohols bearing an alkyne group were exposed to the Ru-catalyzed



Scheme 11 δ -Valerolactones and dihydropyrans from oxidative cyclization and cycloisomerization of bis-homopropargyl alcohols



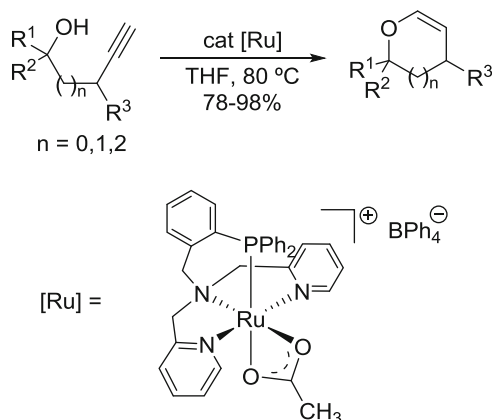
Scheme 12 Chemoselective cycloisomerization of propargyl β,γ -aminoalcohols to dihydropyrans

cycloisomerization conditions [i.e., $\text{CpRuCl}(\text{PPh}_3)_2$, NaHCO_3 , *N*-hydroxysuccinimide and Bu_4NPF_6 in DMF at 80 °C for 8 h] (Scheme 12) [101].

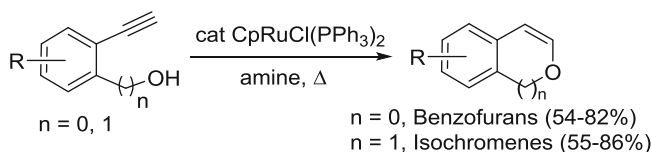
The ruthenium complex $[\text{Ru}(\text{N}_3\text{P})(\text{OAc})][\text{BPh}_4]$, in which N_3P is the N,P mixed tetradentate ligand *N,N*-bis[(pyridin-2-yl)methyl]-[2-(diphenylphosphino)phenyl]methanamine, was found to be catalytically active for the *endo* cycloisomerization of aliphatic alkynols to five-, six-, and seven-membered *endo*-cyclic enol ethers in good to excellent yield (Scheme 13) [102, 103].

On the other hand, cycloisomerization of aromatic homo- and bis-homopropargylic alcohols to benzofurans and isochromenes can be performed using catalytic $\text{CpRuCl}(\text{PPh}_3)_2$ in the presence of an amine as base (Scheme 14) [104]. In a similar manner, benzofurans were also available from homopropargylic aromatic alcohols on using the bifunctional ruthenium catalyst $[\text{RuL}_2\text{Cp}(\text{CH}_3\text{CN})][\text{PF}_6]$ ($\text{L}=\text{AZARYPHOS}$, see Scheme 7) [105].

The proposed mechanism begins with the dissociation of the chloride to afford the starting Ru precatalyst, which upon coordination with the corresponding alkyne would give rise to the key vinylidene intermediate **A** (Scheme 15). Nucleophilic attack by the pendant alcohol to the vinylidene with concurrent removal of a proton by the amine would provide alkenyl ruthenium species **B**, which after protonolysis



Scheme 13 *Endo* cycloisomerization of aliphatic alkynols to five-, six- and seven-membered cyclic enol ethers

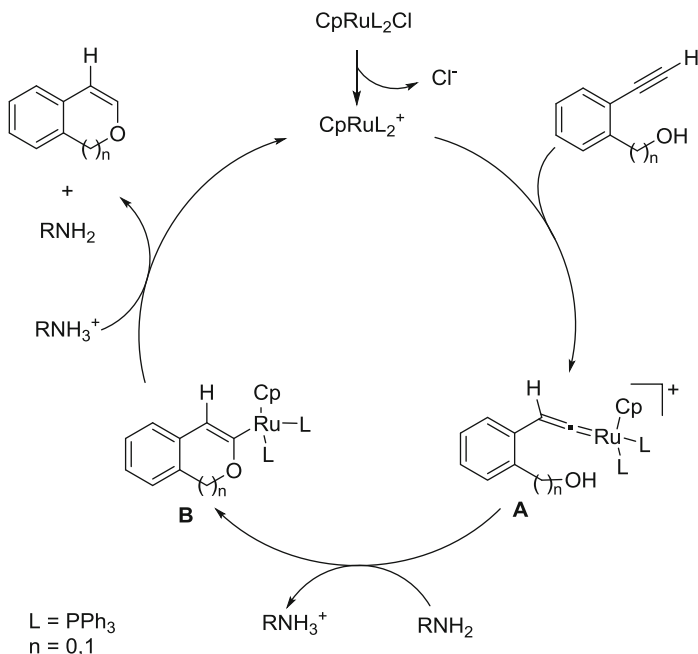


Scheme 14 Cycloisomerization of aromatic homo- and bis-homopropargylic alcohols to benzofurans and isochromenes

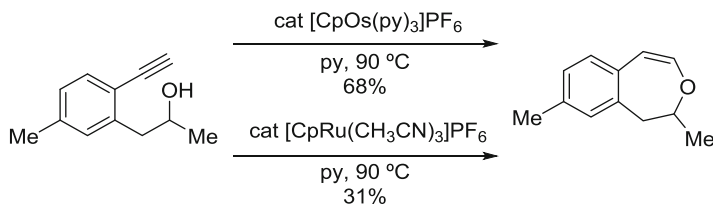
by the ammonium salt formed could provide the final benzofuran or isochromene with regeneration of the active catalyst (Scheme 15).

Seven-membered oxygen heterocycles, 3-benzoxepines, were accessible by a similar methodology involving the use of tungsten vinylidene complexes [106, 107], but catalytic osmium vinylidenes proved to be more efficient than tungsten, ruthenium, and rhodium vinylidenes for the regioselective *7-endo* heterocyclization of aromatic alkynols into benzoxepines (Scheme 16) [108]. The better efficiency could be explained as being due to the more reducing character of osmium compared to ruthenium (Os more easily oxidized), which could result into cleaner osmium-vinylidene formation (see pathway 2, Scheme 1) as compared to the formation of ruthenium-vinylidene via pathways 1 and 2 (Scheme 1), with possible more side reactions.

The oxygen atom from epoxides can also act as a nucleophile in the cycloisomerization of epoxyalkynes to furans catalyzed by $TpRuCl(PPh_3)(CH_3CN)_2$ in the presence of Et_3N [109]. The initial ruthenium vinylidene species **A** would evolve to the ruthenium furylidene **B** by nucleophilic attack of the epoxide oxygen, which in the presence of base would afford ruthenium furyl anion **C**. Protonolysis would give rise to the final product and recovery of the catalytic ruthenium species (Scheme 17).

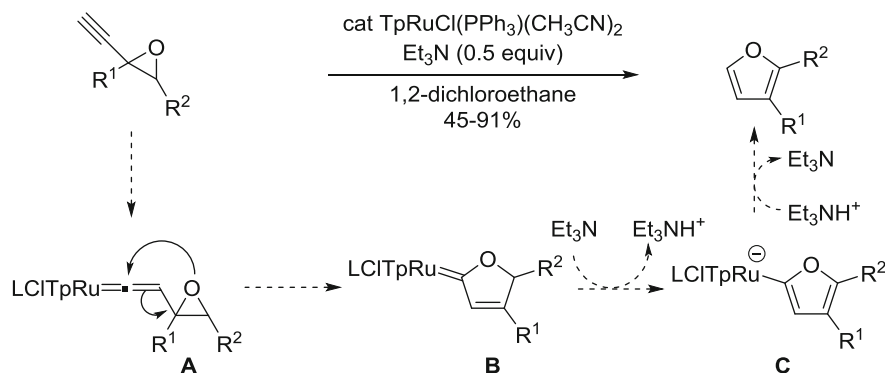


Scheme 15 Proposed mechanism for cycloisomerization of aromatic homo- and bis-homopropargylic alcohols mediated by amines



Scheme 16 Cycloisomerization of aromatic *tris*-homopropargylic alcohols to 3-benzoxepines through catalytic Os- and Ru-vinylidenes

The reaction of (*o*-ethynyl)phenyl epoxides in the presence of $[\text{TpRu}(\text{PPh}_3)(\text{MeCN})_2]\text{PF}_6$ gave different products depending on the epoxide substituents. 1',2'-Disubstituted epoxides gave 2-naphthol derivatives, whereas 1',2',2'-trisubstituted epoxides produced 1-alkylidene-2-indanones in good yields. A possible mechanism for this process involves ketene-alkene intermediates A (Scheme 18), which are generated by an oxygen migration from epoxide to the terminal alkyne initiated by nucleophilic attack of the epoxide to a ruthenium vinylidene. Finally, a 6-*endo-dig* cyclization would afford 2-naphthols and 5-*endo-dig* cyclization would give rise to 1-alkylidene-2-indanones (Scheme 18) [110]. The use of iodoalkynes such as 1-(2'-iodoethynylphenyl)-2-alkyloxiranes in DMF (Scheme 18, X=I) gave rise to 1-iodo-2-naphthols derived from the formation of the corresponding



Scheme 17 Cycloisomerization of terminal epoxyalkynes to furans

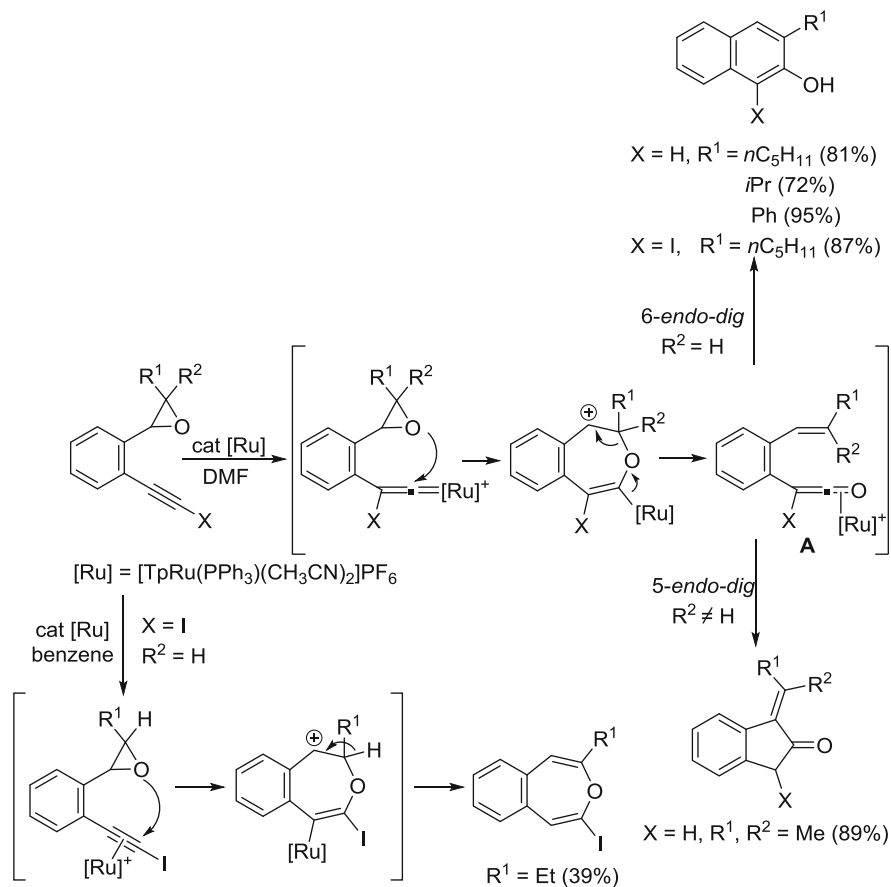
iodovinylidenes. Conversely, the use of benzene as solvent preferentially gave rise to 2-iodobenzo[*d*]oxepines due to the electrophilic activation of the alkyne by the ruthenium catalyst via a π -iodoalkyne species as intermediate [111].

In contrast to oxygen, sulfur has been far less widely used as a nucleophile for addition to ruthenium vinylidenes. The formation of vinyl thioethers from the addition of thiols to alkynes catalyzed by binuclear ruthenium complexes $\text{Cp}^*\text{Ru}(\mu\text{-SR})_2\text{RuCp}^*$ ($\text{R}=\text{Et}$, *i*-Pr, *t*-Bu) and related complex $\text{Cp}^*\text{Ru}(\mu^1\text{-C}_6\text{F}_5)(\mu\text{-S})(\mu\text{-SC}_6\text{F}_5)\text{RuCp}^*$ has been described [112].

2.2 N- and P-Nucleophiles

Nitrogenated nucleophiles can also add to $\text{C}\alpha$ of ruthenium vinylidenes. Although the addition of simple primary or secondary amines to metal-vinylidene intermediates in a catalytic reaction has not been reported to date, probably due to catalyst deactivation by the amine, the $\text{TpRuCl(PPh}_3\text{)}_2$ -catalyzed addition of *N,N*-dialkylhydrazines to alkynes to give nitriles has been reported [113]. In recent years Goossen and coworkers have described a range of customized protocols for the anti-Markovnikov addition of various *N*-nucleophilic amides, thioamides, and imides to terminal alkynes to afford enamides, thioenamides, and enimides in a chemo-, regio-, and stereoselective manner (Scheme 19).

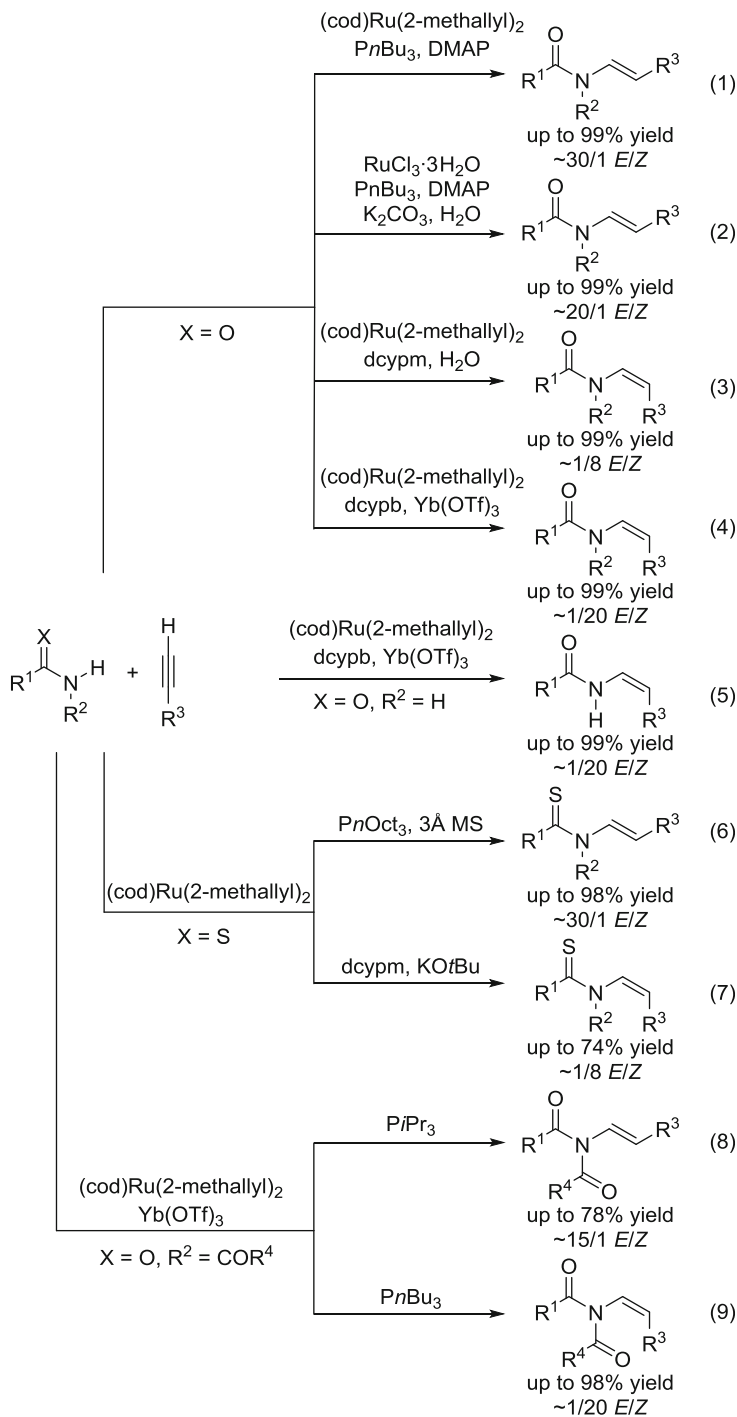
Tertiary (*E*)-enamides can be synthesized by the reaction of secondary amides with terminal alkynes in the presence of a catalyst system generated in situ from bis(2-methallyl)(cycloocta-1,5-diene)ruthenium(II) [(cod)Ru(2-methallyl)₂], tri-*n*-butylphosphine and 4-dimethylaminopyridine (Scheme 19, Eq. 1) [114], or by using a mixture of (RuCl₃·3H₂O), P(*n*-Bu)₃, DMAP, K₂CO₃, and water (Scheme 19, Eq. 2) [115]. The stereoselectivity can be reversed in favor of the corresponding (*Z*)-enamides by employing [(cod)Ru(2-methallyl)₂], bis(dicyclohexylphosphino)methane (dcypm) and water instead of P(*n*-Bu)₃ and DMAP (Scheme 19, Eq. 3) [114], or the Lewis acid ytterbium(III) triflate in combination with [(cod)Ru(2-methallyl)₂] and 1,4-bis(dicyclohexylphosphino)butane dcypb (Scheme 19,



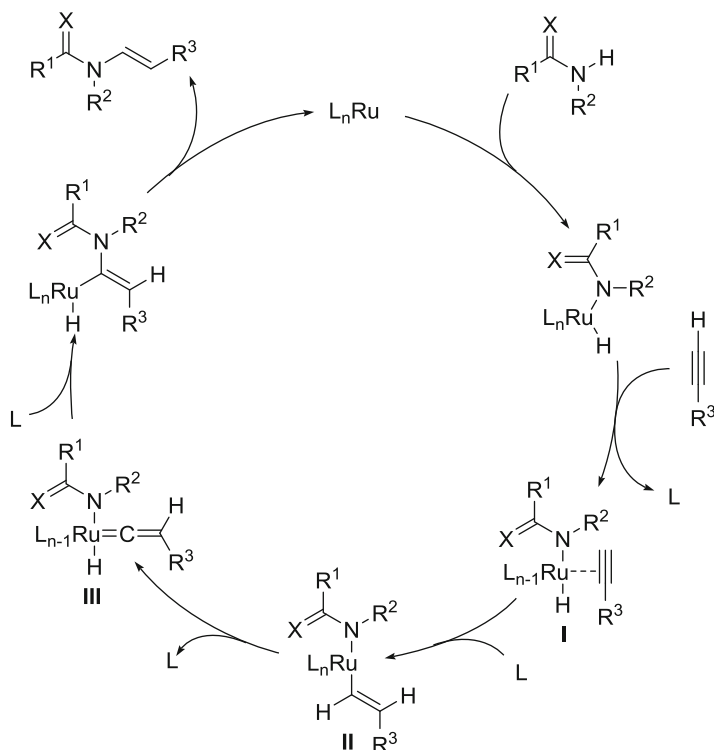
Scheme 18 Cycloisomerization of (*o*-ethynyl)phenyl epoxides to 2-naphthols, 2-indanones and 2-iodobenzo[*d*]oxepines

Eq. 4) [116]. The latter conditions also proved to be efficient for the synthesis of secondary (*E*)-enamides from primary amides and terminal alkynes (Scheme 19, Eq. 5) [117]. The previously described catalytic conditions for the addition of amides to alkynes were also modified to allow the stereoselective addition of thioamides (Scheme 19, Eqs. 6 and 7) [118] and imides to alkynes (Scheme 19, Eqs. 8 and 9) [119].

Mechanistic studies on the Ru-catalyzed hydroamidation of terminal alkynes support the involvement of ruthenium hydride and ruthenium vinylidene species as the key intermediates [120]. The proposed pathway starts with the initial oxidative addition of the amide N–H bond to the ruthenium complex to afford ruthenium-hydride **I** followed by 1,2-insertion of a π -coordinated alkyne to vinyl-ruthenium species **II**. Rearrangement to the vinylidene species **III** followed by nucleophilic attack of the amide and subsequent reductive elimination would give rise to the product (Scheme 20).



Scheme 19 Intermolecular addition of amides, thioamides and enimides to terminal alkynes through Ru vinylidenes

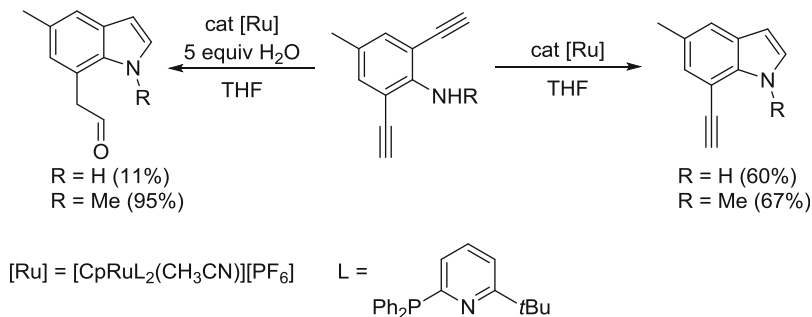


Scheme 20 Proposed mechanism for the hydroamidation of terminal alkynes

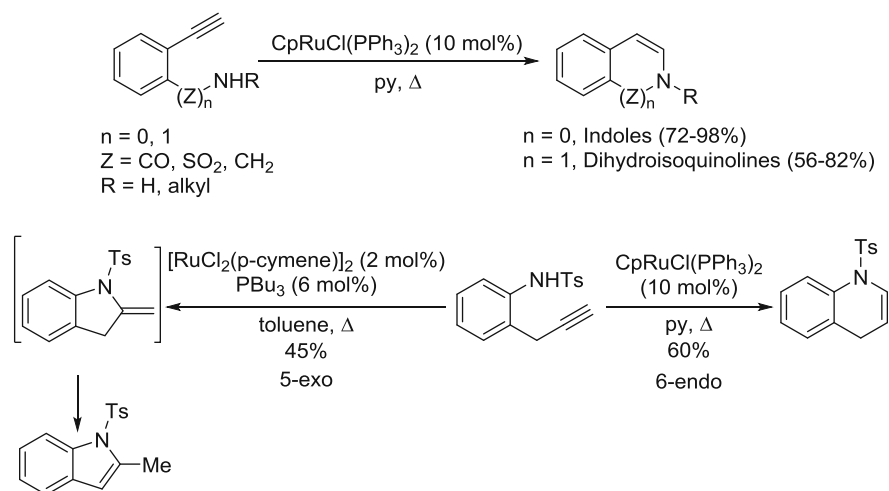
This methodology can be used in an intramolecular fashion to synthesize different nitrogen heterocycles. Ruthenium-catalyzed cycloisomerizations of aromatic homo- and bis-homopropargylic amines/amides to indoles, dihydroisoquinolines, and dihydroquinolines have been developed.

Grotjahn and coworkers used the same ruthenium catalyst as for anti-Markovnikov hydration of terminal alkynes, $[CpRuL_2(CH_3CN)](PF_6)$ ($L=AZARYPHOS$, see Scheme 7) [86], to synthesize indoles from homopropargylic amines/amides in good yields [105]. The use of doubly ethynylated substrates in the presence of water gave rise to the product derived from cyclization to the indole plus anti-Markovnikov hydration of the second terminal alkyne (Scheme 21).

On using $CpRuCl(PPh_3)_2$ as catalyst in pyridine as solvent it was possible to synthesize not only indoles from aromatic homopropargylic amides but also 1,2-dihydroisoquinolines and 1,4-dihydroquinoline from bis-homopropargylic amides (Scheme 22) [121, 122]. Surprisingly, cyclization of the latter amides under other typical conditions used for vinylidene formation, $[RuCl_2(p\text{-cymene})]_2/PBu_3$ [120], gave the 2-methylindole, which indicates that cyclization did not proceed through a ruthenium vinylidene [121, 122].



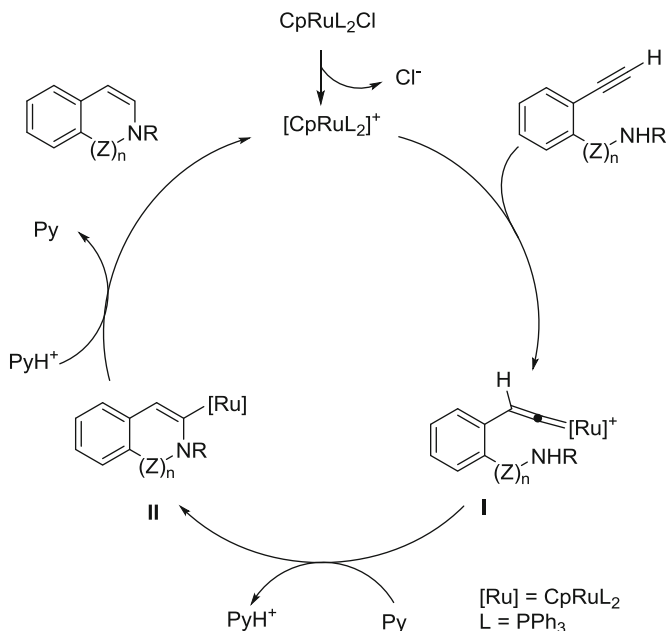
Scheme 21 Simple and double *anti*-Markovnikov hydration of arylacetylenes to indole derivatives



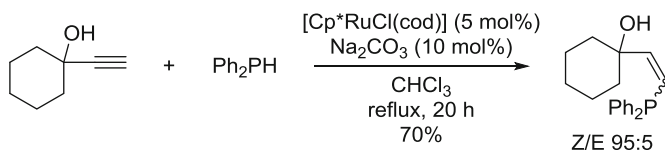
Scheme 22 Cycloisomerization of aromatic propargyl amides to indoles, 1,2-dihydroisoquinolines and 1,4-dihydroquinolines

These results may be interpreted in terms of the proposed mechanism shown in Scheme 23. Dissociation of Cl^- from the starting Ru precatalyst is followed by coordination of the alkyne and subsequent rearrangement leads to Ru vinylidene intermediate **I**. This key intermediate may undergo nucleophilic attack by the pendant amine or amide with concurrent removal of a proton by pyridine to provide the alkenyl Ru species **II**. Finally, protonolysis by the pyridinium salt formed could provide the final indoles or dihydroisoquinolines, with regeneration of the active catalytic species. A similar mechanistic proposal could be invoked for the preparation of dihydroquinolines from bis-homopropargylic amide.

Phosphorus nucleophiles can also be added to $\text{C}\alpha$ of ruthenium vinylidenes. Dixneuf and coworkers reported the efficient Ru-catalyzed *anti*-Markovnikov *cis* hydrophosphination of propargyl alcohols to vinyl phosphines (Scheme 24) [123].



Scheme 23 Proposed mechanism for cycloisomerization of aromatic propargyl amides

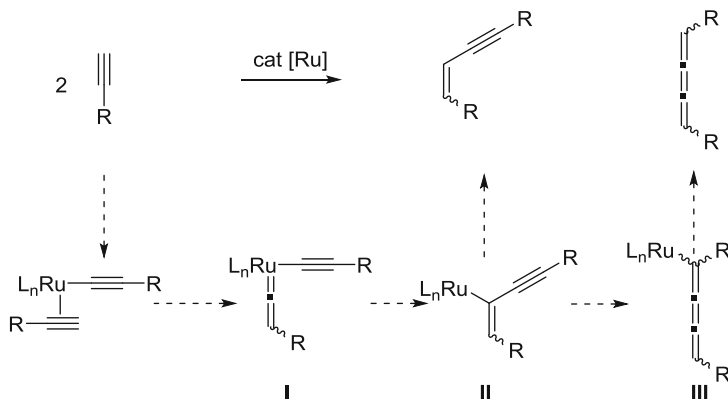


Scheme 24 Hydrophosphination of propargyl alcohols to vinyl phosphines

2.3 C-Nucleophiles

Ruthenium vinylidenes can participate in the formation of C–C bonds by using carbon nucleophiles that are capable of adding to the electrophilic $\text{C}\alpha$ to the metal. Head-to-head dimerization of alkynes can be rationalized by the intramolecular attack of the Csp of one catalytic alkynylrutheniumvinylidene species **I**, generated in situ by treatment of one alkyne with catalytic amounts of a ruthenium complex, followed by acidic protonolysis of the intermediate enynyl **II** to afford the conjugated enyne (Scheme 25) [124, 125]. Depending on the nature of the ligands, complex **II** can rearrange to a cumulenyl ruthenium species **III**, which upon protonolysis gives the butatriene compound (Scheme 25) [126–128].

There have been several reports of ruthenium complexes that are able to catalyze the head-to-head dimerization of alkynes with different *E/Z* selectivities. These compounds include $[\text{TpRuCl}(\text{PPh}_3)_2]$ [129–131], $[\text{TpRu}(\text{Mei-Pr}_2\text{P})\text{C}(\text{Ph})=\text{C}(\text{Ph})$



Scheme 25 Head-to-head dimerization of alkynes involving Ru vinylidenes

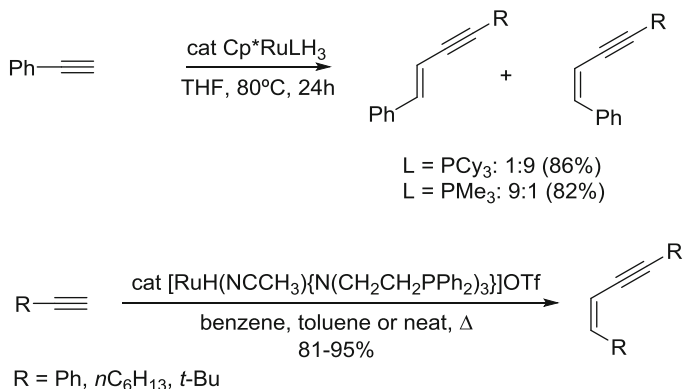
CCPh) [132], [Ru(ma)₂(PPh₃)₂] (ma=maltolate, C₆H₅O₃) [133], [(η⁵-C₉H₇)Ru(PPh₃)₂CCPh] [134], [RuCl₂(PCy₃)₂=CHPh] [135], and RuHXL₂ [X=Cl or N (SiMe₃)₂, L=*Pi*-Pr₃] [136].

The stereoselectivity of the dimerization process can be modulated by changing the nature of the ligands in the catalysts. Yi and Liu reported that the use of [Cp**Ru*(L)H₃] (L=PCy₃) led to dimerization of phenylacetylene to the *Z* isomer, whereas the system with L=PMe₃ gave the product of *E* configuration as the major isomer (Scheme 26) [137, 138]. More recently, Bianchini and coworkers described the synthesis of (*Z*)-enynes from aliphatic and aromatic alkynes with high regio- and stereoselectivity by using [RuH(CH₃CN)(NP₃)OTf] as the catalyst in both aqueous and organic media (Scheme 26) [139].

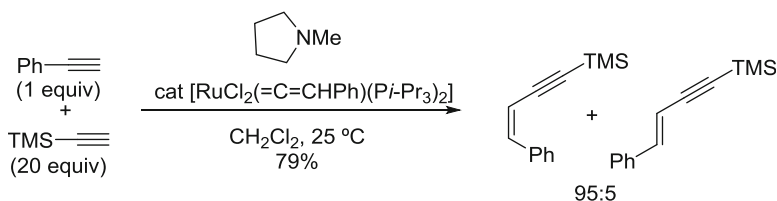
It was also possible to achieve cross-dimerization with (*Z*)-selectivity of two types of alkynes that possess significantly different properties with respect to the tautomerization between alkyne and vinylidene ligands. Cross-dimerization of arylacetylenes and silylacetylenes was reported to proceed on using vinylidene-ruthenium complexes bearing bulky and basic trialkyl phosphine ligands in the presence of methylpyrrolidine (Scheme 27) [140].

In addition to dimerization and cross-dimerization of alkynes, regio-, and stereoselective polyaddition of alkynes catalyzed by ruthenium has also been described. Katayama and Ozawa reported the synthesis of poly(9,9-dioctyl-2,7-fluorene ethynylene vinylene) having (*Z*)-vinylene units by polyaddition of 2,7-diethynyl-9,9-dioctylfluorene catalyzed by RuCl₂(=C=CHPh)(*Pi*-Pr₃)₂ (Scheme 28) [141].

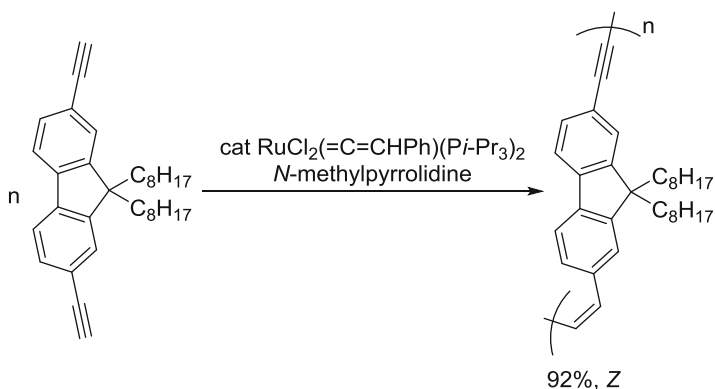
Alkenes are also capable of acting as nucleophiles and can add intramolecularly to ruthenium vinylidenes. Liu and coworkers described the TpRu(PPh₃)(CH₃CN)₂PF₆-catalyzed cycloisomerization of substituted *ortho*-alkynylethynylstyrenes to give different naphthalenes or indenes depending on the nature of the alkene substituents (Scheme 29) [142, 143]. In all cases the reaction begins with the formation of the ruthenium vinylidene **I**. Subsequent 6-*endo-dig* (path a) or 5-*endo-dig* (path b) cyclization by nucleophilic attack of the alkene moiety would afford ruthenium species **II** and **III**, respectively. When monosubstituted iodoalkenes



Scheme 26 Regio- and stereoselective synthesis of (*Z*)-enynes from aliphatic and aromatic alkynes

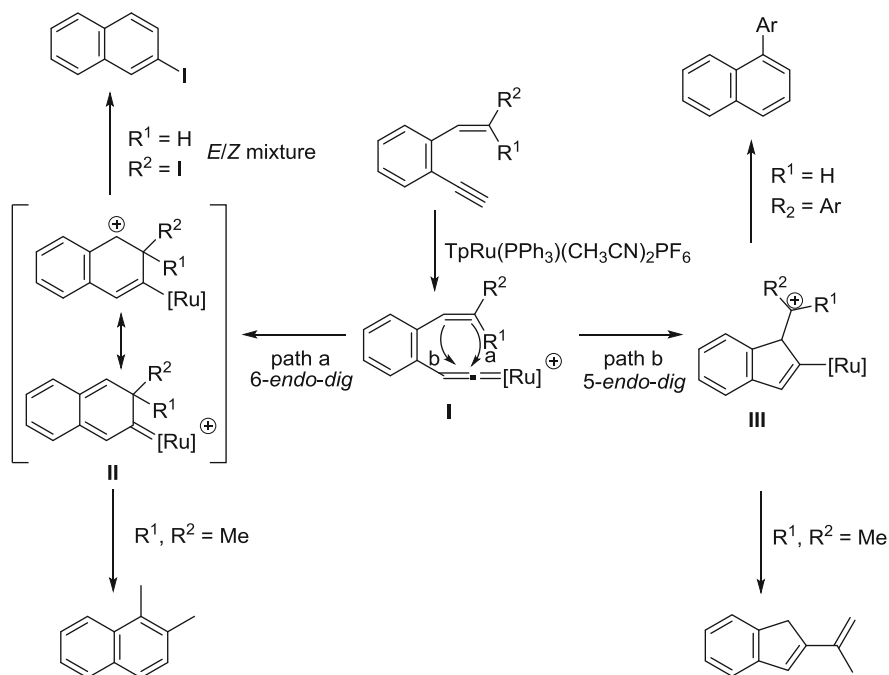


Scheme 27 Cross-dimerization of aliphatic and aromatic alkynes to (*Z*)-enynes



Scheme 28 Regio- and stereoselective polyaddition of aromatic alkynes catalyzed by ruthenium vinylidenes

were used, only path a is operative, while with aryl monosubstituted alkenes the most favorable path was b. The substituted naphthalenes were obtained after a final rearrangement [142]. Both mechanisms are operative when terminal disubstituted alkenes are used, with the naphthalene derivatives obtained from 6-*endo-dig* cyclization and indenenes from 5-*endo-dig* cyclization [143].



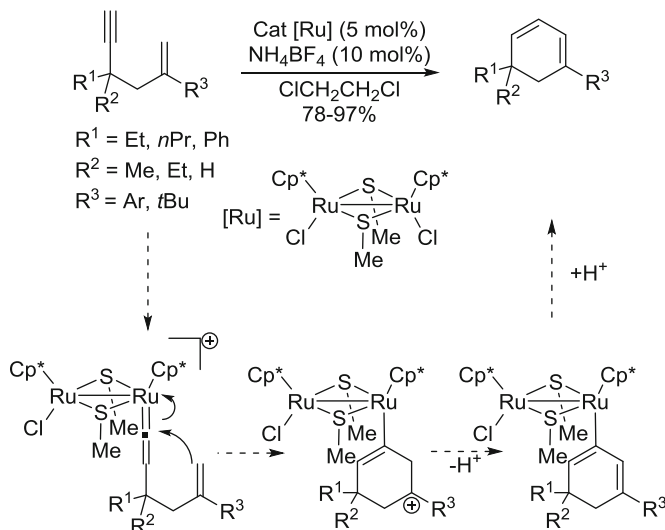
Scheme 29 Cycloisomerization of substituted *ortho*-ethynylstyrenes to different naphthalenes or indenes

Non-conjugated terminal 2-substituted-1,5-enynes also react through a 6-*endo-dig* cyclization to afford 1,3-cyclohexadienes via ruthenium vinylidene intermediates. Nishibayashi and coworkers reported that 2-substituted-1,5-enynes in the presence of 5% methanethiolate-bridged diruthenium complex $[\text{Cp}^*\text{RuCl}(\mu_2\text{-SMe})_2]$ and 10 mol% of NH_4BF_4 afforded the corresponding 1,3-cyclohexadienes in good yields (Scheme 30) [144].

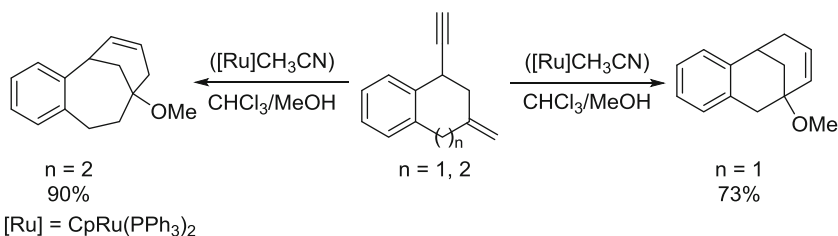
Lin and coworkers described the 6-*endo-dig* cyclization of aromatic 1,5-enynes incorporating a cycle catalyzed by $[\text{CpRu}(\text{PPh}_3)_2\text{CH}_3\text{CN}]^+$ using a mixture of $\text{CHCl}_3/\text{MeOH}$ to afford fused tricyclic rings with the incorporation of MeOH (Scheme 31) [145]. Interestingly, the position of the final double bond varies depending on the size of the ring bearing the enyne.

2.4 B-Nucleophiles

Ruthenium hydride pincer complex $[\text{Ru}(\text{PNP})(\text{H})_2(\text{H}_2)]$ [PNP =1,3-bis(di-*tert*-butyl-phosphinomethyl)pyridine] and its borane analog $[\text{Ru}(\text{PNP})(\text{H})_2(\text{HBpin})]$ (HBpin =pinacolborane) catalyze the hydroboration of terminal alkynes to give selectively *Z*-vinylboronates in high yields (Scheme 32) [146]. Mechanistic studies



Scheme 30 6-*endo-dig* Cyclization of 2-substituted-1,5-enynes to 1,3-cyclohexadienes using a methanethiolate-bridged diruthenium catalyst

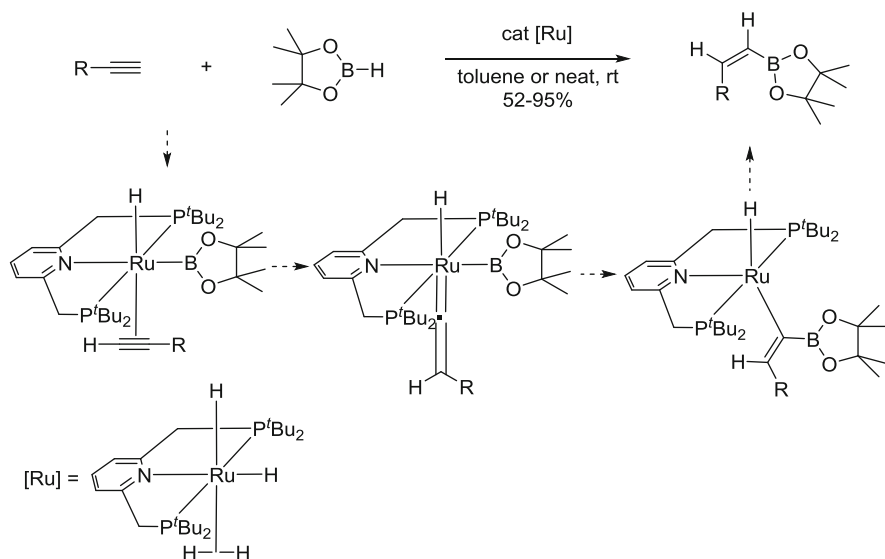


Scheme 31 6-*endo-dig* Cyclization of aromatic 1,5-enynes to fused tricyclic rings

suggest a 1,2-hydrogen shift from a η^2 -alkyne to a vinylidene complex prior to the C–B bond formation.

3 Intramolecular Cyclizations

Cyclizations can be initiated by a nucleophilic attack, e.g. by H₂O or a carboxylic acid, to a catalytic ruthenium vinylidene followed by trapping with an electrophile. Lee and coworkers described the Ru-catalyzed hydrative cyclization of 1,5-enynes (Scheme 33) to give functionalized cyclopentanones [147]. Treatment of 1,5-enynes bearing an internal Michael acceptor with a catalytic amount of [Ru₃Cl₅(dppm)₃]PF₆ in the presence of water initially afforded the corresponding ruthenium vinylidene species. Nucleophilic anti-Markovnikov addition of water

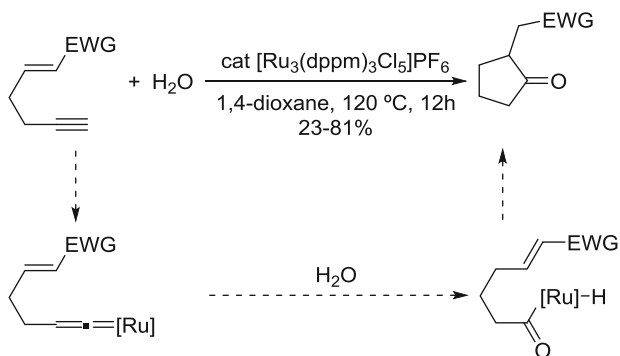
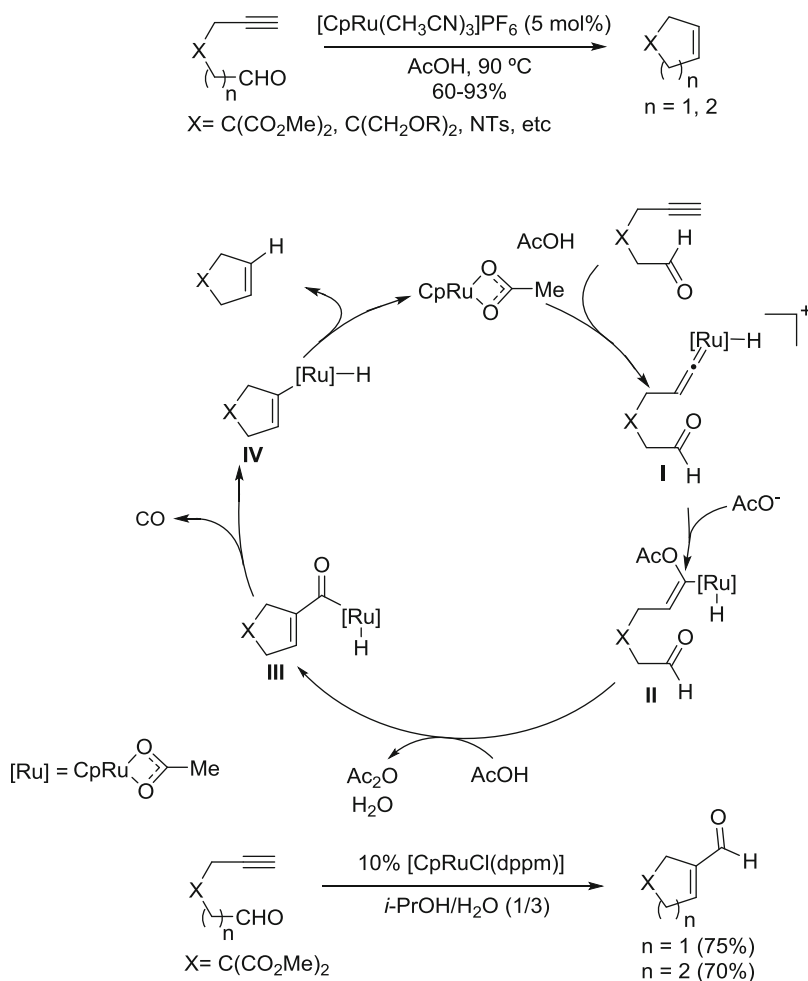


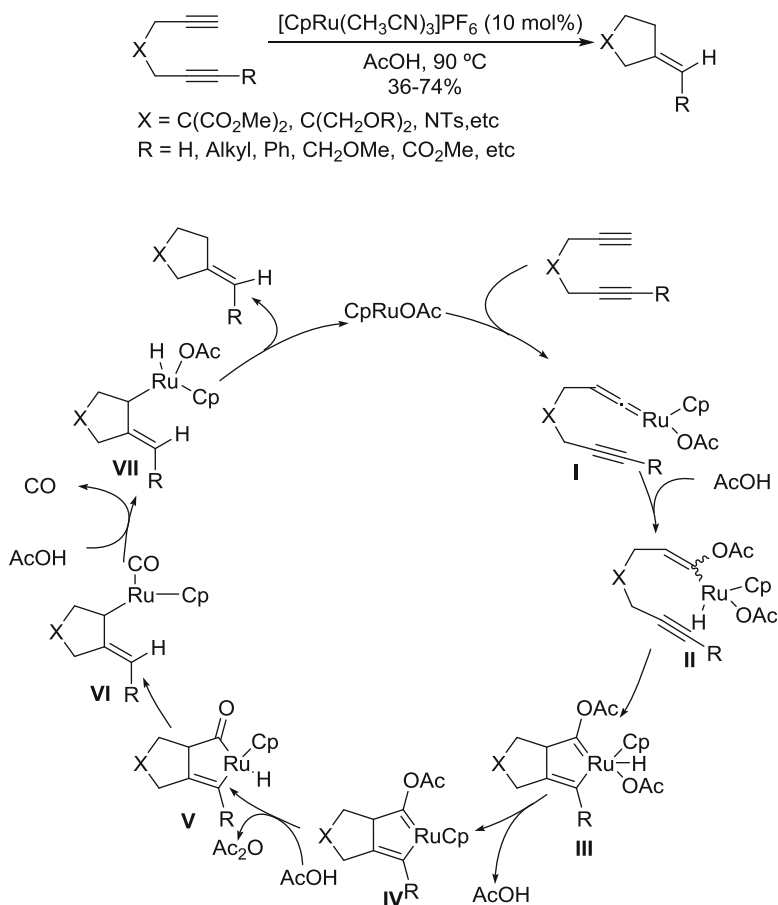
Scheme 32 Hydroboration of terminal alkynes to *Z*-vinylboronates using a ruthenium hydride pincer complex as catalyst

would afford an acyl-ruthenium hydride, which through a hydroacylation or a Michael addition would give rise to the hydrated cycle cyclopentanone.

Cyclization of terminal alkynals to cycloalkenes with loss of a carbon atom through catalytic ruthenium vinylidenes using $[\text{CpRuMeCN}_3]\text{PF}_6$ as catalyst has been described by Saá and coworkers (Scheme 34) [148]. These transformations would be initiated by the nucleophilic attack of acetate to the ruthenium vinylidene **I** to give complex **II** followed by an aldol-type condensation to afford the acyl-ruthenium-hydride **III**. Finally, decarbonylation to **IV** followed by reductive elimination would give rise to the final product, with *the terminal carbon of the alkyne being the one that is lost as CO*. The use of a catalyst bearing a bidentate ligand such as $\text{CpRu}(\text{dppm})\text{Cl}$ prevents the decarbonylative step and this process gives the corresponding α,β -unsaturated aldehyde (Scheme 34).

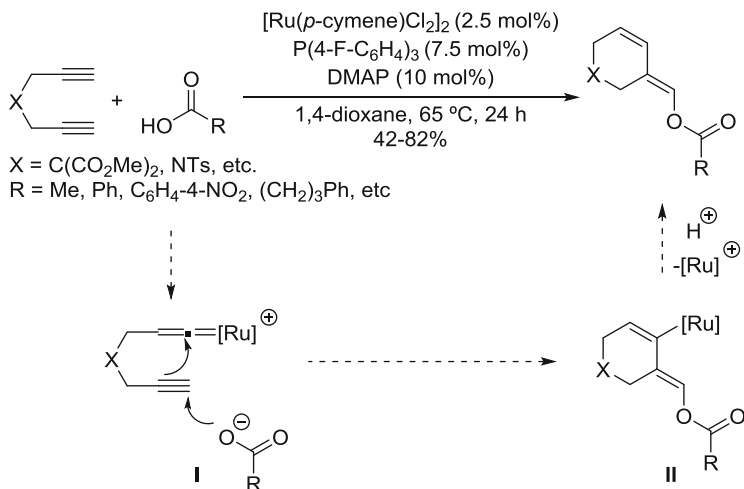
The same catalyst, $[\text{CpRuMeCN}_3]\text{PF}_6$, also performs the *decarbonylative cyclization* of 1,6-diynes to *exo*-alkylidenecyclopentanes through the initial addition of the carboxylic acid to a catalytic ruthenium vinylidene (Scheme 35) [149]. The acyclic vinylruthenium hydride **II** obtained by addition of acetic acid to the initially formed vinylidene would evolve through a [3+2]-type cycloaddition to a cyclic carbene ruthenium-hydride **III**. Reductive loss of AcOH from **III** would give the cyclic carbene **IV**, which undergoes another nucleophilic attack by AcOH to give the acyl-ruthenium-hydride **V**. Reductive opening of ruthenacycle **V** followed by oxidative addition of AcOH with concomitant decarbonylation of **VI** would lead to the ruthenium-hydride **VII**, which affords the observed alkylidenecyclopentane through a reductive elimination (Scheme 35).

**Scheme 33** Ru-catalyzed hydrative cyclization of 1,5-enynes to cyclopentanones**Scheme 34** Ru-catalyzed decarbonylative cyclization of terminal alkynes to cycloalkenes and cycloisomerization to cyclic α,β -unsaturated aldehydes



Scheme 35 Ru-catalyzed decarbonylative cyclization of 1,6-diyne to *exo*-alkylidenecyclopentanes

Variation of the electronic and steric nature of the ruthenium catalysts allow the complementary *carboxylative cyclization* of 1,6-diyne (Scheme 36) [150]. Lee and coworkers described how a variety of carboxylic acids condense with 1,6-terminal diynes in the presence of catalytic amounts of [Ru(*p*-cymene)Cl₂]₂, P(4-F-C₆H₅)₃ and 4-dimethylaminopyridine to give cyclohexylidene enol carboxylates with exclusive (*E*)-selectivity. The proposed mechanism involves the initial formation of a ruthenium vinylidene species **I** followed by intramolecular cyclization induced by the nucleophilic attack of the carboxylate anion to afford a vinylruthenium species **II**. Final protonolysis furnished the product and turns the catalyst over.



Scheme 36 Ru-catalyzed carboxylative cyclization of 1,6-diyne to cyclohexylidene enol carboxylates

4 Pericyclic Reactions

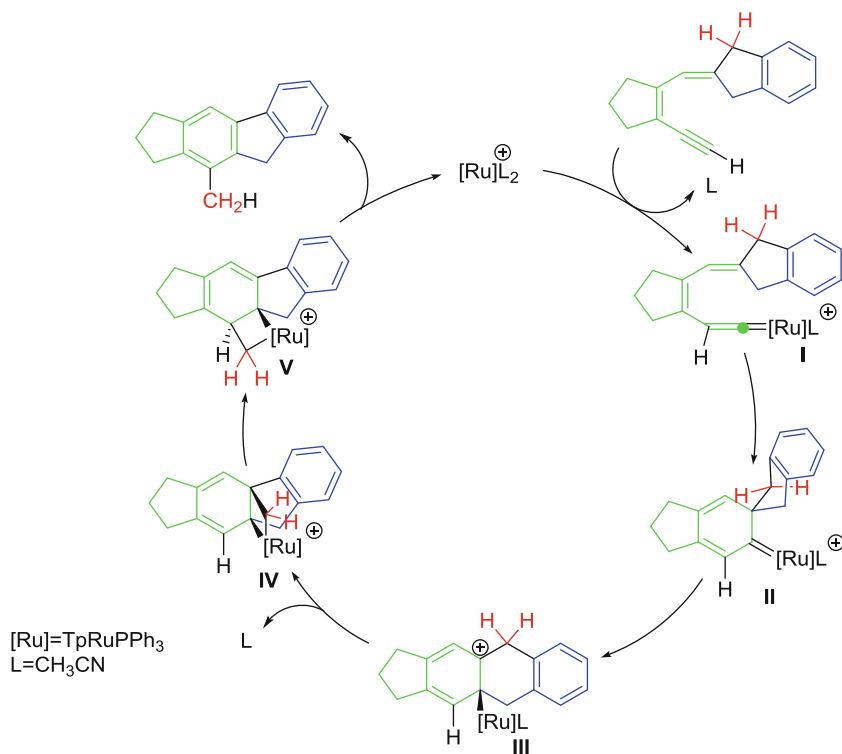
The electronic π system of ruthenium vinylidenes can participate in pericyclic reactions such as electrocyclizations, cycloadditions, and sigmatropic reactions to afford a variety of interesting poly(hetero)cyclic products.

4.1 Electrocyclizations

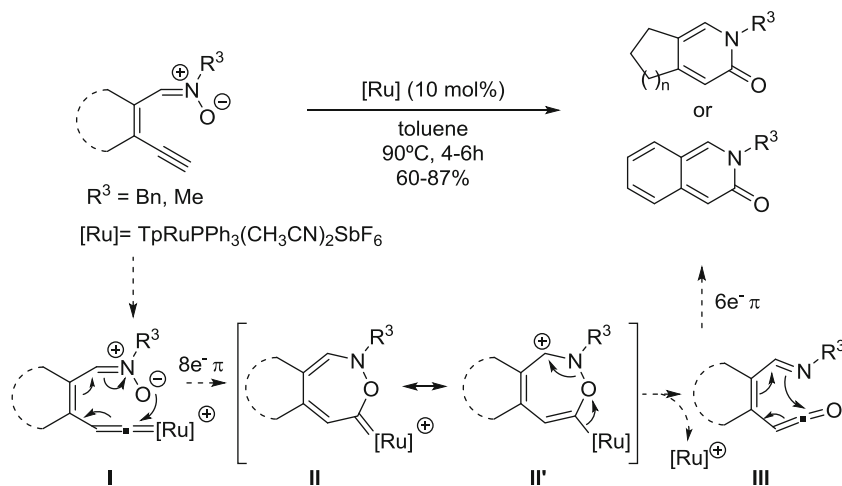
The first example of the participation of the electronic π system of a catalytic ruthenium vinylidene in a $6e^- \pi$ electrocyclization was described by Merlic and Pauly. Treatment of conjugated terminal dienyne with catalytic amounts of $\text{RuCl}_2(\textit{p}\text{-cymene})\text{PPh}_3$ and NH_4PF_6 in refluxing dichloromethane afforded the aromatic benzene derivatives in good yields (Scheme 37) [151]. The proposed mechanism begins with the formation of the conjugated ruthenium vinylidene **I**, which undergoes a $6e^- \pi$ electrocyclization to the ruthenium carbene **II**. Subsequent β -hydride elimination followed by reductive elimination would generate the benzene derivative with recovery of the Ru catalyst.

Liu and coworkers reported a Ru-catalyzed 6-*endo-dig* cyclization of 3,5-dien-1-ynes to rearranged toluene derivatives through a cascade process initiated by the formation of ruthenium vinylidenes (Scheme 38) [152].

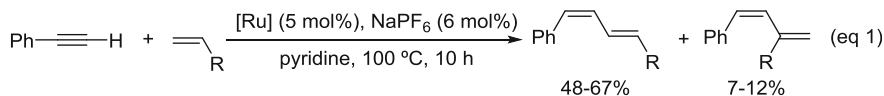
The proposed mechanism for this transformation would start with a $6e^- \pi$ electrocyclization of ruthenium vinylidene **I** to cyclic dienylylcarbene **II** (Scheme 39). A 1,2-alkyl shift in carbene **II** would afford the rearranged cationic intermediate



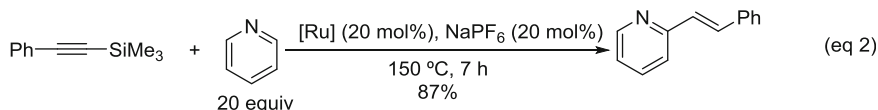
Scheme 39 Proposed mechanism for the 6-*endo-dig* cyclization of 3,5-dien-1-yne to toluene derivatives



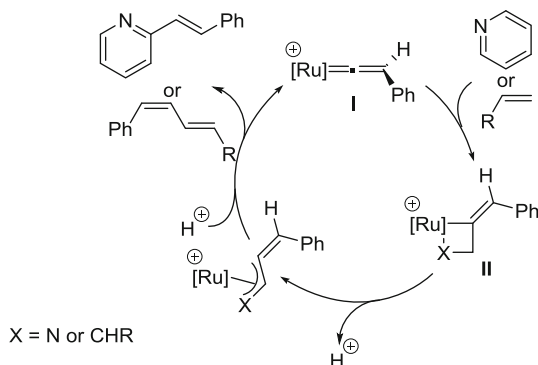
Scheme 40 Conversion of enynyl nitrones to α -pyridones through electrocyclizations of Ru-vinylidenes



R = $n\text{C}_6\text{H}_{13}$, $(\text{CH}_2)_2\text{OH}$, $(\text{CH}_2)_2\text{CO}_2\text{Me}$, $(\text{CH}_2)_2\text{CN}$, $(\text{CH}_2)_4\text{NHAc}$



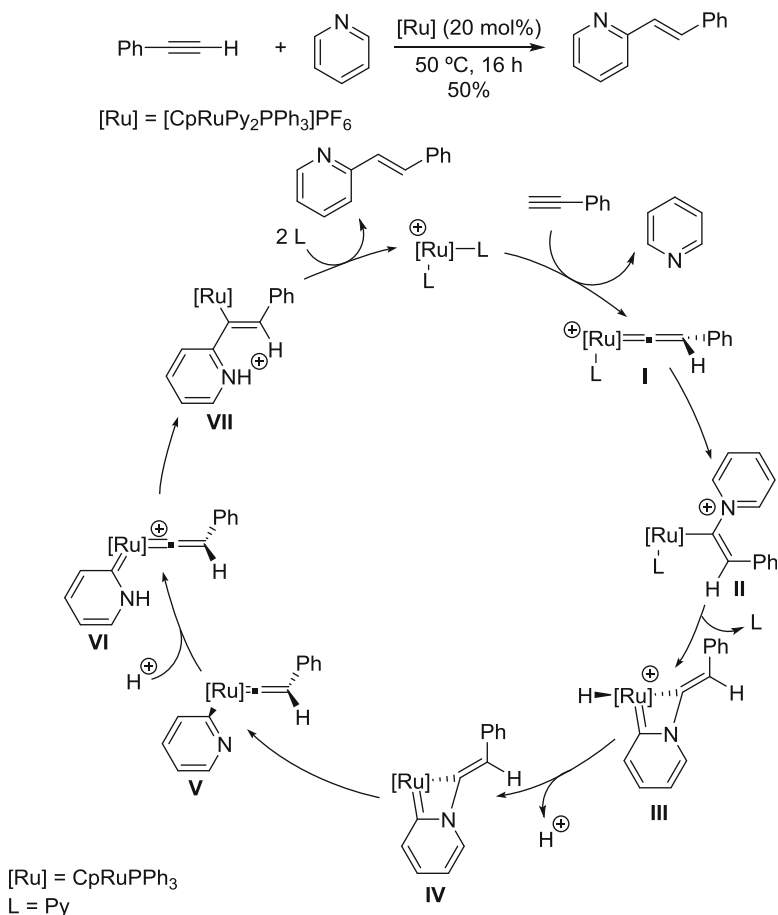
[Ru] = $\text{CpRuCl}(\text{PPh}_3)_2$



Scheme 41 Formation of 1,3-dienes by linear coupling of phenylacetylenes with olefins and regio- and stereoselective α -alkenylation of pyridines

described the formation of 1,3-dienes by reaction of phenylacetylenes with several olefins (Scheme 41, Eq. 1) [154, 155] and the regio- and stereoselective alkylation of pyridines, both catalyzed by the complex $[\text{CpRuCl}(\text{PPh}_3)_2]$ (Scheme 41, Eq. 2) [36]. In both cases the mechanism involves the initial formation of a ruthenium vinylidene **I** followed by a [2+2] cycloaddition with the double bond of either the alkene or the pyridine to afford ruthenacyclobutene species **II**. Finally, deprotonation and protonolysis would afford the corresponding product.

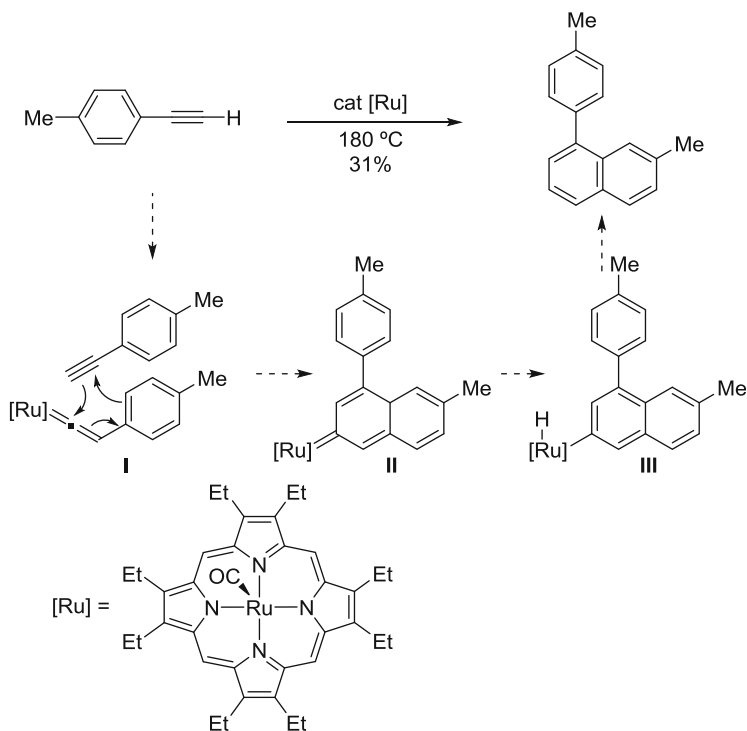
Recently, Slattery and Lynam reported that the formation of 2-styrylpyridine from terminal alkynes and pyridine could also be catalyzed by the cationic ruthenium complex $[\text{CpRuPy}_2(\text{PPh}_3)]\text{PF}_6$ under far milder conditions than the corresponding reaction promoted by $[\text{CpRuCl}(\text{PPh}_3)_2]$ (Scheme 42) [156]. According to experimental and theoretical data, the mechanistic rationale would involve a catalytic ruthenium pyridylidene species without the formation of ruthenacyclobutenes. The initially formed ruthenium vinylidene **I** would undergo nucleophilic attack of the pyridine to give vinyl ruthenium **II**, which would evolve to pyridylidenes **III** and **IV**. C–N bond cleavage and protonation would give rise to vinylidene **VI**, which after C–C bond formation by pyridylidene migration to the α -carbon of the Ru-vinylidene would afford the 2-styrylpyridine with regeneration of the catalytic species.



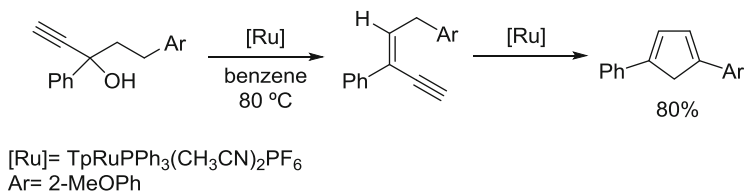
Scheme 42 Proposed mechanism for the formation of 2-styrylpyridine from terminal alkynes and pyridine

4.2.2 [4+2] Cycloadditions

Intermolecular Diels–Alder reactions between catalytic ruthenium vinylidenes **I** and arylacetylenes afforded 1-arylnaphthalenes (cyclodimerization) in moderate yields (Scheme 43) [157]. Tautomerization of the initial cycloadduct, ruthenium carbene **II**, followed by reductive elimination gives rise to the final naphthalene with regeneration of the catalytic porphyrilruthenium complex.



Scheme 43 Cyclodimerization between catalytic ruthenium vinylidenes and arylacetylenes to 1-arylnaphthalenes



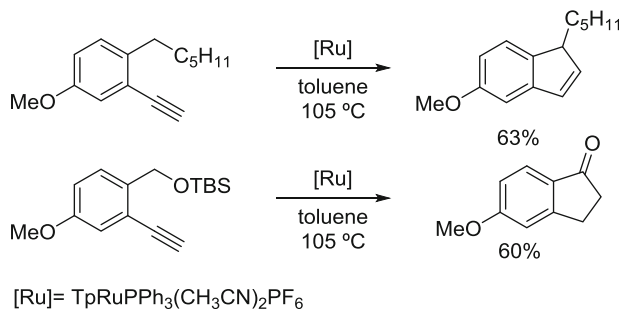
Scheme 44 Cycloisomerization of *cis*-3-en-1-yne to cyclopentadienes

4.3 [1,5] Sigmatropic Rearrangements

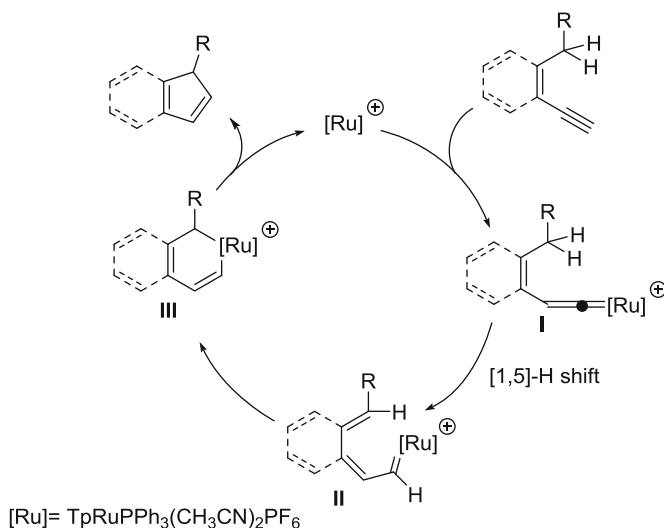
Liu and coworkers reported the cycloisomerization of *cis*-3-en-1-yne to cyclopentadiene derivatives through 1,5-sigmatropic hydrogen shifts of catalytic ruthenium vinylidene intermediates (Scheme 44) [158].

More recently, the cyclizations of 2-alkyl-1-ethynylbenzenes to 1-substituted-1*H*-indenes and 1-indanones have also been developed (Scheme 45) [159].

In both cases the proposed mechanism would start with the formation of vinylidene **I** that evolves to the carbene **II** by a [1,5]-hydrogen shift. Subsequent



Scheme 45 Cyclizations of 2-alkyl-1-ethynylbenzenes to 1-substituted-1*H*-indenes and 1-indanones



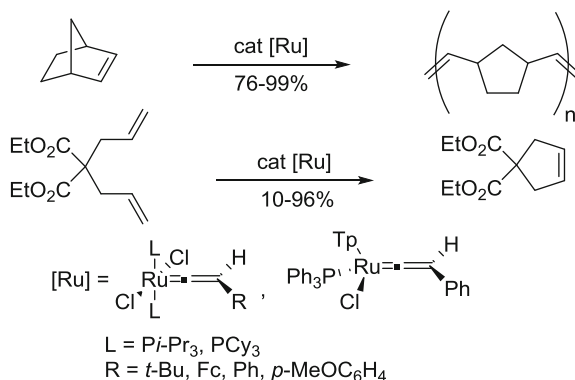
Scheme 46 Proposed mechanism for the cyclizations of 2-alkyl-1-ethynylbenzenes to 1-substituted-1*H*-indenes

$6e^-$ π -electrocyclization of **II** to ruthenacyclohexadiene **III** followed by reductive elimination would afford the final product (Scheme 46).

5 Vinylideneruthenium Catalysts in Metathesis

Some ruthenium vinylidene complexes have been found to serve as good catalyst precursors for olefin metathesis [160]. Although the efficiency of the vinylidene complexes as initiators is lower than those of the well-known Grubbs' alkylidene and indenylidene complexes, the polymerization rate is fast enough for practical use and, more importantly, they are readily prepared from conventional terminal

Scheme 47 ROMP of norbornenes and RCM of α,ω -dienes catalyzed by phosphine ruthenium vinylidene complexes

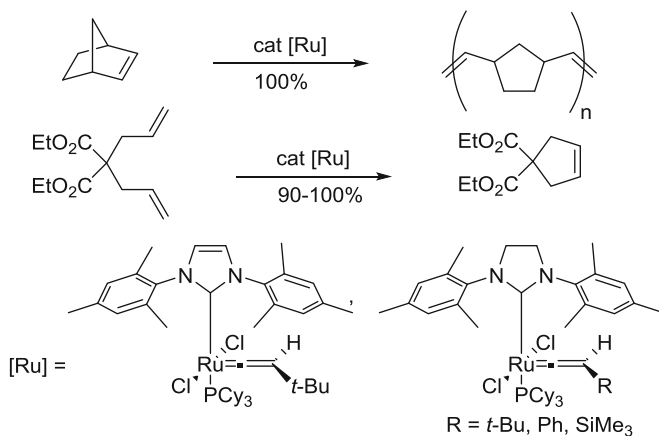


alkynes. Another important feature is the rearrangement of the vinylidene ligand ($[\text{M}]=\text{C}=\text{CHR}$) to an alkylidene moiety ($[\text{M}]=\text{CHR}$) in the presence of an olefin, a process that allows the application of vinylidenes as precursors for selective cross-metathesis (CM), ring-closing metathesis (RCM), and ring-opening metathesis polymerization (ROMP) [161, 162]. Specifically, the use of vinylideneruthenium as a catalyst in metathesis has been subject of several recent reviews [57–59, 65].

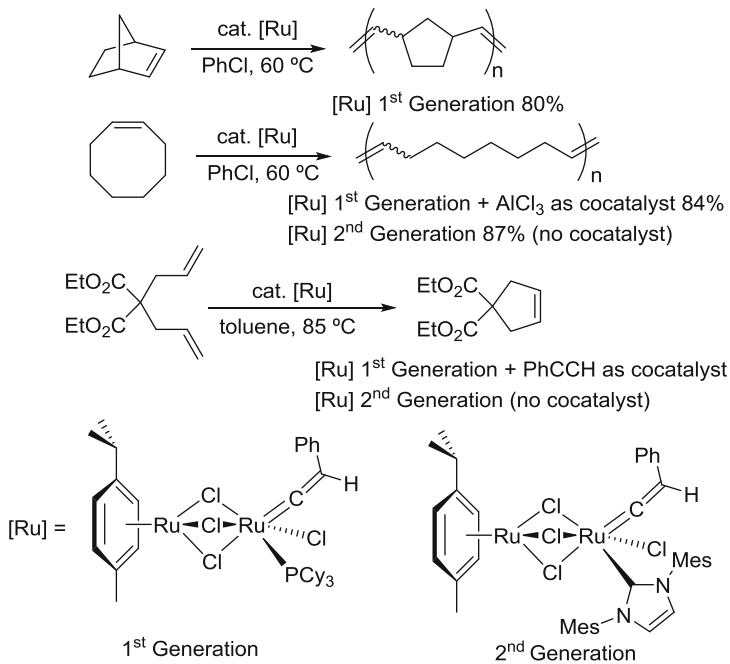
Since the first use of $[\text{RuCl}_2(=\text{C}=\text{CH}_2)(\text{PCy}_3)_2]$ as a catalyst for ROMP [163], several analogs containing other phosphines (such as PPh_3 and Pi-Pr_3) and vinylidene ligands generated from various alkynes (such as *tert*-butylacetylene, phenylacetylene, ferrocenylacetylene, *para*-methoxyphenylacetylene) as well as $\text{TpRuCl}(=\text{C}=\text{CHPh})(\text{PPh}_3)$ have been used to catalyze the ROMP of a variety of norbornene derivatives and in the RCM of α,ω -dienes (Scheme 47) [33, 161, 164–169].

Replacement of a phosphine ligand with an *N*-heterocyclic carbene (NHC) increases the stability and efficiency of the catalyst precursors, thus affording a second generation of monometallic ruthenium initiators. Several vinylidene complexes $[\text{RuCl}_2(=\text{C}=\text{CHR})(\text{PCy}_3)(\text{NHC})]$ bearing mixed ligand sets made up of tricyclohexylphosphine (PCy_3) and *N*-heterocyclic carbenes promoted several RCM and ROMP reactions (Scheme 48) [170, 171].

More recently, Delaude and coworkers described the catalytic application in olefin metathesis of new homobimetallic ruthenium arene complexes bearing vinylidene ligands. The complex $[(\textit{p}$ -cymene) $\text{Ru}(\mu\text{-Cl})_3\text{RuCl}(=\text{C}=\text{CHPh})(\text{PCy}_3)]$ was synthesized and tested in metathesis reactions. Although its reaction with norbornene afforded high molecular weight polymers almost quantitatively, for the ROMP of cyclooctadiene it was necessary to use aluminum chloride as a cocatalyst. For the RCM of 1,6-dienes it was also necessary to use a cocatalyst, in this case phenylacetylene (Scheme 49) [172], homobimetallic ruthenium arene complexes bearing NHC instead of phosphine ligands were also reported as catalysts for metathesis. This second generation of homobimetallic ruthenium arene complexes displayed an enhanced metathetical activity in both the ROMP of cyclooctene and the RCM of 1,6-dienes (Scheme 49) [173].



Scheme 48 ROMP of norbornenes and RCM of α,ω -dienes catalyzed by NHC ruthenium vinylidene complexes



Scheme 49 ROMP of cyclic alkenes and RCM of α,ω -dienes catalyzed by homobimetallic ruthenium arene complexes

6 Ruthenium Allenylidenes in Catalysis

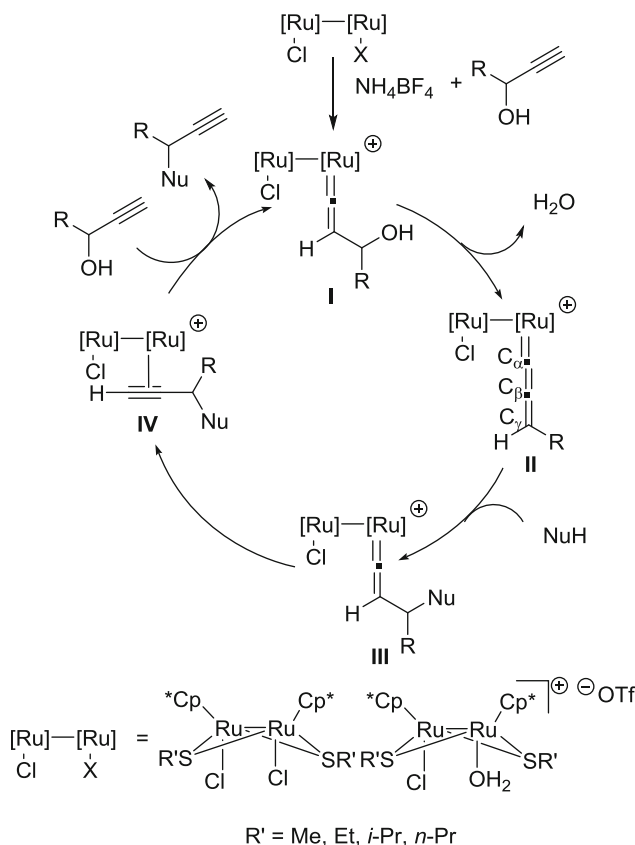
Allenylidenes ligands are divalent radicals derived from allenes and their metal derivatives can be easily obtained from terminal propargylic alcohols by dehydration of initially formed M-hydroxyvinylidenes [174]. Since the first report of the use of transition metal allenylidene complexes in catalytic reactions by Trost [94], significant progress in this field has been made [59, 64, 65, 175]. The reactivities of metal allenylidene complexes are rationalized by considering the electrophilicity of C α and C γ and the nucleophilicity of the M=C=C=CR $_2$ moiety.

6.1 Nucleophilic Addition to Allenylidenes C γ

The ability shown by transition metal allenylidenes to undergo nucleophilic additions at the C γ atom of the cumulenenic chain has been used to develop efficient catalytic processes for the direct substitution of the hydroxyl group in propargylic alcohols [175]. These studies were initiated [176] and further developed by Nishibayashi, Uemura and Hidai using as catalyst precursors the thiolate-bridged diruthenium(III) complexes [Cp* $\text{RuCl}(\mu\text{-SR})_2$] (R=Me, Et, *n*-Pr, *i*-Pr) and [Cp* $\text{RuCl}(\mu\text{-SR})_2\text{-RuCp}^*(\text{OH})_2$]OTf. The proposed mechanism requires the generation of allenylidene **II** by dehydration of the initially formed vinylidene **I** by treatment of the corresponding propargylic alcohol with the diruthenium complex in the presence of NH $_4$ BF $_4$. Nucleophilic attack at the C γ of the allenylidene **II** would afford vinylidene species **III**, which after tautomerization to the η^2 -coordinated alkyne-ruthenium **IV** would afford the propargylic-substituted product with recovery of the catalytic species (Scheme 50).

The nucleophilic substitution of the hydroxy group in propargylic alcohols with a variety of heteroatom-centered nucleophiles, such as alcohols, amines, amides, and diphenylphosphine oxide, to give the corresponding propargylic-substituted products with complete selectivity has been conveniently exploited [177]. One interesting modification of this methodology arises from the reaction of 1-cyclopropyl-2-propyn-1-ols with nitrogen- and oxygen-centered nucleophiles such as anilines and water to afford functionalized conjugated enynes (Scheme 51) [178].

Nishibayashi and Sakata recently described the Ru-catalyzed [3+2] cycloaddition of ethynylcyclopropanes bearing two carboxy groups at the homopropargylic position with aldehydes and aldimines to afford 2-ethynyltetrahydrofurans and pyrrolidines (Scheme 52) [179]. The proposed mechanism requires the formation of the ruthenium allenylidene species **II** by isomerization of the initially formed vinylidene **I**. Nucleophilic attack of species **II** to the aldehyde or aldimine, which are activated by BF $_3$ ·OEt $_2$, would afford allenylidene **III**. Final nucleophilic attack on the C γ by the oxygen or nitrogen followed by tautomerization of the vinylidene

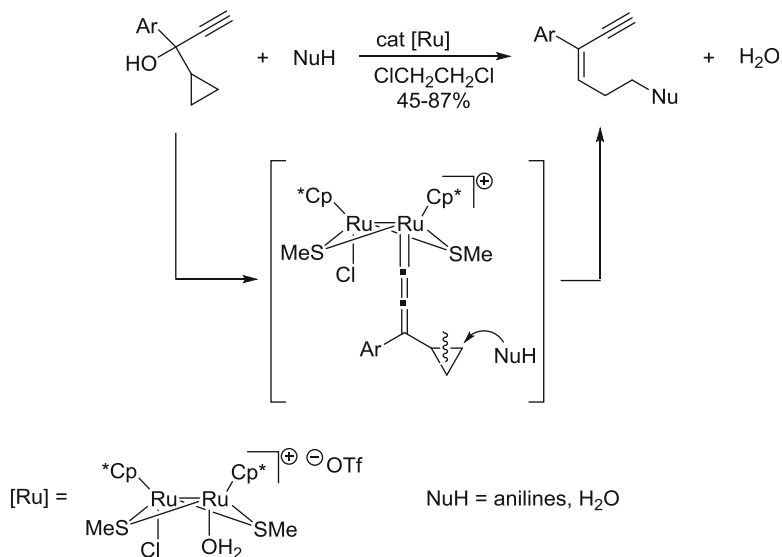


Scheme 50 Nucleophilic substitution of the hydroxy group in propargylic alcohols catalyzed by thiolate-bridged diruthenium(III) complexes

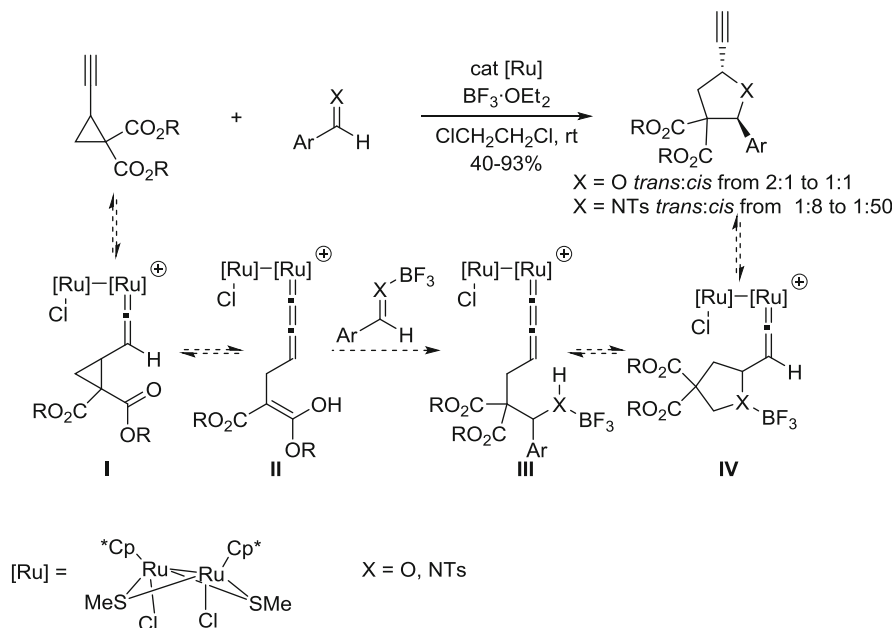
species **IV** would give rise to the corresponding 2-ethynyltetrahydrofurans and pyrrolidines, respectively.

The propargylic substitution with carbon-centered nucleophiles such as acetone has been reported to give γ -ketoalkynes [180, 181], heteroaromatic compounds such as furans, thiophenes, pyrroles, and indoles and electron-rich arenes such as anilines, 1,3,5-trimethoxybenzene, 3,5-dimethoxyacetanilide, and azulene [182, 183]. The asymmetric version of the propargylic alcohol substitution with acetone [184] and hetero- and aromatic compounds [185–187] was achieved using a diruthenium complex incorporating a bridging chiral thiolate ligand (Scheme 53). The chiral induction of the process is believed to be determined by favorable π – π interactions between one of the aromatic rings of the thiolate ligand and the aryl substituent of the alkynol in the corresponding allenylidene intermediate.

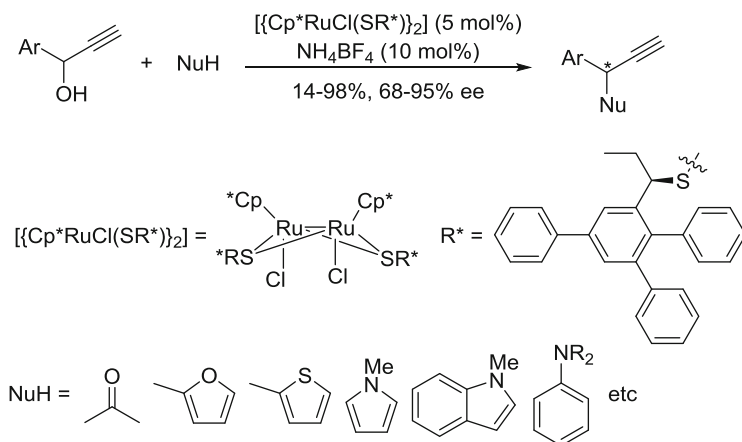
The enantioselective propargylic alkylation of propargylic alcohols with aldehydes [188] or β -ketoesters [189] has recently been accomplished by cooperative catalytic reactions using a thiolate-bridged diruthenium complex and a chiral



Scheme 51 Conjugated enynes from Ru-catalyzed nucleophilic opening of 1-cyclopropyl-2-propyn-1-ols



Scheme 52 Ru-catalyzed [3+2] cycloaddition of ethynylcyclopropanes with aldehydes and aldimines to 2-ethynyltetrahydrofurans and pyrrolidines



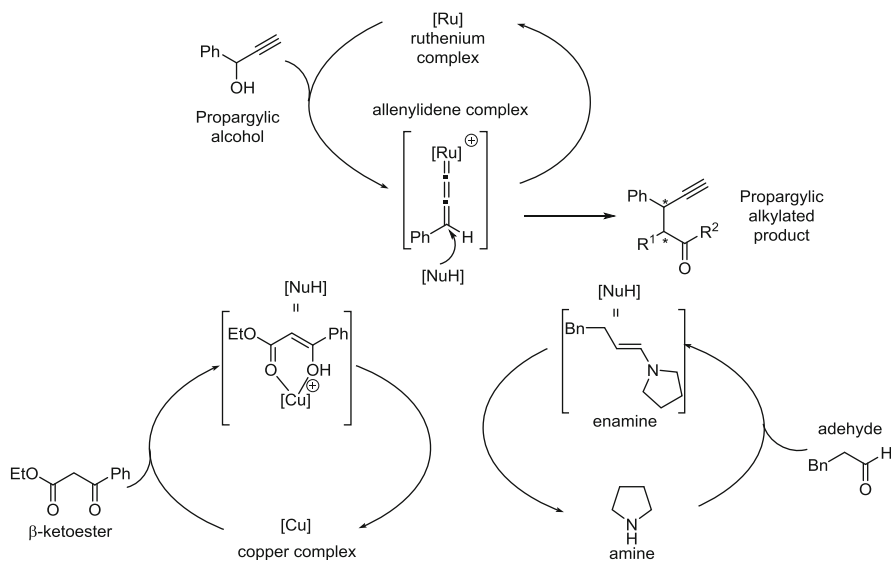
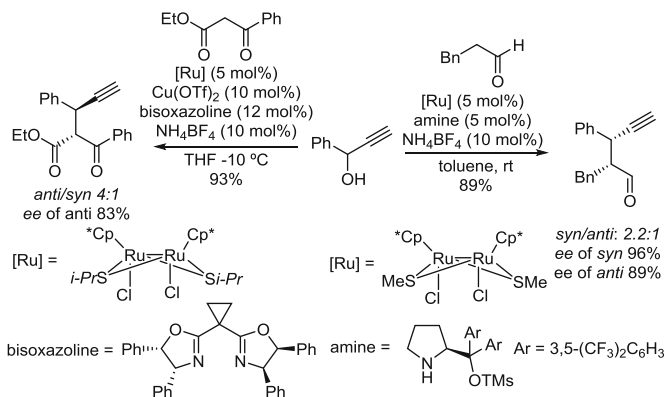
Scheme 53 Enantioselective nucleophilic substitution in aromatic propargylic alcohols catalyzed by chiral thiolate-bridged diruthenium(III) complexes

organocatalyst in the former case or a chiral copper complex in the latter. In both cases, the ruthenium complex activates the propargylic alcohols to afford the corresponding ruthenium allenylidene while aldehydes and β -ketoesters are activated by the chiral organocatalyst and the chiral copper complex, respectively (Scheme 54).

6.2 Nucleophilic Addition to Allenylidenes $\text{C}\alpha$

The electrophilic $\text{C}\alpha$ of allenylidenes is prone to add nucleophiles like ruthenium vinylidenes. The unsaturated $16e^-$ complex $[\text{Ru}(\eta^3\text{-2-C}_3\text{H}_4\text{Me})(\text{CO})(\text{dppf})][\text{SbF}_6]$ efficiently catalyzes the isomerization of both tertiary and secondary terminal propargylic alcohols into the corresponding enals or α,β -unsaturated methyl ketones (Scheme 55) [190, 191]. The proposed mechanism involves the initial formation of the ruthenium vinylidene **I**, which evolves to the corresponding allenylidene **II** if the propargylic alcohol does not bear a hydrogen in the β -position to the hydroxy group. Nucleophilic addition of water to the allenylidene $\text{C}\alpha$ followed by tautomerization would afford acyl-ruthenium species **III**, which after protonolysis would give rise to the corresponding enal. Conversely, if the propargylic alcohol bears a hydrogen in the β -position to the hydroxy group, vinylidene **I** would undergo an elimination to give the new conjugated vinylidene species **IV**. Tautomerization to the corresponding Ru-alkyne complex **V** followed by Markovnikov hydration would afford the corresponding α,β -unsaturated methyl ketone.

If the same reaction is performed in the presence of an enolizable ketone, the initially formed enal can undergo an aldol-type condensation to afford the

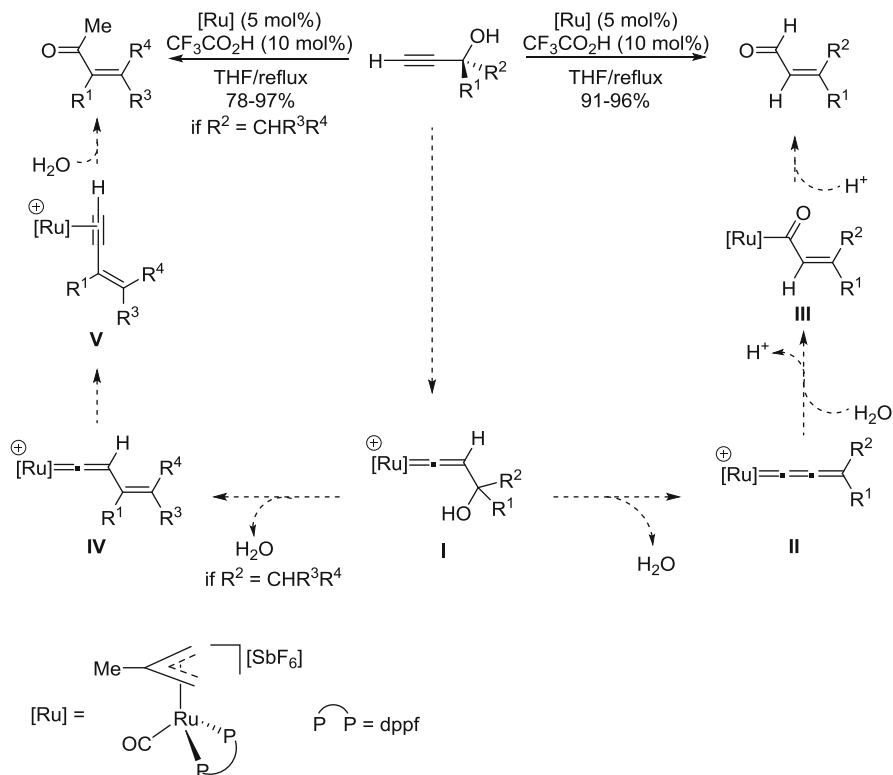


Scheme 54 Enantioselective propargylic alkylation with aldehydes or β -ketoesters catalyzed by chiral thiolate-bridged diruthenium(III) complexes

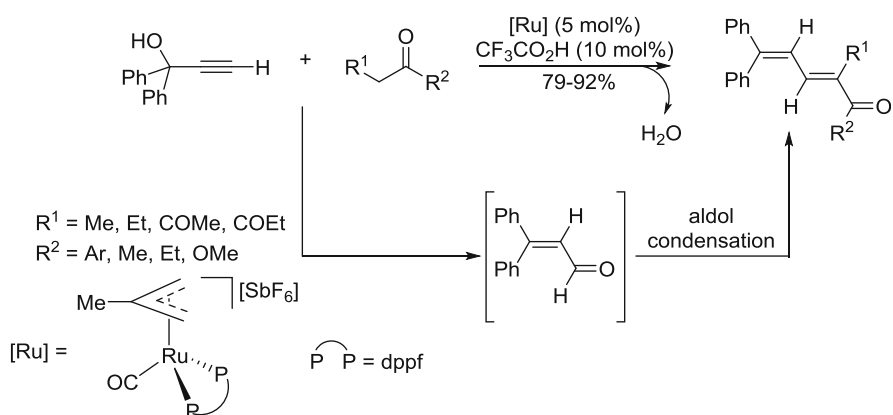
corresponding dienone, which can formally be regarded as a nucleophilic addition of a carbon-centered nucleophile to the $C\alpha$ of an allenylidene (Scheme 56) [192].

6.3 Pericyclic Reactions with Ruthenium Allenylidenes

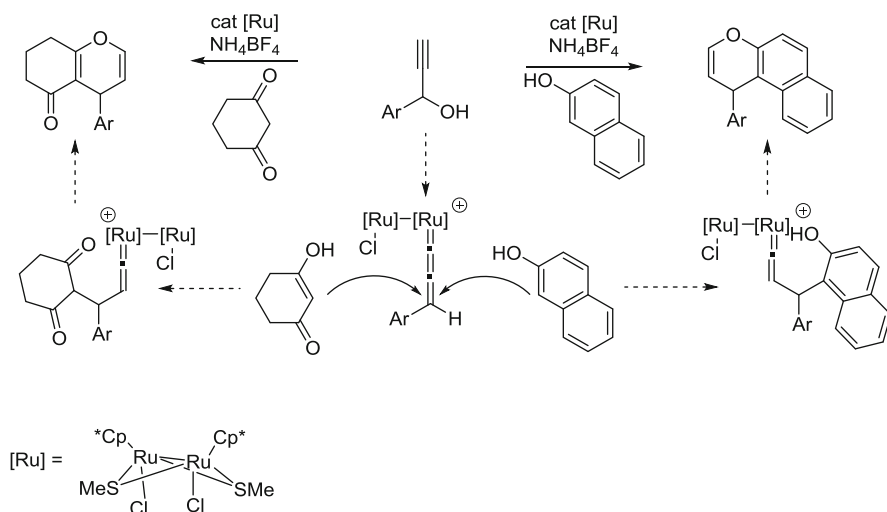
The π system of ruthenium allenylidenes can also participate in pericyclic reactions such as cycloadditions and ene reactions to afford functionalized polycyclic products.



Scheme 55 Ru-catalyzed isomerization of propargylic alcohols into enals or α,β -unsaturated methyl ketones



Scheme 56 Ru-catalyzed condensation of propargylic alcohols with enolizable ketones into dienones



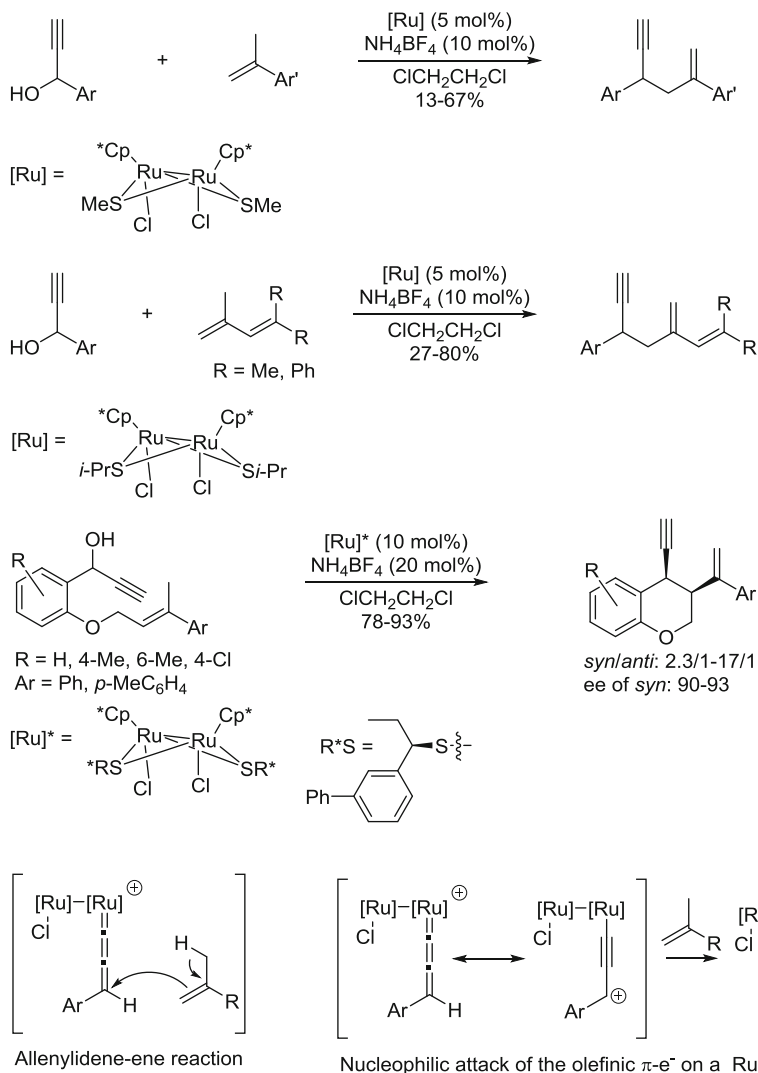
Scheme 57 Ru-catalyzed [3+3] cycloaddition between propargylic alcohols and cyclic 1,3-dicarbonyl compounds to 4,6,7,8-tetrahydrochromen-5-ones and with 2-naphthols to 1*H*-naphtho[2,1-*b*]pyrans

6.3.1 Cycloadditions

Thiolate-bridged diruthenium complexes catalyze the [3+3] cycloaddition reaction between propargylic alcohols and cyclic 1,3-dicarbonyl compounds to afford 4,6,7,8-tetrahydrochromen-5-ones or 4*H*-cyclopenta[*b*]pyran-5-ones [193] and with 2-naphthols or phenols to afford 1*H*-naphtho[2,1-*b*]pyrans and 4*H*-1-benzopyrans, respectively [194]. This cycloaddition is considered to proceed by stepwise propargylation and intramolecular cyclization (carbon and oxygen nucleophile additions) reactions, where ruthenium allenylidene and vinylidene complexes are the key intermediates (Scheme 57). Enantioselective ruthenium-catalyzed [3+3] cycloaddition of propargylic alcohols with 2-naphthols has also been described [195].

6.3.2 Allenylidene-ene Reactions

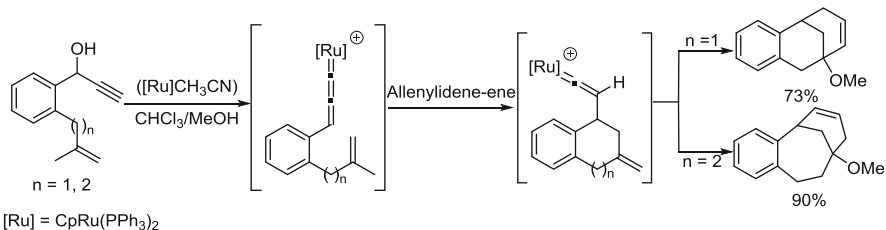
Inter- and intramolecular additions of alkenes and dienes to propargylic alcohols catalyzed by thiolate-bridged diruthenium complexes have been described. The processes, a kind of allenylidene-ene reaction, generate 1,5-enynes and dienynes by reaction of propargylic alcohols with 2-arylpropenes [196] and 1,3-conjugated dienes [197], respectively. The intramolecular version of this reaction has been developed to give diastereo- [196, 198] or enantioselective *syn*-substituted chromanes (Scheme 58) [199]. Recently, the results of DFT calculations indicated that nucleophilic attack of the olefinic π -electrons on a carbocationic



Scheme 58 Ru-catalyzed inter- and intramolecular additions of alkenes and dienes to propargylic alcohols to 1,5-enynes and dienyne

ruthenium-alkynyl $[\text{Ru}]-\text{C}\equiv\text{C}-\text{C}^+\text{HR}$ complex, a resonance structure of the allenylidene intermediate $[\text{Ru}]^+=\text{C}=\text{C}=\text{CHR}$, is clearly involved in the catalytic cycle [200].

Lin and coworkers described the formation of 5,9-methanobenzoannulenes by $[(\text{CpRu}(\text{PPh}_3)_2(\text{CH}_3\text{CN}))^+]$ -catalyzed allenylidene-ene reactions of *ortho*-propenyl and *ortho*-butenylphenyl propargyl alcohols. The processes probably involve the initial formation of aromatic vinylidenes as intermediates and these undergo nucleophilic attack by the pendant olefinic double bonds and final trapping with



Scheme 59 Ru-catalyzed allenylidene-ene reactions of *ortho*-propenyl and *ortho*-butenylphenyl propargyl alcohols to 5,9-methanobenzoannulenes

MeOH (Scheme 59) [145]. Similar cyclizations of enynes containing thioether or ether linkages have recently been described [201].

6.4 Allenylideneruthenium Catalysts in Metathesis

Allenylideneruthenium complexes, which are readily available and easy to handle, have become an alternative to the alkylideneruthenium complexes (the Grubbs catalyst family) in alkene metathesis [56, 59, 64, 65, 202, 203]. The first catalytic applications of allenylidene complexes in alkene metathesis were described by Dixneuf's and Fürstner's groups, who used several well-defined 18-electron cationic ruthenium allenylidene complexes $[\text{RuCl}(\text{=C=C=CAr}_2)(\eta^6\text{-}p\text{-cymene})\text{PR}_3][\text{X}]$ (**A**, Fig. 1) [204–206]. Since then, electronic modifications on these cationic complexes have been studied thoroughly [207, 208]. The following general trends were observed: (1) the activity increases with the electron richness and size of the phosphine ligand in the order $\text{PCy}_3 > \text{P}i\text{-Pr}_3 \gg \text{PPh}_3$; (2) the nature of the counteranion of these ionic precursors has a dramatic influence on the catalytic activity, which increases in the order $\text{TfO}^- \gg \text{PF}_6^- \approx \text{BF}_4^-$; (3) several 3,3-diaryllallenylidene ligands proved to be efficient, but the most simple 3,3-diphenylallenylideneruthenium derivatives led to the best performances. Modifications in the initial 18-electron cationic allenylidene complexes by using a chelate $\eta^6\text{-arene} \eta^1\text{-carbene}$ allenylidene ruthenium complex generated in situ (**B**, Fig. 1) showed high activity and selectivity in some RCM reactions, with a strong influence of the diene and the solvent [209].

Nolan and coworkers reported RCM reactions of neutral allenylideneruthenium complexes with a 16-electron metal center configuration, $(\text{PCy}_3)_2\text{Cl}_2\text{Ru}(\text{=C=C=CPh}_2)$ (**C**, Fig. 1), and its second generation analogs bearing an *N*-heterocyclic carbene ligand, $(\text{PCy}_3)(\text{IMes})\text{Cl}_2\text{Ru}(\text{=C=C=CPh}_2)$ (**D**, Fig. 1) [210]. Other ligand modifications and their influence in RCM reaction were investigated more recently [211, 212].

Cationic allenylideneruthenium complexes with a 16-electron metal center $[\text{RuCl}(\text{=C=C=CPh}_2)(\text{PCy}_3)(\text{DMSO})_2][\text{OTf}]$ and with 18-electron neutral $[\text{RuCl}_2(\text{=C=C=CPh}_2)(\text{PCy}_3)_2(\text{DMSO})]$ and $[\text{RuCl}_2(\text{=C=C=CPh}_2)(\text{PCy}_3)(\text{DMSO})_2]$ and cationic $[\text{RuCl}(\text{=C=C=CPh}_2)(\text{PCy}_3)_2(\text{DMSO})_2][\text{OTf}]$ systems

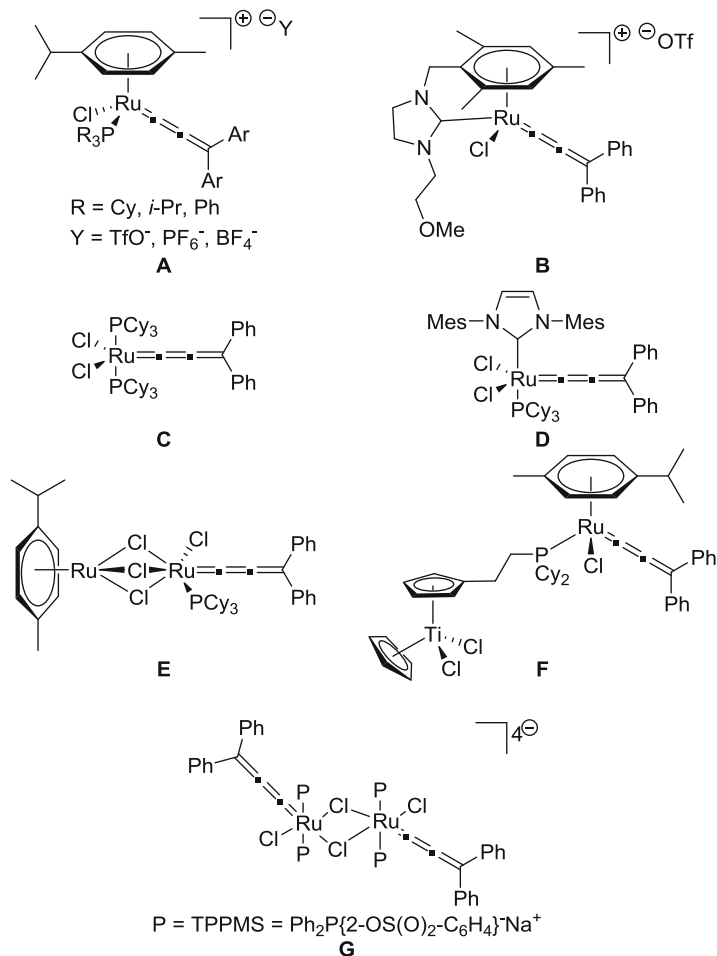


Fig. 1 Allenylideneruthenium catalysts used in metathesis

were tested in ROMP of cyclic olefins, but their efficiencies were found to be lower than those obtained with catalysts of type **A** in Fig. 1 [213, 214].

Homobimetallic ruthenium allenylidene complex [(*p*-cymene)Ru(μ-Cl)₃RuCl(PCy₃)(η²-C₂H₄)] (**E**, Fig. 1) was synthesized and tested in RCM reactions [215]. However, later investigations revealed that the final catalysts formed were actually phenylindenyliideneruthenium complexes rather than allenylidene analogs [216–218]. This latter homobimetallic ruthenium allenylidene complex was finally synthesized along with other ruthenium homobimetallic complexes and they were tested as catalysts in olefin metathesis [219]. Heterobimetallic allenylidene titanium–ruthenium complexes (**F**, Fig. 1) have also shown catalytic activity in RCM reactions [220].

Biocompatible water-soluble ruthenium allenylidenes (**G**, Fig. 1) [166] and complexes of type A in ionic liquids have also been described [207, 221].

7 Conclusion

The formation of catalytic ruthenium vinylidenes and allenylidenes has been revealed as one of the most powerful methods for the activation of compounds bearing terminal alkynes and propargylic alcohols, respectively. The chemical properties of the catalytic ruthenium vinylidenes and allenylidenes generated in situ change to the reactivity of free alkynes, thus allowing new and selective reactions to be carried out with atom economy and significantly increased complexity. This reactivity hinges on the electrophilic character of the C α in vinylidenes as well as C α and C γ of allenylidenes and the capacity of the electronic π -system of both metallic intermediates to participate in pericyclic reactions.

References

1. Bruce MI, Swincer AG (1983) *Adv Organomet Chem* 22:59
2. Antonova AB, Ioganson AA (1989) *Russ Chem Rev* 58:1197
3. Davies SG, McNally JP, Smallridge AJ (1990) *Adv Organomet Chem* 30:1
4. Bruce MI (1991) *Chem Rev* 91:197
5. Bruce MI (1998) *Chem Rev* 98:2797
6. Mills OS, Redhouse AD (1968) *J Chem Soc A* 1282
7. Mills OS, Redhouse AD (1966) *Chem Commun* 444
8. Puerta MC, Valerga P (1999) *Coord Chem Rev* 193–195:977
9. Cadierno V, Gamasa MP, Gimeno J (2004) *Coord Chem Rev* 248:1627
10. Wakatsuki Y (2004) *J Organomet Chem* 689:4092
11. Lynam JM (2010) *Chem Eur J* 16:8238
12. Swennenhuis BHG, Cieslinski GB, Brothers EN, Bengali AA (2010) *J Organomet Chem* 695:891
13. Wang Q, Wang X, Andrews L (2011) *J Phys Chem A* 115:12194
14. Wakatsuki Y, Koga N, Yamazaki H, Morokuma K (1994) *J Am Chem Soc* 116:8105
15. Tokunaga M, Suzuki T, Koga N, Fukushima T, Horiuchi A, Wakatsuki Y (2001) *J Am Chem Soc* 123:11917
16. De Angelis F, Sgamellotti A, Re N (2002) *Organometallics* 21:5944
17. De Angelis F, Sgamellotti A, Re N (2002) *Organometallics* 21:2715
18. Wakatsuki Y, Koga N, Werner H, Morokuma K (1997) *J Am Chem Soc* 119:360
19. Pérez-Carreño E, Paoli P, Ineco A, Mealli C (1999) *Eur J Inorg Chem* 1315
20. Vastine BA, Hall MB (2008) *Organometallics* 27:4325
21. Grotjahn DB, Zeng X, Cooksy AL (2006) *J Am Chem Soc* 128:2798
22. Grotjahn DB, Zeng X, Cooksy AL, Kassel WS, DiPasquale AG, Zakharov LN, Rheingold AL (2007) *Organometallics* 26:3385
23. De Angelis F, Sgamellotti A, Re N (2007) *Organometallics* 26:5285
24. Oliván M, Clot E, Eisenstein O, Caulton KG (1998) *Organometallics* 17:3091
25. Schneider D, Werner H (1991) *Angew Chem Int Ed Engl* 30:700

26. Sakurai H, Fujii T, Sakamoto K (1992) *Chem Lett* 339
27. Werner H, Baum M, Schneider D, Windmüller B (1994) *Organometallics* 13:1089
28. Connelly NG, Geiger WE, Lagunas C, Metz B, Rieger AL, Rieger PH, Shaw MJ (1995) *J Am Chem Soc* 117:12202
29. Naka A, Okazaki S, Hayashi M, Ishikawa M (1995) *J Organomet Chem* 499:35
30. Onitsuka K, Katayama H, Sonogashira K, Ozawa F (1995) *J Chem Soc Chem Commun* 2267
31. Katayama H, Onitsuka K, Ozawa F (1996) *Organometallics* 15:4642
32. Werner H, Lass RW, Gevert O, Wolf J (1997) *Organometallics* 16:4077
33. Katayama H, Ozawa F (1998) *Organometallics* 17:5190
34. Huang D, Streib WE, Eisenstein O, Caulton KG (2000) *Organometallics* 19:1967
35. Foerstner J, Kakoschke A, Goddard R, Rust J, Warchow R, Butenschön H (2001) *J Organomet Chem* 617–618:412
36. Murakami M, Hori S (2003) *J Am Chem Soc* 125:4720
37. Jiménez MV, Sola E, Lahoz FJ, Oro LA (2005) *Organometallics* 24:2722
38. Ilg K, Paneque M, Poveda ML, Rendón N, Santos LL, Carmona E, Mereiter K (2006) *Organometallics* 25:2230
39. Konkol M, Steinborn D (2006) *J Organomet Chem* 691:2839
40. Lass RW, Werner H (2011) *Inorg Chim Acta* 369:288
41. Venkatesan K, Blacque O, Fox T, Alfonso M, Schmalte HW, Kheradmandan S, Berke H (2005) *Organometallics* 24:920
42. Venkatesan K, Fox T, Schmalte HW, Berke H (2005) *Eur J Inorg Chem* 2005:901
43. Miller DC, Angelici RJ (1991) *Organometallics* 10:79
44. Löwe C, Hund H-U, Berke H (1989) *J Organomet Chem* 371:311
45. Miura T, Iwasawa N (2002) *J Am Chem Soc* 124:518
46. Miura T, Murata H, Kiyota K, Kusama H, Iwasawa N (2004) *J Mol Catal A* 213:59
47. Shaw MJ, Bryant SW, Rath N (2007) *Eur J Inorg Chem* 3943
48. Ikeda Y, Yamaguchi T, Kanao K, Kimura K, Kamimura S, Mutoh Y, Tanabe Y, Ishii Y (2008) *J Am Chem Soc* 130:16856
49. Mutoh Y, Ikeda Y, Kimura Y, Ishii Y (2009) *Chem Lett* 38:534
50. de los Ríos I, Bustelo E, Puerta MC, Valerga P (2010) *Organometallics* 29:1740
51. Mutoh Y, Imai K, Kimura Y, Ikeda Y, Ishii Y (2011) *Organometallics* 30:204
52. Singh VK, Bustelo E, de los Ríos I, Macías-Arce I, Puerta MC, Valerga P, Ortuño MA, Ujaque G, Lledós A (2011), *Organometallics* 30:4014
53. Mutoh Y, Kimura Y, Ikeda Y, Tsuchida N, Takano K, Ishii Y (2012) *Organometallics* 31:5150
54. Otsuka M, Tsuchida N, Ikeda Y, Kimura Y, Mutoh Y, Ishii Y, Takano K (2012) *J Am Chem Soc* 134:17746
55. Fishmeister C, Bruneau C, Dixneuf PH (2004) Nucleophilic additions to alkynes and reactions via vinylidene intermediates. In: Murahashi SI (ed) *Ruthenium in organic synthesis*. Wiley-VCH, Weinheim, Chap 8
56. Bruneau C (2004) *Top Organomet Chem* 11:125
57. Katayama H, Ozawa F (2004) *Coord Chem Rev* 248:1703
58. Dragutan V, Dragutan I (2004) *Platin Met Rev* 48:148
59. Bruneau C, Dixneuf PH (2006) *Angew Chem Int Ed* 45:2176
60. Varela JA, Saá C (2006) *Chem Eur J* 12:6450
61. Varela JA, González-Rodríguez C, Rubín SG, Castedo L, Saá C (2008) *Pure Appl Chem* 80:1167
62. Trost BM, McClory A (2008) *Chem Asian J* 3:164
63. Liu R-S (2008) *Synlett* 801
64. Bruneau C, Dixneuf PH (2008) Metal vinylidenes and allenylidenes in catalysis: from reactivity to applications in synthesis. Wiley-VCH, Weinheim
65. Lozano-Vila AM, Monsaert S, Bajek A, Verpoort F (2010) *Chem Rev* 110:4865
66. Sasaki Y, Dixneuf PH (1986) *J Chem Soc Chem Commun* 790

67. Mahe R, Dixneuf PH, Lecolier S (1986) *Tetrahedron Lett* 27:6333
68. Sasaki Y, Dixneuf PH (1987) *J Org Chem* 52:314
69. Bruneau C, Dixneuf PH, Lecolier S (1988) *J Mol Catal* 44:175
70. Mahe R, Sasaki Y, Bruneau C, Dixneuf PH (1989) *J Org Chem* 54:1518
71. Höfer J, Doucet H, Bruneau C, Dixneuf PH (1991) *Tetrahedron Lett* 32:7409
72. Bruneau C, Dixneuf PH (1992) *J Mol Catal* 74:97
73. Ruppin C, Dixneuf PH (1986) *Tetrahedron Lett* 27:6323
74. Doucet H, Höfer J, Bruneau C, Dixneuf PH (1993) *J Chem Soc Chem Commun* 850
75. Doucet H, Martin-Vaca B, Bruneau C, Dixneuf PH (1995) *J Org Chem* 60:7247
76. Doucet H, Höfer J, Derrien N, Bruneau C, Dixneuf PH (1996) *Bull Soc Chim Fr* 133:939
77. Goossen LJ, Paetzold J, Koley D (2003) *Chem Commun* 706
78. Jiménez-Tenorio M, Puerta MC, Valerga P, Moreno-Dorado FJ, Guerra FM, Massanet GM (2001) *Chem Commun* 2324
79. Melis K, Samulkiewicz P, Rynkowski J, Verpoort F (2002) *Tetrahedron Lett* 43:2713
80. Picquet M, Bruneau C, Dixneuf PH (1997) *Chem Commun* 1201
81. Picquet M, Fernández A, Bruneau C, Dixneuf PH (2000) *Eur J Org Chem* 2361
82. Tokunaga M, Wakatsuki Y (1998) *Angew Chem Int Ed* 37:2867
83. Suzuki T, Tokunaga M, Wakatsuki Y (2001) *Org Lett* 3:735
84. Grotjahn DB, Incarvito CD, Rheingold AL (2001) *Angew Chem Int Ed* 40:3884
85. Chevallier F, Breit B (2006) *Angew Chem Int Ed* 45:1599
86. Grotjahn DB, Lev DA (2004) *J Am Chem Soc* 126:12232
87. Labonne A, Kribber T, Hintermann L (2006) *Org Lett* 8:5853
88. Hintermann L, Dang TT, Labonne A, Kribber T, Xiao L, Naumov P (2009) *Chem Eur J* 15:7167
89. Boeck F, Kribber T, Xiao L, Hintermann L (2011) *J Am Chem Soc* 133:8138
90. Labonne A, Zani L, Hintermann L, Bolm C (2007) *J Org Chem* 72:5704
91. Kribber T, Labonne A, Hintermann L (2007) *Synthesis* 2007:2809
92. Trost BM, Dyker G, Kulawiec RJ (1990) *J Am Chem Soc* 112:7809
93. Trost BM, Kulawiec RJ (1992) *J Am Chem Soc* 114:5579
94. Trost BM, Flygare JA (1992) *J Am Chem Soc* 114:5476
95. Trost BM, Kulawiec RJ, Hammes A (1993) *Tetrahedron Lett* 34:587
96. Trost BM, Flygare JA (1994) *J Org Chem* 59:1078
97. McDonald FE (1999) *Chem Eur J* 5:3103
98. McDonald FE, Reddy KS (2001) *J Organomet Chem* 617–618:444
99. Trost BM, Rhee YH (1999) *J Am Chem Soc* 121:11680
100. Trost BM, Rhee YH (2002) *J Am Chem Soc* 124:2528
101. Zacuto MJ, Tomita D, Pirzada Z, Xu F (2010) *Org Lett* 12:684
102. Liu PN, Su FH, Wen TB, Sung HHY, Williams ID, Jia G (2010) *Chem Eur J* 16:7889
103. Liu PN, Wen TB, Ju KD, Sung HHY, Williams ID, Jia G (2011) *Organometallics* 30:2571
104. Varela-Fernández A, González-Rodríguez C, Varela JA, Castedo L, Saá C (2009) *Org Lett* 11:5350
105. Nair RN, Lee PJ, Rheingold AL, Grotjahn DB (2010) *Chem Eur J* 16:7992
106. Alcázar E, Pletcher JM, McDonald FE (2004) *Org Lett* 6:3877
107. Koo B, McDonald FE (2007) *Org Lett* 9:1737
108. Varela-Fernández A, García-Yebra C, Varela JA, Esteruelas MA, Saá C (2010) *Angew Chem Int Ed* 49:4278
109. Lo C-Y, Guo H, Lian J-J, Shen F-M, Liu R-S (2002) *J Org Chem* 67:3930
110. Madhushaw RJ, Lin M-Y, Sohel SMA, Liu R-S (2004) *J Am Chem Soc* 126:6895
111. Lin M-Y, Maddirala SJ, Liu R-S (2005) *Org Lett* 7:1745
112. Koelle U, Rietmann C, Tjoe J, Wagner T, Englert U (1995) *Organometallics* 14:703
113. Fukumoto Y, Dohi T, Masaoka H, Chatani N, Murai S (2002) *Organometallics* 21:3845
114. Goossen LJ, Rauhaus JE, Deng G (2005) *Angew Chem Int Ed* 44:4042

115. Goossen LJ, Arndt M, Blanchot M, Rudolphi F, Menges F, Niedner-Schatteburg G (2008) *Adv Synth Catal* 350:2701
116. Buba AE, Arndt M, Goossen LJ (2010) *J Organomet Chem* 696:170
117. Goossen LJ, Salih KS, Blanchot M (2008) *Angew Chem Int Ed* 47:8492
118. Goossen LJ, Blanchot M, Salih KSM, Karch R, Rivas-Nass A (2008) *Org Lett* 10:4497
119. Goossen LJ, Blanchot M, Brinkmann C, Goossen K, Karch R, Rivas-Nass A (2006) *J Org Chem* 71:9506
120. Arndt M, Salih KSM, Fromm A, Goossen LJ, Menges F, Niedner-Schatteburg G (2011) *J Am Chem Soc* 133:7428
121. Varela-Fernández A, Varela JA, Saá C (2011) *Adv Synth Catal* 353:1933
122. Varela-Fernández A, Varela JA, Saá C (2012) *Synthesis* 44:3285
123. Jérôme F, Monnier F, Lawicka H, Dérien S, Dixneuf PH (2003) *Chem Commun* 696
124. Bianchini C, Peruzzini M, Zanobini F, Frediani P, Albinati A (1991) *J Am Chem Soc* 113:5453
125. Bianchini C, Frediani P, Masi D, Peruzzini M, Zanobini F (1994) *Organometallics* 13:4616
126. Yamazaki H (1976) *J Chem Soc Chem Commun* 841
127. Wakatsuki Y, Yamazaki H, Kumegawa N, Satoh T, Satoh JY (1991) *J Am Chem Soc* 113:9604
128. Wakatsuki Y, Yamazaki H (1995) *J Organomet Chem* 500:349
129. Slugovc C, Mereiter K, Zobetz E, Schmid R, Kirchner K (1996) *Organometallics* 15:5275
130. Slugovc C, Doberer D, Gemel C, Schmidt R, Kirchner K, Winkler B, Stelzer F (1998) *Monatsh Chem* 129:221
131. Pavlik S, Gemel C, Slugovc C, Mereiter K, Schmid R, Kirchner K (2001) *J Organomet Chem* 617–618:301
132. Jiménez-Tenorio MA, Jiménez-Tenorio M, Puerta MC, Valerga P (2000) *Organometallics* 19:1333
133. Fryzuk MD, Jonker MJ, Rettig SJ (1997) *Chem Commun* 377
134. Bassetti M, Marini S, Tortorella F, Cadierno V, Diez J, Gamasa MP, Gimeno J (2000) *J Organomet Chem* 593–594:292
135. Melis K, De Vos D, Jacobs P, Verpoort F (2002) *J Organomet Chem* 659:159
136. Lee J-H, Caulton KG (2008) *J Organomet Chem* 693:1664
137. Yi CS, Liu N (1996) *Organometallics* 15:3968
138. Yi CS, Liu N (1999) *Synlett* 281
139. Chen X, Xue P, Sung HHY, Williams ID, Peruzzini M, Bianchini C, Jia G (2005) *Organometallics* 24:4330
140. Katayama H, Yari H, Tanaka M, Ozawa F (2005) *Chem Commun* 4336
141. Katayama H, Nakayama M, Nakano T, Wada C, Akamatsu K, Ozawa F (2004) *Macromolecules* 37:13
142. Shen H-C, Pal S, Lian J-J, Liu R-S (2003) *J Am Chem Soc* 125:15762
143. Madhushaw RJ, Lo C-Y, Hwang C-W, Su M-D, Shen H-C, Pal S, Shaikh IR, Liu R-S (2004) *J Am Chem Soc* 126:15560
144. Fukamizu K, Miyake Y, Nishibayashi Y (2009) *Angew Chem Int Ed* 48:2534
145. Ma H-W, Lin Y-C, Huang S-L (2012) *Org Lett* 14:3846
146. Gunanathan C, Hölscher M, Pan F, Leitner W (2012) *J Am Chem Soc* 134:14349
147. Chen Y, Ho DM, Lee C (2005) *J Am Chem Soc* 127:12184
148. Varela JA, González-Rodríguez C, Rubín SG, Castedo L, Saá C (2006) *J Am Chem Soc* 128:9576
149. González-Rodríguez C, Varela JA, Castedo L, Saá C (2007) *J Am Chem Soc* 129:12916
150. Kim H, Goble SD, Lee C (2007) *J Am Chem Soc* 129:1030
151. Merlic CA, Pauly ME (1996) *J Am Chem Soc* 118:11319
152. Lian JJ, Odedra A, Wu CJ, Liu RS (2005) *J Am Chem Soc* 127:4186
153. Pati K, Liu R-S (2009) *Chem Commun* 5233
154. Murakami M, Ubukata M, Ito Y (1998) *Tetrahedron Lett* 39:7361

155. Murakami M, Ubukata M, Ito Y (2002) *Chem Lett* 294
156. Johnson DG, Lynam JM, Mistry NS, Slattery JM, Thatcher RJ, Whitwood AC (2013) *J Am Chem Soc* 135:2222
157. Elakkari E, Floris B, Galloni P, Tagliatesta P (2005) *Eur J Org Chem* 889
158. Datta S, Odedra A, Liu RS (2005) *J Am Chem Soc* 127:11606
159. Odedra A, Datta S, Liu RS (2007) *J Org Chem* 72:3289
160. Grubbs, RH (2003) *Handbook of metathesis*. Wiley-VCH, Weinheim
161. del Río I, van Koten G (1999) *Tetrahedron Lett* 40:1401
162. Katayama H, Urushima H, Ozawa F (2000) *J Organomet Chem* 606:16
163. Schwab P, Grubbs RH, Ziller JW (1996) *J Am Chem Soc* 118:100
164. Katayama H, Ozawa F (1998) *Chem Lett* 67
165. Katayama H, Yoshida T, Ozawa F (1998) *J Organomet Chem* 562:203
166. Saoud M, Romerosa A, Peruzzini M (2000) *Organometallics* 19:4005
167. Katayama H, Yonezawa F, Nagao M, Ozawa F (2002) *Macromolecules* 35:1133
168. Maya VG, Contreras AP, Canseco M-A, Tlenkopatchev MA (2001) *React Funct Polym* 49:145
169. Contreras AP, Cerda AM, Tlenkopatchev MA (2002) *Macromol Chem Phys* 203:1811
170. Louie J, Grubbs RH (2001) *Angew Chem Int Ed* 40:247
171. Opstal T, Verpoort F (2003) *J Mol Catal A Chem* 200:49
172. Borguet Y, Sauvage X, Zaragoza G, Demonceau A, Delaude L (2010) *Organometallics* 29:6675
173. Borguet Y, Sauvage X, Zaragoza G, Demonceau A, Delaude L (2011) *Organometallics* 30:2730
174. Selegue JP (1982) *Organometallics* 1:217
175. Nishibayashi Y, Uemura S (2006) *Curr Org Chem* 10:135
176. Nishibayashi Y, Wakiji I, Hidai M (2000) *J Am Chem Soc* 122:11019
177. Nishibayashi Y, Milton MD, Inada Y, Yoshikawa M, Wakiji I, Hidai M, Uemura S (2005) *Chem Eur J* 11:1433
178. Yamauchi Y, Onodera G, Sakata K, Yuki M, Miyake Y, Uemura S, Nishibayashi Y (2007) *J Am Chem Soc* 129:5175
179. Miyake Y, Endo S, Moriyama T, Sakata K, Nishibayashi Y (2013) *Angew Chem Int Ed* 52:1758
180. Nishibayashi Y, Wakiji I, Ishii Y, Uemura S, Hidai M (2001) *J Am Chem Soc* 123:3393
181. Nishibayashi Y, Imajima H, Onodera G, Inada Y, Hidai M, Uemura S (2004) *Organometallics* 23:5100
182. Nishibayashi Y, Yoshikawa M, Inada Y, Hidai M, Uemura S (2002) *J Am Chem Soc* 124:11846
183. Inada Y, Yoshikawa M, Milton MD, Nishibayashi Y, Uemura S (2006) *Eur J Org Chem* 881
184. Inada Y, Nishibayashi Y, Uemura S (2005) *Angew Chem Int Ed* 44:7715
185. Matsuzawa H, Miyake Y, Nishibayashi Y (2007) *Angew Chem Int Ed* 46:6488
186. Matsuzawa H, Kanao K, Miyake Y, Nishibayashi Y (2007) *Org Lett* 9:5561
187. Kanao K, Matsuzawa H, Miyake Y, Nishibayashi Y (2008) *Synthesis* 3869
188. Ikeda M, Miyake Y, Nishibayashi Y (2010) *Angew Chem Int Ed* 49:7289
189. Ikeda M, Miyake Y, Nishibayashi Y (2012) *Chem Eur J* 18:3321
190. Cadierno V, Díez J, García-Garrido SE, Gimeno J (2004) *Chem Commun* 2716
191. Cadierno V, García-Garrido SE, Gimeno J (2006) *Adv Synth Catal* 348:101
192. Cadierno V, Díez J, Garcia-Garrido SE, Gimeno J, Nebra N (2006) *Adv Synth Catal* 348:2125
193. Nishibayashi Y, Yoshikawa M, Inada Y, Hidai M, Uemura S (2004) *J Org Chem* 69:3408
194. Nishibayashi Y, Inada Y, Hidai M, Uemura S (2002) *J Am Chem Soc* 124:7900
195. Kanao K, Miyake Y, Nishibayashi Y (2010) *Organometallics* 29:2126
196. Nishibayashi Y, Inada Y, Hidai M, Uemura S (2003) *J Am Chem Soc* 125:6060

197. Daini M, Yoshikawa M, Inada Y, Uemura S, Sakata K, Kanao K, Miyake Y, Nishibayashi Y (2008) *Organometallics* 27:2046
198. Nishibayashi Y, Yoshikawa M, Inada Y, Hidai M, Uemura S (2004) *J Am Chem Soc* 126:16066
199. Fukamizu K, Miyake Y, Nishibayashi Y (2008) *J Am Chem Soc* 130:10498
200. Sakata K, Miyake Y, Nishibayashi Y (2009) *Chem Asian J* 4:81
201. Feng Y-J, Lo J-X, Lin Y-C, Huang S-L, Wang Y, Liu Y-H (2013) *Organometallics* 32:6379
202. Cadierno V, Gimeno J (2009) *Chem Rev* 109:3512
203. Nishibayashi Y (2012) *Synthesis* 44:489
204. Füstner A, Picquet M, Bruneau C, Dixneuf PH (1998) *Chem Commun* 1315
205. Picquet M, Touchard D, Bruneau C, Dixneuf PH (1999) *New J Chem* 23:141
206. Füstner A, Liebl M, Lehmann CW, Picquet M, Kunz R, Bruneau C, Touchard D, Dixneuf PH (2000) *Chem Eur J* 6:1847
207. Sémeril D, Olivier-Bourbigou H, Bruneau C, Dixneuf PH (2002) *Chem Commun* 146
208. Antonucci A, Bassetti M, Bruneau C, Dixneuf PH, Pasquini C (2010) *Organometallics* 29:4524
209. Çetinkaya B, Demir S, Özdemir I, Toupet L, Sémeril D, Bruneau C, Dixneuf PH (2003) *Chem Eur J* 9:2323
210. Schanz H-J, Jafarpour L, Stevens ED, Nolan SP (1999) *Organometallics* 18:5187
211. Ledoux N, Drozdak R, Allaert B, Linden A, Van DVP, Verpoort F (2007) *Dalton Trans* 5201
212. Lichtenheldt M, Kress S, Blechert S (2012) *Molecules* 17:5177
213. Alaoui AI, Sémeril D, Dixneuf PH (2002) *J Mol Catal A Chem* 182–183:577
214. Özdemir I, Demir S, Çetinkaya B, Toupet L, Castarlenas R, Fischmeister C, Dixneuf PH (2007) *Eur J Inorg Chem* 2862
215. Füstner A, Liebl M, Hill AF, Wilton-Ely JDET (1999) *Chem Commun* 601
216. Jafarpour L, Schanz H-J, Stevens ED, Nolan SP (1999) *Organometallics* 18:5416
217. Füstner A, Guth O, Duffels A, Seidel G, Liebl M, Gabor B, Mynott R (2001) *Chem Eur J* 7:4811
218. Sauvage X, Borguet Y, Zaragoza G, Demonceau A, Delaude L (2009) *Adv Synth Catal* 351:441
219. Sauvage X, Borguet Y, Demonceau A, Delaude L (2010) *Macromol Symp* 293:24
220. Le Gendre P, Picquet M, Richard P, Moïse C (2002) *J Organomet Chem* 643–644:231
221. Csihony S, Fischmeister C, Bruneau C, Horvath IT, Dixneuf PH (2002) *New J Chem* 26:1667

C–C Bond Formation on Activation of Alkynes and Alkenes with $(C_5R_5)Ru$ Catalysts

Sylvie Dérien

Abstract Electron-rich ruthenium(II) catalysts of type $(C_5R_5)XRuL_n$ are used to perform selective carbon–carbon bond formation by combination of simple substrates such as the coupling of functional alkynes and alkenes with a variety of unsaturated molecules (alkynes, diynes, alkenes, dienes) or non-unsaturated molecules such as alcohols or water, often with atom economy. Various selective transformations are developed and can provide access to high multifunctional molecules. These reactions often proceed via an initial oxidative coupling leading to a ruthenacycle intermediate.

Keywords Alkenes · Alkynes · C–C bond formation · Cyclopentadienyl ruthenium(II) catalysts · Ruthenacycle

Contents

1	Introduction	290
2	Intermolecular Coupling of Alkynes	290
2.1	Coupling of Two $C\equiv C$ Bonds	290
2.2	Intermolecular Cyclotrimerization	293
3	Intramolecular Coupling of Diynes	294
3.1	Co-cyclotrimerization with Alkynes	294
3.2	Co-cyclotrimerization with Carbon–Heteroatom Multiple Bonds	295
3.3	Co-cyclotrimerization with Alkenes	296
3.4	Reaction of Diynes with Other Molecules	297
4	Intermolecular Coupling of $C=C$ and $C=C$ Bonds	299
4.1	Linear Coupling	299
4.2	Intermolecular Coupling with Cycle Formation	302
4.3	Cyclization with Carbonylation	305
4.4	Ring Expansion Reaction	305

S. Dérien (✉)

Institut des Sciences Chimiques de Rennes, UMR 6226 CNRS-Université de Rennes1,
Organométalliques : Matériaux et Catalyse, Campus de Beaulieu, 35042, Rennes, France
e-mail: sylvie.derien@univ-rennes1.fr

5	Intramolecular $C\equiv C/C=C$ (or $C=C=C$) Bond Coupling	306
5.1	Enyne Cycloisomerization Involving a Ruthenacycle	306
5.2	Allenyne Cycloisomerization	308
5.3	Enyne Cycloisomerization Involving a π -Allyl Intermediate	309
6	Coupling Involving Two $C=C$ (or $C=C=C$) Bonds	310
7	Addition of Carbene Units to $C\equiv C$ or $C=C$ Bonds	312
7.1	Carbenoid Species Generated from Diazo Compounds	312
7.2	Carbenoid Species Generated from Propargyl Alcohols	314
8	Diels Alder Reactions	314
9	Conclusions	315
	References	316

1 Introduction

During the last years molecular ruthenium complexes have promoted a large variety of catalytic reactions and the creation of novel catalytic combinations of simple molecules to generate high-value chemicals. Especially very simple ruthenium precatalysts have allowed the discovery of new carbon–carbon bond forming reactions by activation of unsaturated molecules. Notably, molecular ruthenium catalysts have appeared to be powerful tools for the activation of alkynes and alkenes providing selective transformations with atom economy. In this field of catalyzed carbon–carbon bond formation $(C_5R_5)Ru$ complexes constitute a very useful family of versatile catalyst precursors as they promote various combinations of alkynes and alkenes to perform new reactions with a large range of applications.

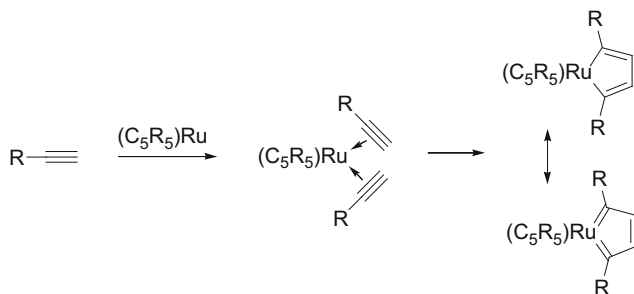
This review outlines the recent advances since 2003 in the catalytic coupling between alkynes and alkenes with carbon–carbon bonds creation by activation with $(C_5R_5)Ru$ catalysts. Reactions which are the topics of other chapters of this volume are not included in this review.

2 Intermolecular Coupling of Alkynes

2.1 Coupling of Two $C\equiv C$ Bonds

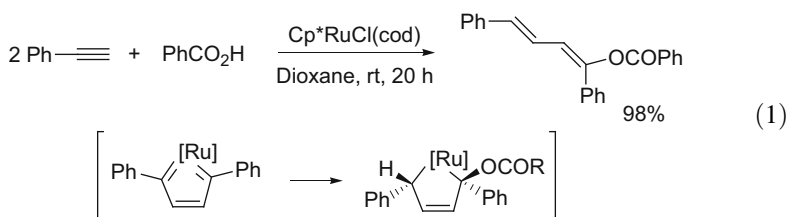
The excellent coordination properties of alkynes with ruthenium catalysts led to their use as partners for the coupling with a large variety of unsaturated molecules. The first examples of dimerization of terminal alkynes involved acetylide or vinylidene intermediates. By contrast, with $(C_5R_5)Ru$ catalysts, a completely different stoichiometric head-to-head coupling of alkynes has been discovered affording ruthenacyclopentatrienes, which are cyclic biscarbenes produced by the oxidative coupling of two alkynes [1–3] (Scheme 1).

The precatalyst $Cp^*RuCl(cod)$, where Cp^* is pentamethylcyclopentadienyl and cod is cycloocta-1,5-diene, allowed the catalytic head-to-head oxidative

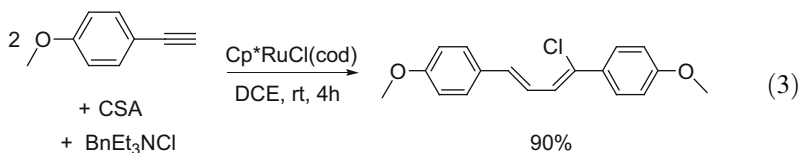
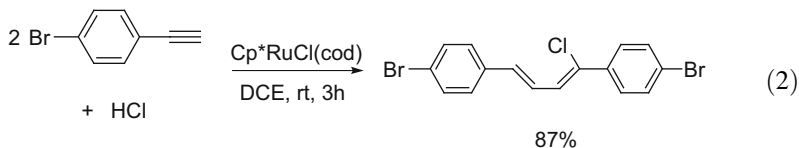


Scheme 1 Oxidative coupling of two alkynes with (C₅R₅)Ru catalysts

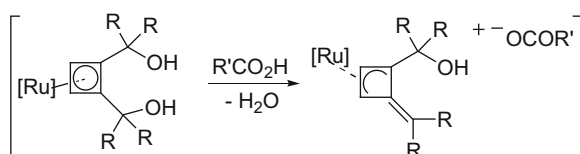
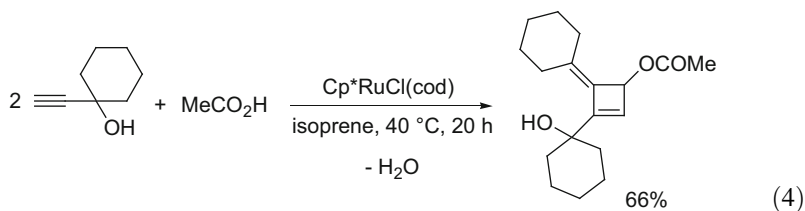
dimerization of terminal alkynes by the concomitant 1,4-addition of carboxylic acids. 1-Acyloxy-1,3-dienes were stereoselectively produced in one step under mild conditions [4] [Eq. (1)]. The ruthenacycle intermediate behaves as a mixed Fischer–Schrock-type biscarbene ruthenium complex, allowing protonation and nucleophilic addition of the carboxylate.



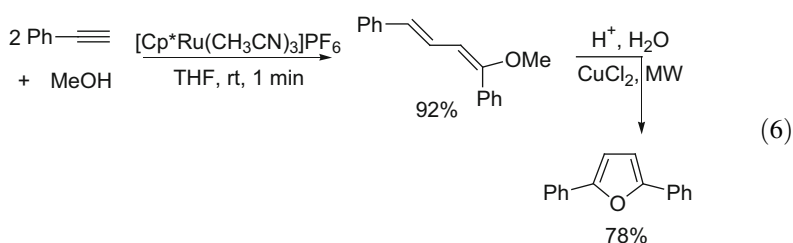
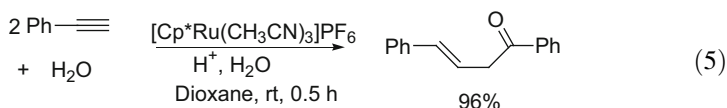
According to this mechanism, the catalytic and selective formation of 1-halo-1,3-dienes could be performed through a hydrohalogenative dimerization of alkynes in one step with the same catalytic system. Di-enylchlorides could be obtained in 1,2-dichloroethane (DCE) by direct addition of HCl or with a hydrohalogenative system consisting of separate proton and halide sources [5] [Eqs. (2) and (3)].



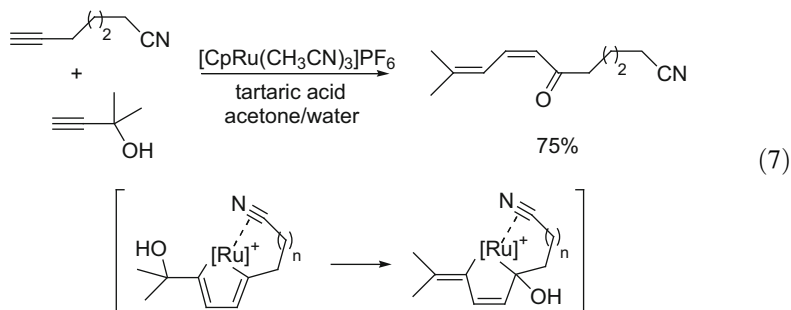
On the other hand, the reaction of carboxylic acids with propargyl alcohols in place of terminal alkynes led to the catalytic head-to-head cyclodimerization of propargyl alcohols and addition of carboxylic acids. Alkylidenecyclobutene derivatives were obtained via cyclobutadieneruthenium and cyclobutenylruthenium intermediates [6] [Eq. (4)].



The linear dimerization of terminal alkynes via ruthenacyclopentatrienes was also carried out in the presence of the cationic $[\text{Cp}^*\text{Ru}(\text{CH}_3\text{CN})_3]\text{PF}_6$ complex and functionalized 1,3-dienes were formed by nucleophilic addition of alcohols [7] or water [8, 9] [Eqs. (5) and (6)]. Further transformations can produce furans or quinoline derivatives.

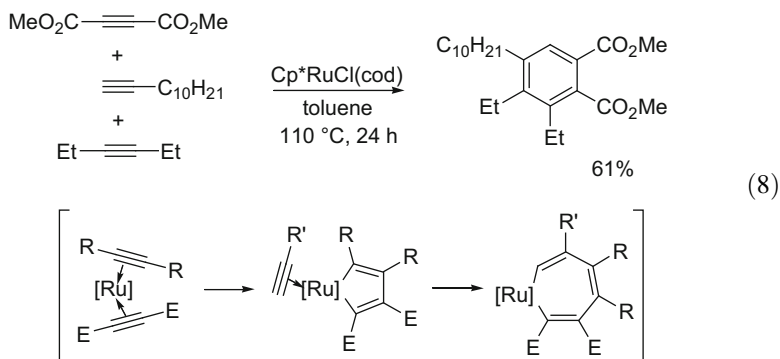


Recently, $[\text{CpRu}(\text{CH}_3\text{CN})_3]\text{PF}_6$ -catalyzed alkyne–alkyne cross coupling between α,ω -cyanoalkynes and tertiary propargyl alcohols was developed in the presence of water and 20 mol% of tartaric acid and produced predominately cyanodienylketones via a nonsymmetric ruthenacyclopentadiene followed by successive dehydration and addition of water [10] [Eq. (7)].

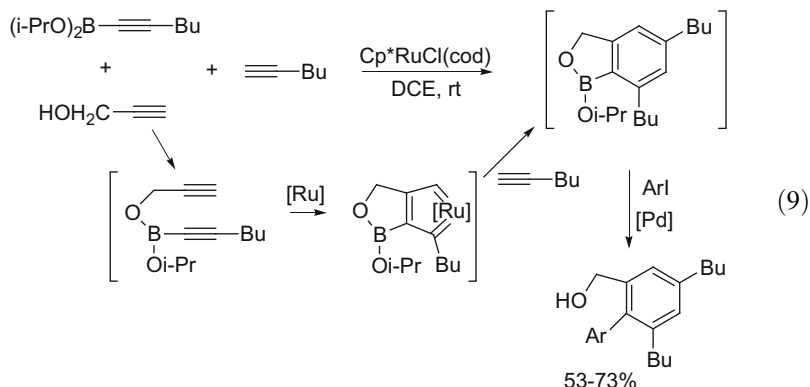


2.2 Intermolecular Cyclotrimerization

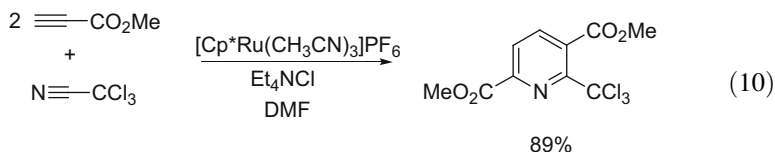
Although ruthenacyclopentadiene intermediates are able to coordinate a third molecule of alkyne to afford benzene derivatives, catalytic intermolecular [2+2+2] cycloadditions involving three nontethered alkynes are seldom because of their low selectivity. For example, substituted *o*-phthalates could be chemoselectively obtained by reaction of two equivalents of terminal alkynes with dimethylacetylenedicarboxylate (DMAD) [11] or by cycloaddition of an internal alkyne, a terminal alkyne and DMAD [12] [Eq. (8)] in the presence of the Cp^{*}RuCl(cod) complex.



Regioselectivity can usually be reliably obtained when two of the alkyne partners are tethered. A Cp^{*}RuCl(cod)-catalyzed intermolecular cyclotrimerization of three different monoalkynes could be performed by an *in situ*-tethering approach with the formation of a temporal C–B–O linkage from alkynylboronates and propargyl alcohols [13–15] [Eq. (9)]. The resultant arylboronates could not be isolated and were further converted to substituted biaryls via the Suzuki–Miyaura coupling or into a sequential one-pot process [14], or to phthalides via a palladium-catalyzed carbonylation [15].



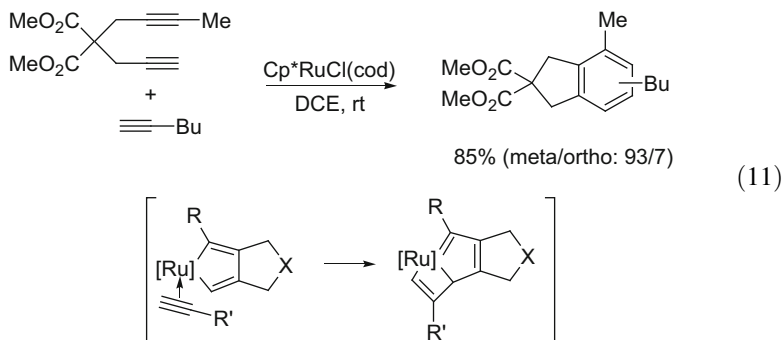
When the third triple bond of the intermolecular cyclotrimerization is a nitrile derivative, pyridines can be obtained [16, 17]. The reaction took place with electron-deficient monoalkynes and electron-poor nitriles [Eq. (10)].



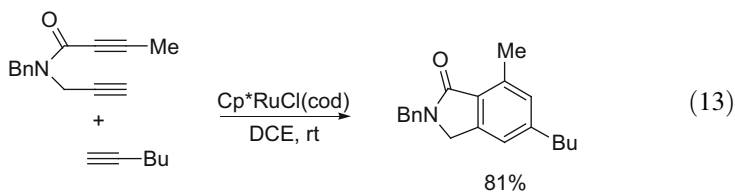
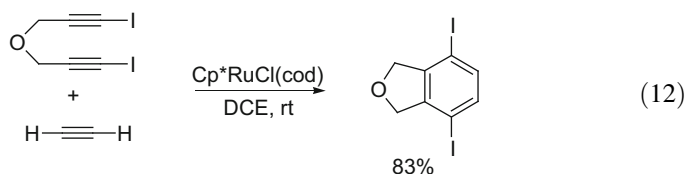
3 Intramolecular Coupling of Diynes

3.1 Co-cyclotrimerization with Alkynes

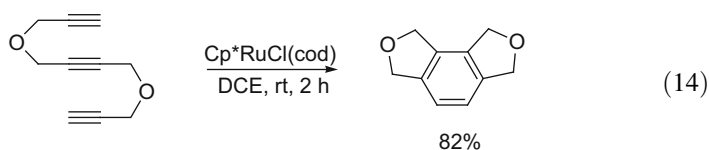
Ruthenium-catalyzed reactions involving diynes generally lead to the intramolecular oxidative coupling of the two $C\equiv C$ bonds. Bicyclic compounds can be synthesized in the presence of another unsaturated molecule. The $Cp^*RuCl(cod)$ -catalyzed reaction of 1,6- and 1,7-diynes in the presence of monoalkynes led to a [2+2+2] cycloaddition. Various substituted benzenes were thus produced in good yields [18–36]. The cycloaddition of unsymmetrical diynes usually favors meta-substituted products by means of judicious choice of substituents as in Eq. (11) [18].



Examples of improved chemoselectivity by immobilized diyne on a solid-support [19–21] or of improved reactivity of less reactive alkynes by use of microwave [21–24] were recently described. A wide variety of diynes and monoynes containing functional groups were applied to this reaction in the past decade. Arylboronates [25, 26] and diiodo benzenes [27, 28] [Eq. (12)] were thus obtained and involved in further transformations. Several types of compounds able to present biological activities could also be synthesized such as benzo-fused lactams and lactones [23, 29] [Eq. (13)], phtalans [19], indanones [20], indanes [21], phenanthridines [22], benzopropine and tetrahydroisoquinoline derivatives [30, 31], C-arylglycosides and C-arylribosides [32–35]. Recently, this ruthenium-catalyzed [2+2+2] cycloaddition between a diyne and a monoalkyne was also used as reaction step in total syntheses [20, 23, 24, 36].



Completely intramolecular alkyne cyclotrimerization was also achieved using triyne substrates to produce tricyclic aromatic compounds [18, 24] [Eq. (14)].

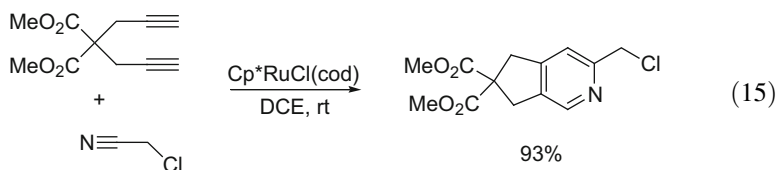


Remarkably, all these above catalytic [2+2+2] cycloadditions involving three C≡C bonds are performed by use of the Cp*RuCl(cod) complex. To our knowledge, just one example of the coupling of a diyne with an alkyne catalyzed by (η^5 -C₅Me_nH_{5-n})RuCl(cod) complexes was described [37].

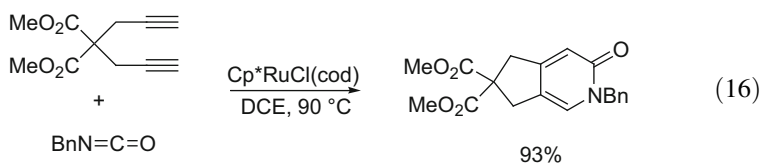
3.2 Co-cyclotrimerization with Carbon–Heteroatom Multiple Bonds

When the [2+2+2] cycloaddition of 1,6-diynes occurred in the presence of C≡N bonds, bicyclic pyridines were regioselectively formed by reaction with

electron-deficient nitriles [16, 17] or nitriles bearing a coordinating group such as dicyanides or α -halonitriles [16, 38, 39] [Eq. (15)]. The synthesis of β - and γ -carbolines was developed by reaction between functionalized yne-ynamides and methylcyanoformate [40] and the pyridine core of cyclothiazomycin was obtained based on a [2+2+2] cyclotrimerization key step of a diyne and an electron-poor thiazole nitrile [36].

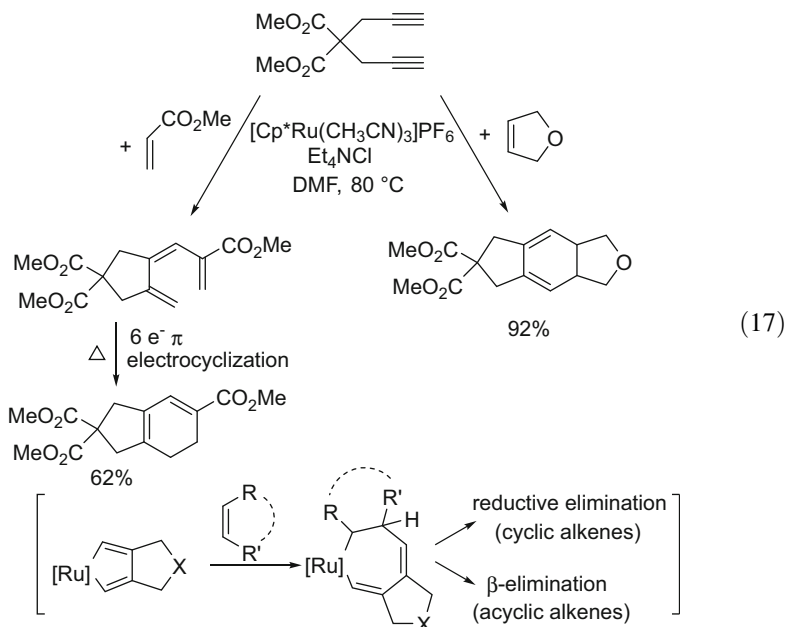


In the presence of catalytic amounts of $\text{Cp}^*\text{RuCl}(\text{cod})$, 1,6-diyne were allowed to react with heterocumulenes such as isocyanates or isothiocyanates to afford bicyclic pyridones or thiopyranimines [17] [Eq. (16)]. When an excess of carbon disulfide was employed in place of isothiocyanates, a bicyclic dithiopyrone was obtained [17].



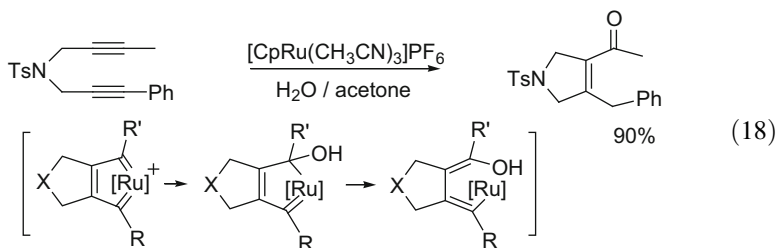
3.3 Co-cyclotrimerization with Alkenes

The [2+2+2] cycloaddition of 1,6-diyne with alkenes can lead to different products. The most recent results about this reaction were obtained by the use of the catalytic system $[\text{Cp}^*\text{Ru}(\text{CH}_3\text{CN})_3]\text{PF}_6/\text{Et}_4\text{NCl}$ which probably generates in situ the neutral complex $\text{Cp}^*\text{RuCl}(\text{CH}_3\text{CN})_2$ [41–45]. If the well-established insertion of a double bond into ruthenacyclopentadiene followed by reductive elimination leading to tricyclic hexadienes was effectively obtained in the case of cyclic alkenes [42–44], a β -elimination affording a ruthenium hydride followed by reductive elimination was produced in the case of acyclic alkenes [41–45] [Eq. (17)]. The obtained open hexatrienes undergo a subsequent thermal $6e^- \pi$ electrocyclozation to give bicyclohexadienes. When 1,3-dienes or *Z*-propenyl(hetero)arenes were used instead of acyclic alkenes, a thermal $8e^- \pi$ electrocyclozation can proceed affording cyclooctatrienes [41, 45].

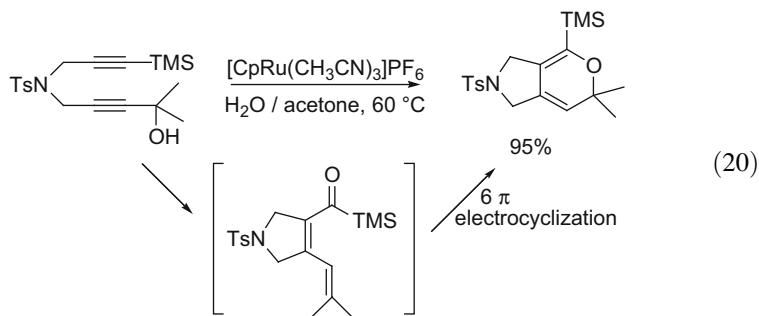
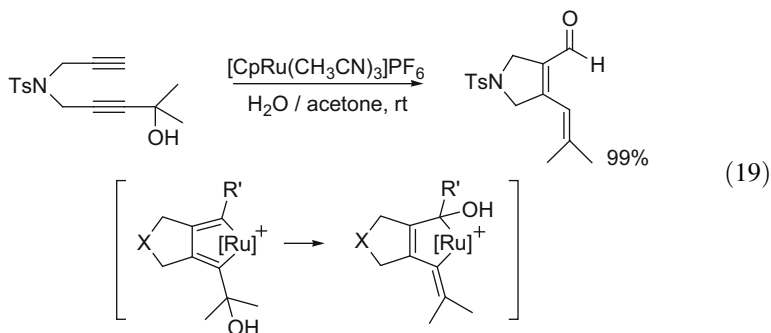


3.4 Reaction of Diynes with Other Molecules

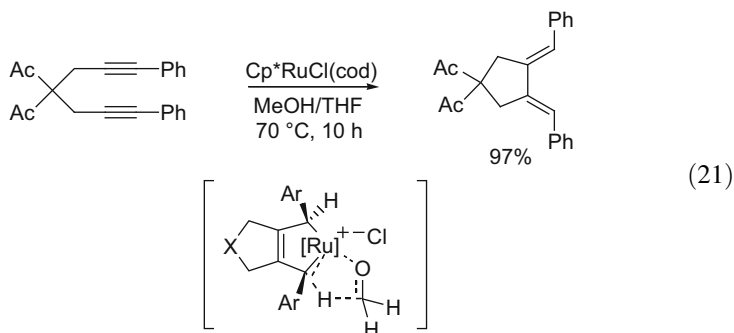
The ruthenacyclopentatrienes, obtained by the oxidative cyclization of diynes, can also undergo an attack of other reagents than unsaturated molecules. In the presence of the complex $[\text{CpRu}(\text{CH}_3\text{CN})_3]\text{PF}_6$ and water, a hydrative diyne cyclization took place leading to α,β -unsaturated ketones [46–49] [Eq. (18)]. This reaction was applied to the total synthesis of (+)-Cylindricine C, D, and E [49].



Conjugated dienones were produced in the case of the cycloisomerization of diynols. The ruthenacyclopentadiene intermediate undergoes an elimination of the hydroxy group and adds water at the resulting carbene carbon [50, 51] [Eq. (19)]. However, the cycloisomerization yielded bicyclic silylpyran derivatives after spontaneous 6π electrocyclicization when diynes containing one silylalkyne and one propargyl alcohol were used [52] [Eq. (20)].

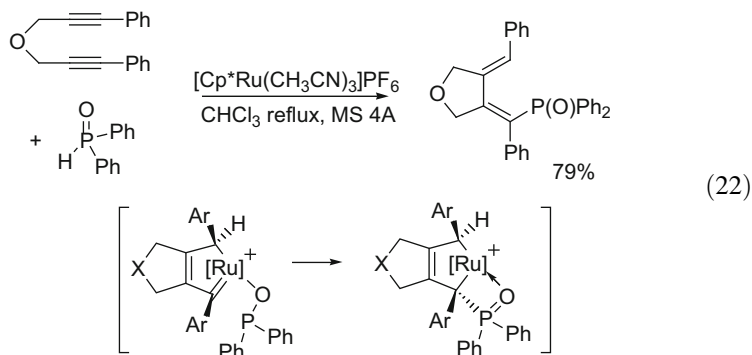


Recently, a catalytic hydrogenative cyclization of 1,6-diyne leading to exocyclic dienes was described involving the $\text{Cp}^*\text{RuCl}(\text{cod})$ catalyst and hydrogen transfer from MeOH or involving a cationic $[(\text{C}_5\text{R}_5)\text{Ru}(\text{CH}_3\text{CN})_3]\text{PF}_6$ catalyst and 1,4-dihydropyridine as a H_2 surrogate [53, 54] [Eq. (21)]. The protonation of a ruthenacyclopentatriene intermediate and the subsequent hydride abstraction from the methoxide ligand by an electrophilic carbene carbon are proposed as mechanism.

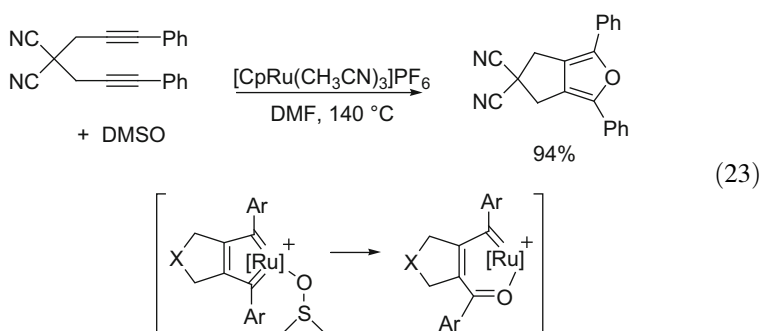


Exocyclic 1,3-dienylphosphine oxides can also be obtained by $[\text{Cp}^*\text{Ru}(\text{CH}_3\text{CN})_3]\text{PF}_6$ -catalyzed hydrophosphinylation of 1,6-diyne via a H-atom transfer on the ruthenacyclopentatriene and subsequent intramolecular

attack of the P center of the phosphinate ligand to the second carbene carbon [55] [Eq. (22)].



On the other hand, the ruthenacyclopentatriene intermediate, produced from diynes and the [CpRu(CH₃CN)₃]PF₆ complex, showed a catalytic activity towards DMSO leading to the direct synthesis of bicyclic furans via an oxygen-atom-transfer process [56] [Eq. (23)].

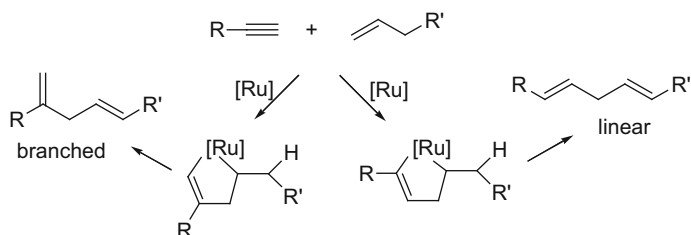


4 Intermolecular Coupling of C≡C and C=C Bonds

4.1 Linear Coupling

One of the most useful pathways for C≡C and C=C bonds coupling involves the oxidative coupling and the ruthenacycle intermediate formation.

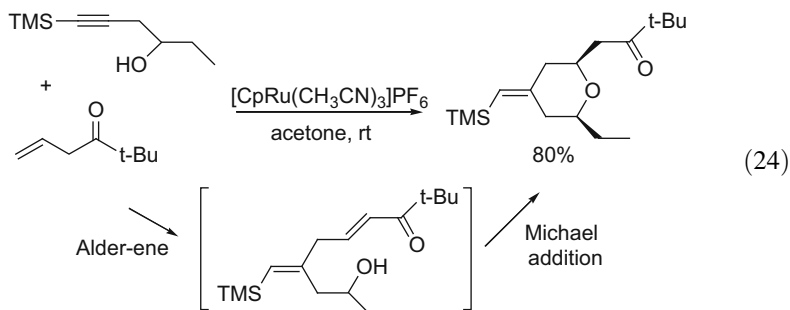
For linear mixed coupling, ruthenium catalysts offered the possibility to develop the potential of the Alder-ene reaction by expanding its scope and selectivity. This C≡C bond/C=C bond coupling afforded a wide variety of linear or branched 1,4-dienes depending on the nature of the substitutions of the starting materials and on the catalyst system based on a (C₅R₅)ruthenium. The presence of two different isomers can be viewed through the competitive ruthenacyclopentene



Scheme 2 Oxidative coupling of C≡C and C=C bonds with (C₅R₅)Ru catalysts

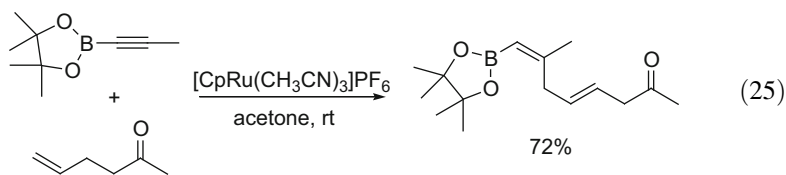
intermediate formation, depending on the orientation of the alkyne. A β -hydride elimination, which is favored with H exocyclic with respect to intracyclic β -hydride, produces the 1,4-dienes (Scheme 2).

In the past decade, using the catalyst [CpRu(CH₃CN)₃]PF₆, the regioselective preference for the formation of the branched isomer by reaction of terminal alkynes and alkenes was applied to the total synthesis of several natural products [57–60]. The reaction of silylalkynes and terminal alkenes usually proceed with complete control of regioselectivity by the silyl substituent to give one isomer similar to the branched isomer [61, 62]. Thus, the reaction of silylated homopropargylic alcohols with β,γ -unsaturated enones gave methylenetetrahydropyrans via a ruthenium-catalyzed tandem alkyne-ene coupling/Michael addition [61] [Eq. (24)].

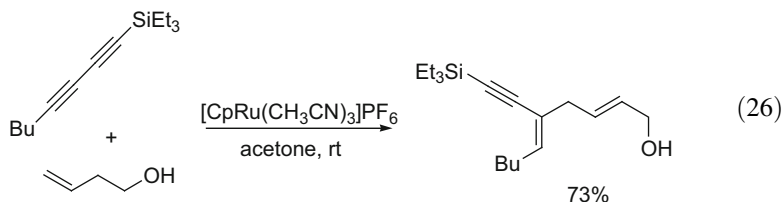


Methylenetetrahydropyrans could also be obtained by [CpRu(CH₃CN)₃]PF₆-catalyzed coupling of allylether with optically active 1-trimethylsilyl-1-alkyn-3-ols followed by in situ ketalization. Further Lewis acid-induced cyclization afforded enantiomerically pure 1,5-oxygen-bridged carbocycles [62].

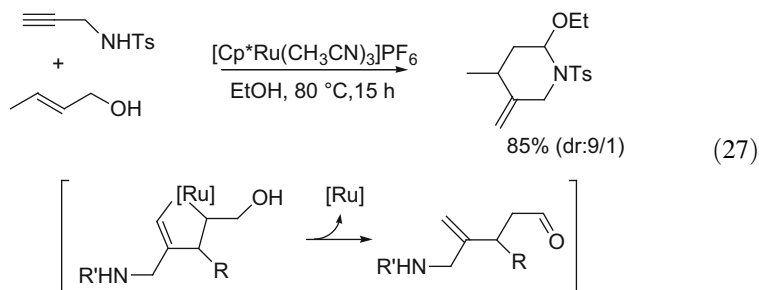
The same regioselectivity in favor of the branched isomer with unusual stereoselectivity was produced with borylated alkynes in place of silylated alkynes to lead to the synthesis of β,β -disubstituted vinyl boronates [63] [Eq. (25)].



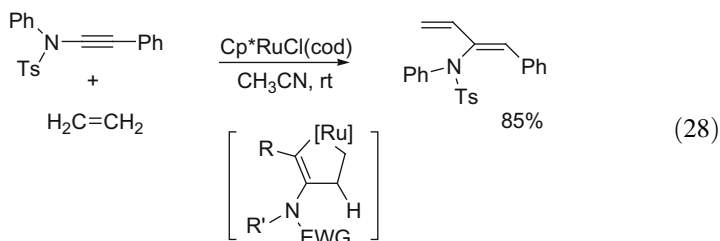
When conjugated diynes or triynes were used in the [CpRu(CH₃CN)₃]PF₆-catalyzed Alder-ene reaction, only one of the alkynyl moieties reacted with terminal alkenes, the other one determining the regioselectivity [64] [Eq. (26)].



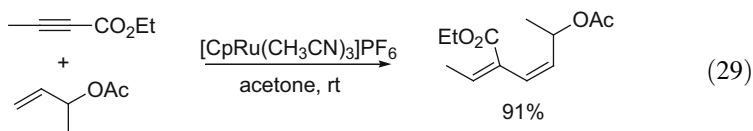
A similar ruthenacyclopentene intermediate can be proposed for the coupling of alkynes and allylic alcohols to lead to γ,δ -unsaturated aldehydes and ketones. When [Cp**Ru*(CH₃CN)₃]PF₆ was used as a catalyst, the catalytic coupling between propargylic amides and allylic alcohols selectively provided piperidine derivatives by cyclization of the highly reactive aminoaldehyde intermediate [65] [Eq. (27)]. Only the branched isomer was formed by oxidative coupling, allowing the intramolecular condensation.



The synthesis of 1,3-dienes via a ruthenacyclopentene intermediate is also a possible pathway. It results from intracyclic β -hydride elimination, and this process takes place only when an exocyclic β -elimination is not possible or not favored. Thus, the Cp**Ru*Cl(cod)-catalyzed hydrovinylation of ynamides proceeded in the presence of ethylene to selectively afford 2-amino-1,3-dienes [66] [Eq. (28)].

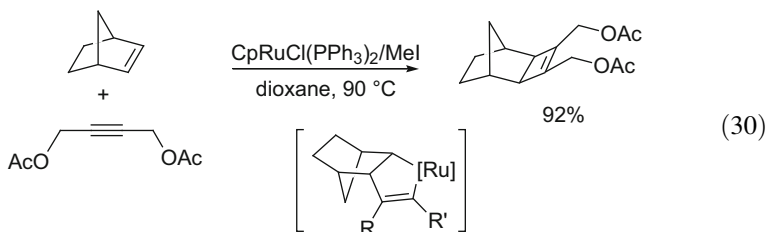


In the same manner, (*Z,Z*)-1,3-dienes were obtained by the [CpRu(CH₃CN)₃]PF₆-catalyzed coupling of internal alkynoates with allylic esters, carbonates, or ethers [67] [Eq. (29)]. The functionalized allylic position seems necessary to lead to this selectivity.

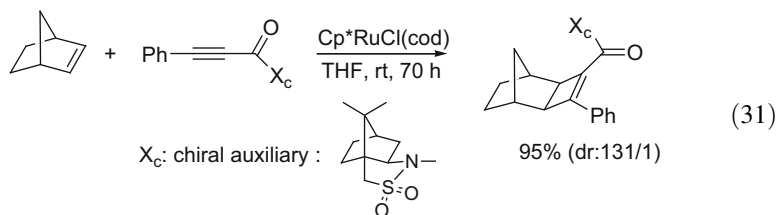


4.2 Intermolecular Coupling with Cycle Formation

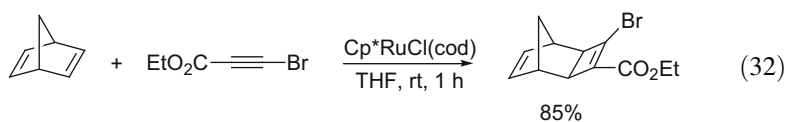
The coupling between alkynes and alkenes can also afford cyclization reactions and leads to strained carbocycles. Most of these reactions are performed via a constrained ruthenacyclopentene intermediate which cannot undergo β -hydride elimination and leads to cyclobutenes via a reductive elimination as in the following example [68] [Eq. (30)].



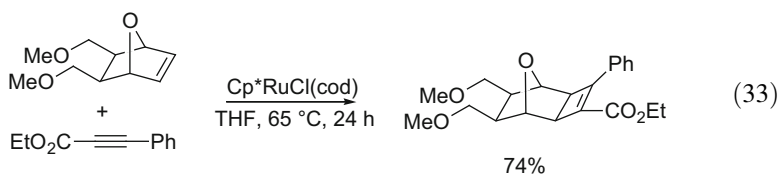
In this area, the complex Cp^{*}RuCl(cod) has shown to be an excellent catalyst for the [2+2] cycloaddition of various internal alkynes with a variety of substituted norbornenes and norbornadienes [69–83]. A number of aspects of this reaction have been studied, notably the reactivity, the chemo- and regioselectivity of unsymmetrical substrates [69–73] and the asymmetric induction with chiral auxiliaries on the alkyne partner [74–77] [Eq. (31)].



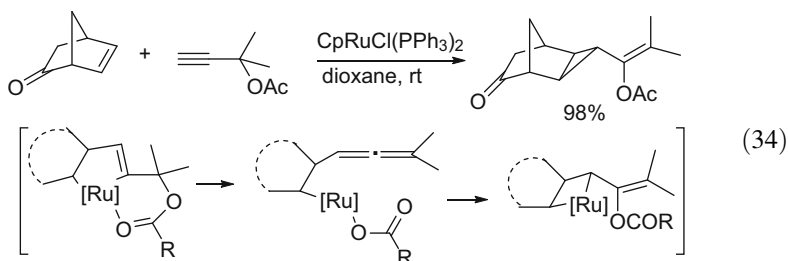
Different heteroatom-substituted alkynes have been involved in this reaction such as alkynyl halides [78, 79] [Eq. (32)], ynamides [76, 77], alkynyl sulfides or sulfones [80], and alkynyl phosphonates [81]. Haloalkynes were found to be the most reactive, proceeding at room temperature, whereas alkynyl phosphonates showed the lowest reactivity.

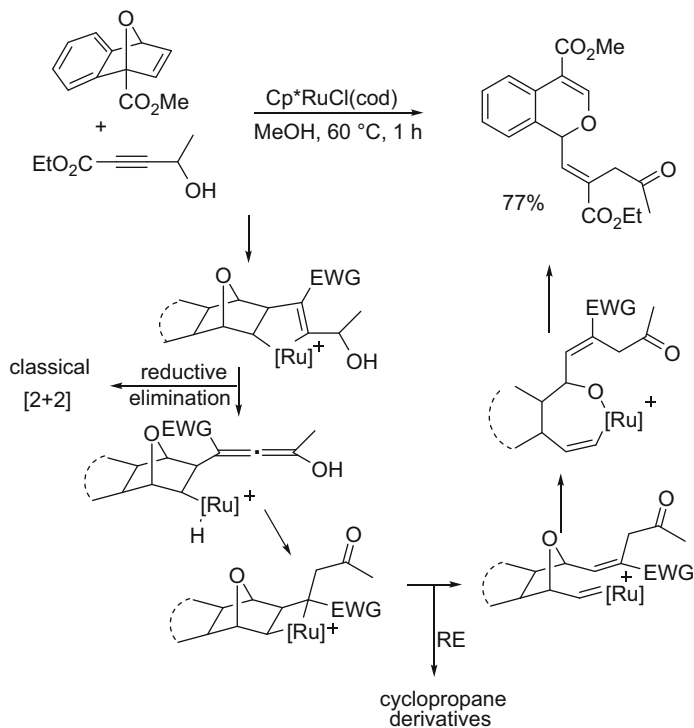


Heteroatom functionalities have also been introduced in bicyclic alkenes. The Cp*₂RuCl(cod)-catalyzed [2+2] cycloaddition of a 2-oxa-3-azabicyclo[2.2.1]hept-5-ene with unsymmetrical alkynes was achieved and the formed cycloadducts could be used to access a functionalized [3.2.0]bicyclic structure through reductive cleavage of the N–O bond [82]. When 7-oxanorbornadienes were reacted with alkynes a [2+2] cycloaddition usually resulted to give cyclobutenes [72, 83] [Eq. (33)].



The expected cyclobutenes are not always formed and other pathways than [2+2] cycloadditions can occur from ruthenacyclopentene intermediate. For example, a cyclopropanation reaction of various bicyclic alkenes could be performed when secondary propargylic alcohols were used as alkynes in the presence of the Cp*₂RuCl(cod) catalyst in THF [84] or when tertiary propargylic acetates were reacted in the presence of the CpRuCl(PPh₃)₂ catalyst in dioxane [85] [Eq. (34)].

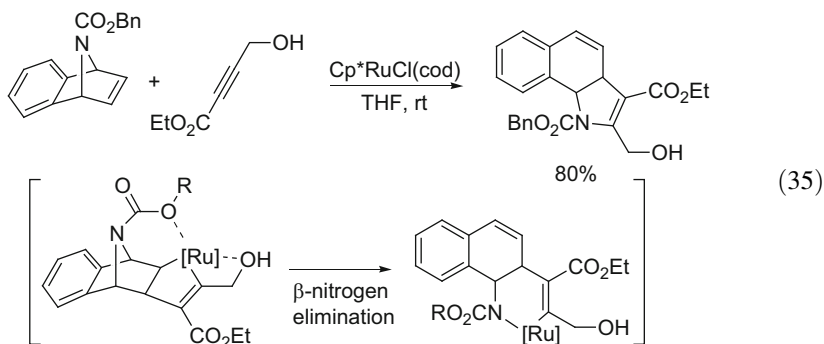




Scheme 3 Reaction of oxabenzonorbornadienes with secondary propargylic alcohols

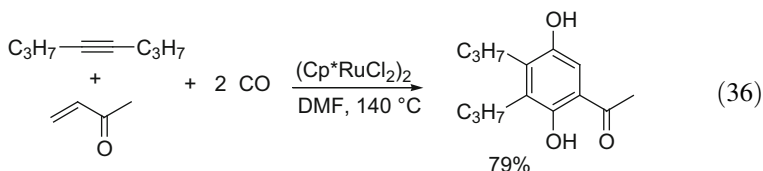
On the other hand, isochromenes were synthesized by reaction of oxabenzonorbornadienes with secondary propargylic alcohols in the presence of the neutral $\text{Cp}^*\text{RuCl}(\text{cod})$ in MeOH or using the cationic $[\text{Cp}^*\text{Ru}(\text{CH}_3\text{CN})_3]\text{PF}_6$ [86, 87]. The proposed mechanism involves oxidative coupling, β -hydride elimination, hydride shift, and [2+2] cycloreversion. The formed ruthenium carbene undergoes an [1,3]-alkoxide shift and reductive elimination generates isochromenes (Scheme 3). Using $\text{CpRuI}(\text{PPh}_3)_2$ as a catalyst in situ generated from the system $\text{CpRuCl}(\text{PPh}_3)_2/\text{MeI}$, oxabenzonorbornadienes were reacted with alkynes bearing oxygen atoms at the propargylic position leading to stereodefined benzenocaradienes [88].

The ruthenium-catalyzed cyclization of 7-azabenzonorbornadienes with alkynes led to a dihydrobenzoindole framework [89, 90]. This reaction was achieved using $\text{CpRuI}(\text{PPh}_3)_2$ as a catalyst generated in situ [89] or with ruthenium catalysts, $\text{Cp}^*\text{RuCl}(\text{cod})$ and $[\text{Cp}^*\text{Ru}(\text{CH}_3\text{CN})_3]\text{PF}_6$ according to substrates [90] and involves a β -nitrogen elimination [Eq. (35)].



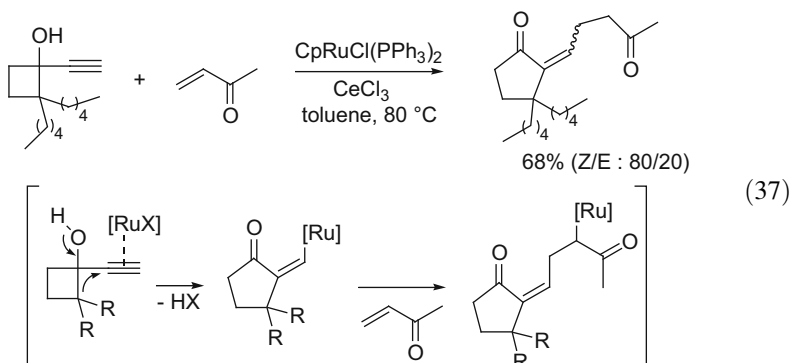
4.3 Cyclization with Carbonylation

Functionalized hydroquinones were obtained via [Cp*RuCl₂]₂-catalyzed cocyclization of alkynes, electron-deficient alkenes, and carbon monoxide [91] [Eq. (36)]. A maleoylruthenium complex is postulated to occur by the reaction of ruthenium with an alkyne and two molecules of carbon monoxide. Subsequent insertion of an electron-deficient alkene and reductive elimination led to hydroquinone derivatives.



4.4 Ring Expansion Reaction

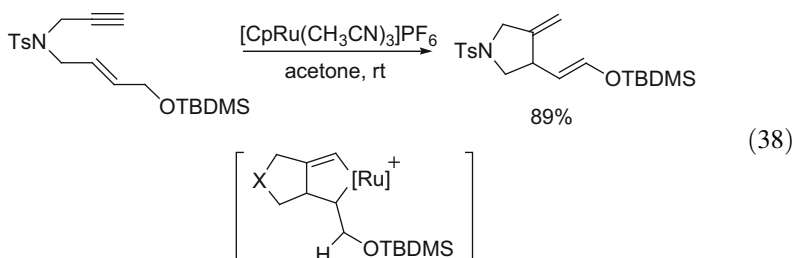
Finally, a novel type of ring expansion reaction was developed by ruthenium-catalyzed activation of alkynylcyclobutanols and methylvinylketone in the presence of Lewis acid to produce 2-alkylidenecyclopentanones [92] [Eq. (37)].



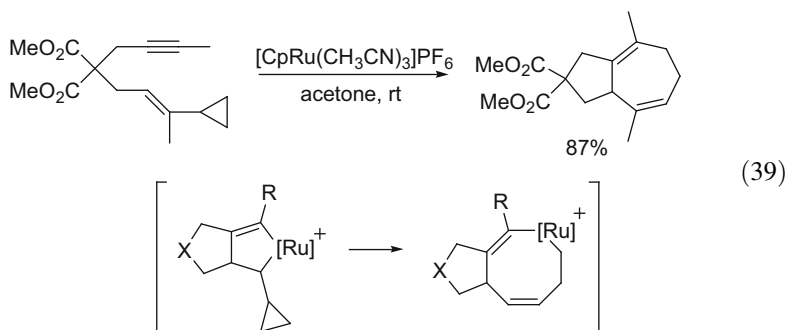
5 Intramolecular $C\equiv C/C=C$ (or $C=C=C$) Bond Coupling

5.1 Enyne Cycloisomerization Involving a Ruthenacycle

Enyne cycloisomerization catalyzed by $(C_5R_5)Ru$ complexes usually proceeds via a ruthenacyclopentene intermediate. Thus, the complexes $[CpRu(CH_3CN)_3]PF_6$ or $[Cp^*Ru(CH_3CN)_3]PF_6$ catalyzed the cycloisomerization of a variety of achiral or chiral 1,6- and 1,7-enynes substituted in the terminal allylic position with a silyl ether group to lead to five- or six-membered rings possessing a geometrically defined enol silane [93] [Eq. (38)]. An exocyclic β -hydrogen elimination on ruthenacyclopentene leads to 1,4-diene product. This reaction was applied to the synthesis of (+)-Allocyathin B₂ [94].

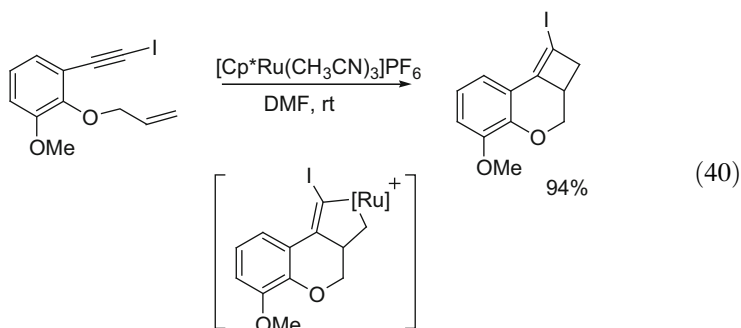


When the double bond of the enyne possesses a cyclopropyl substituent, an intramolecular [5+2] cycloaddition of alkyne and vinylcyclopropane takes place [95–97] [Eq. (39)]. The ruthenacycle does not undergo β -hydride elimination but a rearrangement of the cyclopropane to produce a ruthenacyclooctadiene. Thus, bicyclic and tricyclic cycloheptadienes can be obtained in good yields and high diastereoselectivities. Total synthesis of (+)-Fronodosin A and synthesis of a tricyclic core of Rameswaralide include a ruthenium-catalyzed [5+2] cycloaddition [98, 99].

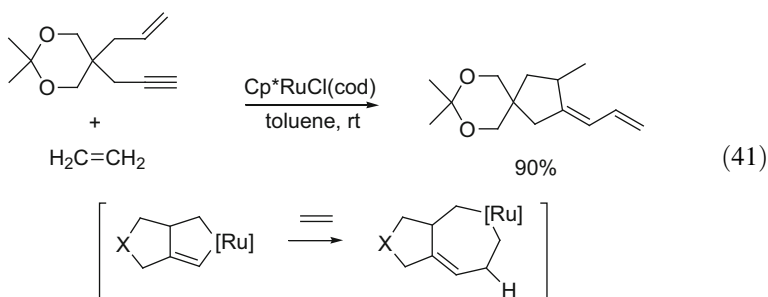


Enynes bearing an iodoalkynyl moiety reacted with catalytic amounts of $[Cp^*Ru(CH_3CN)_3]PF_6$ to lead to strained iodocyclobutene derivatives [100]

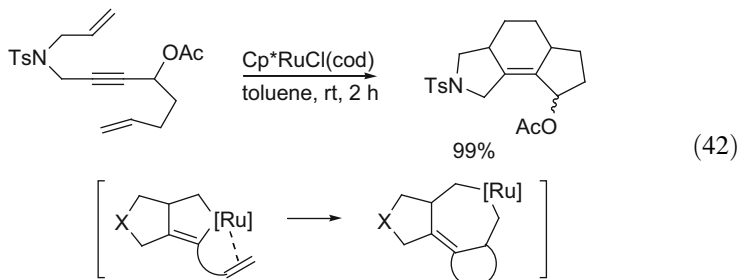
[Eq. (40)]. The proposed ruthenacyclopentene formed by oxidative cyclization undergo a reductive elimination affording stable cyclobutenes when kept cold.



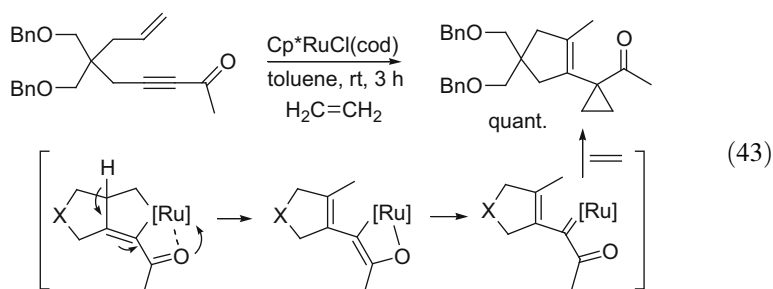
When enyne cycloisomerization takes place in the presence of an unsaturated molecule an insertion reaction can occur. Thus, the ruthenacyclopentene intermediate formed from Cp^{*}RuCl(cod) can undergo insertion of ethylene to give a ruthenacycloheptene. Subsequent β-hydride elimination led to cyclization products with a propenylidene substituent [101] [Eq. (41)]. Various carbo- and heterocyclic compounds were formed in good yields.



A totally intramolecular process is produced in the absence of ethylene if a diene-yne is used by a [2+2+2] cocyclization of two double bonds and one triple bond [102] [Eq. (42)]. Insertion of the second alkene part gave ruthenacycloheptene intermediate and reductive elimination led to tricyclic compounds.

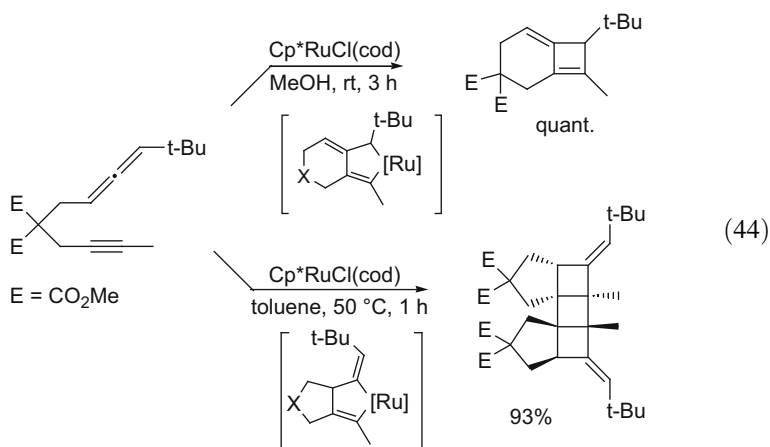


On the other hand, when an enyne having a keto carbonyl group on the triple bond was reacted with $\text{Cp}^*\text{RuCl}(\text{cod})$ under ethylene gas, an unpredicted reaction took place giving cyclized compounds with a cyclopropane ring [103] [Eq. (43)]. Coordination of the carbonyl oxygen to the ruthenium center of the ruthenacyclopentene intermediate is responsible for the formation of a ruthenium carbene able to react with ethylene to form a cyclopropane ring.

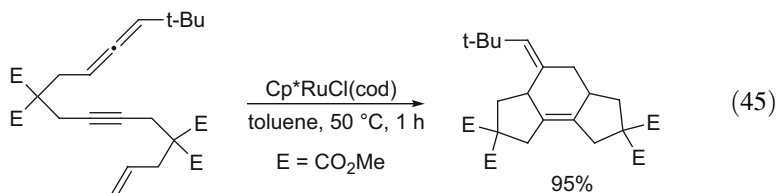


5.2 Allenyne Cycloisomerization

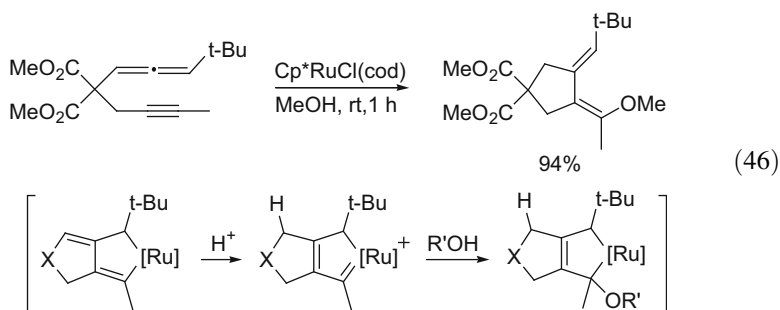
Recently, cycloisomerization reactions could be achieved from allenynes. Indeed, the $\text{Cp}^*\text{RuCl}(\text{cod})$ -catalyzed cyclization of 1,7-allenynes was shown to proceed via an oxidative coupling to form ruthenacyclopentene intermediate. However, the reaction pathway is changed depending on the nature of the solvent employed [104, 105] [Eq. (44)]. In toluene, the ruthenacycle is generated by oxidative cyclization of the triple bond and the internal double bond of allene leading to alkylidene ruthenacyclopentene. Reductive elimination provides cyclobutene derivative which undergoes a cyclodimerization to produce pentacyclic compounds [104]. In methanol, a cationic complex must be generated which coordinates the triple bond and the terminal double bond of allene. A reductive elimination then leads to bicyclo[4.2.0]octadienes [105].



In toluene, an intramolecular [2+2+2] cyclization of allene-yne-enes was performed to produce tricyclic compounds [106] [Eq. (45)].

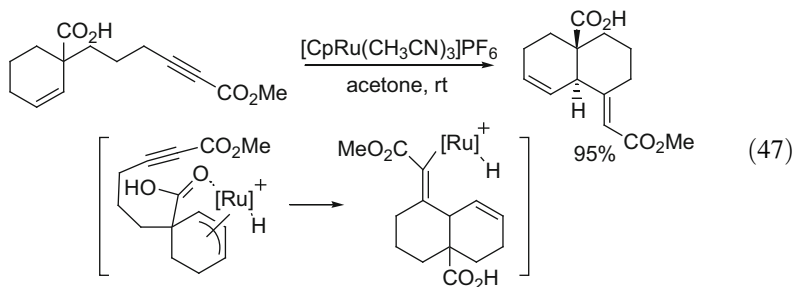


When 1,6-allenynes were reacted with nucleophiles such as alcohols in the presence of Cp^{*}RuCl(cod) in methanol or in the presence of [Cp^{*}Ru(CH₃CN)₃]PF₆ in THF, functionalized 1,2-bisalkylidenecyclopentanes were produced via stereoselective addition of nucleophiles to ruthenacyclopentenes [107] [Eq. (46)]. This ruthenacycle obtained by oxidative coupling of the triple bond and the terminal double bond captures a proton from alcohol at the γ -position of the metal affording a mono-carbene intermediate able to undergo a nucleophilic attack of alcohol.



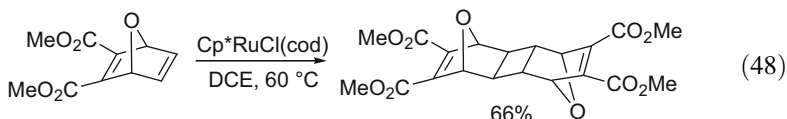
5.3 Enyne Cycloisomerization Involving a π -Allyl Intermediate

If ruthenacycles are invoked as intermediates for the cycloisomerization of enynes containing (E)-olefins [Eq. (38)], enynes containing (Z)-olefins rather undergo an allylic C-H insertion, followed by an intramolecular 1,4-addition to the alkyne forming a vinylruthenium. Reductive elimination affords 1,4-dienes. In this reaction, a coordinating group is required and acts to direct the metal to the same side of the carbocycle, leading to trans diastereoselectivity as in the following example [108, 109] [Eq. (47)].

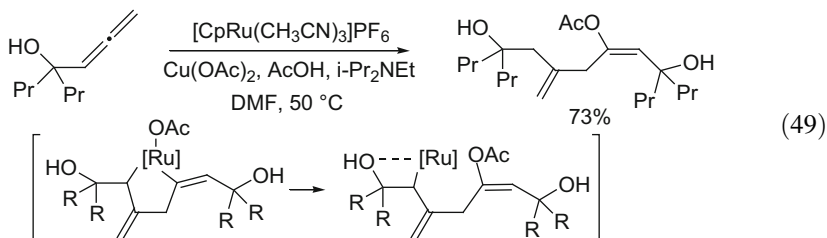


6 Coupling Involving Two C=C (or C=C=C) Bonds

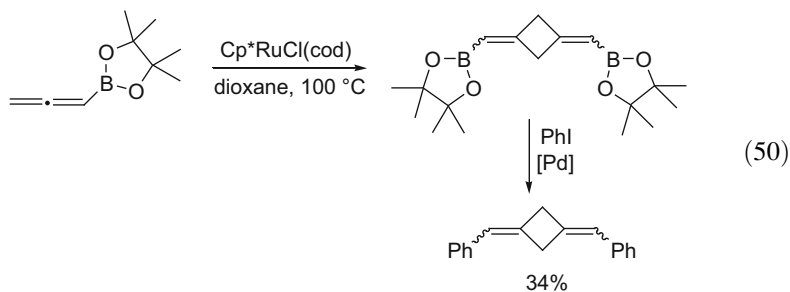
In comparison with C≡C bonds, few examples of coupling between two C=C bonds promoted by (C₅R₅)Ru catalysts are described. The ruthenium-catalyzed dimerization of 7-oxonorbornadienes dicarboxylates was performed in the presence of the Cp^{*}RuCl(cod) complex [110] [Eq. (48)]. Oxidative cyclization provides a ruthenacyclopentane intermediate and subsequent reductive elimination leads to the dimerized oxonorbornadiene with high regioselectivity.



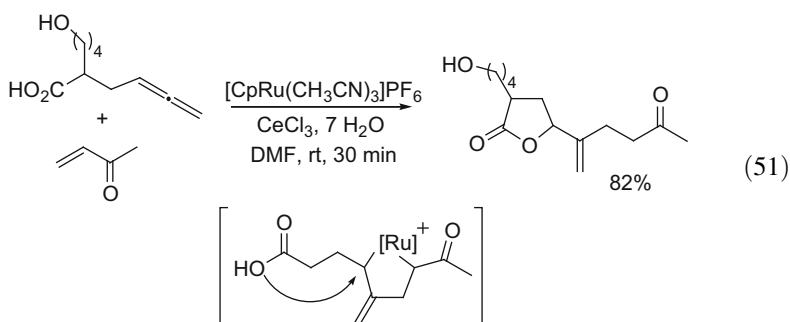
The dimerization of allenic compounds led to linear or cyclic couplings. The [CpRu(CH₃CN)₃]PF₆-catalyzed reaction of allenic alcohols with acetic acid in the presence of Cu(OAc)₂ afforded the corresponding linear dimers with addition of acetate group [111] [Eq. (49)]. An acetoxyruthenacycle formed from an internal and a terminal double bond is proposed as intermediate.



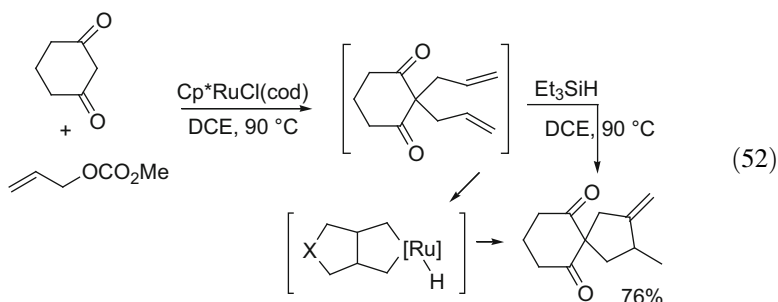
On the other hand, a cyclodimerization of allenylboronates was performed with catalytic amounts of Cp^{*}RuCl(cod) to produce 1,3-dialkylidenecyclobutane derivatives by [2+2] cyclization of the terminal double bonds [112] [Eq. (50)].



Cross coupling of α,β -unsaturated alkenes with allenes could also be promoted. The reaction was catalyzed by the complex [CpRu(CH₃CN)₃]PF₆ with CeCl₃ as a cocatalyst. A ruthenacyclopentane is proposed as an intermediate and this σ -allyl complex allowing nucleophilic additions, an alkylative lactonization was carried out by using allenes with tethered carboxylic acid [113] [Eq. (51)].



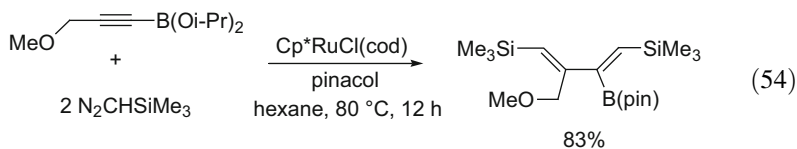
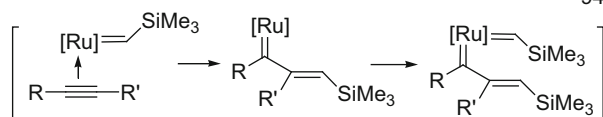
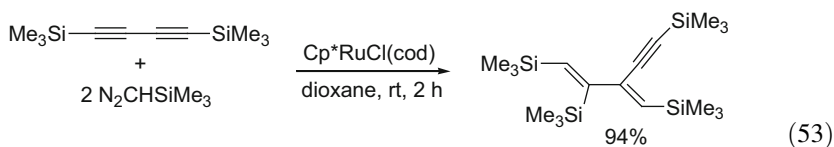
1,6-Dienes were reacted with Cp^{*}RuCl(cod) or Cp^{*}RuCl₂(allyl) in 1,2-dichloroethane in the presence of triethylsilane leading to exo-methylenecyclopentanes. The mechanism suggests the formation of a hydridoruthenacyclopentane intermediate [114]. This reaction was used to develop a ruthenium-catalyzed one-pot double allylation/cycloisomerization of 1,3-dicarbonyl compounds [Eq. (52)].



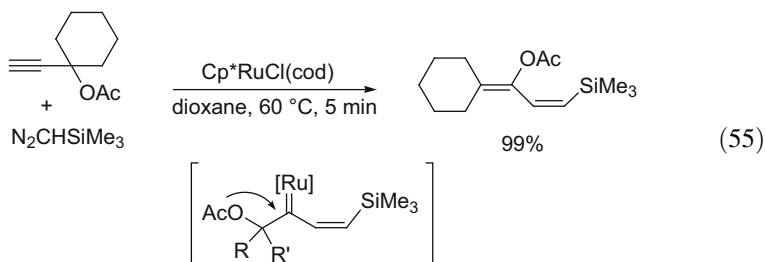
7 Addition of Carbene Units to C≡C or C=C Bonds

7.1 Carbenoid Species Generated from Diazo Compounds

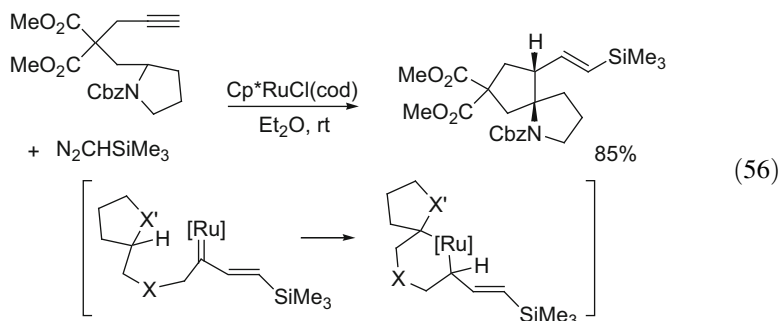
Addition of diazo compounds to metallic complexes allows the formation of metal carbenoid species which can react with unsaturated molecules to form new carbon–carbon bonds. The Cp*RuCl(cod)-catalyzed addition of diazo compounds to alkynes led to the selective synthesis of functional 1,3-dienes by the combination of two molecules of diazoalkane and one molecule of alkyne [115, 116] [Eqs. (53) and (54)]. The ruthenium carbene, generated from diazo compound, reacts with the C≡C bond to produce vinylcarbene intermediate able to add a second molecule of diazo compound to generate dienes. The stereoselective formation of these conjugated dienes results from the selective creation of two C=C bonds, probably due to the possibility for (C₅Me₅)RuCl moiety to accommodate two cis carbene ligands. This reaction occurred with terminal or internal alkynes as well as 1,3-diynes [115] and was applied successfully to alkynylboronates [116].



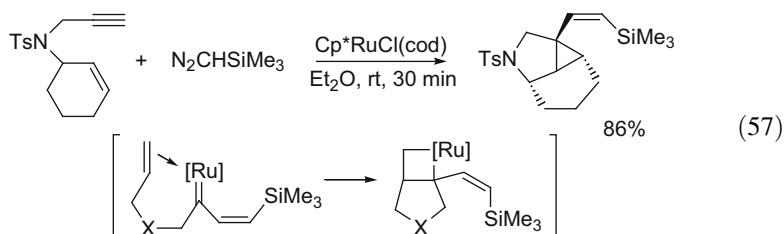
The coupling of diazo compounds was carried out with propargylic carboxylates or propargylic carbonates which led to the synthesis of functional 1,3-dienes. A ruthenium vinylcarbene intermediate is obtained by addition of the carbene unit to the triple bond. A 1,2-shift of the carboxylate or carbonate group onto the carbene carbon can then occur to release conjugated dienylesters or dienylcarbonates [117, 118] [Eq. (55)].



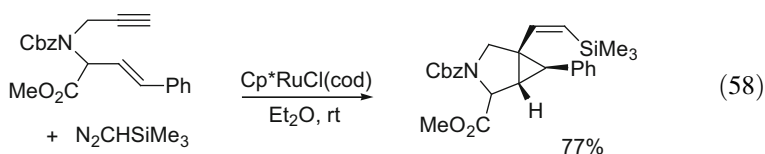
Spiro- and fused bicyclic structures were produced by using linear alkynyl acetals, ethers, or amines by means of a Cp^{*}RuCl(cod)-catalyzed intramolecular carbene insertion into C_{sp3}-H bonds [119] [Eq. (56)]. The proposed mechanism invokes a 1,5- or 1,6-hydride shift onto a ruthenium vinylcarbene intermediate followed by reductive elimination leading to cyclized compounds.



Enynes can also react with diazo compounds allowing the one-step selective synthesis of various alkenylbicyclo[3.1.0]hexane or [4.1.0]heptane derivatives [120–125]. This reaction involves the stereoselective formation of three C–C bonds including a cyclopropanation step. A [2+2] cycloaddition can occur between the vinylcarbene intermediate and the double bond of enyne. At this step the bulky Cp^{*}Ru moiety favors reductive elimination and formation of a cyclopropane derivative with respect to the metathesis reaction [120, 121] [Eq. (57)].

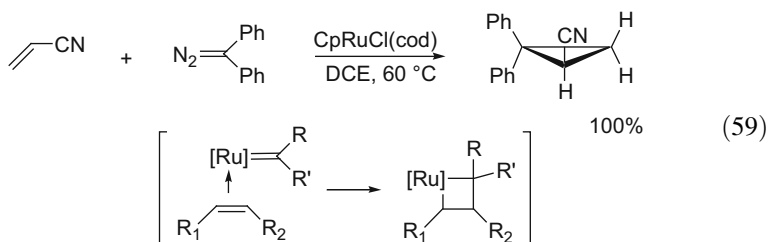


Strained bicyclic carboxylic or boronic amino esters [122] [Eq. (58)] as well as fluorinated amino esters [123, 124] were then synthesized. The reaction could also be applied to allenynes to produce alkenyl alkylidene bicyclo[3.1.0]hexanes [125].



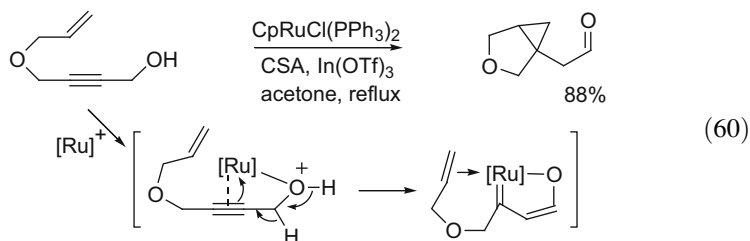
Ruthenium carbenoid species, formed from diazo compounds, can react with alkenes to produce cyclopropane derivatives. For example, the CpRuCl

(cod)-catalyzed addition of unstable aryldiazo compounds to electron-poor olefins was carried out and led to cyclopropanation products rather than metathesis products [126] [Eq. (59)].



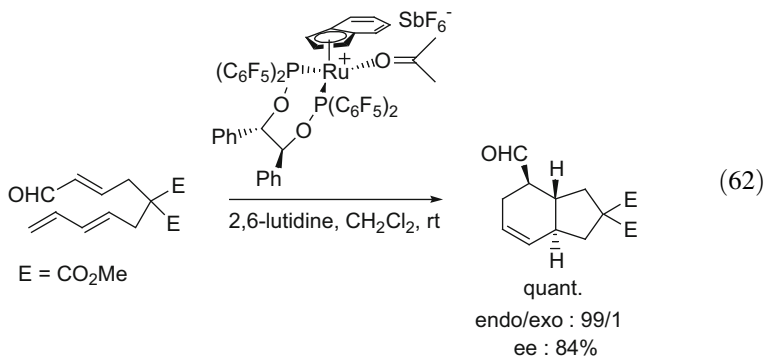
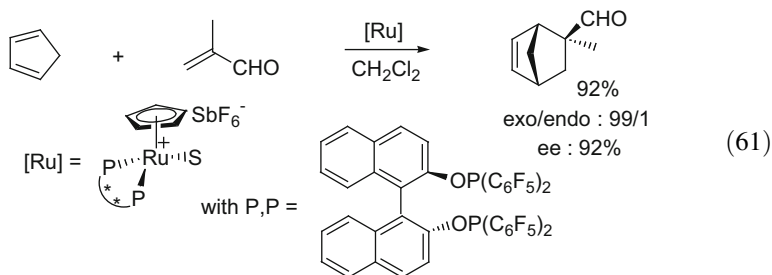
7.2 Carbenoid Species Generated from Propargyl Alcohols

The generation of ruthenium carbenoid intermediates can also arise from propargyl alcohols. In the presence of the $\text{CpRuCl}(\text{PPh}_3)_2$ complex, β -oxoruthenium carbenoids were presumably formed via redox isomerization of propargyl alcohols. This process applied to enynols allowed the synthesis of [3.1.0] and [4.1.0] bicyclic frameworks by [2+2] cycloaddition of the ruthenium carbenoid species with the double bond of enynols followed by reductive elimination [127] [Eq. (60)].

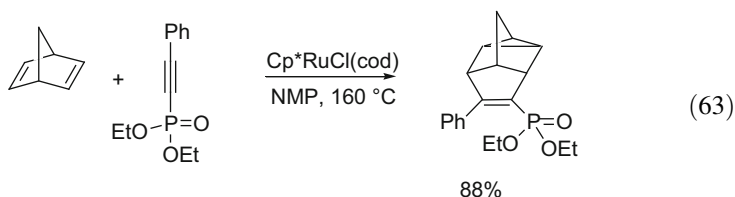


8 Diels Alder Reactions

The moderate Lewis acidity of ruthenium complexes was used to promote catalytic Diels Alder reactions, and notably, enantioselective Diels Alder reactions were performed with ruthenium containing a cyclopentadienyl or indenyl ligand and a chiral P,P-ligand such as (*R*)-BINOP-F or 1,2-bis(diphenylphosphinamino)cyclohexane [128–132]. These mild chiral Lewis acids proved to be excellent catalysts for the intermolecular Diels Alder reactions of dienes with acrolein derivatives [128–130] [Eq. (61)] and enones [131] as well as for the intramolecular Diels Alder reaction of suitable trienes [132] [Eq. (62)].



An example of Cp*RuCl(cod)-catalyzed homo Diels Alder [2+2+2] cycloaddition of alkynylphosphonates with norbornadiene providing the corresponding phosphonate substituted deltacyclenes was also described [133] [Eq. (63)]. This reactivity was found to be dependent on the presence of the phosphonate moiety.



9 Conclusions

The catalytic activation of alkynes and alkenes by (C₅R₅)Ru complexes has been extensively explored during the past decade and can lead to the creation of carbon–carbon bonds, often via the formation of a ruthenacycle intermediate after an oxidative coupling process. [2+2+2] Cycloadditions, cycloisomerizations, or dienes formation are examples of the versatility of these complexes. The diversity and the selectivity (regio- and often stereoselectivity) of these reactions, which can proceed under mild conditions [134–136], show the interest of (C₅R₅)Ru catalysts for new synthetic methodologies and the future potential in organic synthesis.

References

1. Albers MO, de Waal DJA, Liles DC, Robinson DJ, Singleton E, Wiege MB (1986) *J Chem Soc Chem Commun* 1680
2. Gemel C, LaPensée A, Mauthner K, Mereiter K, Schmid R, Kirchner K (1997) *Monatsh Chem* 128:1189
3. Ernst C, Walter O, Dinjus E, Arzberger S, Görls H (1999) *J Prakt Chem* 341:801
4. Le Paih J, Monnier F, Dérien S, Dixneuf PH, Clot E, Eisenstein O (2003) *J Am Chem Soc* 125:11964
5. Klein H, Roisnel T, Bruneau C, Dérien S (2012) *Chem Commun* 48:11032
6. Le Paih J, Dérien S, Demerseman B, Bruneau C, Dixneuf PH, Toupet L, Dazinger G, Kirchner K (2005) *Chem Eur J* 11:1312
7. Zhang M, Jiang H-F, Neumann H, Beller M, Dixneuf PH (2009) *Angew Chem Int Ed* 48:1681
8. Zhang M, Jiang H, Dixneuf PH (2009) *Adv Synth Catal* 351:1488
9. Zhang M, Roisnel T, Dixneuf PH (2010) *Adv Synth Catal* 352:1896
10. Trost BM, Maulide N, Rudd MT (2009) *J Am Chem Soc* 131:420
11. Ura Y, Sato Y, Shiotsuki M, Kondo T, Mitsudo T-A (2004) *J Mol Catal A* 209:35
12. Ura Y, Sato Y, Tsujita H, Kondo T, Imachi M, Mitsudo T-A (2005) *J Mol Catal A* 239:166
13. Yamamoto Y, Ishii J-i, Nishiyama H, Itoh K (2004) *J Am Chem Soc* 126:3712
14. Yamamoto Y, Ishii J-I, Nishiyama H, Itoh K (2005) *Tetrahedron* 61:11501
15. Yamamoto Y, Ishii J-I, Nishiyama H, Itoh K (2005) *J Am Chem Soc* 127:9625
16. Varela JA, Castedo L, Saa C (2003) *J Org Chem* 68:8595
17. Yamamoto Y, Kinpara K, Saigoku T, Takagishi H, Okuda S, Nishiyama H, Itoh K (2005) *J Am Chem Soc* 127:605
18. Yamamoto Y, Arakawa T, Ogawa R, Itoh K (2003) *J Am Chem Soc* 125:12143
19. Young DD, Senaiar RS, Deiters A (2006) *Chem Eur J* 12:5563
20. Senaiar RS, Teske JA, Young DD, Deiters A (2007) *J Org Chem* 72:7801
21. Young DD, Sripada L, Deiters A (2007) *J Comb Chem* 9:735
22. Sripada L, Teske JA, Deiters A (2008) *Org Biomol Chem* 6:263
23. Teske JA, Deiters A (2008) *Org Lett* 10:2195
24. Zou Y, Deiters A (2010) *J Org Chem* 75:5355
25. Yamamoto Y, Hattori K, Ishii J-I, Nishiyama H, Itoh K (2005) *Chem Commun* 4438
26. Yamamoto Y, Hattori K, Ishii J-I, Nishiyama H (2006) *Tetrahedron* 62:4294
27. Yamamoto Y, Hattori K, Nishiyama H (2006) *J Am Chem Soc* 128:8336
28. Yamamoto Y, Hattori K (2008) *Tetrahedron* 64:847
29. Yamamoto Y, Kinpara K, Saigoku T, Nishiyama H, Itoh K (2004) *Org Biomol Chem* 2:1287
30. Shchetnikov GT, Osipov SN, Bruneau C, Dixneuf PH (2008) *Synlett* 578
31. Zotova MA, Vorobyeva DV, Dixneuf PH, Bruneau C, Osipov SN (2013) *Synlett* 24:1517
32. Yamamoto Y, Saigoku T, Ohgai T, Nishiyama H, Itoh K (2004) *Chem Commun* 2702
33. Yamamoto Y, Saigoku T, Nishiyama H, Ohgai T, Itoh K (2005) *Org Biomol Chem* 3:1768
34. Yamamoto Y, Hashimoto T, Hattori K, Kikuchi M, Nishiyama H (2006) *Org Lett* 8:3565
35. Yamamoto Y, Yamashita K, Hotta T, Hashimoto T, Kikuchi M, Nishiyama H (2007) *Chem Asian J* 2:1388
36. Zou Y, Liu Q, Deiters A (2011) *Org Lett* 13:4352
37. Yamamoto Y, Yamashita K, Harada Y (2010) *Chem Asian J* 5:946
38. Yamamoto Y, Kinpara K, Nishiyama H, Itoh K (2005) *Adv Synth Catal* 347:1913
39. Yamamoto Y, Kinpara K, Ogawa R, Nishiyama H, Itoh K (2006) *Chem Eur J* 12:5618
40. Nissen F, Richard V, Alayrac C, Witulski B (2011) *Chem Commun* 47:6656
41. Varela JA, Castedo L, Saa C (2003) *Org Lett* 5:2841
42. Varela JA, Rubin SG, Gonzalez-Rodriguez C, Castedo L, Saa C (2006) *J Am Chem Soc* 128:9262
43. Varela JA, Rubin SG, Castedo L, Saa C (2008) *J Org Chem* 73:1320

44. Garcia-Rubin S, Varela JA, Castedo L, Saa C (2008) *Chem Eur J* 14:9772
45. Garcia-Rubin S, Varela JA, Castedo L, Saa C (2009) *Org Lett* 11:983
46. Trost BM, Rudd MT (2003) *J Am Chem Soc* 125:11516
47. Trost BM, Huang X (2005) *Org Lett* 7:2097
48. Trost BM, Huang X (2006) *Chem Asian J* 1:469
49. Trost BM, Rudd MT (2003) *Org Lett* 5:4599
50. Trost BM, Rudd MT (2005) *J Am Chem Soc* 127:4763
51. Trost BM, Gutierrez AC (2007) *Org Lett* 9:1473
52. Trost BM, Rudd MT, Gulias Costa M, Lee PI, Pomerantz AE (2004) *Org Lett* 6:4235
53. Yamashita K, Nagashima Y, Yamamoto Y, Nishiyama H (2011) *Chem Commun* 47:11552
54. Yamamoto Y, Mori S, Shibuya M (2013) *Chem Eur J* 19:12034
55. Yamamoto Y, Fukatsu K, Nishiyama H (2012) *Chem Commun* 48:7985
56. Yamashita K, Yamamoto Y, Nishiyama H (2012) *J Am Chem Soc* 134:7660
57. Trost BM, Papillon JPN (2004) *J Am Chem Soc* 126:13618
58. Trost BM, Papillon JPN, Nussbaumer T (2005) *J Am Chem Soc* 127:17921
59. Trost BM, Yang H, Probst GD (2004) *J Am Chem Soc* 126:48
60. Trost BM, Seganish WM, Chung CK, Amans D (2012) *Chem Eur J* 18:2948
61. Trost BM, Yang H, Wuitschik G (2005) *Org Lett* 7:4761
62. Lopez F, Castedo L, Mascarenas JL (2005) *Org Lett* 7:287
63. Hansen EC, Lee D (2005) *J Am Chem Soc* 127:3252
64. Cho EJ, Lee D (2007) *J Am Chem Soc* 129:6692
65. Murugesan S, Jiang F, Achard M, Bruneau C, Dérien S (2012) *Chem Commun* 48:6589
66. Saito N, Saito K, Shiro M, Sato Y (2011) *Org Lett* 13:2718
67. Trost BM, Martos-Redruejo A (2009) *Org Lett* 11:1071
68. Tenaglia A, Giordano L (2003) *Synlett* 2333
69. Jordan RW, Khoury PR, Goddard JD, Tam W (2004) *J Org Chem* 69:8467
70. Liu P, Jordan RW, Kibbee SP, Goddard JD, Tam W (2006) *J Org Chem* 71:3793
71. Jordan RW, Villeneuve K, Tam W (2006) *J Org Chem* 71:5830
72. Burton RR, Tam W (2007) *J Org Chem* 72:7333
73. Jordan RW, Le Marquand P, Tam W (2008) *Eur J Org Chem* 80
74. Villeneuve K, Jordan RW, Tam W (2003) *Synlett* 2123
75. Villeneuve K, Tam W (2004) *Angew Chem Int Ed* 43:610
76. Riddell N, Villeneuve K, Tam W (2005) *Org Lett* 7:3681
77. Villeneuve K, Riddell N, Tam W (2006) *Tetrahedron* 62:3823
78. Villeneuve K, Riddell N, Jordan RW, Tsui GC, Tam W (2004) *Org Lett* 6:4543
79. Allen A, Villeneuve K, Cockburn N, Fatila E, Riddell N, Tam W (2008) *Eur J Org Chem* 4178
80. Riddell N, Tam W (2006) *J Org Chem* 71:1934
81. Cockburn N, Karimi E, Tam W (2009) *J Org Chem* 74:5762
82. Durham R, Mandel J, Blanchard N, Tam W (2011) *Can J Chem* 89:1494
83. Burton RR, Tam W (2006) *Tetrahedron Lett* 47:7185
84. Villeneuve K, Tam W (2006) *Organometallics* 25:843
85. Tenaglia A, Marc S (2006) *J Org Chem* 71:3569
86. Villeneuve K, Tam W (2006) *Eur J Org Chem* 5449
87. Villeneuve K, Tam W (2007) *Organometallics* 26:6082
88. Tenaglia A, Marc S, Giordano L, De Riggi I (2011) *Angew Chem Int Ed* 50:9062
89. Tenaglia A, Marc S (2008) *J Org Chem* 73:1397
90. Burton RR, Tam W (2007) *Org Lett* 9:3287
91. Fukuyama T, Yamaura R, Higashibeppu Y, Okamura T, Ryu I, Kondo T, Mitsudo T-A (2005) *Org Lett* 7:5781
92. Sugimoto K, Yoshida M, Ihara M (2006) *Synlett* 1923
93. Trost BM, Surivet J-P, Toste FD (2004) *J Am Chem Soc* 126:15592
94. Trost BM, Dong L, Schroeder GM (2005) *J Am Chem Soc* 127:2844

95. Trost BM, Shen HC, Schulz T, Koradin C, Schirok H (2003) *Org Lett* 5:4149
96. Trost BM, Shen HC, Horne DB, Toste FD, Steinmetz BG, Koradin C (2005) *Chem Eur J* 11:2577
97. Hong X, Trost BM, Houk KN (2013) *J Am Chem Soc* 135:6588
98. Trost BM, Hu Y, Horne DB (2007) *J Am Chem Soc* 129:11781
99. Trost BM, Nguyen HM, Koradin C (2003) *Tetrahedron Lett* 51:6232
100. Fürstner A, Schlecker A, Lehmann CW (2007) *Chem Commun* 4277
101. Mori M, Tanaka D, Saito N, Sato Y (2008) *Organometallics* 27:6313
102. Tanaka D, Sato Y, Mori M (2007) *J Am Chem Soc* 129:7730
103. Tanaka D, Sato Y, Mori M (2006) *Organometallics* 25:799
104. Saito N, Tanaka D, Sato Y (2009) *Organometallics* 28:669
105. Saito N, Tanaka D, Sato Y (2009) *Org Lett* 11:4124
106. Saito N, Ichimaru T, Sato Y (2012) *Chem Asian J* 7:1521
107. Saito N, Kohyama Y, Tanaka Y, Sato Y (2012) *Chem Commun* 48:3754
108. Trost BM, Ferreira EM, Gutierrez AC (2008) *J Am Chem Soc* 130:16176
109. Trost BM, Gutierrez AC, Ferreira EM (2010) *J Am Chem Soc* 132:9206
110. Jack K, Tam W (2013) *J Org Chem* 78:3416
111. Yoshida M, Gotou T, Ihara M (2003) *Tetrahedron Lett* 44:7151
112. Bustelo E, Guérot C, Hercouet A, Carboni B, Toupet L, Dixneuf PH (2005) *J Am Chem Soc* 127:11582
113. Trost BM, McClory A (2006) *Org Lett* 8:3627
114. Yamamoto Y, Nakagai Y-I, Itoh K (2004) *Chem Eur J* 10:231
115. Le Paih J, Vovard-Le Bray C, Dérien S, Dixneuf PH (2010) *J Am Chem Soc* 132:7391
116. Morita R, Shirakawa E, Tsuchimoto T, Kawakami Y (2005) *Org Biomol Chem* 3:1263
117. Vovard-Le Bray C, Dérien S, Dixneuf PH (2009) *Angew Chem Int Ed* 48:1439
118. Moulin S, Zhang H, Raju S, Bruneau C, Dérien S (2013) *Chem Eur J* 19:3292
119. Cambeiro F, Lopez S, Varela JA, Saa C (2012) *Angew Chem Int Ed* 51:723
120. Monnier F, Castillo D, Dérien S, Toupet L, Dixneuf PH (2003) *Angew Chem Int Ed* 42:5474
121. Monnier F, Vovard-Le Bray C, Castillo D, Aubert V, Dérien S, Dixneuf PH, Toupet L, Ienco A, Mealli C (2007) *J Am Chem Soc* 129:6037
122. Vovard-Le Bray C, Klein H, Dixneuf PH, Macé A, Berrée F, Carboni B, Dérien S (2012) *Adv Synth Catal* 354:1919
123. Eckert M, Monnier F, Shchetnikov GT, Titanyuk ID, Osipov SN, Toupet L, Dérien S, Dixneuf PH (2005) *Org Lett* 7:3741
124. Eckert M, Moulin S, Monnier F, Titanyuk ID, Osipov SN, Roisnel T, Dérien S, Dixneuf PH (2011) *Chem Eur J* 17:9456
125. Vovard-Le Bray C, Dérien S, Dixneuf PH, Murakami M (2008) *Synlett* 193
126. Basato M, Tubaro C, Biffis A, Bonato M, Buscemi G, Lighezzolo F, Lunardi P, Vianini C, Benetollo F, Del Zotto A (2009) *Chem Eur J* 15:1516
127. Trost BM, Breder A, O'Keefe BM, Rao M, Franz AW (2011) *J Am Chem Soc* 133:4766
128. Alezra V, Bernardinelli G, Corminboeuf C, Frey U, Kündig EP, Merbach AE, Saudan CM, Viton F, Weber J (2004) *J Am Chem Soc* 126:4843
129. Anil Kumar PG, Pregosin PS, Vallet M, Bernardinelli G, Jazzar RF, Viton F, Kündig EP (2004) *Organometallics* 23:5410
130. Arena CG, Bruno G, Nicolo F (2010) *Polyhedron* 29:2822
131. Rickerby J, Vallet M, Bernardinelli G, Viton F, Kündig EP (2007) *Chem Eur J* 13:3354
132. Thamapipol S, Bernardinelli G, Besnard C, Kündig EP (2010) *Org Lett* 12:5604
133. Kettles TJ, Cockburn N, Tam W (2011) *J Org Chem* 76:6951
134. Severa L, Vavra J, Kohoutova A, Cizkova M, Salova T, Hyvl J, Saman D, Pohl R, Adriaenssens L, Teply F (2009) *Tetrahedron Lett* 50:4526
135. Adriaenssens L, Severa L, Salova T, Cisarova I, Pohl R, Saman D, Rocha SV, Finney NS, Pospisil L, Slavicek P, Teply F (2009) *Chem Eur J* 15:1072
136. Xu F, Wang C, Li X, Wan B (2012) *ChemSusChem* 5:854

Organometallic Ruthenium Nanoparticles and Catalysis

Karine Philippot, Pascal Lignier, and Bruno Chaudret

Abstract Due to a high number of possible applications in various domains, metal nanoparticles are nowadays the subject of an extensive development. This interest in metal nanoparticles is related to their electronic properties at the frontier between those of molecular species and bulk compounds which are induced by their nanometric size. Regarding the field of catalysis, the growing attention for metal nanoparticles also results from the high proportion of surface atoms present in the upper layer of the metallic core which gives rise to numerous potential active sites. Thus, nanocatalysis (which involves the use of catalysts with at least one dimension at the nanoscale) has emerged in the field of modern catalysis as a domain on the borderline between homogeneous and heterogeneous catalysis. Present developments aim at multifunctionality which can be achieved by the proper design of complex nanostructures also named nanohybrids. In nanohybrid the term “hybrid” refers to the appropriate association between a metal core and a stabilizing shell such as a polymer, a ligand, an ionic liquid, or even a support (inorganic materials, carbon black, carbon nanotubes, etc...). This association can be considered as crucial to tune the surface properties of nanostructures and consequently their catalytic performance. The main expectation for the scientific community is that precisely designed nanoparticles (in terms of size, shape, and composition including surface ligands) should offer the benefits of both homogeneous and heterogeneous catalysts, namely high efficiency and better selectivity.

K. Philippot (✉) and P. Lignier
Laboratoire de Chimie de Coordination, CNRS, LCC, 205 Route de Narbonne, 31077
Toulouse, France

Université de Toulouse, UPS, INPT, LCC, 31077 Toulouse, France
e-mail: karine.philippot@lcc-toulouse.fr

B. Chaudret
Laboratoire de Physique et Chimie des Nano-Objets (LPCNO), UMR5215 INSA-CNRS-UPS,
Institut des Sciences appliquées, 135, Avenue de Rangueil, 31077 Toulouse, France

In that context, we have been developing an efficient and versatile synthesis method using common tools from organometallic chemistry to produce well-controlled nanostructures which have been proved to be of interest for application in catalysis. A high number of studies have been focused on ruthenium nanosystems due to the use of a very convenient organometallic precursor, namely [Ru(COD)(COT)], as the metal source. This Ru complex is easily decomposed under dihydrogen atmosphere at room temperature. In addition, it is a complex of choice to prepare “naked” ruthenium nanostructures since the olefinic ligands present in the coordination sphere of ruthenium are hydrogenated into alkanes which exhibit no interaction with the metal surface. As a consequence, the metallic surface of the obtained nanoparticles is only covered by hydrides and the stabilizer which was deliberately added. This is highly convenient for studying the influence of the stabilizer on the morphology of the nanoparticles as well as their surface chemistry and related catalytic performance.

This chapter gives an overview of our experience in the preparation of ruthenium nanoparticles of controlled size and surface state. Insights are given on the study of their surface chemistry by using simple techniques, mainly IR and NMR, both in solution and in solid state, as well as model hydrogenation reactions. We also discuss the performances of the Ru nanoparticles in catalysis which have been investigated both in solution (in organic or aqueous phases) and after their deposition on a support (alumina, silica, or carbon supports).

Keywords Catalysis · Colloid · Ligand · Nanocluster · Nanohybrid · Nanoparticle · Nanostructure · Organometallic synthesis · Ruthenium · Surface chemistry

Contents

1	Introduction	321
2	Organometallic Synthesis of RuNPs and Surface Chemistry Studies	324
2.1	Polymer-Stabilized RuNPs	324
2.2	Alcohol-Stabilized RuNPs	326
2.3	Ligand-Stabilized RuNPs	329
2.4	Bimetallic RuPt, RuFe, and RuSn NPs	340
3	Investigation of RuNPs in Organic Colloidal Catalysis	342
3.1	β -Aminoalcohols and Oxazoline-Stabilized RuNPs	343
3.2	Diphosphite-Stabilized RuNPs	343
3.3	Diphosphine-Stabilized RuNPs	345
3.4	Secondary Phosphine Oxide (SPO)-Stabilized RuNPs	346
3.5	APTS-Stabilized RuNPs for Dehydrogenation Reactions of Amine-Boranes	347
4	Water-Soluble RuNPs for Investigation in Aqueous Colloidal Catalysis	349
4.1	PTA-Stabilized RuNPs	349
4.2	Sulfonated Diphosphine-Stabilized RuNPs	351
4.3	Sulfonated Diphosphine/Cyclodextrin-Stabilized RuNPs	353
5	Ionic Liquid-Stabilized RuNPs	354

6	Investigation of RuNPs in Supported Catalysis	359
6.1	Alumina-Supported RuNPs for Hydrogenation and Oxidation Reactions	359
6.2	Silica-Supported RuNPs for Oxidation of Carbon Monoxide and Benzylalcohol ..	360
6.3	Carbon Material-Supported RuNPs for Hydrogenation and Oxidation Reactions ..	362
7	Conclusions and Perspectives	362
	References	366

1 Introduction

Due to a high number of potential applications in various fields such as optoelectronics, sensors, medicine, catalysis [1, 2], metal nanoparticles, also named nanoclusters, nanostructures or colloids are nowadays the subject of an extensive development. This growing attention for metal nanoparticles (MNPs) results mainly from their particular electronic properties induced by their nanometric size and situated at the frontier between those of molecular species and bulk compounds. Present developments aim at multifunctionality at the nanoscale and this can be achieved by the proper design of nanohybrids. In nanohybrids, the term “hybrid” refers to the appropriate association between a metal core and a stabilizing shell which can be a polymer, a ligand, or even a support. This association can be considered as a key parameter to tune the surface properties of nanostructures. When catalysis is the target application, the high proportion of surface atoms present in the upper layer of metal nanoparticles is also of high interest since it gives rise to numerous potential active sites [3–6]. Thus, in the modern area of catalysis, nanocatalysis which involves the use of catalysts with at least one dimension at the nanoscale has emerged as a domain on the borderline between homogeneous and heterogeneous catalysis [7–11]. The main expectation for the scientific community is that precisely designed nanoparticles (in terms of size, shape, and composition including surface ligands) should offer the benefits of both homogeneous and heterogeneous catalysts, namely high efficiency and better selectivity.

For applications in catalysis, the production of metal nanoparticles mainly deals with (1) chemical or electrochemical reduction of the corresponding metal salts, (2) decomposition of organometallic complexes through reduction and/or displacement of ligands from the coordination sphere. These syntheses require the presence of a stabilizer (also called capping agent) [12, 13] which can be a wide range of functional organic ligands [14, 15], surfactants [16], polymers [17, 18], dendrimers [19–21], ionic liquids [22, 23], inorganic ligands [24] as reported in the literature. The choice of the stabilizing agent is crucial since this can influence the nucleation, growth, stability, and surface chemistry of MNPs [25]. Thus, the synthesis and characterization of metal-based nanocatalysts have experienced a huge development during the past decade, e.g., to determine the influence of the stabilizer on the catalytic properties. Since the surface properties of MNPs are related to their size, shape, crystalline structure, chemical composition, efficient synthetic methods are required to have MNPs of well-defined characteristics. This will enable to precisely

study the influence of MNP morphology on their surface properties and catalytic performances. In parallel to these methods for the preparation of MNPs, heterogeneous catalysis has developed powerful tools to model and characterize the surface of the nanoparticles. Interestingly, these studies can be achieved during the catalytic process (Transmission Electron Microscopy (TEM), powder X-Ray Diffraction (DRX), X-ray Photoelectron Spectrometry (XPS), Extended X-Ray Absorption Fine Structure (EXAFS), IR in operando) [26–34]. However, simple spectroscopic methods, such as UV/Vis, IR, or NMR both in solution and in solid state, which are adapted from molecular chemistry and homogeneous catalysis, offer interesting alternatives to precisely characterize the metallic surface of MNPs.

For 25 years, our team has been developing a versatile approach for the synthesis of metal nanoparticles starting from organometallic precursors. This approach was inspired by previous results on the preparation of hydrogen-rich complexes [35]. It takes advantage of previous knowledge on organometallic complexes which are not very thermally stable, and prone to oxidation, sometimes energetically. This leads to the formation of black solutions or residues as observed for various metals. Whilst these observations seemed very detrimental for molecular reactions, this has prompted chemists to take profit of this decomposition tendency. As a consequence, organometallic complexes have been used as precursors for the preparation of metal nanoparticles. Since organometallic derivatives are not always easy to prepare and most often sensitive to both air and moisture, this may seem both senseless and expensive to decompose them to prepare metal nanoparticles. However, this approach exhibits two main advantages. First, their decomposition requires milder conditions which allow a better control of the nanoparticle formation. Second, organometallic derivatives offer access to clean procedures which avoid the presence of contaminants such as salts, halides, main group oxides, on the surface of the nanostructures [36, 37].

The interest of high energy organometallic complexes to synthesize otherwise inaccessible species was demonstrated in the early 1980s by John Spencer who reported the synthesis of polyhydrido platinum clusters from platinum (0) olefin complexes [38, 39]. This work served as an inspiration for the subsequent synthesis of polyhydrido ruthenium complexes. Besides the bis(styrene) ruthenium derivative, $[\text{Ru}(\text{C}_8\text{H}_8)_2(\text{PPh}_3)_2]$ [40], the scope of which was found to be too limited, the possibility of using a new ruthenium(0) complex $[\text{Ru}(\text{COD})(\text{COT})]$ (COD = 1,5-cyclooctadiene; COT = 1,3,5-cyclooctatriene) was explored [41]. This resulted in the preparation of the $[\text{RuH}_2(\text{H}_2)_2(\text{PCy}_3)_2]$ complex at room temperature by bubbling dihydrogen into a solution containing the $[\text{Ru}(\text{COD})(\text{COT})]$ precursor and two molar equivalents of a bulky phosphine, PCy_3 [35]. When testing the generality of this synthesis, it was noticed that in certain cases the solution turned black and that, in the absence of any ligand, a black deposit of pyrophoric ruthenium powder precipitated. Following this observation, and fascinated by previous pioneering works (see, for example, the works of Chini et al. on very large organometallic clusters [42–44], Basset et al. on the use of organometallic complexes to prepare heterogeneous catalysts [45], Schmid et al. on the preparation of Gold 55 clusters through borane reduction of

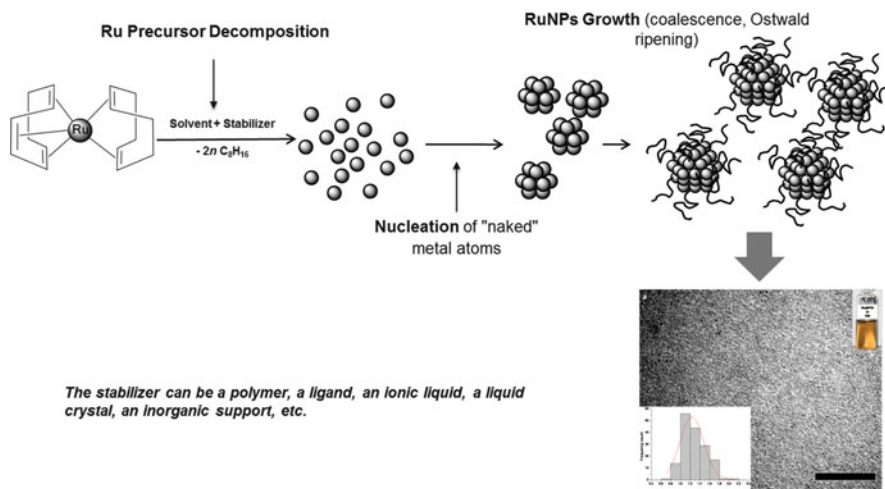


Fig. 1 Synthesis of ruthenium nanoparticles from [Ru(COD)(COT)] organometallic precursor. (Adapted from [37] with permission from the CNRS and RSC)

AuCl(PPh₃) (see for example: [46–50]), and Bradley et al. who decomposed carbonyl clusters to produce nanoparticles in solution [51]), we attempted the controlled decomposition of [Ru(COD)(COT)] in the presence of various stabilizers in order to prepare hydride containing large clusters. As a result, we first obtained diverse polymer-stabilized ruthenium nanoparticles (RuNPs) and then extended the approach to both different stabilizers (mainly ligands) and different metals [52]. Thus, in addition to noble metals (Au, Ag, Pt, Rh, Pd, Ru) which are of interest in catalysis, this approach could be extended to magnetic metals (Fe, Co, Ni, and their alloys) via a judicious choice of precursors. The resulting materials may display interesting magnetic properties for potential applications as hard magnets which are relevant for tunnel magnetoresistance or for hyperthermia. In addition copper may be used for applications in micro-electronics (see for example: [53–57]). This implies to employ precursors, such as [Co(COE)(COD)], [Ni(COD)₂]; COE = cyclooctenyle, which are similar to [Ru(COD)(COT)]. Aryl (Cu(Mes)₄; Mes = mesityl) and amido (M[N(SiMe₃)₂]₂; M = Fe, Co) complexes are also relevant. For example, the amine ligand could be easily displaced from the nanoparticle surface.

About ruthenium, a strong activity has been maintained all over the years since ruthenium is a metal of interest in catalysis (it is a very good hydrogenation and oxidation catalyst). In addition, ruthenium can easily accommodate ligands which allow us to study the influence of ligands on the growth of nanoparticles. Furthermore, this metal hardly displays any Knight shift which makes it a metal of choice to study the coordination of the ligand by solution or solid-state NMR. Finally, the olefinic complex [Ru(COD)(COT)] is particularly convenient since its decomposition easily occurs below room temperature (RT) under low dihydrogen pressure (Fig. 1). Under dihydrogen, the unsaturated ligands present in the coordination

sphere are reduced in corresponding alkanes which are inert towards the metallic surface and thus do not interact with the growing nanoparticles. As a consequence, Ru(COD)(COT)] is a source of “naked” Ru atoms in very mild conditions in solution. The resulting particles are, however, not totally naked since they are covered with hydrides (resulting from the synthesis conditions). In addition, the nanoparticles interact with the added stabilizers present in solution. This makes possible to precisely tune the surface properties of metal nanoparticles by an appropriate choice of the stabilizer as discussed later. Then, the question is related to the stabilization of the nanoparticles. What do we need to stabilize nanoparticles, allow them to react but not to coalesce up to the point where they will agglomerate and precipitate? The ruthenium is again ideal since there are only hydrides on the ruthenium surface. This enables us to study a wide range of stabilizers including the stabilizing agents which exhibit very weak interactions with the metal surface.

In this chapter, we present an overview of our experience in the organometallic synthesis of ruthenium nanoparticles of controlled size and surface state. We also give insights on the study of their surface chemistry by using simple techniques, mainly IR and NMR both in solution and in solid state. In addition, model hydrogenation reactions have been used. We also discuss the performances of these materials as catalysts in solution (organic and aqueous phases) and on a support (alumina, silica, or carbon materials).

2 Organometallic Synthesis of RuNPs and Surface Chemistry Studies

2.1 *Polymer-Stabilized RuNPs*

Polymers have long been used to stabilize metal nanoparticles giving rise to a steric protection [58]. In fact, an organic polymer may display a structure containing voids which results in the formation of “nanoreactors” inside which the nanoparticles can grow depending on the amount of precursor present. As a consequence, the size distribution of the particles is controlled by the concentration of the solution as well as both the size and monodispersity of these “nanoreactors.” In these cases, the nanoparticles display little or no chemical interaction with the polymer, i.e. they are ligand-free except both solvent and hydrogen. These materials appear ideal for catalysis and surface studies.

Our synthesis procedure was developed originally using [Ru(COD)(COD)] as a precursor under mild conditions of pressure and temperature (3 bar H₂, RT). The dihydrogen atmosphere acts as a reducing agent in the presence of a polymer (Fig. 2), namely nitrocellulose (NC), cellulose acetate (CA), or polyvinylpyrrolidone (PVP). The hydrogen treatment allows the reduction of the olefin ligands of the ruthenium precursor into cyclooctane which is inert towards the metal surface. This is a crucial point since the metal surface of these polymer-stabilized

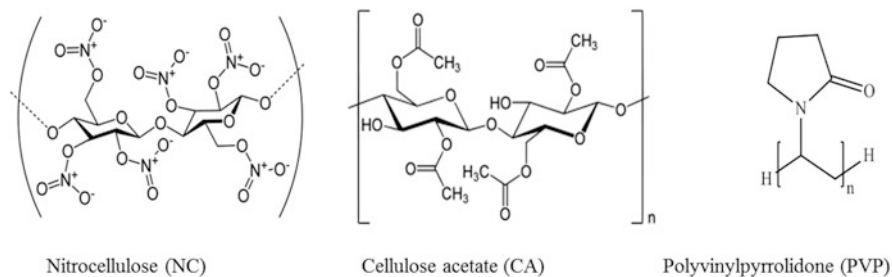


Fig. 2 Formula of polymers used for the synthesis of polymer-stabilized RuNPs

systems is “naked”. In collaboration with J. Bradley, we showed that nanoparticles of ruthenium of very small size (ca. 1 nm) could be obtained by bubbling hydrogen through a solution of $[\text{Ru}(\text{COD})(\text{COT})]$ in THF in the presence of PVP. Interestingly, intriguing ^{13}C NMR results were obtained following the addition of ^{13}CO [59]. The preparations of RuNPs stabilized by nitrocellulose and cellulose acetate were the first results entirely obtained in the group on this topic [60]. The resulting nanoparticles were very small in size, exhibiting a mean diameter between 1 and 2 nm, which depends on both the nature of the polymeric matrix and the metal/polymer ratio (wt.%). These results showed that small RuNPs can remain well dispersed in the reaction medium using polymers which weakly interact with this surface.

The stable nanoparticles were used to study the surface reactivity of nano-objects. To probe the surface state of these RuNPs, the adsorption of carbon monoxide (CO) was studied by IR. This shows that CO can coordinate at the surface of the particles in two different coordination modes: linear at $2,030\text{ cm}^{-1}$ and bridging at $1,968\text{ cm}^{-1}$.

The synthesis of RuNPs in the presence of polyvinylpyrrolidone was then revisited using our now standard procedure (3 bar H_2) giving rise to 1.1 nm nanoparticles (Fig. 3) [61].

Characterization by WAXS showed crystalline nanoparticles displaying the expected hexagonal close packed (hcp) structure of bulk ruthenium. Reactivity studies were carried out in particular with CO to show the availability of the nanoparticles surface for reactivity. Recently, the synthesis of these PVP-stabilized RuNPs has been reproduced to perform an exhaustive study of the coordination of CO to their surface by a combination of IR and NMR techniques [62]. It has been observed that: (1) the coordination mode of the CO to the NP surface depends on the reaction time and (2) CO is mobile. Low reaction-times give rise to CO adsorption in the bridging mode while longer reaction times result in the adsorption of more CO molecules only adsorbed in the linear or multicarbonyl modes.

These PVP-stabilized RuNPs were also shown to be of interest for chemical transformations. In a recent work with Rousseau et al., these NPs appeared as a highly active catalyst for the deuteration of nitrogen-containing compounds [63].

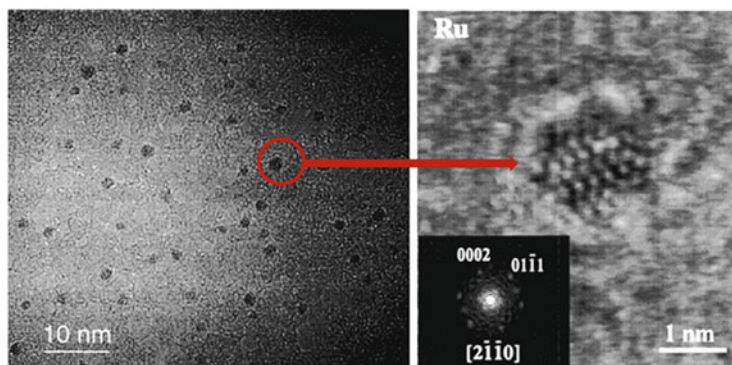


Fig. 3 TEM (*left*) and HRTEM (*right*) micrographs of RuNPs in PVP. (Reproduced from [61] with permission from ACS)

In the presence of D_2 as the isotopic source, the PVP-stabilized RuNPs allowed an efficient H/D exchange which resulted in the deuteration of a large diversity of aza compounds such as pyridines, quinolines, indoles, and alkyl amines. A total of 22 compounds could be isotopically labeled in good yields with high chemo- and regioselectivities following a simple procedure, i.e. mild reaction conditions (1–2 bar of D_2 ; $55^\circ C$) and simple filtration to recover the labeled product. The viability of this procedure was demonstrated by the labeling of eight biologically active compounds. Remarkably, conservation of the enantiomeric purity of the labeled compounds was observed, even though labeling took place in the vicinity of the asymmetric center. The level of isotopic enrichment that could be reached is suitable for metabolomic studies in most cases. In addition to these applications to molecules of biological interest, this study reveals a rich and underestimated chemistry on the surface of RuNPs, which can be further exploited as novel reagents in organic chemistry.

In summary, simple organic polymers can be efficiently used for the organometallic synthesis of RuNPs, giving rise to the formation of very small nanoparticles (down to ca. 1 nm) which are stable under inert atmosphere. These nanoparticles can be isolated as a powder and dissolved when required. This steric stabilization is a great advantage for reactivity and mechanistic studies. A new way for catalysis and organic chemistry has recently been opened due to novel results in the regioselective and stereospecific isotopic labeling of nitrogen-containing compounds.

2.2 Alcohol-Stabilized RuNPs

Similarly to numerous data in the literature, our initial results showed that RuNPs could be stabilized in a simple polymer matrix which exhibits very weak chemical interactions with the NP surface. The next questions were: (1) how weak a stabilizer

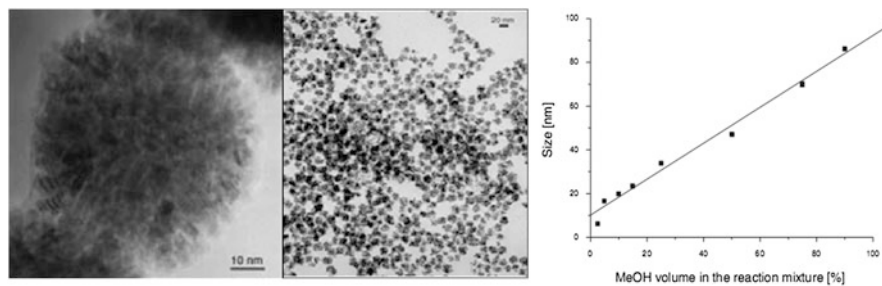


Fig. 4 Polycrystalline “spongelike” RuNPs obtained in pure methanol (*left*), in a 10/90 mixture of methanol and THF (*middle*) and linear correlation between the MeOH/THF volume ratio and the particle size (*right*). (Adapted from [64, 65] with permission from Wiley)

can be? (2) under very mild conditions, can we prepare nano-objects displaying their own stability (giant clusters)? For this purpose, the organometallic precursor [Ru(COD)(COT)] was dissolved in various solvents to then react with an H_2 atmosphere. Whilst only a black ruthenium precipitate was obtained in neat pentane, dichloromethane and THF, a stabilization was observed in some neat alcohols and THF/alcohol mixtures in the absence of further stabilizer [64, 65]. The particles were characterized by TEM, XRD, WAXS, and XPS. TEM micrographs revealed the presence of polycrystalline sponge-like particles of regular spherical shape and homogeneous size. In addition, both isolated and well-dispersed monocrystalline particles were sometimes observed depending upon the solvent mixture and the alcohol alkyl chain length (from C1 for methanol to C5 for pentanol). In all cases, size distributions were relatively narrow. WAXS and XRD analyses indicated the exclusive presence of hcp ruthenium in these materials. The size of the particles could be controlled by adjusting the reaction temperature or the composition of the solvent mixture. In pure methanol, the formation of large polycrystalline particles of 76 nm mean size was observed (Fig. 4, left). Smaller nanostructures are formed by decreasing the quantity of methanol in a MeOH/THF reaction mixture. As examples, nanostructures of mean size 16 nm were formed for a MeOH/THF/ratio of 10/90 in volume (Fig. 4, middle) and nanostructures of a size range of 3–6 nm for a 2.5/97.5 MeOH/THF ratio. A surprising linear correlation was established between the solvent composition and the size of the particles in the range 4–85 nm (Fig. 4, right).

In addition, the particles display different spongelike morphologies depending upon the medium composition. In MeOH-rich mixtures, this spongelike aspect is more pronounced than in MeOH poor media. The colloidal solutions obtained in these reaction conditions are surprisingly very stable, i.e. they can be kept under argon for very long periods of time. The less stable solutions were prepared in MeOH-rich solutions which also contain the largest particles. The size and morphology variations observed upon changing the solvent mixtures were also unexpected. These observations were related to the increase in polarity of the solution upon adding MeOH in THF. This led us to suspect the segregation of cyclooctane,

which is synthesized from the reduction of the precursor, within the more polar solvents. In this respect, larger droplets are likely to be formed in the most polar solvent systems which are consequently expected as the most segregated medium. This hypothesis was confirmed following further experiments, i.e. adding excess of cyclooctane to a MeOH/THF 10/90 solution while keeping other parameters constant. The addition of 2 or 20 equiv. cyclooctane (equiv./initial Ru) led to an increase of the particle size of a factor 1.5 or 2, respectively. These results were consistent with the formation of ruthenium particles within the cyclooctane droplets (“nanoreactors”), i.e. the stabilization of the RuNPs in these systems results from a segregation phenomenon in the reaction mixture. Interestingly, this result implies that the nanoparticles are more soluble in cyclooctane than in alcohols. Although the origin of this phenomenon was not clear at that time, we have then demonstrated that the surface of the particles prepared in our conditions under H₂ accommodate between 1 and 2 hydrides per surface Ru atom. Since the polarity of the Ru–H bond is comparable to that of a C–H bond in molecular chemistry, these experiments suggest that the RuNPs prepared according to our procedure can be viewed as large grease bowls.

Using alcohols displaying longer alkyl chains than methanol, an important change in the nature of the particles was observed. Whilst the particles are homogeneous in size, their size drops to 2–5 nm for propanol, isopropanol, and pentanol. The particles are monocrystalline in pentanol and display a mean size of 3 nm. In *n*- and iso-propanol, the particles are slightly larger (4.8 nm in *n*-propanol) and may be polycrystalline. In all these cases, the solutions are stable (3–4 months in *n*-propanol). In pure heptanol [66], small and single crystalline RuNPs of 3 nm mean size were obtained, displaying the compact hcp structure. These NPs could be isolated as a black powder by: (1) evaporation of the solution to dryness, (2) concentration of the solution and precipitation from pentane. Microanalytical data on this powder indicated the presence of ca. 70% Ru and ca. 1 heptanol: 7.5 Ru. Considering these data and the RuNPs mean size of 3 nm, a calculation provided an estimation of 123 heptanol molecules present in the vicinity of the particles made of 923 Ru atoms (whose 362 are located on the surface). Whilst these heptanol ligands are associated with the ruthenium surface, some heptanol molecules may not be directly coordinated on this surface. However, the characterization of these purified particles by ¹H and ¹³C solution NMR in THF-d⁸ revealed the coordination of heptanol on their surface. Whilst the protons located on the carbon in α -position to oxygen were not visible, the protons located on the β carbon were very broad and not distinguishable from the other –CH₂– of the alkyl chain. These observations were attributed to the presence of a fast exchange between free heptanol and heptanol coordinated to the surface of a large particle tumbling slowly in the solution. In addition, the presence of dihydrogen desorbing from the RuNPs surface was detected by ¹H NMR. This was attributed to the presence of hydrides on the RuNPs surface as a result of their synthesis conditions. All these observations were in favor of the concomitant presence of both “X” functional ligands (hydrides) and “L” labile ligands (heptanol molecules) at the RuNP surface. This suggested the possibility to develop a novel complex chemistry

using the traditional concepts of organometallic chemistry and monodisperse particles as “super-atoms.” Finally, all these particles prepared in alcohols appeared extremely reactive when isolated in the solid state since they burned in contact with air. Catalytic studies performed with the nanoparticles prepared in 10% MeOH showed that these RuNPs are active for the reduction of benzene to cyclohexane in mild conditions (20 bar, 80°C, 15 h) and remain unaltered following their evaluation in catalysis.

All these results obtained with alcohols suggested the presence of hydrogen on the surface of the particles and raised the question of the nature of the stabilization mechanism of the particles prepared by hydrogenation of [Ru(COD)(COT)] in alcoholic medium. It appeared that depending on the nature of the alcohol, i.e. the length of the alkyl chain and the polarity, the control of the growth of the nanoparticles may result (1) from the size of “nanoreactors” formed in the reaction medium due to a segregation phenomenon and (2) from a weak-coordinating effect of a ligand when the alkyl chain of the alcohol is long enough.

2.3 *Ligand-Stabilized RuNPs*

Following our achievements with polymers and alcohols, our research widely focused on the preparation of well-defined RuNPs stabilized by ligands of different natures [67]. Some of our aims were to better understand how a ligand can affect the surface chemistry of the nanoparticles as well as how the stabilization of the nanoparticles depends on the interaction of the ligand with the metallic surface. Another interest for us in using ligands was their potential to orientate the course of a catalytic reaction by inducing selectivity, a well-known phenomenon in homogeneous catalysis. Whilst numerous efforts have been devoted to the use of simple ligands, more sophisticated molecules have also been selected for the development of nanocatalysts with improved catalytic performances in comparison with already known homogeneous and heterogeneous catalysts. Our studies to develop novel RuNP nanocatalysts mainly involved ligands containing nitrogen (amines, aminoalcohols, oxazolines), phosphorus (diphosphites, phosphines, secondary phosphine oxides), or carbon (carbenes) as coordinating atoms to the metal surface. Here, we discuss how the ligand can control different properties of the nanoparticles such as their size, shape, and surface reactivity. Some RuNPs have been applied in catalysis, mainly in hydrogenation reactions of model substrates and also in dehydrogenation of amine-boranes.

2.3.1 *Amine-Stabilized RuNPs*

Amines are frequently used for the synthesis of metal nanoparticles. Amines can act as reducing agent and as stabilizers due to their σ -type coordination mode to the metallic surface (see for example: [68–70]). The use of simple amines for the

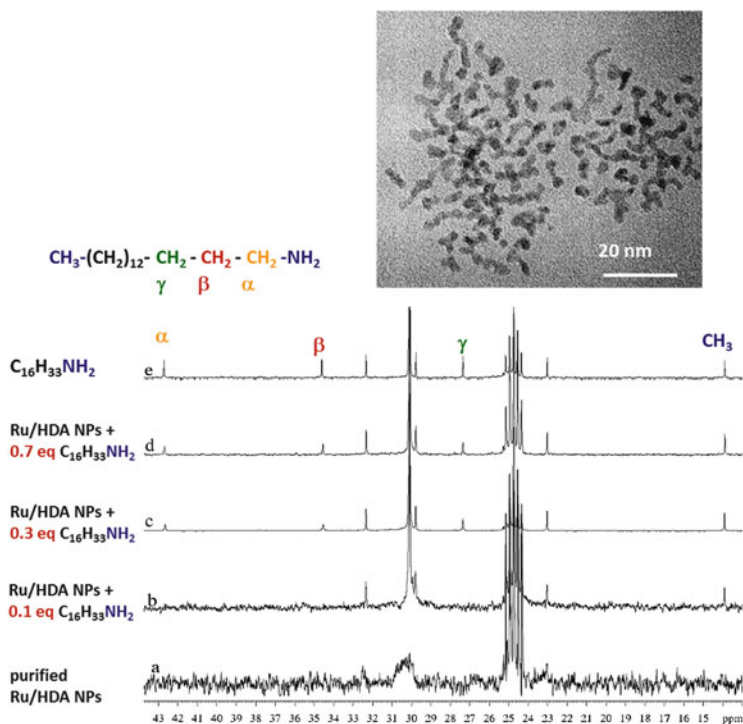


Fig. 5 TEM image of RuNPs stabilized with 0.2 equiv. of hexadecylamine (*top*) and ^{13}C NMR studies (100.71 MHz, THF-d^8 , 303 K) (*bottom*): (a) purified colloid, (b) colloid + 0.1 equiv. HDA, (c) colloid + 0.3 equiv. HDA, (d) colloid + 0.7 equiv. HDA, (e) pure HDA. (Adapted from [61] with permission from ACS)

stabilization of RuNPs was described by our group in 2001 [61]. The decomposition of the $[\text{Ru}(\text{COD})(\text{COD})]$ complex was performed under the same reaction conditions as with polymers or alcohols (3 bar H_2 , RT) but using $\text{C}_8\text{H}_{17}\text{NH}_2$, $\text{C}_{12}\text{H}_{25}\text{NH}_2$ or $\text{C}_{16}\text{H}_{33}\text{NH}_2$ (0.2, 0.5 and 1 M equiv./Ru) as stabilizers. Whilst hcp RuNPs are formed in all cases, both the nature and concentration of the ligand control the size and dispersion of the nanoparticles. For example, using 0.2 equiv. of octylamine led to the formation of superstructures of 100 nm which results from the agglomeration of isolated nanospheres with a mean size of 2.3 nm. Interestingly, higher concentrations of octylamine yields more agglomerated structures. Using hexadecyl- and dodecylamine results in the formation of nanoparticles with elongated shape, whose size is dependent upon the molar ratio Ru:L (in all cases the sizes are found between 1.8 and 2.6 nm). When the concentration of ligands in the solution is increased (Fig. 5), the nanoparticles show a tendency to agglomerate which leads to worm-like nanoparticles with a large size distribution.

Since the size and shape of the nanoparticles are not well controlled, these results demonstrate that amines do not ensure a strong stabilization of the particles. This is also consistent with the tendency of these nanoparticles to display a vermicular

aspect. This lack of control was thought to result from a weak coordination of the amine ligand to the surface of the particles via the nitrogen atom. To study the behavior of the amines, these colloids were analyzed by liquid ^1H and ^{13}C NMR which confirmed the coordination of the amine ligand to the surface of the nanoparticles (Fig. 5). It is worth mentioning that the signals corresponding to the carbons located in the α , β , and γ positions relative to the amino group are not observed on the NMR spectra of the RuNPs stabilized with hexadecylamine (0.2 equiv.). These peaks correspond to the carbons located in close vicinity of the metal surface which are not visible. As previously discussed for the stabilization of the nanoparticles by heptanol, this is related to a very short T_2 resulting from the slow tumbling of the particles in solution due to their large size. To shed more light on the interaction of the amine with the NP surface, extra ligand was progressively added in the NMR tube. This study demonstrated that a fast equilibrium occurs between the free amine and the amine coordinated at the NP surface at the NMR time scale. As a consequence, the coordination of the ligand at the surface of the colloids is a dynamic process which implies a weak interaction between the ligand and the metallic surface of the nanoparticles. The mobility of the amines favors the coalescence of the initial nanospheres particles. In addition, the wormlike shape may result from a self-organization of the ligands in the solution.

The ability of long alkyl chain amines to induce a shape control of ruthenium nanostructures from ruthenium complexes has been explored by other groups and significant advances have recently been described. Different protocols in organic medium leading to monodisperse nanoparticles such as stars, urchins, and hourglass, from $\text{Ru}(\text{acac})_2$ [71] and $\text{Ru}_3(\text{CO})_{12}$ [72], have been reported. These syntheses require the presence of an amine or a mixture of an amine plus a carboxylic acid which play a crucial role in controlling the shape of ruthenium nanocrystals

For example, Tilley and coworkers recently achieved the synthesis of ruthenium nanocrystals which can exhibit a sophisticated hourglass morphology, i.e. two truncated hexagonal pyramids connected at their vertices (Fig. 6) [71]. The hourglass nanocrystal consists of $\{101\}$ facets at the sides and $\{001\}$ facets at the ends while truncated corners are $\{101\}$ facets. These nanocrystals were prepared in a yield of 77% from the reduction of ruthenium(II) acetylacetonate in mesitylene under hydrogen atmosphere at 140°C for 70 h in the presence of dodecylamine (DDA). They are 18 ± 3 nm in length, 11 ± 2 nm wide, and exhibit intermediate necks which are 4 ± 1 nm thick. During the synthetic process, 19% of rod-like and 4% of near-spherical nanocrystals were also synthesized. It is worth mentioning that a mixture of hourglasses and spheres can self-assemble in a binary superlattice (Fig. 6, right). Interestingly, a three-step growth process has been observed by HRTEM during the formation of the hourglass nanocrystals: (1) formation of partially crystallized rod-like nanoparticles from the coalescence of ruthenium nanoparticles to decrease their surface free energy, (2) crystallization of the rod-like nanoparticles resulting in single crystalline nanocrystals, this is possibly driven by the high strength of Ru–Ru bonds which compensates the entropic cost required to eliminate defects, (3) overgrowth leading to nanocrystals with a well-defined hourglass morphology which exposes facets of low surface energy.

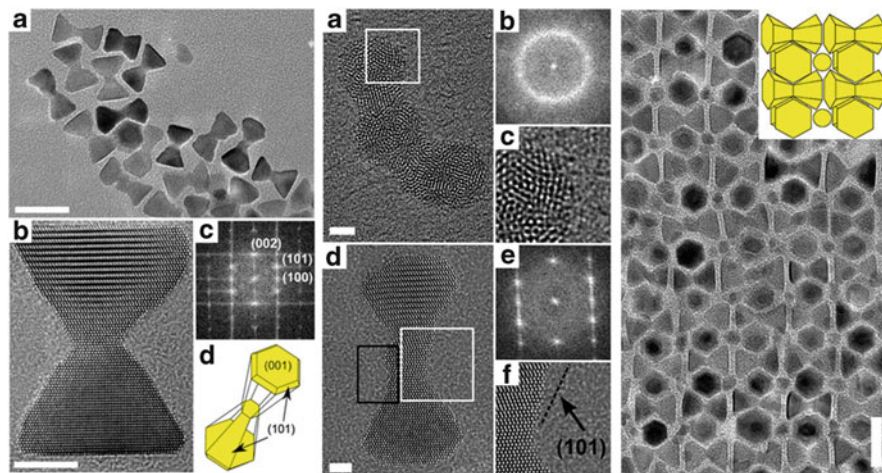


Fig. 6 *Left*: Ruthenium hourglass nanocrystals synthesized after 70 h. (a) TEM image of ruthenium hourglass nanocrystals, scale bar = 20 nm. (b) HRTEM image of a single, highly crystalline, ruthenium hourglass nanocrystal, scale bar = 5 nm. (c) FFT of the ruthenium hourglass nanocrystal shown in (b). (d) Schematic of a single ruthenium hourglass nanocrystal showing termination by {001} and {101} facets; *Center*: Ruthenium hourglass nanocrystal intermediates. (a) HRTEM image of a partially crystalline ruthenium rod-like nanocrystal intermediate isolated after 48 h, scale bar = 2 nm. (b) FFT of the ruthenium rod-like nanocrystal shown in (a). (c) High magnification HRTEM image of the surface of the rod-like nanocrystal as shown by the white box in (a). (d) HRTEM image of a single crystal ruthenium hourglass-like nanocrystal intermediate isolated after 52 h, scale bar = 2 nm. (e) FFT of the ruthenium hourglass-like nanocrystal shown in (d). (f) High magnification HRTEM image of the surface of the hourglass-like nanocrystal as shown by the white box in (d); *Right*: TEM image of a binary nanocrystal superlattice formed by the evaporation of a mixture of ruthenium hourglass nanocrystals and spherical ruthenium nanocrystals. Scale bar = 20 nm. (Reproduced from [71] with permission from ACS)

Lignier et al. achieved the synthesis of Ru nanostars (Fig. 7) from the decomposition of $\text{Ru}_3(\text{CO})_{12}$ in toluene at 160°C under dihydrogen in the presence of hexadecylamine (HDA) and hexadecanoic acid (PA) [72]. Under these conditions, the nanoparticles are catalysts for both arene hydrogenation, e.g. toluene, and the Fischer–Tropsch reaction. Whilst the direction, location, and number of branches are not identical in all nanostars, the uniformity of the particle size is high, especially in view of their complex three-dimensional morphology. The metallic state and hcp structure of the Ru nanostars, which are approximately 15 nm across, were determined by XRD, X-ray photoelectron spectroscopy (XPS), and HRTEM. Following the extension of the reaction time to 24 h, the nanostar shape is preserved which reveals the stability of these branched nanocrystals.

An increase of HDA concentration led to a higher rate of nanoparticle formation from $\text{Ru}_3(\text{CO})_{12}$, while an increase of PA concentration had the opposite effect. This is likely to be related to the presence of ruthenium–amine and ruthenium–carboxylate complexes as intermediates in the synthetic process. Before the formation of the nanostars, quasi-spherical and unbranched nanoparticles were first

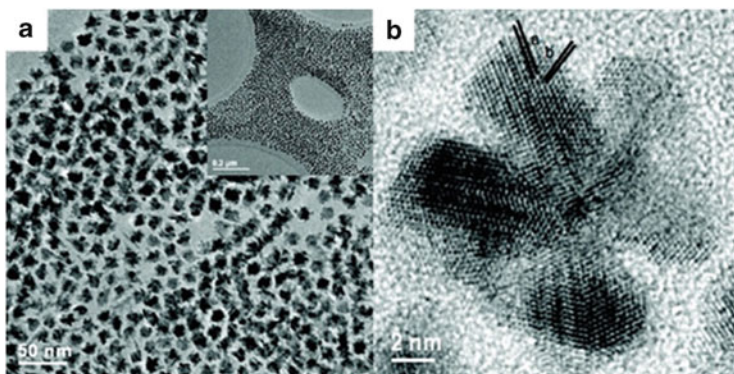


Fig. 7 (a) TEM images of Ru nanostar particles prepared from $\text{Ru}_3(\text{CO})_{12}$ with a 1:3 ratio of PA/HAD at 160°C for 6 h. (b) HRTEM image of a typical Ru nanostar. The d -spacings of parts (a) and (b) are 0.21 and 0.20 nm, respectively, and can be indexed to the (002) and (101) planes of hexagonal ruthenium. Twin defects and stacking faults are clearly present. (Reproduced from [72] with permission from ACS)

obtained. No discernible grain boundaries were present in these polycrystalline nanoparticles which constitute the core of nanostars. Then, the formed branches are single crystalline or exhibit twin defects and stacking faults. These defects, which are parallel to the crystal growth direction, result from the propagation of the defects during the growth of the branches. This reveals that the growth of the branches proceeds by addition of monomer from solution and not by oriented attachment or agglomeration of smaller nanoparticles. Since the nucleation and growth of the branches occur on the cores, the size uniformity of the nanostars is related to the monodispersity of the cores. In addition, the location of the branches results from both the morphology and crystallinity of these cores. Unexpectedly, a novel crystallization step occurs in the nanostar formation since single crystalline nanostars are formed from polycrystalline seeds.

Interestingly, a dramatic increase in the length of the branches is obtained following the additional injection of ruthenium precursor in the solution containing the nanostars, i.e. by seeded growth. This results in the formation of monodisperse nanourchins (Fig. 8). A molar ratio of acid/amine/Ru of 1/2/1 is required to achieve the slow decomposition of the metal precursor which favors heterogeneous nucleation. Similarly to the nanostars, the controlled addition of monomers results in the formation of the branches which are single crystalline or exhibit defects oriented in the direction of the growth.

In summary, simple amines are weakly coordinated ligands which are not appropriate for the synthesis of small spherical RuNPs in our reaction conditions. Nevertheless, interesting worm-like shapes were observed. In addition, the presence of amines allows the growth of preformed nuclei, which suggest the potential of amines for a shape-controlled synthesis of MNPs. This advantage was confirmed by results from other groups which reported sophisticated nanostructures displaying

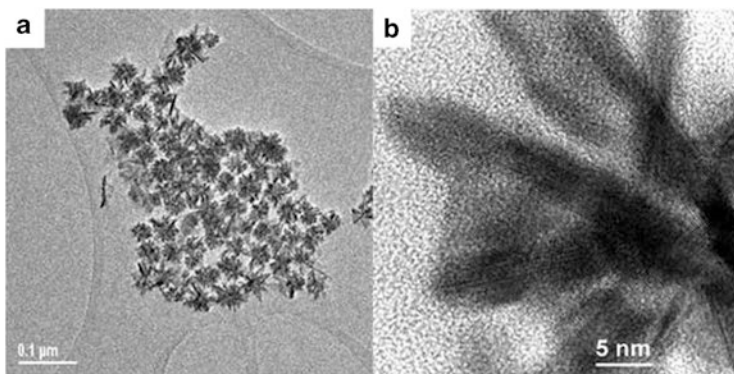


Fig. 8 (a) TEM and (b) HRTEM images of Ru nanourchins prepared from Ru nanostars by adding $\text{Ru}_3(\text{CO})_{12}$ with a 1:2 ratio of PA/HDA at 160°C. (Reproduced from [72] with permission from ACS)

well-defined crystalline faces. As a consequence, these novel nano-objects are of high interest for catalysis as they may induce a different selectivity.

2.3.2 Diphosphine-Stabilized RuNPs

It is well known from molecular chemistry that phosphine ligands are usually strong σ -donor ligands and only weak π -acceptors. Interestingly, this effect can be increased by the presence of electron-donating substituents. In addition, the size and steric hindrance of the phosphine ligands is approximately described by the cone-angle (θ) of the phosphine. In the field of metal nanoparticles, the phosphines are not often used as stabilizers. From our experience, the use of phosphine gave rise to a very efficient stabilization of the RuNPs which are generally well defined with a spherical shape and a small size. By playing with the substituents on the phosphorus atom, it was possible to tune the surface properties of RuNPs and the related catalytic reactivity of this surface.

Since polyphosphines were efficient ligands for the synthesis of PdNPs [73], a similar methodology was applied to RuNPs. As discussed in the introduction, this metal presents a lower Knight-shift than Pt and Pd. This facilitates the characterization of the surface state of the particles using NMR. For that purpose, the study was focused on simple diphosphines, i.e. 1,4-bis(diphenylphosphino)butane (dppb) and 1,10-bis(diphenylphosphino)decane (dppd) [74]. The nanoparticles were prepared from $[\text{Ru}(\text{COD})(\text{COT})]$ in the presence of 0.1 equiv. of the corresponding diphosphine (the diphosphine/Ru ratio was optimized to add the lower quantity of ligand as possible; it gives rise to 0.2 equiv. of P/Ru), in THF under 3 bar of dihydrogen at RT. This resulted in the formation of stable, crystalline, and mono-disperse hcp nanoparticles which exhibit a mean size of 1.5 (dppb) and 1.9 nm (dppd). The presence of the ligand at the surface of the NPs was confirmed by

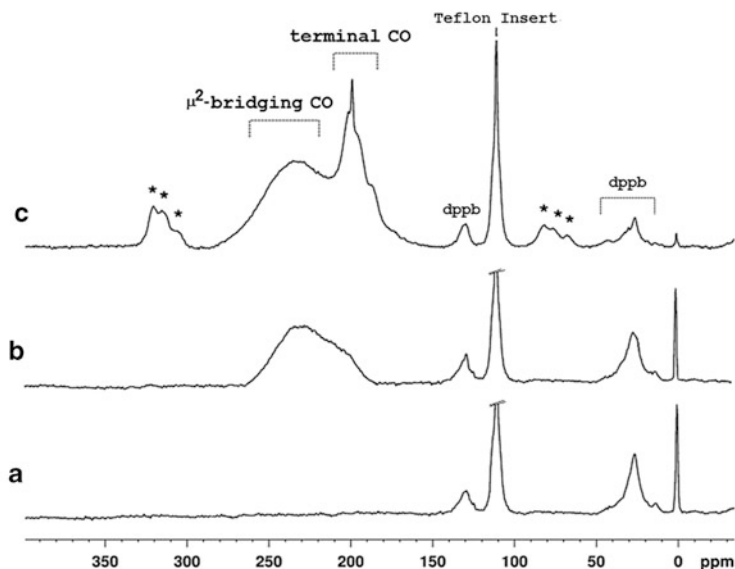


Fig. 9 ^{13}C MAS NMR spectra of dppb-stabilized RuNPs after adsorption of ^{13}CO : 0 h (a), 2 h (b), 12 h (c), (*asterisk*: spinning side-band). (Reproduced from [75] with permission from Wiley)

solution ^{31}P NMR following the treatment of the NPs with H_2O_2 to release the oxidized phosphine. This result was also confirmed by MAS ^{31}P NMR. The quantification of the hydrides present at the surface of the Ru/dppd particles was performed by titration with an olefin, leading to a reproducible value of 1.1 hydrides by surface ruthenium atom. This value is lower than for HDA or PVP ligands since 1.3 hydrides by surface ruthenium atom were measured for both Ru/HDA and Ru/PVP.

The surface state of the dppb-stabilized RuNPs was investigated using ^{13}CO as a probe molecule via IR and MAS NMR techniques [62]. These studies demonstrated that, in contrast to the case of ^{13}CO adsorbed on Ru/PVP NPs, the CO ligands are not fluxional. This is related to the presence of the ancillary phosphines ligands at the surface of the RuNPs (Fig. 9). In addition, the presence of bridging terminal and multicarbonyl group was evidenced. Unexpectedly, similar studies carried out with labeled ethylene demonstrated the breaking of the C–C bond to produce methyl groups firmly attached to the surface [74].

In continuity of this study, the reactivity of dppb and PVP-stabilized RuNPs was compared using standard reactions, i.e. CO oxidation, CO_2 reduction and styrene hydrogenation [75]. The aim of the work was: (1) to study the effect of ligands on the intrinsic reactivity of metal nanoparticles and (2) to identify the sites of reactivity on the nanoparticles by using NMR and IR spectroscopies. Through simple experiments, it was demonstrated that CO oxidation proceeds at RT on RuNPs. However, a rapid deactivation of this system occurred in the absence of ligands (RuPVP NPs) because of the formation of RuO_2 . In the presence of dppb

ligands, the reaction involved exclusively the bridging CO groups and no bulk oxidation was observed at RT under catalytic conditions. The reverse reaction, CO₂ reduction, was achieved at 120°C in the presence of H₂ and led to CO, which coordinated exclusively in a bridging mode. This demonstrates the competition between hydrides and CO for the coordination on RuNPs. The effect of ligands localized on the surface was also evidenced in catalytic reactions. In Ru/PVP and Ru/dppb systems, styrene is slowly hydrogenated at RT: first into ethylbenzene and then into ethylcyclohexane. Whilst the selective poisoning of the nanoparticles with bridging CO groups led to catalysts only able to reduce the vinyl group of styrene, a full poisoning of the surface with both terminal and bridging CO groups led to inactive catalysts. These results evidenced that bridging CO groups and arenes compete for the same sites on the surface of the particles. This also suggested that the sites accommodating both arenes and bridging CO groups are present on the faces. In addition, this work showed that: (1) diphosphine ligands are located in the proximity of terminal CO groups, (2) hydrides can selectively displace the terminal CO groups and not the bridging ones. About CO oxidation and arene reduction, the selectivity could be related to the availability of the faces. While it was expected that arene hydrogenation occurs on compact faces, the necessity of bridging groups for CO oxidation was not obvious.

Diphosphine ligands strongly coordinate at the surface of RuNPs forming a system of choice to compare the surface properties of polymer- and ligand-stabilized RuNPs. CO oxidation, CO₂ reduction, and styrene hydrogenation provided a picture of small RuNPs at the molecular level: (1) CO preferably binds in a bridging mode on face atoms which are also the sites for the hydrogenation of arenes. These face atoms are also the preferred sites for CO oxidation. (2) Hydrides and terminal CO compete for sites located near the bulky diphosphine ligands. These sites are likely to be apexes and edges since they are inactive for arene hydrogenation.

2.3.3 Phenyl Pyridine-Stabilized RuNPs

In a collaborative work with Gomez et al. we reported the synthesis of RuNPs using the 4-(3-phenylpropyl)pyridine (PPy) as a stabilizing ligand [76]. This unusual ligand was selected due to its simple structure containing a pyridine group, which can favor the approach of the flat phenyl to the metallic surface upon σ -coordination. As a consequence, this ligand was relevant to elucidate π -interactions between the ligand and the metallic surface. In fact, previous investigations of the Heck coupling reactions with PdNPs showed that a phenyl group is required in the ligand or the substrate [77, 78]. RuNPs were prepared via the decomposition of [Ru(COD)(COT)] under dihydrogen in the presence of PPy (0.2 M equiv./Ru). Optimized conditions led to reproducible NP syntheses, giving rise to small nanoparticles with a mean diameter of 1.3 ± 0.3 nm (Fig. 10).

Whilst this result contrasted with our synthesis of large and agglomerated particles using simple pyridines as stabilizers, this was consistent with previous

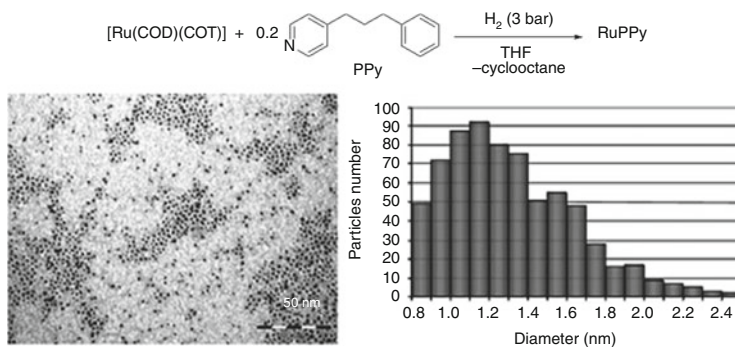


Fig. 10 Synthesis, TEM image and size histogram for RuNPs stabilized with 4-(3-phenylpropyl)pyridine (PPy). (Adapted from [76] with permission from RSC)

reports on gold particles using pyridine [79]. The coordination of the PPy ligand to the ruthenium surface was attested by ^{13}C CP-MAS NMR. Narrow aliphatic peaks and a broad signal in the aromatic region showed that an aromatic group in PPy participates to the stabilization of the particles. In addition, this favors their dispersion probably as a result of the coordination of the phenyl group on the metallic surface. Following the treatment of RuNPs under deuterium atmosphere, ^2H MAS NMR experiments revealed the presence of two signals: one attributed to Ru–D bonds and one attributed to C–D bonds with a 120 kHz quadrupolar splitting, which is consistent with previously reported data [80]. This evidenced the presence of organic stabilizers on the RuNPs surface which are able to exchange their hydrogen with surface deuterides. Finally, a quantitative release of unreduced PPy could be achieved after 24 h of reaction, showing both the effective presence of the ligand at the surface of the particles and the strong interaction of this ligand with the metallic surface. The ligand coordination to RuNPs was studied by ^1H NMR under the conditions of the NP preparation. This technique enabled us to follow the decomposition of the ruthenium complex as well as the evolution of the ligand once coordinated at the surface of the particles. This allowed us to observe that the signal broadening was faster for the *ortho*-pyridinyl protons than for the aromatic protons. This can be related to the interaction of the ligand with the metallic surface, first via the nitrogen atom of pyridinyl group and then via a π -interaction, which is consistent with the absence of Ru–N absorption band in the IR spectrum.

These RuPPy NPs appeared to us as a model of choice to develop surface reactivity studies based on NMR. This approach was expected to improve our understanding of mechanistic aspects of hydrogenation reactions catalyzed by RuNPs [80]. For that purpose, the surface reactivity of the RuPPyNPs was explored with various aromatic substrates using different NMR experiments. First, the high stability of RuPPy NPs has been demonstrated in the presence of several aromatic substrates during hydrogenation studies. The hydrides present on the surface reacted selectively with the vinyl functions of substituted arenes, the aromatic

group being not hydrogenated. No hydride transfer from the metallic surface to aromatic rings agrees with a high coverage of the metallic surface by PPy molecules. Mechanistic studies by NOE NMR experiments using proton selective excitations evidenced the coordination of the pyridine derivatives (4-(3-phenylpropyl)pyridine, 4-vinyl-pyridine and 4-ethyl-pyridine) in contrast to styrene and ethylbenzene. Since the magnetization exchanges are faster than residential times on the metallic surface at the NMR time scale of the experiences, intermolecular NOE effects were observed between 4-vinylpyridine and 4-ethylpyridine. In the presence of an excess of dihydrogen, all substituted aromatic substrates were hydrogenated under mild conditions, probably through transient displacement of the coordinated phenyl ring.

In summary, 4-(3-phenylpropyl)-pyridine efficiently stabilizes very small RuNPs. A precise analysis of the behavior of RuPPyNPs in solution by NMR investigations revealed that 4-(3-phenylpropyl)pyridine acts as a “bidentate” ligand which is strongly coordinated to the metallic surface through π,π -interaction. This can be considered as a novel and specific mode of coordination on the nanoparticle surface although such π -coordination has previously been proposed, e.g. for the coordination of cinchonidine on Pt nanoparticles. In addition, this study demonstrated the potential of specific ligands, such as PPy, to efficiently stabilize the nanoparticles while preserving their reactivity.

2.3.4 Carbene-stabilized RuNPs

Since the achievements of Grubbs on metathesis, N-heterocyclic carbene ligands (NHCs) are strongly related to ruthenium in molecular chemistry. However, these ligands had not been used for the stabilization of ruthenium nanoparticles despite the work of Tilley et al. on AuNPs [81]. It was therefore of interest, following a comprehensive study of phosphine coordination on nanoparticles, to investigate the interaction between RuNPs and NHCs [82]. The ruthenium nanoparticles were prepared by decomposition of [Ru(COD)(COT)] in pentane (3 bar H₂; RT) in the presence of a carbene, i.e. 1,3-bis(2,6-diisopropylphenyl)imidazol-2-ylidene (IPr) or *N,N*-di(*tert*-butyl)imidazol-2-ylidene (I^tBu), as shown in Fig. 11.

Different colloids were obtained depending on the amount and the type of carbene. Whilst RuNPs with a mean size of 1.7 nm were formed using 0.2 equiv. of IPr or 0.5 equiv. of I^tBu, the mean diameter of the RuNPs is 1.5 nm using 0.5 equiv. of IPr. In all these cases, the Ru/NHC NPs are homogeneous in size and shape. In addition, WAXS analysis demonstrated that these NPs present the expected hcp structure. Since it was not possible to displace the carbene ligand at the surface of the nanoparticles in the presence of thiol, amine, or phosphine ligands, the carbenes are strongly attached to the metal surface. With the aim to study the coordination of the carbenes by IR and NMR spectroscopies, the synthesis of the RuNPs has been performed using NHCs ligands which are ¹³C labeled in the carbene position. By this way, MAS NMR analysis (Fig. 11) allows us to detect the signals of the bonded carbene to the Ru surface in the 195–205 ppm range

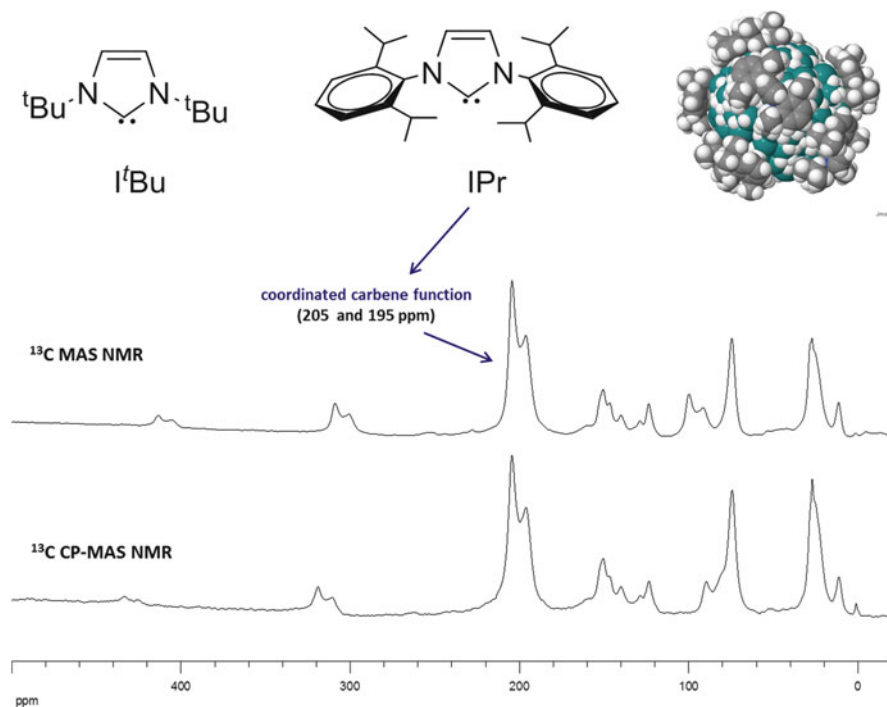


Fig. 11 Top Left: NHCs employed to stabilize RuNPs (left); Right: Space filling model of a 1.8 nm hcp RuNP stabilized by 8 IPr NHC ligands and accommodating 1.5 hydrides per surface Ru (right); Bottom: ^{13}C MAS and CP-MAS NMR spectra of RuNPs/ iPr^* ($[iPr^*]/[Ru]_0 = 0.5$). (Adapted from [82] with permission from Wiley)

(depending on the type and amount of carbene used). Carbon monoxide was used to probe the sites available at the surface of the NHC-stabilized RuNPs since it was expected that CO resonances would inform us on the coordination of the carbenes. For the nanoparticles prepared with 0.5 equiv. of I^tBu , the CO is predominantly present in bridging mode. Whilst this coordination mode is also observed when CO is added to the colloid prepared with 0.2 equiv. of IPr, the colloids prepared using 0.5 equiv. of IPr only exhibit linear and multicarbonyl adsorption (i.e. no bridging CO). From these results, the location of the different carbene ligands at the surface of the RuNPs can be proposed. For the nanoparticles prepared using 0.5 equiv. of I^tBu or 0.2 equiv. of IPr, CO is located on the faces while the ligand is located on edges and apexes. In contrast, for the RuNPs prepared with 0.5 equiv. of IPr, the absence of bridging CO is in agreement with the full coverage of the nanoparticle surface by the IPr ligand. These carbene-stabilized RuNPs showed a moderate activity in the hydrogenation of styrene under mild conditions. As expected for RuNPs, the hydrogenation of the vinyl bond is followed by the hydrogenation of the aromatic ring. In collaboration with P. van Leeuwen *and coworkers*, these NHC-stabilized RuNPs were used as catalysts in the hydrogenation of different

substrates (benzene derivatives, methylanisoles, acetophenone) under various reaction conditions (solvent, substrate concentration, substrate/metal ratio, temperature) [83]. The Ru/NHC NPs appeared as active catalysts in the hydrogenation of aromatics and showed an interesting ligand effect, i.e. Ru/IPr NPs were generally more active than Ru/*t*Bu NPs.

In summary, carbene ligands, known to be excellent ligands for molecular Ru complexes, are equally efficient for the stabilization of RuNPs. The strong binding of the NHC ligands to the surface was evidenced by NMR via ^{13}C labeling of the carbenes and addition of ^{13}CO . In addition, we were able to identify the probable location of these NHC ligands on the nanoparticles (Fig. 11 right). Finally, we demonstrated that the substituents of the carbenes influence the reactivity of the nanoparticles which is mainly due to steric effects.

2.4 Bimetallic RuPt, RuFe, and RuSn NPs

Bimetallic NPs are emerging as an important class of material offering a vast number of possible structures and compositions. As a consequence, these materials are expected to exhibit superior performances and even novel properties [84]. Usually, bimetallic NPs are classified on the basis of the chemical distribution of the two metals in the NPs. One can distinguish (1) bimetallic alloys characterized by the formation of a statistical distribution of the two elements and (2) bimetallic heterodimers or core-shell nanostructures in which monometallic domains are segregated. The NPs can exhibit synergetic effects resulting from the intimate contact between the two metals, or can fulfil multifunctional tasks due to the association of two metal domains with different properties. This diversity of structure raises issues about the control of the chemical order in bimetallic NPs [85–87]. First, perfect bimetallic alloys require comparable kinetics of decomposition of the precursors. However, as reported by Bradley et al. [88], surface chemistry has also a huge impact on the final distribution of each metal in the NPs. As a consequence, molecular chemistry appears as a powerful tool to engineer the synthesis of complex nano-objects as illustrated by the synthesis of various alloys in our group including Ru-based bimetallic nanostructures, e.g. RuPt [89–92], RuFe [93] and RuSn [94].

Varying the kinetics of decomposition of the precursors was profitable for the controlled synthesis of RuPt NPs. Whilst the co-decomposition of [Ru(COD)(COT)] and [Pt(dba)₂] in the presence of polyvinylpyrrolidone as stabilizer led to a RuPt alloy with a *fcc* structure, core-shell RuPt NPs were obtained in PVP, using [Pt(CH₃)₂(COD)] (i.e., [dimethyl(1,5-cyclooctadiene) platinum (II)]) instead of [Pt(dba)₂] [91]. This is related to the slower rate of decomposition of [Pt(CH₃)₂(COD)]. In summary, the chemical order can be controlled via the choice of the precursor. The chemical segregation leading to core-shell RuPt results from kinetic (decomposition rate of the metal precursors) and thermodynamic (preferred location of each metal in the particle) parameters as well as from the steric

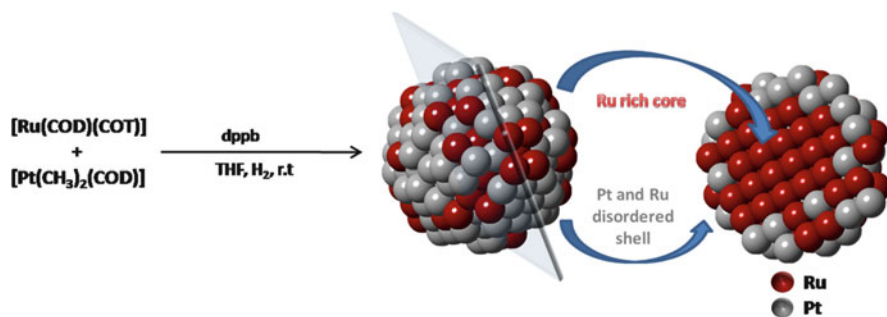


Fig. 12 Schematic representation of RuPt nanostructures synthesized from $[\text{Ru}(\text{COD})(\text{COT})]$ and $[\text{Pt}(\text{CH}_3)_2(\text{COD})]$ and stabilized by diphenylphosphinobutane ligand. (Reproduced from [92] with permission from RSC)

properties of the polymer, taking into account that PVP has little or no chemical interaction with metals. In addition, it is worth mentioning the influence of the electronic properties of a diphosphine ligand on the size and chemical composition of RuPtNPs [92]. Using a strongly coordinating ligand (diphenylphosphinobutane; dppb) instead of a neutral stabilizer while keeping the same metal sources (i.e., $[\text{Ru}(\text{COD})(\text{COT})]$ and $[\text{Pt}(\text{CH}_3)_2(\text{COD})]$) and reaction conditions), nanostructures display a ruthenium-rich core and a disordered shell containing both ruthenium and platinum (Fig. 12). The complexity observed in the structure of these NPs arises from the high chemical affinity of the diphosphine ligand for both metals. These results show how a simple ligand, such as a diphosphine, can add a significant degree of complexity since the ligand significantly affects the chemical order of these bimetallic nanoparticles.

Associating a platinum metal displaying good catalytic properties, such as Ru, with a metal displaying much poorer catalytic properties may be of interest for controlling the selectivity of a catalytic reaction when several functions are accessible. In this respect, ultrasmall FeRu bimetallic nanoparticles (NPs) were prepared by the co-decomposition of two organometallic precursors, $\{\text{Fe}[\text{N}(\text{Si}(\text{CH}_3)_3)_2]_2\}_2$ and $\text{Ru}(\text{COD})(\text{COT})$, under dihydrogen at 150°C in mesitylene [93]. A series of FeRu NPs of sizes of ca. 1.8 nm, which exhibit different ratios of iron to ruthenium, were obtained by varying the added quantity of ruthenium complex (FeRu : 1/1, 1/0.5, 1/0.2 and 1/0.1). The surface of the particles was shown by titration to contain ca. 0.5 hydride by surface metal atom. In addition, IR spectroscopy after CO adsorption evidenced the presence of both Fe and Ru at the surface of the particles. These FeRu NPs were used as catalyst for the hydrogenation of styrene and 2-butanone. The results indicated that the selectivity of the NPs catalysts can be modulated according to their composition. For example, whereas, in contrast to Ru NPs, Fe NPs are inactive for ketone and arene reduction in mild conditions, bimetallic NPs of composition Fe:Ru = 1:0.2 can efficiently reduce olefins and ketones but preserve the aromatic rings. This result therefore represents a case

study which demonstrates the possibility of fine-tuning the reactivity of nanocatalysts and adjusting their selectivity for a given reaction.

In another study aiming at selectively poisoning the surface of the RuNPs for modulating their reactivity, tributyltin hydride $[(n\text{-C}_4\text{H}_9)_3\text{SnH}]$ was added in a solution of preformed RuNPs stabilized by either a polymer (polyvinylpyrrolidone; Ru/PVP) or a ligand (bisdiphenylphosphinobutane; Ru/dppb) [94]. The idea was to take advantage of the presence of hydrides at the metallic surface to perform a simple organometallic reaction with the tin complex at the surface of the RuNPs. By this way, we could obtain tin-decorated ruthenium nanoparticles with a mean size similar to that of the preformed RuNPs. Different Sn/Ru molar ratio enabled us to study the influence of the surface tin content on the properties of these new nanoparticles and to compare them with Ru/PVP and Ru/dppb systems. In addition to HREM, WAXS, IR, NMR and Mössbauer studies, theoretical calculations and a model catalytic reaction (styrene hydrogenation) allowed us to evidence the formation of μ^3 -bridging “SnR” groups on the ruthenium surface as well as to rationalize their influence on surface chemistry and catalytic activity. Whilst in the case of dppb-stabilized RuNPs, the reaction with the tin precursor was limited by the surface coverage induced by the coordination of the bulky diphosphine ligand, it was possible to vary the amount of tin deposited on the Ru surface using PVP instead of dppb. The resulting modification of the ruthenium surface led to a tuning of the surface properties of the particles, as observed through the coordination of CO as well as the catalytic hydrogenation of styrene. Ru/PVP/Sn cannot accommodate CO after the addition of even a very small amount of tin while Ru/dppb/Sn can still accommodate terminal CO groups. In addition, the Ru/PVP/Sn NPs showed a gradual variation of selectivity with increasing tin loading while only a small quantity of tin was sufficient to impede the arene hydrogenation ability of Ru/dppb NPs. These results evidence that the presence of tin adatoms on the metallic surface block some reactive sites. This approach may be a way to tune selectivity in hydrogenation reactions.

In summary, the organometallic approach is also efficient to prepare bimetallic nanoparticles. By precisely selecting the reaction conditions (precursor, stabilizer, reactant), we could access to ruthenium-based bimetallic nanoparticles displaying a controlled chemical order, i.e. alloy, core-shell, or even nanoparticles decorated with a second metal such as platinum, iron, or tin. These nanoparticles, which display different surface properties, can pave the way towards synergetic and selective catalytic performances.

3 Investigation of RuNPs in Organic Colloidal Catalysis

To pursue our work on ruthenium nanoparticles, we have investigated their surface reactivity in colloidal catalysis via the hydrogenation of model substrates. In addition, RuNPs showed promising performances for the dehydrogenation of

amine-borane in comparison with previously known homogeneous and colloidal systems.

3.1 *β -Aminoalcohols and Oxazoline-Stabilized RuNPs*

Asymmetric catalysis involving nanoparticles remains an important challenge since only a few examples of efficient heterogeneous catalysts have been reported [95]. With Gomez et al., we evaluated chiral β -amino alcohols and oxazolines for the stabilization of RuNPs and their applications as catalysts in the hydrogenation of unsaturated substrates [96]. The nanoparticles were prepared by decomposing [Ru(COD)(COD)] (3 bar H₂; RT) in the presence of 0.2 M equiv. of the chosen ligand. In all cases, the nanoparticles appeared stable in solution under argon atmosphere. 2-aminobutanol led to nearly spherical monodisperse RuNPs of 2.5 nm which exhibit a strong tendency to self-assemble. Amino(oxazolines) led to anisotropic RuNPs with a mean size of 2.5 nm which tend to agglomerate. The use of hydroxyl(oxazoline) yielded to well-dispersed and slightly elongated nanoparticles of 2.7 nm). Finally, well-defined nanoparticles of very small mean size (1.6 nm) and isotropic shape were obtained with bis(oxazoline) ligands. These nanoparticles are crystalline as determined by WAXS and show a tendency to aggregate into large and regular mesoscopic superstructures which result from the coordination of the ligand to different nanoparticles. NMR spectroscopy showed the coordination of the oxazoline ligands to the metal surface using methodologies previously developed to study the dynamic exchange of the amine ligand on the ruthenium surface. In addition, some dihydrogen, released in the solution, was detected, as similarly observed for ruthenium colloids stabilized with heptanol [66] or hexadecylamine [61]. This suggested that nanoparticles contain mobile hydrides at their surface. Using isopropanol as hydrogen source for the transfer of hydrogen to acetophenone, the catalytic behavior of these RuNPs was compared to Ru molecular complexes prepared in situ with the same ligands. Depending on the stabilizing ligand, the particles showed moderate to high activities. In all these cases, the formation of the *trans*-product was observed. Only Ru/amino(oxazoline) colloidal system gave asymmetric induction with a modest value of ca. 10% enantiomeric excess (ee). This very low but reproducible asymmetric induction confirmed the fluxional behavior of the amino(oxazoline) ligands at the surface of RuNPs, as previously described for Ru/amine colloids.

3.2 *Diphosphite-Stabilized RuNPs*

Following previous studies with diphosphite-stabilized PdNPs which led to interesting and intriguing results in Heck-coupling reactions [77, 78], the synthesis of RuNPs using carbohydrate-based diphosphites was carried out for their application

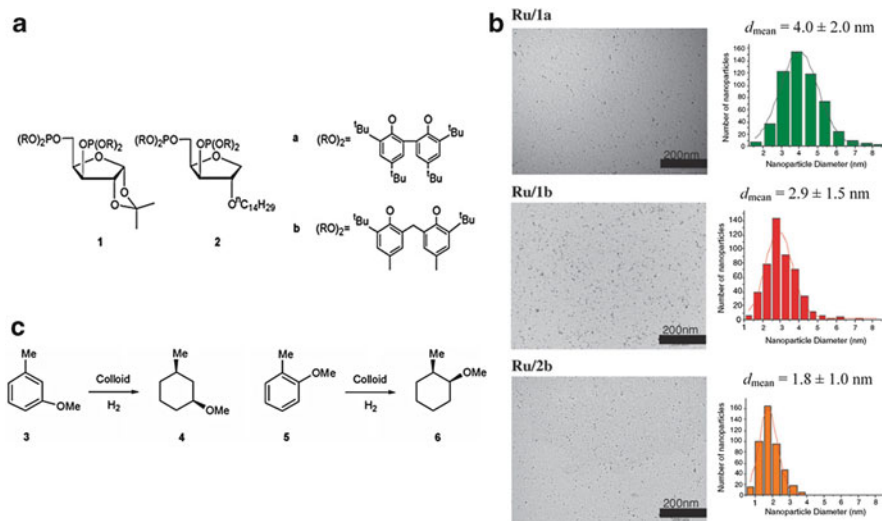


Fig. 13 (a) Carbohydrate-based diphosphites used for the synthesis of the RuNPs, (b) TEM images, and (c) catalytic hydrogenation of *o*- and *m*-methylanisoles with RuNPs. (Adapted from [97] with permission from RSC)

as catalysts in the hydrogenation of anisole derivatives [97]. This study was performed in collaboration with the groups of Roucoux, Claver and Castillon et al. The RuNPs were prepared as usual from [Ru(COD)(COD)] and a ligand/Ru ratio of 1:0.1 was selected, as previously used with diphosphines. Different diphosphite ligands (Fig. 13a) were employed with the objective to analyze the influence of their structure on the characteristics of the nanoparticles as well as on their catalytic activity. The question was: are such ligands adapted to induce asymmetric catalysis at the surface of the nanoparticles? TEM analysis showed the formation of RuNPs of mean size between 1.8 and 4 nm, depending on the diphosphite, thus demonstrating the influence of the ligand on the size of the particles (Fig. 13b). The smallest RuNPs were prepared in the presence of ligands which exhibit a long lipophilic chain on the sugar part or one carbon atom between the aromatic rings of the diol part.

These particles were evaluated as nanocatalysts in the hydrogenation of *o*- and *m*-methyl anisoles (Fig. 13c). As the result of a competition between the substrate and a coordinating solvent at the surface of the NPs, no conversion was observed using THF and CH₃CN as solvents for the reaction. In pentane, the particles were active and this activity was related to the nature of the ligand. The best activity was reported for the most flexible ligand which contains one carbon between the aromatic rings. The introduction of a long lipophilic chain in the ligand increased further the activity of the particles which is related to the smaller mean size and higher solubility of the nanoparticles in pentane. Contrary to the results previously obtained with aminooxazoline-stabilized RuNPs, the hydrogenation of *o*-methyl anisole gave a total selectivity for the *cis*-product. This opposite selectivity shows

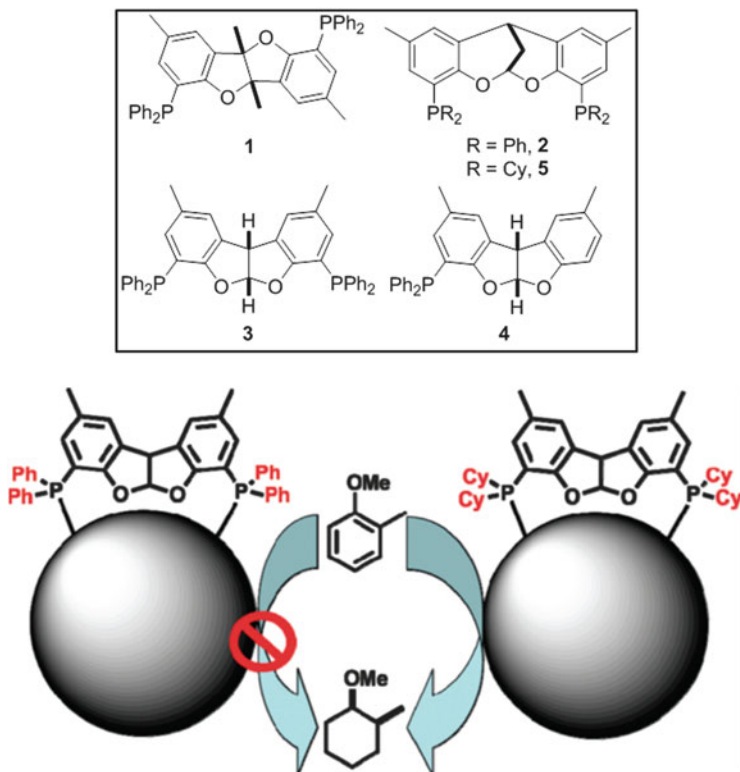


Fig. 14 Phosphine ligands used as stabilizers for the RuNPs (*top*) and difference in reactivity during hydrogenation *o*-methylanisole (*bottom*). (Adapted from [98] with permission from ACS)

that the ligand can induce different reactivities. No significant enantioselectivity was observed with diphosphites; this is probably related to the sterical hindrance of these ligands which restricts the approach of the substrate near the metal surface.

3.3 *Diphosphine-Stabilized RuNPs*

In nanocatalysis, an important issue is to determine whether and how ancillary phosphine ligands may influence the reactivity of the nanoparticles. In this respect, in collaboration with the group of Van Leeuwen, we investigated the design of new roof-shape phosphine ligands for the stabilization of RuNPs and their application as catalysts for the hydrogenation of aromatics [98]. The particles were prepared as usual by hydrogen-assisted decomposition of $[\text{Ru}(\text{COD})(\text{COT})]$ in THF in the presence of various mono or diphosphines (Fig. 14, top) at different L/M ratios. In all cases, the prepared RuNPs have a mean size in the 1.1–2.1 nm range. Whilst

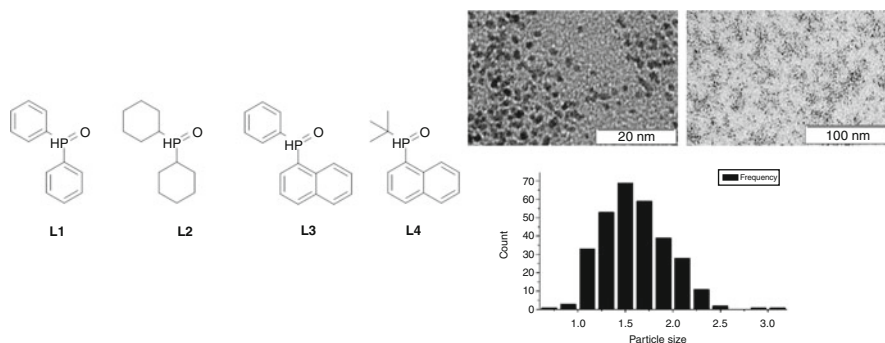


Fig. 15 Secondary phosphine oxide (SPO) used as stabilizers for the RuNPs (*left*) and TEM images of RuNPs and particle size distribution obtained with ligand L1. (Adapted from [102] with permission from RSC)

^{31}P -HRMAS NMR evidenced the coordination of the triarylphosphines, dialkylphosphines, or trialkylphosphines ligands at the surface of the particles, this also indicated the partial or total hydrogenation of the substituents due to the presence of hydrogen for the synthesis of the particles. This phenomenon was previously observed with simple diphosphine ligands [74]. The resulting nanoparticles were active in the hydrogenation of *o*-methylanisol. The nature of the ligands strongly influences the catalytic performances of these nanoparticles. It was observed that colloids containing triarylphosphines were not or very poorly active, while colloids containing dialkylarylyphosphines led to the full hydrogenation of the substrate (Fig. 14, bottom). This work pointed out the interest of designing appropriate ligands to control the catalytic properties of the particles.

3.4 Secondary Phosphine Oxide (SPO)-Stabilized RuNPs

Whilst it is well established that secondary phosphine oxides (SPOs) form very strong complexes of coordination, it has been recently reported that SPOs can be efficient pre-ligands for catalytic applications [99–101]. Depending on the solvent, substituents and metal coordination, these SPOs compounds are in equilibrium which could lead to the pentavalent phosphorus oxide pre-ligand and the trivalent phosphinous acid ligand. In collaboration with van Leeuwen et al., SPO were used as ligands to prepare RuNPs (Fig. 15) [102]. These easily accessible ligands allowed the formation of air-stable small nanoparticles in the size range of 1–2 nm. The characterization of these particles employing FT-IR, liquid and solid-state NMR techniques led to insights into the structure and dynamics of surface species.

In the case of SPO ligand L1, the RuNPs were further tested for the hydrogenation of model substrates (Table 1) in acidic or basic conditions using different

Table 1 RuL1 NPs as catalysts for hydrogenation of aromatics. (Reproduced from [102] with permission from RSC)

Substrate	S/C ^a	Time	Solvent	Conversion	TOF ^b
Toluene	2,400	16	THF	83	124
Cyclohexene	2,400	16	THF	100	150
Benzene	2,400	16	THF	100	150
Acetophenone	2,400	16	THF	87	130
Toluene	13,500	16	None	89	750
Toluene	13,500	6	None	59	1,330
Benzene	16,200	6	None	100	2,700
Anisole	13,300	6	None	16	350
Acetophenone	12,300	6	None	56	1,150
1,1,1-Trifluorotoluene	11,800	6	None	35	690

^aSubstrate/catalyst molar ratio. Catalyst: 1 mg of Ru-L1^{0,1}. 25 mL Berghof reactor connected with a 300 mL reservoir of 40 bar H₂

^bAverage turnover frequency calculated relative to hydrogenated products. TOF = mol substrate converted/mol catalyst⁻¹ h⁻¹. Rate calculated by conversion not gas uptake

solvents. In homogeneous SPOs catalysis, acids and bases usually play an important role. The absence of such an effect for Ru/L1 NPs indicated that the oxygen atom is not involved in the reactions with H₂ using these nanocatalysts. The particles were highly active for the hydrogenation of aromatics with the highest hydrogenation rates achieved utilizing neat reagents (TOFs up to 2,700 mol h⁻¹). This method could be used with very low catalyst loadings (i.e., <0.01 mol% of nanoparticles) and no further additives. This work is a proof of concept that secondary phosphine oxides can be successfully used as strong ligands for nanoparticle stabilization.

3.5 APTS-Stabilized RuNPs for Dehydrogenation Reactions of Amine-Boranes

In the field of the materials for the storage of hydrogen, amine-boranes are interesting candidates due to their high hydrogen contents (19.6 wt.%) [103]. In a collaborative work with Zahmakiran and Ozkar et al., we prepared 3-aminopropyltriethoxysilane-stabilized Ru nanoclusters (Ru/APTS) of different sizes. The mean size of Ru/APTS NPs decreased with increasing APTS ligand concentration in the

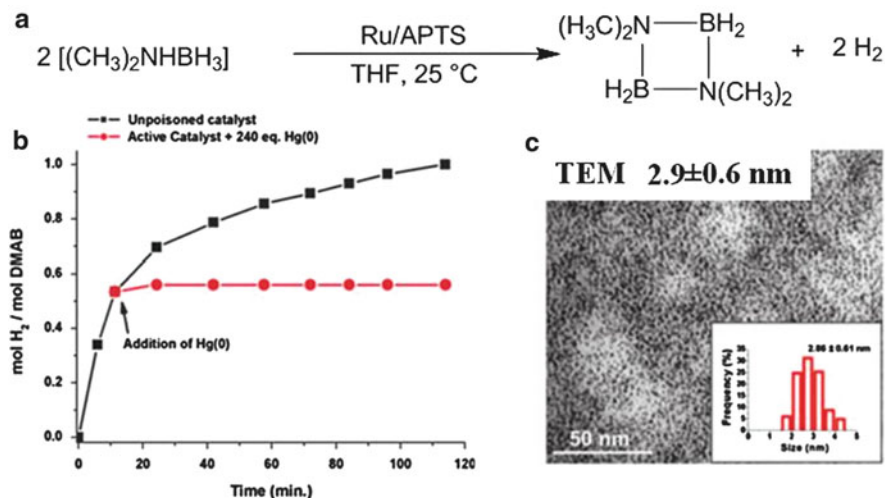


Fig. 16 (a) Dehydrogenation of dimethylamine-borane catalyzed by Ru/APTS NPs in THF at r.t. (b) mol H₂/mol DMAB vs. time graph ([Ru] = 2.24 mM; [DMAB] = 54 mM; 240 equiv. of Hg(0) after ~50% conversion of DMAB), and (c) TEM image of Ru/APTS NPs (~2.9 nm) after the third catalytic run. (Adapted from [104] with permission from RSC)

1.2–2.4 nm range. The catalytic performance of these Ru/APTS NPs was studied in the catalytic dehydrogenation of dimethylamine-borane (Me₂NHBH₃; DMAB) under mild conditions (Fig. 16a) [104, 105]. Following the addition of DMAB into a THF solution of Ru/APTS NPs, hydrogen evolution immediately started with an initial turnover frequency (TOF) of 53 h⁻¹ and continued until 1 equiv. H₂ per mol DMAB was released. To determine the homogeneous or heterogeneous nature of the catalytic reactivity, Hg(0), a poison for heterogeneous metal(0) catalysts, was added into the reaction mixture. The suppression of the catalysis in the presence of Hg(0) demonstrated that the catalyst was heterogeneous: the reaction occurred at the surface of the nanoparticles (Fig. 16b). The initial TOF value of 53 h⁻¹ obtained with this system was comparable to that of the prior best heterogeneous catalyst of rhodium nanoclusters (TOF = 60 h⁻¹). In addition, it was the first example of an isolable, bottleable, and reusable transition metal nanocatalyst for the dehydrogenation of dimethylamine-borane (Fig. 16c). An increase of APTS concentration resulted in a significant decrease of the catalytic activity as a result of a higher coverage of the metallic surface. The maximum catalytic activity was achieved with Ru/APTS = 3 which appeared as the best compromise between the NP mean size and the surface accessibility.

By varying the nature of the ligands used for the synthesis of RuNPs, we could obtain various colloidal solutions which are stable in organic media. Precise characterization by IR and NMR techniques allowed us to understand better how the ligand affects the characteristics of the obtained particles, such as their size, shape, and surface state. Depending on the strength of coordination of the ligands at

the metal surface, we can expect different nanostructures and consequently different surface properties. In summary, ligands which are strongly coordinated at the metal surface, such as phosphorus molecules and phenylpyridine, lead to very small and spherical RuNPs. On the contrary, amines and aminoalcohols are weakly coordinating ligands but this can be exploited to induce a specific morphology. Some of our RuNPs were investigated in colloidal catalysis leading to encouraging results although there is still a long way to go in the field of enantioselective catalysis. Since we can prepare various nanostructures displaying different surface chemistry, we now have different tools to deeply explore the world of well-defined nanocatalysts with the aim to find catalytic systems of high selectivity and activity in the near future.

4 Water-Soluble RuNPs for Investigation in Aqueous Colloidal Catalysis

Due to sustainability issues, we have been interested in the synthesis of water-soluble MNPs for their use as catalysts in water. For this purpose, we took inspiration from organometallic catalytic systems in water and considered ligands, such as 1,3,5-triaza-7-phosphaadamantane (PTA) and sulfonated diphosphines, which are frequently employed to stabilize complexes.

4.1 PTA-Stabilized RuNPs

PTA is a versatile ligand which combines a strong basicity and a very small cone angle to a high solubility in both organic solvents and water. The synthesis of PTA-stabilized RuNPs was carried out by decomposition of the [Ru(COD)(COT)] precursor in the presence of 0.8 equiv. of PTA ($P(H_2) = 3$ bar; THF; $70^\circ C$) (Fig. 17) [106, 107]. The resulting NPs displayed a spherical shape and low size dispersity, with a mean diameter of 1.3 nm. These NPs were purified by washing with pentane and filtration, and then dissolved in water with no change in dispersion and mean diameter (~ 1.4 nm). Aqueous suspensions of these NPs were stable for weeks under argon atmosphere. The coordination of the ligand at the Ru surface was investigated by NMR; 1H , ^{13}C , ^{31}P solution and solid-state NMR studies showed the strong coordination of PTA at the surface of the particles via the phosphorous atom. DOSY experiments excluded the presence of exchange processes at the NMR time scale. In addition, PTA was not released following the addition of excess dodecanethiol, showing the strong interaction of PTA with the nanoparticles' surface. In the presence of air, an excess of PTA resulted in low quantity of PTA-oxide. Interestingly, in addition to the signals of PTA ligands, the 1H MAS NMR spectrum of Ru@PTA showed a weak signal at -14 ppm which is a typical

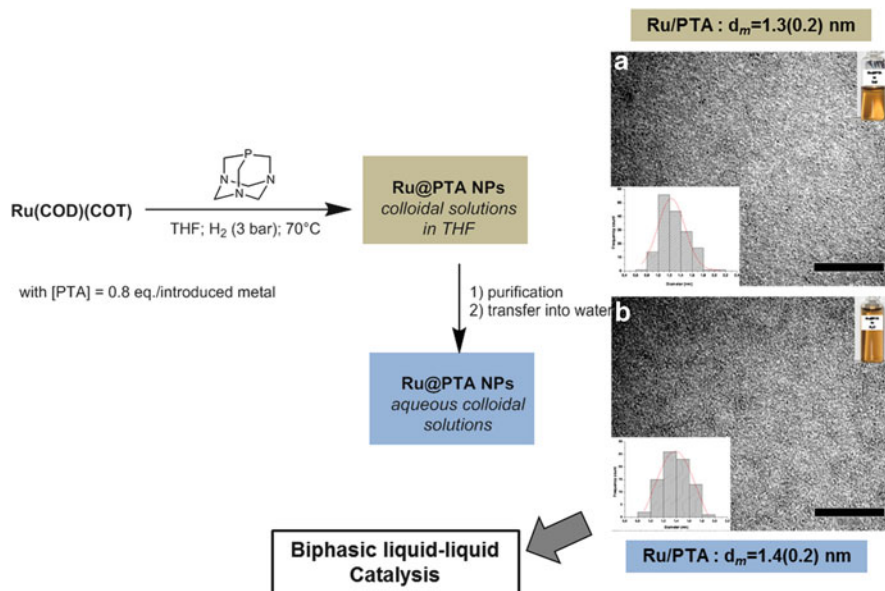


Fig. 17 Synthesis of PTA-stabilized RuNPs and TEM images in THF (*top*) and in water (*bottom*). (Adapted from [106] with permission from RSC)

value for hydrides. It is worth mentioning the disappearance of this peak following the exposure of the nanoparticles to air or deuterium atmospheres. As the presence of hydrides at the surface of various RuNPs was previously demonstrated through indirect methods as well as by static ²D NMR, this peak was attributed to surface hydrides. For the first time hydrides were observed on the nanoparticles' surface via direct ¹H NMR.

In collaboration with Buntkowsky et al., ³¹P-¹³C REDOR NMR measurements allowed a reasonable approximation of distances between PTA ligands and carbon monoxide (CO) molecules on the surface of PTA-stabilized RuNPs following the adsorption of ¹³CO on these particles [108]. REDOR data evidenced that ¹³C and ³¹P nuclei form complex spin systems with distributions of multiple dipolar couplings on the surface of the NPs. However, the ³¹P and ¹³C REDOR curves at short dephasing times are dominated by nearest neighbor interactions. This allowed us to determine the nearest neighbor distance between the PTA ligand and CO to be 3.1 Å, which is in good agreement with the results of quantum chemical DFT calculations about small cluster compounds. This work shed light on the interactions between CO and phosphine as well as on the binding geometries of these molecules on the surface of the RuNPs. As information on the ligand location and mobility is precious for the understanding of the chemical and catalytic properties of nanoparticles, these results support the interest of using sophisticated NMR tools to investigate the surface chemistry of nanoparticles.

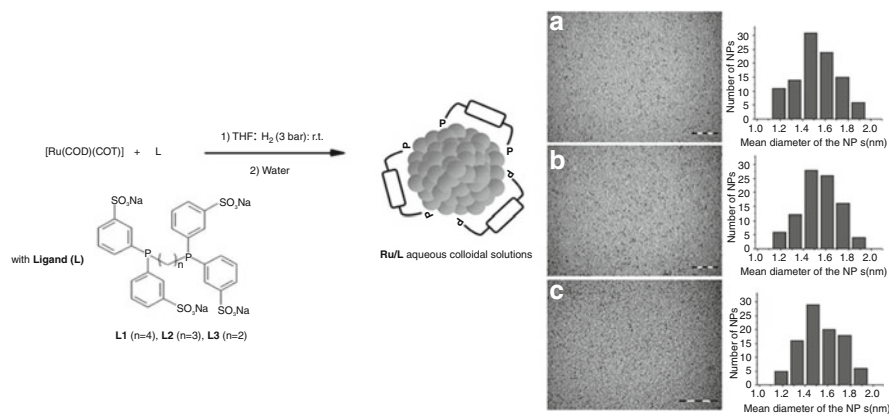
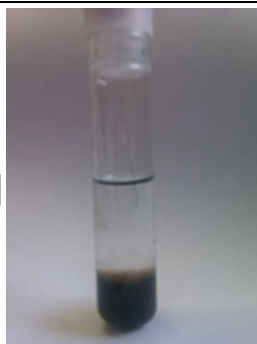
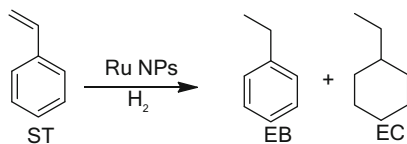


Fig. 18 Synthesis and TEM images of sulfonated diphosphine-stabilized RuNPs in water with (a) dppb-TS (b) dppp-TS, and (c) dppe-TS with $[\text{L}]/[\text{Ru}] = 0.1$. (Adapted from [109] with permission from Elsevier)

Finally, these aqueous colloidal solutions were used as catalysts for the hydrogenation of simple olefins and arenes with Roucoux et al. [107]. These nanocatalysts appeared efficient in mild conditions, evidencing that these materials are active despite the evolution of their environment related to their dissolution into water. For example, octene and dodecene were fully converted into the corresponding alkanes (r.t.; 1 bar H_2) with moderate activities. An increase in the hydrogen pressure ($P(\text{H}_2) = 10$ bar) was not detrimental for the stability of the colloidal suspension. The complete hydrogenation of toluene into cyclohexane was observed overnight with Ru/PTA, whereas 60% of *m*-methoxymethylcyclohexane was formed from methoxymethylanisole. Nevertheless, preliminary recycling tests showed that an improvement of the stability and recovery of these materials was necessary to increase their interest in catalysis.

4.2 Sulfonated Diphosphine-Stabilized RuNPs

By applying the procedure previously described for PTA ligand, we used sulfonated diphosphines to stabilize RuNPs [109]. In this collaborative work with Roucoux and Monflier et al., the RuNPs were prepared from $[\text{Ru}(\text{COD})(\text{COT})]$ and different diphosphines, (1,4-bis[(di-*m*-sulfonatophenyl)phosphine]butane = dppb-TS; 1,4-bis[(di-*m* sulfonatophenyl)phosphine]propane = dppp-TS; 1,4-bis[(di-*m* sulfonatophenyl)phosphine]ethane = dppe-TS) in THF (3 bar H_2 ; RT). Various ligand/Ru ratios were employed in order to analyze the effect of both the backbone and the diphosphine concentration on the stability, size, and catalytic properties of the NPs. Depending on the amount of ligand, this resulted in the formation of well-crystallized RuNPs which exhibit a mean size in the range of 1.2–1.5 nm (Fig. 18). The coordination of

Table 2 Hydrogenation of styrene with Ru/sulfonated diphosphine aqueous colloidal solutions and picture of the reaction medium. (Adapted from [109] with permission from Wiley)

Nanocatalysts	<i>T</i> (°C)	Time (h)	Products selectivity (%)		
			ST	EB	EC
Ru/dppb-TS	20	1	25	75	0
	20	20	0	45	55
	20	40	0	3	97
Ru/dppp-TS	20	1	59	40	1
	20	20	0	47	53
	20	40	0	2	98
Ru/dppe-TS	20	1	75	24	1
	20	20	0	41	59
	20	40	0	1	99
Ru/dppb-TS	50	1	10	90	0
	50	2	0	82	18
	50	3	0	0	100

Reaction conditions: [Ligand]/[Ru] = 0.1; Ruthenium (3.9×10^{-5} mol), styrene (3.9×10^{-3} mol), 1 bar H_2 , water (10 mL)

the sulfonated diphosphines at the surface of the RuNPs allowed their facile dispersion in water giving rise to very homogeneous and stable aqueous colloidal solutions (up to several months) with no change in their mean sizes.

The catalytic evaluation of these aqueous colloidal solutions showed promising reactivities for the hydrogenation of unsaturated substrates (tetradecene, styrene and acetophenone) in biphasic liquid–liquid conditions. Interestingly, minor structural differences in the diphosphine ligands, such as the alkyl chain length, influenced the catalytic activity in styrene hydrogenation in addition to the positive effect of temperature (from 20°C to 50°C) or pressure (from 1 to 10 bar H_2) increase (Table 2). As the [Ligand]/[Ru] ratio increased, conversion and selectivity (expressed as ethylbenzene (EB)/ethylcyclohexane (EC) ratio) also increased at short reaction times. The best results were obtained with the dppb-TS ligand which

exhibits the longest alkylchain giving rise to 75% EB after 1 h; dppp-TS led to 40% EB and dppe-TS resulted in the formation of 20% of EB. As all these RuNPs display similar mean sizes, their different performances in catalysis may result from different flexibilities of their alkyl chain. Due to the highest number of carbon atoms, dppb-TS ligand had the highest flexibility and therefore favored a better diffusion of the substrate towards the metal surface. Although the mean size (1.25 nm) of the RuNPs remained similar with the increase of [dppe-TS]/[Ru] from 0.2 to 0.5, an evolution of the selectivity is observed. The aromatic substrate could have a more limited access to the NP surface since the presence of a higher density of ligands coordinated to this surface increases the sterical hindrance. A molar ratio of 0.1 appeared to be a good compromise between the stabilization and catalytic activity of the NPs. Finally, as for Ru/PTA NP systems, preliminary studies offered encouraging results about the recovery of these water-soluble Ru/sulfonated diphosphine nanocatalysts. These results confirmed the high versatility of the organometallic approach for the synthesis of metal nanoparticles since efficient preparations of nanoparticles can be achieved to get in aqueous solutions.

4.3 Sulfonated Diphosphine/Cyclodextrin-Stabilized RuNPs

The combined presence of both a sulfonated diphosphine and a cyclodextrin (CD) led to very stable water-soluble RuNPs which displayed suitable performances in the catalytic hydrogenation of unsaturated substrates due to a supramolecular control effect of the cyclodextrin (Fig. 19) [110]. The so-obtained nanoparticles were fully characterized and compared to sulfonated diphosphine-stabilized RuNPs. Interestingly, deep NMR investigations evidenced: (1) the strong coordination of the sulfonated diphosphine ligand at the metallic surface, (2) in the presence of cyclodextrin, the formation of an inclusion complex between the sulfonated diphosphine and the cyclodextrin which modified the coordination mode of the diphosphine. Indeed, an interaction between the sulfonated diphosphine and the cyclodextrin was unambiguously observed by NMR spectroscopy (both in solution and in solid state). This interaction was even stronger at higher cyclodextrin content which hugely disrupted the coordination properties of the diphosphine on the metal surface. However, this interaction only took place when the cyclodextrin was present during the synthesis of the particles.

The catalytic properties of the sulfonated diphosphine-stabilized RuNPs and sulfonated diphosphine/cyclodextrin-stabilized RuNPs were compared in the hydrogenation of unsaturated model substrates (styrene, acetophenone, and *m*-methylanisole) in biphasic liquid–liquid conditions (i.e., ruthenium aqueous colloidal solution and organic substrate; no added solvent). Whilst all of these RuNPs displayed suitable performances in catalysis, different activities and selectivities were observed. This highlighted that supramolecular interactions on the metallic surface in the presence of a cyclodextrin control the catalytic reactivity of the nanocatalysts. Interestingly the CD acts as a phase-transfer promotor, which

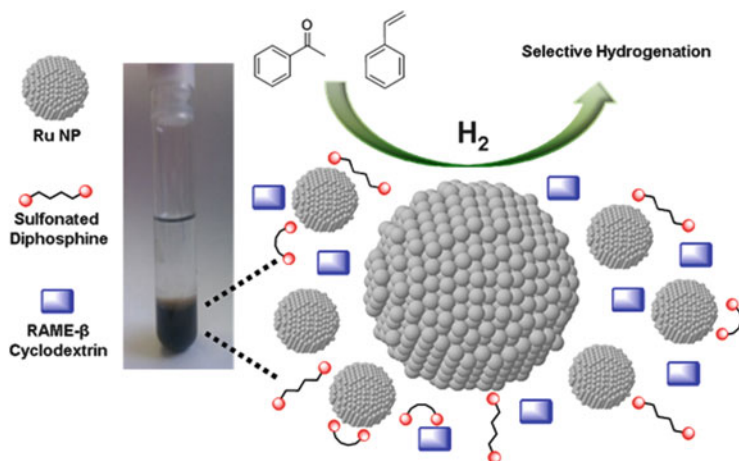


Fig. 19 RuNPs stabilized by a mixture of sulfonated diphosphine + Rame-β-cyclodextrin as selective catalyst for hydrogenation of styrene and acetophenone. (Reproduced from [110] with permission from Wiley)

increases the activity and affects the selectivity. As evidenced via NMR studies, the influence of CD on the selectivity may result from the formation of an inclusion complex between the CD and the diphosphine ligand at the RuNPs surface. This original work takes advantage of the supramolecular properties of a cyclodextrin to modulate the surface reactivity of diphosphine-stabilized RuNPs which is expected to offer novel opportunities to the field of nanocatalysis.

All these results point out the high versatility of the organometallic approach for the synthesis of metal colloidal solutions in aqueous media. The recent results obtained by combining organometallic complexes as precursors and hydrosoluble molecules as stabilizers open the way for catalytic applications in water. As previously reported using complexes in molecular chemistry, the catalytic performance of Ru nanocatalysts can be controlled at a supramolecular level in the presence of both a sulfonated diphosphine and a cyclodextrin. This highlights that metal nanoparticles can be considered as organometallic objects of large size; the surface chemistry of which can be modified by selecting the ligands similarly to molecular complexes.

5 Ionic Liquid-Stabilized RuNPs

Providing more environmentally friendly conditions than usual solvents, the use of ionic liquids (ILs), acting as both the solvent and the stabilizer, has emerged as an alternative for the preparation of nanocatalysts [22, 23, 111–113]. Both experiments and simulations reported in literature have evidenced the segregation phenomenon

that exists between polar and non-polar domains in imidazolium-based ILs [114, 115]. The organometallic synthesis of MNPs in ionic liquids has been initiated by Dupont et al. who followed our method to produce nanoparticles directly from organometallic precursors in the ILs [116–118]. This route is also applied by the group of Gomez [119, 120].

In collaboration with Santini et al., we investigated the stabilization of RuNPs in the presence of imidazolium-derived ionic liquids [121–126]. The synthesis of RuNPs was first performed in 1-butyl methylimidazoliumbis(trifluoromethanesulfonyl)imide ([RMIm][NTf₂]; R = C₄H₉) [121]. This implied to control the decomposition of [Ru(COD)(COT)] under 4 bar of H₂ without adding any further stabilizer. To study their influence on the NPs formed different temperatures of reaction (0°C and 25°C) and stirring rates were selected. At 25°C under stirring, homogeneously dispersed RuNPs were observed with a mean size of ~2.4 nm. At 0°C, the RuNPs, which had a smaller size of ~0.9 nm, tend to agglomerate to form larger clusters of 2–3 nm. When no stirring was applied at 0°C, the NPs displayed a slightly larger mean size, ~1.1 nm and no agglomeration was observed. These results showed the influence of the temperature on the mean size of the NPs: the smallest NPs were obtained at the lowest temperature. The size of RuNPs is governed by the degree of self-organization of the imidazolium-based ionic liquid. The 3D organization of the ionic liquid is better maintained at low temperature which led to a better confinement of the Ru nuclei and finally smaller nanoparticles.

This observation was further confirmed by using a series of imidazolium-derived ionic liquids: [RMIm][NTf₂] (R = C_nH_{2n+1} with n = 2; 4; 6; 8; 10), [R₂Im][NTf₂] (R = Bu) and [BMMIm][NTf₂] (with BMMIm = 1-butyl-2,3-dimethylimidazolium) [122]. In all of these ILs, the size of the RuNPs was smaller at 0°C than at 25°C, and the stirring induced their agglomeration. Additionally, the increase in alkyl chain lengths was found to be linearly proportional with the mean size of the RuNPs (Fig. 20). In parallel, simulation of the molecular dynamics evidenced a relationship between the size of IL non-polar domains and the mean diameter of RuNPs, which highlights the role of the organization of the ILs on the control of the RuNPs size. Crystal growth occurs inside the pockets created by the non-polar domains of the ILs, giving rise to a confinement effect which leads to the control of the growth of the particles. Finally, the addition of a polar solute like water to the ionic liquid induced the aggregation of the particles due to the disruption of the ionic liquid 3D structure.

The use of spectroscopic methods evidenced the presence of hydrides at the surface of the nanoparticles [123]. As part of the labeling experiments, H/D exchange was studied at the surface of the RuNPs prepared in 1-butyl-3-methylimidazolium bis(trifluorosulfonyl)imide by exposing the colloidal solution to a D₂ atmosphere. After several days, an analysis of the gas atmosphere by NMR revealed the formation of HD in agreement with the initial presence of hydrides on the ruthenium nanoparticles. The quantification of hydrides, by hydrogenation of ethylene at room temperature, gave a value of 0.6H/Ru_{surf}. In addition, the hydrides present at the surface of the particles display a stabilizing effect since a more important coalescence is observed under stirring in the presence of argon

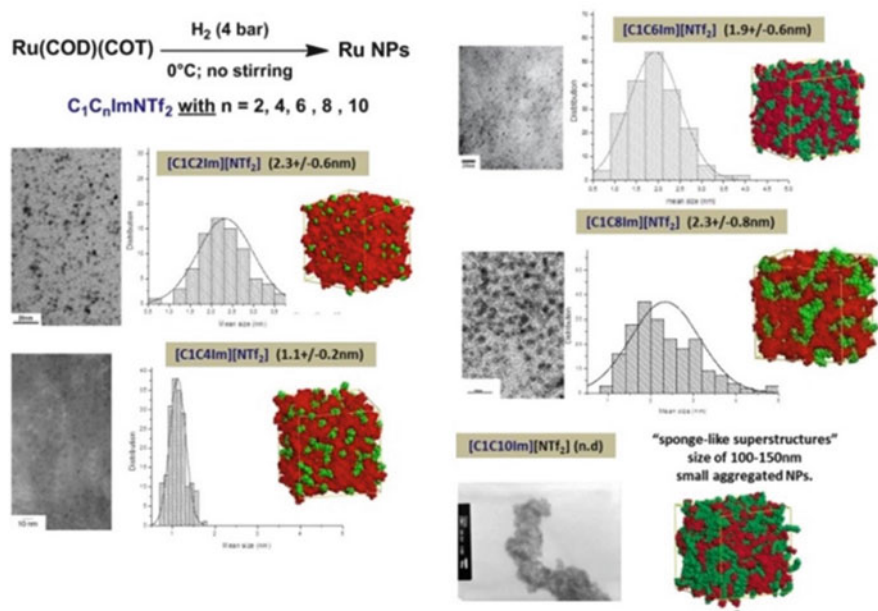


Fig. 20 Influence of the ionic liquid chain length on the size of the RuNPs. (Adapted from [122] with permission from RSC)

atmosphere instead of H₂ atmosphere. When the synthesis of the nanoparticles was performed under deuterium, an H/D exchange occurred for all of the carbons of the imidazolium ring. This shows that the RuNP surface is active and in the near environment of the side alkyl group (Fig. 21).

In addition, we studied the influence of the addition of amines on both the size control of IL-prepared RuNPs and the stability of these NPs [124, 125]. Whilst RuNPs are reference catalysts in hydrogenation reactions, IL-stabilized RuNPs are generally not stable in the conditions required for catalytic hydrogenation. For this study, the ionic liquids [RMIm][NTf₂] (R = C_nH_{2n+1}, n = 2, 4, 6, 8, 10) were used in the presence of octylamine (OA) or hexadecylamine (HDA) as additional ligands. The synthesis of the NPs was performed following the previously described conditions, and 0.2 M equiv. of the selected ligand. Regardless of the alkyl chain length of the IL, well-dispersed and well-crystallized NPs were obtained with a mean size in the range of 1.1–1.3 nm (Fig. 22). These RuNPs displayed a better size dispersity than the corresponding RuNPs only stabilized with an amine ligand [61]. Whilst IL prevents particles from agglomeration through a confinement effect, amines also play an important role in controlling the size and dispersion of these NPs. This demonstrates the interest of using ionic liquids to confine nanoparticles in the non-polar domains (*nanoreactors*) in the presence of a ligand which stabilizes the particles at a very small size.

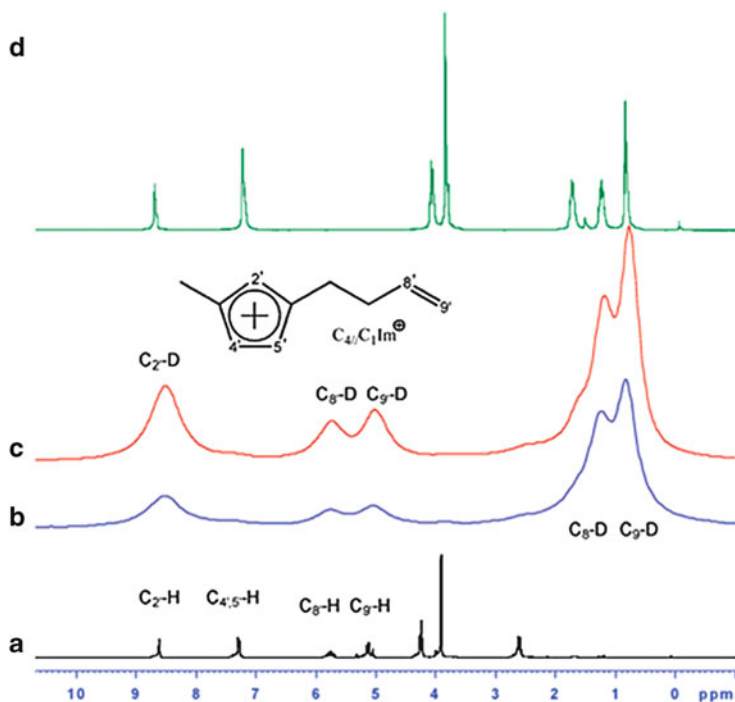


Fig. 21 (a) ^1H NMR spectra of $\text{C}_4/\text{C}_1\text{Im NTf}_2$, neat IL_2 ; (b) ^2H NMR spectra of IL_2 after RuNP formation at 0°C under deuterium; (c) ^2H NMR spectra of IL_2 after RuNP formation at 50°C under deuterium; (d) ^1H NMR spectra of $\text{C}_4/\text{C}_1\text{Im NTf}_2$, neat. (Reproduced from [123] with permission from RSC)

Hydrogenation of toluene was first performed at different temperatures with the RuNPs synthesized in $\text{C}_1\text{C}_4\text{ImNTf}_2$ in the presence of octylamine, (Table 3). The conversion obtained was low but reproducible. A temperature of 75°C was then selected to evaluate the catalytic properties of the Ru colloids. Since Ru/HDA and Ru/OA have similar size and shape, the slightly lower conversion obtained by hexadecylamine was explained by viscosity changes in the reaction mixtures and by a higher steric hindrance of HDA once coordinated on the RuNP surface.

These systems were also tested in the hydrogenation of 1,3-cyclohexadiene (CYD), styrene (STY), and R-(+)-limonene (LIM). Whilst the activity of the RuNPs in these hydrogenation reactions increased with σ -donor ligands, such as $\text{C}_8\text{H}_{17}\text{NH}_2$ and H_2O , a decrease of the activity was observed using bulkier and π -acceptor ligands, i.e. PPhH_2 , PPh_2H and CO . This underlined the quasi-molecular nature of sub-3 nm NPs since their activity can be tuned by the σ - π -ligand character similarly to homogeneous catalysis.

In summary, imidazolium-based ILs display a high degree of self-organization in the liquid state. Both theoretical and experimental studies showed that a three-dimensional ionic network dominated by electrostatic interactions coexists with

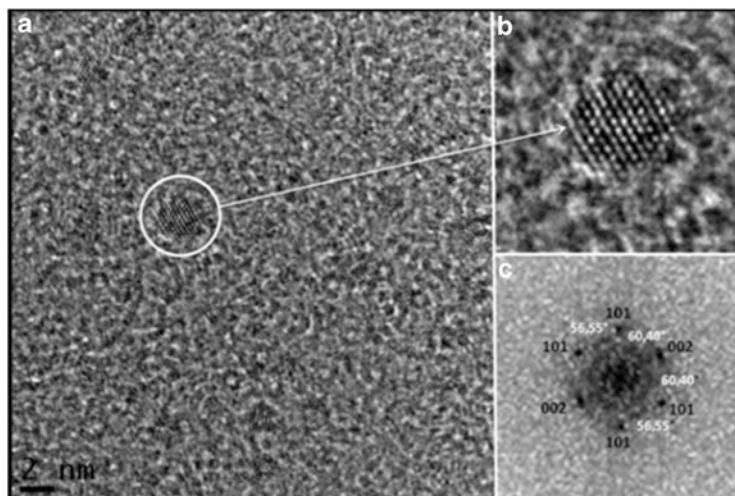


Fig. 22 (a) General HREM image of *C4OA*-stabilized RuNPs in $C_1C_4ImNTf_2$, (b) HREM image of an isolated and well-crystallized *C4OA*-stabilized RuNP with (c) FFT. (Reproduced from [124] with permission from RSC)

Table 3 Hydrogenation of toluene with RuNPs synthesized in $C_1C_4ImNTf_2$ + octylamine. (Reproduced from [124] with permission from RSC)

Nanocatalyst IL/ligand	T ($^{\circ}C$)	PhMe/ Ru_T	PhMe/ Ru_S	Ru_S / Ru_T	Conversion (%)	TON ^a	$k_{initial}$ ^b
<i>C4OA</i>	30	38/1	46/1	0.82	4	2	
<i>C4OA</i>	50	38/1	46/1	0.82	9	4.5	
<i>C4OA</i>	75	38/1	46/1	0.82	17	8	12 ± 1
<i>C4OA</i>	100	38/1	46/1	0.82	17	8	
<i>C4HDA</i>	75	38/1	52/1	0.73	14	6.5	
<i>C4OA</i>	75	38/1	46/1	0.82	17	8	12 ± 1
<i>C6OA</i>	75	38/1	49/1	0.77	16	8	8 ± 1
<i>C8OA</i>	75	38/1	49/1	0.77	11	5.5	5 ± 1
<i>C10OA</i>	75	38/1	52/1	0.73	14	7	7 ± 1

Reaction conditions: $P(H_2) = 1.2$ bars; reaction time = 5 h; Ru_T = total amount of Ru atoms; Ru_S = amount of surface Ru atoms

^aTurn over number (moles of product converted per mol of Ru_S)

^bEstimated initial rates in $10^{-2} \text{ mol L}^{-1} \text{ h}^{-1}$

non-polar domains resulting from the lipophilic alkyl side chains. Due to a confinement effect, this phenomenon facilitated the growth control of the RuNPs. The catalytic performance of these RuNPs was further improved via the addition of an amine as co-stabilizer. As expected, the amine played an important role in controlling the size, shape, and stability of the RuNPs.

6 Investigation of RuNPs in Supported Catalysis

In the last 15 years, the application of supported metal nanoparticles as catalysts in organic synthesis has received a renewed interest. The association between a metal and a support could result in synergistic effects which would precisely drive the reactivity of these nanocatalysts, e.g. supported-gold NPs for the oxidation of carbon monoxide [127]. The recyclability and recovery from the reaction medium still remains one of the major drawbacks to a widespread use of NPs in catalysis. To overcome these problems, the immobilization of MNPs on solid supports appears as a promising alternative. Synthetic methods are also developed to achieve the direct synthesis of MNPs in the presence of a support in a controlled manner. Intensive work is made on the functionalization of the support to increase the anchorage of the particles, inspired by the ligands which are used to stabilize MNPs in solution.

The organometallic approach for the synthesis of MNPs can also be applied for the preparation of composite materials. Some results were obtained using alumina membranes, mesoporous silica, and carbon materials as templates for the deposition of MNPs, mainly for hydrogenation and oxidation reactions. Metal oxide ruthenium nanoparticles could be obtained after a calcination step on the preformed nanoparticles under air without change in size and dispersion. The inclusion of MNPs was performed following two different approaches: (1) either by impregnation of the support using a colloidal solution of preformed NPs or (2) by direct synthesis of the nanoparticles in the presence of the support, with or without a ligand.

6.1 Alumina-Supported RuNPs for Hydrogenation and Oxidation Reactions

In a collaborative work with Schmid et al., the filling of nanoporous alumina membranes of various pore widths was carried out in two different ways from the decomposition of $[\text{Ru}(\text{COD})(\text{COT})]$ in THF/MeOH mixtures in the absence of stabilizer [128]. The first approach involved the impregnation of alumina support with colloidal solutions of RuNPs of different sizes which were dependent on the ratio of MeOH/THF in the reaction mixture. Colloidal solutions were transferred into membranes by vacuum induction. Only a few agglomerates were observed outside of the pores whereas dense areas were located within the membrane channels. The second approach consisted of the room-temperature decomposition of $[\text{Ru}(\text{COD})(\text{COT})]$ under 3 bar of H_2 following the deposition of this metal precursor inside the pores. In this way, homogeneous materials displaying well-dispersed RuNPs were obtained in the pores of alumina membranes. The size of the particles depended on the pore diameter of the template. These materials were evaluated in two catalytic reactions, i.e. the hydrogenation of 1,3-butadiene and

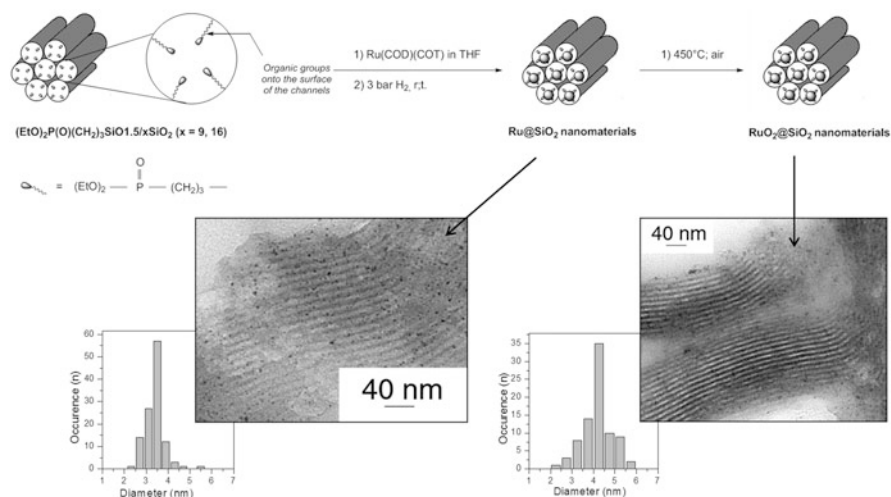


Fig. 23 Synthesis and TEM images of Ru and RuO₂NPs inside the pores of a phosphonate-functionalized mesoporous silica. (Adapted from [130] with permission from Wiley)

the gas-phase oxidation of CO [129]. For both reactions the decrease of the particle size resulted in an increase of activity.

6.2 Silica-Supported RuNPs for Oxidation of Carbon Monoxide and Benzylalcohol

In collaboration with Corriu et al., organized mesoporous silica materials containing phosphonate groups were used as a host for controlling the growth of RuNPs [130]. $[\text{Ru}(\text{COD})(\text{COT})]$ was first impregnated into the support and then decomposed (3 bar H_2 ; RT). The phosphonate groups present in the pores of the solid acted as a stabilizer for the Ru/SiO₂ NPs which allowed their organization in the channels of the host material. A calcination step (air; 400°C) led to RuO₂/SiO₂ nanomaterial (Fig. 23). The use of RuO₂/SiO₂ composite nanomaterials, as catalytic filters for gas sensors, has been successful since these materials efficiently achieved the preferential detection of propane in a propane/CO/NO₂/air mixture. The sensitivity of the propane sensing was dependent on the metal content of the nanocomposite materials: higher Ru/Si_w induced higher $S_{\text{C}_3\text{H}_8}/S_{\text{CO}}$ sensitivity ratios. The RuO₂/SiO₂ nanomaterials partially removed CO from the gas mixture via the selective oxidation of CO into CO₂, while the hydrocarbon content remained unaltered.

To control the size of the NPs inside the silica matrix, the organometallic approach was combined with the sol-gel method for the preparation of RuO₂/SiO₂ nanocomposite materials (Fig. 24) [131]. The key-point of this new

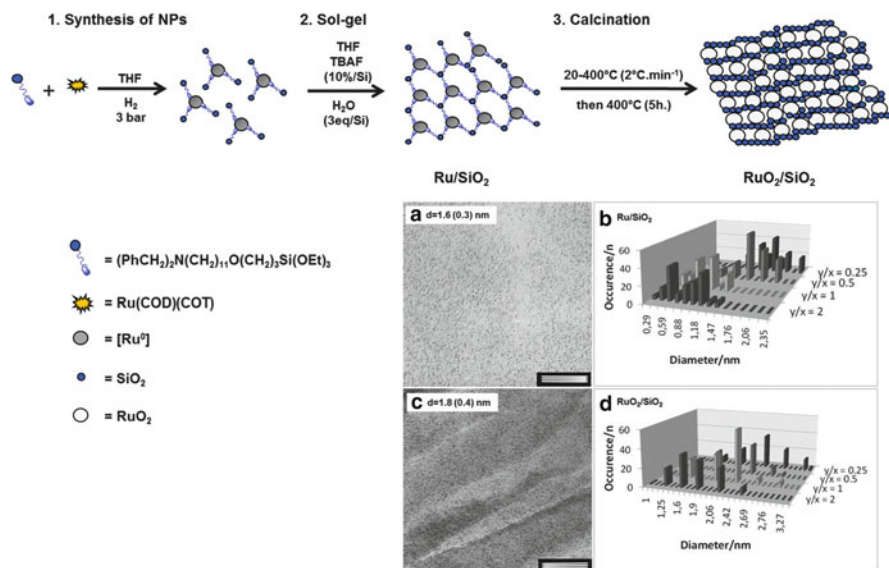


Fig. 24 Synthesis of Ru and RuO₂ NPs embedded in silica using a polycondensable amine; (a) TEM image of Ru/SiO₂ nanocomposites with L/Ru(COD)(COT) ratio of 2. (b) Distribution histograms of Ru/SiO₂ NPs. (c) TEM image of RuO₂/SiO₂ NPs with L/Ru(COD)(COT) ratio of 0.5. (d) Distribution histograms of RuO₂/SiO₂ nanocomposites with L/Ru(COD)(COT) = 2, 1, 0.5, 0.25 (Scale bars of TEM images = 50 nm). (Adapted from [131] with permission from Wiley)

methodology was to use a ligand ((PhCH₂)₂N(CH₂)₁₁O(CH₂)₃Si(OEt)₃; benzenemethanamine; L) which plays a double role: (1) a stabilizing agent for the synthesis of NPs, (2) a precursor for the silica matrix. This approach led to hybrid materials with high Ru contents, displaying well-dispersed and small size RuNPs in the silica matrix. A calcination step (air; 400°C) gave rise to mesoporous silica materials containing RuO₂ NPs. The mean size of the NPs was related to the [L]/[Ru(COD)(COT)] ratio. In addition, the addition of tetraethylorthosilicate (TEOS) to the initial [L]/[Ru(COD)(COT)] solution led to materials which exhibit higher proportions of silica and higher specific surface areas. These hybrid nanomaterials displayed a good dispersion inside the silica matrix and interesting surface-specific area properties, which made them attractive materials to be used as catalytic filters for gas sensors. This has been illustrated by an interesting increase of the sensitivity for the detection of propane.

Once adapted to 3-aminopropyltriethoxy-silane and 11-aminoundecyltriethoxysilane, this methodology gave rise to very small and reactive RuO₂ NPs [132]. Studies in the aerobic oxidation of benzyl alcohol showed promising results for further development of this type of nanomaterials.

6.3 Carbon Material-Supported RuNPs for Hydrogenation and Oxidation Reactions

Carbon materials are often used for the immobilization of MNPs as these solid supports offer multiple advantages including easy availability, relatively low cost, high mechanical strength and chemical stability. In addition, their porous structure makes them attractive for surface chemistry since important modifications can be simply achieved, e.g. the facile functionalization of these materials favors the immobilization of the NPs.

In a collaborative work with Serp et al., we studied how the confinement of MNPs inside carbon nanotubes (CNTs) may influence their catalytic properties. Using CNTs with various functionalization, the synthesis of RuPtL/CNTs (L = 4-(3-phenylpropyl)pyridine) was performed, in different conditions of reaction, from a couple of organometallic precursors, i.e. [Ru(COD)(COT)] and [Pt(CH₃)₂(COD)] (Fig. 25) [133]. One option consisted in the preparation of the NPs through the stabilization by the ligand first and then their impregnation on the CNTs. An alternative route was the co-decomposition of the two organometallic precursors in the presence of both the ligand L and the CNTs. The best results in terms of confinement of the particles were obtained by the impregnation method employing amide-functionalized CNTs. The resulting hybrid material had ~2–2.5 nm NPs which were located inside the CNTs (80% of NPs for a 23 wt.% of metal). In addition to the non-supported RuPt/L NPs, all of the prepared systems were evaluated as catalysts in the hydrogenation of cinnamaldehyde (Table 4). The catalytic activity and the selectivity of CNTs-supported RuPt/L NPs were higher than those of the non-supported NPs. For the NPs mainly located inside the CNTs, a remarkable selectivity towards the formation of cinnamyl alcohol was achieved.

In another work, NP/carbon hybrid systems were obtained by the impregnation of different mesoporous carbons with colloidal solutions of RuNPs previously prepared by the decomposition of [Ru(COD)(COT)], (P(H₂) = 3 bar; THF) in the presence of 4(3-phenylpropyl)pyridine ligands [134]. The supported RuNPs were well dispersed on the carbon materials with a mean size of 1.2–1.3 nm. These hybrid systems were successfully used as catalysts in the oxidation of benzyl alcohol in water at 80°C, giving rise to excellent conversion and selectivity (>99%) towards the aldehyde. The catalytic activity of these systems was found to be influenced by the hydrophilicity of the carbon support.

7 Conclusions and Perspectives

During the past decade, the design and characterization of ligand-stabilized metal nanostructures have experienced a huge development for their application in catalysis. The association between a metal core and a stabilizing ligand to form nanohybrids can be considered as crucial to control the surface properties of these

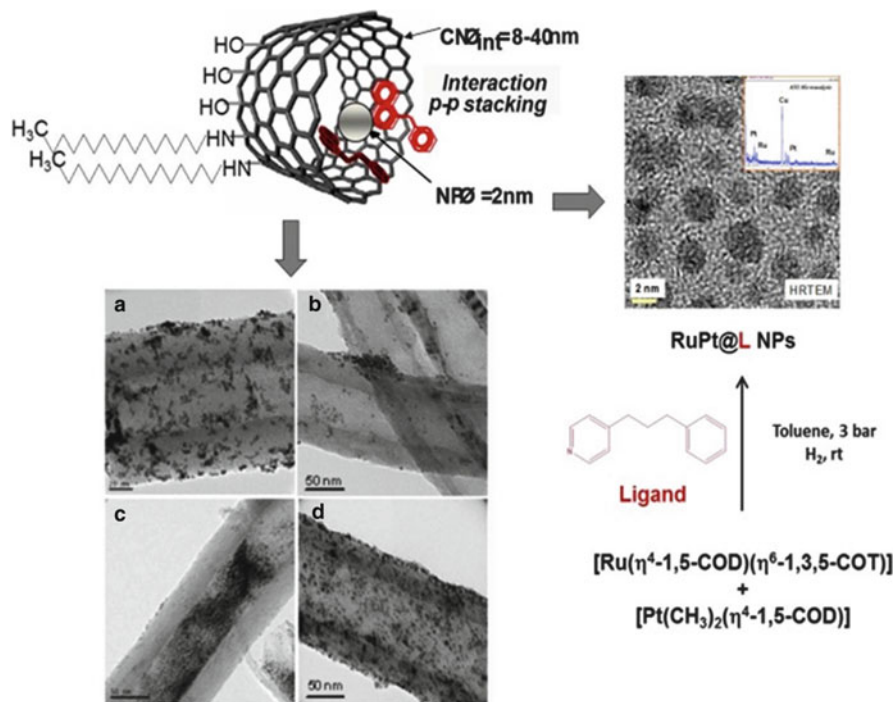
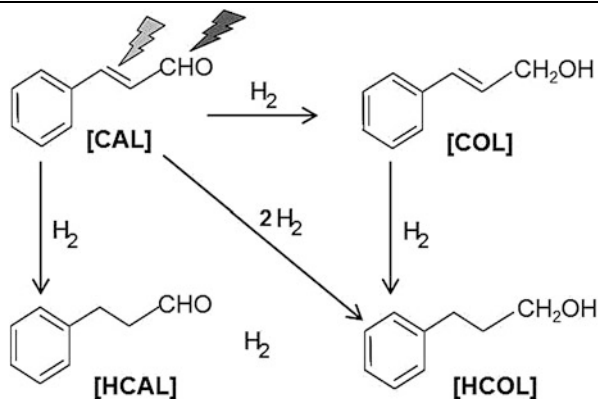


Fig. 25 Top left: Schematic representation of the confinement of the RuPt NPs in the channels of the CNTs. Bottom left: TEM images of the RuPt/L/CNTs nanomaterials with (a) 11% w/w PtRu/L/CNT, (b) 5% w/w PtRu/L/CNT-COOH, (c) 23% w/w PtRu/L/CNT-CO-NH-R (impregnation), and (d) 5% w/w PtRu/L/CNT-COOH (direct decomposition). Right: Synthesis and HREM image of the RuPt/L NPs. (Adapted from [133] with permission from Wiley)

nanostructures and their catalytic performance. Whilst a wide range of ligands can be used as stabilizers, their selection is guided by the similarity between the behavior of ligands on molecular complexes and on nanoparticles. This chapter overviews our contributions in this field giving representative results on ruthenium nanoparticles of interest in catalysis both in solution and in supported conditions, mainly for hydrogenation reactions. These results highlight our recent achievements in the field of ruthenium nanostructure to: (1) control their characteristics such as size, composition, surface state, solubility in organic or aqueous media, and deposition onto supports, (2) characterize their surface chemistry, and (3) explore their chemical properties using these nanoparticles as nanocatalysts.

In summary, we have over the years investigated a wide range of ligands on the surface of ruthenium nanoparticles. The first conclusion is that the behavior of ligands is similar on these nanoparticles and on molecular complexes. Thus, hydrides and CO coordinate on the surface of these nanoparticles, as well as olefins and methyl groups. The hydrides are always fluxional whereas CO appears only fluxional when the surface of the particles is free. Amines are also fluxional and do

Table 4 Catalytic hydrogenation of cinnamaldehyde with RuPt/CNTs nanomaterials. (Adapted from [133] with permission from Wiley)

Catalyst	NPs d_{mean} (nm)	inside/outside	% NP int.	TOF (h^{-1})	HCAL	HCOL	COL
PtRu/L NPs	2,2		–	30	50	15	35
PtRu/CNT2	2,2/2,2		10	56	33	8	59
PtRu/CNT1	1,6/2,2		30	75	18	12	69
PtRu/CNT3	2/2,5		80	85	0	5	95

Reaction conditions: isopropanol; 20 bar H_2 ; 343 K; 2 h

not stabilize the particles unless they are added in excess. However, what is a drawback in molecular chemistry can be used here as an advantage since amines allow the growth of nanoparticles. This may lead to shape-controlled nano-objects, as reported by other groups. Phosphines and N-heterocyclic carbenes are, as in molecular chemistry, very promising since their steric and electronic properties can be modulated. Consequently, phosphines and N-heterocyclic carbenes are suitable ligands to precisely control the surface chemistry of the nanostructures, and further tune their properties. Using the same principle, hydrosoluble molecules can favor the dissolution of organometallic nanoparticles into aqueous media with no change in size, dispersion, or surface reactivity. This paves the way towards application in sustainable nanocatalysis. In addition, bimetallic, such as nano-objects alloys, core-shell or heterostructures, can also be prepared. Finally, the organometallic approach provides nanostructures which exhibit a “clean” surface since the only molecules coordinated to the surface are selected for the synthesis of these nanoparticles. As a consequence, these systems are suitable for precisely studying the properties of the ligands coordinated to the particle surface and the influence of the ligands on the properties of the nanoparticles’ surface. For this purpose, in combination to other techniques, the nuclear magnetic resonance spectroscopy is a very helpful tool, well known in molecular chemistry to characterize precisely molecules and complexes. About the immobilization of nanoparticles on supports, the most promising results evidenced the important role of the functionalization of the support to increase the

anchorage of the particles. This improves the catalytic performances of these nanoparticles, such as selectivity, and facilitates the recovery of the catalyst.

On the basis of our long experience, i.e. 25 years, here exemplified with different metals, mainly ruthenium, we can affirm that the concepts and techniques of organometallic chemistry allow the design of nano-objects which display remarkable surface properties. This chapter describes new organometallic objects covered by different species: hydrides, CO, ancillary ligands, such as phosphines or N-heterocyclic carbenes. The location and dynamics of the ligands can be studied as well as the influence of the ligand location on the surface reactivity of the NPs. Due to advances in the field of characterization, including NMR techniques, the full characterization of the surface of catalytically active nanoparticles could be achieved at the molecular level. This achievement would drive the emergence of a complex chemistry on the surface of nanoparticles.

Recent results illustrate the possibility to perform selective chemistry on the surface of nanoparticles. Whilst we started with simple ligands (i.e., the hydride-carbonyl-phosphine triad which was the basis of the molecular organometallic chemistry in the 1970s), it is now required to develop both an understanding of this chemistry in collaboration with theoretical chemists and a more complex chemistry leading to highly selective transformations. Considering the recent advances, and predicting even more progress in the understanding of the formation and surface properties of NPs, we propose that future developments will provide novel hybrid nanocatalysts of interest in catalysis. Whilst other well-known methods often use commercially available metal sources, the organometallic approach requires the synthesis of the metal precursors. Even if an additional step may be perceived as a drawback, this efficient method is very complementary to other possibilities. The organometallic method is a highly versatile approach which is particularly attractive for its ability to afford precise control over the characteristics of nanostructures (size dispersion, chemical composition) and surface properties.

In terms of perspectives, many challenges remain to be met in nanocatalysis. The first one is probably the understanding of the influence of ligands on the course of catalytic reactions, e.g. how ligands could modify the selectivity of selected reactions. This would help in the preparation of nanocatalysts displaying catalytic performance of desire. Although numerous efforts have already been done with various capping agents all over the world, future progress will probably require the design of molecules more appropriate for the metal surface. As a consequence, it will be possible to produce nanoparticles designed for specific applications in catalysis. In this respect, one of the most interesting and challenging fields is asymmetric catalysis. Only a few examples of enantioselective reactions are presently known to be catalyzed by nanoparticles. Another area of importance is the activation and functionalization of C–H bonds which has been studied in heterogeneous catalysis and is rapidly developing in homogeneous catalysis. However, although nanoparticles seem to be perfectly fitted for these reactions, this field remains to be explored. However, recent results in the regioselective and stereospecific isotopic labeling of nitrogen-containing compounds may open a new way

for organic chemistry. Finally, for sustainable development issues, the recycling and the recovery of the nanocatalysts are also to be improved.

Acknowledgments All our collaborators are greatly acknowledged for their fruitful contributions. We also thank CNRS, University Paul Sabatier at Toulouse University, Institut des Sciences Appliquées at Toulouse (INSA), the Midi-Pyrénées region (including CTP program), ANR (SIDERUS-ANR-08-BLAN-0010-03; SUPRANANO-ANR-09-BLAN-0194), ANR-DFG (MOCA-NANO-ANR-11-INTB-1011 and DFG-911/19-1), INTERREG SUDOE (TRAIN 2 project), EU (ARTIZYMES STREP-FP6-2003-NEST-B3-0151471; SYNFLOW FP7-NMP2-Large program 2010-246461; NANOSONWINGS ERC Advanced Grant-2009-246763), CAPES-COFECUB, CONACyT, ANRT and Sasol for financial supports.

References

1. Schmid G (ed) (1994) Clusters and colloids. From theory to applications. Wiley, Weinheim
2. Schmid G (ed) (2004) Nanoparticles. From theory to application. Wiley, Weinheim
3. Zhou B, Han S, Raja R, Somorjai G (eds) (2003) Nanotechnology in catalysis. Kluwer Academic/Plenum Publisher, New York
4. Ulrich H, Uzi L (eds) (2007) Nanocatalysis. Series Nanoscience and Technology. Springer Berlin and Heidelberg
5. Roucoux A, Philippot K (2007) In: de Vries JG, Elsevier CJ (eds) Handbook of homogeneous hydrogenations, vol 9. Wiley, Weinheim, pp 217–255
6. Astruc D (ed) (2008) Nanoparticles and catalysis. Wiley-Interscience, New York
7. Somorjai GA, Frei H, Park JY (2009) *J Am Chem Soc* 131:16589–16605
8. Somorjai GA, Aliaga C (2010) *Langmuir* 26:16190–16203
9. Somorjai GA, Park JY (2009) *Surf Sci* 603:1293–1300
10. Somorjai GA, Li Y (2010) *Top Catal* 53:311–325
11. Zhang Y, Grass ME, Kuhn JN, Tao F, Habas SE, Huang W, Yang P, Somorjai GA (2008) *J Am Chem Soc* 130:5868–5869
12. Cushing BL, Koleschnichenko VL, O'Connor CJ (2004) *Chem Rev* 104:3893–3946
13. Tao AR, Habas S, Yang P (2008) *Small* 4:310–325
14. Pradhan SM, Pal T (2010) *J Colloid Interface Sci* 341(2):333
15. Mourdikoudis S, Liz-Marzán LM (2013) *Chem Mater* 25:1465
16. Guyonnet Bilé E, Cortelazzo-Polisini E, Denicourt-Nowicki A, Sassine R, Launay F, Roucoux A (2012) *ChemSusChem* 5:91
17. Grubbs RB (2007) *Polym Rev* 47(2):2015
18. Yan N, Zhang J, Yuan Y, Chen G-T, Dyson PJ, Li Z, Kou Y (2010) *Chem Commun* 46:1631
19. Myers VS, Weir MG, Carino EV, Yancey DF, Pande S, Crooks RM (2011) *Chem Sci* 2:1632
20. Astruc D (2003) *CR Chimie* 6:709
21. Astruc D, Diallo AK, Ornelas C (2013) In: Serp P, Philippot K (eds) Nanomaterials and catalysis. Wiley, Weinheim, Chap 3, p 101
22. Dupont J, Scholten JD (2010) *Chem Soc Rev* 39:1780
23. Scholten JD, Prechtl MG, Dupont J (2012) Handbook of green chemistry, vol 8. Wiley, Weinheim, p 1
24. Nag A, Kovalenko MV, Lee J-S, Liu W, Spokoyny B, Talapin DV (2011) *J Am Chem Soc* 133:10612–10620
25. Philippot K, Chaudret B (2003) *CR Chim* 6:1019–1034
26. Baumer M, Libuda J, Neyman KM, Rosch N, Rupprechterz G, Freund H-J (2007) *Phys Chem Chem Phys* 9:3541–3558
27. Corma A, García H (2008) *Chem Soc Rev* 37:2096–2126

28. Risse T, Shaikhutdinov S, Nilius N, Sterrer M, Freund H-J (2008) *Acc Chem Res* 41:949–956
29. Freund H-J (2010) *Chem Eur J* 16:9384–9397
30. Nilius N, Risse T, Schauermaann S, Shaikhutdinov S, Sterrer M, Freund H-J (2011) *Top Catal* 54:4–12
31. Primo A, Corma A, García H (2011) *Phys Chem Chem Phys* 13:886–910
32. Serna P, Boronat M, Corma A (2011) *Top Catal* 54:439–446
33. Boronat M, Corma A (2011) *J Catal* 284:138–147
34. López C, Corma A (2012) *ChemCatChem* 4:751–752
35. Chaudret B, Commenges G, Poilblanc R (1982) *J Chem Soc Chem Commun* 1388–1390
36. Cormary B, Dumestre F, Liakakos N, Soulantica K, Chaudret B (2013) *Dalton Trans* 42:12546–12553
37. Amiens C, Chaudret B, Ciuculescu-Pradines D, Collière V, Fajerweg K, Fau P, Kahn M, Maisonnat A, Soulantica K, Philippot K (2013) *New J Chem* 37:3374–3401
38. Gregson D, Howard JAK, Murray M, Spencer JL (1981) *J Chem Soc Chem Commun* 716
39. Frost PW, Howard JAK, Spencer JL, Turner DG (1981) *J Chem Soc Chem Commun* 1104
40. Chaudret B, Cole-Hamilton DJ, Wilkinson G (1978) *J Chem Soc Dalton Trans* 1739
41. Philippot K, Chaudret B (2003) *C R Acad Sci* 6:1019
42. Vranka RG, Dahl LF, Chini P, Chatt J (1969) *J Am Chem Soc* 91:1574–1576
43. Fumagalli A, Martinengo S, Chini P, Albinati A, Bruckner S, Heaton BT (1978) *J Chem Soc Chem Comm* 195–196
44. Washecheck DM, Wucherer EJ, Dahl Lawrence F, Ceriotti A, Longoni G, Manassero Mario M, Sansoni M, Chini P (1979) *J Am Chem Soc* 101:6110–6112
45. Scott SL, Susannah, Basset JM (1994) *J Mol Catal* 86:5–22
46. Schmid G, Boese R, Pfeil R, Bandermann F, Meyer S, Calis GHM, van der Velden JWA (1981) *Chem Ber* 114:3634
47. Wallenberg LR, Bovin JO, Schmid G (1985) *Surf Sci* 156:256–264
48. Van Staveren MPJ, Brom HB, De Jongh LJ, Schmid G (1986) *Solid State Comm* 60:319–322
49. Benfield RE, Creighton JA, Eadon DG, Schmid G (1989) *Zeitschrift fuer Physik D Atoms Mol Clusters* 12:533–536
50. Schmid G (1990) *Inorg Synth* 7:214–218
51. Bradley JS, Hill EH, Leonowicz ME, Wirzke H (1987) *J Mol Catal* 41:59–74
52. Philippot K, Chaudret B (2007) *Comprehensive organometallic chemistry III*. In: Crabtree RH, Mingos MP (Eds-in-Chief) Volume 12 – Applications III: functional materials, environmental and biological applications, Dermot O’Hare (Volume Ed.), Chapter 12–03, Elsevier, Oxford, pp 71–99
53. Mehdaoui B, Carrey J, Stadler M, Cornejo A, Nayral C, Delpech F, Chaudret B, Respaud M (2012) *App Phys Lett* 100:052403/1
54. Barriere C, Piettre K, Latour V, Margeat O, Turrin C-O, Chaudret B, Fau P (2012) *J Mater Chem* 22:2279
55. Meffre A, Lachaize S, Gatel C, Respaud M, Chaudret B (2011) *J Mater Chem* 21:13464
56. Dumestre F, Chaudret B, Amiens C, Fromen M-C, Casanove M-J, Renaud P, Zurcher P (2002) *Angew Chem Int Ed* 41(22):4286
57. Wetz F, Soulantica K, Respaud M, Falqui A, Chaudret B (2007) *Mater Sci Eng C* 27:1162
58. Schmid G (2010) In: In: Schmid G (ed) *Nanoparticles from theory to applications*. Second completely revised and updated edition. Wiley, Weinheim, p 217
59. Bradley JS, Millar JM, Hill EW, Behal S, Chaudret B, Duteil A (1991) *Faraday Discuss* 92:255–268
60. Duteil A, Quéau R, Chaudret B, Mazel R, Roucau C, Bradley JS (1993) *Chem Mater* 5:341–347
61. Pan C, Pelzer K, Philippot K, Chaudret B, Dassenoy F, Lecante P, Casanove M-J (2001) *J Am Chem Soc* 123:7584–7593
62. Novio F, Philippot K, Chaudret B (2010) *Catal Lett* 140:1–7

63. Pieters G, Taglang C, Bonnefille E, Gutmann T, Puente C, Berthet J-C, Dugave C, Chaudret B, Rousseau B (2014) *Angew Chem Int Ed* 53:230–234
64. Vidoni O, Philippot K, Amiens C, Chaudret B, Balmes O, Malm J-O, Bovin J-O, Senocq F, Casanove M-J (1999) *Angew Chem Int Ed* 38:3736–3738
65. Pelzer K, Vidoni O, Philippot K, Chaudret B, Collière V (2003) *Adv Funct Mater* 13:118–126
66. Pelzer K, Philippot K, Chaudret B (2003) *Z Phys Chem* 217:1–9
67. Lara P, Philippot K, Chaudret B (2013) *ChemCatChem* 5:28–45
68. Sun S, Fullerton EE, Weller D, Murray CB (2001) *IEEE Trans Magn* 37:1239–1243
69. Metin O, Mazumder V, Ozkar S, Sun S (2010) *J Am Chem Soc* 132:1468–1469
70. Liu Y, Wang C, Wei Y, Zhu L, Li D, Jiang JS, Markovic NM, Stamenkovic VR, Sun S (2011) *Nano Lett* 11:1614–1617
71. Watt J, Yu C, Chang SLY, Cheong S, Tilley RD (2013) *J Am Chem Soc* 135:606–609
72. Lignier P, Bellabarba R, Tooze RP, Su Z, Landon P, Ménard H, Zhou W (2012) *Cryst Growth Des* 12:939–942
73. Ramirez E, Jansat S, Philippot K, Lecante P, Gomez M, Masdeu-Bulto AM, Chaudret B (2004) *J Organomet Chem* 689:4601–4610
74. García-Antón J, Axet MR, Jansat S, Philippot K, Chaudret B, Pery T, Buntkowsky G, Limbach HH (2008) *Angew Chem Int Ed* 47:2074–2078
75. Novio F, Monahan D, Coppel Y, Antorrena G, Lecante P, Philippot K, Chaudret B (2014) *Chem Eur J* 20:1287–1297
76. Favier I, Massou S, Teuma E, Philippot K, Chaudret B, Gomez M (2008) *Chem Commun* 3296–3298
77. Jansat S, Gomez M, Philippot K, Muller G, Guiu E, Claver C, Castillon S, Chaudret B (2004) *J Am Chem Soc* 126:1592–1593
78. Favier I, Gomez M, Muller G, Axet MR, Castillon S, Claver C, Jansat S, Chaudret B, Philippot K (2007) *Adv Synth Catal* 349:2459–2469
79. Weitz DA, Huang JS, Lin MY, Sung J (1985) *Phys Rev Lett* 54:1416
80. Favier I, Lavedan P, Massou S, Teuma E, Philippot K, Chaudret B, Gómez M (2013) *Top Catal* 56:1253–1261
81. Vignolle J, Tilley TD (2009) *Chem Commun* 7230–7232
82. Lara P, Rivada-Whealaghan O, Conejero S, Poteau R, Philippot K, Chaudret B (2011) *Angew Chem Int Ed* 50:12080–12084
83. Gonzalez-Galvez D, Lara P, Rivada-Whealaghan O, Conejero S, Chaudret B, Philippot K, van Leeuwen PWNM (2013) *Catal Sci Technol* 3:99–105
84. Wang D, Li Y (2011) *Adv Mater* 23:1044
85. Zeng H, Sun S (2008) *Adv Funct Mater* 18:391
86. Jun Y-W, Choi J-S, Cheon J (2007) *Chem Commun* 12:1203
87. Cozzoli PD, Pellegrino T, Manna L (2006) *Chem Soc Rev* 35:1195
88. Bradley JS, Hill EW, Chaudret B, Duteil A (1995) *Langmuir* 11:693
89. Pan C, Dassenoy F, Casanove M-J, Philippot K, Amiens C, Lecante P, Mosset A, Chaudret B (1999) *J Phys Chem B* 103:10098
90. Dassenoy F, Casanove M-J, Lecante P, Pan C, Philippot K, Amiens C, Chaudret B (2001) *Phys Rev B* 63:235407
91. Lara P, Casanove M-J, Lecante P, Fazzini P-F, Philippot K, Chaudret B (2012) *J Mater Chem* 22:3578
92. Lara P, Ayvali T, Casanove M-J, Lecante P, Fazzini P-F, Philippot K, Chaudret B (2013) *Dalton Trans* 42:372
93. Kelsen V, Meffre A, Fazzini P-F, Lecante P, Chaudret B (2014) *ChemCatChem*. doi:10.1002/cctc.201300907
94. Bonnefille E, Novio F, Gutmann T, Poteau R, Lecante P, Jumas J-C, Philippot K, Chaudret B (2014) *Nanoscale*. doi:10.1039/C4NR00791C
95. Baddeley CJ, Jones TE, Trant AG, Wilson K (2011) *Top Catal* 54:1348–1356

96. Jansat S, Picurelli D, Pelzer L, Philippot K, Gomez M, Muller G, Lecante P, Chaudret B (2006) *New J Chem* 30:115–122
97. Gual A, Axet MR, Philippot K, Chaudret B, Denicourt-Nowicki A, Roucoux A, Castellón S, Claver C (2008) *Chem Commun* 2759–2761
98. Gonzalez-Galvez D, Nolis P, Philippot K, Chaudret B, van Leeuwen PWNM (2012) *ACS Catal* 2:317–321
99. Ackermann L (2006) *Synthesis* 1557–1571
100. Ackermann L, Born R, Spatz JH, Althammer A, Gschrei CJ (2006) *Pure Appl Chem* 78:209–214
101. Wolpers A, Ackermann L, Vana P (2010) *Macromol Chem Phys* 212:259–265
102. Raffter E, Gutmann T, Löw F, Buntkowsky G, Philippot K, Chaudret B, van Leeuwen PWNM (2013) *Catal Sci Technol* 3:595–599
103. Stephens FH, Pons V, Baker RT (2007) *Dalton Trans* 25:2613–2626
104. Zahmakiran M, Philippot K, Özkar S, Chaudret B (2012) *Dalton Trans* 41:590–598
105. Zahmakiran M, Tristany M, Philippot K, Fajerweg K, Özkar S, Chaudret B (2010) *Chem Commun* 46:2938–29540
106. Debouttière PJ, Martinez V, Philippot K, Chaudret B (2009) *Dalton Trans* 10172–10174
107. Debouttière PJ, Coppel Y, Denicourt-Nowicki A, Roucoux A, Chaudret B, Philippot K (2012) *Eur J Inorg Chem* 1229–1236
108. Gutmann T, Bonnefille E, Breitzke H, Debouttière P-J, Philippot K, Poteau R, Buntkowsky G, Chaudret B (2013) *PCCP* 15:17383–17394
109. Guerrero M, Roucoux A, Denicourt-Nowicki A, Bricout H, Monflier E, Collière V, Fajerweg K, Philippot K (2012) *Catal Today* 183:34–41
110. Guerrero M, Coppel Y, Chau NTT, Roucoux A, Denicourt-Nowicki A, Monflier E, Bricout H, Lecante P, Philippot K (2013) *ChemCatChem* 12:3802–3811
111. Yan N, Xiao C, Kou Y (2010) *Coord Chem Rev* 254:1179–1218
112. Hallett JP, Welton T (2011) *Chem Rev* 111:3508–3576
113. Pârvulescu VI, Hardacre C (2007) *Chem Rev* 107:2615–2665
114. Pádua AAH, Costa Gomes MC, Canongia Lopes JNA (2007) *Acc Chem Res* 40:1087–1096
115. Pensado AS, Pádua AAH (2011) *Angew Chem Int Ed* 50:8683–8687
116. Prechtl MHG, Scariot M, Scholten JD, Machado G, Teixeira SR, Dupont J (2008) *Inorg Chem* 47:8995–9001
117. Prechtl MHG, Scholten JD, Dupont J (2009) *J Mol Chem* 313:74–78
118. Scholten JD, Leal BC, Dupont J (2012) *ACS Catal* 2:184–200
119. Raluy E, Favier I, Lopez-Vinasco AM, Pradel C, Martin E, Madec D, Teuma E, Gomez M (2011) *Phys Chem Chem Phys* 13:13579–13584
120. Rodriguez-Perez L, Pradel C, Serp P, Gomez M, Teuma E (2011) *ChemCatChem* 3:749–754
121. Gutel T, Garcia-Anton J, Pelzer K, Philippot K, Santini CC, Chauvin Y, Chaudret B, Basset JM (2007) *J Mater Chem* 17:3290–3292
122. Gutel T, Santini CC, Philippot K, Padua A, Pelzer K, Chaudret B, Chauvin Y, Basset J-M (2009) *J Mat Chem* 19:3624–3631
123. Campbell PS, Santini CC, Bouchu D, Fenet B, Philippot K, Chaudret B, Padua AAH, Chauvin Y (2010) *Phys Chem Chem Phys* 12:4217–4223
124. Salas G, Santini CC, Philippot K, Colliere V, Chaudret B, Fenet B, Fazzini PF (2011) *Dalton Trans* 40:4660–4668
125. Salas G, Podgorsek A, Campbell PS, Santini CC, Padua AAH, Gomes MFC, Philippot K, Chaudret B, Turmine M (2011) *Phys Chem Chem Phys* 13:13527–13536
126. Salas G, Campbell PS, Santini CC, Philippot K, Costa Gomes MF, Padua AAH (2012) *Dalton Trans* 41:13919–13926
127. Bond GC, Louis C, Thompson DT (2006) *Catalysis by gold*. Imperial College Press, London
128. Pelzer K, Philippot K, Chaudret B, Meyer-Zaika W, Schmid GZ (2003) *Anorg Allg Chem* 629:1217–1222

129. Kormann H-P, Schmid G, Pelzer K, Philippot K, Chaudret B (2004) *Z Anorg Allg Chem* 630:1913–1918
130. Jansat S, Pelzer K, García-Antón J, Raucoules R, Philippot K, Maisonnat A, Chaudret B, Guari Y, Medhi A, Reyé C, Corriu RJP (2007) *Adv Funct Mater* 17:3339–3347
131. Matsura V, Guari Y, Reyé C, Corriu RJP, Tristany M, Jansat S, Philippot K, Maisonnat A, Chaudret B (2009) *Adv Funct Mater* 19:3781–3787
132. Tristany M, Philippot K, Guari Y, Collière V, Lecante P, Chaudret B (2010) *J Mater Chem* 20:9523–9530
133. Castillejos E, Debouttière P-J, Roiban L, Solhy A, Martinez V, Kihn Y, Ersen O, Philippot K, Chaudret B, Serp P (2009) *Angew Chem Int Ed* 48:2529–2533
134. García-Suárez EJ, Tristany M, García AB, Collière V, Philippot K (2012) *Micropor Mesopor Mater* 153:155–162

Visible-Light-Induced Redox Reactions by Ruthenium Photoredox Catalyst

Takashi Koike and Munetaka Akita

Abstract Photoredox catalysis by well-known ruthenium(II) polypyridine complexes is a versatile tool for redox reactions in synthetic organic chemistry, because they can effectively catalyze single-electron-transfer (SET) processes by irradiation with visible light. These favorable properties of the catalysts provide a new strategy for efficient and selective radical reactions. Salts of tris(2,2'-bipyridine)ruthenium (II), $[\text{Ru}(\text{bpy})_3]^{2+}$, were first reported in 1936. Since then, a number of works related to artificial photosynthesis and photofunctional materials have been reported, but only limited efforts had been devoted to synthetic organic chemistry. Remarkably, since 2008, this photocatalytic system has gained importance in redox reactions. In this chapter, we will present a concise review of seminal works on ruthenium photoredox catalysis around 2008, which will be followed by our recent research topics on trifluoromethylation of alkenes by photoredox catalysis.

Keywords Electron transfer · Photoredox catalysis · Radical reaction · Redox economy · Trifluoromethylation

Contents

1	Introduction	372
2	Photo- and Electro-Chemistry of $[\text{Ru}(\text{bpy})_3]^{2+}$	372
3	A “Renaissance” in Photoredox Catalysis	374
4	Trifluoromethylation of Alkenes by Photoredox Catalysis	381
4.1	A New Strategy for Generation of the Trifluoromethyl Radical Through SET Photoredox Processes	381

4.2 Oxy- and Amino-Trifluoromethylation of Alkenes with Electrophilic CF ₃ Reagents	382
4.3 Trifluoromethylation of Vinylborates by Photoredox Catalysis	387
5 Conclusions and Outlook	389
References	390

1 Introduction

Radical chemistry is the source of various technologies [1]. In particular, many radical reactions utilized in the field of synthetic organic chemistry have been recognized as useful and practical methodologies. Outstanding breakthroughs in radical reactions have arisen from developments of new systems for generating radical species. In general, the smooth generation of a radical is triggered by application of a simple stimulus, such as heat, light, or redox. Conventional systems, however, are often associated with disadvantages, such as the need to use toxic or explosive reagents (e.g., tin reagents and peroxides), the need for high-energy UV light, the formation of considerable amounts of wastes derived from oxidants or reductants, or the need for special equipment for photochemical or electrochemical processes. In modern synthetic organic chemistry, protocols need to be easy and safe to use, and efficient and selective outcomes should be provided.

The use of visible light as the stimulus is fascinating because visible light, which is the main component of sunlight (Fig. 1), is freely available on the earth. In addition, photoinduced electron transfer (PET) is one of the useful strategies for producing radicals; especially, visible-light-induced electron transfer has become a strong synthetic tool. Recently, well-investigated ruthenium polypyridine complexes (e.g., [Ru(bpy)₃]²⁺ (bpy: 2,2'-bipyridine)) have been paid attention from the viewpoint of photocatalysts, which can readily catalyze single-electron transfer (SET) processes under visible light irradiation. In this chapter, we will describe recent developments of radical reactions through photoredox processes of the ruthenium polypyridine complexes.

2 Photo- and Electro-Chemistry of [Ru(bpy)₃]²⁺

In this section, we will refer to photo- and electro-chemical properties of the most thoroughly investigated [Ru(bpy)₃]²⁺ photoredox catalyst [2, 3]. Firstly, its absorption maximum (around 450 nm) is in the visible-light region (Fig. 1), indicating that it can be easily excited by visible light. Secondly, the lifetime of the luminescent triplet excited state (τ = approximated 1 μ s), *[Ru(bpy)₃]²⁺, resulting from photochemical electron transfer from the $d\pi$ orbital of the ruthenium center to the π^* orbital of the 2,2'-bipyridine ligand, i.e., MLCT (metal-to-ligand charge-transfer transition), is sufficiently long enough for chemical transformations to proceed.

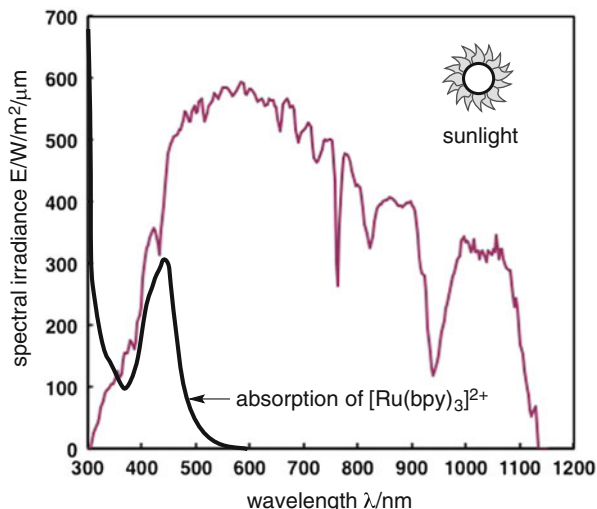
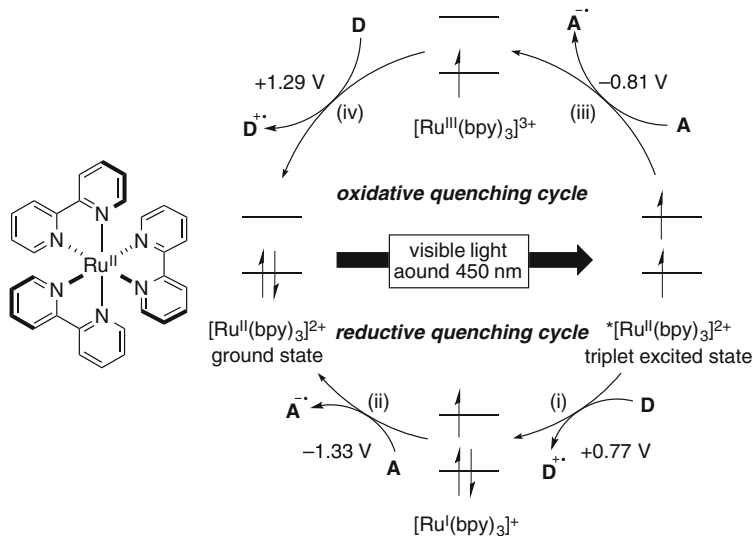


Fig. 1 The direct normal spectral irradiance on February 21, 2012, at Suzukakedai Campus of Tokyo Institute of Technology and UV-vis spectrum of $[\text{Ru}(\text{bpy})_3]^{2+}$



Scheme 1 Photoredox cycle of $[\text{Ru}(\text{bpy})_3]^{2+}$

Thirdly, the triplet excited state, $*[\text{Ru}(\text{II})(\text{bpy})_3]^{2+}$, undergoes single-electron-transfer (SET) to/from organic molecules, i.e., this triplet state can serve as either a 1e-oxidant or a 1e-reductant before returning to the initial ground state $[\text{Ru}(\text{II})(\text{bpy})_3]^{2+}$ (Scheme 1).

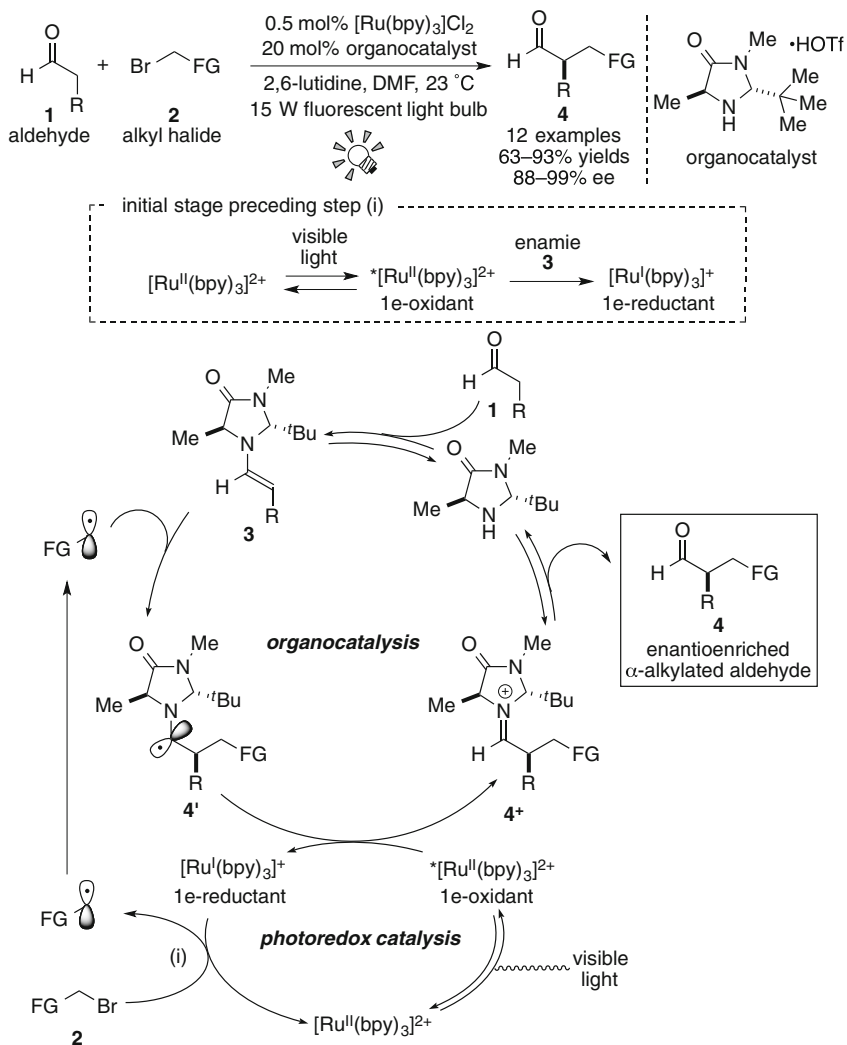
Therefore, photoredox processes catalyzed by this complex should be useful and powerful tools for redox reactions of organic compounds. The cycle consisting of a sequence of (i) electron transfer from an electron donor **D** to $^*[\text{Ru}(\text{II})(\text{bpy})_3]^{2+}$ associated with formation of reduced $[\text{Ru}(\text{I})(\text{bpy})_3]^+$ and (ii) reduction of an electron acceptor **A** associated with regeneration of the ground state of the catalyst is called *reductive quenching cycle*. On the other hand, the cycle consisting of a sequence of (iii) electron transfer from $^*[\text{Ru}(\text{II})(\text{bpy})_3]^{2+}$ to an electron acceptor **A** associated with formation of high-oxidation-state $[\text{Ru}(\text{III})(\text{bpy})_3]^{3+}$ and (iv) oxidation of an electron donor **D** associated with regeneration of the ground state of the catalyst is called *oxidative quenching cycle*. Both these cycles produce D^+ and A^- radicals in a single reactor through SET processes to make, overall, the transformation redox neutral. The terms *reductive* and *oxidative* are confusing and require explanation. *Reductive* refers to reduction of the photoexcited species, whereas the external electron donor **D** is oxidized in the same process. *Oxidative* means oxidation of the photoexcited species concomitant with reduction of external electron acceptor **A**.

Redox potential of each catalytic species is one of the most important factors to design visible-light-induced photoredox reactions. As shown in Scheme 1, the highly reduced species, $[\text{Ru}(\text{I})(\text{bpy})_3]^+$, generated upon reductive quenching serves as a 1e-reductant (-1.33 V vs. SCE = Standard Calomel Electrode, in MeCN) stronger than the photoexcited species itself (-0.81 V vs. SCE in MeCN). On the other hand, oxidative quenching cycle produces the Ru(III) species, $[\text{Ru}(\text{III})(\text{bpy})_3]^{3+}$, which turns out to be a stronger 1e-oxidant. In the field of photoredox chemistry using $[\text{Ru}(\text{bpy})_3]^{2+}$, it is well known that the combined use of sacrificial donors (e.g., triethylamine) and acceptors (e.g., methyl viologen: *N,N'*-dimethyl-4,4'-bipyridinium) efficiently leads to redox reactions mediated by $[\text{Ru}(\text{I})(\text{bpy})_3]^+$ and $[\text{Ru}(\text{III})(\text{bpy})_3]^{3+}$, respectively. But it should be noted that a *stoichiometric* amount of *sacrificial* reagent is used for the catalytic reactions by $[\text{Ru}(\text{bpy})_3]^{2+}$ and, as a result, a *stoichiometric amount of waste* is formed as a by-product. From the viewpoint of green chemistry, this type of catalytic reaction is obviously *less green*.

The redox potentials of the catalytic species can be modified by ligands and changing central metal. In particular, relevant cyclometalated Ir catalysts such as *fac*-Ir(ppy)₃ (ppy: 2-phenylpyridine) have been often used as alternative photoredox catalysts.

3 A “Renaissance” in Photoredox Catalysis

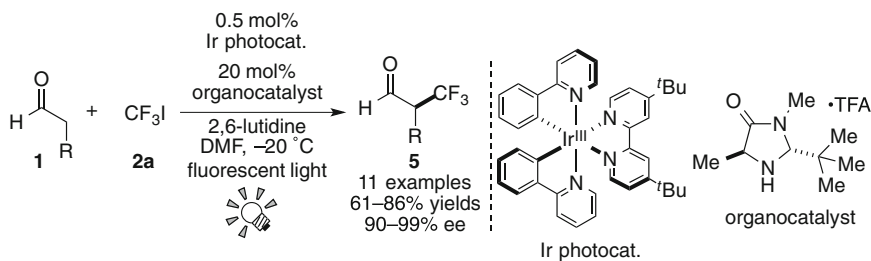
Before 2008, a limited number of works about photoredox catalysis by $[\text{Ru}(\text{bpy})_3]^{2+}$ had been reported in the field of synthetic organic chemistry [4–17]. After publication of the undermentioned seminal works during 2008–2010, however, a great number of reports on redox reactions by photoredox catalysis have appeared [18–29]. In this section, we will concisely review redox reactions by photoredox catalysts around 2008.



Scheme 2 Merger of catalysis for asymmetric α -alkylation of aldehydes

Nicewicz and MacMillan reported an elusive asymmetric intermolecular α -alkylation of aldehydes by elegantly merging Ru photoredox catalysis with chiral amine organocatalysis [30]. The reaction mechanism proposed for the synergistic catalysis is illustrated in Scheme 2.

At the initial stage, the Ru catalyst, $[\text{Ru}(\text{II})(\text{bpy})_3]^{2+}$, is excited by irradiation with a 15 W fluorescent light bulb to form the excited species, $*[\text{Ru}(\text{II})(\text{bpy})_3]^{2+}$, which is reduced by enamine **3** derived from the reaction of the secondary chiral amine catalyst with aldehydes **1** [31, 32]. The resulting strong reductant, $[\text{Ru}(\text{I})(\text{bpy})_3]^+$, undergoes SET to alkyl halide **2**, leading to formation of alkyl radical and



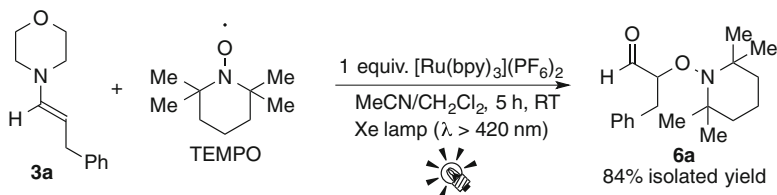
Scheme 3 Synthesis of α -trifluoromethylaldehydes by photoredox catalysis

regeneration of the ground state, $[\text{Ru}(\text{II})(\text{bpy})_3]^{2+}$. The alkyl radical reacts with the preformed enamine **3** to give the C–C coupled radical intermediate **4'**. The 1e-oxidation of the radical intermediate **4'** by the photoactivated Ru catalyst proceeds in the mainstream to afford the iminium intermediate **4⁺** and the Ru reductant, which follows abovementioned SET event for generation of alkyl radical. Subsequent hydrolysis produces α -alkylated aldehyde **4** as the product together with the organocatalyst.

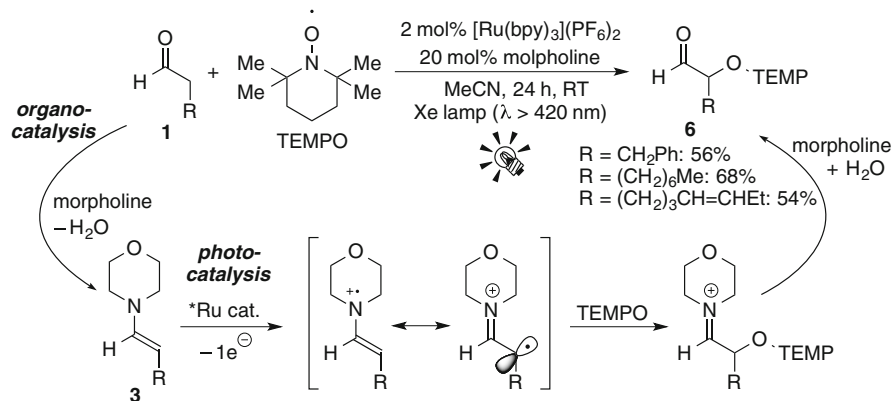
The mechanism proposed by them is based on the reaction of a SOMOphilic enamine **3** with an electron-deficient radical, which is the converse mechanism to their previously reported SOMO activation studies [33]. It is noteworthy that the present catalytic system can allow us an easy access to various optically active α -alkylated aldehydes **4** in high yields with excellent enantioselectivity.

Furthermore, the group of MacMillan extended the present photocatalytic protocol to the trifluoromethylation using CF_3I (**2a**) as a CF_3 source and a strongly reducing Ir photocatalyst, leading to the synthesis of valuable enantioenriched α -trifluoromethylated aldehydes **5** (Scheme 3) [34]. In this reaction, the Ru catalyst, $[\text{Ru}(\text{bpy})_3]^{2+}$, also afforded the product but in a lower yield.

Almost at the same time, our group was working on development of photocatalytic reactions using enamine as a substrate because we envisaged that enamine, a tertiary amine derivative which can work as a sacrificial reagent (*vide supra*), can also be oxidized by the triplet excited state, $*[\text{Ru}(\text{bpy})_3]^{2+}$, to generate a cationic amine radical (SOMO activation) [35, 36]. As we expected, the ruthenium photocatalyst effected stoichiometric oxidative coupling of 4-[(1*E*)-3-phenylprop-1-en-1-yl]morpholine (**3a**) with (2,2,6,6-tetramethylpiperidin-1-yl)oxyl (TEMPO) at room temperature under visible-light irradiation (an Xe lamp with a cutoff filter; $\lambda > 420\text{ nm}$) to give the α -oxyaminated aldehyde **6a** in a 84% isolated yield after hydrolysis (Scheme 4). Moreover, this system was extended to a photocatalytic system. Catalytic amounts of $[\text{Ru}(\text{bpy})_3](\text{PF}_6)_2$ (2 mol%) and morpholine (20 mol%) effected direct α -oxyamination of aldehydes **1**. A plausible reaction mechanism, involving a cooperative catalytic cycle consisting of photocatalysis and organocatalysis, is shown in Scheme 5. Morpholine first reacts with aldehydes **1** to give enamine **3**, which then undergoes 1e-oxidation by the photoactivated $*[\text{Ru}(\text{bpy})_3]^{2+}$. Final radical coupling of the cationic radical intermediates with TEMPO, followed by hydrolysis, gives the product **6** and morpholine.

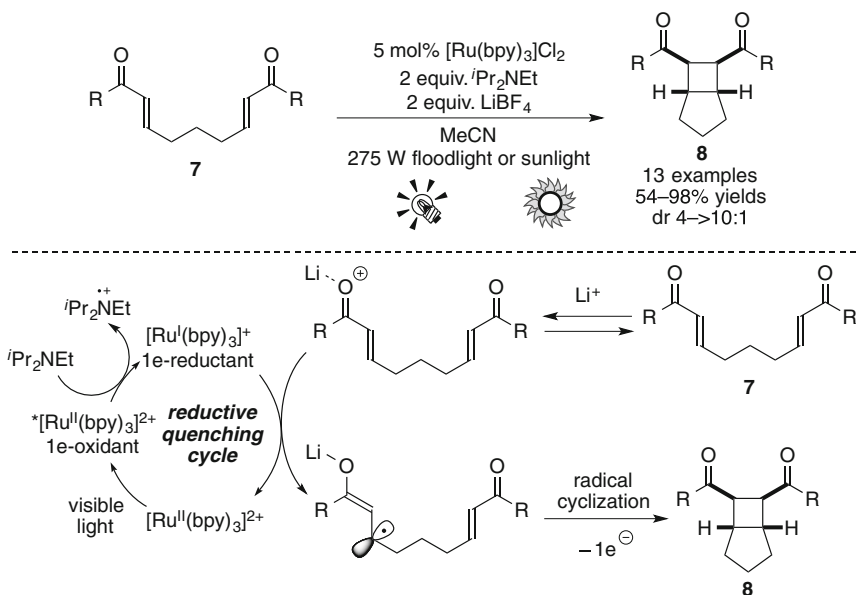


Scheme 4 Oxyamination of enamine by photoredox catalysis



Scheme 5 Merger of photo- and organo-catalysis for α -oxyamination of aldehydes

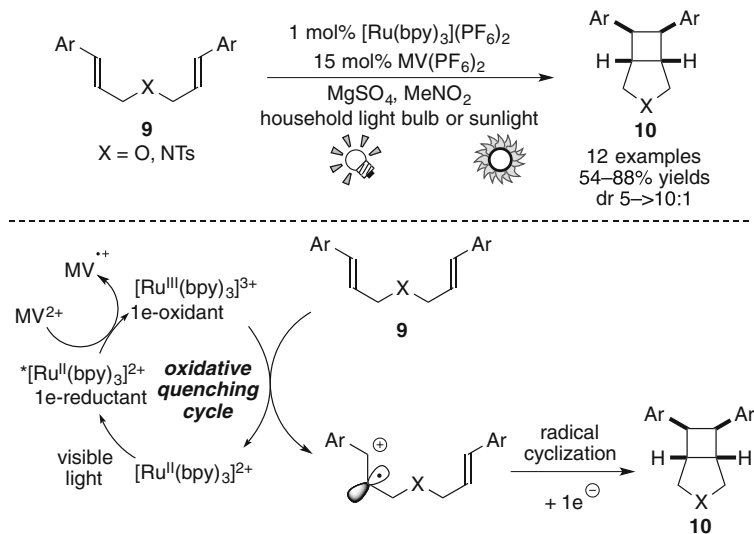
On the same date when the abovementioned MacMillan's work was published in *Science*, another work on photoredox catalysis by the group of Yoon appeared. They reported [2+2] cycloaddition of bis(enone) **7** in the presence of the Ru catalyst under visible light irradiation (a 275 W floodlight) (Scheme 6) [37]. In this reaction, addition of an electron donor, $^i\text{Pr}_2\text{NEt}$, and a Lewis acid, LiBF_4 , is essential to produce a strong reductant, $[\text{Ru}(\text{I})(\text{bpy})_3]^+$, from the photoactivated species, $^*[\text{Ru}(\text{II})(\text{bpy})_3]^{2+}$, and lower the LUMO level of **7**, respectively. In addition, sunlight induced a gram-scale reaction, leading to the product **8** with less efficiency but with the same diastereoselectivity, compared to the reaction with a 275 W floodlight. Analogous [2+2] cyclizations by high-energy UV photolysis [38, 39] and electrochemical methods [40] were reported, but these reaction systems usually require special reactors. In contrast, the present photocatalytic protocol allows us to conduct the reaction by the use of usual glassware and easily available visible light. Furthermore, the group of Yoon extended the present reaction to crossed intermolecular [2+2] cycloaddition of enones [41] and intramolecular [3+2] cycloaddition of aryl cyclopropyl ketones [42]. The latter reaction is induced by the action of photocatalyst, $[\text{Ru}(\text{bpy})_3]^{2+}$, and Lewis acid, $\text{La}(\text{OTf})_3$. Their report described that choice of Lewis acids is critical for the SET event from $[\text{Ru}(\text{I})(\text{bpy})_3]^+$ to carbonyl groups.



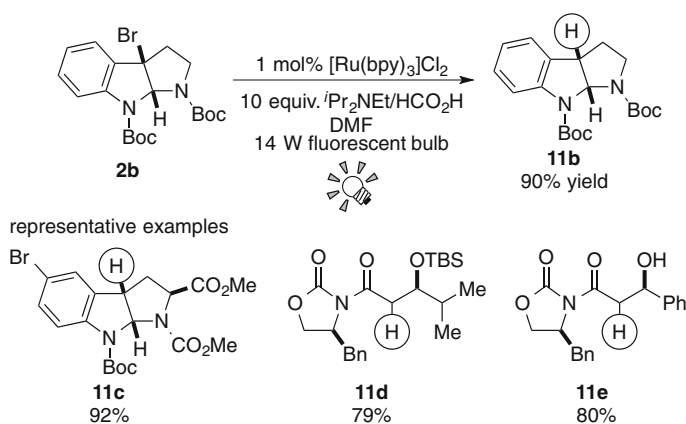
Scheme 6 [2+2] Enone cycloadditions through the reductive quenching cycle

After the development of cycloaddition for electron-deficient alkenes such as **7**, they designed complementary methods for electron-rich alkenes. The cycloaddition product **10** was obtained from the reaction of electron-rich bis(alkene) **9** through the oxidative quenching cycle in the presence of MV^{2+} (methyl viologen) as an electron acceptor (Scheme 7) [43]. More recently, it was reported that direct oxidation of styrenes by $[\text{Ru}(\text{bpm})_3](\text{BArF})_2$ (bpm: 2,2'-bipyrimidine, BArF: tetrakis[3,5-bis(trifluoromethyl)phenyl]borate), under visible light irradiation, which forms the oxidizing excited state (+1.20 V vs. SCE) stronger than $[\text{Ru}(\text{bpy})_3]^{2+}$ (+0.77 V vs. SCE), affected crossed intermolecular [2+2] cycloadditions of styrenes [44]. It is noteworthy that careful tuning of the redox properties of the Ru photocatalyst enables these [2+2] cycloadditions of both electron-rich and -deficient alkenes.

Another seminal work was reported by Stephenson and coworkers in 2009. They reported environmentally benign tin-free reductive dehalogenation of alkyl halides **2** in the presence of $[\text{Ru}(\text{bpy})_3]\text{Cl}_2$ and an amine as the hydrogen atom source under visible light irradiation (a 14 W fluorescent bulb) (Scheme 8) [45]. It is proposed that alkyl radicals are formed via 1e-reduction of alkyl halides **2** by the action of photocatalyst, leading to the product **11**. Furthermore, they extended their tin-free method for generation of organic radicals to radical C–C bond formation with alkenes [46, 47] and electron-rich heteroarenes [48]. After the reports by the group of Stephenson, Gagné et al. described intermolecular radical addition of glycosyl halide **2f** to electron-deficient alkenes **12** based on reductively induced generation of organic radicals from alkyl halides **2**, leading to C-glycosides **13** in good yields with high diastereoselectivity (Scheme 9) [49]. These reports show that



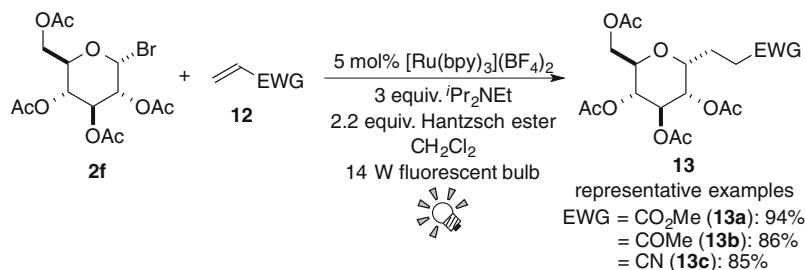
Scheme 7 Photooxidative [2+2] cycloadditions



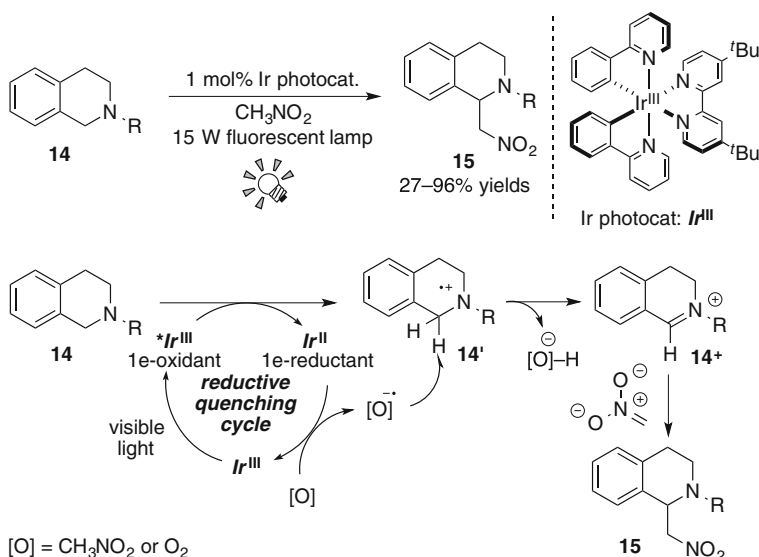
Scheme 8 Tin-free reductive dehalogenation using photoredox catalysis

visible-light-driven photoredox catalysis is a suitable alternative to the tin-mediated radical reaction system.

In 2010, Stephenson and coworkers developed aza-Henry reactions of tetrahydroisoquinolines **14** on the assumption that electron-rich tertiary alkylamines serve as electron donors to be converted into iminium ion through SET photoredox processes [50]. They showed that the Ir photocatalyst is more efficient than the Ru photocatalyst, $[\text{Ru}(\text{bpy})_3]\text{Cl}_2$. Proposed reaction mechanism based on the reductive quenching cycle is illustrated in Scheme 10. The photoexcited Ir species $^*\text{Ir}^{\text{III}}$ undergoes SET from tetrahydroisoquinoline **14** to give the



Scheme 9 Tin-free Giese reaction



Scheme 10 Photoredox-catalyzed aza-Henry reaction

radical cation **14'** and the powerful reducing agent Ir^{II} . Subsequent reduction of nitromethane and/or adventitious oxygen by Ir^{II} generates the corresponding radical anion and the ground state of the Ir catalyst Ir^{III} . The formed radical anion may abstract a hydrogen atom from **14'** to produce the iminium intermediate **14⁺**. Final nucleophilic attack of alkylnitrate to **14⁺** affords aza-Henry product **15**. After their report, a great number of related works on the photoredox reaction of tertiary amines have been reported [51–60]. Furthermore, these reports lead to photoredox aminoalkylation via oxidatively induced generation of α -aminoalkyl radical from electron-rich alkylamines [61–65].

These findings stimulated many researchers to join this field, leading to several recent breakthroughs [18–29]. Let us point out that some works still require

sacrificial electron donors/acceptors, but this photocatalytic system has potential to achieve a unique redox neutral process like the abovementioned work by the group of MacMillan. More recently, we found some redox neutral reactions by photoredox catalysis, which are the subjects of the next section. Trifluoromethylation of alkenes can be achieved by photoredox catalysis in the absence of *sacrificial* electron donors/acceptors.

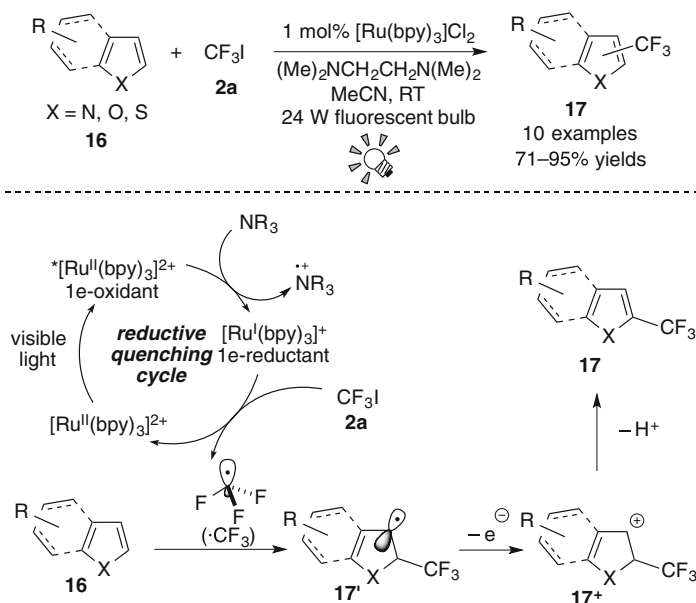
4 Trifluoromethylation of Alkenes by Photoredox Catalysis

4.1 A New Strategy for Generation of the Trifluoromethyl Radical Through SET Photoredox Processes

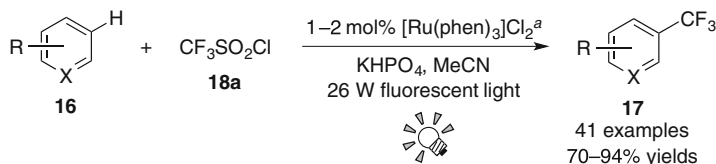
Organofluorine compounds are of vital importance, especially in the pharmaceutical and agrochemical fields, because fluorine atom can often enhance the effect of medicine in terms of chemical and metabolic stability, lipophilicity, and binding selectivity. In particular, the trifluoromethyl group (CF_3) is considered to be a useful structural motif in many bioactive molecules [66, 67]. Thus, the development of new methodologies for efficient and selective introduction of the CF_3 group into diverse skeletons has become an active and hot topic in synthetic chemistry [68–77]. Recently, photoredox-catalyzed radical trifluoromethylation has received great attention [78]. It has been proved that the trifluoromethyl radical ($\cdot\text{CF}_3$) can be readily generated by photoredox reactions of conventional CF_3 sources such as CF_3I (**2a**), $\text{CF}_3\text{SO}_2\text{Cl}$ (**18a**) and $\text{CF}_3\text{SO}_2\text{Na}$ [34, 79–85].

In 2009 and 2011, the groups of MacMillan and Stephenson independently suggested that, in the case of reductively induced generation of $\cdot\text{CF}_3$ from CF_3I (**2a**), more strongly reducing Ir photoredox catalysts such as *fac*-Ir(ppy)₃ derivatives are effective [34, 80]. On the other hand, Cho and coworkers showed that the Ru photocatalysts such as $[\text{Ru}(\text{bpy})_3]\text{Cl}_2$ and $[\text{Ru}(\text{phen})_3]\text{Cl}_2$ (phen: phenanthroline) can efficiently reduce CF_3I (**2a**) in the presence of electron-rich tertiary amines (a sacrificial reducing agent) to produce the CF_3 radical, leading to radical trifluoromethylation [83–85]. For example, they reported trifluoromethylation of electron-rich heteroarenes by photoredox catalysis (Scheme 11). The photoactivated Ru species undergoes SET from tertiary amine, TMEDA (*N,N,N',N'*-tetramethylethylenediamine), to give the strongly reducing Ru species, $[\text{Ru}(\text{I})(\text{bpy})_3]^+$. This Ru(I) species reduces CF_3I (**2a**) smoothly to produce $\cdot\text{CF}_3$. The addition of $\cdot\text{CF}_3$ to heteroarenes **16** provides valuable CF_3 -substituted heteroarenes **17**.

Just before Cho's report, Nagib and MacMillan reported a high-impact work on direct C–H trifluoromethylation of arenes by photoredox catalysis [79]. The use of $[\text{Ru}(\text{phen})_3]\text{Cl}_2$ as photocatalyst and $\text{CF}_3\text{SO}_2\text{Cl}$ (**18a**) as a CF_3 source enables the reaction with the broad scope with respect to the arenes, i.e., electron-rich/electron-deficient heteroarenes and unactivated arenes, in the absence of *sacrificial* electron



Scheme 11 Trifluoromethylation of electron-rich heteroarenes by photoredox catalysis



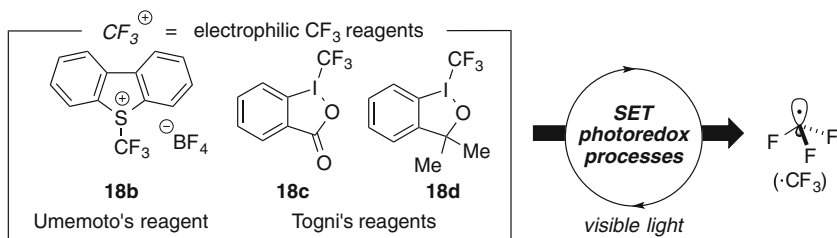
^aIr photocatalyst, Ir(Fppy)₃ (Fppy = 2-(2,4-difluorophenyl)pyridine) was also used.

Scheme 12 Direct C–H trifluoromethylation of arenes by photoredox catalysis

donor (Scheme 12). The detailed factors in the success still leave room for discussion, but these results imply that further exploration of photocatalysts and CF₃ precursors leads to new radical trifluoromethylation by photoredox catalysis.

4.2 Oxy- and Amino-Trifluoromethylation of Alkenes with Electrophilic CF₃ Reagents

During our exploration of new radical precursors [29], we envisaged facile generation of organic radicals through 1e-reduction of electrophilic *organic onium salts* by photoredox catalysis. Our attention was directed to *electrophilic trifluoromethylating reagents* (Scheme 13) such as 5-(trifluoromethyl)dibenzo[*b,d*]



Scheme 13 Generation of the CF_3 radical from electrophilic trifluoromethylating reagents through SET photoredox processes

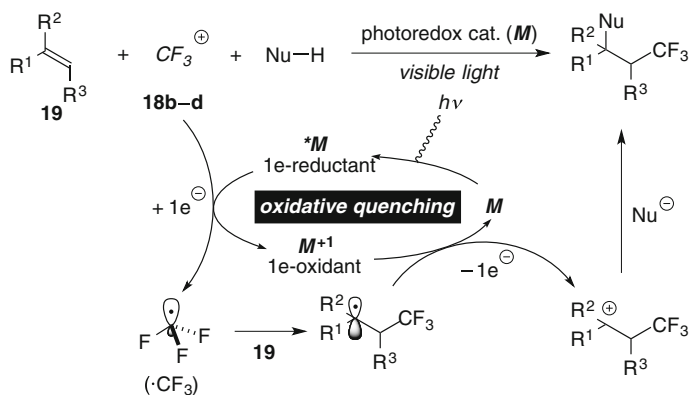
thiophenium tetrafluoroborate (**18b**; Umamoto's reagent) and Togni's reagents, 1-(trifluoromethyl)- $1\lambda^3$,2-benziodoxol-3(1*H*)-one (**18c**) and 3,3-dimethyl-1,3-dihydro- $1\lambda^3$,2-benziodoxole (**18d**) [86–88]. We expected that electrophilic trifluoromethylating reagents (CF_3^+) also serve not only as precursors for the trifluoromethyl radical but also as *direct* electron acceptors from the photoexcited Ru species. Additionally, they are easy-handling and shelf-stable reagents at room temperature. In this section, we will present our recent results on photoredox-catalyzed trifluoromethylation of $\text{C}=\text{C}$ bonds.

Alkene difunctionalization, particularly regio- and stereo-selective introduction of two different functional groups across a double bond, is an attractive method for construction of diverse structures by a single transformation. Therefore, there have been a large number of studies on transition-metal-catalyzed 1,2-difunctionalization of alkenes [89–91]. Transformations involving construction of $\text{C}-\text{CF}_3$ bonds, however, are still limited [80–82, 85, 92–105]. We expected trifluoromethylative difunctionalization of alkene proceeds in the presence of the electrophilic CF_3 reagents (CF_3^+) and a nucleophile ($\text{Nu}-\text{H}$) through the oxidative quenching cycle as shown in Scheme 14. By this design, the reaction does not require any sacrificial electron donors/acceptors.

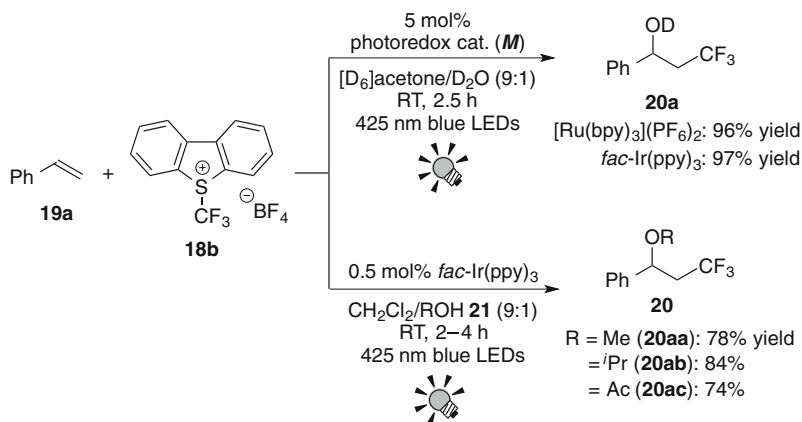
We initially examined photocatalytic hydroxytrifluoromethylation of styrene (**19a**) with Umamoto's reagent **18b** using $[\text{Ru}(\text{bpy})_3](\text{PF}_6)_2$ in a mixture of acetone and H_2O (Scheme 15). As was expected, irradiation by blue LEDs ($\lambda = 425 \text{ nm}$) afforded the desired hydroxytrifluoromethylated product, 3,3,3-trifluoro-1-phenyl-1-propanol (**20a**), in a 96% yield as the sole regioisomer. Another photocatalyst, *fac*- $\text{Ir}(\text{ppy})_3$, also promoted the present reaction in a manner similar to $[\text{Ru}(\text{bpy})_3](\text{PF}_6)_2$.

When a CH_2Cl_2 solution of other O nucleophiles (ROH **21**) such as alcohols and carboxylic acids is used as the solvent, oxytrifluoromethylation took place. We chose the Ir photocatalyst for the present oxytrifluoromethylation because of its solubility. Reactions of styrene (**19a**) with MeOH (**21a**), *t*PrOH (**21b**), and acetic acid (**21c**) afforded the corresponding CF_3 -containing products (**20aa–20ac**) in good yields with regioselective fashions, respectively (Scheme 15).

Representative results of the hydroxytrifluoromethylation are summarized in Table 1. Styrene derivatives with halogen atoms, F (**19b**), Cl (**19c**), and Br (**19d**),

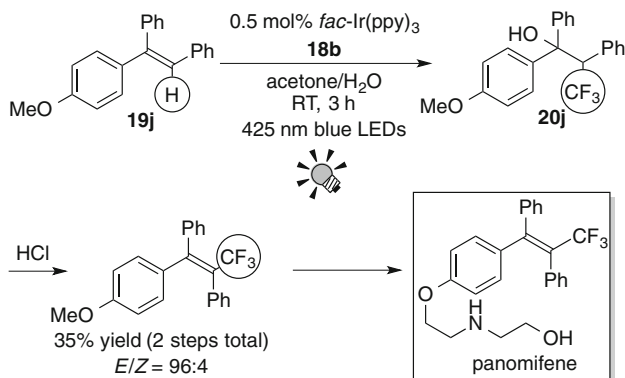
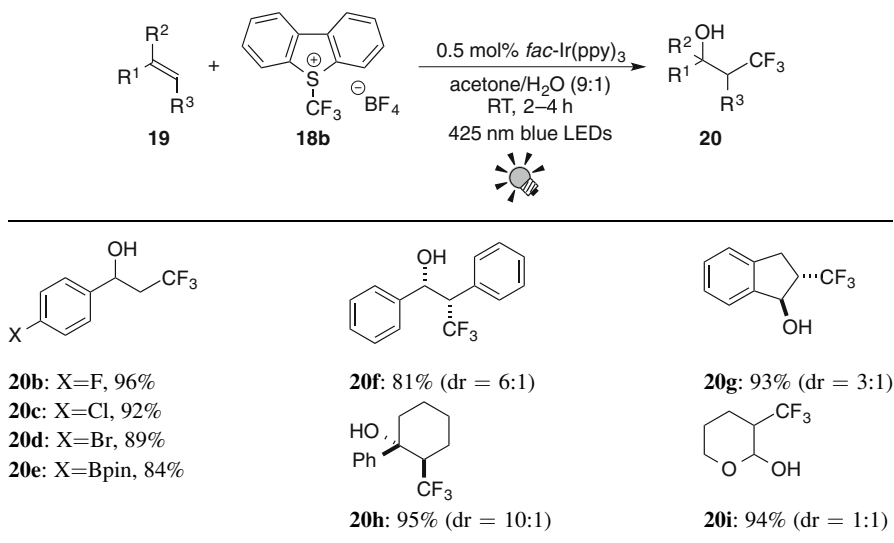


Scheme 14 Photoredox-catalyzed difunctionalization of alkenes through construction of a C- CF_3 bond



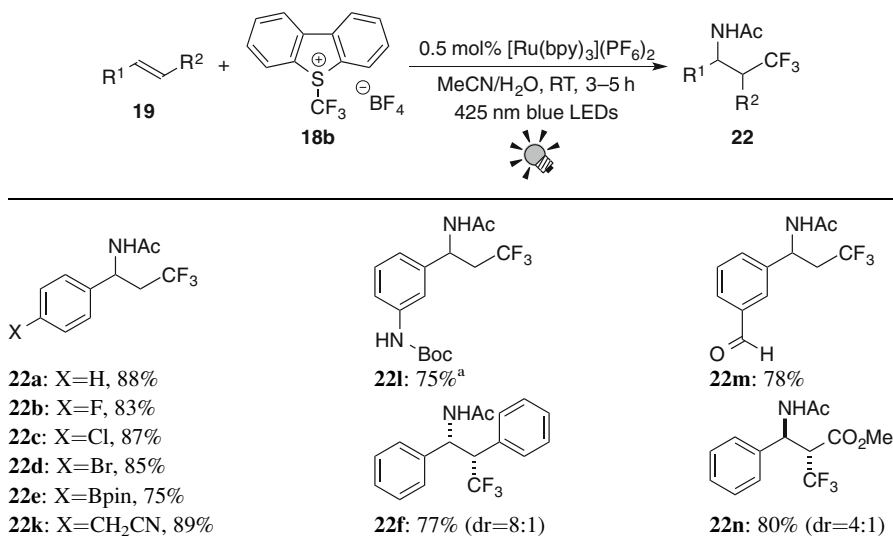
Scheme 15 Photoredox-catalyzed oxytrifluoromethylation of styrene

and a boronic acid ester, Bpin (**19e**), smoothly produced the corresponding products in good yields (84–96%) without any loss of the functional groups. In the case of internal alkenes, *trans*-stilbene (**19f**) and indene (**19g**), reactions gave single regioisomers but mixtures of two diastereomers. Remarkably, the reaction of a trisubstituted alkene, 1-phenylcyclohexene (**19h**), proceeded in a highly regio- and diastereoselective manner (*dr* = 10/1), i.e., with an *anti*-fashion, in a 95% yield. Furthermore, an electron-rich alkene, 3,4-dihydro-2*H*-pyran (**19i**), can be applied to this photocatalytic system. These results show that the present hydroxytrifluoromethylation is regioselective for both terminal and internal electron-rich alkenes. We have expanded this transformation to the reaction of 1,1,2-triarylethylene derivative **19j**. The hydroxytrifluoromethylation of **19j** and subsequent dehydration

Table 1 Representative results for photocatalytic hydroxytrifluoromethylation**Scheme 16** Application to the synthesis of panomifene

gave the olefinic product, a key intermediate for panomifene, which is reported to exhibit anti-estrogenic activity and be a well-known drug for treatment of breast cancer [106, 107]. Indeed, the CF_3 -containing tetrasubstituted alkene was obtained in a 35% yield (Scheme 16) [108]. This result suggests that a hydrogen atom on a $\text{C}=\text{C}$ bond can be replaced by CF_3 group through the consecutive hydroxytrifluoromethylation and dehydration processes.

Encouraged by these findings, we extended our study to develop aminotrifluoromethylation of alkenes. Acetonitrile (MeCN) is an *N*-nucleophile known as an aminative carbocation trapping agent (Ritter-type reaction). We found the

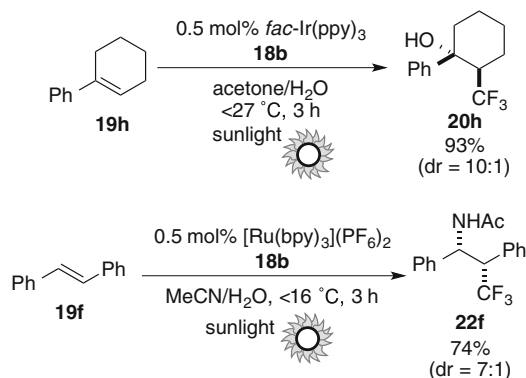
Table 2 Representative results for photocatalytic aminotrifluoromethylation

^a2,6-Dimethylpyridine (1.5 equiv.) was used as an additive

photocatalytic reaction of styrene (**19a**) with Umemoto's reagent **18b** using photoredox catalyst, [Ru(bpy)₃](PF₆)₂, in MeCN containing H₂O (1 equiv. to **18b**) under visible light irradiation (blue LEDs) afforded the aminotrifluoromethylated product **22a** in a 88% isolated yield as the sole regioisomer (Table 2).

Representative results of the present aminotrifluoromethylation are summarized in Table 2. Styrenes bearing halogen atoms, F (**19b**), Cl (**19c**), Br (**19d**), a boronic acid ester, Bpin (**19e**), nitrile group (**19k**), a Boc-protected amino group, NHBoc (**19l**), and aldehyde group (**19m**) smoothly produced the corresponding difunctionalized products without any deterioration of the functionalities in good yields (75–89%). In reactions of internal alkenes such as *trans*-stilbene (**19f**) and cinnamic acid esters (**19n**), the corresponding aminotrifluoromethylated products (**22f**, **n**) were obtained as single regioisomers. Interestingly, we can easily access the α-trifluoromethyl-β-amino acid derivatives (**22n**), which is a potentially bioactive substance [109, 110]. These results show that the present photocatalytic reaction gives the aminotrifluoromethylated products in a highly regioselective manner regardless of the position of the double bond, i.e., terminal or internal alkenes [111].

Finally, we examined these photocatalytic reactions under daylight. As a result, the present photocatalytic hydroxy- and amino-trifluoromethylation can harness the ambient sunlight as the light source. It should be noted that efficiency and selectivity of the sunlight-driven reactions are similar to those obtained by irradiation with blue LEDs (Scheme 17).



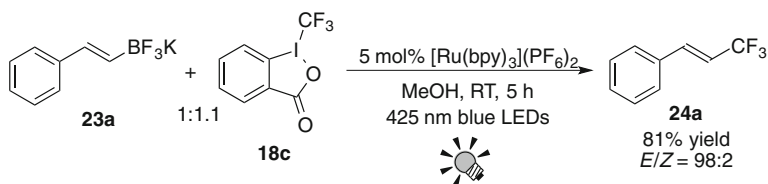
Scheme 17 Sunlight-driven hydroxy- and amino-trifluoromethylation by photoredox catalysis

4.3 Trifluoromethylation of Vinylborates by Photoredox Catalysis

As mentioned in the previous section, trifluoromethylated alkenes are promising building blocks for pharmaceuticals, agrochemicals, and functional materials [112–116]. But reported synthetic methods via trifluoromethylation exhibited limited substrate scopes with respect to hetero-aromatics and functional groups [117–121]. We found that application of potassium vinyltrifluoroborates **23**, which are regarded as electron-rich alkenes, to our photocatalytic oxytrifluoromethylation leads to efficient formation of trifluoromethylated alkenes **24** via deboration. We revealed that our photoredox-catalyzed protocol for construction of $C_{\text{alkenyl}}\text{-CF}_3$ bonds exhibits broad scope in an efficient and stereoselective manner.

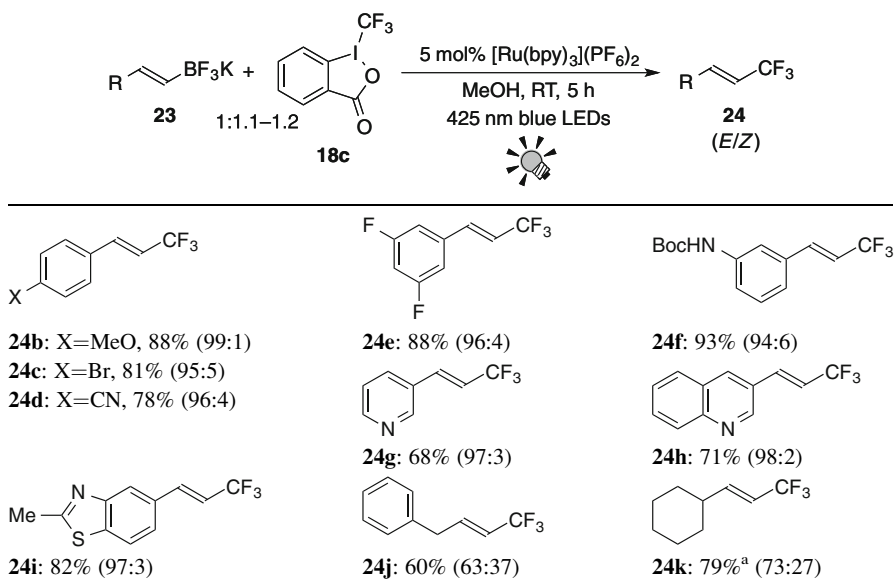
Visible light irradiation of a MeOH solution of potassium (*E*)-styryltrifluoroborate (**23a**) with Togni's reagent **18c** in the presence of $[\text{Ru}(\text{bpy})_3](\text{PF}_6)_2$ afforded β -trifluoromethylstyrene (**24a**) with an *E/Z* ratio of 98/2 in a 81% yield (Scheme 18). Examination of the CF_3 reagents revealed that **18c** is the best choice in terms of yield and selectivity.

Representative results of the present photocatalytic trifluoromethylation of vinyltrifluoroborates are summarized in Table 3. (*E*)-Styrylborates with MeO (**23b**), Br (**23c**), CN (**23d**), F (**23e**), and NHBoc (**23f**) substituents smoothly produced the corresponding β - CF_3 -styrene products (**24b–f**) with high *E/Z* selectivities in good yields. This broad applicability to vinylborates is remarkable. In addition, reactions of vinylborates containing heteroaromatic groups such as pyridine, quinoline, and benzothiazole were also successful. The photocatalytic reactions of vinylborates (**23g–i**) gave the corresponding CF_3 -substituted alkenes (**24g–i**) with excellent *E/Z* selectivities (>97/<3) in good yields (68–82%).



Scheme 18 Trifluoromethylation of styrylborate by photoredox catalysis

Table 3 Representative results for photocatalytic trifluoromethylation of alkenylborates

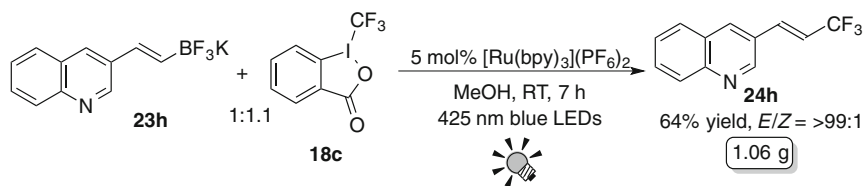


^aNMR yield

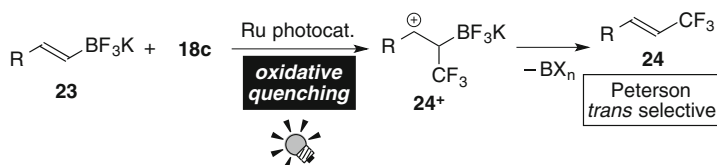
Furthermore, reactions of alkenylborates (**23j** and **k**) afforded the trifluoromethylated alkenes (**24j** and **k**) with moderate selectivities and good yields.

Photoreaction often provokes an issue of scalability because efficient reaction requires a transparent reaction system. As a demonstration of scalability of the present reaction, the trifluoromethylation of **23h** was carried out on a gram scale (Scheme 19). As a result, the trifluoromethylated alkene with quinoline moiety **24h**, which is a herbicide-related molecule [116], was obtained in a good yield (64%, 1.06 g) with an excellent *E/Z* selectivity (>99/<1).

A plausible reaction mechanism for the photocatalytic trifluoromethylation of vinylborates **23** is shown in Scheme 20. According to the previous oxy- and amino-trifluoromethylation, $\cdot\text{CF}_3$ could be generated from 1e-reduction of electrophilic Togni's reagent **18c**. The resultant $\cdot\text{CF}_3$ reacts with a C=C bond of vinylborates **23** in a regioselective manner to give β -borato cation intermediates (**24⁺**) [122] through the oxidative quenching cycle in a manner similar to Scheme 14. Finally



Scheme 19 Gram-scale synthesis of 3-[(*E*)-3,3,3-trifluoroprop-1-en-1-yl]quinolone



Scheme 20 A plausible mechanism for *E*-selective formation of trifluoromethylated alkenes

predominant *trans*-selective Peterson elimination of the boron-based group provides (*E*)-trifluoromethylated alkenes **24** [123].

5 Conclusions and Outlook

In conclusion, photoredox catalysis with the well-known Ru polypyridine complexes has emerged as a powerful tool for redox reactions because they can achieve not only easier, safer, and economical redox processes but also useful and selective transformations. Both of the reductive quenching cycle and the oxidative quenching cycle can be designed by appropriate choice of photocatalyst and substrate. In particular, well-designed photocatalytic system enables redox neutral transformations without an excess amount of oxidizing/reducing agents. We have developed photoredox-catalyzed radical trifluoromethylation using electrophilic trifluoromethylating reagents as the CF_3 radical precursors. No *sacrificial* reagents have been used in these reactions. In addition, our trifluoromethylative transformations are elusive by other synthetic methods. The present photocatalytic processes require a source of visible light, but, blue LED, standard fluorescent light and even natural sunlight can be utilized. Additionally, redox reactions mediated by photocatalyst proceed under mild conditions compared to conventional methods. Thus, a wide variety of functional molecules have chances to be explored. We expect the present new protocol to expand the radical reactions of more diverse and complex architectures and stimulate development of novel reactive but storable radical precursors.

Acknowledgment This work was supported financially by Grants-in-Aid for Scientific Research from the Ministry of Education, Culture, Sports, Science of the Japanese Government (Nos. 23750174, 22350024, and 24108101).

References

1. Chatgililoglu C, Studer A (eds) (2012) Encyclopedia of radical in chemistry, biology and materials. Wiley, Chichester
2. Juris A, Balzani V, Barigelletti F, Campagna S, Belser P, von Zelewsky A (1988) Ru (II) polypyridine complexes: photophysics, photochemistry, electrochemistry and chemluminescence. *Coord Chem Rev* 84:85–277
3. Roundhill DM (1994) Photochemistry and photophysics of metal complexes. Plenum, New York
4. Hedstrand DM, Kruizinga WH, Kellog RM (1978) Light induced and dye accelerated reductions of phenyl onium salts by 1,4-dihydropyridines. *Tetrahedron Lett* 19:1255–1258
5. Pac C, Ihama M, Yasuda M, Miyauchi Y, Sakurai H (1981) Ru(bpy)₃²⁺-mediated photoreduction of olefins with 1-benzyl-1,4-dihydronicotinamide: a mechanistic probe for electron-transfer reactions of NAD(P)H-model compounds. *J Am Chem Soc* 103:6495–6497
6. Ishitani O, Pac C, Sakurai H (1984) Redox-photosensitized reactions. 11. Ru(bpy)₃²⁺-photosensitized reactions of 1-benzyl-1,4-dihydronicotinamide with aryl-substituted enones, derivatives of methyl cinnamate, and substituted cinnamitriles: electron-transfer mechanism and structure-reactivity relationships. *J Org Chem* 49:26–34
7. Goren Z, Willner I (1983) Photochemical and chemical reduction of vicinal dibromides via phase transfer of 4,4'-bipyridinium radical: the role of radical disproportionation. *J Am Chem Soc* 105:7764–7765
8. Cano-Yelo H, Deronzier A (1984) Photocatalysis of the Pschorr reaction by tris-(2,2'-bipyridyl) ruthenium(II) in the phenanthrene series. *J Chem Soc Perkin Trans 2*:1093–1098
9. Hironaka K, Fukuzumi S, Tanaka T (1984) Tris(bipyridyl)ruthenium(II)-photosensitized reaction of 1-benzyl-1,4-dihydronicotinamide with benzyl bromide. *J Chem Soc Perkin Trans 2*:1705–1709
10. Mashraqui SH, Kellog RM (1985) 3-Methyl-2,3-dihydrobenzothiazoles as reducing agents. Dye enhanced photoreactions. *Tetrahedron Lett* 26:1453–1456
11. Tomioka H, Ueda K, Ohi H, Izawa Y (1986) Photochemical and chemical reduction of nitroalkenes using viologens as an electron phase-transfer catalyst. *Chem Lett* 1359–1362
12. Fukuzumi S, Mochizuki S, Tanaka T (1990) Photocatalytic reduction of phenacyl halides by 9,10-dihydro-10-methylacridine: control between the reductive and oxidative quenching pathways of tris(bipyridine)ruthenium complex utilizing an acid catalysis. *J Phys Chem* 94:722–726
13. Okada K, Okamoto K, Morita N, Okubo K, Oda M (1991) Photosensitized decarboxylative Michael addition through N-(acyloxy)phthalimides via an electron-transfer mechanism. *J Am Chem Soc* 113:9401–9402
14. Hamada T, Ishida H, Usui S, Watanabe Y, Tsumura K, Ohkubo K (1993) A novel photocatalytic asymmetric synthesis of (*R*)-(+)-1,1'-bi-2-naphthol derivatives by oxidative coupling of 3-substituted-2-naphthol with Δ -[Ru(menbpy)₃]²⁺[menbpy = 4,4'-di(1*R*,2*S*,5*R*)-(-)-menthoxy-carbonyl-2,2'-bipyridine], which possesses molecular helicity. *J Chem Soc Chem Commun* 909–911
15. Barton DHR, Csiba MA, Jaszberenyi JC (1994) Ru(bpy)₃²⁺-mediated addition of *Se*-phenyl *p*-tolueneselenosulfonate to electron rich olefins. *Tetrahedron Lett* 35:2869–2872
16. Zen JM, Liou SL, Kumar AS, Hsia MS (2003) An efficient and selective photocatalytic system for the oxidation of sulfides to sulfoxides. *Angew Chem Int Ed* 42:577–579

17. Hasegawa E, Takizawa S, Seida T, Yamaguchi A, Yamaguchi N, Chiba N, Takahashi T, Ikeda H, Akiyama K (2006) Photoinduced electron-transfer systems consisting of electron-donating pyrenes or anthracenes and benzimidazolines for reductive transformation of carbonyl compounds. *Tetrahedron* 62:6581–6588
18. Yoon TP, Ischay MA, Du J (2010) Visible light photocatalysis as a greener approach to photochemical synthesis. *Nat Chem* 2:527–532
19. Narayanam JMR, Stephenson CRJ (2011) Visible light photoredox catalysis: applications in organic synthesis. *Chem Soc Rev* 40:102–113
20. Teplý F (2011) Photoredox catalysis by $[\text{Ru}(\text{bpy})_3]^{2+}$ to trigger transformations of organic molecules. Organic synthesis using visible-light photocatalysis and its 20th century roots. *Collect Czech Chem Commun* 76:859–917
21. Tucker JW, Stephenson CRJ (2012) Shining light on photoredox catalysis: theory and synthetic applications. *J Org Chem* 77:1617–1622
22. Xuan J, Xiao W-J (2012) Visible-light photoredox catalysis. *Angew Chem Int Ed* 51:6828–6838
23. Maity S, Zheng N (2012) A photo touch on amines: new synthetic adventures of nitrogen radical cations. *Synlett* 23:1851–1856
24. Shi L, Xia W (2012) Photoredox functionalization of C–H bonds adjacent to a nitrogen atom. *Chem Soc Rev* 41:7687–7697
25. Xi Y, Yi H, Lei A (2013) Synthetic applications of photoredox catalysis with visible light. *Org Biomol Chem* 11:2387–2403
26. Hari DP, König B (2013) The photocatalyzed Meerwein arylation: classic reaction of aryl diazonium salts in a new light. *Angew Chem Int Ed* 52:4734–4743
27. Prier CK, Rankic DA, MacMillan DWC (2013) Visible light photoredox catalysis with transition metal complexes: applications in organic synthesis. *Chem Rev* 113:5322–5363
28. Reckenthäler M, Griesbeck AG (2013) Photoredox catalysis for organic syntheses. *Adv Synth Catal* 355:2727–2744
29. Koike T, Akita M (2013) Visible-light-induced photoredox catalysis: an easy access to green radical chemistry. *Synlett* 24:2492–2505
30. Nicewicz DA, MacMillan DWC (2008) Merging photoredox catalysis with organocatalysis: the direct asymmetric alkylation of aldehydes. *Science* 322:77–80
31. Lelais G, MacMillan DWC (2006) Modern strategies in organic catalysis: the advent and development of iminium activation. *Aldrichimica Acta* 39:79–87
32. MacMillan DWC (2008) The advent and development of organocatalysis. *Nature* 455:304–308
33. Beeson TD, Mastracchio A, Hong J-B, Ashton K, MacMillan DWC (2007) Enantioselective organocatalysis using SOMO activation. *Science* 316:582–585
34. Nagib DA, Scott ME, MacMillan DWC (2009) Enantioselective α -trifluoromethylation of aldehydes via photoredox organocatalysis. *J Am Chem Soc* 131:10875–10877
35. Koike T, Akita M (2009) Photoinduced oxyamination of enamines and aldehydes with TEMPO catalyzed by $[\text{Ru}(\text{bpy})_3]^{2+}$. *Chem Lett* 38:166–167
36. Yasu Y, Koike T, Akita M (2012) Sunlight-driven synthesis of γ -diketones via oxidative coupling of enamines with silyl enol ethers catalyzed by $[\text{Ru}(\text{bpy})_3]^{2+}$. *Chem Commun* 48:5355–5357
37. Ischay MA, Anzovino ME, Du J, Yoon TP (2008) Efficient visible light photocatalysis of [2+2] enone cycloadditions. *J Am Chem Soc* 130:12886–12887
38. Crimmins MT (1988) Synthetic applications of intramolecular enone-olefin photocycloadditions. *Chem Rev* 88:1453–1473
39. Bach T (1998) Stereoselective intermolecular [2+2]-photocycloaddition reactions and their application in synthesis. *Synthesis* 683–708
40. Roh Y, Jang H-Y, Lynch V, Bauld NL, Krische MJ (2002) Anion radical chain cycloaddition of tethered enones: intramolecular cyclobutanation and Diels–Alder cycloaddition. *Org Lett* 4:611–613

41. Du J, Yoon TP (2009) Crossed intermolecular [2+2] cycloadditions of acyclic enones via visible light photocatalysis. *J Am Chem Soc* 131:14604–14605
42. Lu Z, Shen M, Yoon TP (2011) [3+2] Cycloadditions of aryl cyclopropyl ketone by visible light photocatalysis. *J Am Chem Soc* 133:1162–1164
43. Ischay MA, Lu Z, Yoon TP (2010) [2+2] Cycloadditions by oxidative visible light photocatalysis. *J Am Chem Soc* 132:8572–8574
44. Ischay MA, Ament MS, Yoon TP (2012) Crossed intermolecular [2 + 2] cycloaddition of styrenes by visible light photocatalysis. *Chem Sci* 3:2807–2811
45. Narayanam JMR, Tucker JW, Stephenson CRJ (2009) Electron-transfer photoredox catalysis: development of a tin-free reductive dehalogenation reaction. *J Am Chem Soc* 131:8756–8757
46. Tucker JW, Nguyen JD, Narayanam JMR, Krabbe SW, Stephenson CRJ (2010) Tin-free radical cyclization reactions initiated by visible light photoredox catalysis. *Chem Commun* 46:4985–4987
47. Tucker JW, Narayanam JMR, Krabbe SW, Stephenson CRJ (2010) Electron transfer photoredox catalysis: intramolecular radical addition to indoles and pyrroles. *Org Lett* 12:368–371
48. Furst L, Matsuura BS, Narayanam JMR, Tucker JW, Stephenson CRJ (2010) Visible light-mediated intermolecular C-H functionalization of electron-rich heterocycles with malonates. *Org Lett* 12:3104–3107
49. Andrew RS, Becker JJ, Gagné MR (2010) Intermolecular addition of glycosyl halides to alkenes mediated by visible light. *Angew Chem Int Ed* 49:7274–7276
50. Condie AG, González-Gómez JC, Stephenson CRJ (2010) Visible-light photoredox catalysis: Aza-Henry reactions via C-H functionalization. *J Am Chem Soc* 132:1464–1465
51. Rueping M, Vila C, Koenigs RM, Poscharyn K, Fabry DC (2011) Dual catalysis: combining photoredox and Lewis base catalysis for direct Mannich reactions. *Chem Commun* 47:2360–2362
52. Xuan J, Cheng Y, An J, Lu L-Q, Zhang X-X, Xiao W-J (2011) Visible light-induced intramolecular cyclization reactions of diamines: a new strategy to construct tetrahydroimidazoles. *Chem Commun* 47:8337–8339
53. Rueping M, Zhu S, Koenigs RM (2011) Photoredox catalyzed C–P bond forming reactions—visible light mediated oxidative phosphorylations of amines. *Chem Commun* 47:8679–8681
54. Zou Y-Q, Lu L-Q, Fu L, Chang N-J, Rong J, Chen J-R, Xiao W-J (2011) Visible-light-induced oxidation/[3+2] cycloaddition/oxidative aromatization sequence: a photocatalytic strategy to construct pyrrolo[2,1-*a*]isoquinolines. *Angew Chem Int Ed* 50:7171–7175
55. Freeman DB, Furst L, Condie AG, Stephenson CRJ (2012) Functionally diverse nucleophilic trapping of iminium intermediates generated utilizing visible light. *Org Lett* 14:94–97
56. Maity S, Zhu M, Shinabery RS, Zheng N (2012) Intermolecular [3+2] cycloaddition of cyclopropylamines with olefins by visible-light photocatalysis. *Angew Chem Int Ed* 51:222–226
57. Rueping M, Koenigs RM, Poscharyn K, Fabry DC, Leonori D, Vila C (2012) Dual catalysis: combination of photocatalytic aerobic oxidation and metal catalyzed alkynylation reactions—C–C bond formation using visible light. *Chem Eur J* 18:5170–5174
58. Cai S, Zhao X, Wang X, Liu Q, Li Z, Wang DZ (2012) Visible-light-promoted C–C bond cleavage: photocatalytic generation of iminium ions and amino radicals. *Angew Chem Int Ed* 51:8050–8053
59. Zhao G, Yang C, Guo L, Sun H, Chen C, Xia W (2012) Visible light-induced oxidative coupling reaction: easy access to Mannich-type products. *Chem Commun* 48:2337–2339
60. DiRocco DA, Rovis T (2012) Catalytic asymmetric α -acylation of tertiary amines mediated by a dual catalysis mode: N-Heterocyclic carbene and photoredox catalysis. *J Am Chem Soc* 134:8094–8097
61. McNally A, Prier CK, MacMillan DWC (2011) Discovery of an α -amino C–H arylation reaction using the strategy of accelerated serendipity. *Science* 334:1114–1117

62. Kohls P, Jadhav D, Pandey G, Reiser O (2012) Visible light photoredox catalysis: generation and addition of *N*-aryltetrahydroisoquinoline-derived α -amino radicals to Michael acceptors. *Org Lett* 14:672–675
63. Miyake Y, Nakajima K, Nishibayashi Y (2012) Visible-light-mediated utilization of α -aminoalkyl radicals: addition to electron-deficient alkenes using photoredox catalysts. *J Am Chem Soc* 134:3338–3341
64. Ju X, Li D, Li W, Yu W, Bian F (2012) The reaction of tertiary anilines with maleimides under visible light redox catalysis. *Adv Synth Catal* 354:3561–3567
65. Zhu S, Das A, Bui L, Zhou H, Curran DP, Rueping M (2013) Oxygen switch in visible-light photoredox catalysis: radical additions and cyclizations and unexpected C–C bond cleavage reactions. *J Am Chem Soc* 135:1823–1829
66. Hiyama T (2000) *Organofluorine compounds: chemistry and applications*. Springer, Berlin
67. Ojima I (ed) (2009) *Fluorine in medicinal chemistry and chemical biology*. Wiley, Oxford
68. Ma J-A, Cahard D (2004) Asymmetric fluorination, trifluoromethylation, and perfluoroalkylation reactions. *Chem Rev* 104:6119–6146
69. Shimizu M, Hiyama T (2005) Modern synthetic methods for fluorine-substituted target molecules. *Angew Chem Int Ed* 44:214–231
70. Ma J-A, Cahard D (2007) Strategies for nucleophilic, electrophilic, and radical trifluoromethylations. *J Fluorine Chem* 128:975–996
71. Tomashenko OA, Grushin VV (2011) Aromatic trifluoromethylation with metal complexes. *Chem Rev* 111:4475–4521
72. Furuya T, Kamlet AS, Ritter T (2011) Catalysis for fluorination and trifluoromethylation. *Nature* 473:470–477
73. Besset T, Schneider C, Cahard D (2012) Tamed arene and heteroarene trifluoromethylation. *Angew Chem Int Ed* 51:5048–5050
74. Studer A (2012) A “Renaissance” in radical trifluoromethylation. *Angew Chem Int Ed* 51:8950–8958
75. Hollingworth C, Gouverneur V (2012) Transition metal catalysis and nucleophilic fluorination. *Chem Commun* 48:2929–2942
76. Liu H, Gu Z, Jiang X (2013) Direct trifluoromethylation of the C–H bond. *Adv Synth Catal* 355:617–626
77. Liang T, Neumann CN, Ritter T (2013) Introduction of fluorine and fluorine-containing functional groups. *Angew Chem Int Ed* 52:8214–8264
78. Koike T, Akita M (2014) Trifluoromethylation by visible-light-driven photoredox catalysis. *Top Catal*. DOI: 10.1007/s11244-014-0259-7
79. Nagib DA, MacMillan DWC (2011) Trifluoromethylation of arenes and heteroarenes by means of photoredox catalysis. *Nature* 480:224–228
80. Nguyen JD, Tucker JW, Konieczynska MD, Stephenson CRJ (2011) Intermolecular atom transfer radical addition to olefins mediated by oxidative quenching of photoredox catalysts. *J Am Chem Soc* 133:4160–4163
81. Wallentin C-J, Nguyen JD, Finkbeiner P, Stephenson CRJ (2012) Visible light-mediated atom transfer radical addition via oxidative and reductive quenching of photocatalysts. *J Am Chem Soc* 134:8875–8884
82. Wilger DJ, Gesmundo NJ, Nicewicz DA (2013) Catalytic hydrotrifluoromethylation of styrenes and unactivated aliphatic alkenes via an organic photoredox system. *Chem Sci* 4:3160–3165
83. Iqbal N, Choi S, Ko E, Cho EJ (2012) Trifluoromethylation of heterocycles via visible light photoredox catalysis. *Tetrahedron Lett* 53:2005–2008
84. Iqbal N, Choi S, Kim E, Cho EJ (2012) Trifluoromethylation of alkenes by visible light photoredox catalysis. *J Org Chem* 77:11383–11387
85. Kim E, Choi S, Kim H, Cho EJ (2013) Generation of CF₃-containing epoxides and aziridines by visible-light-driven trifluoromethylation of allylic alcohols and amines. *Chem Eur J* 19:6209–6212

86. Umemoto T (1996) Electrophilic perfluoroalkylating agents. *Chem Rev* 96:1757–1777
87. Eisenberger P, Gischig S, Togni A (2006) Novel 10-I-3 hypervalent iodine-based compounds for electrophilic trifluoromethylation. *Chem Eur J* 12:2579–2586
88. Kieltch I, Eisenberger P, Togni A (2007) Mild electrophilic trifluoromethylation of carbon- and sulfur-centered nucleophiles by a hypervalent iodine(III)–CF₃ reagent. *Angew Chem Int Ed* 46:754–757
89. Wolfe JP (2008) Stereoselective synthesis of saturated heterocycles via palladium-catalyzed alkene carboetherification and carboamination reactions. *Synlett* 2913–2937
90. Jensen KH, Sigman MS (2008) Mechanistic approaches to palladium-catalyzed alkene difunctionalization reactions. *Org Biomol Chem* 6:4083–4088
91. McDonald RI, Liu G, Stahl SS (2011) Palladium(II)-catalyzed alkene functionalization via nucleopalladation: stereochemical pathways and enantioselective catalytic applications. *Chem Rev* 111:2981–3019
92. Fuchikami T, Shibata Y, Urata H (1987) Transition-metal complex catalyzed polyfluoroalkylation. A facile synthesis of fluorine-containing oxiranes and enynes. *Chem Lett* 521–524
93. Kamigata N, Fukushima T, Yoshida M (1989) Reaction of trifluoromethanesulphonyl chloride with alkenes catalysed by a ruthenium(II) complex. *J Chem Soc Chem Commun* 1559–1560
94. Kamigata N, Fukushima T, Terakawa Y, Yoshida M, Sawada H (1991) Novel perfluoroalkylation of alkenes with perfluoroalkanesulphonyl chlorides catalysed by a ruthenium (II) complex. *J Chem Soc Perkin Trans 1*:627–633
95. Ignatowska J, Dmowski W (2007) Sodium dithionite initiated addition of CF₂Br₂, CF₃I and (CF₃)₂CFI to allylaromatics synthesis and the reactivity of 4-aryl-1,1-difluorodienes and 4-aryl-1,1-bis(trifluoromethyl)dienes. *J Fluorine Chem* 128:997–1006
96. Mu X, Wu T, Wang H-Y, Guo Y-L, Liu G (2012) Palladium-catalyzed oxidative aryltrifluoromethylation of activated alkenes at room temperature. *J Am Chem Soc* 134:878–881
97. Janson PG, Ghoneim I, Ichenko NO, Szabó KJ (2012) Electrophilic trifluoromethylation by copper-catalyzed addition of CF₃-transfer reagents to alkenes and alkynes. *Org Lett* 14:2882–2885
98. Zhu R, Buchwald SL (2012) Copper-catalyzed oxytrifluoromethylation of unactivated alkenes. *J Am Chem Soc* 134:12462–12465
99. Li Y, Studer A (2012) Transition-metal-free trifluoromethylaminoxylation of alkenes. *Angew Chem Int Ed* 51:8221–8224
100. Egami H, Shimizu R, Sodeoka M (2012) Oxytrifluoromethylation of multiple bonds using copper catalyst under mild conditions. *Tetrahedron Lett* 53:5503–5506
101. Feng C, Loh T-P (2012) Copper-catalyzed olefinic trifluoromethylation of enamides at room temperature. *Chem Sci* 3:3458–3462
102. Wu X, Chu L, Qing F-L (2013) Silver-catalyzed hydrotrifluoromethylation of unactivated alkenes with CF₃SiMe₃. *Angew Chem Int Ed* 52:2198–2202
103. Egami H, Shimizu R, Kawamura S, Sodeoka M (2013) Alkene trifluoromethylation coupled with C–C bond formation: construction of trifluoromethylated carbocycles and heterocycles. *Angew Chem Int Ed* 52:4000–4003
104. Egami H, Kawamura S, Miyazaki A, Sodeoka M (2013) Trifluoromethylation reactions for the synthesis of β-trifluoromethylamines. *Angew Chem Int Ed* 52:7841–7844
105. Mizuta S, Verhoog S, Engle KM, Khotavivattana T, O'Duill M, Wheelhouse K, Rassias G, Médebielle M, Gouverneur V (2011) Catalytic hydrotrifluoromethylation of unactivated alkenes. *J Am Chem Soc* 135:2505–2508
106. Nemeth G, Kapiller-Dezsofi R, Lax G, Simig G (1996) New practical synthesis of panomifene. The effect of 2-trifluoromethyl substituent on the stereoselectivity of dehydration of 1,1,2-triarylethanol. *Tetrahedron* 52:12821–12830
107. Liu X, Shimizu M, Hiyama T (2004) A Facile stereocontrolled approach to CF₃-substituted triarylethenes: synthesis of panomifene. *Angew Chem Int Ed* 43:879–882

108. Yasu Y, Koike T, Akita M (2012) Three-component oxytrifluoromethylation of alkenes: highly efficient and regioselective difunctionalization of C=C bonds mediated by photoredox catalysts. *Angew Chem Int Ed* 51:9567–9571
109. Nie J, Guo H-C, Cahard D, Ma J-A (2011) Asymmetric construction of stereogenic carbon centers featuring a trifluoromethyl group from prochiral trifluoromethylated substrates. *Chem Rev* 111:455–529
110. Qiu X-L, Qing F-L (2011) Recent advances in the synthesis of fluorinated amino acids. *Eur J Org Chem* 3261–3278
111. Yasu Y, Koike T, Akita M (2013) Intermolecular aminotrifluoromethylation of alkenes by visible-light- driven photoredox catalysis. *Org Lett* 15:2136–2139
112. Rivkin A, Chou T-C, Danishefsky SJ (2005) On the remarkable antitumor properties of fludelonone: how we got there. *Angew Chem Int Ed* 44:2838–2850
113. Shimizu M, Takeda Y, Higashi M, Hiyama T (2009) 1,4-Bis(alkenyl)-2,5-dipiperidino-benzenes: minimal fluorophores exhibiting highly efficient emission in the solid state. *Angew Chem Int Ed* 48:3653–3656
114. Shimizu M, Takeda Y, Higashi M, Hiyama T (2011) Synthesis and photophysical properties of dimethoxybis(3,3,3-trifluoropropen-1-yl)benzenes: compact chromophores exhibiting violet fluorescence in the solid state. *Chem Asian J* 6:2536–2544
115. Shi Z, Davies J, Jang S-H, Kaminsky W, Jen AK-Y (2012) Aggregation induced emission (AIE) of trifluoromethyl substituted distyrylbenzenes. *Chem Commun* 48:7880–7882
116. Selby TP (1995) Preparation of substituted fused heterocyclic herbicides. PCT international patent application US5,389,600 (A)
117. Xu J, Luo D-F, Xiao B, Liu Z-J, Gong T-J, Fu Y, Liu L (2011) Copper-catalyzed trifluoromethylation of aryl boronic acids using a CF_3^+ reagent. *Chem Commun* 47:4300–4302
118. Liu T, Shen Q (2011) Copper-catalyzed trifluoromethylation of aryl and vinyl boronic acids with an electrophilic trifluoromethylating reagent. *Org Lett* 13:2342–2345
119. Parsons AT, Senecal TD, Buchwald SL (2012) Iron(II)-catalyzed trifluoromethylation of potassium vinyltrifluoroborates. *Angew Chem Int Ed* 51:2947–2950
120. He Z, Luo T, Hu M, Cao Y, Hu J (2012) Copper-catalyzed di- and trifluoromethylation of α , β -unsaturated carboxylic acids: a protocol for vinylic fluoroalkylations. *Angew Chem Int Ed* 51:3944–3947
121. Li Y, Wu L, Neumann H, Beller M (2013) Copper-catalyzed trifluoromethylation of aryl- and vinylboronic acids with generation of CF_3 -radicals. *Chem Commun* 49:2628–2630
122. Kim H, MacMillan DWC (2008) Enantioselective organo-SOMO catalysis: the α -vinylation of aldehydes. *J Am Chem Soc* 130:398–399
123. Yasu Y, Koike T, Akita M (2013) Visible-light-induced synthesis of a variety of trifluoromethylated alkenes from potassium vinyltrifluoroborates by photoredox catalysis. *Chem Commun* 49:2037–2039

Index

A

- Acetoxyruthenacycle, 310
- N*-Acylimidazole, 123
- 1-Acyloxy-1,3-dienes, 291
- Acylpyrrolidine, decarbonylation, 201
- Adiponitrile, 93
- Alcohols, 45
 - amidation, 104
 - dehydrogenation, 45, 49
- Aldehydes, coupling with hydroxylamine, 81
 - dehydrogenative amidation, 105
- Aldimines, 122, 131, 179, 184, 272
- Aldoximes, rearrangement, 81, 95
 - Ru-catalyzed rearrangement, 95
- Alkenes, 289
 - hydroarylation, 119, 145
 - trifluoromethylation, 381
- Alkenyl alkylidene bicyclo[3.1.0]hexanes, 313
- Alkenyl carbamates, 243
- Alkenylation, 119, 121, 142, 153–174, 188, 266
- Alkylation, 119, 121, 142, 196, 215, 223, 273, 375
- 1-Alkylidene-2-indanones, 249
- Alkylidenecyclopentanes, 260
- 2-Alkylidenecyclopentanones, 305
- Alkylidenes, 1
- Alkynes, 289
 - hydroarylation, 119
 - intermolecular coupling, 290
- Alkynyl acetals, 313
- Alkynyl halides, 303
- Alkynyl phosphonates, 303, 315
- Alkynyl sulfides, 303
- Alkynylations, 245
- Alkynylboronates, 293, 312
- Alkynylcyclobutanols, 305
- o*-Alkynylethynylstyrenes, 256
- o*-Alkynylphenyl nitrones, 264
- Alkynylrutheniumvinylidene, 255
- Allenylboronates, cyclodimerization, 310
- Allenynes, cycloisomerization, 308
- Allocyathin, 306
- Allylbenzene, 4
- Amidations, 93, 99
 - aldehydes, 105
 - alcohols, 104
 - dehydrogenative, 81, 98–108
 - hydroamidation, 251, 253
 - hydrolytic, 81, 93
 - Ru-catalyzed dehydrogenative, 98
- Amide-bond formation, 81
- Amides, 19, 20, 25, 48, 83, 98–110, 155, 188, 203, 272
 - aromatic, 138, 148
 - hydrogenation, 30
 - intramolecular carbonylation, 204
 - secondary, 97, 250
 - tertiary, 93, 103
- Amines, 30, 62, 69, 93–111, 272, 313, 329–333, 349, 356, 363
 - secondary, 50, 250
 - tertiary, 381
- Aminoalcohols, 99, 349
- 2-Amino-1,3-dienes, 301
- 2-Aminomethylpyridine, 50
- Anacetrapib (MK-0859), 136
- Angiotensin II receptor blockers (ARBs), 136
- Anilines, 104, 161, 177, 214, 272
- Annulations, 119
- Antihypertensive drugs, 136

- Arene-ruthenium(II) complexes, 87
 Arenes, arylation, sp^2 C–H bond activation, 122
 Aromatization–dearomatization, 20
 Aryl tosylates, 140
 Arylation, 119, 121, 205–212
 Asymmetric ring opening cross metathesis (AROCM), 10
 7-Azabenzonorbornadienes, 304
 AZARYPHOS, 244
- B**
 BArF (tetrakis[(3,5-trifluoromethyl)phenyl]borate), 24
 Benzalacetone, 99
 Benzofurans, 142, 150, 247, 248
 Benzonitrile, 84, 86, 88, 91
 Benzothiophene, 142
 Benzoxazolylacetamide, 90
 Benzoxazolylacetoneitrile, 90
 3-Benzoxepines, 249
 2-(3-Benzoylphenyl)propionitrile, 89
 Benzyl alcohol, oxidation, 49, 361
 Benzyl carbamates, hydrogenation, 35
 α -Benzyl- α -methylmalononitrile, 90
 Bicyclo[4.2.0]octadienes, 308
 Bis(allyl)-ruthenium(II) complex, 87
 Biscarbenes, cyclic, 290
 1,4-bis(5*H*-dibenzo[a,d]cyclohepten-5-yl)-1,4-diazabuta-1,3-diene, 65
 1,3-bis(2,6-diisopropylphenyl)imidazol-2-ylidene (IPr), 338
 1,2-bis(diphenylphosphinamino)cyclohexane, 314,
 314,
 Born-Oppenheimer molecular dynamics (BO-MD), 67
 Boronic acids, arylation, 141
 Boronic amino esters, 313
 Bottom-bound metallacycles, 3
 2-Butyne, hydroacylation, 230
- C**
 C–C bonds, cross-couplings, 119
 formation 195, 289
 C–H bond activation, sp^2 , 119
 C–H bond activation, sp^3 , 195
 Carbenes, 1, 270, 329, 338, 364
 Carbon dioxide (CO₂), 19, 54, 71, 351
 Carbon nanotubes (CNTs), 319, 362
 carbonylation, 33, 138, 151, 202, 305
 Carboxylative cyclization, 262
 Cascade catalysis, 37
 Catalysis, 45, 119, 195, 237, 319
 Cellulose acetate (CA), 324
 Chlorobenzene, 129
 Chloroformate, 151
 Chlorosulfolipid, 14
 2-Chlorothiophene, 129
 2-Chlorotoluene, 129
 Chromane, 146
 Citronellamide, 97
 Colloids, 319
 Continuous flow methods, 68
 Cross-couplings, 119
 Cross metathesis, 9
 Cyanodienylketones, 292
 Cyanohydrins, 90
 Cyclizations, intramolecular, 259
 Cycloadditions, 260, 264, 278, 294, 303,
 314, 377
 Cyclobutadieneruthenium, 292
 Cyclodextrin, 353
 1,3-Cyclohexadiene, 357
 Cyclohexanol, dehydrogenation, 49
 Cyclohexylidene enol carboxylates, 262
 Cyclooctane, 324
 Cyclopentadienyl ruthenium(II) catalysts, 289
 Cyclopentanes, 146
 chiral-substituted, 10
 Cyclopentanones, 259
 Cycloversion, 3
 Cyclotrimerization, intermolecular, 293
 Cylindricines, 297
- D**
 Decarbonylative cyclization, 260
 Dehydrogenation, 45
 Dehydrogenative amidation, 81
N,N-Di(*tert*-butyl)imidazol-2-ylidene, 338
cis-1,4-Diacetoxybutene, 4
 1,3-Dialkylidenecyclobutane, 310
 Diastereoselectivity, 1
 Dichloroethane, 162, 291, 311
 Dichloromethane, 9, 263, 327
 Diels Alder reactions, 267, 314
 Dienones, conjugated, 297
 Dienylchlorides, 291
 1,3-Dienylphosphine oxides, 298
 Dihydrobenzoindole, 304
 Dihydrocoumarin, 146
 Dihydroisoquinolines, 253
 Dihydropyrans, 246
 Dihydroquinolines, 253
 Dimethyl carbonate (DMC), hydrogenation to
 methanol, 33
 Dimethylacetylenedicarboxylate (DMAD), 293

2-Dimethylaminoethanol, 51
1,3-Dimethylimidazolium formate, 67
2,2-Dimethylpropanol, 102
1,2-Diols, 19, 27
Di-*O*-silyl-6-arylpyrimidine, 138
2-Di-*tert*-butylphosphinyl-1-phenyl-1*H*-pyrrole, 50
Dynes, intramolecular coupling, 294
1-Dodecene, 14

E

Electrocyclizations, 263
Electron transfer, 371
Enamides, 110, 250
Ene-lactams, 85
Enimides, 250
Enol esters, 243
Enyne cycloisomerization, 306
Esters, 19
 dehydrogenative amidation, 107
Ethanol, dehydrogenation, 47, 49, 53
Ethenolysis, *Z*-selective, 9, 12
Ethyl acetate, 53
Ethyl mandelate, prenylation, 227
1-Ethyl-2,3-dimethylimidazolium (EMMim), 67
1-Ethyl-3-methylimidazolium (EMim), 67

F

Formamides, 36, 38, 104, 199
Formates, 29, 58–72
Formic acid, 45, 48, 51
 dehydrogenation, 58
Formic acid/amine, dehydrogenation, 62
Fronodosin A, 306

G

Geranylation, 227
Giese reaction, 380
Glucose, 51, 73
Glycolonitrile, 90
Gypsy moth, 14

H

2-Heptanamine, 102
Heptanol, 328, 331, 343
Heteroarenes, arylation, sp^2 C–H bond
 activation, 122
Heteroarylation, 119, 121
Hexadecylamine (HDA), 356
Hexamethylbenzene, 89

Homopropargyl alcohols, cyclization, 246
Hydridophilicity, 25
Hydrido-ruthenium(II) catalysts, 86
Hydrogen, 19, 322
 ionic liquid-assisted evolution 65
 shift, 241, 259, 268
 storage devices, 71
Hydrogenation, 19, 323
 amides, 30
 carbamates, 35
 carbonates, 33
 carbonyl groups, 25
 CO₂, 37
 esters, 25
 urea, 36

I

Ibuprofenamide, 89
Imidazoles, 123
Imidazolylphosphanes, 244
Imidazo[1,2-*a*]pyridines, 137
Indanones, 268
Indenes, 256, 268
Indoles, 164, 231, 254, 273, 326
Indolo-cyclohexane, 146
1-Iodo-2-naphthols, 249
Ionic liquids, 45, 354
2-(4-Isobutylphenyl)propionitrile, 89
Isochromenes, 248
Isocyanates, 110, 296
Isocyanides, 231
Isopropanol, 198, 224, 229, 328, 343
 dehydrogenation, 47, 50

K

Ketoprofenamide, 89
Ketoximes, reductive acylation, 111

L

Lactams, 93, 99, 157
Lactones, 156, 242, 244, 295
Lactonitrile, 90
Ligands, 319
Limonene, 357
Lupasol FG, 69

M

Macrocycles, RCM, 10
Markovnikov addition, 242
Maytenine, 93

- Metal-hydroxyvinylidenes, 237
 Metal–ligand cooperation (MLC), 19, 20, 34
 Metathesis, 1, 269
 Methanol, 19, 29, 33–37, 104
 amidation, 104
 aqueous-phase reforming, 54
 dehydrogenation, 56
 Methyl formate, hydrogenation, 30
 10-Methyl undecenoate, 8
 6-Methyl-2-bromopyridine, 129
trans-2-Methyl-6-undecylpiperidine, 202
 2-Methylbutanol, 102
 Methylene-cyclopentanes, 311
 Methylene-cyclopropanes, 147
 Methylenetetrahydropyrans, 300
 7-Methylindole, 232
 Methylvinylketone, 305
 Monoarylations, selective, 132
 Myrtenamide, 97
 Mytilipin A, 14
- N**
- Nanocatalysts, 91, 93, 319, 352
 Nanoclusters, 319, 347
 Nanohybrids, 319
 Nanoparticles, 67, 91, 104, 319, 323
 Nanoreactors, 356
 Nanostructures, 319
N-Heterocyclic carbene (NHCs), 270, 338–340, 365
 Nitrile ylides, 220
 Nitriles, 81, 104, 250, 294, 296
 hydration, 81, 84
 hydrolytic amidation, 93
 Nitrocellulose (NC), 324
 Norbornadienes, 11, 159, 160, 302, 315
 Norbornenes, 10, 11, 270, 271
 AROCM, 10
 Nylon-6,6, 93
- O**
- 1-Octanol, 53
 Octylamine (OA), 356
 Olefins, 1, 121, 149, 196, 200, 216, 233, 266, 309, 341, 351, 363
 cyclic, 281
 metathesis catalysts, Z-selective, 1
 Oleyl alcohol, 13
 Organometallic synthesis, 319
 2-Oxa-3-azabicyclo[2.2.1]hept-5-ene, 303
 Oxabenzonorbornadienes, 304
 7-Oxanorbornadienes, 303
 2-Oxazoline, 123
 Oxidative quenching cycle, 374
 Oxonorbornadiene dimerized, 310
- P**
- Pentanenitrile, 93
 4-Pentenol, 14
 Perillamide, 97
 Pest control agents, 13
 1-Phenyl-1-cyclopentanecarboxylic acid, 129
 2-Phenylethanol, 106
 2-Phenyloxazoline, 123
 Phenylpyridine, 122
 Phenyltetrazoles, arylation, 137
 Pheromones, 13
 Phosphonium ILs, 51
 Phosphorane ester, 220
 Photoinduced electron transfer (PET), 372
 Photoredox catalysis, 371
 Pincer complexes, 19, 45
 Piperazine-2,5-diones, 3,6-disubstituted, 102
 Pivalate ligand, 10
 Platinum, 47, 48, 322, 340–342
 PNN-pincer, 101
 Polyamides, 101
 Polyvinylpyrrolidone (PVP), 324
 Potassium phthalimide (KPI), 129
 Prenylation, 227
 Proline derivatives, decarboxylative arylation, 207
 α -Propanoyl amines, 202
 PTA (1,3,5-triaza-7-phosphaadamantane), 88
 Pumiliotoxin C, 84
 (*N*-Pyridin-2-yl)piperidine, selective monoarylation, 207
- R**
- Radial distribution functions (RDF), 67
 Radical reactions, 371
 Rearrangements, 81
 Redox economy, 371
 Reductive quenching cycle, 374
 Renewable feedstocks, 45
 Ring closing metathesis (RCM), 7, 237
 Ring expansion, 305
 Ring opening metathesis polymerization (ROMP), 11, 237
 Ru(II) hydridoborohydride, 23
 Ru/tppts, 70
 Ru-pincer-type complexes, 45

Ruthenacycles, 5, 135, 187, 289, 309
 side-bound, 5
Ruthenacyclobutanes, 3
 side-bound, 5
Ruthenacyclopentatrienes, 290, 297–299
Ruthenium allenylidenes, 237, 272
Ruthenium nanoparticles (RuNPs), 323
Ruthenium vinylidenes, 237

S

Secondary phosphine oxide (SPO), 346
2-Silylbutadienes, hydrohydroxylation, 226
Single-electron transfer (SET), 372
Sodium bicarbonate, 71
Sodium formate, 71
Solenopsin A, 202
Steam reforming, 54
Styrene, 160, 163, 199, 335, 357, 386
2-Styrylpyridine, 266
Surface chemistry, 319

T

Tetrahydroisoquinolines, 233, 379
Tetrahydroquinoline, 146
Tetralin, 146
Thiazoles, 123

Thioenamides, 250
Toluene, 99, 127, 332, 347
Triethylamine, 62
Trifluoromethylation, 371
N-(3-Trifluoromethylpyridin-2-yl)piperidine,
 monoarylation, 209,
 1-Trimethylsilyl-1-alkyn-3-ols, 300,
Triphos, 63
Tris(5-(2-aminothiazolyl))-phosphine
 trihydrochloride, 89
Tris(2,2'-bipyridine)ruthenium (II), 371
Tris(dimethylamino)phosphine, 89
Tris(2-pyridyl)benzene, 130

U

Urea, hydrogenation, 36
Urotropin, 69

V

δ -Valerolactones, 247
Vinyl boronates, β,β -disubstituted, 300
Vinylidenes, 237, 240, 290

Y

Ynamides, 301, 303